



GEOLOGICAL SURVEY OF CANADA
COMMISSION GÉOLOGIQUE DU CANADA

This document was produced
by scanning the original publication.

Ce document est le produit d'une
numérisation par balayage
de la publication originale.

MEMOIR 387

**MESOZOIC AND TERTIARY GEOLOGY
OF BANKS ISLAND, ARCTIC CANADA**
The history of an unstable craton margin

Andrew D. Miall



Energy, Mines and
Resources Canada

Énergie, Mines et
Ressources Canada

1979

**MESOZOIC AND TERTIARY GEOLOGY
OF BANKS ISLAND, ARCTIC CANADA**
The history of an unstable craton margin



**GEOLOGICAL SURVEY
MEMOIR 387**

**MESOZOIC AND TERTIARY GEOLOGY
OF BANKS ISLAND, ARCTIC CANADA
The history of an unstable craton margin**

Andrew D. Miall

© Minister of Supply and Services Canada 1979

Available by mail from

Printing and Publishing
Supply and Services Canada
Hull, Québec, Canada K1A 0S9

and from

Geological Survey of Canada
601 Booth Street
Ottawa, Canada K1A 0E8

or through your bookseller

A deposit copy of this publication is also available
for reference in public libraries across Canada

Catalogue No. M46-387
ISBN 0-660-00848-3

Canada: \$25
Other countries: \$30

Price subject to change without notice

Addendum

Recent stratigraphic compilation and re-examination of biostratigraphic data suggest that the Jurassic strata in the Banks Island area may all be Upper Jurassic in age. They are correlated with the Husky Formation of the Beaufort-Mackenzie Basin (A.F. Embry, T.P. Poulton, *pers. com.*, 1978).

Errata

Figure 8: Location of Columbia et al Ikkariktok M-64 well should read 74°24', not 74°24°.

Map 1455A, Sheet 3: Locations 74-MLA-37 and 74-MLA-38 (near Eames River) should be 73-MLA-37 and 73-MLA-38, respectively.

Scientific Editor

E.J.W. IRISH

Critical Readers

D.W. MYHR

J.R. McLEAN

Editor

VALERIE DONNELLY

Text printed on Kelmscott offset, smooth (brilliant white)

Set in Times Roman with News Gothic captions

by SOUTHAM MURRAY, Toronto

Artwork by CARTOGRAPHIC UNIT, ISPG

1300-1977-6693-11

Preface

One of the principal aims of the Geological Survey is the estimation of the potential abundance and probable distribution of the mineral and fuel resources available in Canada. Such estimates depend on the continued refinement of the geological framework by detailed studies such as the one on Banks Island described in this report.

The main object of this investigation is to demonstrate, through a combination of surface and subsurface stratigraphic data and detailed facies and paleocurrent studies, that sedimentation was controlled by a series of small basins and highs which were on the margins of stable areas. These show a history of instability throughout Cretaceous and Paleogene time. The sedimentary record contains evidence of fluvial, deltaic, marginal marine and open-marine sedimentary facies.

D.J. McLaren
Director General
Geological Survey of Canada

Ottawa, September 1977

Contents

Abstract/Résumé	1
1. Introduction	3
Source of data	3
Previous work	3
Acknowledgments	5
Regional geological setting	5
2. Stratigraphy	10
Introduction	10
Description of formations	12
Jurassic and Lower Cretaceous	12
Wilkie Point Formation	12
Definition, distribution and thickness	12
Lithology	12
Age and correlation	12
Mould Bay Formation	13
Definition, distribution and thickness	13
Lithology	13
Age and correlation	14
Lower Cretaceous	14
Isachsen Formation	14
Definition, distribution and thickness	14
Contacts	16
Lithology	16
Age and correlation	24
Christopher Formation	25
Definition, distribution and thickness	25
Contacts	25
Lithology	27
Age and correlation	28
Hassel Formation	33
Definition, distribution and thickness	33
Contacts	33
Lithology	33
Age and correlation	33
Upper Cretaceous	37
Kanguk Formation	37
Definition, distribution and thickness	37
Contacts	37
Lithology	37
Age and correlation	40
Upper Cretaceous and Paleogene	44
Eureka Sound Formation	44
Definition, distribution and thickness	44
Contacts	44
Lithology	47
Age and correlation	48
Neogene	55
Beaufort Formation	55
Definition, distribution and thickness	55
Contacts	55
Lithology	55
Age and correlation	56

3. Sedimentology	57
Methods	57
Stratigraphic sections	57
Lithological percentages, ratios	57
Analysis of cyclic sedimentation	57
Assemblages of sedimentary structures	57
Paleocurrent studies	57
Sand petrography	58
Grain size analyses	58
Grain roundness	59
X-ray diffraction	59
Computer methods	59
Sedimentological synthesis	59
Wilkie Point and Mould Bay Formations	59
Isachsen Formation	60
Lithofacies and sedimentary structures	60
Coarse sand facies	60
Sand-shale facies	65
Summary	67
Paleocurrent analysis	67
The field sampling hierarchy	67
Interpretation 1. Areal paleocurrent variation	68
Interpretation 2. Vertical paleocurrent variation	72
Grain size analysis	76
Causes of grain size variability	76
Environmental interpretation	76
Local and regional grain size variations	78
Petrographic analysis	80
Description of clast types	80
Matrix and cement	87
Texture	87
Quantitative analysis	88
Sediment sources	90
Summary	97
Paleoclimate analysis	97
Paleohydrological analysis	97
Discharge as a function of climate	97
Paleohydrology of the meandering streams	97
Paleohydrology of the braided streams	100
Paleogeographic implications	103
Christopher Formation	103
Lithofacies and sedimentary structures	103
Depositional environment	104
Grain size analysis of sand units	104
Petrographic analysis	105
Sand, sandstone	105
Shale, silty shale	106
Hassel Formation	106
Lithofacies and sedimentary structures	106
Facies types	106
Depositional environment	107
Paleocurrent analysis	109
Analysis of ripple-mark morphology	110
Modal analysis	110
Grain size analysis	111
Petrographic analysis	111
Description of clast types	111
Matrix and cement	112
Texture	112
Quantitative analysis	112
Sediment sources	112

Kanguk Formation	115
Bituminous shale member	115
Petrographic analysis	115
Tuff beds	115
Bentonite beds	115
Manganese spherulites	115
Depositional environment	116
Silty shale member	119
Petrographic analysis	119
Shale, silty shale	119
Concretions	119
Depositional environment	120
Lower and upper sand members	120
Lithofacies and sedimentary structures	120
Depositional environment	120
Paleocurrent analysis	120
Grain size analysis	120
Petrographic analysis	121
Description of clast types	121
Matrix and cement	122
Texture	122
Sand classification	122
Sediment sources	122
Eureka Sound Formation	124
Lithofacies and sedimentary structures – 1. General description	124
Analysis of cyclic sedimentation	126
Markov chain analysis of surface sections	126
Fourier analysis of subsurface sections	131
Lithofacies and sedimentary structures – 2. Regional variation	132
Vertical variation	132
Lateral variation	133
Depositional environment	135
Cyclic models	136
Small-scale cycles	137
Noncyclic units	143
Regional variability in small-scale cycles	143
The delta model	144
Paleocurrent analysis	144
Interpretation	144
Grain size analysis	147
Interpretation	147
Petrographic analysis	147
Description of clast types	147
Matrix and cement	149
Texture	149
Quantitative analysis	151
Sediment sources	152
Paleohydrological analysis	153
An analysis based on epsilon crossbedding	153
An analysis based on trough crossbedding	156
Estimation of river discharge and drainage area	157
Paleogeographic implications	157
Beaufort Formation	158
4. Structural geology	159
Introduction	159
Folds	159
Faults	159
Superficial structures	165
5. Economic geology	166
Oil and gas	166
Coal	167

6. Synthesis and conclusions	168
Regional paleogeographic evolution	168
Jurassic and early Neocomian	168
Barremian and Aptian	168
Albian	170
Cenomanian to Santonian	172
Campanian and Maastrichtian	172
Paleocene and Eocene	173
Oligocene and Miocene	177
Post-Miocene	177
Detrital flow chart	178
Regional tectonic considerations	178
Assessment of sedimentological methods	179
 References	 181
 Appendices	
1. Summary of subsurface Mesozoic and Tertiary stratigraphy	189
2. Subsurface logs	191
3. Stratigraphic sections	207
 Maps	
1454A. 1:1,000,000 geological map of Banks Island, with structural cross-section	<i>in pocket</i>
1455A. 1:250,000 geological map of northern Banks Island, in four sheets (88C, 88F, 98D, 98E)	<i>in pocket</i>
1456A. 1:250,000 geological map of De Salis Bay area (97H)	<i>in pocket</i>
 Tables	
1. Table of formations, Banks Island and adjacent areas	7
2. Nomenclature changes, Upper Cretaceous and Paleogene rocks of Banks Island	38
3. Paleocurrent data, Isachsen Formation	67
4. Summary of field data for five vertical profiles through the coarse sand facies, Isachsen Formation	72
5. Grain size data, Isachsen Formation	76
6. Petrographic analyses of sand and sandstone, Isachsen Formation	81
7. Conglomerate clast types, Isachsen Formation	82
8. Paleohydrology of meandering river at Orksut I-44	99
9. Paleohydrology of braided streams, Isachsen Formation	99
10. Hydrology of some modern braided rivers	99
11. Petrographic analyses of sand and sandstone, Christopher Formation	105
12. X-ray diffraction analyses of fine-grained rocks, Christopher Formation	106
13. Derivation of wave parameters from field observations on ripple marks, Hassel Formation	110
14. Petrographic analyses of sand and sandstone, Hassel Formation	112
15. Chemical analyses of tuff samples, basal Kanguk Formation	115
16. X-ray diffraction analyses of bentonitic beds, basal Kanguk Formation	115
17. Spherulitic carbonate, basal Kanguk Formation: partial chemical analyses	115
18. X-ray diffraction analyses of fine-grained rocks, silty shale member, Kanguk Formation	120
19. X-ray diffraction analyses of concretions, silty shale member, Kanguk Formation	120
20. Petrographic analyses of sand and sandstone, Kanguk Formation	122
21. Transition count matrix, grouped Paleocene data, Cyclic Member, Eureka Sound Formation	126
22. Transition count matrix, grouped Eocene data, Cyclic Member, Eureka Sound Formation	126
23. Difference probability matrix, grouped Paleocene data, Cyclic Member, Eureka Sound Formation	126

24. Difference probability matrix, grouped Eocene data, Cyclic Member, Eureka Sound Formation	126
25. Tests of significance, Markov chain analysis of stratigraphic successions, Cyclic Member, Eureka Sound Formation	131
26. Vertical variations in stratigraphic parameters, Cyclic Member, Eureka Sound Formation	132
27. Stratigraphic data, Cyclic Member, Eureka Sound Formation	133
28. Paleocurrent data, Eureka Sound Formation	144
29. Grain size data, Eureka Sound Formation	147
30. Petrographic analyses of sand and sandstone, Eureka Sound Formation	148
31. Conglomerate clast types, Eureka Sound Formation	149
32. Paleohydrology of the distributary channel at Station 74-MLA-156 (Castel Bay)	157
33. Paleohydrology of an average distributary channel at Stations 73-MLA-19, 20, 21 (Nangmagvik Lake)	157
34. Drillstem test results, Mesozoic rocks, Banks Island	166

Plates

1. Planar crossbedded sands, Isachsen Formation, Cape Vesey Hamilton	17
2. General views of the Isachsen Formation, northern Banks Island	19
3. The Isachsen-Christopher contact, Baker Creek	20
4. General views of the Isachsen Formation, Nelson Head	21
5. Pebble and boulder conglomerates, basal Isachsen Formation, Nelson Head	22
6. Uppermost Isachsen Formation, Colquhoun River	23
7. Lower part of the Christopher Formation	29
8. Upper part of the Christopher Formation	30
9. The Hassel Formation	35
10. The basal Kanguk Formation	36
11. Silty shale member, Kanguk Formation	41
12. Kanguk-Eureka Sound transition beds	49
13. Cyclic Member, Eureka Sound Formation	50
14. Plant remains and coal, Eureka Sound Formation	51
15. The Eureka Sound-Beaufort contact	52
16. Deformed crossbedding, Isachsen Formation	62
17. Planar and trough crossbedding, Isachsen Formation	63
18. Ripple marks, Isachsen Formation	64
19. Photomicrographs of quartz grains, Isachsen Formation	83
20. Photomicrographs of quartz grains, Isachsen Formation	84
21. Quartz, sandstone and chert grains, Isachsen Formation	85
22. Chert, feldspar and zircon grains, Isachsen Formation	86
23. Small-scale ripple marks, Hassel Formation	108
24. Tuffaceous rocks, basal Kanguk Formation	116
25. Manganese spherulites, basal Kanguk Formation	117
26. Sedimentary structures, upper sand member, Kanguk Formation	118
27. Photomicrographs of sand, Hassel and Kanguk formations	123
28. Photomicrographs of sandstone, Kanguk Formation	124
29. Planar crossbedding, Cyclic Member, Eureka Sound Formation	127
30. Trough crossbedding, Cyclic Member, Eureka Sound Formation	128
31. Small-scale sedimentary structures, Cyclic Member, Eureka Sound Formation	129
32. Ball and pillow structures, Cyclic Member, Eureka Sound Formation	130
33. Features of deltaic sedimentation, Cyclic Member, Eureka Sound Formation	141
34. Plant and lignite remains, Cyclic Member, Eureka Sound Formation	142
35. Photomicrographs of sand, Eureka Sound Formation	150
36. Faults	160
37. Superficial structures, Eureka Sound Formation	163
38. Small-scale structures	164

Figures

1. Index map, western Canadian Arctic	<i>facing</i> 1
2. Index map of Banks Island	4
3. Structural-stratigraphic provinces, western Canadian Arctic	6
4. Structural elements in Banks Island, based on Bouguer gravity data	8
5. Restored stratigraphic cross-section, Mesozoic and Tertiary rocks, northern Banks Island	<i>in pocket</i>
6. Restored stratigraphic cross-section, Mesozoic and Tertiary rocks, central Banks Island	<i>in pocket</i>
7. Restored stratigraphic cross-section showing distribution of Lower Cretaceous rocks along the edge of the Central Stable Region	<i>in pocket</i>
8. Stratigraphic cross-section showing subsurface Mesozoic and Tertiary stratigraphy	<i>in pocket</i>
9. Isachsen Formation: distribution, thickness and lithologies	15
10. Lateral changes within the Isachsen Formation, Nelson Head	18
11. Christopher Formation: distribution, thickness and lithologies	26
12. Hassel Formation: distribution, thickness and lithologies	34
13. Kanguk Formation: distribution, thickness and lithologies	39
14. Eureka Sound Formation, Shale Member: distribution, thickness and lithologies	45
15. Eureka Sound Formation, Cyclic Member: distribution, thickness and lithologies	46
16. Lateral changes within the Cyclic Member, Eureka Sound Formation, Nangmagvik Lake	48
17. Generalized paleogeography, Jurassic Period	60
18. Location of five vertical profiles through the coarse sand facies, Isachsen Formation	61
19. Interpretation of the Isachsen Formation at Orksut I-44 in terms of cyclic sequences	66
20. Plot of ripple index and ripple symmetry index for five ripple marks at Station 73-MLA-35, Colquhoun River	66
21. Paleocurrent rose diagrams, Isachsen Formation	69
22. Interpreted transport directions and facies distribution, Isachsen Formation	70
23. Geological sketch map, Nelson Head Graben	71
24. Geological sketch map, Cape Vesey Hamilton area	71
25. Cross-section of Figure 24	72
26. Vertical profile at Station 74-MLA-18	73
27. Vertical profile at Station 73-MLA-26	73
28. Vertical profile at Station 73-MLA-29	73
29. Vertical profile at Station 73-MLA-30	74
30. Vertical profile at Station 73-MLA-31	74
31. Grain size distribution curves, Station 73-MLA-26A	77
32. Grain size distribution curves, Station 73-MLA-26B	77
33. Grain size distribution curves, Station 73-MLA-30A	77
34. Grain size distribution curves, Station 73-MLA-30B	77
35. Variations in phi mean grain size, Isachsen Formation	79
36. Variations in grain size parameters in two vertical profiles	80
37. Sand petrography, Isachsen Formation, showing sand classification scheme of Okada (1971)	88
38. Q-mode cluster analysis of 59 petrographic samples, Isachsen Formation	89
39. Sand petrography, Isachsen Formation, showing the composition of Q-mode cluster analysis groupings	90
40. Areal distribution of cluster analysis groupings, sand petrography, Isachsen Formation	91
41. Sand petrography, minor constituents, Isachsen Formation	92
42. Distribution of some rare components, Isachsen Formation	93
43. Upward changes in petrographic composition, two vertical profiles, Isachsen coarse sand facies: major constituents	94
44. Upward changes in petrographic composition, two vertical profiles, Isachsen coarse sand facies: minor constituents	94

45. Source rocks, Isachsen Formation	95
46. Development of a fining-upward sequence by lateral accretion	98
47. Main drainage pattern, east side of Banks Basin	101
48. Estimated drainage area, meandering stream at Orksut I-44	102
49. Plot of ripple index and ripple symmetry index for 16 ripple marks, Stations 74-GAS-4 (Rufus River) and 74-GAS-13 (Atitok River)	104
50. Grain size distribution curves, sand from the Christopher Formation	104
51. Typical sections through the Hassel Formation	107
52. Plot of ripple index and ripple symmetry index for 23 ripple marks, Stations 73-MLA-15, 17 (lower Thomsen River)	110
53. Paleocurrent rose diagrams, Hassel Formation	110
54. Grain size distribution curves, sand from the Hassel Formation	111
55. Sand petrography, Hassel Formation, showing composition of Q-mode cluster analysis groupings	113
56. Q-mode cluster analysis of 14 samples, Hassel Formation	113
57. Areal distribution of cluster analysis groupings, sand petrography, Hassel Formation	114
58. Paleocurrent rose diagrams, upper sand member, Kanguk Formation	121
59. Grain size distribution curves, upper sand member, Kanguk Formation	121
60. Sand petrography, Kanguk Formation	125
61. Transition path diagrams, Cyclic Member, Eureka Sound Formation	131
62. Comparison of cycles, surface and subsurface	132
63. Amplitude spectra for parts of four gamma ray logs through the Cyclic Member, Eureka Sound Formation	133
64. Location numbers and age of sections, Cyclic Member, Eureka Sound Formation	134
65. Sand/shale ratio, Cyclic Member, Eureka Sound Formation	135
66. Mean sand bed thickness, Cyclic Member, Eureka Sound Formation	136
67. Mean cycle thickness, Cyclic Member, Eureka Sound Formation	137
68. Sand/shale ratio within the clastic cycles, Cyclic Member, Eureka Sound Formation	138
69. Percentage of section that is cyclic, Cyclic Member, Eureka Sound Formation	139
70. Distribution of sedimentary structure assemblages, Cyclic Member, Eureka Sound Formation	140
71. Variations in cycle thickness, Cyclic Member, Eureka Sound Formation	143
72. Paleocurrent rose diagrams, Eureka Sound Formation	145
73. Sedimentary structure assemblages and paleocurrent trends, Eureka Sound Formation	146
74. Grain size distribution curves, sand from the Eureka Sound Formation	147
75. Sand petrography, Eureka Sound Formation, showing sand classification scheme of Okada (1971)	151
76. Q-mode cluster analysis of 42 samples, Eureka Sound Formation	152
77. Sand petrography, Eureka Sound Formation, showing composition of Q-mode cluster analysis groupings	153
78. Areal distribution of cluster analysis groupings, sand petrography, Eureka Sound Formation	154
79. R-mode cluster analysis, sand samples, Eureka Sound Formation	155
80. Ternary plot of chert, mafic minerals (micas plus iron oxides) and feldspars, sand from the Eureka Sound Formation	155
81. Source rocks, Eureka Sound Formation	156
82. The main drainage pattern for rivers entering Northern Banks Basin	158
83. Structural contour map, base of the Mesozoic	161
84. Structural contour map, base of the Beaufort Formation	162
85. Paleogeographic synthesis, Barremian and Aptian time	169
86. Paleogeographic synthesis, Albian time	171
87. Paleogeographic synthesis, Cenomanian to Santonian time	173
88. Paleogeographic synthesis, Campanian and Maastrichtian time	174
89. Paleogeographic synthesis, Paleocene time	175
90. Paleogeographic synthesis, Eocene time	176
91. Detrital flow chart	177

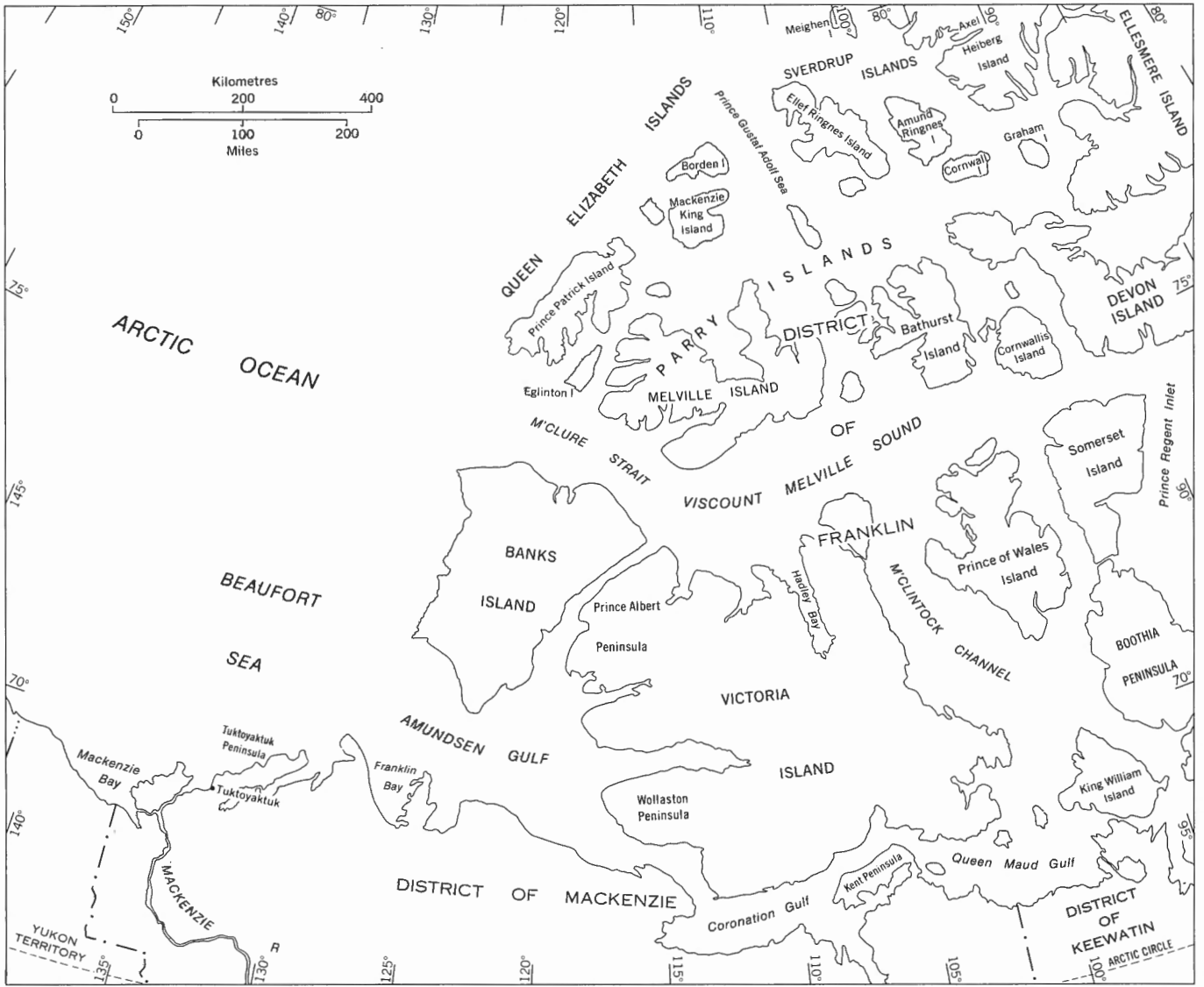


Figure 1. Index map of the western Canadian Arctic.

MESOZOIC AND TERTIARY GEOLOGY OF BANKS ISLAND, ARCTIC CANADA

The History of an Unstable Craton Margin

Abstract

More than 80 per cent of the surface area of Banks Island is underlain by Mesozoic and Tertiary rocks, the maximum thickness of which probably does not exceed 3000 m (10 000 ft). The disposition of these strata led to the definition of the term 'Banks Island Basin' by Thorsteinsson and Tozer, but gravity and subsurface data show that the basin is divisible into a series of structural lows and highs, including Banks Basin, Big River Basin, Cardwell Basin and Storkerson Uplift. These structural elements have been in existence at least since the Early Cretaceous, as shown by facies and paleocurrent trends.

Post-Paleozoic sedimentation commenced in the Early or Middle Jurassic with the accumulation in Banks Basin of 400 m (1320 ft) of marine silty shale correlated with the Wilkie Point and Mould Bay formations. Most of Valanginian to Barremian time is not represented in the sedimentary record. In the Barremian-Aptian interval, differential uplift of Minto Arch and, probably, Storkerson Uplift caused erosion of coarse, quartz-rich detritus, which was transported into Banks and Cardwell basins by braided and meandering streams. The Isachsen Formation, up to 200 m (660 ft) thick, was the result. A transgression in the Albian inundated the existing topography, and the shales of the Christopher Formation overlap the Isachsen at several localities and lie directly on the Devonian basement. The Christopher Formation ranges from 30 to 460 m (110–1500 ft) thick. It is followed by a regressive unit, the Upper Albian Hassel Formation, which represents a barrier island environment. The Hassel is present only on the margins of Northern Banks Basin where it is up to 50 m (165 ft) thick. Most of the detritus in the formation was derived from the Upper Devonian Melville Island Group.

A major disconformity occurs above the Hassel Formation. Locally, much or all of the Lower Cretaceous succession is absent as a result of post-Albian, pre-Campanian erosion. Sedimentation may, however, have continued with a much shorter break in Big River Basin.

The Kanguk Formation (Upper Cretaceous), ranging from 90 to 380 m (300–1250 ft) in thickness, is a transgressive unit consisting mainly of silty shale. Tuff, bentonite beds and manganese spherulites occur in a distinctive bituminous shale member at the base. Littoral marine sand units comprise lower and upper sand members. It grades upward into the predominantly nonmarine Eureka Sound Formation, of late Maestrichtian to Eocene age. Lowermost beds of the Eureka Sound comprise a shale of prodelta origin, but delta lobes, consisting of coarser sediments derived mainly from Devonian rocks, prograded into Banks and Big River basins during the Paleogene. The deltaic

Résumé

Plus de 80 pour cent de la superficie de l'île Banks repose sur des roches mésozoïques et tertiaires dont l'épaisseur maximale n'excède probablement pas 3000 m (10 000 pieds). La disposition des strates a amené Thorsteinsson et Tozer à définir le terme 'Banks Island Basin', mais les données concernant le sous-sol et la gravitation montrent que le bassin peut être divisé en une succession de dépressions et d'élévations structurales, dont le bassin de Banks, le bassin de Big River, le bassin de Cardwell et le soulèvement de Storkerson. Ces éléments structuraux existent au moins depuis le Crétacé inférieur comme l'indiquent les faciès et les directions des paléocourants.

La sédimentation post-paléozoïque a commencé pendant le Jurassique inférieur ou le Jurassique moyen par l'accumulation, dans le bassin de Banks, de 400 m (1320 pieds) de schiste silteux marin relié aux formations de Wilkie Point et de Mould Bay. La plus grande partie de l'intervalle comprise entre le Valanginien et le Barrémien n'est pas représentée dans les sédiments. Dans l'intervalle comprise entre le Barrémien et l'Aptien, le soulèvement différentiel de l'arche de Minto et, probablement, le soulèvement de Storkerson, ont provoqué l'érosion de débris grossiers riches en quartz qui ont été transportés dans les bassins de Banks et de Cardwell par des cours d'eau anastomosés et sinueux. La formation qui en a résulté, celle d'Isachsen, peut atteindre une épaisseur de 200 m (660 pieds). Durant l'Albien, une transgression a inondé le relief existant; les schistes argileux de la formation de Christopher, qui reposent directement sur le socle dévonien, ont alors recouvert la formation d'Isachsen en plusieurs endroits. L'épaisseur de la formation de Christopher se situe entre 30 et 460 m (110 à 1500 pieds). La formation de Hassel, unité régressive de l'Albien supérieur, fait suite à cette formation et constitue un milieu d'île-barrière. On ne la trouve qu'aux limites nord du bassin de Banks où elle peut atteindre jusqu'à 50 m (165 pieds) de profondeur. La majeure partie des débris de cette formation proviennent du groupe de Melville Island du Dévonien supérieur.

Au-dessus de la formation de Hassel, on note la présence d'une importante discordance d'érosion. Localement, une érosion post-albienne et pré-campanienne a fait disparaître une grande partie ou la totalité de la succession du Crétacé inférieur. La sédimentation peut s'être poursuivie, cependant, avec une interruption beaucoup plus courte dans le bassin de Big River.

La formation de Kanguk (Crétacé supérieur), dont l'épaisseur se situe entre 90 et 380 m (300 à 1250 pieds), est une unité transgressive constituée surtout de schiste silteux. A la base, on y trouve du tuf, des lits de bentonite et des sphérolites de manganèse dans un niveau distinctif de schiste bitumineux. Les unités littorales de sable marin comprennent des niveaux inférieurs et supérieurs de sable. Celui-ci se transforme graduellement de bas en haut pour donner naissance à la formation d'Eureka Sound qui est surtout non marine et qui date du Maestrichtien à l'Éocène. Les lits les plus bas de la formation d'Eureka Sound sont constitués de schistes argileux d'origine prodeltaïque, mais les lobes du delta, constitués de sédiments grossiers provenant en grande partie de roches dévoniennes ont avancé vers la mer pour former les bassins de Banks et de Big River durant le Paléogène. Les successions deltaïques sont caractérisées par des cycles de roches clastiques qui sont de plus en plus grossières de bas en haut et dont l'épaisseur moyenne est de 7,4 m (24,2 pieds). L'épaisseur de la formation d'Eureka Sound se situe entre 200 et 1200 m (650 à 3900 pieds).

Manuscript received 19 November 1975
Manuscript accepted for publication 2 September 1977

Andrew D. Miall is with the Institute of Sedimentary and Petroleum Geology, 3303 - 33rd Street, NW, Calgary, Alta, T2L 2A7

successions are characterized by coarsening-upward clastic cycles averaging 7.4 m (24.2 ft) in thickness. The Eureka Sound ranges from 200 to 1200 m (650–3900 ft) thick.

The report-area underwent major fault movements during the Oligocene or early Miocene. Most faults are oriented between north and northeast and displacements are normal. The maximum recorded throw is 900 m (3000 ft) on a fault at Nelson Head, where the Eureka Sound Formation is juxtaposed with the Proterozoic basement. Uplift and erosion, which followed this tectonic activity, resulted in deposition of sand, gravel and clay of the Beaufort Formation during the mid to late Miocene by rivers flowing westward across the report-area. The formation thickens to the west, reaching 260 m (860 ft) in Big River Basin, and several thousands of metres offshore to the west of the report-area. Post-Beaufort events include a gentle structural warping, glaciation, and dissection of the Beaufort surface by erosion during the Quaternary.

Oil and gas prospects are poor in the Mesozoic-Tertiary rocks although good reservoir rocks are present. The best reservoir probably is the Isachsen Formation, but this unit is absent over at least some of the major structural highs, probably because they formed topographically elevated areas during sedimentation. Geochemical results indicate that most or all of the Mesozoic-Tertiary section is immature. Lignitic coals are abundant in the Eureka Sound Formation, but their volume and heat value are estimated to be of little economic interest.

Durant l'Oligocène ou le Miocène inférieur, des déplacements de failles importants se sont produits dans la région considérée. La plupart des failles sont orientées entre le nord et le nord-est et leurs déplacements sont normaux. Le rejet vertical maximal enregistré sur la faille est de 900 m (3000 pieds) au promontoire Nelson, où la formation d'Eureka Sound est juxtaposée au socle protérozoïque. Par suite du soulèvement et de l'érosion qui ont suivi cette activité tectonique, les rivières s'écoulant vers l'ouest dans la région étudiée ont déposé, durant le Miocène moyen et le Miocène supérieur, le sable, le gravier et l'argile qui constituent la formation de Beaufort. Celle-ci s'épaissit vers l'ouest, pour atteindre 260 m (860 pieds) d'épaisseur dans le bassin de Big River et plusieurs milliers de mètres au large, à l'ouest de la région étudiée. Parmi les événements qui ont fait suite à la formation de Beaufort, on distingue un léger gauchissement structural, une glaciation et une dissection de la surface de la formation de Beaufort par érosion durant le Quaternaire.

Dans les roches mésozoïques-tertiaires, les zones productives possibles de pétrole et de gaz naturel sont pauvres malgré la présence de bonnes roches réservoirs. Le meilleur réservoir est probablement la formation d'Isachsen, mais cette unité manque sur au moins une partie des principales élévations structurales, probablement à cause du fort relief de celles-ci durant la sédimentation. Les résultats géochimiques indiquent que la majeure partie ou la totalité de la coupe mésozoïque-tertiaire n'a pas atteint la maturité. Les charbons lignitiques abondent dans la formation d'Eureka Sound, mais on estime qu'à cause de leur volume et de leur pouvoir calorifique, leur intérêt économique est faible.

1. Introduction

Source of data

Banks Island is the southwesternmost island of the Canadian Arctic Archipelago (Fig. 1); it comprises an area of 60 100 km² (23 200 sq mi) and is the fifth largest island in Canada. The island was sighted first in 1820 by Lieutenant F.W. Beechey of the Royal Navy and was named Banks' Land after Sir Joseph Banks, President of the Royal Society.

The present report is concerned with the geology of the Mesozoic and Tertiary rocks, both at the surface and in the subsurface. Data from eight of the first nine wells to be drilled on the island are incorporated with data obtained in the field during the summers of 1973 and 1974. The first six wells have been studied in detail. Their names, locations and completion dates are listed below. Locations are shown in Figure 2.

Elf et al Storkerson Bay A-15; lat. 72°54'00"N, long. 124°33'29"W; 10 December 1971

Elf Nanuk D-76; lat. 73°05'13"N, long. 123°23'45"W; 4 March 1972

Elf Uminmak H-07; lat. 73°36'29"N, long. 123°00'30"W; 7 May 1972

Deminex CGDC FOC Amoco Orksut I-44; lat. 72°23'45"N, long. 122°42'09"W; 28 March 1973

Elfex Texaco Tiritchik M-48; lat. 72°47'51"N, long. 120°44'48"W; 6 April 1974

Columbia et al Ikkariktok M-64; lat. 72°23'46"N, long. 121°50'49"W; 16 April 1974

Preliminary results from the following two wells also are incorporated:

Panarctic Tenneco et al Castel Bay C-68; lat. 74°07'11"N, long. 120°49'00"W; 1 April 1975

Panarctic Elf Bar Harbour E-76; lat. 75°15'28"N, long. 123°53'50"W; 29 December 1975

The first six wells have been logged by the author, using the chip samples and cores stored at the Institute of Sedimentary and Petroleum Geology, Calgary. Because very few cores are available from any of the wells, lithological descriptions and age determinations must rely mainly on data obtained from the surface. Chip samples are necessarily small and, owing to the different densities of the various lithologies, they rise to the surface in the mud stream at different rates. Thus lithological and depth determinations are imprecise unless they are coupled with interpretations of geophysical log character, as has been done in the present study. The softness of the post-Paleozoic rocks creates additional problems: soft

shales and mudstones may disperse into the mud stream, so that the final sample may contain an undue proportion of coarser clastic material such as sand grains, or excessive quantities of less abundant lithologies such as concretions. Caving is also a problem. The returning mud stream may pick up fragments from high in the well and these may mask the characteristics of the lower (older) rock types. This has proved to be a particularly difficult problem during palynological and micropaleontological studies. As an example, caved Jurassic pelecypod fragments and foraminifera were recovered from apparent depths down to 2100 m (6890 ft) at the Orksut I-44 well, which is 270 m (890 ft) below the base of the Mesozoic at this locality.

Approximately ten weeks were spent in the field on Banks Island. The party commenced work on foot in June 1973 with a ten-day stay at Antler Cove. Base camp was then moved to Nangmagvik Lake, where a river terrace provides an excellent landing strip much used by scientific parties during the last few years. The remainder of the 1973 field work (three and a half weeks) was carried out from this camp, using a Piper Super Cub to visit many of the more extensive or more geologically significant outcrops in the northern part of the island. In 1974 field work was conducted first from a base camp at De Salis Bay, with the aid of a G3B1 helicopter. A three-week stay was sufficient to visit virtually all the significant outcrops of the Cretaceous and lower Tertiary rocks exposed in the De Salis Bay map-area (NTS 97H), with the aid of a senior field assistant A.S. Greene, who operated independently. Subsequently the party moved to the Nangmagvik Lake camp site and mapping of the northern part of the island was completed.

A total of ten weeks' field work was found to be sufficient because a very large part of the island is covered by thick surficial deposits. With the exception of the area of Devonian outcrop, less than a quarter of the surface area contains sufficient exposure for geological mapping at the scale of 1:250 000.

Previous work

The first systematic geological investigations on Banks Island were carried out by Thorsteinsson and Tozer (1962) in co-operation with R.L. Christie and J.G. Fyles. That party spent two and a half months in Banks Island and Victoria Island and mapped the entire area at a scale of 1:1 000 000. Their final report has provided the basis for all subsequent geological endeavours on the two islands. A summary of earlier geological investigations and a brief history of exploration are provided by the same authors (*ibid.*, p. 4-6).

Field work on Banks Island has been carried out by several oil companies in recent years, notably by geologists of Petropar Canada Ltd. (later Elf Oil Exploration and Production Canada Ltd.), who first visited the area in July 1966. Summaries of their findings have been published by Plauchut (1971), Jutard and Plauchut (1973) and Cassan and Evers (1973). Several important revisions in stratigraphic correlation were included in these reports and the first major attempt was made to understand the sedimentology of some of the units.

Hills (1969), Hills and Ogilvie (1970) and Hills and Fyles (1973) studied the Beaufort Formation of northwestern Banks Island.

Exploratory drilling activity commenced in 1971 and up to the date of writing (April 1976) nine wildcat wells had been drilled on the island. No hydrocarbon shows were found in any of these wells and all were abandoned. However, the geological data they provide are invaluable.

Equally valuable is a gravity survey of Banks Island published by Stephens *et al.* (1972), which has assisted considerably in the compilation of the regional subsurface geology. The area has been much explored seismically by industry but all of the results remain confidential to the present.

Parts of the work carried out by the writer have appeared elsewhere. Preliminary results of the field work were published (Miall, 1974*b*, 1975*a*), and the subsurface stratigraphy of several of the wells was described as each was released from confidential status (Miall, 1974*a*, 1974*c*, 1975*c*). Some manganese carbonate spherulites that occur in the subsurface were described (Miall, 1974*d*), and the methods of paleocurrent analysis and some of the detailed results also have been discussed previously (Miall, 1974*e*, 1976*b*, *c*). A preliminary synthesis of the post-Paleozoic geology (Miall, 1975*b*) and a final report on the Proterozoic and Paleozoic geology have been published (Miall, 1976*a*). Work on the Paleozoic rocks by other authors is summarized in the 1976*a* reference.

Acknowledgments

Able assistance in the field and in the office was provided by A.S. Greene (senior assistant) and by D. Wiens, T. Gallagher and W. George (junior assistants). The co-operation and expertise of Super Cub pilot Bob Mackenzie (in 1973) and helicopter pilot-engineer Wiley Miuse (in 1974) contributed much to the success of field operations. Expediting, radio-communications services and fixed-wing air time for camp moves were provided by Polar Continental Shelf Project through their base at Tuktoyaktuk. Thanks are due in particular to Frank Hunt, base manager, for his efficiency in managing our logistic support. Aircraft were chartered from Reindeer Air Services of Inuvik (Piper Cub), and from Shirley Helicopters, Edmonton.

Seismic shothole samples used in the regional mapping were provided by Elf Oil Exploration and Production Canada Ltd. Palynological and micropaleontological studies of these samples were carried out by Robertson Research (North America) Ltd. R. Arnold of Elf Oil co-ordinated the project. Several additional field samples and field observations were very kindly contributed by B.P. Plauchut (Ste. Nat. Pétroles Aquitaine), H. Evers (Elf Oil) and J.S. Vincent (Terrain Sciences Division, Geological Survey of Canada).

XRD and wet-chemical analyses were carried out at the Institute of Sedimentary and Petroleum Geology by A.J. Heinrich and R.R. Barefoot, under the supervision of A.E. Foscolos. Computing services were provided by Digitech Corp. Ltd. and Geodigit, both of Calgary. Most of the computer programs used in this report were written by the author but N. Thompson (Digitech) carried out the Fourier analyses, M. Oldershaw (Geodigit) supplied the grain size distribution probability plots, and Dilsher Virk (ISPG) wrote a program for plotting paleocurrent rose diagrams.

The writer is grateful to many of his colleagues for discussions of the subject matter, particularly F.G. Young, H.R. Balkwill and H.P. Trettin. D.W. Myhr and J.R. McLean critically read an earlier version of the manuscript; thanks are extended to them for their numerous suggestions for its improvement.

Regional geological setting

The structural setting of the Banks Island area is shown in Figure 3, which is based on the work of numerous authors, notably Thorsteinsson and Tozer (1960), Kerr (1974) and Lerand (1973). Most of the detail pertaining to Banks Island itself has been omitted from Figure 3 and is shown separately in Figure 4.

In the southeast corner of Figure 3 is the edge of the Canadian Shield, which is covered partly by Proterozoic sedimentary rocks. The Shield also projects northward along a linear feature named Boothia Uplift, the northern end of which is shown at the right-hand edge of the figure. A large area of exposed Proterozoic rocks is present also in Victoria Island; it has been named Minto Uplift.

Most of the craton which borders the Shield is underlain by Cambrian to Devonian rocks, composing the Central Stable Region. Epeirogenic movements of uncertain, but probably in part post-Devonian, age divided the Central Stable Region into broad basins, platforms and highs and erosion on the highs subsequently has revealed the Proterozoic rocks beneath. Structural units made up of Paleozoic cratonic sequences include Mackenzie Platform, Wollaston Basin, Prince Albert Homocline, Melville Basin and M'Clintock Basin (Christie, 1972). Part of Banks Island is underlain by the rocks of Prince Albert Homocline, which was estimated by Thorsteinsson and Tozer (1962) to comprise at least 2400 m (8000 ft) of Cambrian to Devonian strata. The author (Miall, 1976*a*) has shown that on Banks Island the Devonian succession alone is probably double this thickness.

The cratonic sequences pass laterally into geosynclinal rocks west of the Mackenzie River and in the central Arctic Islands. The Cordilleran Orogen has had a complex stratigraphic and tectonic history spanning the late Proterozoic and most of Phanerozoic time (Norris, 1974). Geosynclinal conditions in the Arctic Islands, however, were confined as far as is known to the late Proterozoic to Devonian time interval (Trettin *et al.*, 1972). The shallower-water, miogeosynclinal portions of the geosyncline were deformed during Early to Late Devonian time, giving rise to Cornwallis Fold Belt, and again in the Late Devonian or Early Mississippian Ellesmerian Orogeny, creating Parry Islands Fold Belt and Central Ellesmere Fold Belt (not shown in Fig. 3). The deeper-water,

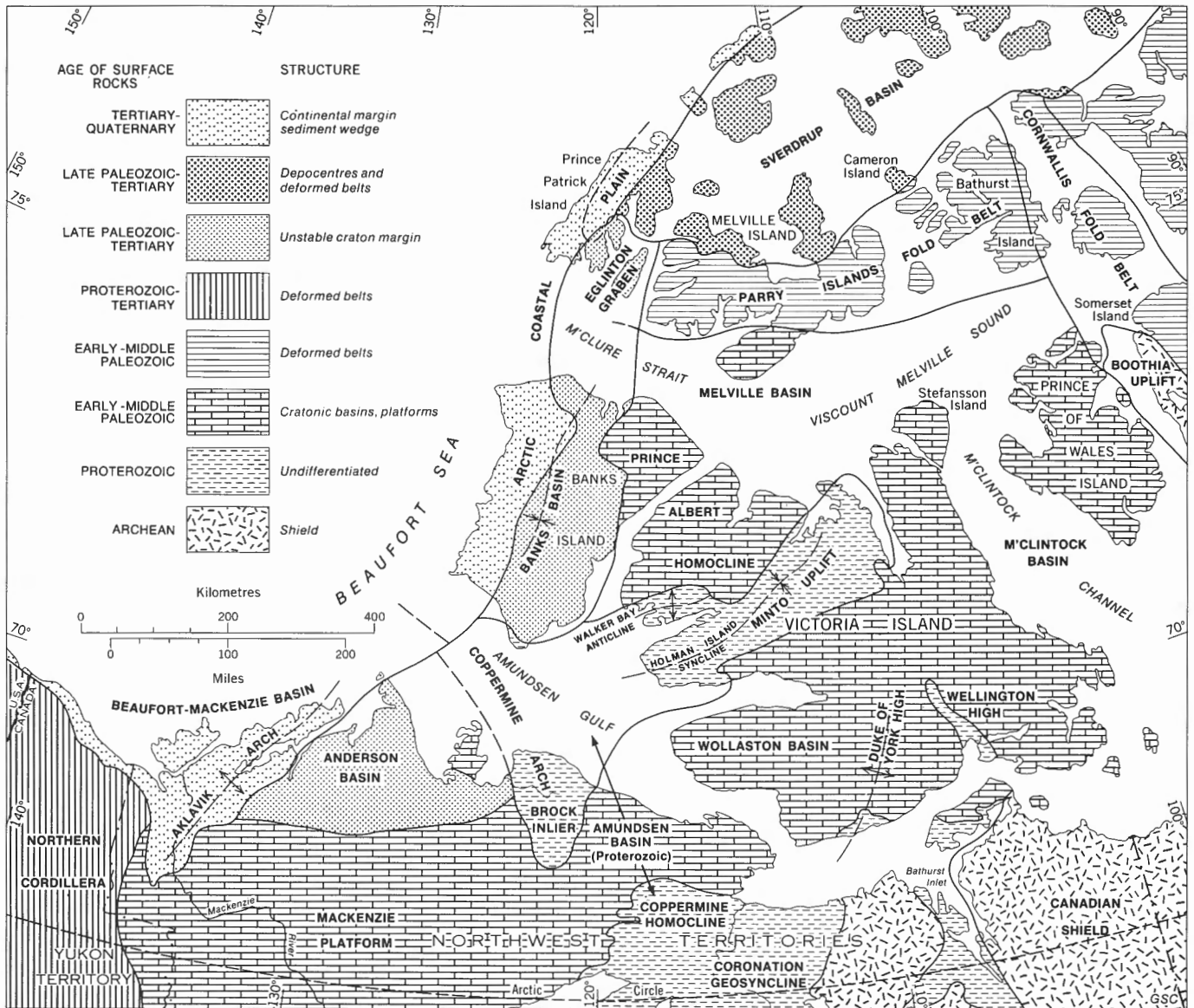


Figure 3. Structural-stratigraphic provinces in the western Canadian Arctic.

axial portion of the geosyncline (Hazen Trough) now is largely covered by upper Paleozoic to upper Tertiary deposits of Sverdrup Basin.

The Sverdrup is a successor basin. The rocks within it reach thicknesses as great as 12 000 m (40 000 ft) (Trettin *et al.*, 1972). Of similar age is Beaufort-Mackenzie Basin, which contains approximately 9000 m (30 000 ft) of Jurassic to upper Tertiary sediments (Lerand, 1973; Young *et al.*, 1976).

Between these two major depocentres is an area which is herein termed the Unstable Craton Margin. The reasons for proposing this new name are as follows: (1) The thickness of post-Paleozoic sediments in the Unstable Craton Margin is less than in the two major contemporaneous depocentres, but is greater than in the Central Stable Region (where there are only isolated remnants of Cretaceous and Tertiary rocks). The maximum thickness in the Banks Island area probably does not exceed 3000 m (10 000 ft). (2) The detailed work described

in this report shows that the Banks Island area underwent several periods of minor epeirogenic uplift during the interval of time from Jurassic to Tertiary. Evidence for these periods of movement is sparse or absent within Sverdrup Basin and Beaufort-Mackenzie Basin (e.g., see stratigraphic column for the Ringnes islands in Table 1). (3) The structural style of the Unstable Craton Margin is distinctive, comprising a series of relatively small pericratonic basins and highs.

Units included within the Unstable Craton Margin are Anderson Basin (Lerand, 1973), Banks Island Basin (as originally defined by Thorsteinsson and Tozer, 1960) and Eglinton Graben. The main theme of this report is to describe the distinctive stratigraphic and sedimentological history of that part of the Unstable Craton Margin encompassed by Banks Island. Eglinton Graben is discussed by Tozer and Thorsteinsson (1964) and Miall (1975*b*), and the Anderson Basin area by Yorath *et al.* (1975).

Table 1. Table of formations in Banks Island and adjacent areas, showing thicknesses, map symbols and rock types

	ANDERSON BASIN	BIG RIVER BASIN	STORKERSON UPLIFT	CAPE LAMBTON UPLIFT	CARDWELL BASIN	SHELF EDGE	CENTRAL BANKS BASIN	CAPE CROZIER UPLIFT	NORTHERN BANKS BASIN	RINGNES ISLANDS
	From Yorath, Balkwill and Klassen, 1975	Storkerson Bay A-15	Uminmak H-07 Nanuk D-76	Surface Sections	Surface Sections	Tiritichik M-48 Ikkariktok M-64	Orksut I-44	Surface Sections	Surface Sections	Stott, 1969 Hopkins and Balkwill, 1973
Glacial and post-glacial deposits										
QUATERNARY										
TERTIARY	PLIOCENE									
	MIOCENE									
	OLIGOCENE									
EOCENE										
PALEOCENE										
MAASTRICHTIAN										
CAMPAIAN										
SANTONIAN										
CONIACIAN										
TURONIAN										
CENOMANIAN										
ALBIAN										
APTIAN										
BARREMIAN										
HAUTERIVIAN										
VALANGINIAN										
BERRIASIAN										
UPPER JURASSIC										
MIDDLE JURASSIC										
LOWER JURASSIC										

Thickness in metres (feet) 30 (100) Rock types (sand or sandstone, siltstone, shale, conglomerate, coal, manganese spherulites) ss, silt, sh, cg, c, ● Map-unit symbols Te

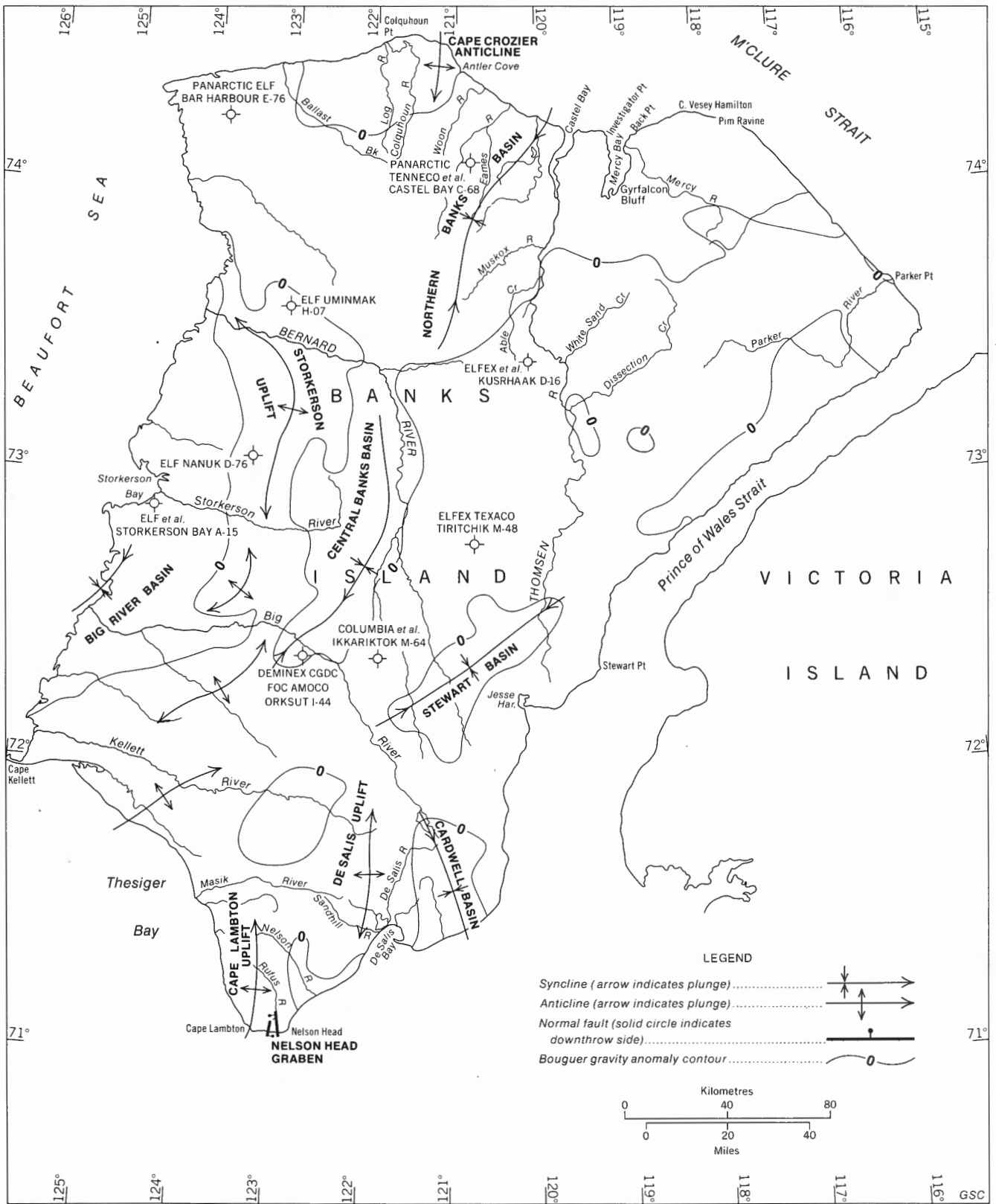


Figure 4. Structural elements in Banks Island, based on Bouguer gravity data of Stephens *et al.* (1972).

The structural geology of the report-area is considered in detail in Chapter 4 but for a fuller understanding of the local variations within the Mesozoic and Tertiary rocks the second-order structural features within the broad outline of Banks Island Basin must be described briefly, because most of these features have been in existence at least since Cretaceous time. Figure 4 is a structural trend map of Banks Island based on subsurface well control and on gravity data (Stephens *et al.*, 1972). All the available evidence suggests that the Bouguer gravity anomalies reflect the configuration of the Paleozoic-Mesozoic unconformity.

Banks Island Basin, as defined by Thorsteinsson and Tozer (1960), was believed to be a broad, shallow feature open toward the west. Gravity and well data show that, in fact, the structure is somewhat more complex. A prominent structural high named Storkerson Uplift (Miall, 1974b) extends from north to south near the western edge of the report-area and divides Banks Island Basin into two smaller troughs. West of the uplift lies Big River Basin, most of which is located offshore. The Storkerson Bay A-15 well is located near the axis of this feature. The Nanuk D-76 and Uminmak H-07 wells are located on the flanks of the basin. East of Storkerson Uplift is Banks Basin, as defined by the writer (Miall, *ibid.*), a long linear feature, which may be subdivided into Central Banks Basin and Northern Banks Basin. The latter contains the thickest section of post-Paleozoic rocks in the report-area, as shown by the section at the Castel Bay C-68 well. Jurassic to upper Tertiary strata total 1977 m (6486 ft) of beds, slightly thicker than the 1830 m (6000 ft) of Jurassic to upper Tertiary strata in the Orksut I-44 well, which is located on the axis of Central Banks Basin. Most of the Mesozoic and Tertiary section probably is absent over Storkerson Uplift.

Stewart Basin and Cardwell Basin are minor features located in southeastern Banks Island. The former is known only from gravity data, because the area underlain by the basin is covered almost entirely by surficial deposits. A small structural low of local importance is Nelson Head Graben, described but not formally named by Thorsteinsson and Tozer (1962). De Salis Uplift and Cape Lambton Uplift are expressed at the surface by exposures of Proterozoic rocks.

Lerand (1973, Fig. 7) defined a northwesterly trending feature in Amundsen Gulf south of Banks Island which he named Coppermine Arch. Sedimentological evidence indicates that this arch plus Cape Lambton Uplift were active, positive areas during at least part of Mesozoic time.

North of Banks Island, Northern Banks Basin probably connects with Eglinton Graben, although gravity trends suggest a left-lateral offset between the two troughs in the order of 50 km (30 mi). Bourne and Pallister (1973, p. 50) estimate from gravity data a "post-Paleozoic carbonate" sediment thickness of 2100 m (7000 ft) in Eglinton Graben, which is comparable to that of Banks Basin.

Thorsteinsson and Tozer (1960) applied the term Prince Patrick Uplift to a series of Paleozoic and Precambrian inliers aligned in a north-south trend through Prince Patrick and Banks Islands. They included a large inlier of Devonian rocks in southeastern Prince Patrick Island characterized by strong north-south faulting (Plauchut, 1971, Fig. 1), the Devonian inlier of Cape Crozier Anticline in northern Banks Island, and the Precambrian inlier now named Cape Lambton Uplift. It was suggested (Thorsteinsson and Tozer, 1962, p. 73), also, that the Precambrian rocks of Darnley Bay may be part of the same trend, which was thought to represent a large, buried structural feature comparable to Boothia or Minto arches. Gravity data now show that a more complex pattern prevails. Storkerson Uplift is close to the proposed alignment of Prince Patrick Uplift, but its southern end is continued in a southwesterly direction by a series of *en echelon* uplifts which probably link up with Aklavik Arch (Lerand, 1973, Fig. 7).

Overlapping the Unstable Craton Margin and the Beaufort-Mackenzie and Sverdrup basins is the Arctic Coastal Plain. This comprises a wedge of virtually undeformed Miocene sediments which thickens markedly offshore, and probably includes younger units of from Pliocene to Recent ages. Remnants of the coastal plain sediments (Beaufort Fm.) are found far inland to the east of the western coast of Banks Island, suggesting that in comparatively recent times the Coastal Plain as a structural unit occupied most of the present report-area. In the Beaufort-Mackenzie Basin this unit has been named Kugaluk Homocline by Norris (1974).

2. Stratigraphy

Introduction

Detailed descriptions of the units in Banks Island are provided later in this chapter. The purpose of this section is to present a brief summary, with a description of regional correlations (see Table 1). Restored stratigraphic cross-sections through the report-area are provided in Figures 5, 6 and 7 (*in pocket*). Figure 8 (*in pocket*) is a detailed graphic log of the six subsurface sections described in detail in this report.

The oldest Mesozoic unit exposed at the surface in Banks Island is the Isachsen Formation, of Early Cretaceous age. However, drilling now has shown that Jurassic rocks are present at depth in Banks Basin. In the Orksut I-44 well 401 m (1317 ft) of beds are present above the Devonian rocks and below the Isachsen. Microforaminiferal studies indicate that they range in age from late Early Jurassic to Valanginian. The beds consist predominantly of silty shale with minor amounts of interbedded siltstone. In age, but not in lithology they are correlated with the Wilkie Point Formation (Tozer, 1956, p. 18) and the Mould Bay Formation (*ibid.*, p. 23) of Prince Patrick Island. The Wilkie Point of southern Prince Patrick Island comprises up to 180 m (600 ft) of sand and sandstone that is in part glauconitic, ferruginous and phosphatic. According to Tozer and Thorsteinsson (1964, p. 124) the lower part of the formation is marine and the upper part nonmarine. These beds may represent shoreline deposits or a prograding delta marginal to Sverdrup Basin. The Mould Bay Formation in the type area (Mould Bay, on Prince Patrick Island) and on northern Eglinton Island consists predominantly of sandstone, but increasing amounts of shale appear to the northeast, into Sverdrup Basin (*ibid.*, p. 136).

The Jurassic strata in Banks Island are overlapped by the Isachsen Formation and nowhere reach the surface. Whether they extended beyond the present confines of Banks Basin in pre-Isachsen time is unknown. Their fine-grained character at the Orksut I-44 well suggests that no source areas with any marked relief were located nearby. However, the stratigraphy and sedimentology of the Cretaceous and lower Tertiary rocks suggest that the present margins of Banks, Big River and Cardwell basins correspond fairly closely to the original limits of the depositional areas of the various units and the same may have been true of the Jurassic rocks. The thickness of Jurassic strata is thought to be considerable throughout Banks Basin, and they probably are coextensive with Jurassic strata underlying Eglinton Island. At the Castel Bay C-68 well only the Mould Bay Formation is present, comprising 102 m (334 ft) of sandstone and shale.

The Isachsen Formation probably disconformably overlies the Mould Bay strata in Banks Island, although fossil

evidence for the age of the Isachsen is very sparse. The formation is assigned herein a Barremian or Aptian to Early Albian age, and there is evidence to suggest that the formation may be diachronous locally. The Mould Bay–Isachsen contact is reported to be conformable within much of Sverdrup Basin; on Ellef Ringnes Island the base of the Isachsen is probably Valanginian in age (Stott, 1969, p. 25).

The name Isachsen Formation was given first by Heywood (1955, p. 28; 1957, p. 11) to a succession of essentially nonmarine, arenaceous strata in the Isachsen area of Ellef Ringnes Island. The formation is known now to occur throughout Sverdrup Basin, and similar rocks have been recognized also on the Arctic mainland south of Banks Island, where they have been assigned to the Gilmour Lake Member of the Langton Bay Formation (Yorath *et al.*, 1975). The formation represents a period of great expansion of sedimentation beyond the confines of Sverdrup Basin but it would be misleading to call this event a transgression because the sediments which resulted are almost entirely nonmarine. At least within Banks Island, and probably also along the margins of Sverdrup Basin, this increased sedimentation is thought to have been caused by a period of epeirogenic disturbance and rejuvenation of source areas on the craton.

The initial surface on which the Isachsen Formation was deposited displayed considerable relief, as will be described in detail in later sections. As a result the formation shows considerable local variation in thickness. South of Mercy Bay, along Dissection Creek, in part of the Cape Crozier region, and near Cape Lambton the formation is absent; the Christopher Formation rests directly on the basement rocks (Fig. 7). These regions probably represent parts of the local Isachsen source area. The formation is absent also in the vicinity of Storkerson Uplift, as shown by the four wells drilled on western Banks Island (Fig. 8; Miall, 1974c).

The typical Isachsen Formation consists of medium- to coarse-grained, unconsolidated quartzose sand, with occasional pebble beds and rare cobbles and boulders. A transitional unit with the overlying Christopher Formation is present; it consists of fine-grained sand and silty sand with carbonaceous beds. The formation includes beds of boulder conglomerate in Nelson Head Graben, whereas at Sandhill River and at Orksut I-44 silty shale with some coal beds compose a minor but significant part of the section.

The thickest section through the Isachsen Formation on Banks Island is at Nelson Head, where boulder conglomerates and pebbly sands increase the thickness locally to at least 200 m (660 ft). However, this is considerably thinner than in parts of central Sverdrup Basin, where the formation generally is more

than 1000 m (3300 ft) thick. In the Ringnes islands the Isachsen is interpreted as the deposit of a major delta system (Roy, 1973, 1974), whereas the Isachsen of Banks Island is a more proximal deposit formed mainly by relatively small, meandering and braided rivers (Miall, 1976b). The distinctiveness of the Isachsen lithofacies and its mode of accumulation in partly fault-bounded basins are two of the characteristic features of the Unstable Craton Margin.

The Early Albian was marked by a widespread marine transgression throughout western and Arctic Canada (Jeletzky, 1971, p. 42), resulting in an extension of the sea over and beyond most of the areas which had been undergoing nonmarine sedimentation in Isachsen time. Deposition of the ammonite- and pelecypod-bearing shale, silty shale and siltstone of the Lower to Upper Albian Christopher Formation followed this transgression. The formation reaches its maximum thickness within the report-area of at least 460 m (1500 ft) in the Masik River and Atitok River region of southern Banks Island. Elsewhere, as at Nelson Head, at Orksut I-44 and south of Mercy Bay, the formation thins to 60 m (200 ft) or less, either as a result of post-Christopher, pre-Kanguk erosion or as a result of the persistence of the coarse, fluvial Isachsen facies into Albian time (Figs. 6, 7). The Christopher Formation is the oldest Mesozoic unit yet detected by drilling west of Storkerson Uplift, where it rests directly on Devonian strata (Fig. 8). It is correlated in part with the Horton River Formation of the Anderson Plains area (Yorath *et al.*, 1975).

A sandy shoreline facies developed along what was probably the margins of the Christopher sea and on the east side of Northern Banks Basin, and also may have occurred on shoals corresponding to partly or fully submerged Cape Crozier and Storkerson uplifts. Of this shoreline facies only part is preserved, corresponding to the end of Christopher time when the sea was beginning to retreat to the west. This is the Upper Albian Hassel Formation, which consists of glauconitic, very fine to medium-grained sand with rare small pebbles and a few clay laminae. Ironstone nodules containing ammonites and pelecypods are present locally. The formation is typically 25 m (82 ft) thick and within the report-area it is, at present, known only in Northern Banks Basin. Elsewhere its absence may be the result of nondeposition or erosion in pre-Kanguk time (Figs. 5, 7).

The Hassel Formation of Banks Island was described first by Plauchut (1971) and Jutard and Plauchut (1973). It is of a different facies from most of the Hassel of the type area on Ellef Ringnes Island and also is considerably thinner. The Hassel of Sverdrup Basin ranges in thickness from 90 to 550 m (300–1800 ft) and consists of sandstone with minor amounts of carbonaceous shale and coal. Glauconitic sands are present at the base. Hopkins and Balkwill (1973, p. 4) interpret the unit as fluvial and marine- to nonmarine-deltaic in origin.

The Christopher and Hassel formations are succeeded by the Kanguk formation throughout Banks Island. This predominantly argillaceous unit was defined first by Souther (1963, p. 442–444) from exposures on Axel Heiberg Island. The Banks Island exposures were included with the Eureka Sound Formation by Thorsteinsson and Tozer (1962) but were assigned correctly to the Kanguk Formation by Plauchut (1971) and Jutard and Plauchut (1973). Throughout most of Sverdrup Basin, the Kanguk Formation is Santonian to Maastrichtian

in age (Plauchut, 1971). In Banks Basin the age range is Campanian to Maastrichtian but west of Storkerson Uplift there is evidence that the base of the formation is as old as Turonian. The Kanguk represents a marine transgression following a mid-Cretaceous period of erosion and at several localities the underlying Cretaceous units are thin or absent. At Orksut I-44 the Christopher Formation is 43 m (140 ft) thick; at the Tiritchik M-48 and Ikkariktok M-64 locations, the Christopher and Isachsen formations are absent. Both are probably absent south of Mercy Bay, although exposure in this area is poor and therefore the stratigraphy is not known completely.

At the base of the Kanguk throughout Banks Island there is a distinctive black, bituminous, sulphurous shale member containing one or more bentonitic clay layers. Thin tuff beds also are present in southern Banks Island. Near Mercy Bay and in four of the well sections (Storkerson Bay A-15, Nanuk D-76, Uminmak H-07 and Orksut I-44), manganese carbonate spherulites are present at the base of the section (Miall, 1974d). The bituminous shale member is thin, reaching a maximum of 12.5 m (41 ft) at Able Creek, but is readily recognizable at the surface because on long-continued exposure to the air the unit oxidizes to a dark red. The same lithology has been mapped over much of the Arctic, including the Ringnes islands (Balkwill, *pers. com.*, 1975), Graham Island (Plauchut, 1971, p. 675), Eglinton Island (*ibid.*), Anderson Plains (part of Smoking Hills Fm. of Yorath *et al.*, 1975), northern Yukon (Boundary Creek Fm. of Young, 1975), Mackenzie Delta (Myhr, 1975), and northeast Alaska (part of Seabee Fm., see Detterman *et al.*, 1975, p. 32). The unit may not be precisely of the same age everywhere but it indicates the widespread occurrence of unusual geochemical and paleogeographic conditions, including much contemporaneous volcanism.

The remainder of the Kanguk Formation comprises shale with minor silty beds. Prominent but thin marine sand members are present locally, as at Antler Cove and in the Uminmak H-07, Orksut I-44 and Ikkariktok M-64 sections. The Kanguk varies in thickness, reaching a maximum of 463 m (1520 ft) at the Castel Bay C-68 well and a minimum of approximately 120 m (400 ft) in outcrop sections south of Castel Bay and west of De Salis Bay.

The Kanguk Formation grades upward without apparent break into the Eureka Sound Formation, which includes both marine and nonmarine beds. The name Eureka Sound was applied first by Troelsen (1950, p. 78) to outcrops in central Ellesmere Island, although no type section of the unit (named a 'group' by Troelsen) was designated. The Eureka Sound Formation is predominantly Paleocene and Eocene although in the Ringnes islands much of the lower part of the section has been dated as Late Cretaceous (Stott, 1969, p. 28) or, more specifically, Maastrichtian (W.S. Hopkins, Jr., *pers. com.*, 1974). In Banks Island the basal Eureka Sound Formation west of Storkerson Uplift and south of Orksut I-44 is probably Maastrichtian in age but everywhere else the base of the formation is Paleocene.

A typical Eureka Sound section, representing a deltaic environment, comprises interbedded sand (unconsolidated), silt, soft shale, soil beds and lignitic coal. Throughout most of Banks Basin, except for an area east of Musko River, there is

also a basal member that is lithologically similar to the Kanguk Formation, which probably is mainly marine and is of Paleocene age according to palynological studies (Figs. 5, 6, 8). This member reaches a maximum thickness of 241 m (790 ft) in the Tiritchik M-48 well. The upper, sandy member ranges in thickness from a minimum of approximately 60 m (200 ft) southwest of Colquhoun Point, where it has been subjected to a mid-Tertiary period of erosion, to a possible maximum of 939 m (3080 ft) at the Castel Bay C-68 well (the two members of the Eureka Sound cannot be separated in this well).

The Eureka Sound Formation is overlain unconformably by the Beaufort Formation, a succession of unconsolidated sand, gravel, clay and peat, with abundant unaltered fragments of wood. The unit was named by Tozer (1956) and is recognized now throughout the Arctic Coastal Plain from Meighen Island in the north to Anderson Plains in the south. Hills and Fyles (1973) assigned a middle to late Miocene age to the formation on northwestern Banks Island. Over much of central and northern Banks Island, the Beaufort Formation is a thin veneer capping an elevated, much dissected plateau. The formation thickens to the west, reaching 100 m (330 ft) at Ballast Brook (Hills, 1969) and possibly as much as 260 m (860 ft) in the Storkerson Bay A-15 well and 276 m (905 ft) in the Bar Harbour E-76 well, although the accurate delineation of formation boundaries in the subsurface in completely unconsolidated deposits is a difficult undertaking and subject to error.

In summary the Jurassic to upper Tertiary section comprises eight formations, although not all are present in every locality. Two, or possibly three, regional, low-angle unconformities are present within the succession, indicating periods of movement in the late Neocomian (questionable), the beginning of the Late Cretaceous and in mid-Tertiary, possibly Oligocene time. Thicknesses are considerably less than in the major depocentres of Sverdrup Basin or Beaufort-Mackenzie Basin, the total Mesozoic and Tertiary section reaching a recorded maximum of 1977 m (6486 ft) at the Castel Bay C-68 well in Northern Banks Basin.

Description of formations

Jurassic and Lower Cretaceous

Wilkie Point Formation

Definition, distribution and thickness

The Jurassic strata which have the most extensive area of outcrop on Prince Patrick Island were named the Wilkie Point Formation by Tozer (1956, p. 18). The outcrops on Prince Patrick Island and those on Melville, Borden and Mackenzie King islands were described more fully by Tozer and Thorsteinsson (1964, p. 124–135). On Prince Patrick Island, the Wilkie Point comprises up to 180 m (600 ft) of sand and sandstone with some glauconitic, dusky red ferruginous bands, and grey phosphatic nodules. The lower part of the formation is marine and the upper part nonmarine in origin. Toward Sverdrup Basin the formation becomes entirely marine and the proportion of shale increases. The Wilkie Point ranges in age from late Early Jurassic to Oxfordian.

The presence of this formation throughout Sverdrup

Basin has been known for a long time. Exploratory drilling now has demonstrated that the Wilkie Point also underlies at least part of Banks Island. The Orksut I-44 well, which was drilled near the axis of Central Banks Basin, penetrated 201 m (660 ft) of Lower to lower Upper Jurassic strata, herein assigned to the Wilkie Point Formation. The formation is absent in the other seven well sections described in this report. Elsewhere in the report-area it is overstepped or overlapped by younger, Jurassic or Cretaceous units. At the Orksut I-44 location the Wilkie Point rests unconformably on calcareous shale and limestone of the Orksut Formation (Early and Middle Devonian in age, *see* Miall, 1975c, 1976a) and is succeeded by the Mould Bay Formation (Late Jurassic to Neocomian). The contact with the latter is marked by a slight change in lithology, as shown by geophysical log character (Fig. 8).

Lithology

The lowermost 16 m (52 ft) of the Wilkie Point Formation at Orksut I-44 consist of sandstone with minor amounts of silty shale interbeds. The sandstone is pale to medium brownish grey, fine to very fine grained and mineralogically supermature, containing in excess of 99 per cent quartz. Chert and rare glauconite grains constitute the remainder of the detrital grains. Grains are subangular to well rounded, cementation is poor, and porosity and permeability are both excellent. A core through part of the sandstone (core #4) shows faint crossbedding and rare burrows. The interbedded silty shale contains wood fragments and traces of disseminated pyrite. The shale units are typically a few millimetres thick.

The remaining 185 m (608 ft) of the formation consist of dark grey, slightly calcareous, silty shale interbedded with rare beds of dark grey, argillaceous siltstone. Traces of glauconite are present. Pelecypod fragments and arenaceous foraminifera are abundant except near the base of the section.

The Wilkie Point shale is virtually indistinguishable from that of the Mould Bay Formation when seen in well chip samples, but geophysical logs indicate that it is characterized at Orksut I-44 by a slightly greater radioactivity and a slightly lesser resistivity than the latter.

Age and correlation

Chamney (*in* Brideaux *et al.*, 1975) has studied the micropaleontology of the Wilkie Point Formation in the Orksut I-44 well by taking successive channel samples of the cuttings over 30 m (100 ft) intervals throughout the section. Two samples also were taken from core #4 at the base of the Mesozoic succession. The faunal assemblages and interpreted ages are listed below.

Depth m (ft)	Fauna	GSC loc.
1646–1676 (5400–5500)	<i>Astacohus</i> cf. <i>A. pediacus</i> Tappan—few	C-30099
	<i>Nodosaria</i> sp. (pyritized)—few	
cuttings	<i>Trochammina</i> ex gr. <i>T. sablei</i> Tappan —common	
	<i>T. spp.</i> —common	
	<i>Ammobaculites barrowensis</i> Tappan —common	
	<i>Haplophragmoides kingakensis</i> Tappan —common	

	<i>Arenoturrispirillina</i> ex gr. <i>A. intermedia</i> Chamney—few <i>Gravellina?</i> sp. age: Jurassic, Late	
1676–1707 (5500–5600) cuttings	as above with addition of: <i>Ammodiscus</i> sp. (small)—few <i>Gravellina</i> n. sp. (dwarf)—common <i>Bolivina?</i> sp. (pyrite fragment)—rare = ex gr. <i>B. lathetica</i> Tappan age: Jurassic, Late	C-30100
1707–1737 (5600–5700) cuttings	<i>Discorbis?</i> sp.—rare <i>Lenticulina</i> cf. <i>Astacolus connudatus</i> Tappan—few <i>Haplophragmoides</i> spp.—common <i>Hippocrepina</i> sp.—few pelecypod shell fragments—common age: Jurassic, Late, Oxfordian?	C-30101
1737–1768 (5700–5800) cuttings	<i>Ammobaculites</i> n. sp.—few (giant) <i>Haplophragmoides</i> spp.—abundant <i>Astacolus</i> sp.—few <i>Trochamminoides</i> n. sp.—common (giant) <i>Glomospirella</i> sp.—few spines—common age: Jurassic, Late	C-30102
1768–1798 (5800–5900) cuttings	<i>Trochamminoides</i> spp. as above —common <i>Haplophragmoides</i> n. sp.—abundant <i>H.</i> spp.—abundant <i>Ammodiscus</i> ex gr. <i>A. thomsii</i> Chamney —few <i>Bathysiphon</i> sp. <i>Astacolus</i> cf. <i>A. connudatus</i> Tappan—few age: Jurassic, Middle to Late boundary	C-30103
1817–1820 (5960–5970) cuttings	<i>Haplophragmoides</i> spp.—abundant <i>H.</i> n. sp. 95—common <i>Arenoturrispirillina</i> sp. 6—few <i>Ammobaculites</i> ex gr. <i>A. alaskensis</i> Tappan—few pyrite rods—common age: Jurassic undifferentiated, possibly cavings	C-30104
1820–1823 (5970–5980) cuttings	no microfossils	C-30105
1823–1826 (5980–5992) core	plant megaspores: II A sp. 12—common	C-30106
1826–1829 (5992–6000) core	<i>Ammodiscus</i> cf. <i>A. orbis</i> Lalicker —common <i>Haplophragmoides</i> sp.—common pyrite replacing organic remains —common age: Jurassic, Early? to Middle	C-30107

the latter is placed at 1628 m (5340 ft) because of a slight change in lithological character, as shown by geophysical logs, at that level.

In summary, the Wilkie Point Formation is assigned an Early, possibly late Early, Jurassic to early Late Jurassic (Oxfordian?) age range at Orksut I-44. This is similar to the age range of the formation throughout Sverdrup Basin (Plauchut, 1971). Unnamed beds of similar age also occur in Beaufort-Mackenzie Basin (Young *et al.*, 1976).

Mould Bay Formation

Definition, distribution and thickness

The Mould Bay Formation, as first described by Tozer (1956, p. 23), included all the beds between the Wilkie Point and Christopher formations on Prince Patrick Island. Subsequently it was recognized that the upper part of the formation corresponded to the Isachsen Formation, as had been defined by Heywood (1955); therefore Tozer and Thorsteinsson (1964, p. 136–146) excluded these beds in their description of the formation as it occurs in the western Queen Elizabeth Islands.

Throughout most of Sverdrup Basin, the Mould Bay Formation rests with an abrupt but apparently conformable contact on the Wilkie Point Formation. South of Mould Bay on Prince Patrick Island the formation rests unconformably on the Wilkie Point Formation, and in the southern part of the island the Mould Bay oversteps the Wilkie Point and rests directly on Devonian rocks.

In the type area of the formation near Mould Bay the strata consist of marine sand and sandstone with a thin shale unit at the base. Toward the northeast, into Sverdrup Basin, increasing amounts of shale appear and the formation passes into the predominantly argillaceous Deer Bay Formation.

The Mould Bay Formation also crops out on northern Eglinton Island, where it consists of sand and sandstone (*ibid.*, p. 141). The base of the formation is not exposed in this area.

It is anticipated that within the report-area the formation will be found, by continued drilling, to occupy all the deeper parts of Northern and Central Banks basins. The formation is overstepped by the Isachsen Formation along the flanks of Banks Basin and is nowhere exposed at the surface.

At Orksut I-44 the Mould Bay Formation is 200 m (657 ft) thick, and at Castel Bay C-68 it is 102 m (334 ft) thick. This compares with a thickness of 60 to 120 m (200–400 ft) on Prince Patrick Island.

Lithology

The Mould Bay Formation at Orksut I-44 consists predominantly of medium grey to grey-green, slightly micaceous, noncalcareous silty shale. The uppermost 33 m (107 ft) comprise dark brownish grey, soft, plastic mudstone. Thin beds of glauconitic sandstone and siltstone are present, especially in the 1493 to 1496 m (4900–4910 ft) interval of the well. Disseminated pyrite, pelecypod fragments and arenaceous foraminifera are common throughout.

This lithological assemblage is quite different from that of the Mould Bay Formation of the type area; it resembles the exposures in eastern Prince Patrick Island and Mackenzie King Island (*ibid.*, p. 140, 144–146) where the Mould Bay interfingers with the Deer Bay Formation. The section in the

The first three samples, from the 1646 to 1737 m (5400–5700 ft) interval of the section, may represent cavings from the overlying Mould Bay Formation. The contact with

Castel Bay C-68 well is more similar to that of the type area; it consists of interbedded sand and shale.

Age and correlation

Micropaleontological assemblages from the Orksut I-44 well have been identified by Chamney (*in* Brideaux *et al.*, 1975). These are listed below, with their respective age assignments.

Depth m (ft)	Fauna	GSC loc.
1432-1463 (4700-4800) cuttings	<i>Haplophragmoides</i> ex gr. <i>H. canui</i> Cushman—abundant <i>H. spp.</i> —common <i>Lituotuba</i> ex gr. <i>L. gallupi</i> Chamney—few <i>Reophax</i> sp.—few (coarse, inflated) <i>Glomospirella</i> cf. <i>G. elongata</i> Chamney—few <i>Ammodiscus</i> ex gr. <i>A. silicea</i> Terquem—few age: Early Neocomian	C-30092
1463-1493 (4800-4900) cuttings	<i>Haplophragmoides</i> ex gr. <i>H. canui</i> Cushman—abundant <i>H. cf. H. barrowensis</i> Tappan—common <i>H. spp.</i> —abundant <i>Arenoturrspirillina waltoni</i> Chamney—common <i>Ammodiscus</i> spp.—common <i>Glomospirella?</i> sp.—few <i>Lenticulina</i> ex gr. <i>L. excavata</i> (Terquem)—few pelecypod shell fragments—common age: Cretaceous/Jurassic boundary	C-30093
1493-1524 (4900-5000) cuttings	<i>Haplophragmoides barrowensis</i> Tappan—common <i>H. spp.</i> (coarse, small)—abundant <i>Eoguttulina</i> cf. <i>E. liassica</i> (Strickland)—few <i>Trochammina</i> ex gr. <i>T. canningensis</i> Tappan—common megaspores—few ostracode—few (smooth elongate) age: Jurassic, Late, Tithonian?	C-30094
1524-1554 (5000-5100) cuttings	<i>Haplophragmoides</i> spp. and <i>Ammodiscus</i> spp. (similar to 1554 to 1585 m) age: Jurassic, Late	C-30095
1554-1585 (5100-5200) cuttings	<i>Haplophragmoides</i> ex gr. <i>H. canui</i> Cushman—common <i>H. cf. H. barrowensis</i> Tappan—common <i>H. spp.</i> —abundant <i>Ammodiscus</i> cf. <i>A. orbis</i> Lalicker—few <i>Bathysiphon</i> cf. <i>B. anomalocoelia</i> Tappan—few pelecypod shell fragments—common megaspores—few ostracode sp.—few (slipper-shape) trixion spines (radiolaria?)—few age: Jurassic, Late	C-30096
1585-1615 (5200-5300) cuttings	<i>Textularia</i> cf. <i>T. areoplecta</i> Tappan—few <i>Eoguttulina</i> cf. <i>E. liassica</i> (Strickland)—few <i>Sagoplecta?</i> sp. (pyritized)—rare	C-30097

Haplophragmoides ex gr. *H. canui*
Cushman—common
H. cf. H. barrowensis Tappan—common
megaspores and plant rootlets—common
age: Jurassic, Late

1615-1646 (5300-5400) cuttings	<i>Ammobaculites</i> cf. <i>A. barrowensis</i> Tappan—common <i>Lenticulina</i> sp.—rare <i>Trochammina</i> sp.—few <i>Arenoturrspirillina</i> ex gr. <i>A. jeletzkyi</i> Chamney—few <i>Haplophragmoides</i> spp. (small, coarse, n. sp.)—abundant <i>H. cf. H. kingakensis</i> Tappan—common age: Jurassic, Late	C-30098
--------------------------------------	--	---------

Based on these identifications the formation is assigned a Late Jurassic to early Neocomian age at Orksut I-44. This compares with the late Oxfordian to late Valanginian age range of the formation in western Sverdrup Basin (Tozer and Thorsteinsson, 1964, p. 137).

Lower Cretaceous

Isachsen Formation

Definition, distribution and thickness

The Isachsen Formation was defined first by Heywood (1955, 1957) following his reconnaissance work in the area of Isachsen Dome on Ellef Ringnes Island. According to Heywood (1957, p. 11) the formation consists of grey to red, quartzose sandstone, fine to medium grained and containing pebble beds, beds of siltstone and claystone and some coal seams. The formation was estimated to be 900 m (3000 ft) thick and was assigned an Early Cretaceous age on the basis of pelecypods found in the lower 30 m (100 ft) of the succession.

Subsequently the formation was recognized throughout the Arctic Islands from Prince Patrick Island in the west (Tozer and Thorsteinsson, 1964) to Ellesmere Island in the east (Tozer, 1960). The almost complete absence of fossils in the formation has been interpreted to indicate a nonmarine origin. Roy (1973, 1974) showed from sedimentological studies that the Isachsen Formation of the Ringnes islands is of fluviodeltaic origin.

The outcrops of the formation on Banks Island were described by Thorsteinsson and Tozer (1962, p. 59-62), who recognized two informal members: a lower unit of fine-grained to mainly coarse grained sandstone with grit and pebble-conglomerate sandstone, and containing thin coal laminae; and an upper unit comprising fine- to coarse-grained, crossbedded sandstone. The formation was estimated to be 75 to 90 m (250-300 ft) thick in northern Banks Island. Similar descriptions of the outcrops on northern Banks Island were provided by Jutard and Plauchut (1973, p. 208, 209) although they estimated a somewhat greater thickness for the formation, at 140 m (460 ft).

The distribution, thickness and lithologies of the Isachsen Formation on Banks Island are summarized in Figure 9. The thickest section through the formation in Banks Island is at the southern tip of the island, within Nelson Head Graben.

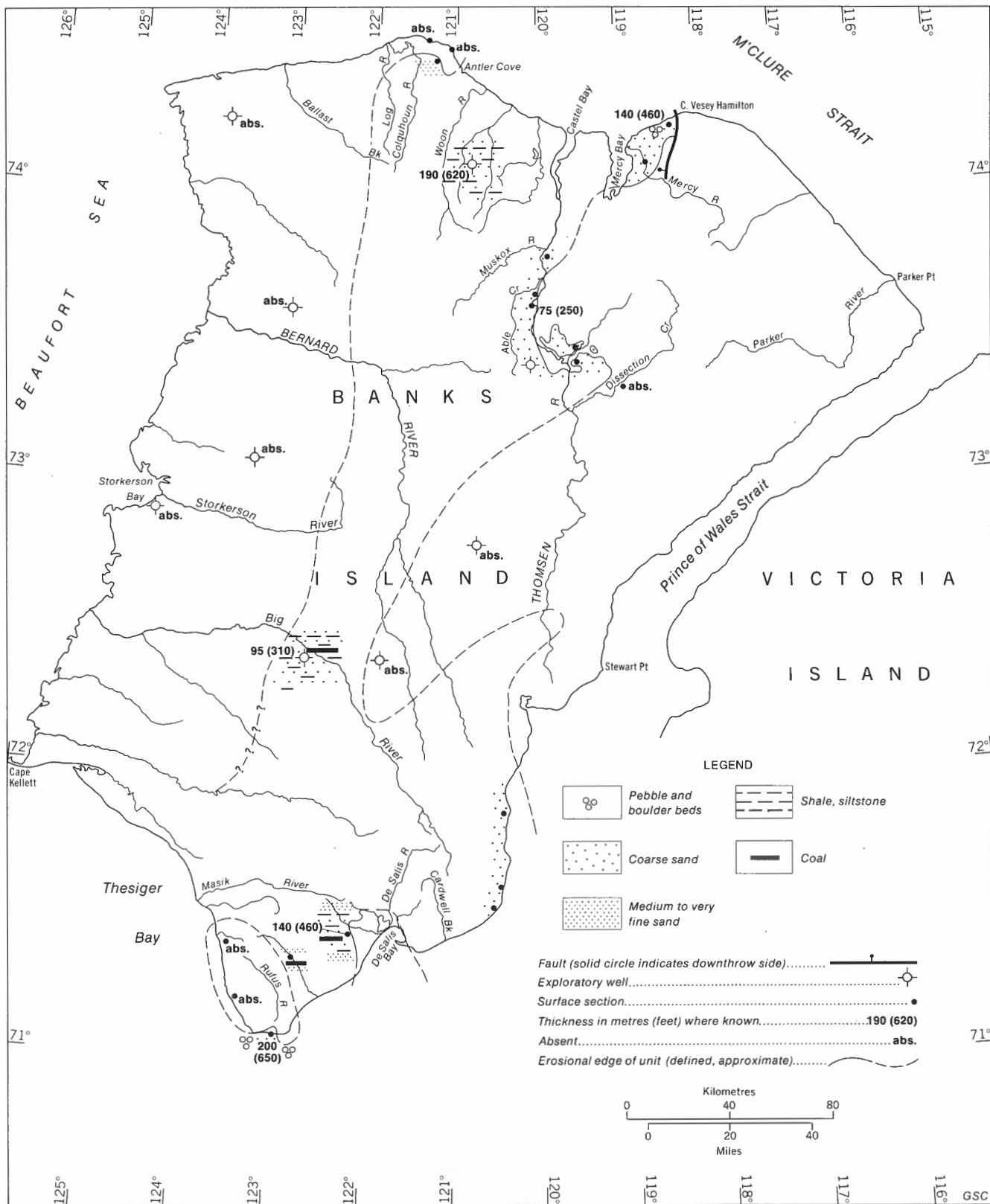


Figure 9. Isachsen Formation: distribution, thickness and lithologies. Thicknesses are rounded off for convenience.

The formation shows a marked lateral change in thickness over less than 2 km (1.2 mi), as will be discussed in the next section. The thickest section at this locality comprises 200 m (660 ft) of beds*. Elsewhere within the outcrop belt of the formation, thicknesses range from 75 m (250 ft) at Able and Baker creeks to 140 m (460 ft) at Sandhill River. Thin erosional remnants of the formation are present beyond its main outcrop area, within a hollow on the top of Gyrfalcon Bluff and on the top of the Devonian plateau south of Cape Vesey Hamilton (not shown on Fig. 9, see Map 1455A). According to J.S. Vincent (*pers. com.*, 1975), there are many thin outliers of the Isachsen southeast of Pim Ravine.

In several areas the Isachsen Formation is absent and the Christopher Formation rests directly on the basement rocks. This is the case at Cape Crozier southwest of Mercy Bay, at Dissection Creek and at Rufus River. A single exposure of Isachsen Formation, 9 km (5.6 mi) south of Cape M'Clure, exposes 13 m (43 ft) of the uppermost part of the formation, indicating that the overlap of the Isachsen at Cape Crozier is not laterally extensive. The formation is absent in six of the eight wells described in this report, whereas at Orksut I-44 the Isachsen is 95 m (313 ft) thick, and at Castel Bay C-68 it is 188 m (616 ft) thick. These wells are located on the central axis of Banks Basin. Elsewhere, on the east flank of Central Banks Basin at Ikkariktok M-64 and Tiritchik M-48, the Isachsen is absent, probably because of nondeposition over a contemporaneous, structurally uplifted area. The formation is absent also over Storkerson Uplift and in Big River Basin (Storkerson Bay A-15, Nanuk D-76, Uminmak H-07 and Bar Harbour E-76 wells), probably for the same reason.

The outcrop and well data suggest that the Isachsen was deposited only within and on the immediate flanks of the principal basins within the report-area, including Northern and Central Banks basins, Cardwell Basin and probably Stewart Basin, although no evidence is available from the last area. Beyond the confines of these basins the formation may never have been more than a few metres thick, as suggested in Figure 5.

Contacts

Throughout most of Banks Island, the basal contact of the Isachsen Formation is a major regional unconformity. Along the east flank of Northern Banks Basin and at Cape Crozier the formation rests on the Upper Devonian Melville Island Group. At Pass Brook and Nelson Head in the southern part of the island, the basal contact is underlain by Proterozoic rocks of the Glenelg Formation or by diabase sills which intrude the Glenelg. In the two well sections the Isachsen is underlain, probably disconformably, by the Jurassic to Lower Cretaceous Mould Bay Formation.

The upper contact of the Isachsen with the Christopher Formation is conformable and, to a greater or lesser degree, gradational. The Christopher consists predominantly of shale and the contact is drawn where argillaceous beds become predominant. Throughout Northern Banks Basin this transi-

tion takes place within a few centimetres but elsewhere a somewhat arbitrary boundary must be drawn between the two formations, as will be discussed in greater detail in the section on lithology. The contact may be diachronous regionally but this cannot be demonstrated from the available biostratigraphic evidence.

Lithology

The present study has indicated that earlier attempts to subdivide the formation into two or more units on the basis of lithology (Thorsteinsson and Tozer, 1962, p. 60, 61; Jutard and Plauchut, 1973, p. 208; Miall, 1975b) are inappropriate because of the marked lateral variations. At most localities there is an upward decrease in gross grain size and the formation may be subdivided locally into two or more members, but there is no evidence that these members correlate with one another. Therefore formal subdivision of the Isachsen into stratigraphic subunits is not attempted in this report.

An alternative type of subdivision has been attempted which is believed to have a greater sedimentological and paleogeographic significance. At each outcrop locality the entire formation has been assigned to one of two gross lithofacies types, a coarse sand facies or a sand-shale facies (the term 'sand' is used in preference to sandstone because the bulk of the Isachsen sands are completely unconsolidated). The coarse sand facies appears to be typical of outcrops along the margins of the depositional basins, whereas the sand-shale facies is in the centres of the basins.

A section exposed 5.5 km (3.5 mi) west of Cape Vesey Hamilton (Field Station 73-MLA-30*) is typical of the coarse sand facies. It consists of 95 m (313 ft) of mainly medium- to coarse-grained, white, quartzose sand with abundant planar and trough crossbedding and rare pebble beds. Boulders up to 34 cm (13.2 in.) and wood fragments up to 50 cm (20 in.) are present (see Appendix 3 for detailed description). The uppermost 2 m (6.6 ft) of the section consist of very fine grained, silty sand containing argillaceous streaks and showing a 'castellated' weathering appearance typical of the beds immediately below the Christopher Formation (which is not exposed at this locality). There are an estimated 45 m (140 ft) of Isachsen below the exposed section, bringing the estimated total thickness of the formation to 140 m (450 ft).

The medium to coarse, crossbedded sands are illustrated in Plate 1. A general view of the upper part of the section, including the characteristically castellated exposures of the uppermost part of the Isachsen is shown in Plate 2A.

A very similar partial section 28 m (92 ft) thick is exposed 5 km (3 mi) southwest of the Cape Vesey Hamilton exposures and another exposure totalling 46.5 m (153 ft) of beds is 7 km (4.4 mi) from the mouth of Mercy River. These sections (Stations 73-MLA-29 and 73-MLA-31, respectively) are described in Appendix 3. In addition there are numerous small exposures of the coarse, quartzose sands in this area extending from Gyrfalcon Bluff in the southwest, to the top of the Devonian plateau in the northeast. In both of these cases, as

* All field measurements were made in metric units. Conversions to imperial units also are included. Small inconsistencies may appear as a result of the conversion and where measurements have been rounded off for convenience.

* Stations identified with the letters MLA were measured and described by A.D. Miall; those identified by GAS were studied by A.S. Greene. All sections identified by station number are shown on the 1:250 000 coloured geological maps (*in pocket*).

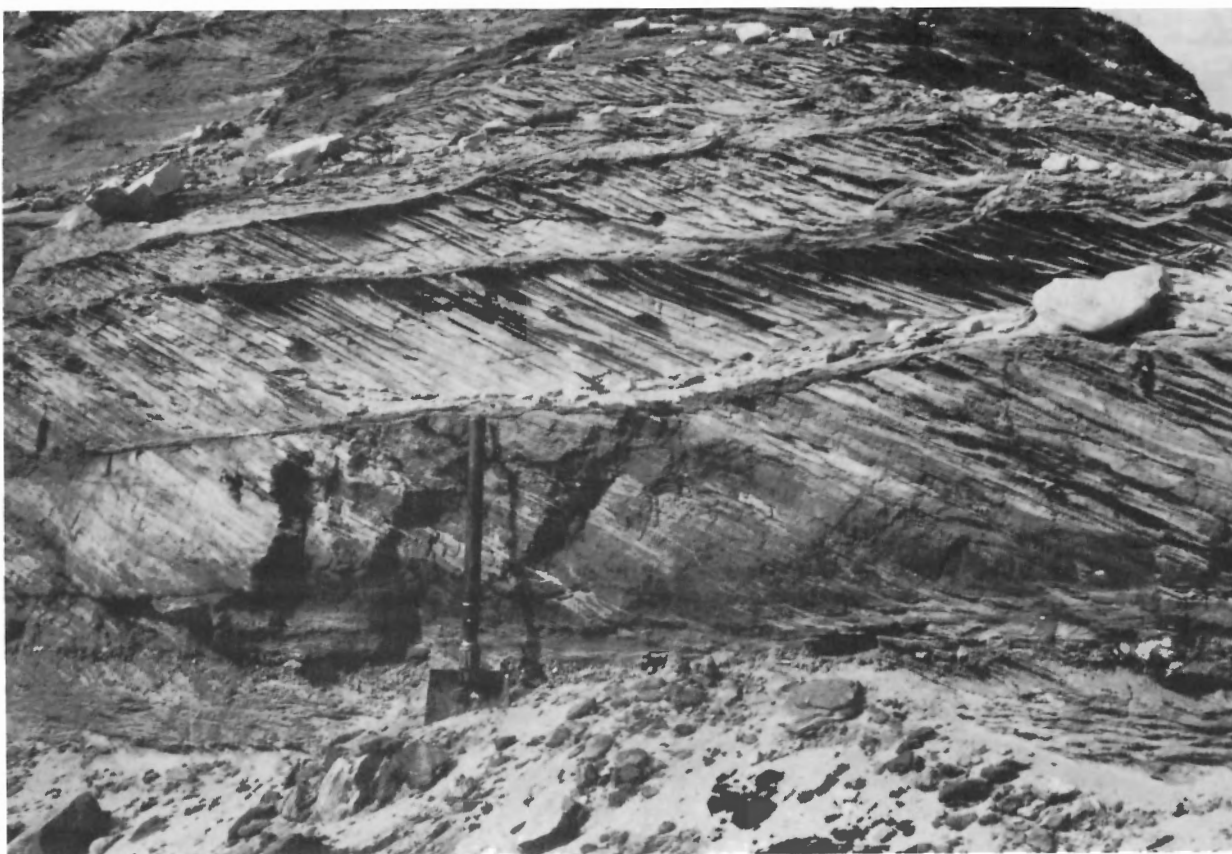


Plate 1. Superimposed sets of planar crossbedded sand in the Isachsen Formation, at Station 73-MLA-30, Cape Vesey Hamilton. Such structures are common in several of the Mesozoic and Tertiary units, particularly the Isachsen Formation. Note the local preservation of curved topsets. Shovel handle is 50 cm long. GSC 199209.

discussed in more detail later in this report, the patches of Isachsen are present in hollows eroded in the Devonian rocks, which are interpreted as representing exhumed, Cretaceous, topographic relief. According to J.S. Vincent (*pers. com.*, 1975), there are many thin outliers of the Isachsen sand on the Devonian plateau southeast of Pim Ravine.

Mapping indicates that the Isachsen Formation is absent between Mercy Bay and Thomsen River, but reappears near the junction of Thomsen River and MuskoX River and is exposed extensively upstream along Thomsen River and its immediate tributaries as far as White Sand Creek. All the exposures are of the coarse sand facies. The best exposure is located at the junction of Baker Creek and Thomsen River, where a section 21.5 m (70.5 ft) thick has been measured (Station 73-MLA-26, *see* Appendix 3 for a detailed description). A general view of the outcrop is given in Plate 2B; note the abundance of planar crossbedding. Pebble beds and lignite streaks also are common and the succession is very similar generally to that at Cape Vesey Hamilton. The finer grained, upper part of the formation is 7.5 m (24.6 ft) thick at this locality and is, in part, weathered in the typical castellated form. The formation is estimated from graphic reconstruction to be 75 m (250 ft) thick in the Baker Creek area. The contact with the Christopher Formation is well exposed and is abrupt, as shown in Plate 3 (*see also* Thorsteinsson and Tozer, 1962, Pl. XXVI).

Numerous patchy exposures of the coarse sand facies are present in the vicinity of White Sand Creek. They consist of medium to coarse, commonly pebbly, quartzose sand and, from the air, appear characteristically pale. Clay ironstone concretions are rare.

The third main area of outcrop of the coarse sand facies extends between Schuyter Point and Alexander Milne Point, in southeastern Banks Island. Rock types and sedimentary structures are similar to those in northern Banks Island, as described above. Crossbedded sands predominate, pebbles of quartz, chert and silicified carbonate sediments are present, as are sideritic clay ironstone concretions, carbonized logs, and lignitic coal seams up to 10 cm (4 in.) thick. A partial section through the upper, finer grained part of the formation was measured at Alexander Milne Point (Station 74-MLA-17). Fine-grained to very fine grained sand with interbedded shale and siltstone, totalling 52.5 m (172.2 ft) of beds, are exposed. A similar section 36 m (118 ft) thick is exposed 8 km (5 mi) along the coast to the north (Station 74-GAS-8, *see* Appendix 3), whereas 3 km (2 mi) to the south is an exposure of the typical medium to coarse sands of the lower part of the Isachsen (Station 74-MLA-18, *see* Appendix 3).

The fourth area in Banks Island where the coarse facies of the Isachsen is preserved is at Nelson Head, where three closely spaced outcrops indicate a marked lateral change in thickness and rock types (Stations 74-MLA-2, 4, 6, *see*

Appendix 3). At Station 74-MLA-6, there is a basal unit 75 m (246 ft) thick, consisting of pink, quartzose, medium-grained to very coarse grained sandstone with numerous beds of pebble-, cobble- and boulder-conglomerate. Clasts reach 50 cm (20 in.) in diameter and consist predominantly of Proterozoic quartz sandstone (Pl. 5). The remainder of the section, which is 199 m (653 ft) thick, comprises medium-grained to very fine grained sand with abundant argillaceous partings and thin beds of coal. The conglomeratic unit thins to the east, and at Station 74-MLA-4, 1.5 km (0.9 mi) distant, it is virtually absent (Pl. 4B). The lateral facies changes are summarized in Figure 10.

Thorsteinsson and Tozer (1962, p. 64) assigned only 21 m (70 ft) of beds at Nelson Head to the Isachsen Formation. This is approximately the thickness of the basal, coarse unit at Station 74-MLA-2 (Appendix 3). The overlying beds at this locality were assigned to the Christopher Formation by Thorsteinsson and Tozer (*ibid.*) but here are reassigned tentatively to the Isachsen Formation, although they contain considerably less sand than the laterally equivalent beds at Station 74-MLA-6.

As stated at the beginning of this section, there is a second gross lithofacies within the Isachsen Formation. This is the sand-shale facies, and much of the section at Stations 74-MLA-2 and 74-MLA-4 may be assigned to it. A more complete section through this type of lithological sequence is present at Sandhill River (Station 74-GAS-11); a detailed description is provided in Appendix 3. Clay or soft shale composes approximately half of the total thickness. Thin seams of coal and carbonaceous shale and layers of siderite concretions are common. Beds of sand up to 7.5 m (24.6 ft) contain abundant planar crossbedding and rare ripple marks. The base of the section is an estimated 30 m (98.4 ft) above the Isachsen-Precambrian contact and the total exposed thickness of the Isachsen is 112 m (367.5 ft). There is a gradational contact with a clay, sand and coal succession composing the basal Christopher Formation.

Plate 4B shows the typical appearance of this facies.

At Orksut I-44, sample and log interpretation indicates that the Isachsen in this area also should be assigned to the sand-shale facies. Gamma ray log response (Fig. 8) indicates a general upward-fining, from coarse-grained, pebbly sandstone at the base to fine- to medium-grained sandstone with siltstone and shale interbeds at the top. A sample description is given as part of the complete well section in Appendix 2 and an interpretative graphic log is shown in Figure 8. A similar succession is present in the Castel Bay C-68 well.

In two localities only, the upper few metres of the Isachsen are exposed and it is uncertain to which of the two gross lithofacies the outcrops should be assigned. The first of these exposures is located on Nelson River (Station 74-MLA-8), where 25 m (82 ft) of beds were studied in sections along the river bluffs. The principal rock type consists of silt to very fine sand, which is white, quartzose, and contains laminae of medium to dark grey clay and coal. Mud pebbles are rare and planar crossbeds are abundant.

Near Colquhoun River in northern Banks Island 13 m (43 ft) of the uppermost Isachsen Formation are exposed (Station 73-MLA-35), consisting of faintly laminated, fine-grained sand with ripple marks and rare solitary trough

crossbeds. Thin argillaceous laminae also are present. Other structures include horizontal burrow structures and very low angle planar crossbedding, in which the foresets dip at angles of 2 or 3 degrees (Pl. 6). The base of the Christopher is a few metres above this outcrop but is not well exposed. The outcrop may represent most of the formation at this locality since immediately to the north, at Cape M'Clure and Cape Wrottesley, the Isachsen is absent beneath the Christopher Formation as a result of northward thinning and overlap against the Devonian.

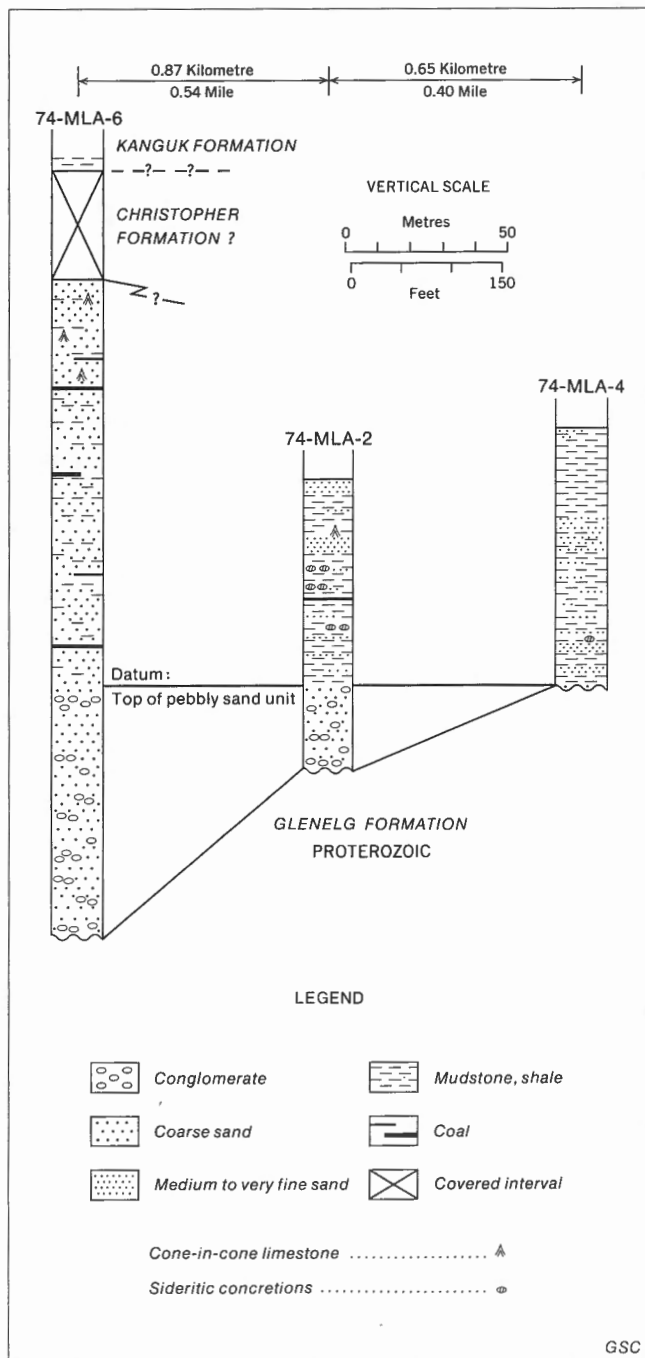


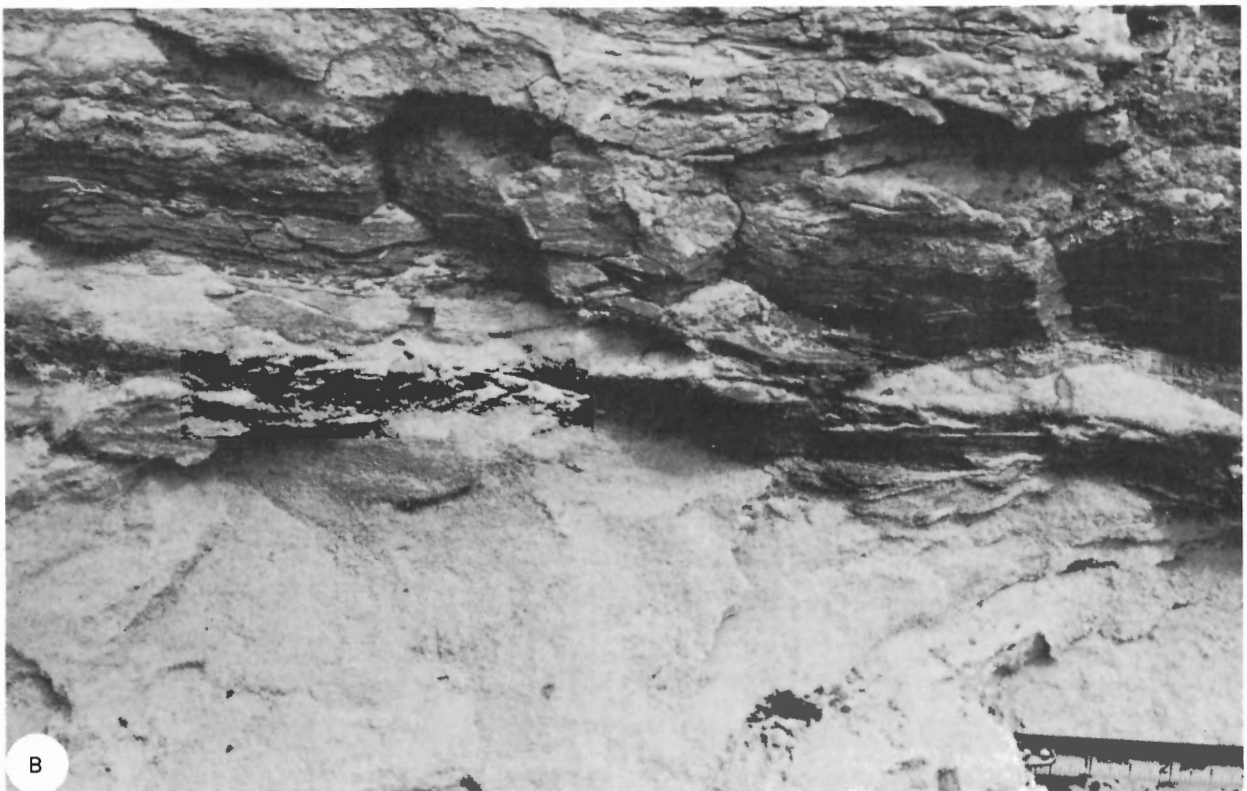
Figure 10. Lateral changes within the Isachsen Formation at Nelson Head.



Plate 2. General views of the Isachsen Formation in northern Banks Island. A: Station 73-MLA-30, Cape Vesey Hamilton. Note the characteristic castellated appearance of the uppermost part of the formation at top right. Outcrop is approximately 25 m (82 ft) high. GSC 199178. B: Station 73-MLA-26, Baker Creek. Note the abundance of planar crossbedding. Outcrop is 21 m (69 ft) high. GSC 199174.



A



B

Plate 3. The Isachsen–Christopher contact (Ki–Kc) at Baker Creek (Station 73-MLA-27).
 A: General view. The contact lies immediately above the white sand unit. Outcrop is 15 m (49 ft) high. GSC 199175. B: Closeup view, showing basal Christopher shales in fairly abrupt contact with fine-grained Isachsen sand. GSC 199176.

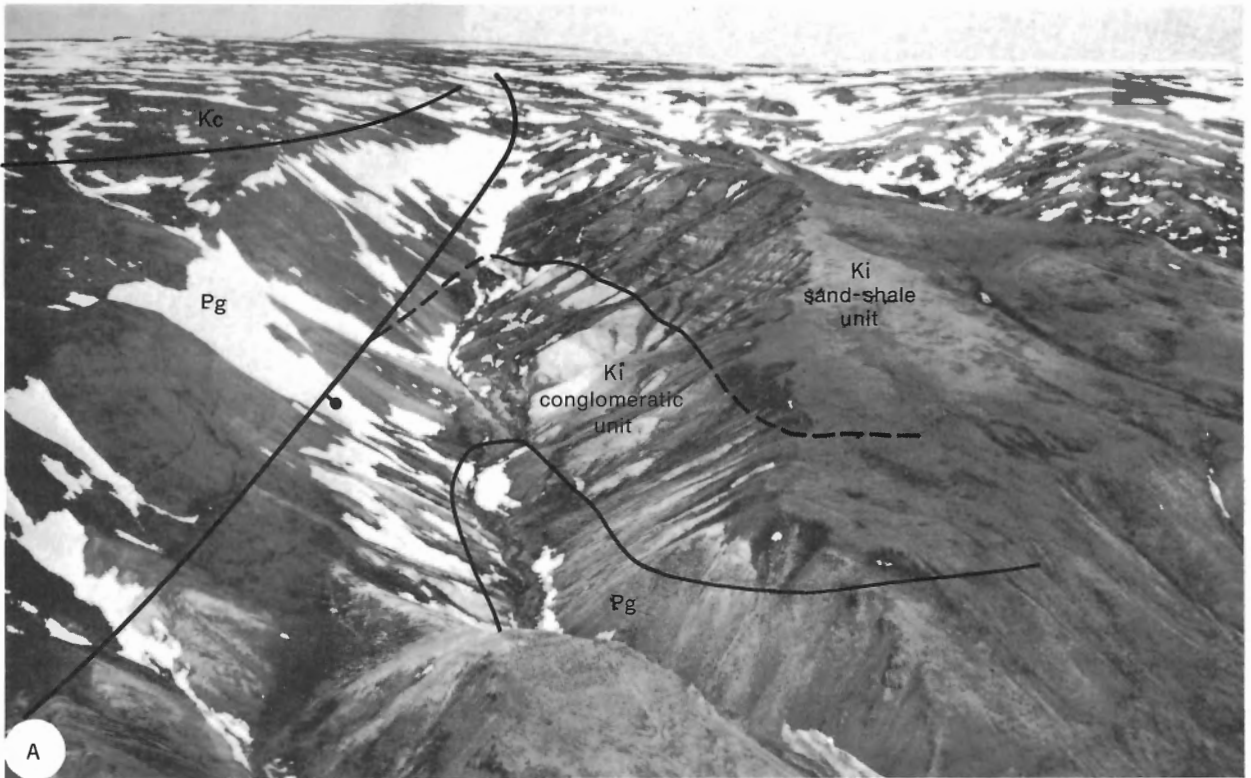


Plate 4. General views of the Isachsen Formation (Ki) at Nelson Head. A: The basal conglomeratic unit and the overlying sand-shale unit at Station 74-MLA-6 juxtaposed against the Proterozoic Glenelg Formation (Pg) along the westerly bounding fault of the Nelson Head Graben. (Kc=Christopher Formation.) GSC 199190. B: The Isachsen-Glenelg contact at Station 74-MLA-4. The basal conglomeratic unit virtually is absent at this locality. GSC 199188. Locations are shown in Figure 23.



Plate 5. Pebble and boulder conglomerates, basal Isachsen Formation, Nelson Head.
A: Boulder conglomerate with interbedded sandstone, Station 74-MLA-6. GSC 199191.
B: Pebble conglomerate, Station 74-MLA-6. GSC 199192.

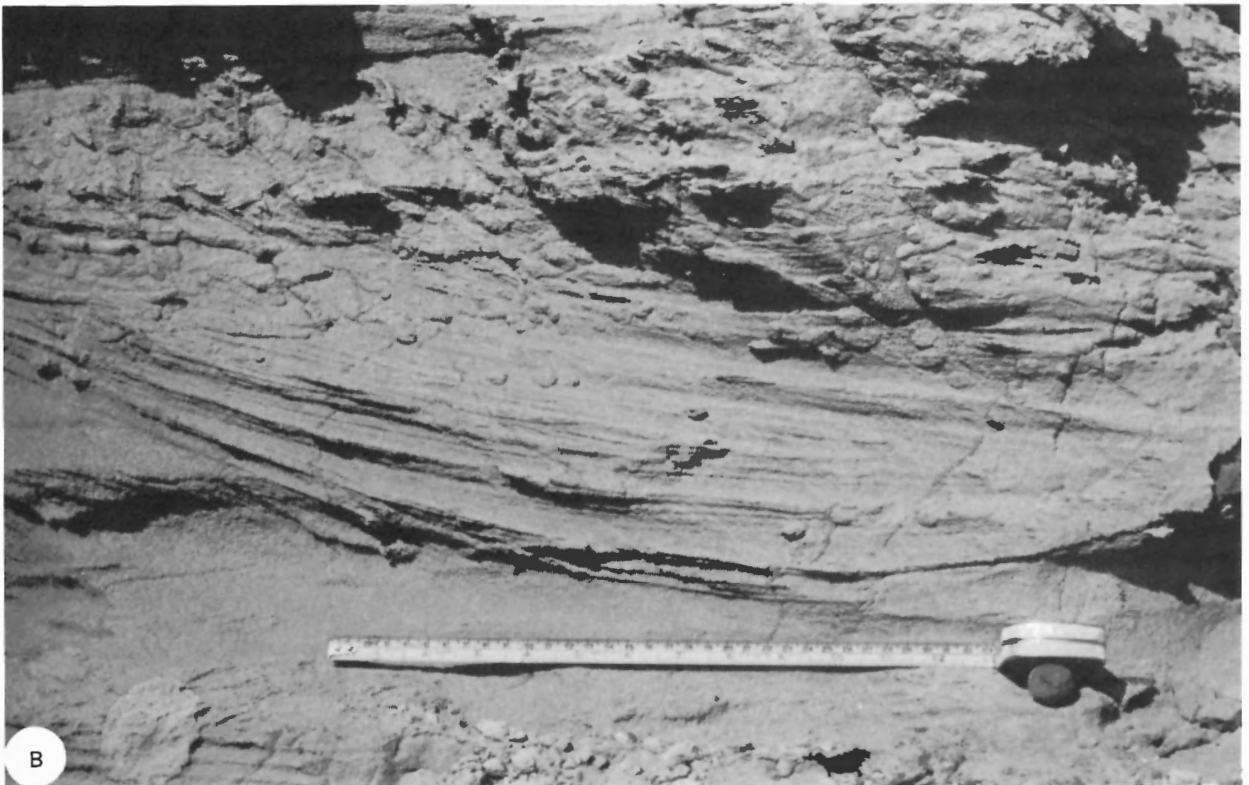
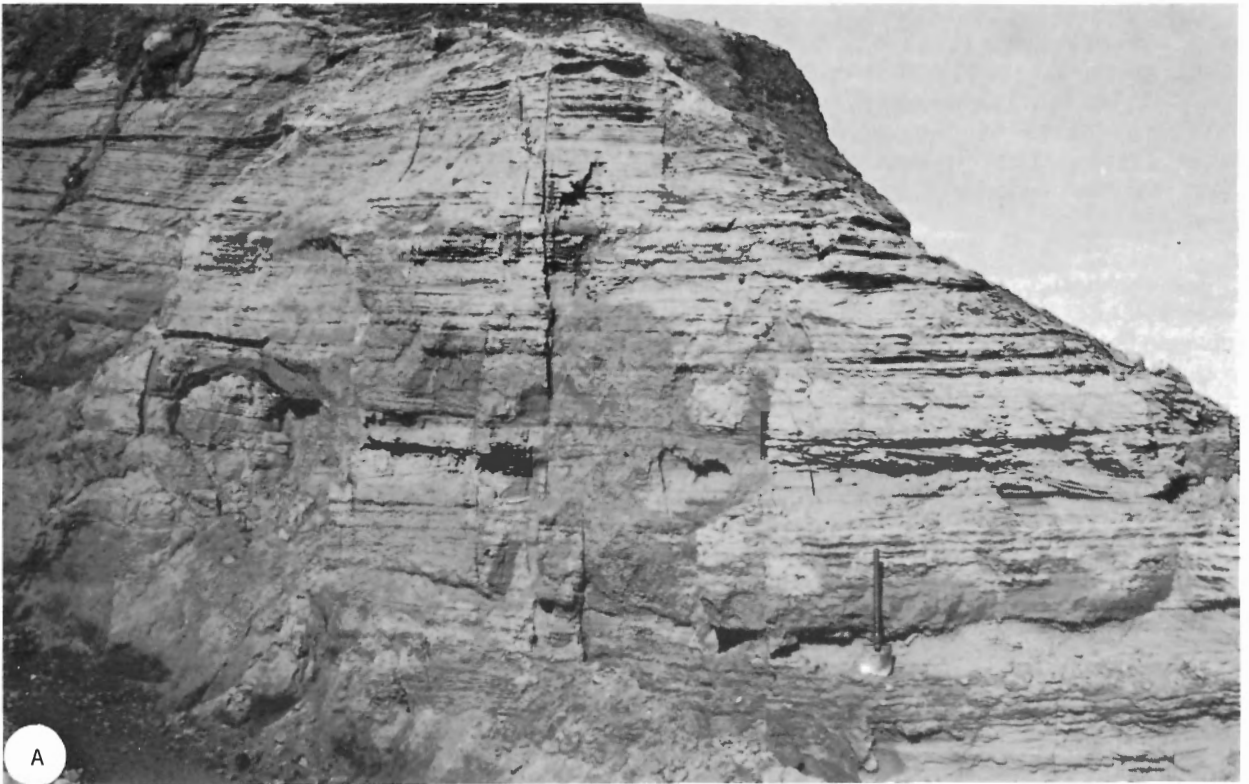


Plate 6. Uppermost Isachsen Formation at Colquhoun River (Station 73-MLA-35). A: Fine-grained, planar bedded sands. Note low-angle planar crossbedding, particularly at top left. Shovel handle is 50 cm long. GSC 199185. B: Closeup of trough-crossbed with abundant trace fossils (*centre right, 6A*). GSC 199184.

An outcrop 16 km (10 mi) north of Cape Lambton and another series of outcrops along the lower Rufus River were included in the Isachsen Formation by Thorsteinsson and Tozer (1962) but are reassigned tentatively to the Christopher Formation on the basis of greater lithological similarity with the latter formation. These exposures will be described together with the other outcrops of the Christopher in a later section.

Age and correlation

Fossils of all types are sparse in the Isachsen Formation and it is necessary in some instances to assign an age on the basis of the age of the overlying and underlying units. No megafossils have been found in the Isachsen on Banks Island; the formation is predominantly nonmarine and rarely contains foraminifera or dinoflagellates. However, sparse spore and pollen assemblages have been obtained from a few samples, as described below.

A sample 10 m (33 ft) above the base of Station 73-MLA-26 at Baker Creek yielded the following assemblage (GSC loc. C-26404):

Sphagnum antiquasporites Wilson and Webster
Gleicheniidites senonicus Ross
Concavissimisporites sp.

W.S. Hopkins, Jr., who identified this flora, assigned to it an Early Cretaceous age (*pers. com.*, 1974).

A sample from the uppermost Isachsen at the same locality, 14 m (46 ft) above the base of the section, contains the following flora (GSC loc. C-26405):

Sphagnum antiquasporites Wilson and Webster
Appendicisporites sp.
Cicatricosisporites sp.
Lycopodium sp.
Cyathidites sp.
Osmundacidites sp.
Gleicheniidites senonicus Ross
Trilobosporites sp.
Tsuga sp.
Eucommiidites sp.
Classopollis sp.

Hopkins (*ibid.*) assigned an Early Cretaceous age to the assemblage and stated that there are strong affinities between this flora and those obtained from the Isachsen Formation of the Sverdrup Basin.

A sample from 2 m (6.6 ft) above the base of Station 73-MLA-29 near Cape Vesey Hamilton contains the following flora (GSC loc. C-26408):

Sphagnum antiquasporites Wilson and Webster
Deltoidospora sp.
Baculatisporites sp.
Cicatricosisporites sp.
Appendicisporites sp.
Lycopodium sp.
Gleicheniidites senonicus Ross
Vitreisporites sp.
Eucommiidites sp.
Tsuga sp.
cf. Taxodiaceae

Hopkins (*ibid.*) compares this assemblage also with those found in the Isachsen Formation of Sverdrup Basin.

Eight samples from Station 74-GAS-11 at Sandhill River were processed for microforaminifera by C.A. Pollock and C.B. Mahdeo of Amoco Canada Petroleum Company Ltd. Surprisingly, two samples were found to contain foraminifera; they were assigned an Albian age and were interpreted as indicating an open-marine environment. The results are listed below, using unit numbers allocated in the formal description of the outcrop in Appendix 3.

Unit	Results	GSC loc.
2	barren	C-30719
5	barren	C-30721
7	<i>Miliammina awunensis</i> Tappan <i>Pallaimorphina ruckerae</i> Tappan <i>Vaginulina exilis</i> (Reuss) <i>Globulina prisca</i> Reuss <i>Rectoglandulina kirschneri</i> Tappan <i>Haplophragmoides topagorukensis</i> Tappan <i>Vaginulinopsis grata</i> (Reuss) <i>Saracenaria grandstandensis</i> Tappan	C-30723
7	<i>Miliammina awunensis</i> Tappan <i>Uvigerinammina manitobensis</i> (Wickenden) <i>Verneulinoides borealis</i> Tappan <i>Arenobulimina paynei</i> Tappan	C-30724
10	barren	C-30726
16	barren	C-30728
17	barren	C-30729

Sample C-30729 was taken from beds assigned to the Christopher Formation.

Two samples from the exposures of the Isachsen Formation at Nelson Head were processed for microfossils by J.H. Wall. They were obtained 35 m (115 ft) above the base of the formation at Station 74-MLA-2 (GSC loc. C-30464) and 7.5 m (25 ft) above the base of Station 74-MLA-4 (GSC loc. C-30473). Both samples were barren.

A sparse foraminifera fauna from probably caved material was obtained from the upper part of the Isachsen Formation in the Orkut I-44 well. J.H. Wall (*pers. com.*, 1974) commented that a channel sample from the 1402 to 1432 m (4600–4700 ft) interval of the well contains a distinctively different fauna from that in samples taken higher in the succession, and he tentatively assigned to it an early Neocomian age. The fauna includes the following (GSC loc. C-30109):

Ammodiscus sp. cf. *A. southeyensis* (Wall)
Haplophragmoides sp. cf. *H. barrowensis* Tappan—one
H. sp. cf. *H. canui* Cushman
Trochammina sp., compressed, indistinct
ostracode, indeterminate

The interval of the well from which this sample was taken includes the uppermost 5 m (17 ft) of the Mould Bay Formation and the entire fauna possibly was derived from this pre-Isachsen unit.

Jutard and Plauchut (1973, p. 209) reported the following from their studies of the Isachsen Formation in northern Banks Island:

Pollen, mainly disaccate, are very common: *Alisporites*, *Cedripites*, *Podocarpidites* and *Cerebropollenites*. The relative percentage of genus *Classopollis* decreases from bottom to top. Moreover, two associations of spores were observed in samples of the Isachsen Formation: in the lower part, a rather poor microflora without any *Trilobosporites trioreticulosus*, *Lycopodiumsporites austroclavaiidites* and *Aequitriradites spinulosus*; in the upper part, a very rich microflora characterized by *T. trioreticulosus* and *L. austroclavaiidites*. Correlations with the Deville and Ellerslie members of Mannville Group of Alberta are possible and indicate a Barremian-Aptian age for the Isachsen Formation.

The proposed Barremian to Aptian age range of the Isachsen Formation is adopted in this report, except for parts of southern Banks Island, as at Sandhill River, where part of the formation may be as young as Albian. Locally, the Isachsen probably shows an interfingering relationship with the base of the Christopher Formation, as Figure 7 suggests.

The Isachsen Formation of Ellef Ringnes Island contains *Buchia* (*Aucella*) cf. *B. bulloides* (Lahusen) and *Buchia* cf. *B. terebratuloides* (Lahusen) in the lowest 30 m (100 ft) of the succession. The fossils have been assigned an Infravalangian to Valangian age by J.A. Jeletzky, as reported by Heywood (1957, p. 11). The base of the formation, therefore, appears to be older in the Sverdrup Basin.

Based on similar stratigraphy and lithology the Isachsen Formation is correlated with the Gilmour Lake Member of the Langton Bay Formation in the Anderson Plains area (Yorath, Balkwill and Klassen, 1975, Fig. 17). The Gilmour Lake Member is predominantly arenaceous and is partly Aptian and partly Valangian in age.

Christopher Formation

Definition, distribution and thickness

The Christopher Formation was described first by Heywood (1955; 1957, p. 12), who applied the name to a succession comprising shale and silty shale with minor amounts of limestone overlying the Isachsen Formation in the Isachsen area of Ellef Ringnes Island. Stott (1969, p. 25, 26) stated that the formation ranges up to 760 m (2500 ft) in thickness in Ellef Ringnes Island, and is of Albian and possibly latest Aptian age. The formation now is known to be widespread in the Arctic Islands. The outcrops which occur throughout the western Queen Elizabeth Islands have been described by Tozer and Thorsteinsson (1964) and those in parts of Axel Heiberg Island have been described by Tozer (1963b, p. 454) and Souther (1963, p. 440).

The Christopher Formation of Banks Island was first described by Thorsteinsson and Tozer (1962), who estimated the thickness to be between 300 and 370 m (1000–1200 ft) and stated that the formation comprises a succession of shale with lesser amounts of sandstone and beds and concretions of clay

ironstone. A similar description was provided by Jutard and Plauchut (1973, p. 209, 210), based on their work in northern Banks Island.

As shown in Figure 11, the formation underlies most of the report-area, with the exception of those parts of the island where Recent erosion has penetrated to older rocks. The formation is absent also within two long narrow areas within the subsurface along which uplift and removal of the Christopher is interpreted to have taken place in early Late Cretaceous time. The formation is thickest in southern Banks Island, where it has an extensive area of outcrop. An incomplete section 300 m (984 ft) thick was measured at Nelson River, and graphic reconstructions in this area suggest a thickness for the complete formation in the order of 460 m (1500 ft). The formation thins to the south and to the north (Fig. 7). At Nelson Head Graben only 30 m (110 ft) of beds are assigned to the Christopher Formation although the upper part of the Isachsen Formation may be of Christopher (Albian) age as at Sandhill River. On Durham Heights the original thickness of the Christopher Formation may be even less, as shown by outcrop patterns of the enclosing units.

At the Orksut I-44 well the Christopher Formation is 40 m (140 ft) thick, probably as a result of pre-Kanguk erosion.

Elsewhere, within Big River Basin and Northern Banks Basin, the Christopher ranges in thickness from 79 m (260 ft) at the Bar Harbour E-76 well to an estimated 240 m (800 ft) in outcrop along lower Thomsen River. Between Thomsen River and Mercy Bay, mapping indicates that the Christopher thins to a few metres or disappears altogether beneath the Kanguk Formation (Fig. 7).

Thin but extensive erosional remnants of the Christopher rest on the Devonian rocks along Dissection Creek. Between this creek and Johnson Point photogeological interpretation suggests a further broad area thinly covered by Christopher strata, although there are extensive surficial deposits in this region and the evidence is ambiguous. According to J.S. Vincent (*pers. com.*, 1975), there are also thin outliers of the Christopher Formation between Dissection Creek and Parker Point.

Contacts

The contact between the Isachsen and Christopher formations is gradational in most localities and therefore a somewhat arbitrary boundary must be drawn between the two units. A sharp contact between Isachsen sands and Christopher shales was observed at Baker Creek (Pl. 3) and log interpretation suggests a similar sharp contact in the Orksut I-44 well (Fig. 8). Elsewhere, lithologies typical of each formation are interbedded over intervals of several or many metres. Secondary criteria may be resorted to, such as the presence of large-scale crossbedding in the Isachsen Formation and ripple marks, pelecypods and foraminifera in the Christopher Formation, but such criteria are not infallible, as shown by the foraminifera in a 'typical' Isachsen section at Sandhill River.

The upper contact of the Christopher Formation is more distinctive. On the east flank of Northern Banks Basin and at Cape Crozier the formation grades upward, through an interval of a few metres, into the sands of the Hassel Formation. Elsewhere the Hassel is absent and the Christopher is

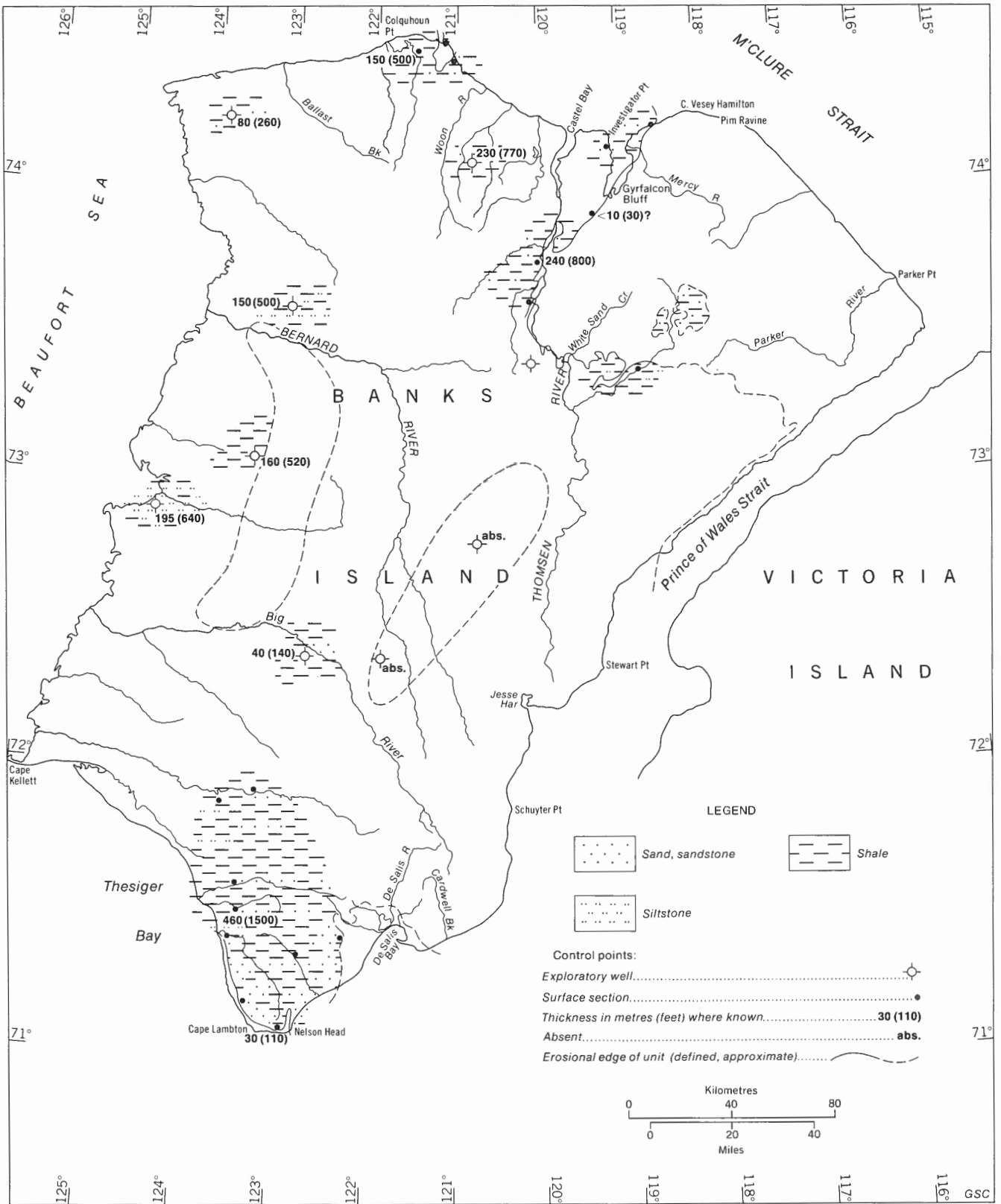


Figure 11. Christopher Formation: distribution, thickness and lithologies. Thicknesses are rounded off for convenience.

overlain sharply and unconformably by the basal beds of the Kanguk Formation. In most areas these are characterized by black bituminous shale or by small manganese-bearing spherulites (Miall, 1974*d*). The latter are particularly useful as a marker horizon in the subsurface although, as noted below, they have been recorded also from near the top of the Kanguk Formation at two localities and therefore their presence in a section should be interpreted with care.

Lithology

The Christopher Formation was divided into two members by Thorsteinsson and Tozer (1962) and Jutard and Plauchut (1973). As with the Isachsen Formation, the implication was that these members persist throughout Banks Island. The basis of the subdivision was that, although the Christopher Formation consists predominantly of shale, the lower part of the formation contains a considerable proportion of interbedded sandstone. These sand-bearing beds were defined as a lower member and the shale above constituted the upper member.

This subdivision is followed informally in the present report, since there is no doubt that in some areas an upward gradation from a sandstone-shale succession to a shale succession does occur. However, it is doubtful if the facies change is of more than local stratigraphic significance, and it cannot be recognized in the three wells drilled on western Banks Island.

The gradational contact with the Isachsen Formation is best seen at Sandhill River (Station 74-GAS-11), where the lowermost 22 m (73 ft) of the Christopher Formation are exposed. The contact is drawn where argillaceous beds predominate in the section, although beds of fine-grained sand up to 4 m (13.1 ft) thick are in the section. Most of the exposed beds consist of grey to buff, silty clay with thin sand and coal seams.

Successions rather similar to this are present in Nelson Head Graben (Stations 74-MLA-2, 4) where they overlie the basal coarse sand of the Isachsen Formation and pass laterally within a distance of less than 1 km (0.6 mi) into medium to coarse sands of typical upper Isachsen aspect (Fig. 10). Stations 74-MLA-2 and 4 (see Appendix 3 for complete descriptions) are assigned to the Isachsen Formation but the existence of this marked lateral facies change demonstrates that the lithofacies types, and the members of the Christopher Formation that are based on them, are diachronous in their distribution.

A more complete section through the lower part of the Christopher Formation is exposed along the lower reaches of the Rufus River. Station 74-GAS-4 is typical. At this locality, rocks of typical lower Christopher aspect – shale with thin beds of silt and medium to very fine sand – rest directly on the Proterozoic basement. There is a basal unit 1 m (3.3 ft) thick consisting of medium- to coarse-grained, limonite-stained sand which probably represents a soil zone on the Proterozoic erosion surface. A total of 80.5 m (264.1 ft) of the Christopher Formation are exposed at this locality. Pyrite nodules and siderite concretions are abundant, and there is one bedding-plane exposure of a siderite-cemented sandstone covered with a field of small-scale asymmetric ripple marks. Plate 7A gives a view of the Christopher-Glenelg contact at this locality. The typical appearance of the interbedded clays, silts and sands

in the lower part of the Christopher Formation is shown in Plate 7B.

Several good but incomplete exposures of the upper part of the Christopher Formation are present in southern Banks Island, notably in the bluffs along Masik, Atitok and Nelson rivers (Stations 74-GAS-12, 13 and 7, respectively). Detailed descriptions are provided in Appendix 3. Soft grey shale predominates and beds a few metres thick of fine-grained sand or silt also are present. Pelecypods and ammonites are the most common fossil types but gastropods and wood fragments also are present, and one fragmentary decapod was found (by W. George) near Masik River.

The typical appearance of these predominantly shale successions is shown in Plate 8A, which is a view of Station 74-GAS-13 on the lower Atitok River. Near the middle of this exposure a thin, resistant and laterally persistent unit is visible. This is unit 5 in Station 74-GAS-13 (see Appendix 3), a calcareous and sideritic sandstone with symmetrical ripple marks and abundant pelecypods. The unit can be traced laterally for at least 8 km (5 mi) without any significant alteration of lithology or thickness. Plate 8B gives a view of another calcareous sandstone at the base of the section at Atitok River. Note the bulbous, concretionary nature of the upper surface of this bed and the abundant small-scale, superimposed ripple marks.

Several small exposures of the Christopher Formation are present on Kellett River. They are all of the upper part of the formation, consisting of uniform soft, dark grey shale with sideritic nodules and small 'hedgehog' concretions.

In Central Banks Basin much of the Christopher Formation has been removed by pre-Kanguk erosion. At the Orksut I-44 well the lower 40 m (140 ft), consisting of sandstone and silty shale, are preserved. A complete description is included with the detailed log of this well in Appendix 2 and a graphic log is included in Figure 8. Sections through the formation are more complete in Big River Basin (Storkerson Bay A-15 well) and on the flanks of Storkerson Uplift (Nanuk D-76 and Uminmak H-07 wells, see Appendix 2 and Fig. 8). At Storkerson Bay the formation consists predominantly of argillaceous siltstone but includes minor sandstone and shale beds; at the Nanuk and Uminmak locations the Christopher consists mainly of silty shale.

Numerous exposures of the formation are present on the east flank of Northern Banks Basin, between Dissection Creek and Cape Vesey Hamilton, and also in the vicinity of Cape Crozier (Fig. 11). None of these exposures shows more than a few tens of metres of section and therefore the general character of the formation is difficult to determine. Several small exposures along Dissection Creek show the Christopher Formation strata resting directly on the Devonian Melville Island Group. The basal Christopher beds comprise pale buff, quartzose silt; soft, dark grey shale; thin coal seams; and scattered clay-ironstone concretions.

Exposures are better along Thomsen River northward from the junction with Baker Creek. At the latter locality, the Christopher Formation rests abruptly on the Isachsen Formation, as seen in Plate 3 (Stations 73-MLA-26, 27, Appendix 3). The lower 16 m (52 ft) of the formation comprise medium grey, bioturbated shale and some interbedded fine-grained sand. Rare ironstone concretions also are present. Similar rock

types, with fewer arenaceous interbeds, are visible in several tributary creeks along the west side of Thomsen River north of Able Creek. Pelecypods are common and ammonites are rare in these beds. Several good exposures of the upward transition into the Hassel Formation also are found in this area and will be described in the section on that formation.

Additional exposures are on the west and east sides of Mercy Bay. Station 74-GAS-25, in the sea cliffs 9 km (6 mi) east of Back Point, exposes 72 m (236.2 ft) of the lower part of the formation, consisting of interbedded grey-brown shale and very fine grained, quartzose sand.

The uppermost part of the Christopher Formation is well exposed in Station 74-GAS-26 near Investigator Point. Here the Christopher is followed directly by the Kanguk Formation; the uppermost Christopher beds are probably a lateral equivalent of the Hassel and represent a local continuation of the Christopher facies into latest Albian time. They consist of silty clays with abundant ironstone concretions. A total thickness of 52.3 m (171.6 ft) of beds is exposed below the Kanguk Formation.

The lower Christopher Formation is well exposed in a downfaulted area between the cliffs of Devonian Melville Island Group at Cape M'Clure and Cape Crozier (Station 74-GAS-46, see Appendix 3). A succession of soft shale, siltstone and sandstone 67 m (220 ft) thick is exposed and includes concretionary masses of calcareous siltstone up to 6 m (20 ft) in diameter and numerous hedgehog concretions.

Age and correlation

Numerous macrofossil, microfossil and palynological collections indicate that the Christopher Formation is Albian in age. Only at the Nanuk D-76 well is there evidence that the lowermost Christopher Formation is Aptian. H. Evers of Elf Oil Exploration and Production Canada Ltd. (*pers. com.*, 1974) reported that the palynological studies by his company indicate that in the Storkerson Bay A-15 and Nanuk D-76 wells the lower part of the Mesozoic section is Late Cretaceous and he correlated it with the Kanguk Formation. Evers states (*see also* Clowser in Brideaux *et al.*, 1976) that a similar situation prevails at the Uminmak H-07 well, except that the lower few metres of the Mesozoic section are of Late Jurassic or Neocomian age, indicating a correlation with the Mould Bay Formation. These correlations are not followed in the present report. Faunal and floral lists and age assignments for the three wells as determined by GSC paleontologists are listed and referenced below.

Micropaleontology of the Christopher Formation in the Storkerson Bay A-15 well by Sliter (*in* Barnes *et al.*, 1974):

Depth m (ft)	Fauna	GSC loc.
1341-1372 (4400-4500)	<i>Haplophragmoides topagorukensis</i> Tappan <i>Bathysiphon vitta</i> Nauss <i>Ammodiscus mangusi</i> (Tappan) <i>A. rotalarius</i> Loeblich and Tappan charaphytes age: Albian, Middle to Late	C-24434

1372-1387 (4500-4550)	<i>Haplophragmoides topagorukensis</i> Tappan <i>Bathysiphon vitta</i> Nauss <i>Ammodiscus mangusi</i> (Tappan) <i>Psammimopelta bowsheri</i> Tappan <i>Verneulinoides borealis</i> Tappan age: Albian, Middle to Late	C-24435
--------------------------	--	---------

1387-1393 (4550-4570)	<i>Haplophragmoides topagorukensis</i> Tappan <i>H. gigas</i> Cushman <i>Ammodiscus rotalarius</i> Loeblich and Tappan (large) <i>Bathysiphon vitta</i> Nauss <i>Verneulinoides borealis</i> Tappan age: Albian, Middle to Late	C-24436
--------------------------	---	---------

1393-1402 (4570-4600)	as above plus large (1 mm) <i>Ammodiscus</i>	C-24437
--------------------------	---	---------

1402-1432 (4600-4700)	as above, abundant foraminifera large (1 mm) <i>Ammodiscus</i> <i>Glomospirella gaultina</i> Berthelin <i>Saccammina lathrami</i> Tappan age: Albian, Middle	C-24438
--------------------------	--	---------

1432-1463 (4700-4800)	<i>Ammodiscus rotalarius</i> Loeblich and Tappan (large, 1 mm) <i>Haplophragmoides topagorukensis</i> Tappan <i>H. gigas</i> Cushman <i>Bathysiphon vitta</i> Nauss <i>B. broegei</i> Tappan <i>Verneulinoides borealis</i> Tappan <i>Saccammina lathrami</i> Tappan age: Albian, Middle	C-24439
--------------------------	--	---------

1463-1493 (4800-4900)	as above	C-24440
--------------------------	----------	---------

1493-1524 (4900-5000)	as above <i>Saracenaria</i> sp. cf. <i>S. dutroi</i> Tappan	C-24441
--------------------------	--	---------

1524-1554 (5000-5100)	as above	C-24442
--------------------------	----------	---------

1554-1570 (5100-5150)	as above <i>Saccammina lathrami</i> Tappan, abundant, large (1 mm) <i>Gavelinella</i> sp. cf. <i>G. awunensis</i> Tappan age: Albian, Early to Middle	C-24443
--------------------------	---	---------

Palynology of the Christopher Formation in the Storkerson Bay A-15 well by Hopkins (*in* Barnes *et al.*, 1974):

Depth m (ft)	Flora	GSC loc.
1341-1372 (4400-4500)	<i>Ulmus</i> sp. <i>Carya</i> sp. <i>Paraalnipollenites confusus</i> Hills and Wallace <i>Baculatisporites</i> sp. <i>Aquilapollenites</i> sp. (spinulos) age: Maastrichtian	C-24195

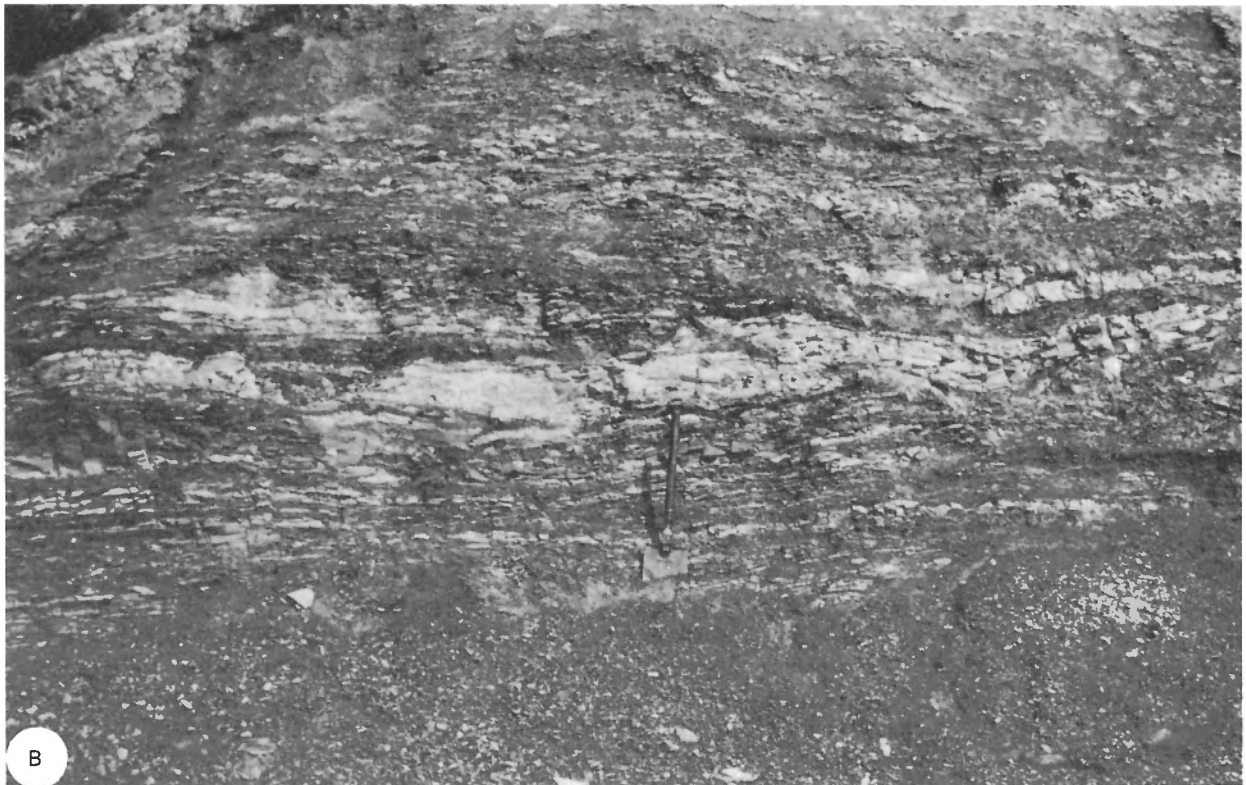


Plate 7. The lower part of the Christopher Formation (Kc). A: At Rufus River (Station 74-GAS-4); the river is cut into resistant Proterozoic gabbro and the Christopher Formation underlies the rounded bluffs above. (Pg=Glenelg Formation.) GSC 199189. B: Interbedded shale and fine-grained, silty sand near Station 73-MLA-30, Cape Vesey Hamilton. GSC 199198.



Plate 8. The upper part of the Christopher Formation. A: At Atitok River (Station 74-GAS-13); approximately 200 m (660 ft) of section are exposed. The thin, resistant sandstone unit half way up the hillside can be traced laterally for at least 8 km (5 mi). GSC 199195. B: Calcareous siltstone at Atitok River, with abundant small-scale ripple marks. GSC 199213.

- 1372–1402 *Ulmus* sp.
(4500–4600) *Carya* sp.
Wodehouseia spinata Stanley
cf. Proteaceae
Aquilapollenites sp. (spinulos)
age: Maastrichtian
- 1402–1432 *Paraalnipollenites confusus* Hills and
(4600–4700) Wallace
Alnus sp. 1
cf. *Gleicheniidites* sp.
age: Maastrichtian
- 1432–1463 *Carya* sp.
(4700–4800) *Aquilapollenites* sp. (spinulos)
Orbiculapollis globosus Khlonova
Expressipollis accuratus Khlonova
miscellaneous phytoplankton
age: Campanian
- 1463–1493 *Lycopodiacidites* sp.
(4800–4900) *Wodehouseia spinata* Stanley
Aquilapollenites sp. (reticulate)
Aquilapollenites sp. (spinulos)
Orbiculapollis globosus Khlonova
Expressipollis accuratus Khlonova
miscellaneous phytoplankton
Aquilapollenites sp. (scabrate)
Extratripoporipollenites sp.
age: Campanian
- 1493–1524 *Lycopodiacidites* sp.
(4900–5000) *Aquilapollenites* sp. (reticulate)
Aquilapollenites sp. (spinulos)
Orbiculapollis globosus Khlonova
Expressipollis accuratus Khlonova
miscellaneous phytoplankton
Extratripoporipollenites sp.
Osmunda sp. 2
age: Campanian
- 1524–1554 *Lycopodiacidites* sp.
(5000–5100) *Aquilapollenites* sp. (spinulos)
cf. *Gleicheniidites* sp.
Orbiculapollis globosus Khlonova
Expressipollis accuratus Khlonova
miscellaneous phytoplankton
Aquilapollenites sp. (scabrate)
cf. *Staplinisporites* sp. (Singh) Singh
age: Albian
- 1554–1569 *Lycopodiacidites* sp.
(5100–5150) *Aquilapollenites* sp. (reticulate)
Cicatricosisporites sp.
Aquilapollenites sp. (spinulos)
Orbiculapollis globosus Khlonova
Expressipollis accuratus Khlonova
miscellaneous phytoplankton
Aquilapollenites sp. (scabrate)
Extratripoporipollenites sp.
Osmunda sp. 2
Distaltriangulisporites perplexus (Couper)
Pocock
Dictyotriletes cf. *D. pseudoreticulatus*
Triporetetes reticulatus (Pocock) Playford
age: Albian
- C-24196 identified much lower in the well using palynological methods than they are on the basis of foraminifera. The reasons for this are not clear but presumably are related to sample caving and contamination. Hopkins (*pers. com.*, 1974) stated that the last three species listed for GSC loc. C-24204 are found exclusively in Albian rocks but that their true first appearance may be much higher than indicated. Contamination in these samples was severe and Tertiary palynomorphs are abundant throughout the entire Mesozoic section.
- C-24199 Additional fauna lists and age determinations for the Banks Island wells are available as follows: Nanuk D-76 micropaleontology by Chamney (*in* Brideaux *et al.*, 1975); Uminmak H-07 palynology by Hopkins (*unpubl.* GSC report), micropaleontology by Clowser (*in* Brideaux *et al.*, 1976) and Sliter (*unpubl.* GSC report); Orkut I-44 micropaleontology by Wall (*in* Brideaux *et al.*, 1976).
- C-24200 The thin sequence of Christopher Formation in the Orkut I-44 well yielded only caved Late Cretaceous foraminifera or long-ranging forms, according to Wall (*in* Brideaux *et al.*, 1976). However, core number 3, from a silty shale in the Christopher at a depth of 1303 to 1313 m (4274–4307 ft), yielded the following palynomorph assemblage, according to W.S. Hopkins, Jr. (GSC loc. C-29058):
- C-24201
- Klukisporites* sp.
Concavissimisporites sp.
Classopollis sp.
Tsuga sp.
?Tricolpites sp.
- C-24202 Hopkins (*pers. com.*, 1974) stated that this sample is nearly barren but that the first two forms named are typically Early Cretaceous.
- C-24203 Numerous fragmentary macrofossils, mainly pelecypods and ammonites, were collected from outcrops in the Christopher Formation and several have yielded useful age information. The faunal assemblages are similar to those described by Thorsteinsson and Tozer (1962, p. 64, 65) and Jutard and Plauchut (1973, p. 210) and indicate an Early to Late Albian age; the reader is referred to these references for the details. Numerous outcrop samples were collected by the writer for micropaleontological and palynological analysis to assist with regional mapping. Some of the principal results of this work are described below.
- C-24204 Twelve samples from Station 74-GAS-7 on Nelson River were processed for microfauna by C.A. Pollock and C.B. Mahadeo of Amoco Canada Petroleum Company Ltd. (*pers. com.*, 1975), with the following results:
- | Height above
base of
section
m (ft) | Fauna | GSC loc. |
|--|---|----------|
| 269 (882) | barren | C-30704 |
| 255 (837) | indet. foraminifera | C-30702 |
| 237 (778) | indet. foraminifera | C-30701 |
| 193 (633) | <i>Ammodiscus</i> sp.
<i>Haplophragmoides topagorukensis</i>
Tappan | C-30700 |

A comparison between the micropaleontological and palynological results shows that successively older stages are

173 (568)	<i>Pallaimorphina ruckerae</i> <i>Marginulinopsis jonesi</i> (Reuss) <i>Globulina lacrima canadensis</i> Mellon and Wall <i>Saracenaria spinosa</i> Eichenberg <i>Ammodiscus</i> sp. <i>Gavelinella stictata</i> Tappan	C-30699	70.5 (231)	foraminiferal assemblage: <i>Hippocrepina barksdalei</i> (Tappan) <i>Haplophragmoides</i> sp. cf. <i>H. sluzari</i> Mellon and Wall ?" <i>Tritaxia</i> " <i>athabascensis</i> Mellon and Wall – one small specimen <i>Quadriformina albertensis</i> Mellon and Wall – weathered specimens	C-30735
152 (499)	<i>Ammodiscus</i> sp. <i>Haplophragmoides topagorukensis</i> Tappan	C-30652	62.5 (205)	?" <i>Tritaxia</i> " <i>athabascensis</i> Mellon and Wall – fragment pyritized cylindrical objects	C-30734
130 (427)	as above, plus <i>Miliammina awunensis</i> Tappan	C-30697	65.5 (215)	agglutinated foraminifera: <i>Ammodiscus</i> sp. of Stelck and Wall, 1956 <i>Hippocrepina barksdalei</i> (Tappan) – one <i>Miliammina</i> sp. – one <i>Haplophragmoides gigas minor</i> Nauss <i>H.</i> sp. cf. <i>H. sluzari</i> Mellon and Wall ?" <i>Tritaxia</i> " <i>athabascensis</i> Mellon and Wall gastropod fragments (Recent appearance)	C-30733
115 (377)	<i>Haplophragmoides topagorukensis</i> Tappan	C-30696			
95.5 (313)	<i>Uvigerinammina manitobensis</i> (Wickenden) <i>Bathysiphon vitta</i> Nauss <i>Miliammina awunensis</i> Tappan <i>Haplophragmoides topagorukensis</i> Tappan <i>Tritaxia athabascensis</i> Mellon and Wall <i>Trochammina</i> sp.	C-30695			
80.5 (264)	<i>Pallaimorphina ruckerae</i> Tappan <i>Marginulinopsis jonesi</i> (Reuss) <i>Globulina lacrima canadensis</i> Mellon and Wall <i>G. prisca</i> Reuss <i>Saracenaria spinosa</i> Eichenberg <i>S. grandstandensis</i> Tappan <i>Vaginulina exilis</i> (Reuss)	C-30693	32 (105)	foraminiferal faunule: <i>Haplophragmoides</i> sp. cf. <i>H. sluzari</i> Mellon and Wall <i>Quinqueloculina</i> sp. – two <i>Saracenaria projectura</i> Stelck and Wall – one <i>Quadriformina albertensis</i> Mellon and Wall – one shell fragments (Recent appearance)	C-30731
72 (236)	barren	C-30686			
66.5 (218)	<i>Pallaimorphina ruckerae</i> Tappan <i>Globulina prisca</i> Reuss	C-30685			

Pollock and Mahadeo (*pers. com.*, 1975) stated that the faunas show several species in common with the *Verneuilinoides borealis* zone of the Topagoruk–Grandstand formations of Alaska and the Grand Rapids–Peace River formations of Alberta. An Albian age is indicated.

J.H. Wall (*pers. com.*, 1974) provided the following identifications of microfauna in Station 74-GAS-12 on Masik River:

Height above base of section m (ft)	Fauna	GSC loc.	
139 (456)	agglutinated foraminiferal faunule: <i>Glomospira subarctica</i> Chamney <i>Glomospirella scaphoides</i> (McGill and Loranger) <i>Haplophragmoides</i> sp. – two	C-30742	agglutinated foraminifera: <i>Glomospirella</i> sp. – large <i>Haplophragmoides</i> sp. cf. <i>H. topagorukensis</i> Tappan – very large form, common <i>Ammobaculites</i> sp. – wide coil ?" <i>Ammobaculites</i> sp. – uniserial portion of a very large form with prominent central aperture age: Cretaceous, probably Albian
105 (345)	agglutinated foraminiferal faunule: <i>Bathysiphon</i> sp. – one <i>Ammodiscus</i> sp. of Stelck and Wall, 1956 <i>Glomospirella</i> sp. <i>Miliammina</i> sp. – one	C-30738	Two samples from the Christopher Formation on lower Able Creek (GSC locs. C-30628, C-30629) yielded the following (combined) fauna: <i>Saracenaria dutroi</i> Tappan – one only <i>S. projectura</i> Stelck and Wall <i>S.</i> spp. <i>Dentalina</i> sp. – fragments <i>Globulina lacrima canadensis</i> Mellon and Wall <i>Pyruiloides thurrelli</i> Tappan <i>Quadriformina albertensis</i> Mellon and Wall – abundant <i>Ammodiscus</i> sp. <i>Haplophragmoides</i> sp. cf. <i>H. sluzari</i> Mellon and Wall <i>Verneuilinoides(?)</i> sp. – fragment age: Early to Middle Albian

Many similar faunal and floral assemblages were obtained from other outcrop samples collected in the report-area. All these confirm an Albian age for the Christopher Formation. As far as biostratigraphic precision permits intra-stage comparisons, it can be stated that the Christopher Formation of Banks Island is identical in age range with that of the Christopher Formation throughout Sverdrup Basin and also is virtually the same age as the Horton River Formation of Anderson Basin. Sliter (*in Barnes et al.*, 1974, p. 6) stated that foraminiferal assemblages in the Storkerson Bay A-15 well are similar to those in the Torok, Topagoruk and Grandstand formations of Alaska and the Clearwater, Joli Fou and Ashville formations of the Western Interior.

Hassel Formation

Definition, distribution and thickness

The formation was defined by Heywood (1955; 1957, p. 13) to consist mainly of a thick succession of sandstone occurring in the vicinity of Isachsen Dome, Ellef Ringnes Island. Stott (1969, p. 26) showed that the formation ranges from 90 to 550 m (300–1800 ft) thick in Ellef Ringnes Island, and is of Early to Late Cretaceous age. Work subsequent to that carried out in the original type area has shown that the unit is widespread throughout the Arctic Islands.

The Hassel Formation was not recognized on Banks Island by Thorsteinsson and Tozer (1962) because the critical exposures were not visited. Jutard and Plauchut (1973, p. 210) showed that the formation is present on lower Thomsen River, where it was estimated to be 50 m (165 ft) thick.

The present study has demonstrated that within Banks Island the Hassel Formation probably is confined to Northern Banks Basin (Fig. 12). In part, this may be the result of a lateral facies change into the Christopher Formation and in part it may be the result of pre-Kanguk erosion. The Hassel is considerably thinner in the report-area than in the Sverdrup Basin, and consists of a lithofacies that is only in the lower part of the formation in the type area (K.J. Roy, *pers. com.*, 1974). For this reason Miall (1975b) proposed earlier to assign this lithofacies to a new formation. However, difficulties in mapping the facies as a separate unit in the Ringnes Islands (H.R. Balkwill, *pers. com.*, 1975) indicate that such a reassignment is impractical at present.

The thickest section through the formation is located in a faulted inlier 7 km (4 mi) southeast of Cape Crozier. The Hassel is 48 m (158 ft) thick at this locality but thins to 20 m (65 ft) near Colquhoun River, 14 km (9 mi) to the southwest. On the east flank of Northern Banks Basin, the Hassel ranges from 21 m (69 ft) on the lower Thomsen River near Castel Bay, to a minimum of 30 m (98 ft) on a tributary of Muskox River (incomplete exposure). The Hassel Formation is absent in seven of the eight wells described in this report, and at Investigator Point and in southern Banks Island (*see* Fig. 12). At most of these localities the Kanguk Formation rests directly on the Christopher Formation, except at Ikkariktok M-64 and Tiritchik M-48, where the Kanguk rests directly on Devonian rocks.

Contacts

The contact of the Hassel with the Christopher Formation is invariably gradational, indicating a gradual facies change. The

contact between the Hassel and the Kanguk is abrupt and represents a disconformity. No angularity or evidence of deep erosion of the Hassel was observed at this disconformity.

Lithology

A complete section, from the overlying Kanguk Formation to the underlying Christopher Formation, is exposed southeast of Cape Crozier, at Station 74-MLA-44. The upper part of the Hassel is particularly well exposed at Station 74-MLA-104 near Muskox River (Pl. 10A). Appendix 3 gives detailed descriptions of these sections. Several other partial sections through the formation were measured on lower Thomsen River and on Muskox River.

The distinctive characteristics of the Hassel Formation include the following: greenish buff, glauconitic sands, low-angle planar crossbedding, small-scale ripple marks, and reddish brown or yellowish brown ironstone lenses and nodules containing ammonites and pelecypods. Some of these characteristics are illustrated in Plate 9. At Castel Bay C-68, in the centre of Northern Banks Basin, the formation includes a considerable proportion of interbedded shale.

Age and correlation

Two macrofossil collections from lower Thomsen River have been studied by J.A. Jeletzky (*pers. com.*, 1974). The assemblages are as follows:

GSC loc. C-26198

Neogastropiles n. sp. aff. *selwyni* McLearn
? *Granocardium* sp. indet.
indeterminate pelecypods

GSC loc. C-26200

Neogastropiles n. sp. aff. *selwyni* McLearn
Pecten (*Entolium*) sp. indet.
Arctica? sp. indet.
Astarte? (sensu lato) sp. indet.
Mya? (sensu lato) sp. indet.
indeterminate pelecypods and gastropods

Regarding these collections Jeletzky (*pers. com.*, 1974) stated that they probably represent the lower part of the *Neogastropiles* zone of the Western Interior region of Canada, corresponding to the *N. selwyni* (= *N. haasi*) subzone (Jeletzky, 1968, p. 19–23; 1971, p. 47). A Late Albian age is indicated.

Two samples from the Christopher-Hassel transition beds at Station 74-MLA-44 near Cape Crozier were processed for palynomorphs by W.S. Hopkins, Jr., A.R. Sweet and W.W. Brideaux. A small macrofossil collection also was made (GSC locs. C-26388, C-30551, C-30552):

microspores:

Cingulatisporites sp.
Sphagnum antiquasporites Wilson and Webster
S. regium Drozhastchich
Cicatricosisporites sp.
Baculatisporites sp.
Gleicheniidites senonicus Ross
Lycopodiacidites sp.
Laevigatosporites sp.
Osmundacidites sp.
Sestrosporites pseudoalveolatus (Couper) Dettmann
Tsuga sp.
Glyptostrobus
Taxodiaceae

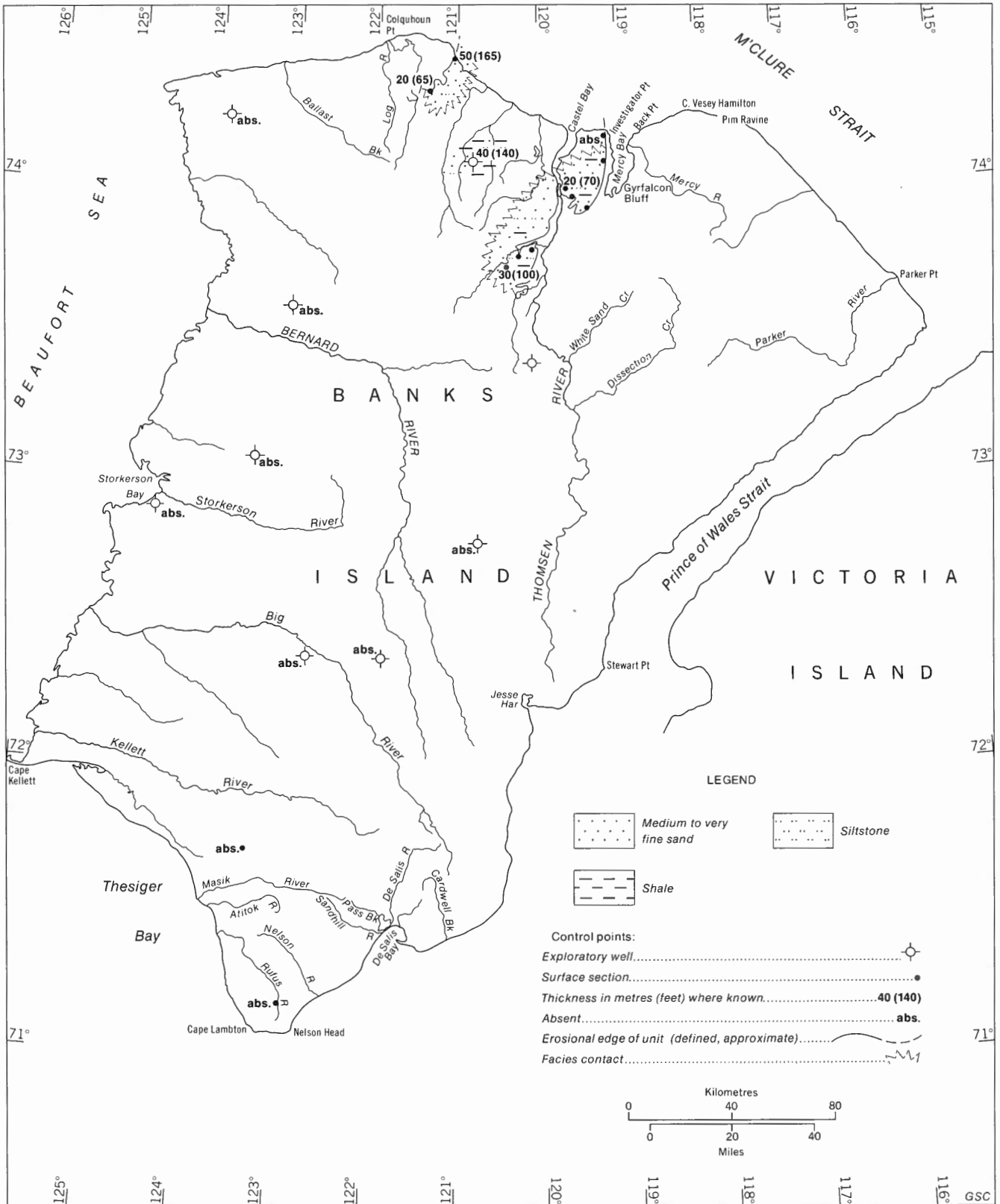


Figure 12. Hassel Formation: distribution, thickness and lithologies. Thicknesses are rounded off for convenience.

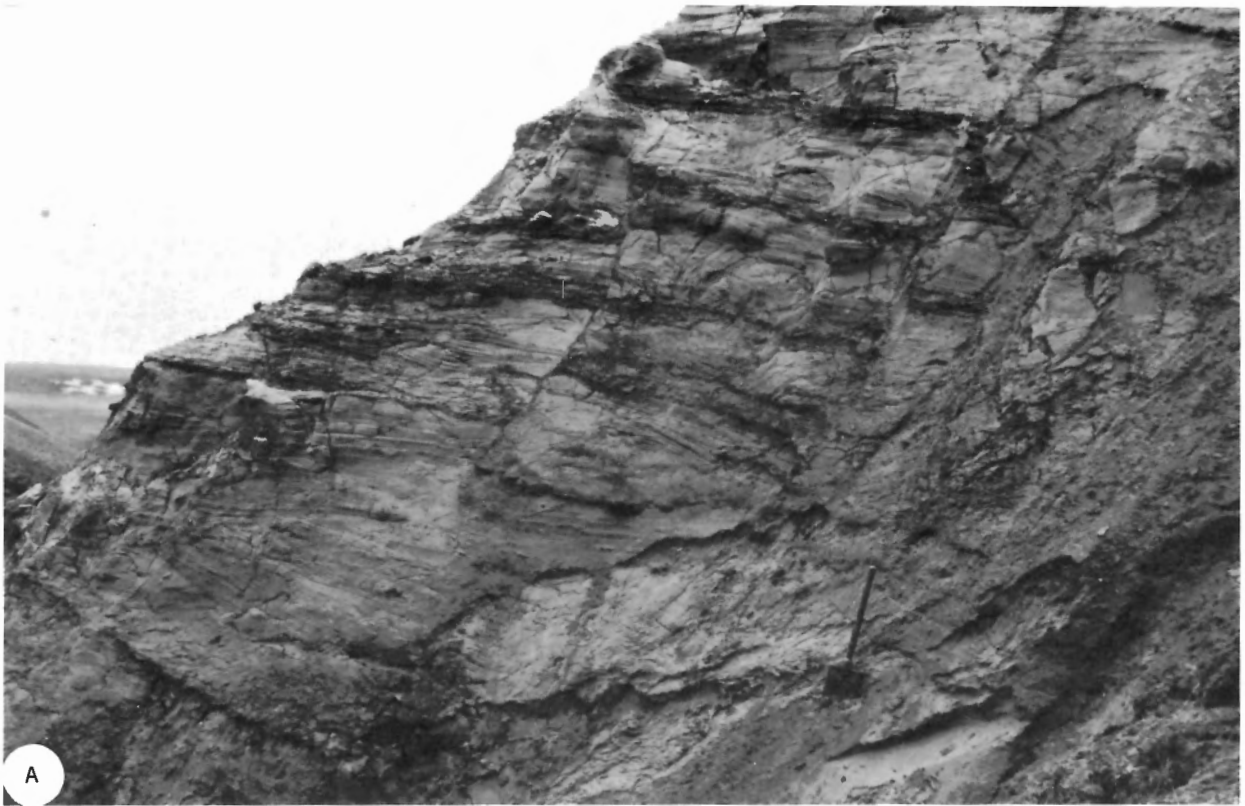


Plate 9. The Hassel Formation. A: At Able Creek (near Station 73-MLA-24), showing sand with abundant low-angle planar crossbedding. Shovel handle is 50 cm long. GSC 199200. B: Pelecypod shell bed at Muskox River (Station 74-MLA-119). GSC 199204.

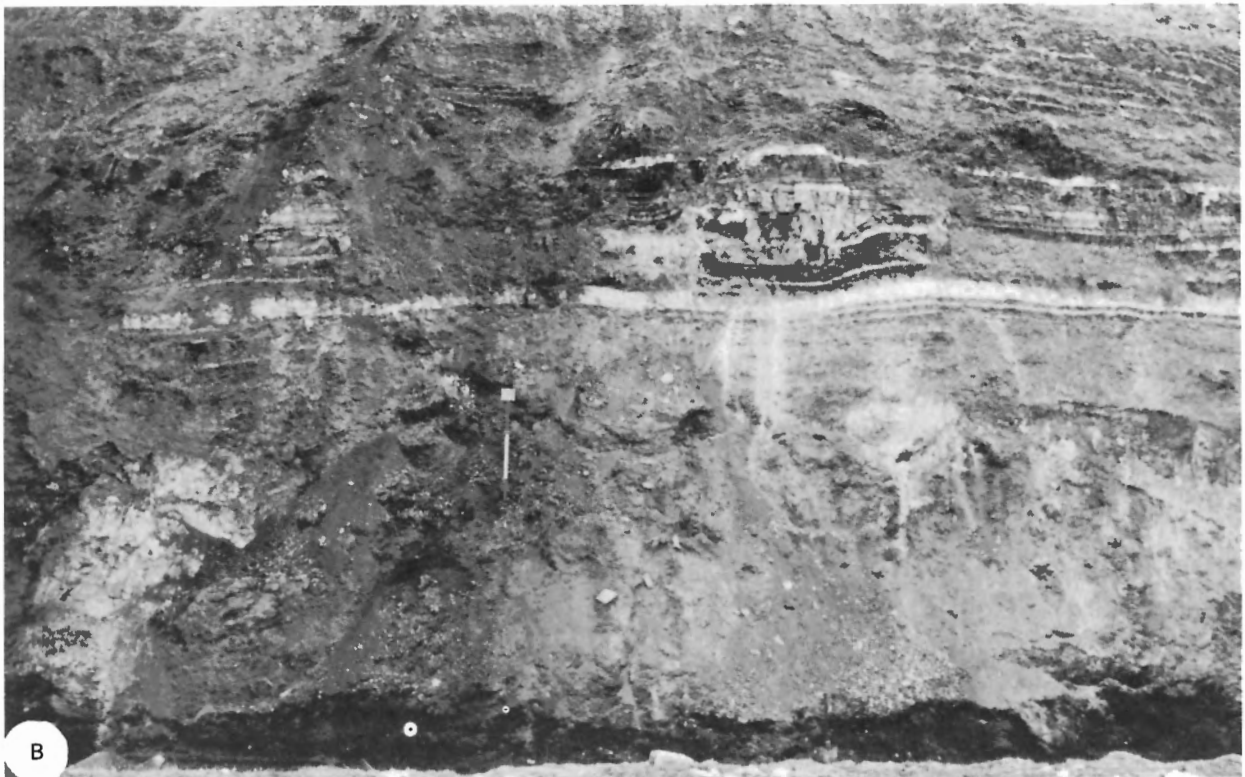
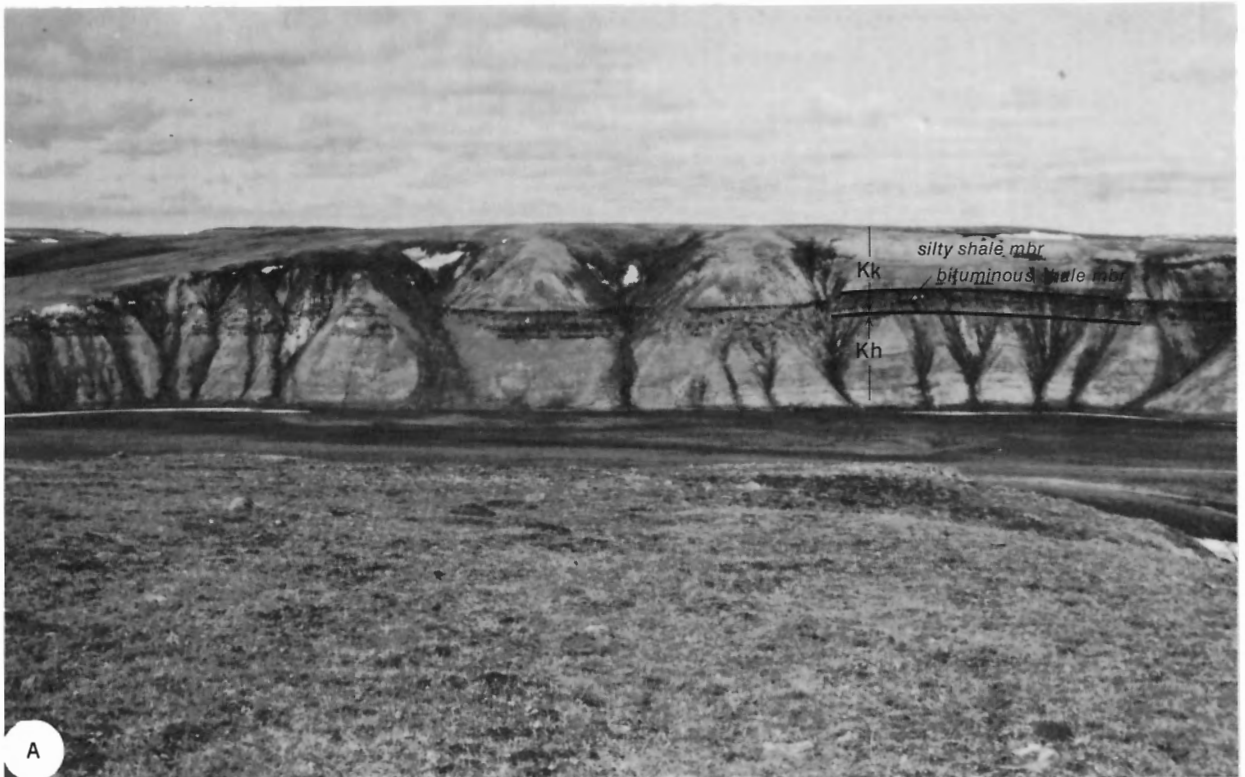


Plate 10. The basal Kanguk Formation (Kk). A: The basal Kanguk bituminous shale, 4.2 m (13.8 ft) thick, is overlain by recessive silty shale and underlain by silty sand of the Hassel Formation (Kh), Muskox River (Station 74-MLA-104). GSC 199203. B: Tuffaceous and bentonitic beds (white) in the basal Kanguk shale at upper Sachs River (Station 74-MLA-28). Measuring rod subdivisions are 50 cm. GSC 199194.

megaspores:

Balmeisporites holodictyus Cookson and Dettmann
Arcellites disciformis Miner
A. incipiens Singh
Echitriletes sp.
Dijkstraisporites sp.
Minerisporites venustus Singh
M. macroreticulatus Singh
M. cf. M. marginatus (Dijkstra) Potonié
Erlansonisporites spp.
Maexisporites sp.
Spermatites cf. *S. ellipticus* Miner

dinoflagellates: numerous forms, including

Luscadinium propatulum

macrofauna:

Gastropoditid
 cf. n. sp. aff. *G. spiekeri* McLearn or
Neogastropodites cf. n. sp. aff. *selwyni* McLearn
Arctica (sensu lato) sp. indet.
Pleuromya sp. indet.
 indet. pelecypods
 serpulid worm tubes

Only the most diagnostic palynomorphs are listed above. Together the collections indicate a Middle to Late Albian age (Hopkins, *pers. com.*, 1974; Sweet, *pers. com.*, 1974; Brideaux, *pers. com.*, 1975; Jeletzky, *pers. com.*, 1976).

Hopkins and Balkwill (1973, p. 6) assigned an Albian or Cenomanian age to the Hassel Formation of Ellef Ringnes Island. Later work by Balkwill (*pers. com.*, 1975) indicated that the Albian and Cenomanian are both represented and that the Hassel is followed conformably by the Kanguk Formation (Cenomanian to Maastrichtian) throughout much of the Sverdrup Basin. The Hassel of Banks Island compares lithologically with the lower part of the Hassel of the Sverdrup Basin and the younger part of the formation apparently is absent in the report-area, for no indications of a Cenomanian or younger age have been obtained and the basal Kanguk beds are probably Campanian.

The Late Albian to Coniacian time interval is represented by an unconformity in Anderson Basin (Yorath *et al.*, 1975).

Upper Cretaceous***Kanguk Formation****Definition, distribution and thickness*

The Kanguk Formation was defined by Souther (1963, p. 442–444) and based on exposures in the Kanguk Peninsula area of Axel Heiberg Island. In the type area the Kanguk consists of silty shale with minor amounts of sandstone, and contains bentonitic and tuffaceous beds in the lower part of the formation. The thickness ranges from 251 to 365 m (825–1200 ft) and the age from Santonian to early Campanian. The Kanguk has been mapped throughout the Arctic Islands, including Graham Island (Greiner, 1963), Ellef Ringnes Island (Stott, 1969) and Melville Island (Tozer and Thorsteinsson, 1964), but was not recognized on Banks Island until the work of Jutard and Plauchut (1973). On Banks Island, Thorsteinsson and Tozer (1962, p. 65–69) mapped a unit of light grey

shale and fine-grained sandstone 120 m (400 ft) thick, to which they assigned a Cretaceous, possibly Late Cretaceous, age on the basis of limited palynological evidence. This unit was included in the Eureka Sound Formation as the middle of three members. The lower member was estimated to be 8 m (25 ft) thick and comprised sandstone, carbonaceous shale and coal. Locally the beds of the lower member are oxidized to a distinctive red, and Thorsteinsson and Tozer (1962, p. 66) suggested a tentative correlation with similar beds on the southwestern shore of Franklin Bay, which were known to be prone to spontaneous combustion. That area has been named the Smoking Hills because of this local phenomenon.

Jutard and Plauchut (1973) reassigned the lower member and the lower part of the middle member of the Eureka Sound Formation to the Kanguk Formation and confirmed the correlation between the basal unit and the carbonaceous beds of the Smoking Hills area. These correlations are followed in the present report (Table 2).

The Kanguk Formation is present throughout Banks Island, except where it has been removed by erosion in the northeastern and southern parts of the island. It is believed also to be absent over part or all of Storkerson Uplift, as shown in Figure 13. The formation ranges in thickness from 270 m (885 ft) in Big River Basin (Storkerson Bay A-15 well) to 463 m (1520 ft) in Northern Banks Basin (Castel Bay C-68 well). Exposures of the formation near Cape Crozier are poor but graphic reconstruction suggests a much thinner section in this area totalling approximately 90 m (300 ft). The Kanguk is probably of comparable thickness in the Masik River area of southern Banks Island but accurate estimates are, again, difficult to obtain because the exposures are incomplete.

Contacts

The base of the Kanguk Formation marks a disconformity. It is abrupt and unmistakable in the field (Pl. 10A) owing to the distinctive rock types in the basal member of the formation. The upper contact of the Kanguk with the Eureka Sound Formation is conformable, partly gradational, and diachronous. Both on the surface and in the subsurface this contact is difficult to recognize. In Banks Basin it is drawn at the top of a thin, quartzose sand unit but the beds above and below the sand are similar lithologically and, where the sand is not exposed, biostratigraphic information is required for its recognition. In the subsurface the sand unit is poorly expressed on geophysical logs and may be missed easily in the cuttings.

In Big River Basin the single sand unit at the top of the Kanguk is absent. The formation grades almost imperceptibly up into the basal Eureka Sound Formation, which consists of shale with interbedded sand and coal. The contact is drawn arbitrarily at the lower limit of sand or coal beds, whichever is the older.

Lithology

The Kanguk Formation is subdivided in this report into a maximum of five members (Table 2):

Upper sand member
 Silty shale member (upper part)
 Lower sand member
 Silty shale member (lower part)
 Bituminous shale member

Table 2. Nomenclature changes in the Upper Cretaceous and Paleogene rocks of Banks Island

PERIOD	SERIES AND STAGE	THORSTEINSSON AND TOZER, 1962	JUTARD AND PLAUCHUT, 1973 (Northern Banks Island)	MIALL, 1974a, c (Western Banks Island, subsurface)	THIS REPORT			
PALEOGENE	EOCENE	EUREKA SOUND FORMATION	EUREKA SOUND FORMATION	EUREKA SOUND FORMATION	EUREKA SOUND FORMATION			
						Upper Member	Sand-shale Member	Cyclic Member
						Middle Member	Shale-coal Member	Shale Member
	PALEOCENE		Lower Member					
UPPER CRETACEOUS	MAASTRICHTIAN	Middle Member	Sand Unit	KANGUK FORMATION	Upper Sand Member			
			Shale Member		Silty Shale Member			
	CAMPANIAN		Bituminous Member		Sandstone Member	Lower Sand Member		
		Lower Member				Bituminous Shale Mbr		
	SANTONIAN							
	CONIACIAN							
	TURONIAN							
	CENOMANIAN							

Note: Time lines are shown dashed where they were not precisely known

GSC

The lower sand member is known at present in only three subsurface sections; elsewhere within the report-area the silty shale member is not subdivided. The silty shale and bituminous shale members are shown unsubdivided in Table 1. The bituminous shale is too thin to be shown separately on the geological maps; it is found at all exposures of the basal Kanguk that were visited during the present study. The upper sand member has been mapped in the Antler Cove area. It probably is present also to the east and south of Castel Bay but has not been shown separately on the geological map. The members are described below in ascending stratigraphic order.

The bituminous shale member is a distinctive and readily recognizable unit even from the air. It consists predominantly of dark grey to black, laminated, bituminous shale which, when weathered, may be split readily into thin, almost papery fragments along the bedding planes. Ellipsoidal mudstone concretions up to 1 m (3.3 ft) in long diameter commonly are present and gypsum crystals commonly are scattered along bedding planes. A typical outcrop of this unit is shown in Plate 10A. On continued exposure to the air the shale oxidizes to a bright red and becomes blocky, weathering with cindery streaks. Another typical characteristic of this member is the thin beds of bentonitic clay (see Chap. 3 for clay mineral analyses). At least two beds 5 cm (2 in.) or more in thickness generally are present but, at one locality in southern Banks

Island (GSC loc. C-30528) numerous bentonite layers were observed and several beds of vitric tuff up to 20 cm (8 in.) in thickness also are present, as shown in Plate 10B. Siltstone beds interbedded with the tuff contain numerous volcanic shards and abundant radiolarian remains. Other fossil types are extremely rare in the bituminous shale member. At Station 74-MLA-104 concretions contain flattened *Inoceramus* shells and the plates and vertebrae of three species of fish.

Another rock type found commonly, but not exclusively, in the basal Kanguk beds consists of a silty dolomite with abundant manganese in the form of carbonate (rhodochrosite, $MnCO_3$) or amorphous oxide and characterized by a distinctive spherulitic texture. A detailed description of this lithology as it occurs in the Storkerson Bay A-15, Nanuk D-76 and Uminmak H-07 wells has been provided by the author (Miall, 1974d). The spherulites have been found also in the same stratigraphic position at the base of the Kanguk, in the Orksut I-44 well (Miall, 1975c) and in one outcrop section 4 km (2.5 mi) south of Investigator Point. Further descriptions and illustrations of this unusual rock type are included in Chapter 3.

The thickness of the bituminous shale member is variable. Near Cape Crozier at Station 74-MLA-44, the unit is 2 m (6.6 ft) thick. At Muskox River, Station 74-MLA-104, it is 4.2 m (13.8 ft) thick, as described above, and on Able Creek it reaches 12.5 m (41.0 ft). Bentonite-bearing shale is 7.5 m (24.6

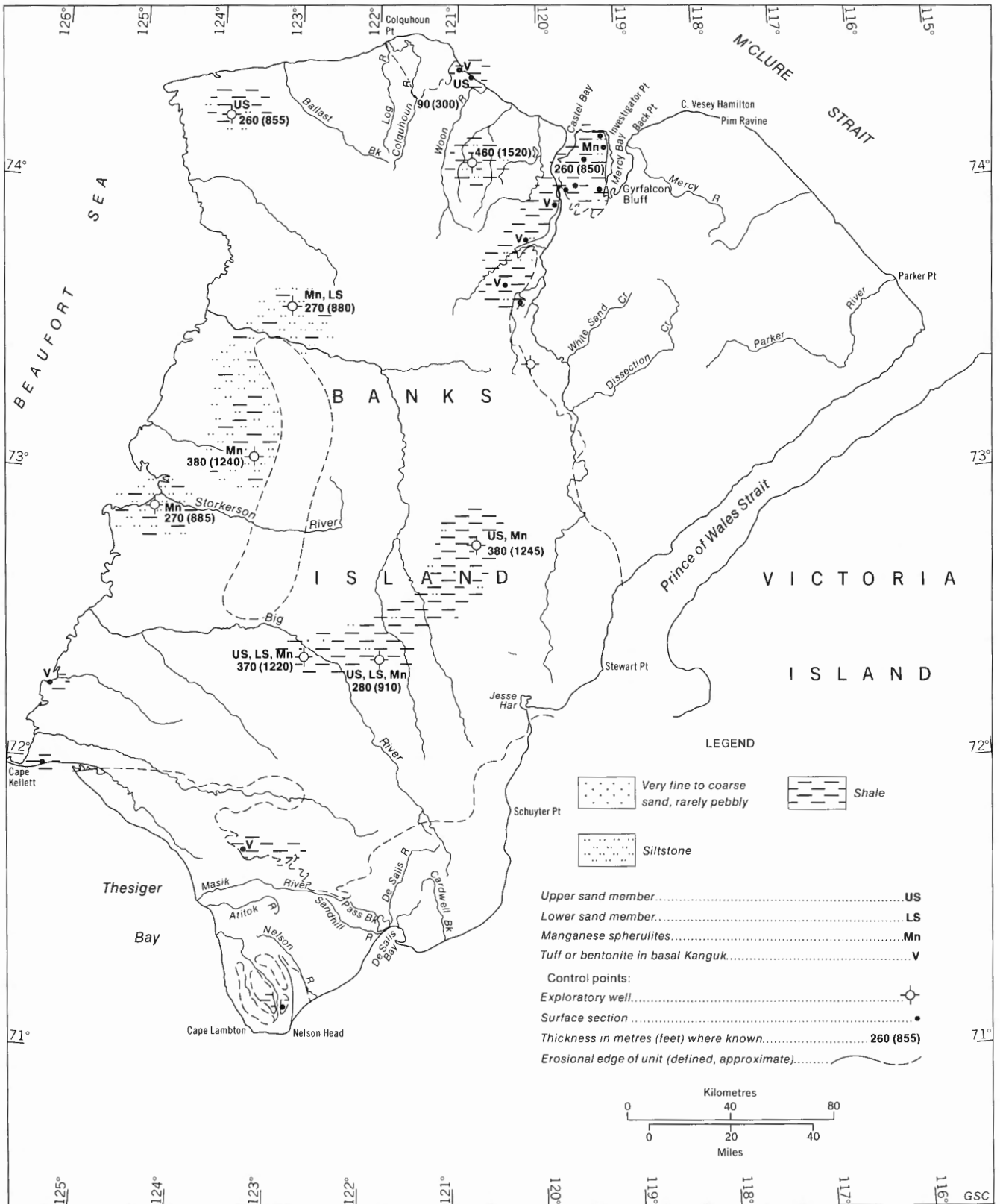


Figure 13. Kanguk Formation: distribution, thickness and lithologies. Thicknesses are rounded off for convenience.

ft) thick near Masik River but the base of the unit is not exposed. Sections through the bituminous shale member are thickest near Investigator Point, where several measurements indicate a range of 13 to 15.2 m (42.7–49.9 ft). The member also is present in the subsurface. It can be recognized by the bentonitic character of shale cuttings from the basal Kanguk and, in some cases, by a distinctive geophysical log response. The radioactive content of the shale causes very large gamma ray deflections in three of the Banks Island wells, Storkerson Bay A-15, Bar Harbour E-76 and Castel Bay C-68. This log response is very characteristic of the member in Tuktoyaktuk Peninsula (Myhr, 1975).

The best exposures of the silty shale member are in the vicinity of Muskox River, and the peninsula between Mercy Bay and Castel Bay. Typical views of these exposures are shown in Plate 11. The member consists predominantly of pale to dark grey, variably micaceous, variably silty shale. Small concretions of dolomite and siderite are abundant and jarosite(?) crystals are scattered along bedding plates. Rare beds of pebbly sand are up to 2.5 m (8.2 ft) thick. The pebbles consist of quartz and chert, are subrounded to well rounded and reach 2 cm (0.8 in.) in diameter. In a few localities these arenaceous beds are lithified with a predominantly clay mineral matrix. Some of the sand and sandstone beds and many of the siltier shale intervals contain abundant siliceous sponge spicules. Reptile bones are present at a few localities.

No complete surface sections through the silty shale member are available. A section on the west side of Thomsen River (Station 74-GAS-21) is the most complete, and is described in Appendix 3. Three other partial sections through the silty shale member, at Station 74-MLA-93 southeast of Castel Bay, and Stations 74-MLA-114 and 73-MLA-42 near Muskox River, also are described in Appendix 3.

Very similar lithologies are displayed in subsurface sections through the silty shale member within Banks Basin, namely in the Castel Bay C-68, Orksut I-44, Ikkariktok M-64 and Tiritchik M-48 wells. At Ikkariktok and Tiritchik, manganese spherulites were recovered from cuttings taken near the top of the formation.

On the flanks of Storkerson Uplift (Nanuk D-76 and Uminmak H-07 wells) and in Big River Basin (Storkerson Bay A-15 well), the Kanguk Formation is generally somewhat more coarse grained, consisting of argillaceous siltstone with lesser amounts of silty shale. Cone-in-cone limestone and siderite concretions are common, except in the Uminmak well. Plant fragments and sponge spicules are present and locally abundant. Appendix 2 gives complete descriptions of these well sections and Figure 8 includes graphic logs.

The lower sand member has been identified in the Uminmak H-07, Ikkariktok M-64 and Orksut I-44 wells, where it is 36, 30 and 29 m (117, 100 and 96 ft) thick, respectively. At Uminmak the member consists of an upward-coarsening succession, comprising interbedded sandstone and shale at the base grading up into coarse-grained to pebbly sandstone at the top. The sandstone is quartzose throughout, poorly cemented, and contains pebbles of quartz, chert and, rarely, silicified oolite up to 1.2 cm (0.5 in.) in diameter. Glauconite grains are rare. A similar, upward-coarsening succession constitutes this member in the Orksut I-44 well, except that the maximum grain size is coarse-grained sand. A

core through part of the interval shows that sandstone and shale are interbedded on a millimetre scale. The sandstone contains scattered muscovite flakes and glauconite grains, abundant small flasers of carbonaceous shale containing comminuted plant debris, and abundant bioturbation. The lower sand member also is exposed near the southwestern corner of Mercy Bay, where it comprises medium-grained sand with large-scale planar crossbedding.

The upper sand member of the Kanguk is well exposed in the vicinity of Antler Cove in northern Banks Island. The predominant rock type is unconsolidated fine- to medium-grained sand, which is pale grey or buff. Pebble beds containing pebbles up to 6 cm (2.4 in.) set in an iron-stained sandstone matrix, are rare. The pebbles consist of grey and, rarely, red and green chert, quartzose sandstone and coral fragments, which E.W. Bamber (*pers. com.*, 1973) has identified as Early Permian in age (*see* section on petrographic analysis of the sand members for a discussion of these coral fragments). Dark grey, carbonaceous shale lenticles and concretions of ironstone containing wood fragments are common and rare pelecypods also have been observed. Sedimentary structures are numerous, including large-scale trough and planar crossbedding and small-scale asymmetrical and near-symmetrical ripple marks. Plate 12A illustrates a typical exposure in this unit. Complete exposures through the member are not available; the greatest thickness measured at any one locality was 12 m (39 ft) at an exposure near the sea, 3 km (1.9 mi) southeast of Antler Cove.

In the subsurface the upper sand member ranges from 11 m (35 ft) thick at Tiritchik M-48, to 21 m (70 ft) at Ikkariktok M-64. Rock types range from micaceous, argillaceous siltstone to very fine grained sandstone. Plant debris is locally abundant.

Age and correlation

Macrofossils are not common in the Kanguk Formation, and those present generally are not diagnostic of age. A collection made in the upper sand member at GSC loc. C-26195 contains the following forms (J. A. Jeletzky, *pers. com.*, 1974):

?*Psilomya* sp. indet.

Donax-like marine pelecypods

age: unknown

Jutard and Plauchut (1973, p. 212) collected plesiosaur remains in the middle part of the silty shale member and D. A. Russell (*in* Jutard and Plauchut, *ibid.*) collected plesiosaur and mosasaur bones from a locality 15 m (49 ft) below the top of the member. They were assigned a Late Cretaceous age (*ibid.*). J.A. Jeletzky (*pers. com.*, 1976) reported the occurrence of *Inoceramus* cf. *I. pictus* Sowerby in two of the writer's collections (GSC locs. C-30771, C-30783) and assigns the collections a Cenomanian or Turonian age, but this does not agree with microfossil determinations, as noted below. Fish remains from the basal Kanguk at Station 74-MLA-104 (Muskox River) have been identified as follows (M.V.H. Wilson, *pers. com.*, 1976):

Ichthyodectes ctenodon Cope

"*Holcolepis*" *transversus* Cockerell

cf. *Leucichthyops* Cockerell

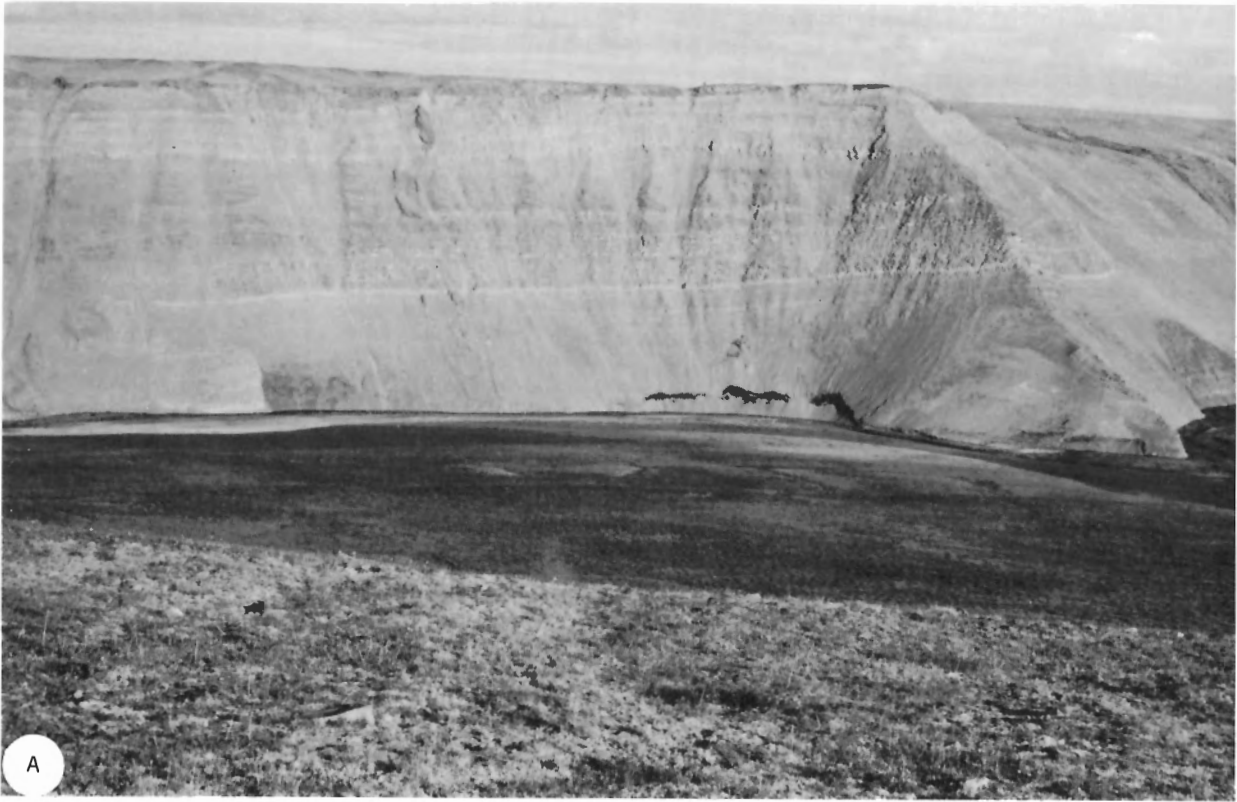


Plate 11. Silty shale member of the Kanguk Formation. A: Very characteristic outcrop 42 m (138 ft) high of pale grey shale, near Thomsen River (Station 73-MLA-22). GSC 199171. B: Shale with sandy and pebbly laminae, near Muskox River (Station 73-MLA-42). Outcrop is 54 m (178 ft) high. GSC 199159.

An Albian to Cenomanian age is indicated but Wilson states that an extension of the age range into the Campanian or Maastrichtian would not be surprising.

More satisfactory results have been obtained using micropaleontology and palynology. Detailed results from the study of the subsurface sections and some key age assignments from surface outcrops are listed or referred to below. Most of the faunal and floral assemblages are of Campanian (probably late Campanian) and Maastrichtian ages but the evidence from Big River Basin indicates that the base of the Kanguk there may be early Late Cretaceous (Turonian to Santonian) in age.

Micropaleontology of the Kanguk Formation in the Storkerson Bay A-15 well by Sliter (*in Barnes et al.*, 1974):

Depth m (ft)	Fauna	GSC loc.
1097-1128 (3600-3700)	<i>Haplophragmoides</i> sp. <i>Hyperamminoides</i> sp. pyritized wood age: Cretaceous(?)	C-24426
1128-1158 (3700-3800)	pyritized wood age: Cretaceous(?)	C-24427
1158-1189 (3800-3900)	<i>Haplophragmoides rota</i> Nauss <i>Bathysiphon vitta</i> Nauss pelecypod fragments age: late Cretaceous, Campanian	C-24428
1189-1219 (3900-4000)	<i>Haplophragmoides rota</i> Nauss <i>Bathysiphon vitta</i> Nauss <i>Ammodiscus crataceus</i> (Reuss) <i>Quinqueloculina</i> sp. cf. <i>Q. sphaera</i> Nauss age: Late Cretaceous, Campanian	C-24429
1219-1250 (4000-4100)	<i>Quinqueloculina</i> sp. cf. <i>Q. sphaera</i> Nauss <i>Vaginulina schraderensis</i> Tappan <i>Globorotalites</i> sp. cf. <i>G. alaskensis</i> Tappan <i>Haplophragmoides rota</i> Nauss <i>Bathysiphon vitta</i> Nauss <i>Saccamina lathrami</i> Tappan <i>Ammodiscus</i> sp. age: Late Cretaceous, Campanian/Turonian	C-24430
1250-1280 (4100-4200)	<i>Haplophragmoides rota</i> Nauss <i>H. bonanzaensis</i> Stelck and Wall <i>Ammodiscus cretaceus</i> (Reuss) <i>Saccamina lathrami</i> Tappan pelecypod fragments age: Late Cretaceous, Turonian	C-24431
1280-1316 (4200-4300)	<i>Marginulina</i> sp. <i>Haplophragmoides rota</i> Nauss <i>H. bonanzaensis</i> Stelck and Wall <i>Hyperamminoides</i> sp. cf. <i>H. barksdalei</i> Tappan age: Late Cretaceous, Turonian	C-24432
1316-1341 (4300-4400)	<i>Haplophragmoides rota</i> Nauss <i>H. bonanzaensis</i> Stelck and Wall <i>Ammodiscus</i> sp. age: Late Cretaceous, Turonian	C-24433

1341-1371 (4400-4500)	<i>Haplophragmoides topagorukensis</i> Tappan <i>Bathysiphon vitta</i> Nauss <i>Ammodiscus mangusi</i> (Tappan) <i>A. rotalarius</i> Loeblich and Tappan charaphytes age: Albian, Middle to Late	C-24434
--------------------------	--	---------

The sample from GSC loc. C-24434 included the topmost 9 m (29 ft) of the Christopher Formation. Sliter commented (*ibid.*, p. 6):

Between 3800 and 4000 feet, a distinctive Campanian *Haplophragmoides-Ammodiscus* fauna occurs, equivalent to that in the Schrader Bluff Formation of Alaska and the Belly River Group of Alberta. From 4000 to 4400 feet the calcareous and agglutinated species indicate correlation with Turonian sections in Alaska and Alberta.

Palynology of the Kanguk in the Storkerson Bay A-15 well by Hopkins (*ibid.*):

Depth m (ft)	Flora	GSC loc.
1097-1128 (3600-3700)	<i>Ulmus</i> sp. <i>Carya</i> sp. <i>Paraalnipollenites confusus</i> Hills and Wallace <i>Alnus</i> sp.	C-24187
1128-1158 (3700-3800)	as above plus: <i>Wodehouseia spinata</i> Stanley <i>Pistillipollenites macgregorii</i> Rouse	C-24188
1158-1189 (3800-3900)	<i>Carya</i> sp. <i>Paraalnipollenites confusus</i> Hills and Wallace <i>Alnus</i> sp. <i>Aquilapollenites</i> sp. (reticulate)	C-24189
1189-1219 (3900-4000)	<i>Ulmus</i> sp. <i>Carya</i> sp. <i>Paraalnipollenites confusus</i> Hills and Wallace <i>Alnus</i> sp. cf. Proteaceae <i>Cicatricosisporites</i> sp.	C-24190
1219-1250 (4000-4100)	<i>Paraalnipollenites confusus</i> Hills and Wallace <i>Alnus</i> sp. cf. Proteaceae	C-24191
1250-1280 (4100-4200)	<i>Paraalnipollenites confusus</i> Hills and Wallace <i>Alnus</i> sp.	C-24192
1280-1316 (4200-4300)	<i>Ulmus</i> sp. <i>Paraalnipollenites confusus</i> Hills and Wallace <i>Alnus</i> sp. <i>Cicatricosisporites</i> sp. <i>Baculatisporites</i> sp.	C-24193
1316-1341 (4300-4400)	<i>Paraalnipollenites confusus</i> Hills and Wallace <i>Baculatisporites</i> sp.	C-24194

1341–1371	<i>Ulmus</i> sp.	C-24195	74 m (243 ft) above base of Kanguk Formation at GSC loc. C-26391, lower Thomsen River:
(4400–4500)	<i>Carya</i> sp.		<i>Laevigatosporites</i> sp.
	<i>Paraalnipollenites confusus</i> Hills and Wallace		<i>Cyathidites</i> sp.
	<i>Baculatisporites</i> sp.		<i>Baculatisporites</i> sp.
	<i>Aquilapollenites</i> sp. (spinulos)		<i>Lycopodiacidites</i> sp.

Hopkins assigned a Maastrichtian age to all these assemblages, but the Campanian is represented in the microflora recovery by assemblages in (caved?) cuttings from the 1432 to 1524 m (4700–5000 ft) interval, which has been assigned to the Christopher Formation on the basis of other evidence. No early Late Cretaceous palynomorphs were identified from the Storkerson Bay A-15 well.

Additional faunal lists and age determinations for the Banks Island wells are available as follows: Nanuk D-76 micropaleontology by Chamney (*in Brideaux et al.*, 1975); Uminmak H-07 micropaleontology by Sliter (*unpubl.* GSC report), palynology by Hopkins (*unpubl.* GSC report); Orksut I-44 micropaleontology by Wall (*in Brideaux et al.*, 1976), palynology by Hopkins (*in Brideaux et al.*, 1975); Tiritchik M-48 micropaleontology by Wall and Clowser (*in Brideaux et al.*, 1976); Ikkariktok M-64 micropaleontology by Wall (*ibid.*).

Microfossil recoveries from surface samples were generally poor. Four samples from Station 74-GAS-21 were processed by J.H. Wall (*pers. com.*, 1974) with the following results:

Height above base of section m (ft)	Fauna	GSC loc.
120 (393.7)	barren	C-30774
80 (262.5)	? <i>Hippocrepina</i> sp. <i>Haplophragmoides</i> sp. cf. <i>H. howardense</i> Stelck and Wall ? <i>Ammomarginulina</i> sp. age: Cretaceous, probably Late	C-30773
49.5 (162.4)	? <i>Haplophragmoides</i> sp., poorly preserved age: unknown	C-30772
11 (36.1)	siliceous sponge spicules	C-30770

A sample from the basal, bentonitic and tuffaceous sediments near Masik River yielded the following microfauna (J.H. Wall, *pers. com.*, 1974; GSC loc. C-30528):

radiolarian faunule:
Spongodiscus (*Spongodiscus*) sp.
Cenosphaera (*Cenosphaera*) sp.
Dictyomitra (*Dictyomitra*) *multicostata* Zittel
nasselarian segments
questionable discoidal form with pore
age: Late Cretaceous

Palynological recoveries were generally more satisfactory. A few typical assemblages are listed below, all of which were assigned a Maastrichtian age by W.S. Hopkins, Jr. (*pers. com.*, 1974):

Lycopodium sp.
Cicatricosisporites sp.
Sphagnum antiquasporites sp.
cf. Taxodiaceae
Aquilapollenites sp.
Orbiculapollis sp.
cf. *Cranwellia* sp.
Expressipollis sp.
Tripoporollenites sp.
a few rare and poorly preserved phytoplankton

2 m (6.6 ft) above base of Kanguk Formation at GSC loc. C-26390, lower Thomsen River:

Lycopodiacidites sp.
Sphagnum antiquasporites Wilson and Webster
Sphagnum regium Drozhastchich
Cingulatisporites sp.
Cicatricosisporites sp.
Osmundacidites sp.
cf. *Metasequoia* sp.
Aquilapollenites sp.
Fibulapollis sp.
Expressipollis sp.
cf. *Kurtzipites* sp.
Tricolpites sp.

In summary, the Kanguk Formation of Banks Island is herein assigned a Campanian to Maastrichtian age range, except within Big River Basin where microforaminiferal evidence suggests that the base of the formation is as old as Turonian. Similar results were obtained by the work of Jutard and Plauchut (1973, p. 211, 212), who also stated that the upper sand member contains marine dinoflagellates that are known in Danian strata in northern Europe. The Cenomanian-Turonian age of the two *Inoceramus* collections from northeastern Banks Island is of uncertain significance at this time.

In the Ringnes Islands in the centre of Sverdrup Basin, the Kanguk conformably overlies the Hassel Formation and ranges in age from Cenomanian to Maastrichtian (H.R. Balkwill, *pers. com.*, 1975), as shown in Table 1. Very similar rock types are present in Sverdrup Basin, including the red-weathering shale and thin beds of bentonite, as described by Greiner (1963, p. 411, 412; Graham Island), Souther (1963, p. 443; Axel Heiberg Island), and Stott (1969, p. 27; Ellef Ringnes Island). Map-units 26 and 27 on Eglinton Island (Tozer and Thorsteinsson, 1964, p. 164, 165) also are considered to represent a lithologically similar extension of the Kanguk Formation. They contain several manganese-bearing beds.

Lithologically and biostratigraphically, the Kanguk Formation also is correlated with rocks occurring on the Arctic mainland south of Banks Island (Table 1). The bituminous shale member is correlated with a much thicker "Bituminous Zone" and the silty shale member with a "Pale Shale Zone" in the Anderson Basin area (Yorath *et al.*, 1969). These units

now have been named the Smoking Hills and Mason River formations, respectively (Yorath *et al.*, 1975). Myhr (1975) recognized the same formations in the subsurface of Tuktoyaktuk Peninsula and Chamney (1971, 1973) has described faunal assemblages similar to the Kanguk from the same area. The base of the Smoking Hills Formation is marked by a prominent radioactive horizon in Tuktoyaktuk Peninsula; it is referred to as the "E" marker by Myhr (1975). In Banks Island the Storkerson Bay, Bar Harbour and Castel Bay wells are the only subsurface sections in which the same marker can be recognized (Fig. 8).

In northern Yukon the bituminous shale and silty shale members of the Kanguk are correlated with the Boundary Creek and Tent Island formations (Young, 1975). The characteristic bituminous shale also persists into northern Alaska where it composes the upper part of the Ignek Formation (Keller *et al.*, 1961, p. 206; this formation name has now been abandoned) and the Seabee Formation (Detterman *et al.*, 1975, p. 32).

Upper Cretaceous and Paleogene

Eureka Sound Formation

Definition, distribution and thickness

The name Eureka Sound Group was first proposed by Troelsen (1950, p. 78) for a widespread unit of sandstone, shale and lignitic coal in central Ellesmere Island and Axel Heiberg Island, which he believed to postdate the last orogeny in the area. Tozer (1963a, p. 92–95) pointed out that Troelsen had not established any formations within the Eureka Sound and had not designated a type area or a type section. Tozer redefined the unit as a formation and stated, "it seems reasonable to regard the outcrops on Fosheim Peninsula, adjacent to Eureka Sound, as typical." Tozer also quoted earlier work (Thorsteinsson and Tozer, 1957) which showed that in western Fosheim Peninsula the Eureka Sound represents the highest formation in a structurally conformable, folded sequence of rocks ranging in age from Permian to Tertiary. The formation is known now to be present throughout the Arctic Islands, from northeastern Ellesmere Island to Banks Island. At most localities the Eureka Sound has been assigned an Early Tertiary and possibly a Late Cretaceous age.

The Eureka Sound strata of Banks Island were described first by Thorsteinsson and Tozer (1962, p. 65–69), who divided the formation into three members. The later work of Jutard and Plauchut (1973) showed that the lower member and part of the middle member were of Late Cretaceous age, and they reassigned these beds to the Kanguk Formation. They redefined the Eureka Sound Formation of Banks Island to include the upper part of Thorsteinsson and Tozer's middle member, plus the youngest member. These changes in correlation, plus some additional nomenclature proposals by Jutard and Plauchut (1973) and by the author (Miall, 1974a, c), are shown in Table 2. In this report the author's (Miall, 1974a, c) subsurface subdivisions are modified in an attempt to arrive at a nomenclature that is useable throughout Banks Island, both in the surface and the subsurface. The Cyclic Member (Table 2) includes the two younger members of Jutard and Plauchut (1973) because the writer was unable to confirm by his own

field work that there is any difference in rock types between the two units.

The distribution, thickness and rock types of the Shale Member are shown in Figure 14, and Figure 15 provides the same information for the Cyclic Member. The Shale Member is present throughout Banks Basin and Big River Basin, but may be absent over Storkerson Uplift and also along much of the eastern and southern flanks of the basin, probably as a result of overstep by, or lateral facies change into the Cyclic Member, as suggested in Figure 6. The unit is thickest at the Tiritichik M-48 location, where it reaches 241 m (790 ft).

The complete thickness of the Cyclic Member is nowhere preserved, for throughout much of the island the unit is exposed at the surface and an unknown thickness has been removed by erosion. In the western part of the island the Eureka Sound is succeeded unconformably by the Beaufort Formation, and pre-Beaufort erosion also has reduced the thickness. The thickest sections are preserved in the centres of Big River and Banks Basins. At Storkerson Bay A-15 the member is 683 m (2242 ft) thick and on the north coast of Banks Island, in the centre of Northern Banks Basin, the thickness is estimated graphically at 1100 m (3500 ft). The Castel Bay C-68 well is thought to contain a similar thickness. At Colquhoun River, the Cyclic Member is only 110 m (350 ft) thick because of pre-Beaufort erosion.

Most earlier workers assumed that the Eureka Sound Formation is exclusively nonmarine in origin (Tozer, 1963a, p. 92) but, as discussed in later sections, evidence is now accumulating that a significant proportion of the formation is, in fact, marine.

Contacts

In Banks Basin the lower contact of the Eureka Sound is drawn at the top of the upper sand member of the Kanguk Formation, as discussed in an earlier section. In Big River Basin and on the flanks of Storkerson Uplift, this member is absent. The Kanguk grades upward imperceptibly into the Eureka Sound and the contact is drawn arbitrarily at the lower limit of either coal or sand beds.

In the western part of Banks Island the Eureka Sound is succeeded unconformably by the Beaufort Formation. Where this contact outcrops at the surface it is fairly easily recognized; it can also be traced for considerable distances on aerial photographs because of the slight differences in colour and texture imparted to the terrain by the two units. Areas underlain by Beaufort Formation are commonly slightly darker and the surface is smoother than adjacent areas underlain by the Eureka Sound. In outcrop the two formations may be distinguished on the basis of grain size; the Beaufort Formation includes abundant unconsolidated pebble- and cobble-gravels, which are absent in most surface exposures of the Eureka Sound. Wood fragments and logs are common in both units but those in the Beaufort show very little alteration in contrast to the carbonized or mineralized fragments which typify the older rocks. This is another criterion useful for distinguishing the two units.

In the subsurface the Beaufort–Eureka Sound contact is difficult to define for a variety of reasons. The Beaufort is particularly susceptible to caving because it is unconsolidated. Cuttings therefore tend to contain an abundance of coarse

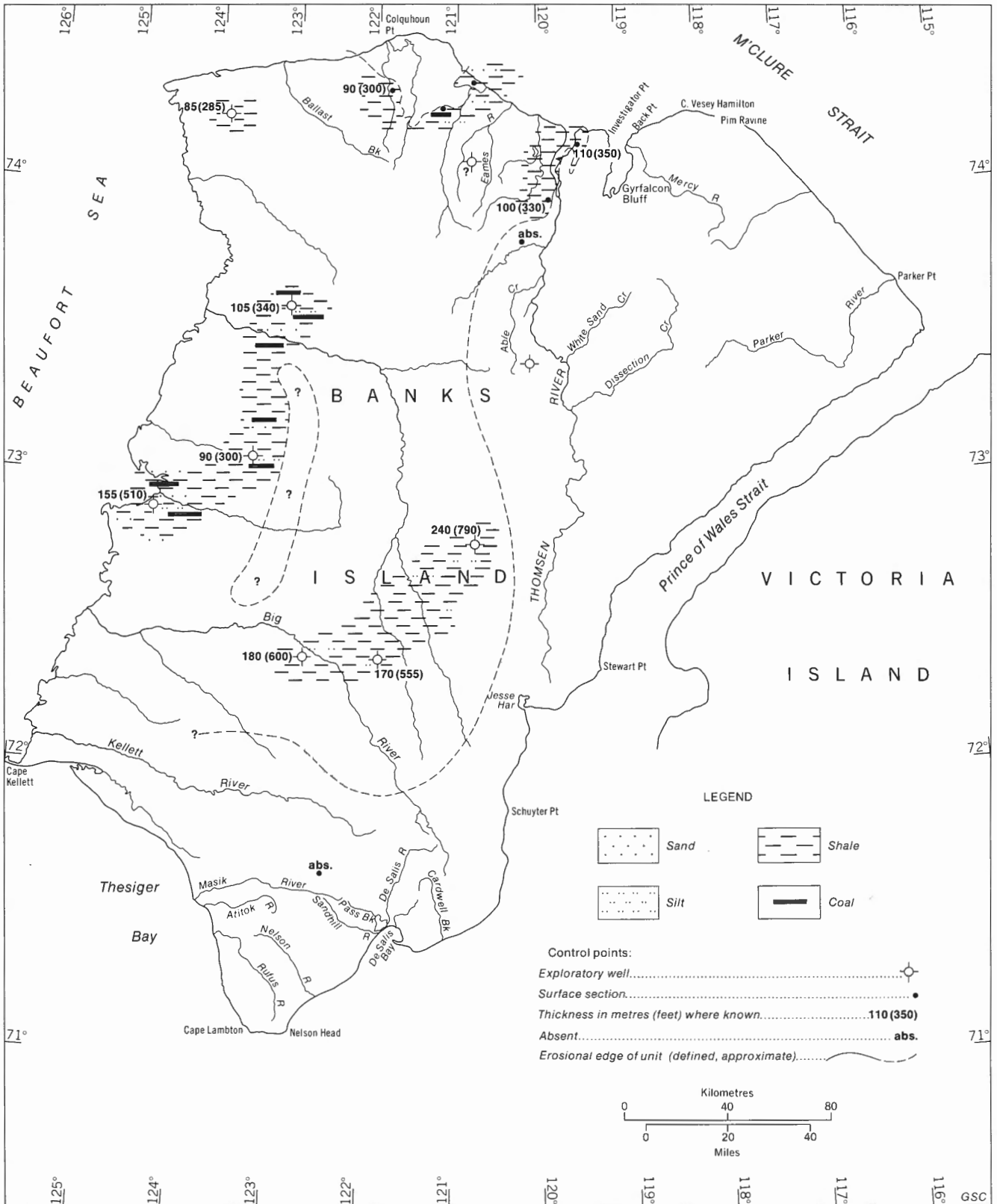


Figure 14. Eureka Sound Formation, Shale Member: distribution, thickness and lithologies. Thicknesses are rounded off for convenience.

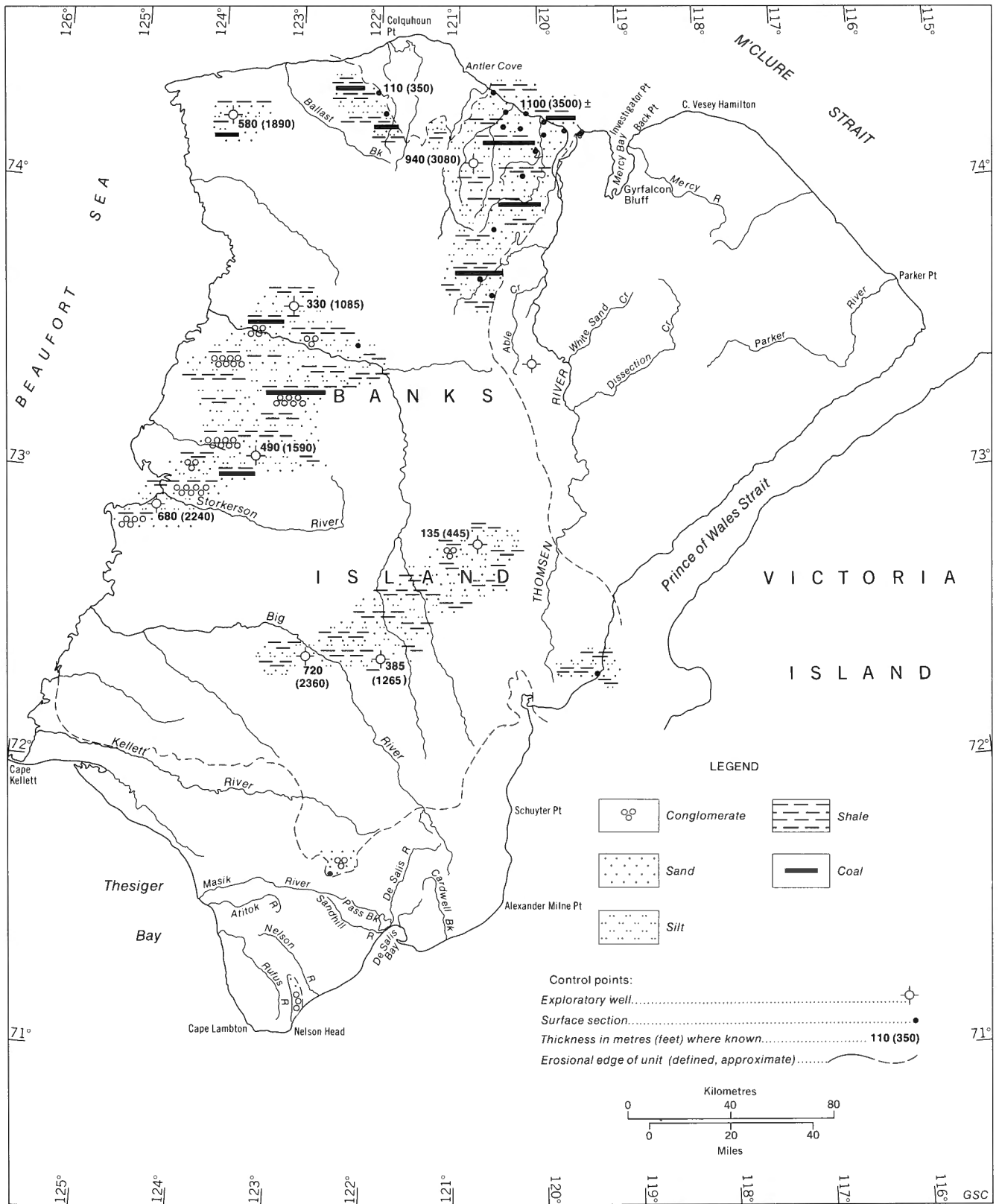


Figure 15. Eureka Sound Formation, Cyclic Member: distribution, thickness and lithologies. Thicknesses are rounded off for convenience.

clastic fragments for tens of metres below the actual base of the formation. Complete geophysical logs of the contact normally are unavailable because the contact occurs at shallow depths and the hole is lined with surface casing before logs are run. Earlier, preliminary reports by the writer (Miall, 1974a, c) assigned considerable thicknesses of beds to the Beaufort Formation in the Storkerson Bay A-15, Nanuk D-76 and Uminmak H-07 wells, but interpretation of aerial photographs and surface mapping in the area, aided by biostratigraphic studies of seismic shothole samples, has shown that, at least in the vicinity of the Nanuk and Uminmak locations, the Beaufort is only a thin veneer capping the Eureka Sound Formation. Consequently in these two wells the Eureka Sound–Beaufort contact has been drawn arbitrarily at a depth of 15 m (50 ft) for the purposes of this report. Owing to a lack of contrary evidence, the position of the contact at Storkerson Bay A-15 is not revised at this time. It was drawn at a depth of 262 m (860 ft) by the writer (Miall, 1974a). A thick Beaufort section is also thought to be present in the Bar Harbour E-76 well. Regional geological considerations indicate a thickening of the Beaufort towards the western coast of Banks Island, so that the presence of the contact at a much deeper level at Storkerson Bay and Bar Harbour is to be expected (*see also* the discussion of the Beaufort Formation at this locality).

Lithology

As remarked earlier in this chapter, the lithology of the Shale Member of the Eureka Sound Formation is very similar to that of the silty shale member of the underlying Kanguk Formation and in areas of poor exposure, such as in the vicinity of Colquhoun River, biostratigraphic control is necessary for a correct formational assignment. The thickest surface section through the shale member is at Station 73-MLA-7 southeast of Antler Cove where 87.5 m (287.1 ft) of beds are exposed. They consist mainly of soft, dark grey shale with several thin but persistent, pelecypod-bearing calcareous sandstone beds.

One of the latter is illustrated in Plate 12B. Other exposures of this member in the Antler Cove–Colquhoun River area show that it consists predominantly of soft grey shale. Pelecypods are found in one outcrop of a calcareous sandstone bed, and Jutard and Plauchut (1973, p. 213) record the presence of marine microplankton. Small hedgehog concretions are abundant locally. Many of the shale beds contain silty laminae and show small-scale asymmetrical and near-symmetrical ripple marks. Similar rock types also are exposed near Castel Bay and on the west side of the lower Thomsen River.

In the subsurface of Banks Basin the Shale Member consists of very similar rock types to those described above. Silty shale predominates, with fewer argillaceous siltstone interbeds. Thin coal seams are present near the base of the member in the Tiritchik M-48 well, and rare foraminifera in the Ikkariktok M-64 well. No sandstone units have been recorded. The member becomes coarser near the top and grades imperceptibly into the Cyclic Member.

Three of the wells in western Banks Island (Storkerson Bay A-15, Nanuk D-76 and Uminmak H-07) display somewhat different rock types at this stratigraphic level. Shale

predominates but is interbedded with very fine grained sandstone, siltstone and lignitic coal; plant debris is abundant. These beds formerly were assigned to a shale-coal member (Miall, 1974a, c, as shown in Table 2 of this report). Sandstone is particularly abundant in the A-15 well and assignment of any beds to the Shale Member is somewhat arbitrary. Appendix 2 gives sample descriptions and Figure 8 shows graphic logs.

Throughout Banks Island the Shale Member shows a gradational contact with the Cyclic Member. The latter is so called because of the abundance of coarsening-upward cycles, which may be seen readily in outcrop and also are apparent from gamma ray logs of the subsurface sections. Some views of this member are shown in Plates 13, 14 and 15.

The cycles are described and analyzed in detail in the next chapter. They consist typically of the following sequence, in upward stratigraphic order: shale, interbedded shale and silt or very fine sand, sand, soil zone, lignitic coal. Average cycle thickness is 7.4 m (24.3 ft). The shale units in the cycles typically are soft, dark brown-grey or mottled, micaceous, and contain abundant plant debris. Thin sand laminae are rare to common and may show contorted bedding as a result of postdepositional density flowage. Sand beds are generally very fine grained, pale, unconsolidated, and contain a wide range of sedimentary structures, including large-scale and very large scale trough and planar crossbedding and small-scale ripple marks. The sands of this member generally display a mottled 'salt and pepper' coloration owing to the abundant dark chert grains. Plate 13B shows part of a low-angle crossbed in which the sand has been penetrated by the burrows of *Ophiomorpha*. This is the only locality at which this trace fossil has been observed. Rare foraminifera are present at two localities near the base of the member, at Stations 74-MLA-113 and 74-MLA-115, and radiolaria were recovered from an exposure higher in the succession, at Station 74-MLA-116. Plant remains are abundant, either as roots and rootlets below a lignite bed, as shown in Plate 14A, or as large logs, as in Plate 14B. The latter commonly are partly replaced by siderite. They are particularly abundant near Nangmagvik Lake and in the bluffs along Log River (hence the choice of name for this feature).

Lignite coal ranges from lensoid bodies a few centimetres thick up to persistent seams reaching 2 m (6.6 ft). The thicker units commonly contain thin, discontinuous shale laminae. Lignite coal beds may or may not be preceded by sandy and iron-stained soil zones. Sideritic ironstone lenses are common. Many contain abundant root and wood impressions and are interpreted as highly reduced soil zones. Rare sandstone beds occur near the base of the Cyclic Member, as in Station 74-MLA-115. They contain an argillaceous matrix and are very resistant. A total of 23 partial sections with an average length of 58 m (190 ft) were measured through the Cyclic Member in northern Banks Island to permit a detailed sedimentological analysis. They are described in detail in Appendix 3. Their locations are shown on the 1:250 000 geological maps. No attempt has been made to correlate any of these sections except for the three near Nangmagvik Lake (Stations 73-MLA-19, 20, 21) because, as shown in Figure 16, most of the beds are laterally discontinuous and such correlation is thought to be impossible. The correlations shown in

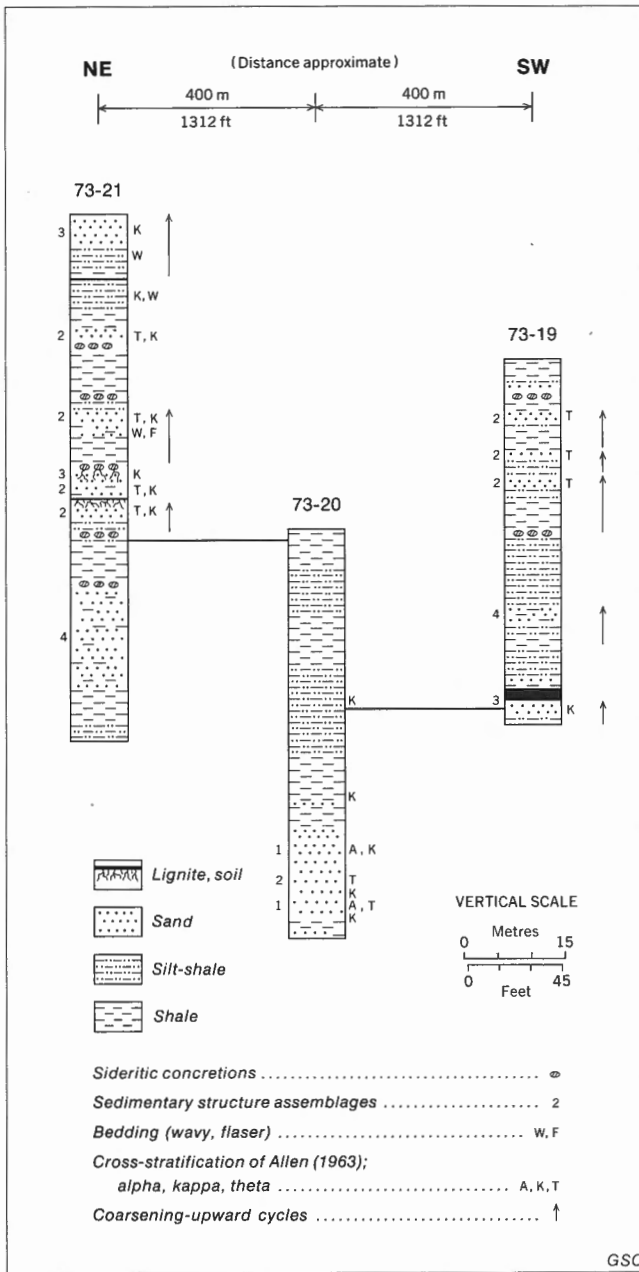


Figure 16. Lateral changes within the Cyclic Member of the Eureka Sound Formation at Nangmagvik Lake.

Figure 16 were 'walked out' on the ground but generally this cannot be done because of a lack of exposure in intervening areas.

The proportions of the various rock types vary slightly across northern Banks Island and this can be related to local differences in depositional environment. Similar rocks also are exposed at Stewart Point in southeastern Banks Island and in small outcrops which occur as inliers eroded in the Beaufort Formation in the western part of the island.

Exposures in southern Banks Island, near Masik River and north of Nelson Head (Fig. 15), show that the formation is much coarser grained. Unconsolidated fine- to coarse-grained sand predominates but also present are pebble- and

cobble-conglomerate beds containing clasts up to 12 cm (4 in.) in diameter. Clast types include silicified carbonate sediments; quartzite; black, brown and grey chert; vein quartz; rare fresh diabase and rare pink granite.

All of these rock types occur also in the subsurface but, owing to sample lag and mixing, it is impossible to determine detailed lithological sequences from cuttings alone (no core is available). Geophysical log interpretation indicates that coarsening-upward cycles are present in these rocks (Fig. 8). The section in the Orksut I-44 well is similar to the surface sections that have been studied in northern Banks Island. Those at Uminmak H-07, Nanuk D-76, Storkerson Bay A-15 and Ikkariktok M-64 contain abundant coarse sand and pebbles, especially in the upper part of the Cyclic Member. The Eureka Sound is followed by the coarse-grained, unconsolidated Beaufort Formation and by surficial deposits, and it is difficult to determine from the samples themselves what proportion of the coarse material is caved from these younger rocks. In all these instances pebble-grade fragments were recovered from the Cyclic Member after surface-casing had been set in the hole and the casing would have reduced or prevented any further caving from the upper levels in the well. Therefore much, perhaps all, of the coarse material must be of Eureka Sound origin. The situation is clearest in the Storkerson Bay A-15 well. The upper 284 m (930 ft) of the Cyclic Member are represented by medium- to coarse-grained sand. At a depth of 546 m (1790 ft) the samples change abruptly to gravel containing clasts up to 6 mm (0.25 in.) in diameter, and this change is accompanied by a sharp, positive deflection in the spontaneous potential log. The typical 'serrated-funnel' shape of the spontaneous potential and gamma-ray logs, indicating coarsening-upward cycles, appears at this level. Most of the samples in the 546 to 972 m (1790-3190 ft) interval consist of pebbles and pebbly sand. All of this material must have been derived from the Eureka Sound Formation, although much of it could have caved from the upper part of the interval.

Age and correlation

Macrofossil collections from the Eureka Sound Formation could not be dated. However, good palynological recoveries from the surface and subsurface permitted reliable age assignments for the two members.

The Shale Member in Northern Banks Basin is Paleocene in age, as shown by the following floral assemblages (identifications and age determinations by W.S. Hopkins, Jr., *pers. com.*, 1974):

Station 73-MLA-7, Antler Cove, 18 m (59.1 ft) above base of section, GSC loc. C-26383:

- Sphagnum antiquasporites* Wilson and Webster
- Sphagnum regium* Drozhastchich
- Sphagnum* spp.
- Baculatisporites* sp.
- Osmundacidites* sp.
- Lycopodium* sp.
- Laevigatosporites* sp.
- Taxodium-Glyptostrobus* sp.
- cf. *Metasequoia* sp.
- cf. *Carpinus* sp.



Plate 12. Kanguk–Eureka Sound transition beds. A: Upper sand member of the Kanguk Formation near Able Creek (Station 73-MLA-11). Note low-angle planar and trough crossbedding. GSC 199164. B: Calcareous sandstone unit in the Shale Member of the Eureka Sound Formation near Antler Cove (Station 73-MLA-7). Measuring rod subdivisions are 50 cm. GSC 199162.

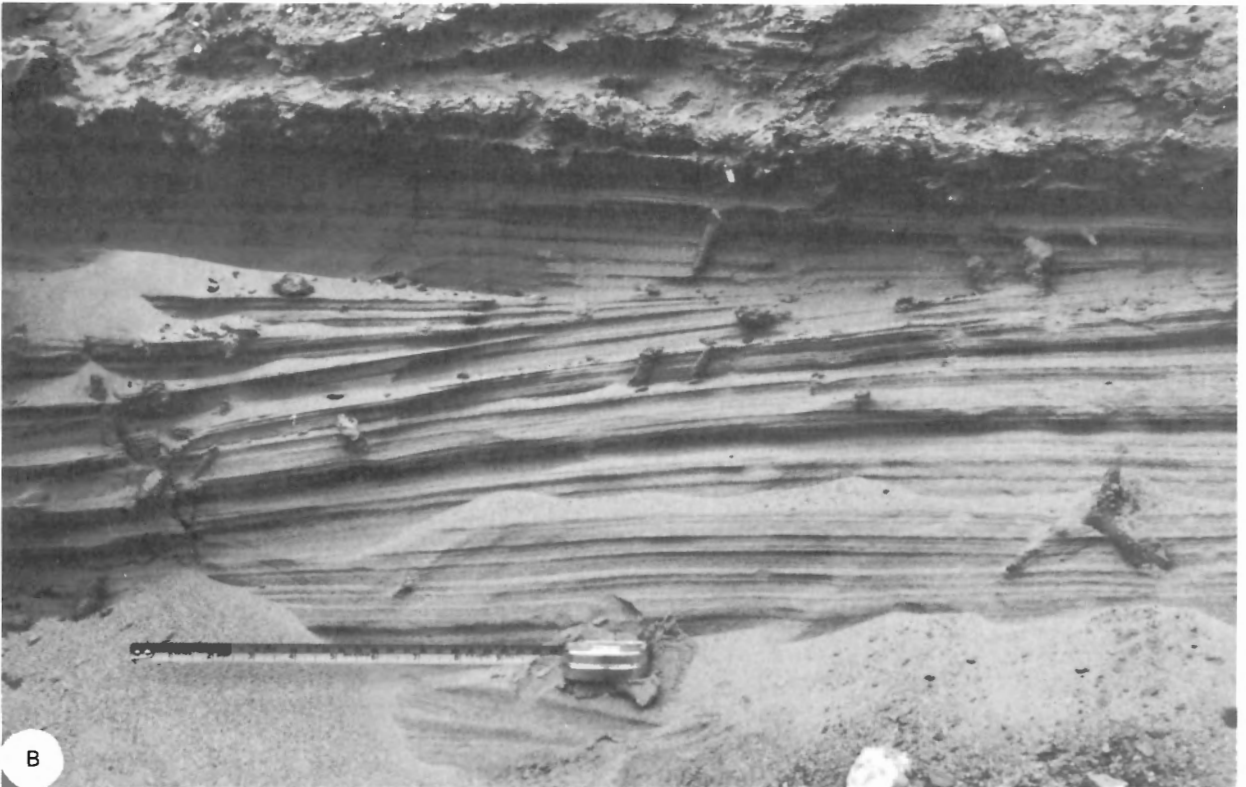


Plate 13. Cyclic Member of the Eureka Sound Formation. A: Typical inland exposure, near Muskox River (Station 73-MLA-39); 71 m (233 ft) of beds are exposed. GSC 199158. B: Low-angle 'hummocky' cross-stratification (Harms *et al.*, 1975, p. 88) in very fine grained sand with numerous *Ophiomorpha*, near Eames River (Station 73-MLA-37). GSC 199181.

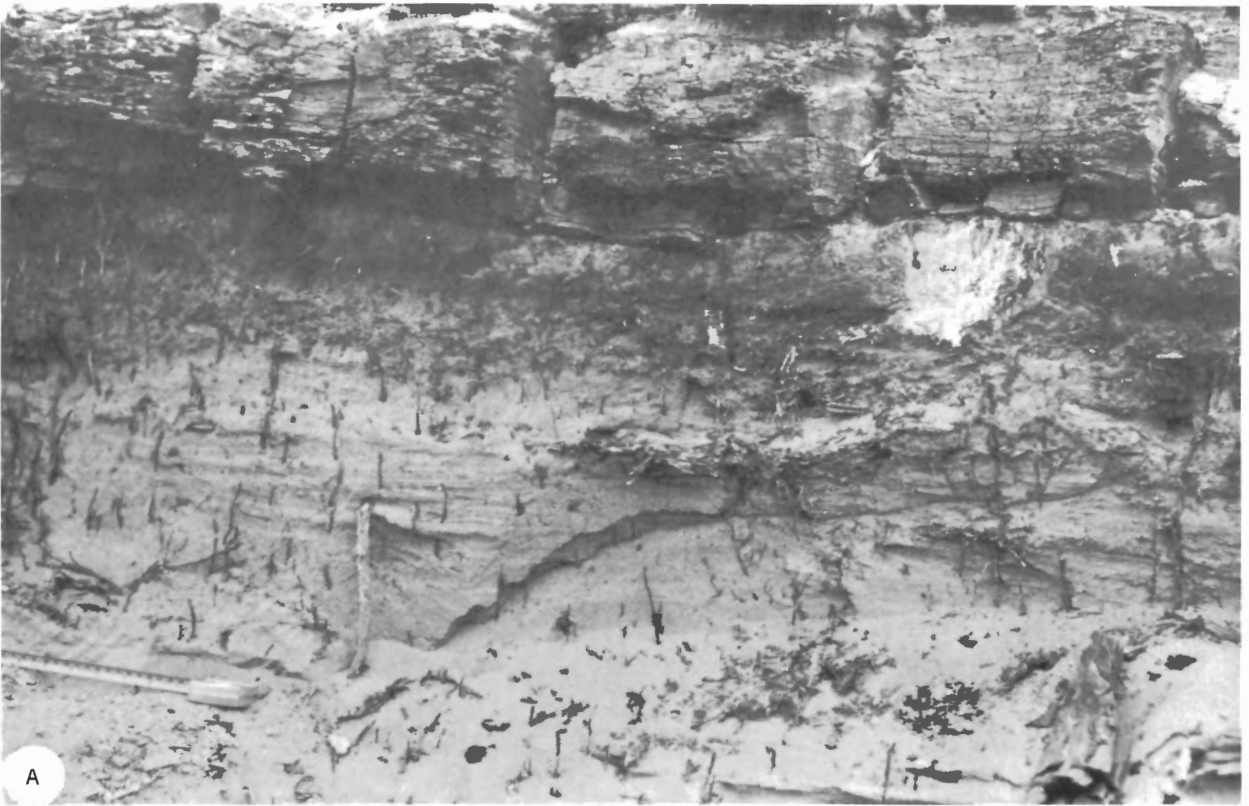


Plate 14. Plant remains and coal, Eureka Sound Formation. A: Sand with abundant roots overlain by a soil, and this by a lignite seam, near Eames River (Station 73-MLA-38). GSC 199180. B: Mineralized log from Nangmagvik Lake (Station 73-MLA-20). GSC 199167.

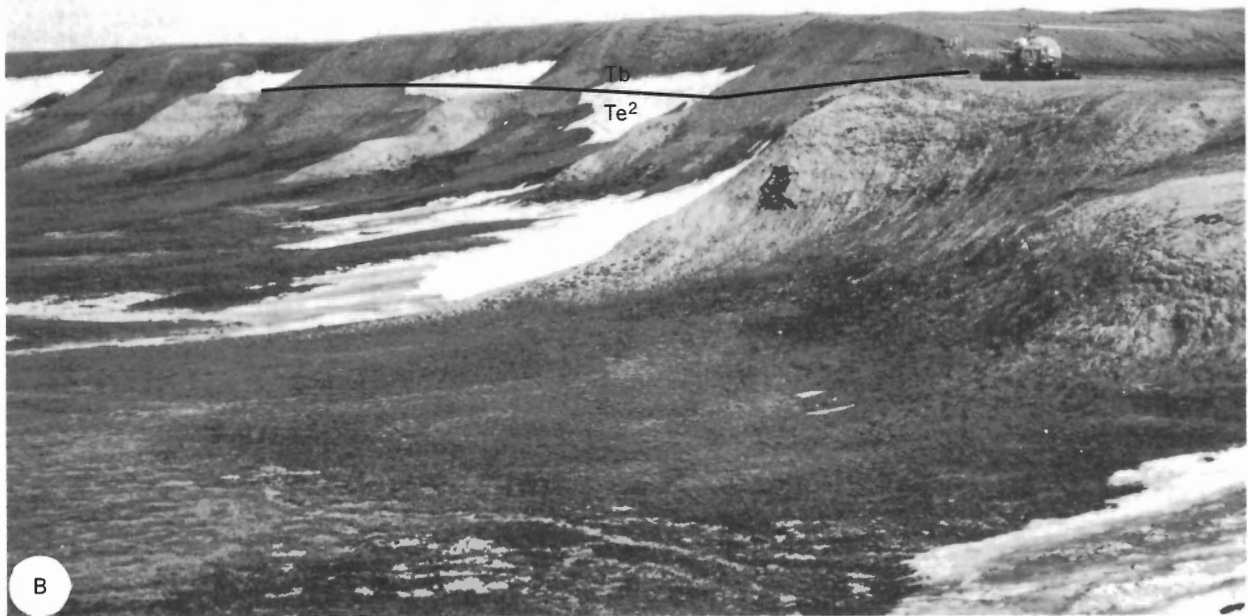
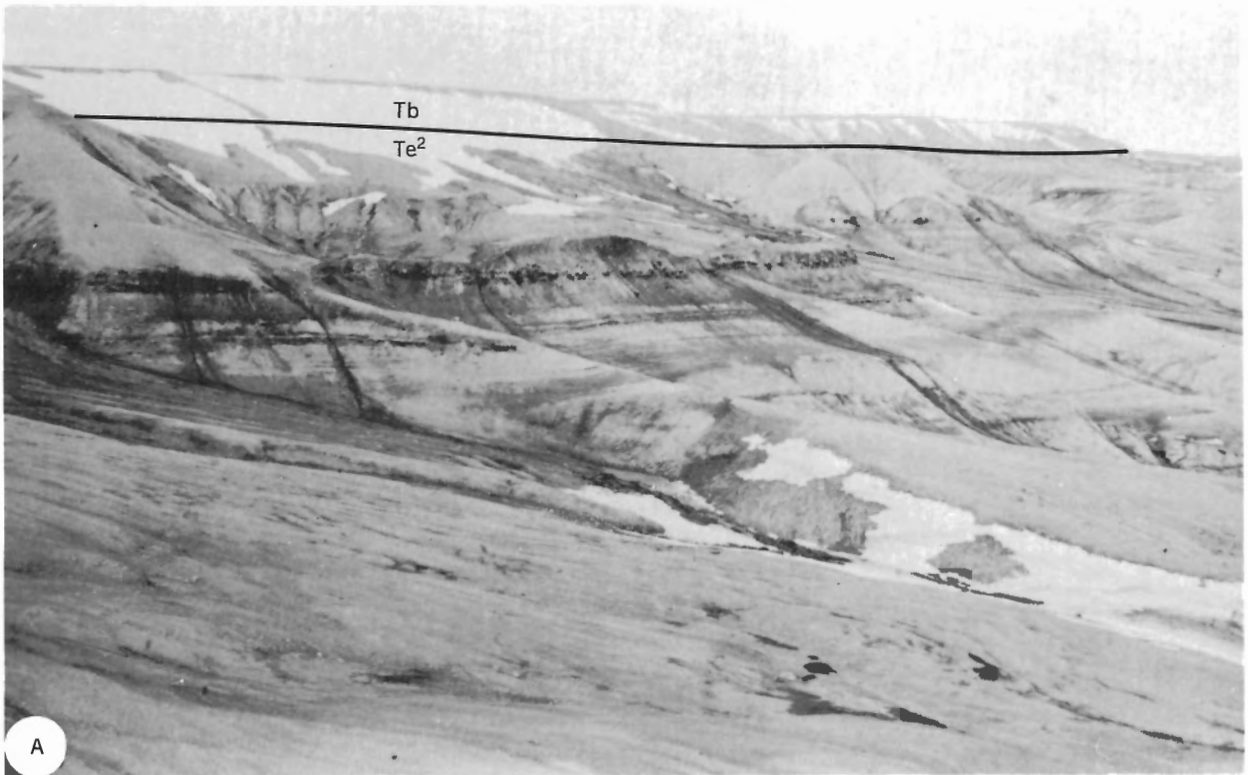


Plate 15. The Eureka Sound–Beaufort contact (Te²-Tb). A: The edge of the Beaufort plateau, near Log River (Station 74-MLA-46). Beaufort gravels, 30 m (98 ft) thick (largely snow covered), overlie the sand-shale-coal succession of the Cyclic Member. GSC 199197. B: The helicopter stands on the Eureka Sound–Beaufort contact north of Bernard River (Station 74-MLA-149). This is typical of many exposures in the low-relief interior of Banks Island. GSC 199208.

Alnus sp.
cf. *Extratropipollenites* sp.
Tricolpites sp.
Tricolporopollenites sp.
Tripoporipollenites spp.

GSC loc. C-30826, Log River:

cf. *Extratropipollenites* sp.
Alnus sp.
Tricolpites sp.
Betula sp.
cf. *Carya* sp.
Paraalnipollenites sp.

Poor recoveries of foraminifera were made from the Shale Member in the Ikkariktok M-64 well (GSC loc. C-33726; identifications and age assignment by Wall, in Brideaux *et al.*, 1976):

Depth m (ft)	Fauna
427-457 (1400-1500)	<i>Florilus</i> sp. — one specimen algal cysts
457-488 (1500-1600)	<i>Haplophragmoides</i> sp. — one fragment
488-518 (1600-1700)	<i>Haplophragmoides</i> spp. — two incomplete or distorted specimens representing two species <i>?Verneulinoides</i> sp. — one
518-549 (1700-1800)	<i>Haplophragmoides</i> spp. — four incomplete to complete specimens representing one large species, and one specimen of a smaller species <i>Florilus</i> sp. — one specimen <i>?bone chip</i>
549-579 (1800-1900)	no microfossils
579-610 (1900-2000)	<i>Saccammina</i> sp. — one <i>Haplophragmoides</i> sp. — three

Wall assigned a probable Early Tertiary age to these assemblages on the basis of the *Florilus* sp.

At Uminmak H-07 the Shale Member contains the following palynomorph assemblages, according to W.S. Hopkins, Jr. (*pers. com.*, 1973):

Depth m (ft)	Flora	GSC loc.
335-366 (1100-1200)	<i>Pterocarya</i> sp. cf. <i>Carpinus</i> sp. <i>Betula</i> sp. <i>Carya</i> sp. <i>Tilia</i> sp. cf. <i>Engelhardtia</i> sp. <i>Pistillipollenites macgregorii</i>	C-24116
366-396 (1200-1300)	<i>Pterocarya</i> sp. <i>Betula</i> sp. <i>Carya</i> sp.	C-24117
396-427 (1300-1400)	<i>Carya</i> sp. <i>Biretisporites</i> sp.	C-24118

427-457 *Betula* sp. C-24119
(1400-1500) *Carya* sp.
Paraalnipollenites confusus

The lowermost sample is assigned a Paleocene age; the remainder are Eocene but may comprise predominantly caved palynomorphs. Similar assemblages are found in the Shale Member in the Storkerson Bay A-15 well (Hopkins, in Barnes *et al.*, 1974).

The lowest sample from the Shale Member at Storkerson Bay is assigned a Maastrichtian age and the remaining samples are Tertiary, indeterminate.

The base of the Cyclic Member ranges from Maastrichtian to Eocene. Beds younger than Eocene have yet to be identified.

The oldest age determination obtained from the Cyclic Member of the Eureka Sound Formation is Maastrichtian. This was assigned to a sample collected at Stewart Point (GSC loc. C-30542; identified by W.S. Hopkins, Jr., *pers. com.*, 1975). The floral assemblage is as follows:

Expressipollis sp.
Orbiculapollis sp.
Fibulapollis sp.
Azonia sp.
Aquilapollenites sp.
Wodehouseia sp.

Hopkins stated that this assemblage resembles that in the lower part of the Eureka Sound Formation in the Ringnes islands.

Another sample, collected very near the base of the member west of Nelson River (GSC loc. C-30505), yielded the following assemblage:

Aquilapollenites sp.
Tricolpites spp.
Betula sp.
Alnus sp.
Carya-type

Hopkins (*pers. com.*, 1975) stated that this sample is late Maastrichtian, or more probably, early Paleocene in age.

On the east flank of Northern Banks Basin, where the Cyclic Member is particularly well exposed, the base of the member is Paleocene. As a considerable thickness of Paleocene beds comprising the Shale Member underlies the Cyclic Member in this area, the base of the latter is assumed to be relatively late Paleocene in age. Two assemblages collected from Station 73-MLA-19 near Nangmagvik Lake are typical. The section is an indeterminate stratigraphic height, above the base of the member:

GSC loc. C-26395, 1 m (3.3 ft) above base of section:
Sphagnum antiquasporites Wilson and Webster
Cyathidites sp.
Laevigatosporites sp.
Lycopodium sp.
Cicatricosisporites sp.
cf. Taxodiaceae

Laricoidites sp.
Glyptostrobus-Taxodium sp.
Vitreisporites sp.
 cf. *Ulmus* sp.
Carya sp.
Paraalnipollenites sp.
 cf. Ericaceae
Alnus sp.
Retitricolpites sp.
Tricolpites sp.
Tripoporollenites sp.

GSC loc. C-26396, 16 m (52 ft) above base of section:

Sphagnum antiquasporites Wilson and Webster
Sphagnum spp.
Gleicheniidites senonicus Ross
Deltoidospora sp.
Cingulatisporites sp.
Baculatisporites sp.
Lycopodium sp.
Glyptostrobus sp.
 cf. Taxodiaceae
 cf. *Metasequoia* sp.
Carya sp.
 cf. *Extratripoporollenites* sp.
 cf. Ericaceae
 cf. *Betula* sp.
Alnus sp.
 cf. *Ulmus* sp.
Tricolpites sp.
Tripoporollenites spp.

W. S. Hopkins, Jr. (*pers. com.*, 1974) assigned a Paleocene age to both these samples.

Younger beds at the centre of the Northern Banks Basin have yielded an Eocene age; for example, at Station 73-MLA-38, where Hopkins (*pers. com.*, 1973) reported the following microflora (GSC loc. C-26411):

Laevigatosporites sp.
Sphagnum spp.
Lycopodium sp.
Taxodium-Glyptostrobus sp.
 cf. Ericaceae
Pistillipollenites sp.
Alnus sp.
 cf. *Acer* sp.
Carya sp.
 cf. *Betula* sp.
 cf. *Typha* sp.
Tilia sp.
Tricolpites spp.
Tricolporopollenites spp.
Tripoporollenites spp.

On₂ the west flank of Northern Banks Basin, in surface sections along Log River and in the Uminmak H-07 well, the Cyclic Member appears to be entirely Eocene. A sample collected 16.5 m (54 ft) above the base of the section at Station 74-MLA-45, and estimated to be less than 30 m (98 ft) above the base of the Cyclic Member, yielded the following microflora:

Triatriopollenites sp.
Paraalnipollenites sp.
Alnus sp.
Engelhardtia sp.
Betula sp.
Ulmus sp.
Carya sp.

Hopkins (*pers. com.*, 1975) assigned an early Eocene age to this assemblage.

Four samples taken from this member in the Uminmak H-07 well have all been assigned Eocene ages by Hopkins (*pers. com.*, 1973). The microflora assemblages are as follows:

Depth m (ft)	Flora	GSC loc.
213-244 (700-800)	<i>Betula</i> sp.	C-24112
244-274 (800-900)	<i>Ilex</i> sp. <i>Pterocarya</i> sp. cf. <i>Carpinus</i> sp. <i>Betula</i> sp. <i>Carya</i> sp. <i>Tilia</i> sp.	C-24113
274-305 (900-1000)	<i>Pterocarya</i> sp. <i>Carya</i> sp. <i>Tilia</i> sp.	C-24114
305-335 (1000-1100)	as above	C-24115

One sample from the base of the Cyclic Member in the Storkerson Bay A-15 well was processed for palynomorphs but yielded only indeterminate Tertiary forms (W.S. Hopkins, Jr., *pers. com.*, 1973; GSC loc. C-24778). The age of the Cyclic Member in this well is assumed to be Eocene.

In summary, the Shale Member of the Eureka Sound Formation is Paleocene in age, except for the basal part of the succession in Big River Basin, where it is Maastrichtian. The Cyclic Member is Paleocene to Eocene on the east side of Northern Banks Basin, and exclusively Eocene on the west side of the basin and probably also in Big River Basin. The base of the member may be as old as latest Maastrichtian in Cardwell and Stewart basins. Marked lateral facies changes within the formation are clearly indicated.

This age range is similar to that reported for the Eureka Sound Formation elsewhere in the Arctic Islands. For example, Stott (1969, p. 28) reported that the formation is Late Cretaceous and Tertiary in age on Ellef Ringnes Island. Plant remains obtained from Ellesmere and Axel Heiberg islands have been dated as Paleocene or Eocene (W.L. Fry *in Tozer*, 1963a, p. 94, 95). Kerr (1974, p. 62) recorded dinoflagellates of Maastrichtian age in the Eureka Sound on Bathurst Island. In Cornwall and Amund Ringnes islands the formation is Maastrichtian to Eocene (Balkwill, 1973, p. 46).

Beds of equivalent age are not present in the areas immediately adjacent to Banks Island, either north in Prince Patrick and Eglinton islands, or south in Anderson Plain. In both cases the youngest strata are Maastrichtian in age and correlate with the Kanguk Formation. The Reindeer Formation of the Richardson Mountains and the Mackenzie Delta

(Mountjoy, 1967; Chamney, 1973; Young, 1975, p. 15–17; Young *et al.*, 1976) is similar in age and lithology. It consists of sand, sandstone, shale and coal, and is Maastrichtian to Eocene.

Neogene

Beaufort Formation

Definition, distribution and thickness

The deposits of crossbedded sand and gravel that cover much of Prince Patrick Island were named the Beaufort Formation by Tozer (1956). The formation underlies the Arctic Coastal Plain from Anderson Plains in the south (Yorath *et al.*, 1969) to Meighen Island in the north (Thorsteinsson, 1961). Recent studies have demonstrated that the formation also is present within the mountains of Axel Heiberg Island (Balkwill and Bustin, 1975).

The Beaufort Formation on Banks Island was described first by Thorsteinsson and Tozer (1962, p. 69, 70). They recognized that outcrops of the formation are scattered widely throughout the island and that it lies unconformably on beds of Early Cretaceous to early Tertiary age. The formation was mapped separately by Thorsteinsson and Tozer (1962) only in northwestern Banks Island, where it reaches its greatest thickness and is not masked by glacial deposits. Elsewhere the Beaufort forms a discontinuous cover, capping hills and locally forming a dissected plateau. In these areas it is difficult to separate the Beaufort Formation from glacial and other surficial deposits. According to J.S. Vincent (*pers. com.*, 1976) much of the region between Bernard River and Big River is underlain by Beaufort sediments that have been reworked by fluvio-glacial processes.

The writer has not studied the formation in detail. A few scattered exposures north of Bernard River and south of Kellett River were visited, and photogeological interpretation has been used to map the distribution of the formation in the intervening areas. Also of great assistance in the mapping of the northern part of the island were the biostratigraphic studies of seismic shothole samples contributed by Elf Oil Exploration and Production Canada Ltd. As shown on the geological maps accompanying this report, the Beaufort Formation forms a thin veneer over much of the island. In the northwest it caps a well developed plateau, the edge of which is a prominent escarpment (Pl. 15A). At the edge of the plateau the formation reaches 30 m (100 ft) in thickness but streams which dissect the plateau such as Ballast Brook, show 100 m (330 ft) of beds locally (Hills, 1969). Near Bernard River the formation has thinned to less than 10 m (30 ft), and similar thicknesses are present on top of many of the higher hills between Bernard River and Castel Bay (Pl. 15B).

The Beaufort Formation has been penetrated by most of the exploratory wells in central and western Banks Island, including Orksut I-44, Bar Harbour E-76, Uminmak H-07, Nanuk D-76 and Storkerson Bay A-15. In all but the Storkerson Bay and Bar Harbour wells, surface geological evidence suggests that only a few metres at the top of the well should be assigned to the Beaufort but, owing to severe caving and the lack of shallow geophysical logs, it is impossible to determine accurately what thickness should be assigned. An arbitrary figure of 15 m (50 ft) has been assigned to the

formation at Nanuk D-76, Uminmak H-07 and Orksut I-44. On the west coast regional geological interpretation suggests a greater thickness; 260 m (860 ft) have been assigned to the formation at Storkerson Bay and 276 m (905 ft) at Bar Harbour. The Beaufort Formation probably thickens markedly offshore to the west. L.V. Hills (*pers. com.*, 1976) reported the discovery, on palynological grounds, of an "older Beaufort" of probable Oligocene age in the 150 to 490 m (500–1600 ft) interval of the Orksut I-44 well. Lithologically this interval is similar to the Eureka Sound Formation and is included with the latter in this report.

Contacts

The Beaufort Formation has an abrupt, unconformable contact with the underlying rocks. In most areas it rests on the Eureka Sound Formation and may be differentiated from the latter by its coarser grain size and the presence of only slightly altered wood, in contrast with the lignitic coal and mineralized wood of the Eureka Sound (Hills, 1969, p. 204). In southern Banks Island the Beaufort rests on the Kanguk and Christopher formations but the contact is rarely exposed. Photogeological mapping of the contact is possible over much of the report-area because the Beaufort Formation generally imparts a darker colour and a smoother texture to the surface than does the Eureka Sound Formation.

Lithology

In the Ballast Brook area, Hills (1969) has subdivided the Beaufort Formation into two units that are separated by an erosional unconformity. The lower unit comprises medium- to coarse-grained, crossbedded sand, clay, silty clay and peat. An incomplete section 40 m (130 ft) thick is exposed but the basal contact with the Eureka Sound Formation is not seen. The upper unit comprises pebble to cobble gravel and medium- to coarse-grained sand with numerous lenses of uncompressed wood. The upper unit is 60 m (200 ft) thick at Ballast Brook. It oversteps the lower unit to the east and at the headwaters of the brook rests directly on the Eureka Sound Formation. The upper unit is widespread. The outcrops of the Beaufort along the edge of the plateau in western Banks Island (Pl. 15) and those on the tops of hills at the headwaters of Woon River and Eames River are all assigned to the upper part of the formation.

Well cuttings from the formation are almost exclusively sand and gravel. It is probable that finer grained lithologies are present but that the unconsolidated cuttings from them were absorbed into the mud stream during drilling. Gravels in the Beaufort both in the surface and the subsurface are characterized by an abundance of orange and brown chert, in contrast with the gravels of the Eureka Sound Formation, which contain much grey and black chert. In the subsurface the transition from orange to grey takes place at the following depths: Uminmak H-07, 58 m (190 ft); Nanuk D-76, 134 m (440 ft); Storkerson Bay A-15, 120 m (400 ft). Whether the grey, chert-bearing gravels below 120 m (400 ft) at Storkerson Bay are Beaufort Formation, or whether they should be reassigned to the Eureka Sound Formation, is impossible to determine at this time. Cuttings suggest the occurrence of peat beds between 250 and 262 m (820–860 ft) and geophysical logs all show a marked change in character below this depth. These

are the main reasons for placing the Beaufort–Eureka Sound contact at 262 m (860 ft) rather than at some shallower depth. In the Nanuk and Uminmak wells the orange chert gravels were recovered well below the assumed base of the Beaufort Formation, probably as a result of caving. In summary, although the colour of the chert in the Beaufort is distinctive, it does not appear to be a reliable guide to the stratigraphy in the subsurface.

Age and correlation

Hills and Ogilvie (1970) report the following assemblage of palynomorphs from the Beaufort Formation of Ellef Ringnes Island and northwestern Banks Island (listed in order of decreasing abundance):

Picea sp.
Tsuga sp.
 Ericaceae (tetrads)
Larix sp.
Lycopodium sp.
Osmunda sp.
Alnus sp.
Pterocarya sp.
Betula sp.
Salix sp.
Acer sp. (rare)
Carya sp. (rare)
 bryophyte spores (rare)

The assemblage is correlated tentatively with the late Homerian or Clamgulchian of Alaska which, according to Wolfe *et al.* (1966), indicates a late Miocene to Pliocene age range. Plant megafossils also were recovered from the Beaufort Formation of the Ballast Brook area in Banks Island. They include the following (Hills and Fyles, 1973):

cones:

Picea banksii Hills and Ogilvie
Pinus cf. *P. strobus*
Larix sp.
Metasequoia alnus sp.

nuts:

Juglans cf. *J. cinerea*

Hills and Fyles (1973) assigned a middle to late Miocene age to the formation on the balance of evidence.

Two samples from the Uminmak H-07 well yielded a Miocene age, according to palynological studies by W.S. Hopkins, Jr. (*pers. com.*, 1973). The samples were derived from below the assumed base of the formation but are believed to have caved from the Beaufort. The assemblages are as follows:

Depth m (ft)	Flora	GSC loc.
67 (220)	<i>Ilex</i> sp. <i>Pterocarya</i> sp. <i>Betula</i> sp.	C-24110
158 (520)	cf. <i>Carpinus</i> sp. <i>Betula</i> sp. <i>Carya</i> sp.	C-24111

Balkwill and Bustin (1975, p. 513) reported that the cone *Picea banksii* Hills and Ogilvie occurs in the Beaufort Formation of Axel Heiberg Island, indicating that at least part of the formation in that area is the same age as on Banks Island.

According to Young *et al.* (1976), the Beaufort Formation is present in Anderson Plains and in the subsurface beneath northeastern Tuktoyaktuk Peninsula and the outer fringe of the Mackenzie Delta. It is Oligocene and Miocene in age.

3. Sedimentology

Methods

Stratigraphic sections

The basis of the work described in this chapter is the detailed, bed-by-bed descriptions of stratigraphic sections. These were measured in the field in metric units to the nearest ten centimetres; a graduated measuring rod was used with an attached clinometer to permit the accurate measurement of dipping rocks (Pl. 12B). Work at this fine scale was found to be essential for the delineation and definition of depositional models. Approximately fifty sections were studied during the two field seasons, in addition to numerous small outcrops where exposure was insufficient to permit a subdivision into different bed types. Some of these sections have been described in the previous chapter; the remainder are listed in Appendix 3 of this report. Few of the sections are long, the longest being 300 m (984 ft), and most are less than a quarter of this length, as exposure in Banks Island is for the most part rather limited.

Longer stratigraphic sections are available from the subsurface but these do not provide the same wealth of detail regarding mesoscopic lithological relationships or sedimentary structures. Bed thicknesses cannot be determined with a greater accuracy than plus or minus one or two metres, except in the rare instances where core is available.

Lithological percentages, ratios

Calculation and plotting of parameters such as per cent sand, mean sand bed thickness, sand:shale ratio, and others, were found to be useful mapping tools for the Cyclic Member of the Eureka Sound Formation. Each surface stratigraphic section through this member was coded onto computer cards, one bed per card. Thus a data set was assembled for each stratigraphic section. These sets were then run through a short, simple computer program named COLUMN*, the output of which consists of *a*) number of beds of each rock type; *b*) mean bed thickness; *c*) per cent of section comprising each rock type; and *d*) an array showing the ratios of total thickness of each lithology to each of the other lithologies.

Analysis of cyclic sedimentation

Field observations in outcrops of the Eureka Sound Formation indicated that a coarsening-upward clastic cycle could be

recognized throughout the Cyclic Member. A statistical study of this cyclicity was carried out with a computer program named MARKOV, which performs single dependency Markov Chain analysis. The 'embedded-chain' method (Krumbein and Dacey, 1969) was used, in which all transitions from one lithology to another are counted, regardless of bed thickness. The same data set as for the program COLUMN was used in the analyses.

Details of analytical procedure and interpretation of the results have been described by many writers, notably Harbaugh and Bonham-Carter (1970), Davis (1973) and the present author (Miall, 1973).

Subsurface sections through the Eureka Sound Formation also were analyzed for cyclicity, using digitized gamma ray logs. Markov chain analysis was found to be unsatisfactory for this purpose, whereas Fourier analysis gave meaningful and useful results. The analyses were performed using a program developed by Digitech Ltd., of Calgary. The purpose of the Fourier analyses was not to provide a statistical description of a set of sections for correlation purposes (Preston and Henderson, 1964), but to test for the most significant harmonics, which could then be interpreted in terms of lithological successions and depositional models.

Assemblages of sedimentary structures

All recognizable sedimentary structures were recorded. Directional structures were classified wherever possible using the system devised by Allen (1963). The recognition of structure assemblages is a useful tool in the development of depositional models, in addition to providing crucial information regarding paleoslope directions, as summarized in the next section.

Wherever possible small-scale ripple marks were measured to enable the calculation of various ripple indices, using the methods described by Tanner (1967) and Reineck and Singh (1973, p. 27). The most useful measures are ripple index (RI), the ratio of length to height, and ripple symmetry index (RSI), the ratio of stoss-side length to lee-side length.

Paleocurrent studies

Two main types of information may be derived from paleocurrent data. The number of directional modes (modality) and their relative strength and relationship to each other are data of considerable environmental significance (Pettijohn, 1962; Selley, 1968; Klein, 1970; Miall, 1974e). Secondly, orientation data can yield critical information regarding paleoslope on both the local and regional scale. Additional work with data

*Except where noted, all computer programs were designed and written (in FORTRAN IV) by the writer.

from the Isachsen Formation (Miall, 1974e, and 1976b) indicates that detailed studies of fluvial paleocurrents can provide further information regarding river type, sinuosity and local tectonic history. Some tentative conclusions regarding paleohydrology also are possible.

The following data were recorded for each measured directional structure: field station number, section bed unit number, indicated current direction (trough axis, direction of foreset dip, perpendicular to ripple crest, wherever appropriate), and thickness or height of structure. For crossbedding maximum foreset dip was recorded and for ripple marks measurements of symmetry were taken, as described earlier in this chapter. The information was entered as soon as possible after measurement on to computer coding sheets (to permit a check on the field notes while still in the field) and was converted into a punched-card deck at the end of the field season. A total of 814 sedimentary structures were measured and described during the two field seasons. In future field programs a specially devised coding card may be used in the field in place of the field notebook for paleocurrent studies.

A general-purpose program named CURRENT was used to analyze the results. This was designed to calculate weighted or unweighted mean azimuth (Miall, 1974e), directional variance (vector strength) and the Rayleigh significance test, using the method of Curray (1956). Corrections for structural dip were not incorporated into the program (although they could be) because they were not needed. A listing also was provided giving the percentage of the readings falling in each of a given number of azimuth classes (eighteen segments with an angular range of 20°) and this was fed into a plotting routine for automated drawing of current rose diagrams on a small flat-bed plotter. The program was designed so that, from the data set, any combination of formations, station numbers and sedimentary structure types could be retrieved for processing by entering a short series of instructions from the computer terminal during program execution.

Paleocurrents were studied in five vertical profiles through the Isachsen Formation and a short computer program, MOVEAV, was written to handle this special type of data. The main function of the program was to calculate a ten-point moving average azimuth, variance and set thickness for each profile.

Sand petrography

A Swift point counter was used to study 155 thin sections of sand and sandstone samples for mineralogical composition. A minimum of 250 grains were counted in each section; in some instances as many as 400 grains were recorded. Most of the thin sections were stained with sodium cobaltinitrite for the identification of potassium feldspars, by using Chayes' method (Allman and Lawrence, 1972, p. 107). Only 34 of the thin sections were of consolidated sandstone samples in which matrix, cement and porosity could be measured. The remainder were made from loose, unlithified sand by impregnation with resin in the laboratory.

One sample was analyzed with the point counter twice, as a basic check on the consistency of the analytical procedure. The two counts, and the differences between them, are as follows (sample from GSC loc. C-30595, 250 points per count):

<i>Mineral</i>	<i>Count 1</i> (%)	<i>Count 2</i> (%)	<i>Difference</i> (%)
quartz	78.2	77.4	-0.8
chert	2.4	1.6	-0.8
plagioclase	tr	tr	0.0
potassium feldspar	5.2	6.8	+1.6
glauconite	tr	tr	0.0
detrital iron oxides	8.8	8.0	-0.8
detrital limestone	0.4	tr	-0.4
muscovite	0.8	0.8	0.0
clay fragments	4.0	5.2	+1.2

The test demonstrates that differences of at least one percentage point may be expected with this number of points counted. Increased accuracy could be gained by increasing the number of points analyzed but it was considered that the increased precision in the level of interpretation that could be gained by, for example, doubling the number of points, would not warrant the extra expenditure of laboratory time. (Tretin, 1969, p. 59, and van der Plaas and Tobi, 1965, provide a further discussion of point count reliability.)

The point counts were converted into percentages with a desk calculator, and a data array was set up on coding sheets and entered into the computer via punched cards. Several types of analysis were then carried out. A simple program, MINLIST, was devised to provide a compact data listing and a second routine, SAND, calculated the necessary values for QRF (quartz, rock-fragments, feldspars) and other ternary plots. This second program also classified each sample into the correct sand type, using the sand classification method of Okada (1971).

Cluster analyses of the data for each formation were carried out using a program, CLUSTR, which incorporated the method described by Parks (1966). The program provides a cluster dendrogram printed out on a 118-space line printer.

Many of the samples were run through a standard heavy mineral separation routine, using heavy liquids. The thin section analyses suggested that little additional data would be gleaned from detailed heavy mineral studies. Little is known regarding heavy mineral suites in any of the potential source rocks, whereas descriptions of some of the light mineral assemblages are available and enable meaningful comparisons. Therefore heavy mineral studies have been carried through to little more than a qualitative level.

Grain size analyses

Sixty-one unconsolidated sand samples were analyzed for grain size distribution, using an Allen-Bradley Sonic Sifter with sieves at ¼ φ intervals. A computer program, GRAINCAL, provided moment measures for each sample, plus a listing of cumulative percentages for computer plotting of grain size curves with a probability distribution. Griffiths (1967, p. 87-89) gives equations for the calculation of moment measures.

The sonic sifter was not very accurate, particularly because static electrical charges caused the silt-size particles to stick to the plastic walls of the sieves. No successful means of overcoming this problem was found other than wet sieving

which was not done during the present project. The silt lag causes a slight skewness toward the coarse end of the distribution and, for this reason, the two moments most sensitive to the tails of the distribution, skewness and kurtosis (Glaister and Nelson, 1974, p. 208–211), are not used in the analysis. Mean, standard deviation, and cumulative curve shape are less affected by this particular type of error.

Grain roundness

A few samples were analyzed for roundness. The 2.25 to 2.5 ϕ fraction of each sample was separated during grain size analysis and a small cut from the fraction was mounted on a glass slide. Roundness was estimated from the visual comparison chart of Krumbein (1941).

X-ray diffraction

Forty samples were analyzed for mineral composition. The samples comprised shale or mudstone (analyzed for clay mineral content) and various concretions. A.G. Heinrich and A.E. Foscolos interpreted the diffractograms; they point out that percentages are based on peak height, which can be influenced by various factors including degree of crystallinity and mineral size. The results therefore are semiquantitative only.

Computer methods

The various programs written for this study and the data files resulting from field and laboratory work were stored on magnetic tape for the duration of the project. Retrievals from the tape were effected by copying the master tape on to disc storage and working only with the disc file. Most of the computer runs were done on a Univac 1106 computer at Digitech Ltd., Calgary, and one or other of two remote terminals (a Vucom and a Datacom) located at the Institute of Sedimentary and Petroleum Geology was used. The availability of peripheral hardware and the large core-storage facilities of a full-size computer such as the 1106 were not required for many of the programs, but using the same computer system for all the necessary operations was found to be both convenient and time-saving.

Sedimentological synthesis

The section on each stratigraphic unit is arranged so that each part of the data analysis allows the overall interpretation to be built on that which has gone before. A review of each formation and a discussion of its significance in a regional context is deferred to a later chapter in this report.

Wilkie Point and Mould Bay formations

Very little can be said regarding the sedimentology of these two Jurassic units; the Wilkie Point is known only in the well section at Orksut I-44 and core is available only from the basal 12 m (40 ft) of the formation. The Mould Bay Formation is present at Orksut I-44 and Castel Bay C-68. Both units are marine throughout, as indicated by the abundant foraminifera and the traces of glauconite in many of the well cuttings. As reported in Chapter 2, foraminiferal assemblages

indicate a fluctuation from open-marine to shallow, restricted marine conditions.

The absence of Jurassic strata in any other surface or subsurface sections is interpreted as the result of nondeposition rather than erosion. The disconformity between the Mould Bay and the overlying Isachsen Formation represents the Hauterivian Stage and part of the Barremian, and there is no evidence here or elsewhere in the Arctic of a major tectonic episode at this time which would have allowed for uplift and removal of the 400 m (1320 ft) of Jurassic strata prior to Isachsen sedimentation. (In the Sverdrup Basin, sedimentation may have been continuous through Neocomian, Barremian and Aptian time.) If this interpretation is correct, the succession at Orksut I-44 and Castel Bay C-68 must represent the deposits of a relatively small basin of deposition, bounded to the east by the craton and to the west, probably, by Storkerson Uplift. It is not clear in which direction the basin connected to the other areas of marine sedimentation, such as the Beaufort–Mackenzie Basin and the Sverdrup Basin. The surrounding land areas near the Orksut I-44 location presumably were of subdued relief, for the only coarse clastic material in the two formations consists of a basal sandstone resting on the Devonian basement.

The basal sandstone is 15 m (50 ft) thick and shows a slight upward increase in coarseness and textural maturity, from very fine grained sand with some argillaceous interbeds at the base, to fine-grained, well sorted, mature sand at the top. A single thin section of the sandstone from core no. 1 consists of the following clastic mineral grains: quartz, 98 per cent; chert, 1 per cent; iron oxides, 1 per cent. Clay matrix comprises 26 per cent of the rock and porosity is virtually nil. Glauconite is rare. The quartz grains are angular to well rounded and rarely show authigenic overgrowths on detrital cores, indicating an earlier sedimentary cycle. Most quartz grains exhibit a thin, red-brown, iron oxide coating, which is common, but not pervasive, between quartz grains that are otherwise in contact. Rare burrows have been observed. The petrography is similar to that of many of the Isachsen sand samples and a discussion of the source of the clastic material is given in detail in the section on that formation.

The basal sandstone is interpreted tentatively as a transgressive shoreline deposit. The lowermost part may represent a nearshore, back-bar environment and the upper, coarser grained part an offshore bar, deposited under relatively higher energy conditions. Coarsening-upward sequences have been documented in several present-day coastal areas, of which Galveston Island, Texas, is probably the best known (Bernard *et al.*, 1963). However, in most cases, the sequences represent prograding bars and are clearly regressive. The basal sandstone at the Orksut location cannot be regressive as it represents the first deposit above an unconformity and probably is marine throughout. Dickinson *et al.* (1972, Fig. 13) illustrate an example of a transgressive barrier island on the coast of Rhode Island.

Coarsening-upward sequences are present in the Mould Bay Formation at Castel Bay C-68, as indicated by geophysical logs, and sandstone becomes more abundant near the top of the formation. These features are interpreted tentatively as the result of deltaic progradation into Northern Banks Basin.

A tentative paleogeographical reconstruction for Jurassic

time is shown in Figure 17. The distribution of the sandstone units is not known and they are not shown on the paleogeographic map.

Isachsen Formation

Lithofacies and sedimentary structures

The Isachsen Formation has been divided into two gross lithofacies (see Chap. 2): coarse sand lithofacies, and sand-shale lithofacies.

Various stratigraphic sections typical of each facies are described in detail in Chapter 2, and the distribution of the rock types is shown in Figure 9. The purpose of the present section is to summarize the lithofacies characteristics, to describe the assemblages of sedimentary structures, and to arrive at an interpretation of the depositional model for each facies.

Coarse sand facies

Lithofacies. The lithological character of the coarse sand facies was described in detail in Chapter 2 and will not be repeated

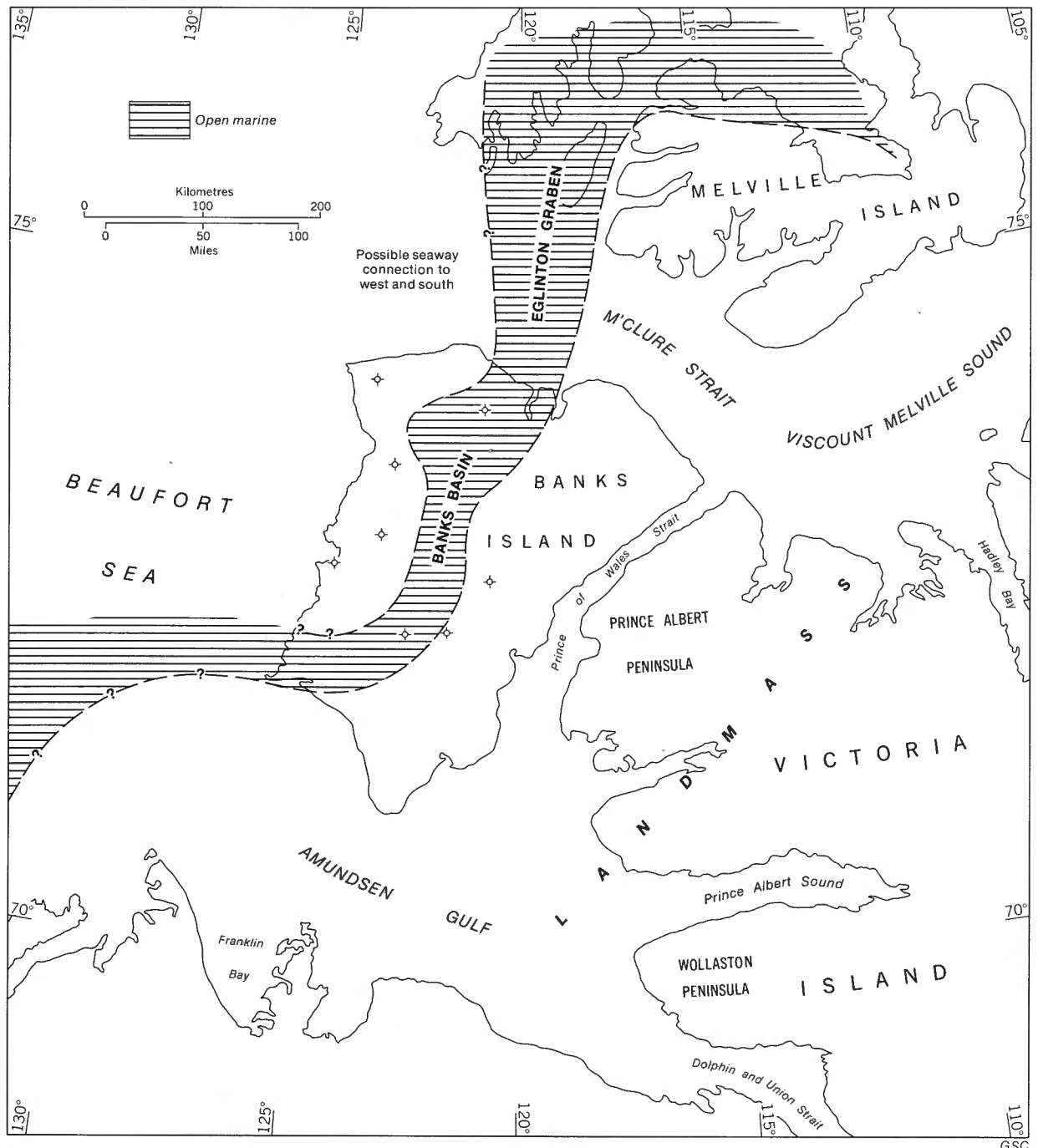


Figure 17. Generalized paleogeography, Jurassic Period.

here. It is important to note that approximately three quarters of the rocks of this facies that were studied in detail consist of crossbedded, medium to very coarse sand. The remainder comprise pebble beds, planar laminated sand, massive sand units and rare lignite beds.

Sedimentary structures. Data from five of the best exposures in the coarse sand facies (Fig. 18) provide adequate information regarding the structure types and their relative importance. The five exposures are the vertical profiles described by the author (Miall, 1976b) and discussed also in the next section on paleocurrents.

Sixty-three per cent of the total vertical thickness of the five profiles consists of planar crossbedded sand. Plate 1 shows a typical view of superimposed crossbeds in one of the outcrops. The crossbeds range in thickness from 4.5 cm (1.8 in.) to 1.5 m (4.8 ft), with a mean of 32 cm (1 ft). They extend laterally for distances up to several tens of metres. Most are of the type Allen (1963, p. 101) described as alpha-crossbedding. They rest on a surface where little or no erosion is evident and as a result the curved topsets of underlying sets are preserved in some places. Bedding within the crossbeds is differentiated on the basis of grain size, alternate laminae showing differences usually in the order of one phi class (for example, medium and coarse sand grade). The lower part of each foreset commonly includes abundant lignite fragments. Foreset dip ranges from 5° to 46° with a mean of 25°. Some of the higher values probably represent syngenetic deformation as a result of sediment fluidization, as described by Allen and Banks (1972). Such deformation ranges from oversteepening and overturning of foresets (Pl. 16A) to locally intense folding (Pl. 16B) but is, in fact, uncommon. Reactivation surfaces, as described by Collinson (1970), are internal erosion surfaces within crossbed sets. They are rare in the coarse sand facies. Superimposed crossbed sets may or may not be separated from one another by thin intervals of planar laminated sand. Examples of each are shown in Plates 1 and 17A. Where planar-bedded intercalations are present, evidence of temporary cessation in sedimentation is provided, in rare instances, by plant rootlets (Pl. 17A).

Trough crossbedding comprises eight per cent of the total thickness of the five vertical profiles. Trough cross-sets are invariably of the theta type (Allen, 1963, p. 105); they are underlain by a trough-shaped erosional surface and are composed of foresets which are curved in plan view. Most troughs occur singly and show at the sides an erosional relationship with a planar crossbed set (Pl. 17B). Troughs show a similar range in size to the planar crossbeds; those in the five vertical profiles have a mean height or thickness of 40 cm (16 in.).

Minor sedimentary structures in the five vertical profiles include various types of small-scale, asymmetrical ripple-marks, as shown in Plate 18. These are infrequent in the coarse sand facies and were not studied in detail.

Similar assemblages of structures are present in other outcrops of this facies except at Nelson Head, where massive or planar bedding is predominant and trough and planar crossbedding are rare.

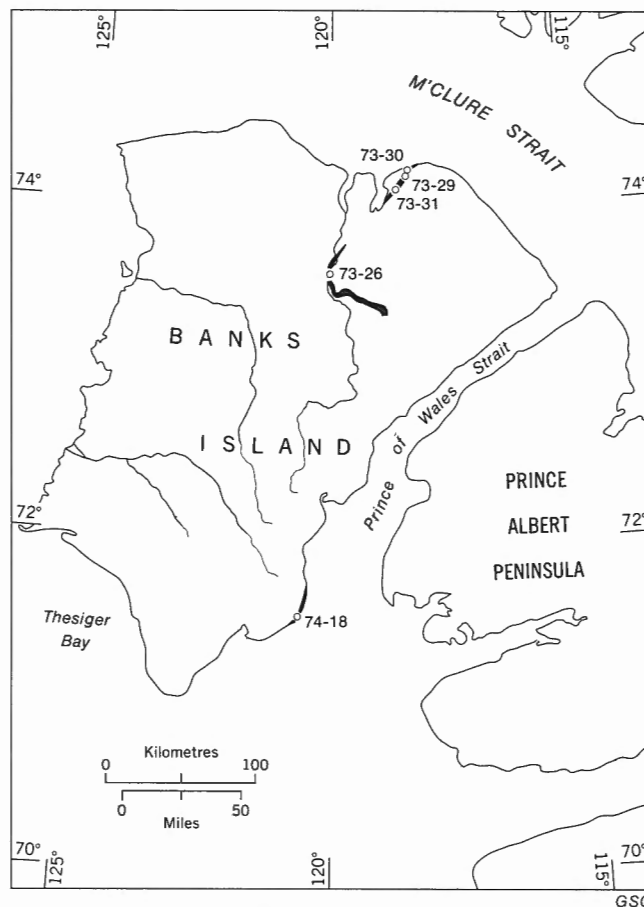


Figure 18. Location of five vertical profiles through the coarse sand facies of the Isachsen Formation. Principal outcrop areas of this facies are shown in black.

Depositional environment. As noted in Chapter 2, evidence of a marine environment is rare in the Isachsen Formation. Foraminifera were recovered from one outcrop in the sand-shale facies. The plant remains, lignite beds and well preserved roots in the coarse sand facies are evidence for a continental origin, and the specific type of vertical sequence and sedimentary structure assemblage is regarded as conclusive evidence of a braided stream environment, as described below.

Several types of continental deposit contain characteristic vertical sequences. For example, deltaic successions may show coarsening-upward cycles as the result of progradation into the sea or a lake (Visher, 1965). By contrast, fluvial deposits formed by meandering streams commonly show a fining-upward cycle, as a result of sedimentation by lateral accretion in a point bar environment (Visher, 1965; Allen, 1964, 1965, 1970b). Braided streams and their deposits display different characteristics. In contrast with the meandering river, which is characterized by relatively few major channels which shift in position slowly, braided rivers consist of many smaller channels showing very rapid migration. Deposits of braided rivers reflect this rapid and random change in the channel patterns by displaying less uniform vertical sequences. Williams and Rust (1969), Williams (1971), Costello and Walker (1972), and Cant and Walker (1976) all provided braided models, most of which consist of fining-upward vertical sequences. However,

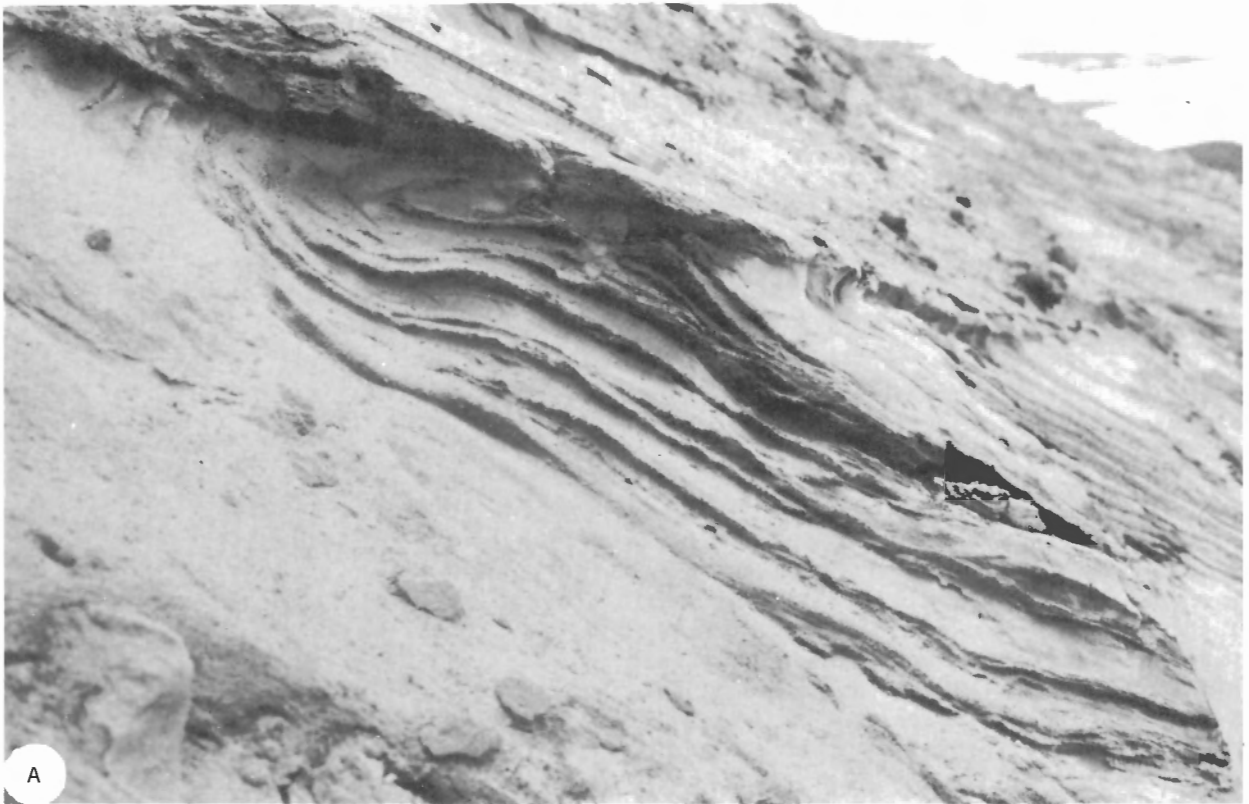


Plate 16. Deformed crossbedding in the Isachsen Formation. A: Overturning of the uppermost few centimetres of a crossbedded unit at Sandhill River (Station 74-MLA-12). GSC 199193. B: Strongly contorted crossbed at Able Creek (Station 73-MLA-24). GSC 199172.



Plate 17. Planar and trough crossbedding in the Isachsen Formation. A: Superimposed planar crossbeds at Baker Creek (Station 73-MLA-26). Note plant roots at upper right. GSC 199173. B: Trough crossbed at Cape Vesey Hamilton, followed by a planar crossbed set and a boulder bed (Station 73-MLA-29). GSC 199177. Shovel handle in both views is 50 cm long.

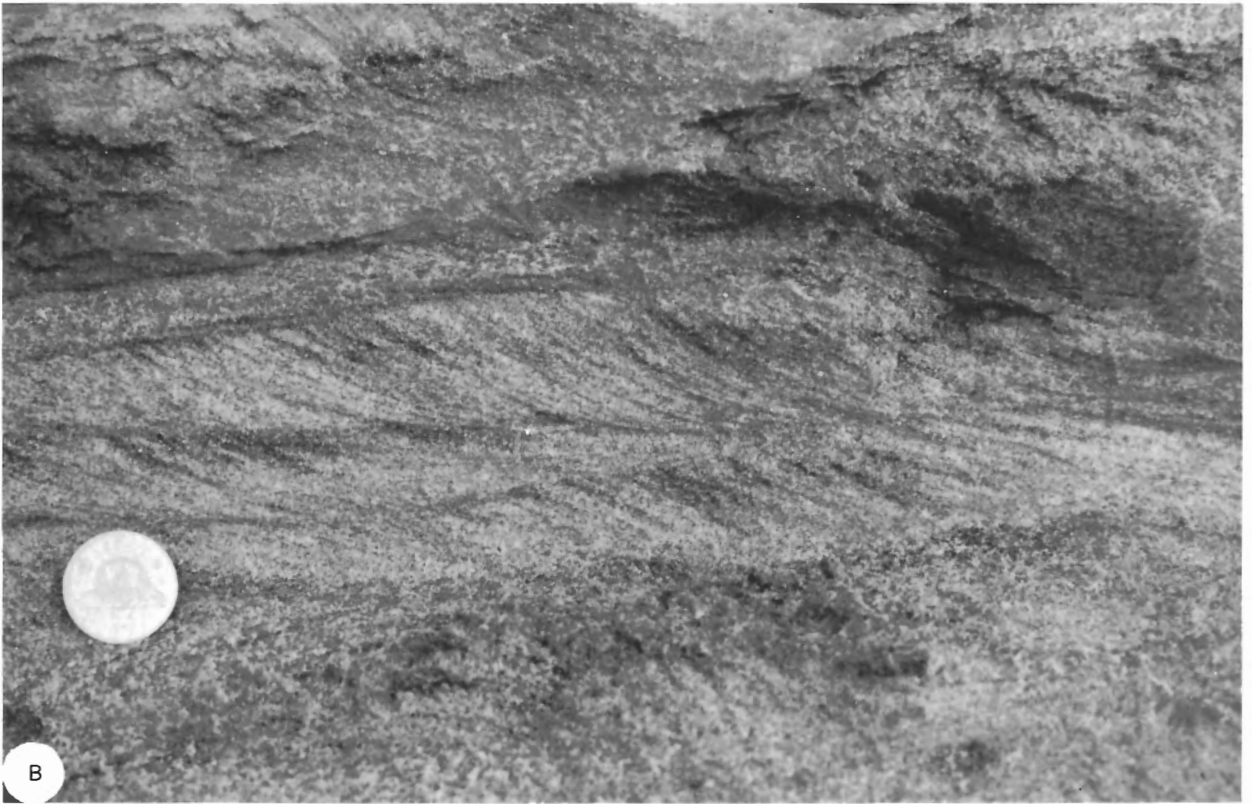
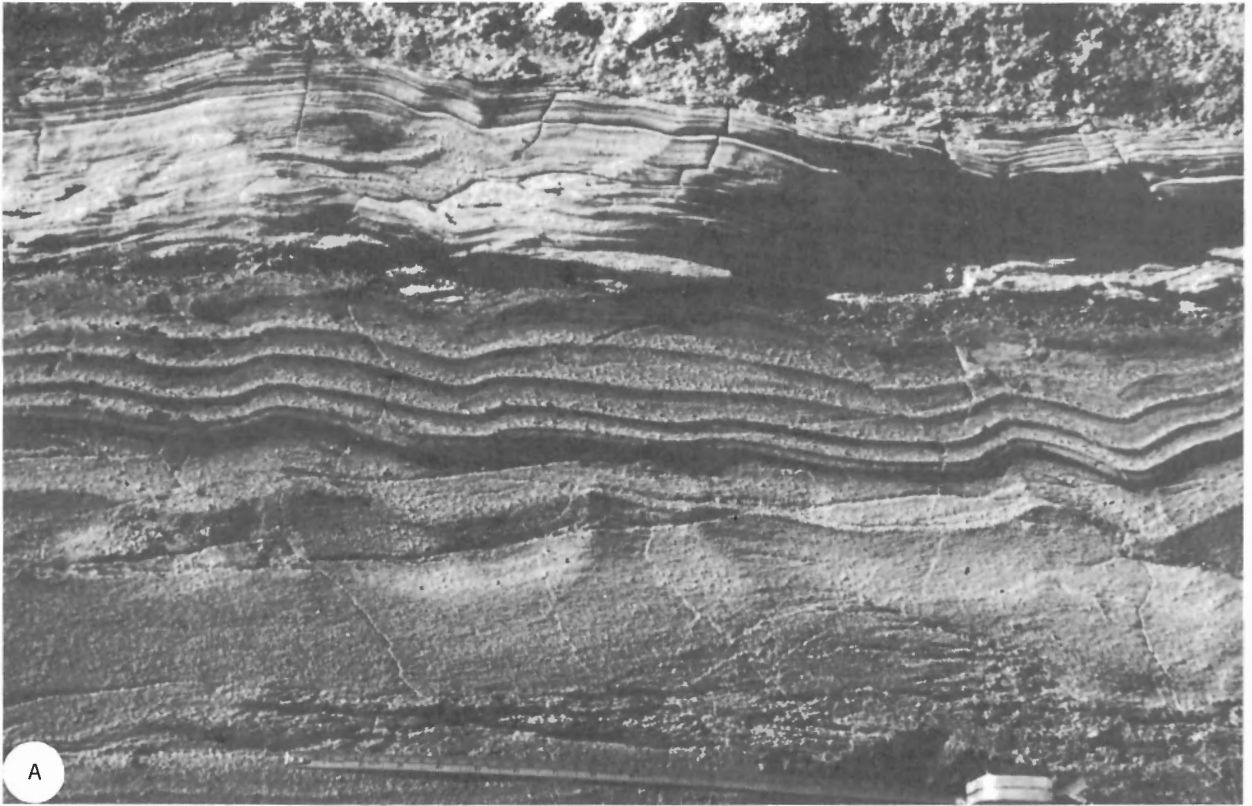


Plate 18. Ripple marks in the Isachsen Formation. A: Low-amplitude climbing ripples near White Sand Creek (Station 74-MLA-107). GSC 199201. B: Asymmetric current ripples at Station 74-MLA-107. GSC 199202.

their applicability may be limited. Other workers studying modern braided streams (e.g., Smith, 1971a, 1972, 1974a) emphasized the ephemeral nature of most braided stream deposits and concluded that in such an environment a generalized vertical sedimentary model is unlikely to be recognized.

Another characteristic feature of the braided environment is the less pronounced differentiation between flood plain and channels. A braided stream consists almost entirely of active or inactive channels and bars which may or may not be colonized by vegetation (Williams and Rust, 1969). The sediments which form in this environment thus may lack the minor but significant thicknesses of fine-grained overbank of flood plain deposits which are characteristic of the meandering environment.

Thirdly, braided streams carry much of their sediment as bedload. Schumm (1963) stated that high-sinuosity rivers typically carry less than 3 per cent of their sediment as bedload whereas, for low-sinuosity, braided streams, the amount is over 11 per cent. Coarse sediment (sand and gravel) is important, therefore, in the final deposits.

In summary, the relevant characteristics of braided stream sediments, both of which are shown by the coarse sand facies of the Isachsen Formation, are random vertical sequence and a predominance of coarse sediment such as sand and gravel.

Planar and trough crossbeds of the type in the Isachsen Formation are formed in several different environments, but work in modern rivers has shown that they are particularly common in braided streams. Large-scale planar crossbedding typically forms as a result of lateral accretion of transverse or linguoid bars. Sediment is carried across the top of the bar and accumulates on avalanche slopes at the downstream end. The avalanche slopes are then preserved as prograding foresets. Examples in modern rivers similar or identical to those in the Isachsen Formation have been illustrated by Williams (1971, Fig. 12), Collinson (1970, Figs. 19, 20), Williams and Rust (1969, Fig. 16) and Smith (1972, Figs. 3, 7; 1974a, Fig. 16B). Trough crossbeds probably represent large-scale migrating dunes formed on the relatively flat and shallow channel bottoms (Williams, 1968; Collinson, 1970).

Most of the coarse sand facies thus represents a complex of migrating, interfering and superimposed braid bars, with some channel bedforms (trough crossbeds) also preserved. One quarter of the total thickness in the five vertical profiles consists of other lithologies, as described earlier. The rare pebble beds probably represent longitudinal gravel bars similar to those described by Williams and Rust (1969) and Smith (1974a). Massive and planar laminated sands, which contain rare, small-scale, asymmetrical ripple marks, probably represent low-energy bar top deposits, and possibly are analogous to facies D of Williams and Rust (1969) and the laminated sand sheet deposits of Smith (1971b). Lignite beds represent rare overbank deposits. The coarse sand facies is a good example of the "Platte type" of braided river lithofacies assemblage (Miall, 1977).

Clasts coarser than pebble grade are uncommon in the Isachsen Formation. Cobbles and boulders in the outcrops at Stations 73-MLA-29 and 73-MLA-30 probably represent material derived very locally, possibly from active fault-line scarps at the edge of the depositional basin. The thick basal

conglomerate at Nelson Head (Station 74-MLA-6) is interpreted as a subaerial alluvial fan deposit (Bull, 1972). As shown in Figure 10, the conglomerate has a very limited lateral extent, indicating a small fan area.

Sand-shale facies

Lithofacies. At Sandhill River (Station 74-GAS-11) four lithofacies are present:

1. Sand, fine- to coarse-grained, locally pebbly, rare thin laminae of coal, abundant planar crossbedding, climbing ripples, low-amplitude ripple marks. This lithofacies represents 20 per cent of the section.
2. Interlaminated fine- to medium-grained, crossbedded sand, grey clay, carbonaceous shale and grey silt; 75 per cent of the section.
3. Clay, brown, laminated; 4 per cent of the section.
4. Lignitic coal; 1 per cent of the section.

Similar lithofacies are present at Orksut I-44 and Castel Bay C-68 although, in the absence of core, an accurate estimate of the relative proportions of the various lithologies is impossible. Two exposures at Nelson Head (Stations 74-MLA-2, 4) also show this type of succession. At the Orksut I-44 location, gamma ray log interpretation suggests two, or possibly, three fining-upward sequences in the lower part of the formation (Fig. 19), with thicknesses of 17.7, 19.8 and 24.4 m (58, 65 and 80 ft). Similar cycles are found in the Castel Bay C-68 section. Units 6 to 9 in the Sandhill River section also comprise a fining-upward sequence, totalling 27.5 m (90 ft) in thickness. It consists of lithologies 1, 2, 3, and 4 (as described above) in vertical stratigraphic order. The remainder of both sections cannot be interpreted readily in terms of any cyclic models. No cycles are recognizable at Nelson Head.

As noted in Chapter 2, silt and fine sand similar to lithofacies 1 above are exposed at two other localities. The exposures are at Stations 74-MLA-8 (Nelson River) and 73-MLA-35 (Colquhoun River). These two outcrops are assigned to the sand-shale facies.

Sedimentary structures. The shale and clay beds in this facies contain few, if any, recognizable current structures. Crossbedding and ripple marks of various kinds, however, are abundant in the sand units.

Planar crossbedding of alpha type (Allen, 1963) and similar to that in the coarse sand facies (described above) is common. Mean height, or thickness, in southern Banks Island (Stations 74-MLA-8, 74-GAS-11) is 28 cm (11 in.). In rare instances carbonaceous laminae and rootlets are present on the foresets, indicating temporary cessation of sedimentation. Trough crossbeds of similar size are present, but rare.

At Pass Brook (Station 74-MLA-11) small-scale asymmetrical ripple marks are predominant. In part they are mutually erosive and crosscutting, in part they are climbing ripples of the kappa type (Allen, 1963, p. 106). The latter represent the migration of trains of ripples with sinuous crests. Mean ripple height at this locality is 2 cm (0.7 in.).

A few large scours and unusually large scale crossbeds are present at Sandhill River. One trough measures 2.3 m (7.5 ft) in depth and probably represents a minor channel.

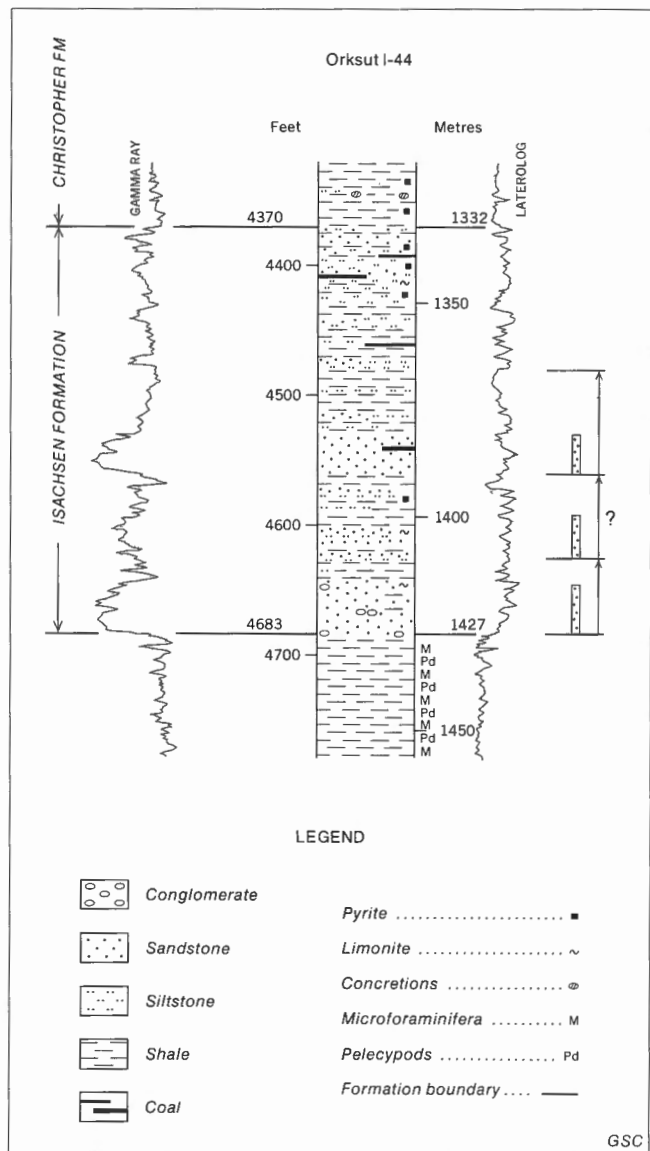


Figure 19. Interpretation of the Isachsen Formation at Orksut I-44 well in terms of cyclic sequences. Lithological sequences as in Fig. 8. Vertical bars at right represent the coarse sand member of each cycle; fining-upward sequences shown by arrows.

At Colquhoun River trough and low-angle planar crossbeds and horizontal burrows are found. These have been described in Chapter 2 and illustrated in Plate 6. Small-scale ripple marks also are seen. Ripple indices were measured on a small sample of these and the results are plotted in Figure 20.

Depositional environment. Fining-upward cycles are very characteristic of meandering-stream deposits. As described by various authors, notably Visher (1965) and Allen (1964, 1965, 1970b), they typically commence with a basal erosion surface, which represents the channel bottom. This generally is followed by a thin lag conglomerate, and then by thick sandstone units showing upward-decreasing grain size and progressively lower energy bedforms. The cycle is capped by a fine-grained unit, typically siltstone, which may contain evidence of

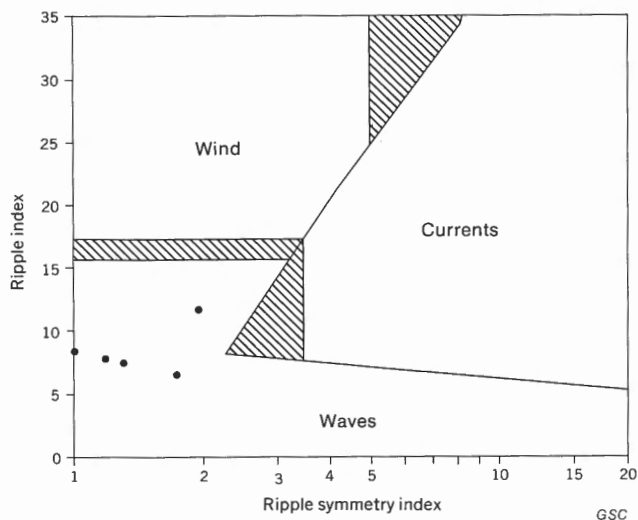


Figure 20. Plot of ripple index and ripple symmetry index for five ripple marks at Station 73-35, Colquhoun River. Environment fields are from Tanner (1967).

bioturbation and paleosol formation. The sandstone beds represent lateral accretion on a point bar and the siltstone unit may include a significant proportion of overbank material. A large suite of typical fining-upward cycles (all of Devonian age) studied by Allen (1970b) showed a mean thickness of 6.46 m (21.2 ft). The cycles in the Orksut well are thicker than Allen's average. In his examples, only 5 per cent were greater than 18 m (59 ft) thick (Allen, 1970b, Fig. 6).

The exposure at Sandhill River may represent deltaic sediments in which marine and nonmarine strata are interbedded. The thick, fining-upward cycle recorded in this section may not be of fluvial origin because marine foraminifera were recorded from the unit of interbedded sand and clay. A detailed analysis of the local environments represented by each bed type is not possible owing to lack of information concerning the geometry of each unit. As Visher (1965, p. 52) pointed out, deltaic sequences are highly variable, and simplified depositional models may not be appropriate in a given case. They certainly do not seem to be useful for interpreting the section at Sandhill River. The presence of a marine element in this area raises paleogeographic problems, unless the interpretation suggested in Figure 7 is correct. In this figure, the author suggests that part of the Isachsen Formation in southern Banks Island is contemporaneous with the marine Christopher Formation. The assignment of an Albian age to the foraminifera at Sandhill River would tend to confirm this interpretation.

There is a rapid lateral facies change within the Isachsen Formation at Nelson Head (see Fig. 10). This is attributed to the proximity of the sediment source area. The coarse sand and boulder conglomerates were discussed in an earlier section and were interpreted as alluvial fan deposits. They wedge out laterally into a succession similar to that at Sandhill River, as exposed at Stations 74-MLA-2 and 4. A meandering stream or, possibly, deltaic mode of origin is postulated for these rocks. Plant remains are the only fossils present and therefore there is no evidence of a marine environment. The rapid lateral facies change is quite characteristic of the alluvial fan environment. Observations of modern alluvial fans show

that there is a sharp break in slope at the outer rim of many alluvial fans and a corresponding abrupt change in modes of sedimentary transport (Bull, 1972, Figs. 1, 12, 13).

The exposure at Colquhoun River is interpreted as a marine upper shoreface deposit. Very low angle crossbedding (Pl. 6A) is characteristic of this environment (Howard, 1972, p. 223; Dickinson *et al.*, 1972, p. 195), for it represents intersecting, gently dipping beach surfaces. Trough crossbeds (Pl. 6B) may represent shallow runoff channels or scours formed in the wave plunge zone (Howard, 1972, p. 223). The presence of abundant burrows strongly suggests a shallow, nearshore marine environment. Ripple marks measured at this exposure have ripple indices (Fig. 20) suggesting a probable wave-formed origin, by comparison with the data of Tanner (1967, Fig. 1) and Reineck and Singh (1973, Figs. 27, 28). The sample is small but the evidence is consistent with the other environmental evidence from this locality.

The exposure at Colquhoun River is of the uppermost Isachsen Formation, immediately below the Christopher shale. The presence of strata of marine beach origin, therefore, is not unexpected, even though the Isachsen normally is considered to be exclusively of continental origin. It indicates a transgressive gradation between the continental rocks below and those of open-marine origin above.

Summary

The bulk of the Isachsen Formation is of fluvial origin. The boulder conglomerates at Nelson Head represent a small alluvial fan deposited very close to the sediment source area. The coarse sand facies, which locally contains pebble beds and boulders, was deposited in a braided stream environment. It too is a relatively proximal (i.e., near source) deposit and it is noteworthy that the outcrops of the facies are restricted to the eastern margins of the present-day Northern Banks and Cardwell basins. Near the centre of the depositional basins, at Orksut I-44 and Castel Bay C-68, the Isachsen Formation is interpreted to be of meandering stream origin. A change from braided to meandering in a downstream direction is a common situation in modern rivers. It represents the response to a progressive decrease in slope and in sediment load. At Sandhill River there is some evidence for a marine, deltaic origin for part of the succession but these beds may be younger than the Isachsen elsewhere, possibly representing a facies variant of the Christopher Formation, which is entirely marine. The upward gradation from nonmarine to marine is typified by the marine, shoreface sands exposed at Colquhoun River.

Paleocurrent analysis

A total of 411 sedimentary structures in the Isachsen Formation were measured to determine paleocurrent directions. Of this total, 363 measurements comprise groups of closely spaced structures at 15 different field stations. Statistical data for these readings are shown in Table 3. At five of the localities, statistics also have been calculated for sublocalities (shown by letters *A*, *B*) within the outcrop. The reasons for doing this will be discussed later. An additional 27 readings were obtained as a result of a special study of one crossbed set, and are discussed below. The remaining 21 readings could not be conveniently grouped into sets of similar structure type

Table 3. Paleocurrent data, Isachsen Formation

STATION NUMBER (MLA)	STATION NAME	STRUCTURE TYPE	n	$\bar{\theta}$	L	p
73-24	Able Creek	<i>a</i> θ	18	018	96	<10 ⁻⁷
73-26	Baker Creek	<i>a</i> θ	55	354	35	0.001
73-26A	Baker Creek	<i>a</i> θ	27	291	83	<10 ⁻⁸
73-26B	Baker Creek	<i>a</i> θ	28	063	93	<10 ⁻¹⁰
73-28	Baker Creek	<i>a</i>	7	049	97	0.001
73-29	Cape Vesey Hamilton	<i>a</i>	31	021	72	<10 ⁻⁶
73-30	Cape Vesey Hamilton	<i>a</i> θ	63	351	90	<10 ⁻²¹
73-30A	Cape Vesey Hamilton	<i>a</i> θ	22	042	89	<10 ⁻⁷
73-30B	Cape Vesey Hamilton	<i>a</i> θ	26	340	96	<10 ⁻¹⁰
73-31	Mercy River	<i>a</i> θ	25	032	78	<10 ⁻⁶
73-35	Colquhoun River	<i>a</i> θ	8	176	94	<10 ⁻⁵
74-4,6	Nelson Head	<i>a</i> θ	5	248	90	0.018
74-4,6	Nelson Head	<i>r</i>	8	234	73	0.014
74-8	Nelson Head	<i>a</i> θ	8	171	87	0.003
74-11	Pass Brook	κ	29	187	26	0.144*
74-11A	Pass Brook	κ	16	231	93	<10 ⁻⁶
74-11B	Pass Brook	κ	13	081	81	<10 ⁻³
74-12	Sandhill River	<i>a</i> θ	29	344	40	0.009
74-12A	Sandhill River	<i>a</i> θ	10	211	71	0.007
74-12B	Sandhill River	<i>a</i> θ	19	000	82	<10 ⁻⁵
74-14	Schuyter Point	<i>a</i>	4	020	54	0.316*
74-14	Schuyter Point	κ	5	303	99	0.008
74-15	Alexander Milne Point	<i>a</i> θ	33	228	36	0.015
74-15A	Alexander Milne Point	<i>a</i> θ	17	049	68	<10 ⁻³
74-15B	Alexander Milne Point	<i>a</i> θ	16	228	89	<10 ⁻⁵
74-16	Alexander Milne Point	<i>a</i> θ	13	262	71	0.001
74-18	Alexander Milne Point	<i>a</i> θ	22	261	88	<10 ⁻⁷

GSC

Number of observations	n
Weighted mean azimuth (Miall, 1974e)	$\bar{\theta}$
Vector magnitude (per cent)	L
Probability of directional randomness (Rayleigh test)	p
Mean azimuth not significant at 95% confidence level	*
Greek-letter structure names assigned by Allen, 1963	<i>a</i> , θ , κ
Small-scale, asymmetric ripple-marks	<i>r</i>

with a limited geographic distribution, and are not used in this report.

The field sampling hierarchy

Olson and Potter (1954) proposed establishing a rigorous sampling hierarchy to allow calculation and comparison of directional variance at different levels of geographical sample scale; for example, bedding plane, bedding unit, outcrop, group of outcrops. The purpose of this method was to determine by statistical techniques the most efficient sampling plan for defining regional transport directions. Few workers have followed this approach because, in most cases, sedimentary structures are not common enough or exposure is too rare. This is the case in the present study, in which the object has been to gather as many paleocurrent readings as possible without attempting to select structures according to a predetermined sampling plan (except for the vertical profiles).

Olson and Potter's (1954) approach takes no account of the sediment structure hierarchy (Allen, 1966; Miall, 1974e) which relates directional variance on different sampling scales to the cause of that variance, in terms of the size of the physical unit (meander belt, channel reach, braid bar) under study. Field data that can be related to the structure hierarchy

clearly will give more information than just regional transport directions. For example, estimates of river size and sinuosity may be obtainable. To gain this type of information, the sampling plan must be empirical; it must be devised to bring out local variations on all scales and should be modified to suit the results as work proceeds. Useful results have been obtained in the Isachsen Formation as a result of using such a method.

It is necessary, however, to use Olson and Potter's approach to test for the validity of individual crossbed readings. One planar crossbed set was studied in detail to assess the importance of within-set (i.e., within-bar) directional variability. The chosen set is at Station 73-MLA-30 (Fig. 18) and is particularly well exposed on two sides of a spur, in the angle between two steep-sided gullies. The exposure extends laterally for 11 m (36 ft) on a north-facing slope and 13 m (43 ft) on an east-facing slope. Part of the latter is shown in Plate 1. At 27 points along this outcrop, approximately every 90 cm (35 in.), measurements were taken of set thickness, angle of foreset dip and foreset dip direction. Accuracy of the orientation measurements to within three or four degrees was obtained by sculpturing the soft sand with a shovel until the outcrop coincided with the strike direction of the dipping foreset bed, and then taking the average of at least three independent measurements of orientation with the Brunton compass held perpendicular to the outcrop. Similar procedures were carried out for all the paleocurrent measurements in the Isachsen Formation.

The statistics of the lateral variability are as follows (calculated using the equations of Curray, 1956):

number of readings	27
vector mean azimuth	045°
variance	93
vector magnitude	99.2%
95% confidence limits on mean	±3.8°
probability of randomness	<10 ⁻¹¹
crossbed set thickness ranges from	13.5 to 42 cm
foreset dip ranges from	24° to 35°

One way of visualizing the directional variability is to consider that if 27 readings were made on a second bar deposit, and assuming a similar variance, *t*-test statistics (one-tail test) show that, at a 95 per cent confidence level, a difference of as little as 4.4° between the mean azimuths of the two bars would be statistically significant.

The degree of directional variability in this crossbed set is similar to that which may be seen in exposures of modern braid bar deposits, as illustrated by Smith (1972, Fig. 7) and the results serve to define the type of variance that probably is present in other crossbed sets in this exposure. Time limitations prevented a detailed study of any other laterally extensive and well exposed crossbed sets in the five vertical profiles.

Five of the localities listed in Table 3 have been divided into sublocalities, because field work demonstrated that separate sets of homogeneous, directionally unimodal data with different azimuth means could be obtained in different parts of the outcrop. At Stations 73-26 and 73-30 the sets are vertically (stratigraphically) separated within the outcrop. These are two of the five vertical profiles discussed in detail

later in this report (and *in* Miall, 1976b). At the other three field stations, the data sets are derived from different parts of the outcrop that are laterally (stratigraphically) equivalent to one another.

Current rose diagrams for each station or substation listed in Table 3 are shown in Figure 21. The diagrams have been drawn with segment radius proportional to square root of per cent of readings. Per cent of total readings is therefore proportional to segment area. Figure 22 is an interpretative map in which local, measured paleocurrent trends are extrapolated to arrive at a regional paleoflow pattern. A discussion of these diagrams follows.

Interpretation 1. Areal paleocurrent variation

Southern Banks Island. In the southeastern part of the island near Alexander Milne Point (Stations 74-MLA-14, 15, 16, 18), measured paleocurrent trends are fairly consistently from the east, with the exception of a local vector at substation 74-MLA-15A that indicates northeasterly directed flow (Fig. 21). These results were derived predominantly from planar crossbedding, which some authors (Agterberg *et al.*, 1967; High and Picard, 1974) have found to be less reliable than trough crossbedding as a paleocurrent indicator. Their interpretation of this difference in reliability was that planar crossbeds represent the slipoff faces of bars oriented obliquely to the current direction, whereas trough axes coincide more closely with stream direction. The results from Alexander Milne Point show a fair degree of internal consistency, which would indicate that planar crossbedding can be a reliable paleocurrent indicator. However, the distributions at Stations 74-MLA-15B, 16 and 18 are bimodal, indicating that the suggested origin of the structures in obliquely oriented bars may be correct in this case.

The current pattern at substation 74-MLA-15A is an anomaly for which there is no immediate explanation. It may represent local meandering but such strongly divergent current directions are not characteristic of the braided stream environment.

It is important to note that the flow directions are perpendicular to the axis of Cardwell Basin, as delineated by gravity data (Fig. 4). This is regarded as strong evidence that the basin was beginning to develop during Isachsen time and that the paleoslope direction along the craton edge (the east side of the basin) was controlled by subsidence along the present axis of the basin. Moreover, the facies of the Isachsen Formation at Alexander Milne Point is proximal; therefore, as their present position would suggest, these deposits may represent sedimentation at the edge of the basin rather than near the centre. There is no evidence that the west side of the present basin, corresponding to the flank of De Salis Uplift, was a distinct topographic feature at this time.

At Pass Brook (Station 74-MLA-11) and Sandhill River (Station 74-MLA-12), current directions are strongly bimodal). At each outcrop the two data sets were derived from sublocalities that are stratigraphically closely equivalent. How a fluvial system could give rise to current directions that are virtually at 180° to each other must therefore be explained. The most probable explanation is that the two modes represent different channel reaches in a strongly meandering river or delta distributary. As discussed in a previous section,

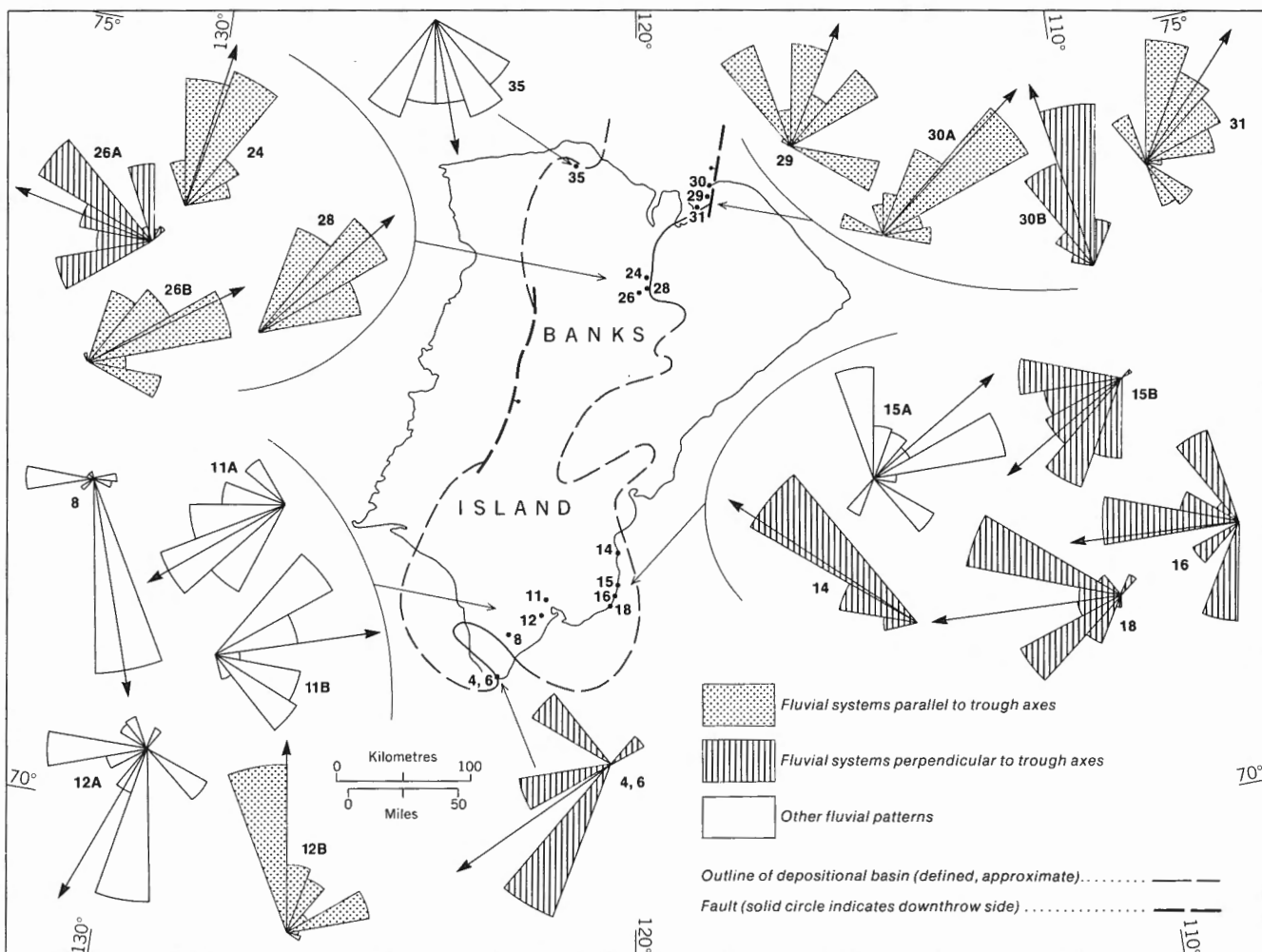


Figure 21. Paleocurrent rose diagrams, Isachsen Formation. (Segment radius proportional to square root of per cent of total readings.) Statistical data are provided in Table 3.

lithofacies types suggest a meandering river or deltaic environment. Bimodal paleocurrent distributions may indicate wave or tidal influences but only if the bimodality is derived from structures that are interbedded with each other, as in herringbone cross-stratification.

The fact that part of the section at Sandhill River is marine and is possibly of early Christopher age does not detract from the regional synthesis shown in Figure 22. The marine transgression at the beginning of Christopher time was probably not accompanied by any tectonic rearrangements, but represents simply a widespread eustatic raising of fluvial base levels. The position and orientation of fluvial systems entering the expanding sea therefore would not have changed; the streams themselves would merely have become more sluggish.

Another anomalous current direction is the southwardly directed flow indicated by the data from Nelson River (Station 74-MLA-8). Statistically the mean direction is significant but it is based on only eight readings and may not have any meaning on a regional scale. It may represent, however, the edge of a fluvial system (for which there is no other

evidence) entering the Banks Island area from the southwest, flowing around the land area from which the Nelson Head fan was derived and merging with northward-flowing rivers in the middle of the alluvial plain near the present Masik River (Fig. 21).

It was noted above that the paleocurrent data at Alexander Milne Point provide evidence for the early appearance of Cardwell Basin. Similar conclusions can be drawn from much of the data derived from northern Banks Island, as discussed below. The outcrops at Sandhill River and Pass Brook are located almost on the crest of De Salis Uplift (Fig. 4) but current directions have no obvious relationship to the configuration of the uplift, and it would seem that the structure is entirely of post-Isachsen age.

Lastly, a limited amount of paleocurrent data was obtained from the Isachsen Formation at Nelson Head. This is shown in Figure 23 together with observations on clast size variations. Paleocurrent information indicates a southwesterly directed paleoslope, at an oblique angle to the trend of the graben. Measurement of stratigraphic sections shows an increase in thickness of the basal coarse unit of the Isachsen

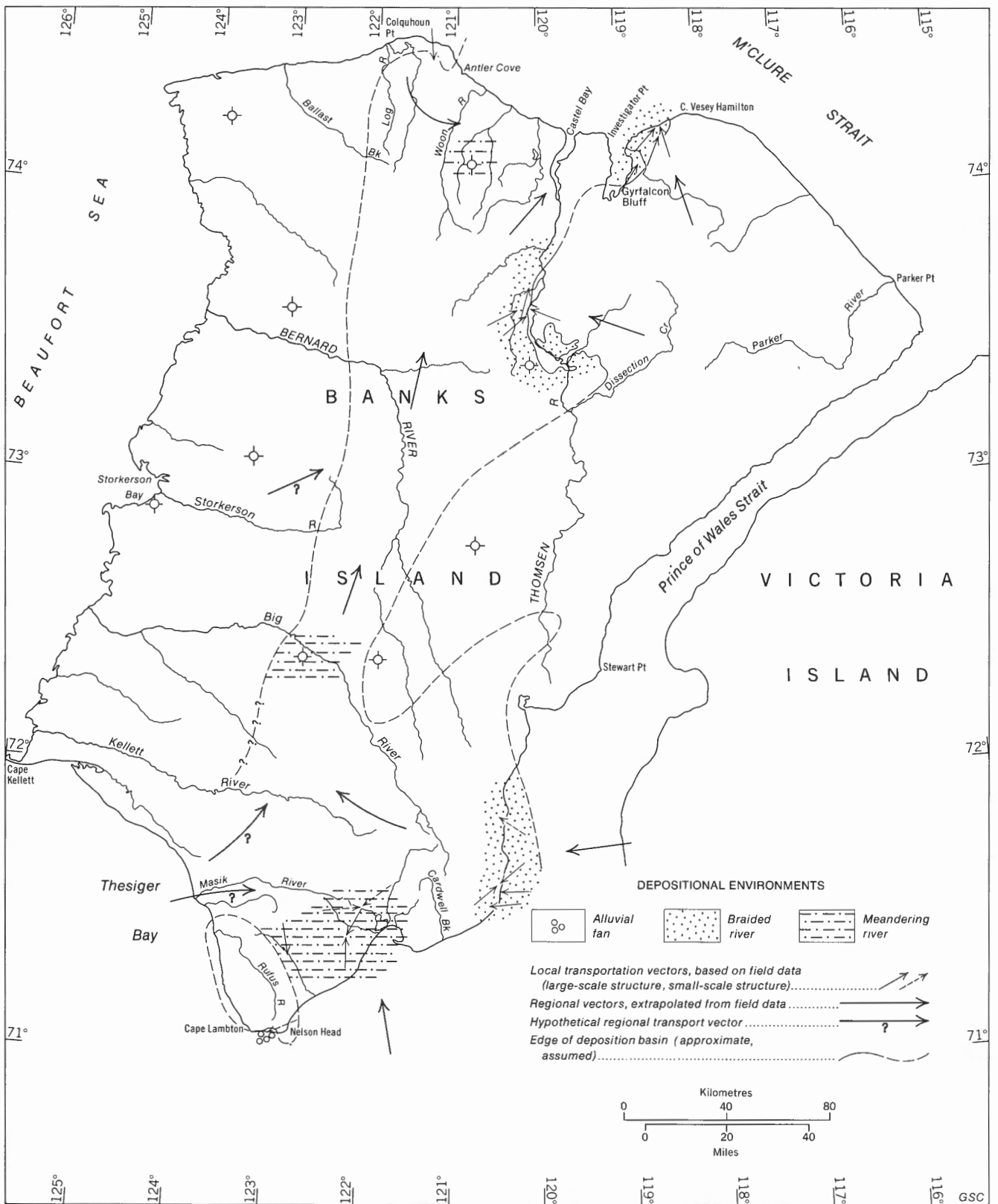


Figure 22. Interpreted transport directions and facies distribution, Isachsen Formation.

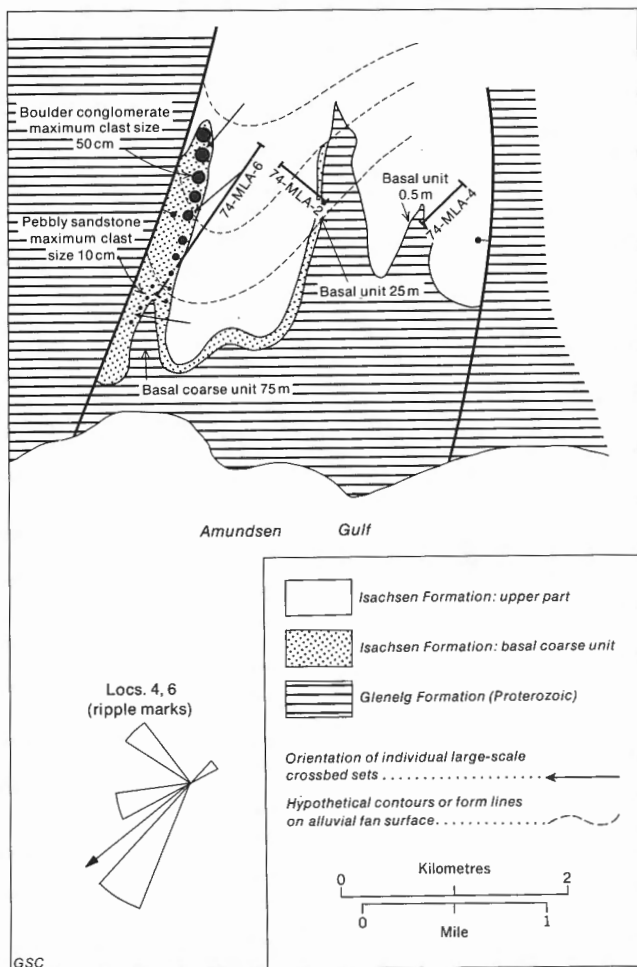


Figure 23. Geological sketch map of the Nelson Head Graben, showing local variations in thickness, clast size and transport directions, Isachsen Formation.

from east to west. A traverse along a small stream valley below Station 74-MLA-6 shows that clast size decreases southward. The interpretation of these data is that the Isachsen Formation in the graben represents a small alluvial fan, which entered the graben from the northeast. There is insufficient evidence to demonstrate conclusively that the graben itself was active at the time but the coarseness of the conglomerates would suggest local, tectonically induced uplift. The Isachsen Formation is absent on either side of the graben and probably was not deposited there, indicating that the sides of the graben were uplifted, as they are now. The alluvial fan may have been channeled toward and alongside the western bounding fault, as suggested by the hypothetical contours, or form lines, in Figure 23.

The thick fining-upward cycles at Castel Bay C-68 and Orksut I-44 indicate a major meandering river at these localities. There may have been a single trunk stream flowing along the axis of Banks Basin but the direction of flow is uncertain. Data from the margin of Northern Banks Basin indicate that northeasterly flow was predominant and, for this reason, the major river system in Banks Basin is assumed to have flowed in the same direction.

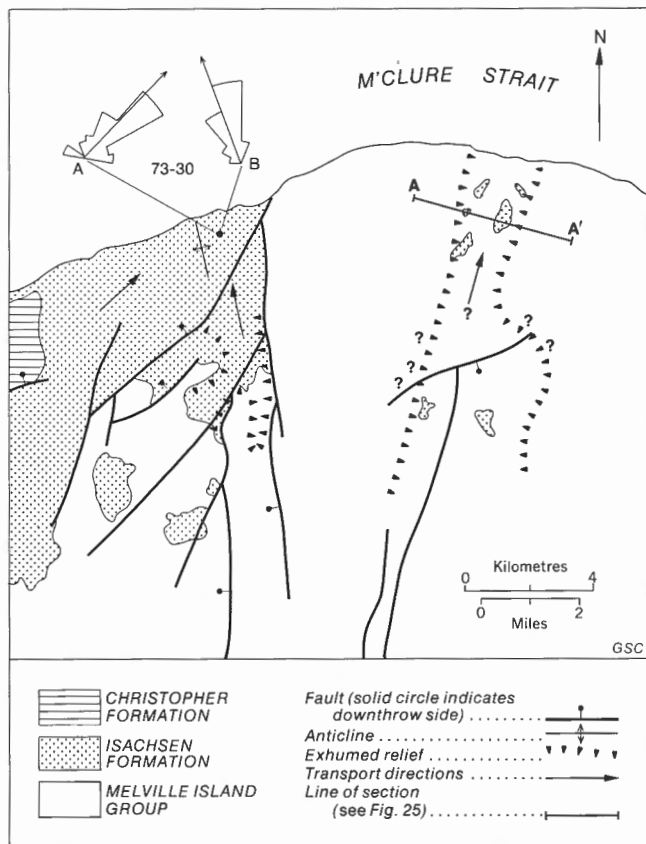


Figure 24. Geological sketch map of Cape Vesey Hamilton area (Station 73-30) showing exhumed Cretaceous relief and local transport directions.

Northern Banks Island. Northeasterly directed flow is indicated consistently by data from Stations 73-MLA-24, 26B, 28, 29, 30A and 31. This trend is parallel to Bouguer anomaly contours and to the axis of Northern Banks Basin (Fig. 4) and suggests that longitudinal flow was predominant. All the control points are located on the edge of the basin and are in the proximal, braided stream facies.

The origin of the longitudinally flowing streams is suggested by data from substations 73-MLA-26A and 30B, where mean azimuth trends show a northwesterly orientation. These two stations are parts of vertical profiles, which are described in greater detail in the next section. A preliminary interpretation of their significance in terms of regional paleocurrent trends follows. At substation 73-MLA-30B the mean current direction differs by 62° from that of the underlying beds, which constitute substation 30A. A geological sketch map of the area is given in Figure 24 and shows the partly fault-controlled contact between the Isachsen Formation and the underlying Melville Island Group (Devonian). Two exhumed Cretaceous stream valleys have been mapped on the eroded Devonian surface. They are broad, shallow features containing outliers of the coarse sand facies; one of the valleys is occupied by a small lake, the other (Fig. 25) has been deeply incised by modern gully erosion. Station 73-MLA-30 lies immediately to the north of one of the two valleys and the mean azimuth in substation 30B is similar to the orientation of this valley. The beds at substation 30B are interpreted as

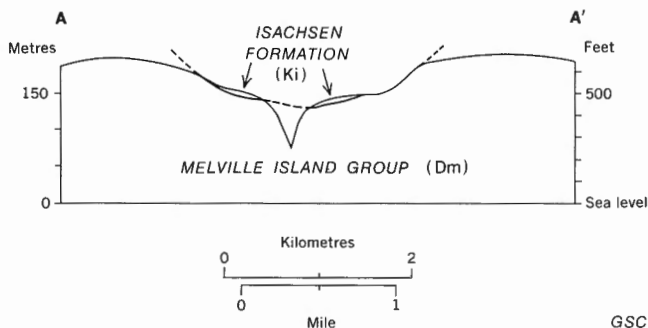


Figure 25. Cross-section along A-A' (Fig. 24) showing exhumed Cretaceous valley incised by modern gully erosion.

the deposits of a braided tributary stream, which flowed across the Devonian plateau and merged with the northeasterly flowing fluvial system of the Banks Basin alluvial plain when it emerged from the uplifted source area at Cape Vesey Hamilton.

A similar situation probably prevailed at Station 26 (Baker Creek) where the substation azimuth means differ by 132°. No clearly demonstrable exhumed valleys have been recognized but the outliers of the coarse sand facies in the White Sand Creek area may represent the fill of a broad, northwest-oriented valley along which sediment was channeled into Banks Basin. The Isachsen Formation is absent at Dissection Creek (Fig. 9), possibly because this area represented part of an elevated watershed to the south of the White Sand Creek valley. Unfortunately paleocurrent directions could not be measured in the White Sand Creek area because good exposure was scarce. (A further discussion and alternative interpretation of the data from Baker Creek are given under the heading Vertical Paleocurrent Variation.)

At Colquhoun River (Station 73-MLA-35) the paleocurrent directions are unimodal and are directed southward. The beds at this locality are interpreted as marine shoreface deposits and paleocurrents probably have a different meaning from the fluvial paleocurrents that have been under discussion up to this point. The Isachsen is absent between Cape Crozier and Cape Wrottesley (two 'abs' control points west of Antler Cove on Fig. 9); the Christopher Formation rests directly on the Melville Island Group (Devonian). What is now the northern part of Banks Island therefore may have represented part of the land area on the west side of Banks Basin. The coastline during the latest Isachsen marine phase, represented by the Colquhoun River exposure, must, therefore, have lain to the north of Station 73-MLA-35. Southward-directed paleocurrents are interpreted as representing sedimentary structures formed during ebb-tide runoff. The trough and planar crossbedding probably formed in tidal channels and the small-scale ripple marks represent late-stage sheet runoff. The internal morphology of the ripple marks indicates an origin under the influence of southward-directed currents, even though their external morphology (Fig. 20) may have been the product of wave action (oscillatory currents).

The marine Isachsen deposits at Colquhoun River probably formed as a result of the drowning of a pre-existing topography during the Albian transgression. Paleogeographic information derived from such rocks therefore is considered to be valid for the remainder of Isachsen time. The coastline

north of Colquhoun River is interpreted as the boundary between the alluvial plain and the elevated source area during the Barremian and Aptian stages.

No information regarding paleocurrent directions is available from any other locality on the west side of Banks Basin because the entire area is covered by younger rocks. The Isachsen Formation is absent at the Bar Harbour E-76, Storkerson Bay A-15, Nanuk D-76 and Uminmak H-07 wells, indicating that the Storkerson Uplift and Big River Basin areas probably were land at the time. How important they were as a sediment source during the Barremian and Aptian is impossible to determine at present.

Interpretation 2. Vertical paleocurrent variation

At five locations in the coarse sand facies (Fig. 18) measurements were made along vertical traverses up the outcrop. Foreset dip and orientation and structure thickness were recorded for every crossbed set encountered on the traverses. At two of the locations, as discussed in the previous section of this report, current directions show a marked change in orientation between the base and the top of the profile. Meandering on a smaller scale is shown by all of the profiles; this and other characteristics are the subject of the next few paragraphs of the report and they lead to some detailed refinements of the braided stream model for the coarse sand facies. (Much of what follows was discussed by Miall, 1976b.) The data are summarized in Table 4 and in Figures 26 to 30.

The figures are each divided into six columns. On the left is a diagrammatic representation of the lithologies and sedimentary structures in the section (lithological legend is given with Fig. 29). Column 2 shows the azimuth of each planar or trough crossbed, with gaps in the graph corresponding to planar-bedded or massive sand units. Column 3 is a plot of the moving average mean azimuth, using a moving set of ten readings, weighted by cube of crossbed set thickness, according to the method of the writer (Miall, 1974e). Column 4 is a

Table 4. Summary of field data for five vertical profiles through the coarse sand facies, Isachsen Formation

Locality	n	$\bar{\theta}$	L	S ²	c	p	M _t	M _d
74-18	22	261	88	900	± 13.2	<10 ⁻⁷	30.2	20.7
73-26	28	054	80	1400	± 14.5	<10 ⁻⁷	27.7	25.1
73-26A	8	346	99	30	± 4.5	<10 ⁻³	25.6	24.1
73-26B	20	068	94	420	± 9.6	<10 ⁻⁷	28.5	25.5
73-29	30	021	72	2260	± 17.7	<10 ⁻⁶	40.3	23.8
73-30	63	351	90	680	± 6.6	<10 ⁻²¹	38.2	25.9
73-30A	22	042	89	840	± 12.8	<10 ⁻⁷	26.1	25.4
73-30B	26	340	96	290	± 6.9	<10 ⁻¹⁰	46.3	26.3
73-31	25	032	78	1680	± 16.9	<10 ⁻⁶	36.4	25.7

GSC

Number of observations	n
Weighted mean azimuth (Miall, 1974e)	$\bar{\theta}$
Vector magnitude (per cent)	L
Variance	S ²
95% confidence interval on the mean	c
Probability of directional randomness at 95% confidence level (Rayleigh test)	p
Mean set thickness	M _t
Mean foreset dip	M _d

ALEXANDER
MILNE POINT

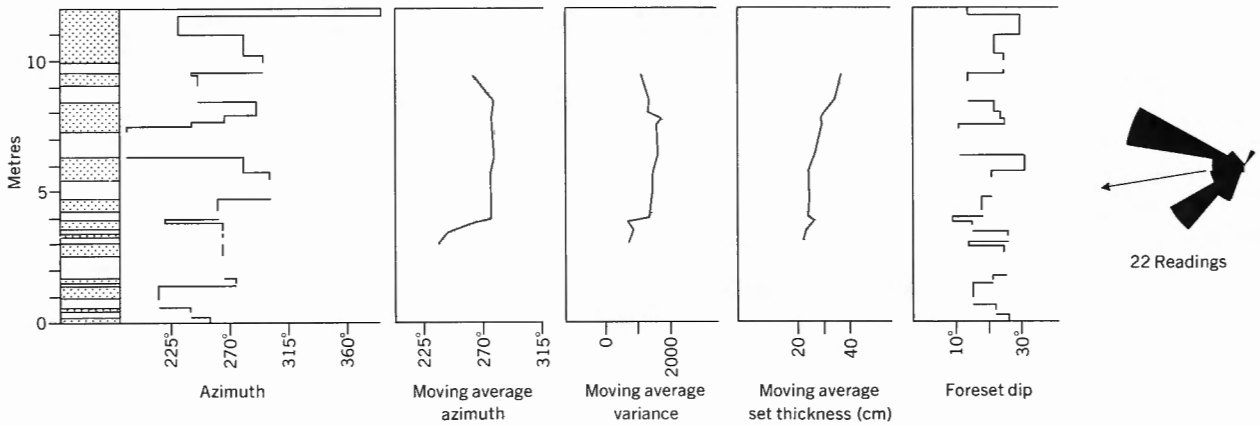


Figure 26. Vertical profile at Station 74-MLA-18.

BAKER
CREEK

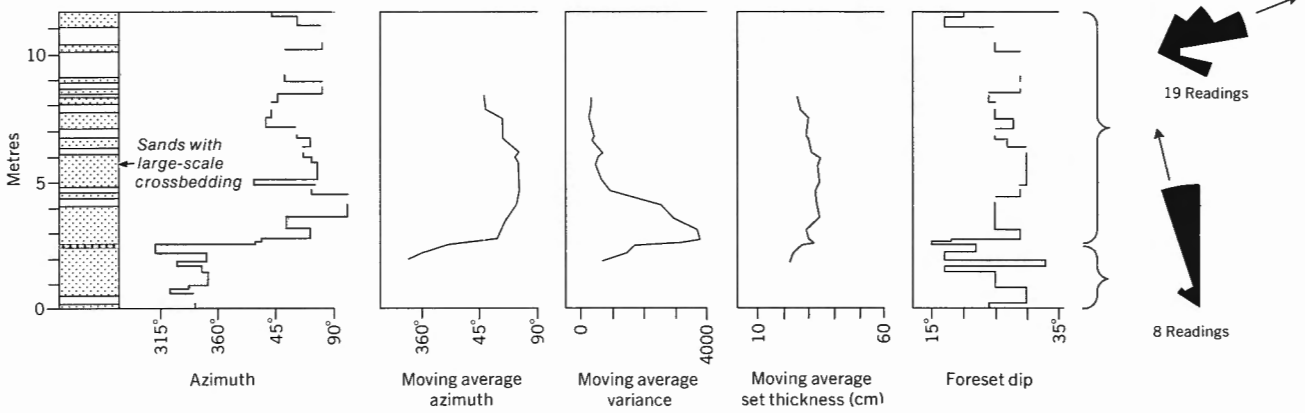


Figure 27. Vertical profile at Station 73-MLA-26.

CAPE VESEY
HAMILTON

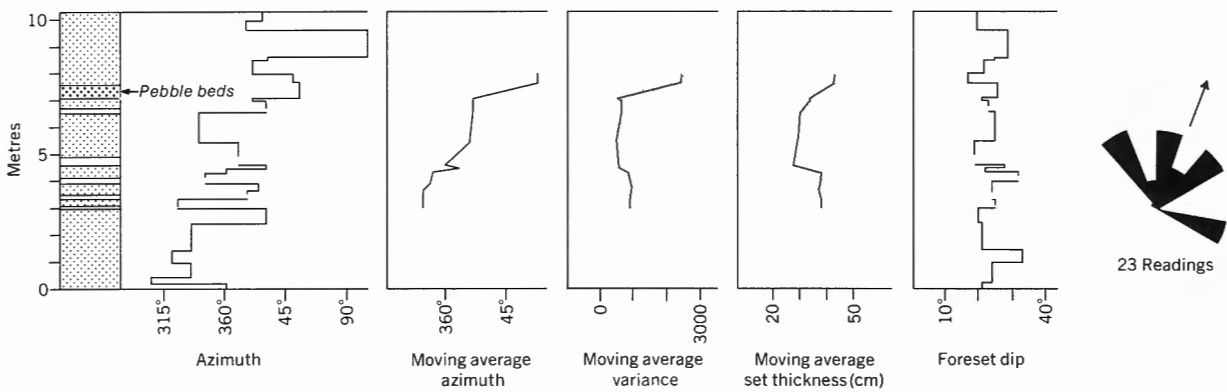


Figure 28. Vertical profile at Station 73-MLA-29.

GSC

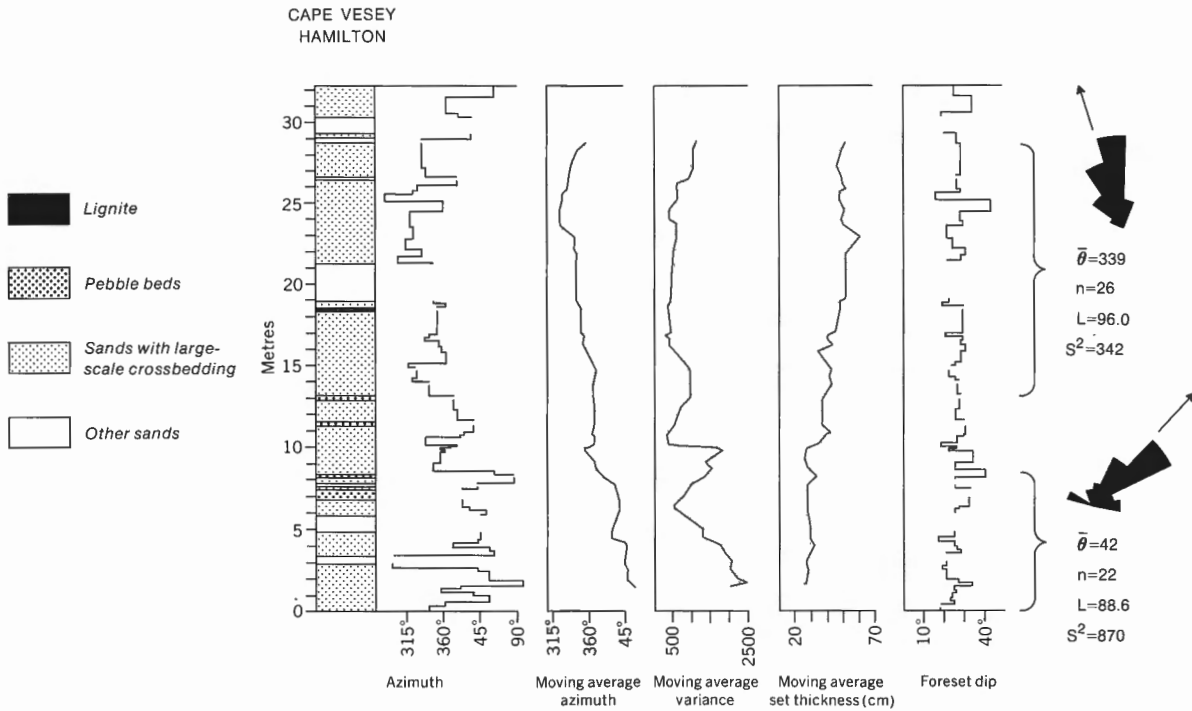


Figure 29. Vertical profile at Station 73-MLA-30.

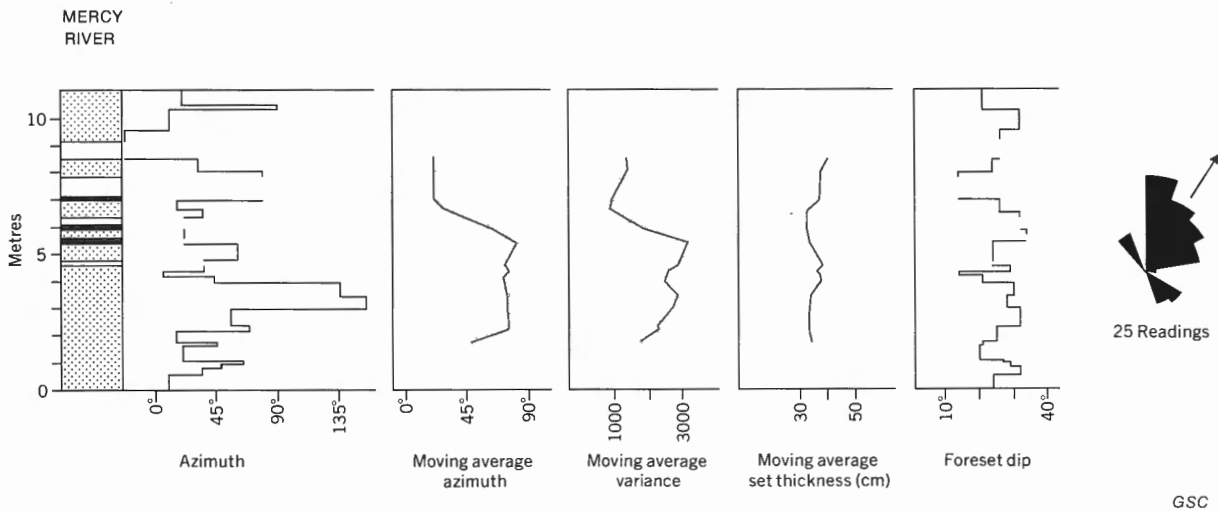


Figure 30. Vertical profile at Station 73-MLA-31.

plot of weighted, moving average directional variance, column 5 shows moving average set thickness, and column 6 shows individual measurements of foreset dip.

All five profiles show marked changes in mean current direction between the base and the top of the exposures. To emphasize these changes the two profiles illustrated in Figures 27 and 29 have been divided into segments and the directional and other parameters have been recalculated for each segment, as shown in Table 4. The differences in azimuth distribution are readily apparent from the current rose diagrams on the right of the figures.

The moving average mean azimuth is interpreted as a measure of the changes in orientation of the entire river tract

(Ranks 2 and 3 variability of Miall, 1974e). The choice of ten readings, rather than some other number, with which to calculate the average, is arbitrary but the fact that the moving average plots as a relatively smooth curve without damping out any of the vertically persistent directional fluctuations suggests that the chosen method is reasonably appropriate.

It is assumed that a measurement of foreset orientation at one point within each crossbed set is sufficient to define the bar orientation. As shown in an earlier section, within-bar variance is small. It may be compared with between-bar variance in the following manner. If it is assumed that moving average azimuth, as calculated, is an accurate measure of orientation of the braided channel system, then within-

channel, between-bar variance may be measured by summing the squared deviations about the moving average. Thus, when the orientation data in the profiles are transformed by subtracting the moving average mean at each point from the actual value at that point, the total range of readings over the five profiles is 186° , the variance is 980, and the 95 per cent confidence limit on the mean is $\pm 5.9^\circ$ (111 readings). Between-bar variance is therefore an order of magnitude greater than within-bar variance. Application of the F-test shows the difference to be significant at the 99.9 per cent confidence level.

The between-bar variance is of a similar order of magnitude to the variance shown by small-scale sedimentary structures and minor channels in low sinuosity reaches of the modern Donjek River, Yukon Territory (Williams and Rust, 1969, Fig. 23 and p. 673; Rust, 1972, Table II). However, it is considerably less than that obtained by measurements on avalanche faces of transverse bars in the Platte River, Nebraska (Smith, 1972, Figs. 12, 13). Other comparisons may be made by examining Table I in Miall (1974e). Smith (1972, 1974b) assumed that measurements on avalanche faces would be a valid way of measuring foreset orientations in planar crossbeds. But, as he stated in his later paper (1974b, p. 269), "the problem of 'preservability' hangs over any study of modern sediments attempting to predict or explain characteristics of ancient deposits." Not all avalanche faces necessarily have an equal chance of preservation as foreset beds, as argued by Banks and Collinson (1974). They suggested that downstream progradation will tend to favour faster growth and greater chances of preservation of foresets which are located on the downstream ends of braid bars, versus those developing on lateral margins. It is felt that the results of the present study, which indicate relatively low within-channel variance, demonstrate the reality of processes of selective preservation such as those described by Banks and Collinson (1974).

Much of the variation in the moving average probably can be attributed to the downstream migration of meanders. Braided streams characteristically are composed of several or many channels, so that what is referred to here is meander migration in the channel system as an entity. At Stations 74-MLA-18 (Fig. 26) and 73-MLA-31 (Fig. 30), the moving average azimuth swings through a maximum angular range of 43° and 61° , respectively. This is similar to the downstream changes in orientation of many modern braided channel systems. For example, a low-sinuosity reach of the braided Donjek River (Williams and Rust, 1969, Figs. 23, 24; Rust, 1972, Fig. 2B) showed a change in mean orientation of approximately 40° over 6 km (3.7 mi).

The next largest vertical changes in mean azimuth are shown by the sections at Stations 73-MLA-26 (Fig. 27) and 73-MLA-29 (Fig. 28), where the mean swings through maximum ranges of 89° and 85° , respectively. These changes also could have been caused by downstream meander migration, although the greater angular changes at these localities indicate greater sinuosities. A comparison with a high-sinuosity reach of the Donjek River is suggested (Area 3 of Rust, 1972, Figs. 2D, 11). The main channel swings through 90° over less than 2 km (1.2 mi) in this example.

At Station 73-MLA-26 (Fig. 27) the vertical change in

azimuth is very abrupt, as shown by the plot of mean azimuth and by the current rose diagrams. The abruptness of the change justifies dividing the vertical profile into two segments A and B and calculating separate directional parameters for each segment (Table 1). The contact between the upper and lower segments is marked by a pebble bed 5 cm (2 in.) thick, although pebbles are scarce throughout the rest of the section. This suggests a temporary raising in energy levels and a resultant rapid but short-lived increase in the rate of change of channel and bar orientations. In a flash flood the channel system could have been altered completely and, when more 'normal' depositional conditions were resumed, the local channel orientation might well have altered by several tens of degrees. As discussed in the previous section, the beds represented by substation 26A may have been deposited by a fluvial system entering Banks Basin from the east. Longitudinal flow at this locality would, under this interpretation, have been established (or re-established) following a flash flood. The angular change of 132° between substations A and B is thought to be too great to be accounted for in terms of rapid downstream meander migration, for braided streams are characteristically of low sinuosity (Schumm, 1963, 1968b). A third possibility, that the divergence at Station 73-MLA-26 represents deposition under falling water conditions following a high flood level, was discussed by the author (Miall, 1976b).

The change in current orientation at Station 73-MLA-30 has been discussed in the previous section. An analysis of Figure 29 provides further important information. The lower part of the section shows northeasterly directed paleocurrents; those in the upper part are north-northwesterly directed. Other vertical changes include an upward decrease in directional variance and an upward increase in set thickness (Table 4, and columns 4, 5 in Fig. 29). The plot of moving average variance shows a peak corresponding to the interval in the section over which the mean direction makes its most sudden change. A comparison of the variance in segments A and B using the F-test shows that the difference is significant at the 99 per cent confidence level. The difference in mean set thickness between segments A and B also is significant at the 99.5 per cent confidence level, as determined using the Welch-Aspin test. (*t*-statistics cannot be used in this case, owing to highly significant differences in the set thickness variances. The Welch-Aspin test is described by Bennett and Franklin, 1954, p. 177.)

The upward decrease in directional variance and the upward increase in set thickness are interpreted as the result of an increase in stream competency with time. The reasons for this are as follows: directional variance is proportional to sinuosity and inversely proportional to meander wavelength. As stated by Schumm (1968b, p. 1579), the greater the flow of water the larger will be channel width, depth and meander wavelength and the smaller will be channel gradient. Allen (1968, Fig. 6.4) shows that crossbed set thickness is a function of mean water depth. Lateral changes in set thickness in ancient rocks have been reported by Schwarzacher (1953), Momin Ul Hoque (1968) and Kumar and Bhandari (1973), all of whom observed that thickness decreases in the direction of indicated current flow when measured over distances in the order of a few tens of kilometres. Set thickness variations, therefore, may be used as a relative proximal/distal indicator.

An increase in stream competency with time is the reverse of what would be expected given conditions of tectonic stability and unchanging climate. There is no reason to suspect climatic changes during Isachsen time but some degree of local tectonic instability is indicated by the fact that the formation consists of medium sand- to boulder-size material, the erosion and transportation of which requires the creation of relatively strong relief. As shown in Figure 24, the contact between the Isachsen and the underlying Devonian rocks is partly fault controlled. The interpretation of the outcrop and sedimentological data is that the beds at substation A were deposited by part of the regional stream system which flowed northeastward along Banks Basin. Uplift within the source area east of Banks Basin, possibly localized along one or more of the faults noted above, had the effect of rejuvenating the streams entering the east side of the basin. The stream to the south of Station 73-MLA-30 probably flowed into and was absorbed by the regional stream system until the rejuvenation took place. At that time, flow along it increased so that its depositional influence extended northward and the deposits of segment B were formed. Pebble beds in the section between the 7 and 13 m (23–43 ft) levels (Fig. 29) suggest that several major flood events took place while the fluvial pattern was changing.

Grain size analysis

Grain size analyses were performed on 34 sand samples from the Isachsen Formation. Sands with a significant proportion of granule or larger clasts (> 2 mm) were not collected owing to the necessity to analyze increasingly larger samples with coarser mean grain sizes. Most of the samples are from large-scale planar crossbed sets. Moment measures calculated from the 34 samples are given in Table 5. Skewness and kurtosis are shown in this table but are not discussed herein owing to doubts concerning the precision of measurements in the fine tails of the distribution (*see* discussion under "Methods").

Causes of grain size variability

Grain size distributions are influenced by three primary independent variables in the fluvial environment: stream power, distance of transport, and size distribution of source material.

The interaction of these variables is liable to yield complex results and only an extremely detailed study may be able to separate the various effects in the deposit that is finally formed. For example, variations in source area geology and day-to-day or longer period fluctuations in discharge both will affect the grain size of the transported sediment.

In the present case a detailed study of the required complexity has not been carried out since most of the information that can be derived from such an analysis is more readily obtainable by other means. The results do, however, serve as independent confirmation of many deductions concerning the sedimentology of the Isachsen Formation.

A first level of interpretation is the analysis of the shape of the grain size distribution to deduce the environment of deposition. Visher (1969) and Glaister and Nelson (1974) discussed the techniques of such an approach. In the present

Table 5. Grain size data, Isachsen Formation (*see* Fig. 5 for location of samples)

MLA STATION NO.	C-NO.	PHI MEAN	MEAN (MM)	PHI VARIANCE	PHI STANDARD DEVIATION	PHI SKEW	PHI KURTOSIS
73-26	33342	1.8214	.2830	.4483	.6696	-.8689	6.8957
	33343	2.3965	.1899	.3933	.6272	-1.1130	11.4438
	33344	1.9315	.2622	.3964	.6296	-.4446	3.1030
	33345	1.7693	.2933	.7330	.8562	-.0673	.5483
	33346	1.6351	.3220	.8520	.9230	-.6197	2.7767
	33347	2.0244	.2458	.7801	.8832	-1.0122	6.1479
73-30	33360	1.5818	.3341	.3889	.6236	-.4247	2.8077
	33338	1.0019	.4993	.1996	.4468	1.1593	9.3500
	33337	1.8757	.2725	.1374	.3707	.2563	1.6127
	33336	1.9979	.2504	.1389	.3726	-.3423	6.0827
74-2	33335	1.8821	.2713	.1733	.4163	.7032	7.2000
	30462	2.0333	.2443	.5248	.7244	.6127	3.1514
	30465	2.2618	.2085	.3486	.5905	.0614	1.5345
74-4	30472	2.2223	.2143	.3348	.5786	.4177	2.5947
	30474	2.1579	.2241	1.0138	1.0069	-.1453	.7910
74-6	30476	1.8998	.2680	.4700	.6856	.4312	2.1091
	30477	1.8480	.2778	1.4240	1.1933	.0965	.0800
	30479	2.5286	.1733	.2935	.5418	.4484	1.9724
	30483	2.4324	.1853	.4189	.6472	.3685	1.6905
	30484	3.5381	.0861	.2057	.4535	-.4821	4.4525
74-8	30486	1.7603	.2952	1.0757	1.0372	-.0374	.4164
74-11	30492	3.3849	.0957	.2586	.5085	-.0939	3.5635
74-13	30495	2.6605	.1582	.2431	.4931	.4269	5.2304
74-14	30497	3.0156	.1237	.3745	.6120	-.2264	1.8454
74-16	30499	1.5594	.3393	.2161	.4649	.0815	4.2951
74-18	30503	1.7383	.2997	.3562	.5968	-.3432	2.6871
74-66	30575	1.6234	.3246	.5834	.7638	-.0743	2.0202
74-71	30576	.7824	.5814	.9672	.9834	.5535	1.8688
74-73	30578	1.5052	.3523	.6089	.7803	.3555	2.5070
74-74	30579	.5483	.6838	1.4901	1.2207	.5415	1.7767
74-90	30587	1.1659	.4457	.6938	.8330	.1712	2.9393
74-107	30595	3.8696	.0684	.5616	.7494	-1.0465	6.5696
74-108	30596	1.4398	.3686	.5186	.7201	.2158	1.3741
74-110	30597	1.4480	.3665	1.7582	1.3260	-.1880	.4949

GSC

case the fluvial, predominantly braided, depositional model has been demonstrated amply on the basis of vertical stratigraphic sequences and sedimentary structure assemblages.

Environmental interpretation

Cumulative distributions of eleven samples from the coarse sand (braided stream) facies are shown in Figures 31 to 34 (stations shown in Fig. 18). The curves have been plotted using a probability function, by which a perfect Gaussian distribution plots as a straight line. Departures from the straight line indicate less than perfect normal populations. Visher (1969) and Glaister and Nelson (1974) have demonstrated that fluvial sand deposits comprise three distinct but intermixed populations representing the three modes of sediment transport: traction, saltation and suspension. Each population is, ideally, log-normally distributed but because they show different degrees of sorting the populations plot with different slopes. The populations therefore should be capable of identification on the basis of recognizing inflexion points in the distribution curve.

Most of the eleven curves shown in Figures 31 to 34 are trimodal. A coarse, poorly sorted fraction and a fine, also

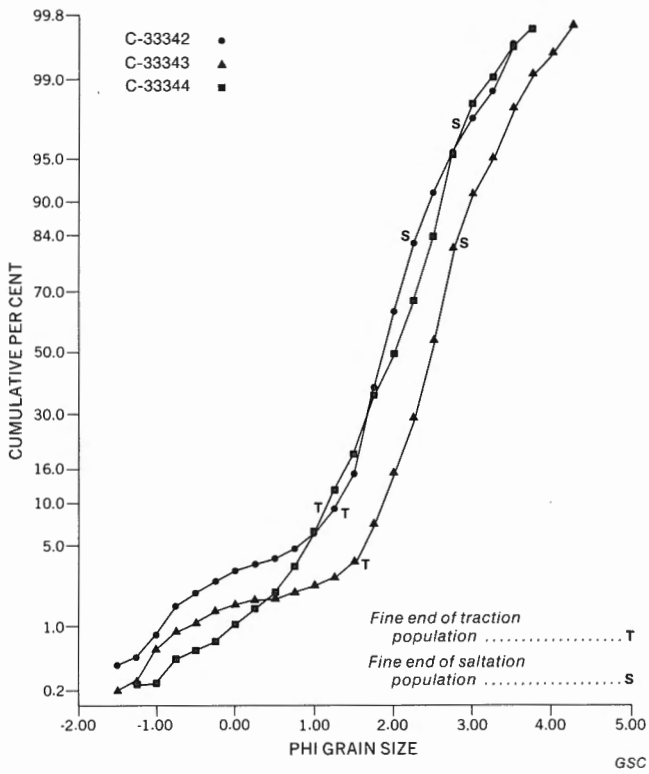


Figure 31. Grain size distribution curves, substation 73-MLA-26A.

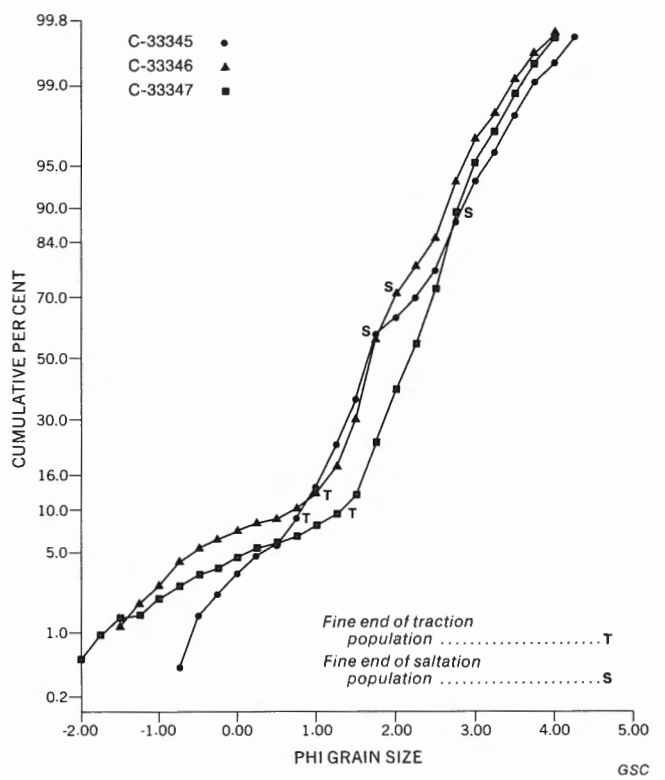


Figure 32. Grain size distribution curves, substation 73-MLA-26B.

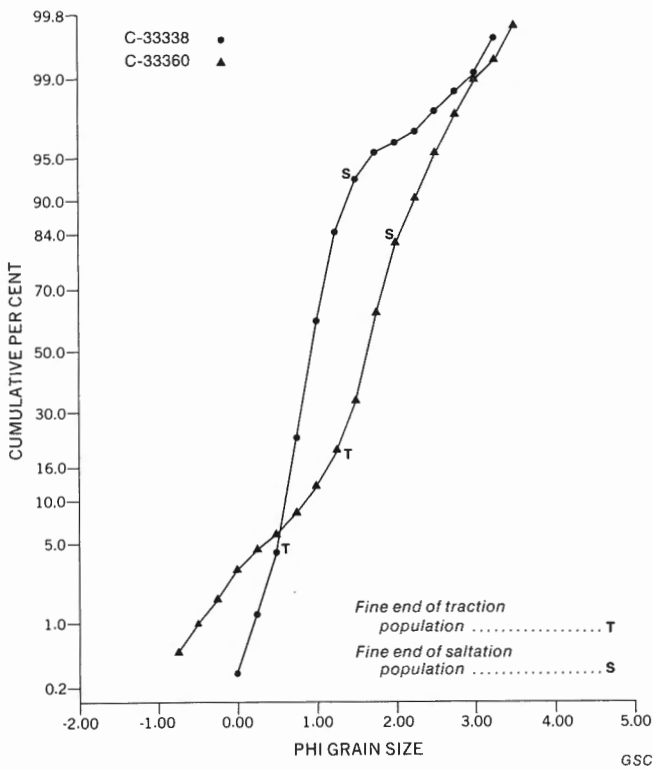


Figure 33. Grain size distribution curves, substation 73-MLA-30A.

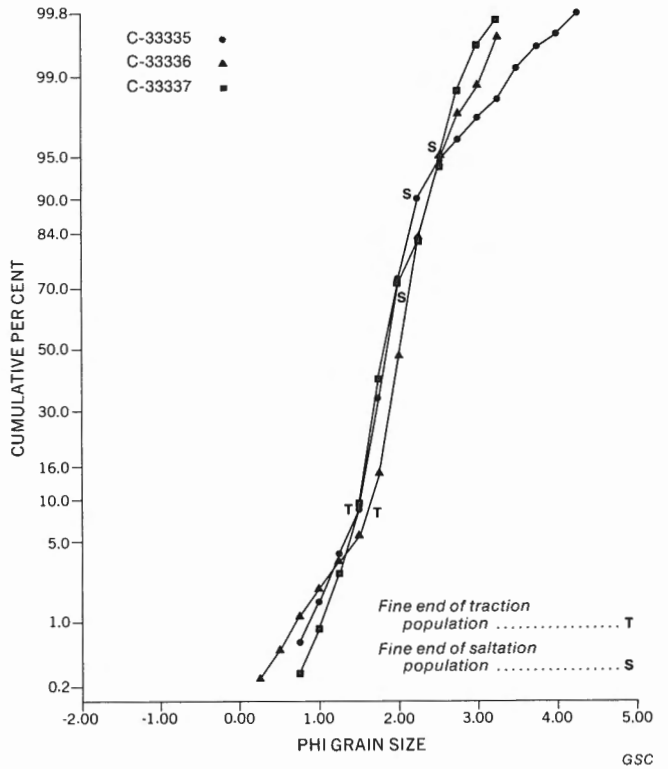


Figure 34. Grain size distribution curves, substation 73-MLA-30B.

poorly sorted fraction (low slope) are separated by a well sorted intermediate grain size fraction (steep slope). In some instances the inflexion points are well defined, as in Figure 34; in others, as in Figure 32, the populations intermix and overlap, and there is no sharp break in slope. Tentative identifications of the population limits are shown on the curves by the letters *T* and *S*. *T* indicates the fine end of the traction load fraction, and the segment *TS* corresponds to the saltation load. According to Visher (1972, p. 91), the size interval for this fraction typically is between 1.75 and 3 ϕ . Estimated proportions of the three fractions are as follows: traction load 5 to 16 per cent; saltation load 47 to 88 per cent; suspension load 5 to 46 per cent.

The rivers which deposited the coarse sand facies of the Isachsen have been interpreted earlier in this chapter as braided streams. According to Schumm (1968*b*), such streams are characterized by deposits containing in excess of 11 per cent bedload (traction load) fraction. Some of the deposits analyzed fall within this category; others are, on the basis of grain size criteria, of the mixed-load type, which contains 3 to 11 per cent bedload material. Sedimentary structure assemblages and sinuosity estimates (see "Paleohydrological Analysis") suggest that all the streams were of the bedload type, which points to a small, unaccountable discrepancy in the interpretations.

Visher (1969, 1972) and Glaister and Nelson (1974) defined typical curve shapes for fluvially deposited sand. Those presented in Figures 31 to 34 show significant differences from some of the supposedly characteristic curves of these authors. Visher (1972, p. 91) stated that saltation and suspension populations are predominant in fluvial sediments unless the sand is particularly coarse. Most of his examples (*ibid.*, Figs. 7–9) in fact show only these two populations; they probably represent mixed load and suspension load streams, in the terminology of Schumm (1968*b*).

Glaister and Nelson (1974, p. 217–219) discuss the curve shapes of deposits that are specifically identified as being of braided stream origin. They state that, except in special cases, the saltation population is of minor importance and typically (*ibid.*, Fig. 12) is less well sorted than the other two fractions. This is the reverse of the present case. The curves shown in Figures 31 to 34 are similar to only two of the nine typical braided stream distributions illustrated by Glaister and Nelson (1974, Fig. 5C, curve 2, Fig. 5D, curve 2). Nevertheless, the Isachsen samples are quite unlike most of those illustrated from other environments (*ibid.*, Figs. 6–12), and to that extent the test of the curve-shape analysis technique could be said to be successful.

Local and regional grain size variations

One of the most distinctive features of the sand analyses shown in Figures 31 to 34 is the predominance and good sorting of the saltation population. This is reflected in the moment measures for the entire distributions. Sorting values for the Isachsen sands range from 0.37 to 1.48, with an average of 0.73, which is the upper end of the "moderate sorting" range of Glaister and Nelson (1974, Fig. 1) and indicates better sorting than most of their braided stream samples. It is possible that the good sorting is inherited from the parent rock from which the Isachsen sands were derived.

The section on petrographic analysis demonstrates that most of the clastic grains are of multicyclic origin; they have been through several cycles of erosion and resedimentation and this will inevitably affect the characteristics of the final deposit. Such factors of regional geological origin may have a major effect on the usefulness of curve-shape studies.

Other local and regional variations in grain size characteristics are shown in Figures 35 and 36. Figure 35 shows the variation in phi mean grain size across Banks Island. No regional trends are apparent, which suggests that the effects of transportation in reducing the mean grain size are masked by other effects, such as local stream competency. The importance of the latter is demonstrated by the finer grained samples showing phi mean grain size of 3 or greater (mean less than 0.125 mm). Four such samples are listed in Table 5. Three of them were derived from beds showing small-scale ripple marks, as in Plate 18; the fourth was from a large-scale planar crossbed set. Simons *et al.* (1965, Fig. 21) and Friend and Moody-Stuart (1972, Fig. 27) showed that small-scale ripple marks are formed generally at lower flow velocities than are medium- and large-scale structures such as dunes, and are more common in finer grained sand.

Some interesting local variations are shown by the plot of mean grain size and sorting for two of the vertical profiles through the braided stream deposits (Fig. 36). Each profile has been divided into two segments, as discussed in the section on paleocurrent analysis. The upper and lower segments are characterized by different paleocurrent trends, as shown by the arrows in Figure 36 (north is toward the top of the diagram). Values for each segment cluster together and the following observations may be made on the arrangement of the clusters:

1. The deposits formed by the northwesterly flowing streams are more texturally mature (finer grained, better sorted) than those laid down by the northeasterly flowing streams.
2. Sorting at Station 73-MLA-30 is equal to or better than that at Section 73-MLA-26.
3. Within the deposits formed by flow along the edge of the basin (northeasterly directed paleocurrents) grain size increases in a downstream direction (i.e., from substation 26B to 30A).

In the section on paleocurrents, analysis of directional variance and structure size showed that the stream which formed the deposits at substation 73-MLA-30B was more competent than that which formed the underlying beds (substation 73-MLA-30A). Yet the sand of substation 30B is marginally more mature texturally. Other things being equal, a more powerful stream would be expected to transport coarser and more poorly sorted detritus. Probably this is not a case of the local availability of material. Petrographic analysis shows that very little local detritus is present in the Isachsen sands of northern Banks Island; probably most was derived from Minto Uplift, several hundred kilometres distant. It is possible, as will be discussed in later sections, that the northwesterly flowing streams in northern Banks Island are farther from source than are those flowing northeastward; this would account for the observed differences in textural maturity.

An added complication is the relationship between samples from substations 26B and 30A. Those substations

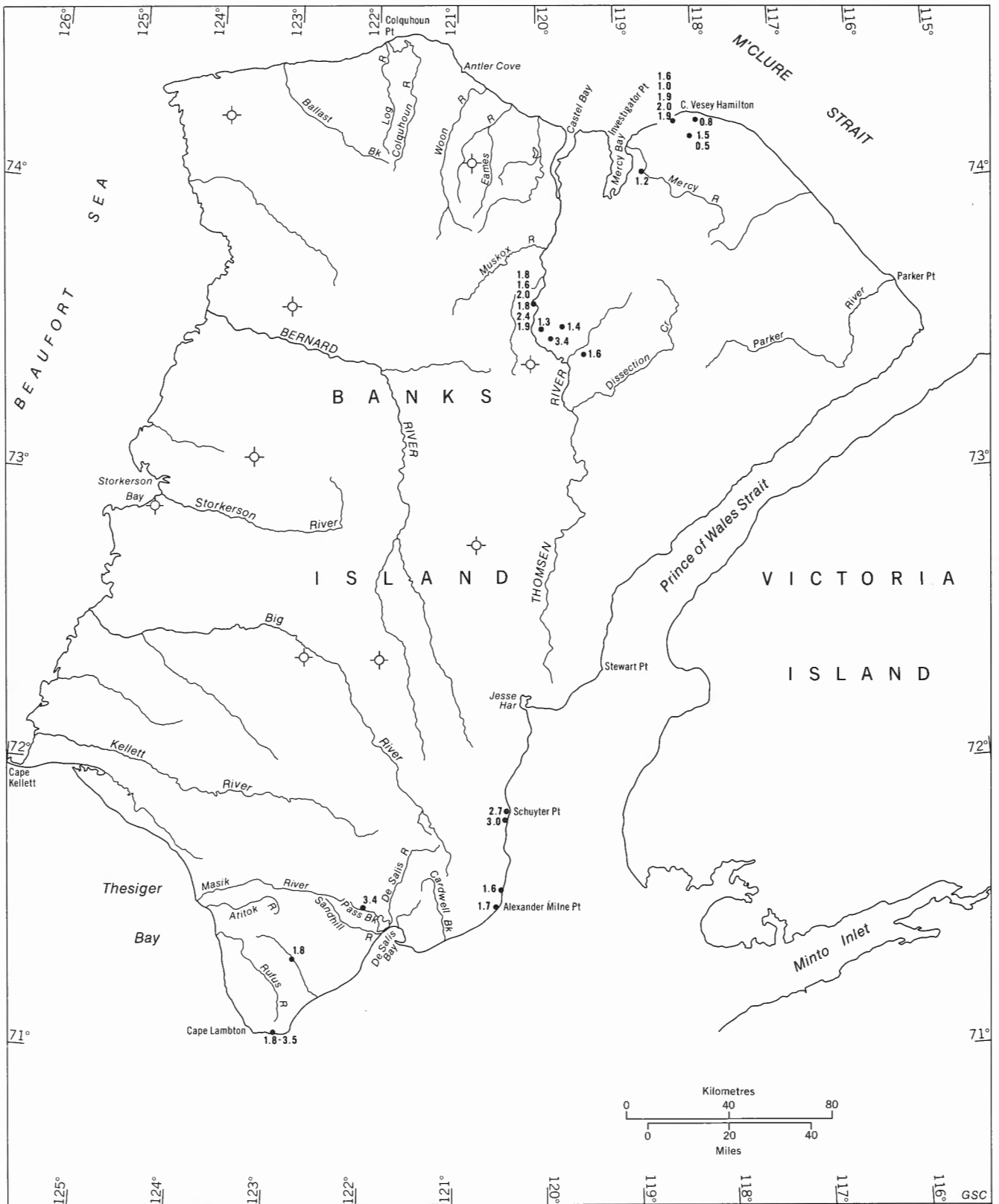


Figure 35. Variations in phi mean grain size, Isachsen Formation. Complete data given in Table 5.

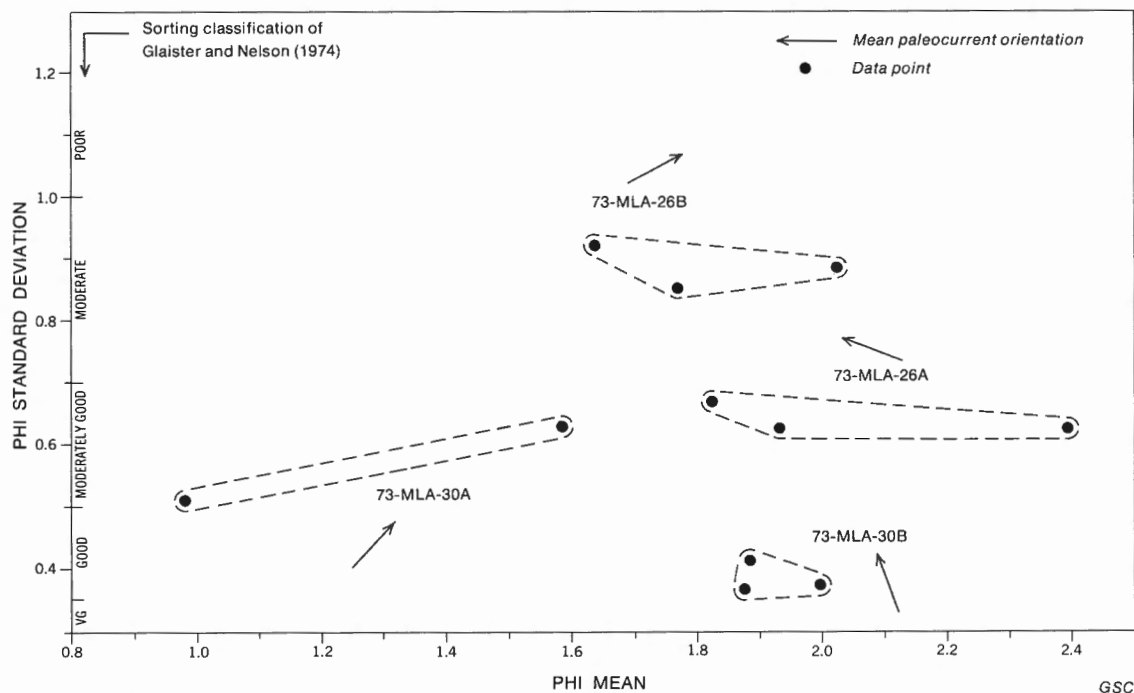


Figure 36. Variations in grain size parameters in two vertical profiles.

represent beds formed by a northeastward-flowing river or rivers, on the edge of Banks Basin. An examination of the paleocurrent trend map (Fig. 22) suggests that substation 73-MLA-30A is directly downstream from substation 73-MLA-26B. Yet the grain size parameters do not show the expected trends. Sorting improves downstream, but the mean grain size increases. The two stations, in fact, may not represent part of the same stream system, or they may represent slightly different time periods between which stream power or sediment load (or both) underwent slight changes.

In summary, sufficient data have been accumulated to show that in the project area grain size parameters are not readily amenable to simple interpretations, but are affected by numerous interrelated factors of varying relative importance. As many as several hundred samples would be necessary for a comprehensive study of the problem, and this is beyond the scope and purpose of the present investigation.

Petrographic analysis

A total of 59 thin sections of sand and sandstone were analyzed for mineral content. The results are given in Table 6. In addition, clast counts were made on several conglomerates (Table 7) and a few heavy mineral recoveries also have been studied.

Description of clast types

Pebbles, cobbles and boulders. Clasts of Proterozoic material have been identified positively only in southern Banks Island but may be present also at Station 73-MLA-29 (quartzite pebbles at this locality are not sufficiently distinctive for a positive identification). In Nelson Head Graben (Station 74-MLA-6; Pl. 5) boulder conglomerates consist almost exclusively of clasts of Glenelg Formation sandstone set in a quartz sand matrix. The sandstone is identical to that the writer

described (Miall, 1976a) from the cliff exposures of the Upper Glenelg at Nelson Head. It is fine to medium grained, pink to medium reddish brown, laminated to thick bedded. Most samples examined are quartz arenite or quartzose arenite (terminology of Okada, 1971) but some contain up to 23 per cent clay matrix and are quartzose wackes. Clasts of shale are rare in the Isachsen Formation at Nelson Head. Those observed at Station 74-MLA-6 are greenish, similar to the greenish shale in the uppermost Glenelg at Nelson Head.

The Proterozoic rocks at Nelson Head and throughout Minto Uplift are intruded by thick gabbro sills and dykes, but clasts of this very distinctive rock type are rare in the Isachsen Formation. Rare pebbles of gabbro are found at Alexander Milne Point (Station 74-MLA-16) but have not been observed elsewhere. The reasons for this scarcity are discussed below.

One of the most abundant clast types in the Isachsen Formation throughout Banks Island is a suite of distinctive grey limestones showing abundant silicification features. Lithotypes present include laminated beds, oolites, flat-pebble conglomerates and stromatolites. Clasts are up to cobble size and generally are angular. Lithologies of this type have been described from the Glenelg and Reynolds Point formations of Minto Uplift (Thorsteinsson and Tozer, 1962; Young, 1974) but also may be present in the unnamed Ordovician-Silurian succession of Prince Albert Peninsula (Thorsteinsson and Tozer, 1962, map-unit 10b).

The other widespread and abundant clast type is sandstone from the Melville Island Group. The lithology is distinctive: it is grey or greenish grey, quartzose, micaceous, laminated to thick bedded, poorly sorted, and contains abundant clay matrix. Grain size ranges from fine to very fine grained, with some medium grain size clasts that probably originated in the Hecla Bay Formation (Klován and Embry, 1971; Miall, 1976a). Clast size ranges up to 75 cm (30 in.).

Table 6. Petrographic analyses of sand and sandstone from the Isachsen Formation

STATION OR WELL	C. NO. OR DEPTH (FT)	PER CENT CLASTIC GRAINS										PER CENT ALL POINTS					PER CENT			ROCK TYPE (follows classification of Okada, 1971)				
		QUARTZ	CHERT	SANDSTONE	K-FELDSPAR	PLAGIOCLASE	MUSCOVITE	BIOTITE	GLAUCONITE	DETRITAL LS/DOL	SHALE, CLAY	DETRITAL FEOX	PYROXENE	OTHER HEAVIES	POROSITY	QUARTZ CEMENT	CARB. CEMENT	CLAY MATRIX	FEOX MATRIX			QUARTZ	ROCK FRAGMENTS	FELDSPAR
73-24	33321	96	3	-	1	-	-	R	-	-	-	-	-	-	-	-	-	-	-	95.5	3.4	1.1	QTZ	AREN
73-24	33322	97	2	-	2	-	-	-	-	-	-	-	-	-	-	-	-	-	-	96.7	1.8	1.5	QTZ	AREN
73-25	33326	59	5	-	3	T	-	-	-	28	R	2	1	-	-	-	-	-	-	59.4	37.1	3.5	LTHC	AREN
73-26	33342	97	T	T	3	-	-	-	-	-	-	-	T	-	-	-	-	-	-	96.9	.3	2.8	QTZ	AREN
73-26	33344	95	5	-	T	T	-	-	-	-	-	-	-	-	-	-	-	-	-	95.1	4.7	.2	QTZ	AREN
73-26	33346	91	7	-	1	1	-	-	-	-	-	-	-	-	-	-	-	-	-	90.9	6.7	2.4	QTZS	AREN
73-26	33347	94	4	-	2	-	-	-	-	-	-	-	T	-	-	-	-	-	-	94.2	3.9	1.9	QTZS	AREN
73-28	33328	93	5	-	1	-	-	-	-	-	-	-	1	-	-	-	-	T	-	93.1	5.8	1.1	QTZS	AREN
73-28	33330	93	5	-	1	-	T	-	-	-	-	-	T	-	-	-	-	-	-	93.0	5.6	1.4	QTZS	AREN
73-29	33331	95	2	-	2	-	-	-	-	-	-	-	1	-	-	-	-	-	-	94.8	3.1	2.1	QTZS	AREN
73-29	33333	89	5	-	6	-	-	-	-	-	-	-	-	-	-	-	-	-	-	88.9	4.8	6.3	QTZS	AREN
73-30	33360	98	2	-	T	T	-	-	-	-	-	-	T	-	-	-	-	-	-	98.0	1.8	.2	QTZ	AREN
73-30	33338	95	4	-	1	-	-	-	-	-	-	-	T	-	-	-	-	-	-	95.0	4.0	1.0	QTZ	AREN
73-30	33336	95	4	-	1	-	-	-	-	-	-	-	-	-	-	-	-	-	-	94.9	4.3	.8	QTZS	AREN
73-30	33335	99	1	-	T	T	-	-	-	-	-	-	-	-	-	-	-	-	-	98.8	1.0	.2	QTZ	AREN
73-30	30564	96	3	-	1	-	-	-	-	-	-	-	-	-	-	-	-	-	24	95.6	3.3	1.1	QTZ	AREN
73-31	33339	98	2	-	T	-	-	-	-	-	-	R	-	-	-	-	-	-	-	97.6	2.3	.1	QTZ	AREN
73-31	33283	94	4	-	1	T	T	-	-	-	-	-	T	-	1	-	-	-	-	93.6	4.9	1.5	QTZS	AREN
73-35	33341	86	12	-	1	-	-	-	-	-	-	1	-	-	-	-	-	-	-	85.9	13.1	1.0	QTZS	AREN
74-2	30462	100	T	-	-	-	-	-	-	-	-	T	-	-	-	-	-	-	-	99.8	.2	.0	QTZ	AREN
74-2	30465	100	-	-	-	-	-	-	-	-	-	T	T	-	-	-	-	-	-	99.8	.2	.0	QTZ	AREN
74-4	30472	100	-	-	-	-	-	-	-	-	-	T	T	-	-	-	-	-	-	99.8	.2	.0	QTZ	AREN
74-4	30474	76	T	6	-	-	-	T	-	-	16	2	-	-	-	-	-	-	-	75.6	24.4	.0	QTZS	AREN
74-6	30476	95	-	2	-	-	-	T	-	-	1	1	-	-	-	-	-	-	-	95.3	4.7	.0	QTZ	AREN
74-6	30477	84	-	1	-	-	T	-	-	-	8	7	-	-	-	-	-	-	-	84.4	15.6	.0	QTZS	AREN
74-6	30478	95	-	5	-	-	-	-	-	-	-	-	-	-	-	-	-	-	14	95.0	5.0	.0	QTZ	AREN
74-6	30479	100	-	T	-	-	-	-	-	-	-	T	T	-	-	-	-	-	-	99.7	.3	.0	QTZ	AREN
74-6	30483	100	-	-	-	-	-	-	-	-	-	-	T	-	-	-	-	-	-	99.9	.1	.0	QTZ	AREN
74-6	30484	88	-	-	2	T	-	R	-	-	9	2	-	-	-	-	-	-	-	87.2	11.1	1.8	QTZS	AREN
74-8	30486	87	3	2	1	T	-	T	-	-	3	4	-	-	-	-	-	-	-	87.2	11.8	1.0	QTZS	AREN
74-11	30492	93	4	-	2	T	T	T	T	-	-	T	-	-	-	-	-	-	-	93.1	4.5	2.4	QTZS	AREN
74-13	30495	92	4	-	3	T	T	-	-	-	1	T	-	-	-	-	-	-	-	91.7	5.0	3.3	QTZS	AREN
74-14	30497	91	3	-	1	T	-	-	-	-	4	1	-	-	-	-	-	-	-	91.0	7.6	1.4	QTZS	AREN
74-16	30499	100	T	T	T	-	-	-	-	-	-	-	-	-	-	-	-	-	-	99.7	.2	.1	QTZ	AREN
74-18	30503	95	3	T	1	-	-	-	-	-	-	T	-	-	-	-	-	-	-	95.0	3.6	1.4	QTZS	AREN
74-48	30563	95	4	-	1	-	-	-	-	-	-	-	-	-	-	-	-	-	-	95.3	3.5	1.2	QTZ	AREN
74-66	30575	97	2	-	1	T	-	-	-	-	-	-	T	-	-	-	-	-	-	97.0	1.9	1.1	QTZ	AREN
74-71	30576	93	4	T	3	-	-	-	-	-	-	-	-	-	-	-	-	-	-	92.9	3.7	3.4	QTZS	AREN
74-73	30578	95	4	-	1	T	-	-	-	-	-	-	T	-	-	-	-	-	-	94.7	4.4	.9	QTZS	AREN
74-74	30579	95	2	1	3	T	-	-	-	-	-	-	-	-	-	-	-	-	-	94.6	2.8	2.6	QTZS	AREN
74-75	30580	97	1	1	1	-	-	-	-	-	-	-	-	-	-	-	-	-	-	97.1	1.6	1.3	QTZ	AREN
74-76	30581	100	T	-	T	-	-	-	-	-	-	-	-	-	-	-	-	-	-	99.8	.1	.1	QTZ	AREN
74-80	30583	96	1	-	3	-	-	-	-	-	-	-	-	-	-	-	-	-	-	95.9	1.5	2.6	QTZ	AREN
74-87	30585	89	-	-	6	T	T	-	-	-	-	5	-	-	-	-	-	-	13	89.1	5.0	5.9	QTZS	AREN
74-90	30587	96	4	-	R	-	-	-	-	-	-	-	-	-	-	-	-	-	-	96.0	3.7	.3	QTZ	AREN
74-107	30595	78	2	-	6	T	1	-	T	T	5	8	-	-	-	-	-	-	-	78.0	15.9	6.1	QTZS	AREN
74-108	30596	94	5	-	1	T	-	-	-	-	-	-	-	-	-	-	-	-	-	94.5	4.7	.8	QTZS	AREN
74-110	30597	99	T	-	1	-	-	-	-	-	-	-	-	-	-	-	-	-	-	98.8	.1	1.1	QTZ	AREN
74-131	30622	77	6	-	1	-	T	-	-	-	-	16	-	-	-	-	-	-	-	76.6	22.1	1.3	QTZS	AREN
74-153	30642	98	T	-	2	-	-	-	-	-	-	-	-	-	-	-	-	-	-	97.8	.1	2.1	QTZ	AREN
GAS 8	30705	86	9	-	4	-	T	-	-	-	-	1	-	-	-	-	-	-	-	85.6	10.5	3.9	QTZS	AREN
GAS 8	30708	96	4	-	1	-	-	-	-	-	-	-	-	-	-	-	-	-	-	95.9	3.6	.5	QTZ	WACK
GAS 8	30710	96	2	-	2	-	-	-	-	-	-	-	T	-	-	-	-	-	-	95.7	2.2	2.1	QTZ	AREN
GAS 11	30717	90	7	-	2	-	-	-	-	-	-	-	-	-	-	-	-	-	-	90.3	7.4	2.3	QTZS	AREN
GAS 11	30722	93	4	-	3	-	-	-	-	-	-	R	-	T	-	-	-	-	-	93.3	4.0	2.7	QTZS	AREN
GAS 11	30730	92	3	3	2	T	T	-	T	-	-	1	-	T	-	-	-	-	-	91.7	6.6	1.7	QTZS	AREN
VH-74-041		98	2	-	-	-	-	-	-	-	-	-	T	-	-	-	-	-	-	98.1	1.9	.0	QTZ	AREN
ORKSUT	(4530)	77	15	7	1	-	-	-	-	-	-	-	-	-	-	-	-	-	-	76.7	22.6	.7	QTZS	AREN
ORKSUT	(4670)	85	4	-	1	-	-	-	-	-	7	4	-	-	-	-	-	-	-	84.7	14.3	1.0	QTZS	AREN

Less than 1% R Trace quantities T Quartz QTZ Quartzose QTZS
 Lithic LTHC Arenite AREN Wacke WACK

Table 7. Conglomerate clast types, Isachsen Formation

STATION NO. (MLA)	Height above base (m)	PROTEROZOIC			PROTEROZOIC OR L. PALEOZOIC	DEVONIAN			?		Maximum clast size (cm)
		Quartzite	Shale	Gabbro	Silicified limestone	Sandstone	Shale	Limestone	Quartz	Chert	
73-24	—	—	—	—	A	A	—	—	—	—	6
73-26	.6	—	—	—	C	C	—	—	C	C	3.5
73-26	2.3	—	—	—	A	—	—	—	C	C	n
73-29	13.3	—	—	—	C	C	—	—	C	—	3.5
73-29	20.6	R?	—	—	A	A	—	—	—	R	73
73-30	—	—	—	—	A	A	—	—	—	—	75
74-6	0-70	A	R	—	—	—	—	—	—	—	50
74-15	—	—	—	—	C	—	—	—	C	C	2
76-16	—	—	—	R	A	—	—	—	C	—	11
74-18	—	—	—	—	—	—	—	—	C	C	1
74-73, 74, 75	—	—	—	—	C	C	—	—	C	—	n
74-90	8	—	—	—	R	A	—	C	—	R	40
74-107	—	—	—	—	—	C	C	—	—	—	5

GSC

Abundant A Rare R
Common C No field record n

These are the largest boulders in the Isachsen Formation and most are angular or subangular. Rare grey shales, probably originating in the Melville Island Group, have been identified at one locality on northern Banks Island.

There remain two clast types of unknown origin: quartz and chert. Quartz clasts are of pebble grade; they generally are milky white and probably originated as vein fillings. Chert clasts are pale to dark grey. Both clast types may have originated in almost any of the Proterozoic or Paleozoic rocks exposed on Victoria Island. Both are abundant as sand grade material in the Isachsen.

Sand. Quartz is ubiquitous in the Isachsen Formation. Strained, unstrained and polycrystalline grains all are present. Strained grains are predominant and polycrystalline grains are rare, but no attempt has been made to quantify the distributions. Blatt and Christie (1963) showed that such a quantification would be of questionable usefulness. Most grains are rounded or well rounded, although some grains are etched and embayed (Pl. 19A–D). The embayments probably are the result of solution in the source area during transportation or following deposition although, as Crook (1968) pointed out, grains with deep embayments are unlikely to withstand for long the wear and tear of transportation. Crook (1968) and Cleary and Conolly (1971) suggested that embayments could develop where a deposit was saturated with waters rich in organic compounds as in a soil deposit. Such a condition could arise easily where a bar or bank in the braided stream system became covered in vegetation. Volcanic quartz grains commonly show embayments (Pettijohn *et al.*, 1972, Fig. 7-5)

but there is no independent evidence of any volcanic activity in the Isachsen Formation. The rounding of the quartz grains probably is inherited partly from previous sedimentary cycles. Many of the grains show detrital cores and authigenic overgrowths (Pl. 19E–J). The detrital cores are always well rounded. Most of the overgrowths must date from a previous sedimentary cycle, because the lack of cementation of most of the Isachsen sands indicates that no diagenetic quartz growth can have taken place. Therefore the rounded cores which the overgrowths enclose must be older still. In a few instances (Pl. 19I, J) there is evidence for several superimposed authigenic overgrowths, indicating a multicyclic origin for the sand grains. Plate 19J shows overgrowths cut by embayments, which also suggests an early origin for the former.

A possible exception to this generalization is shown in Plate 21B, an illustration of a sample from the base of the Christopher Formation immediately above the Isachsen. Some grains showing authigenic growths are in contact at their detrital cores, indicating that at least some of the overgrowths may be of in situ origin. This sample is from a depth of 1295 m (4250 ft) in the Orksut I-44 well, suggesting that cementation may be more extensive in the subsurface, possibly as a result of pressure solution resulting from a greater weight of overburden. No samples of lithified Isachsen Formation were recovered from this well, possibly because of looser cementation.

Some rare quartz types are illustrated in Plates 19K, L, 20A–F. Zoned quartz grains presumably represent vein fillings. The traces of crystal facies shown by trails of inclusions indicate growth into an unconfined space. Quartz grains

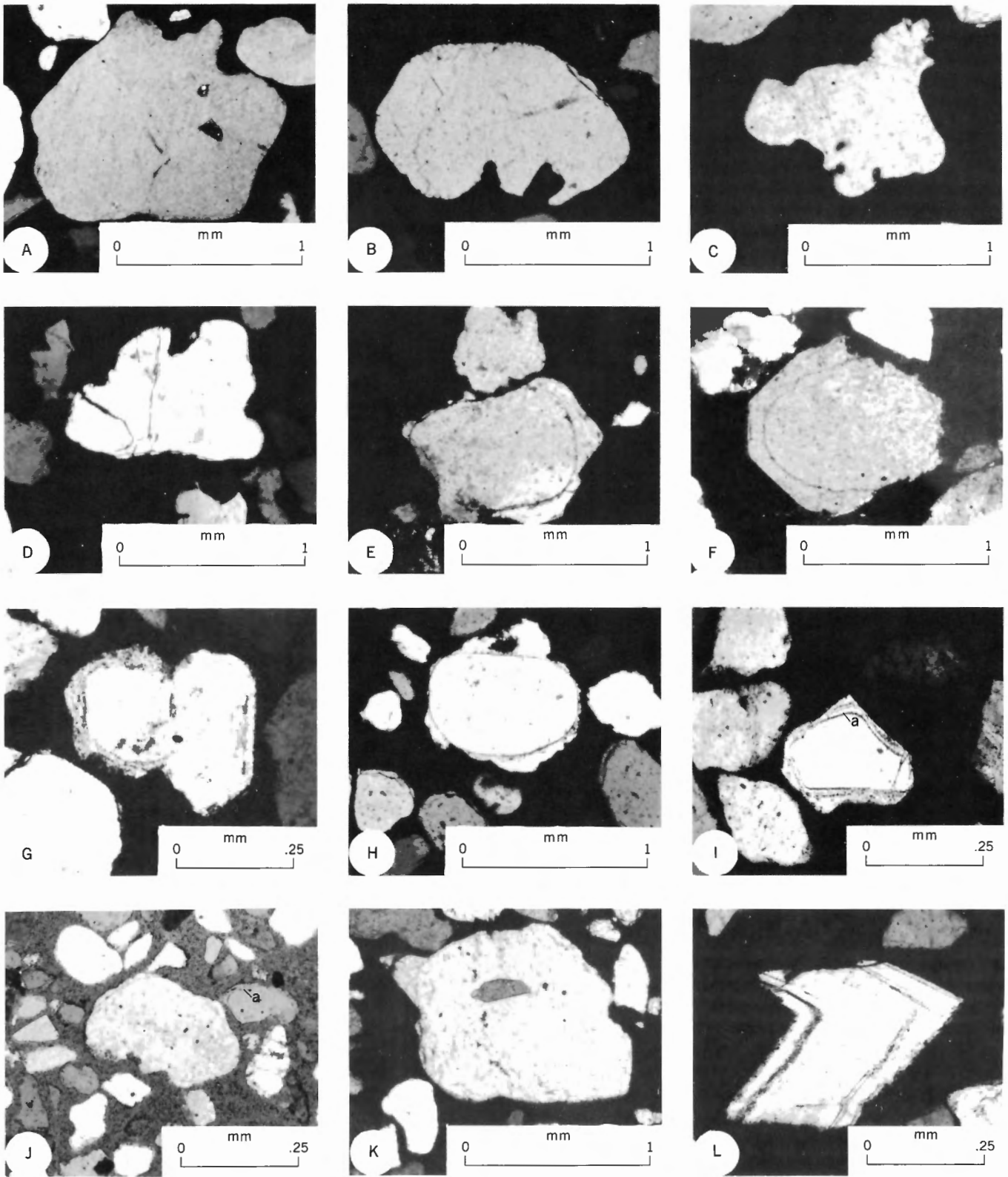


Plate 19. Quartz grains, Isachsen Formation, all under crossed polarizers. A–D: Grains showing solution embayments. E–H: Grains showing inherited authigenic overgrowths; note roundness of the detrital core. I, J: Grains showing multiple (polycyclic) overgrowths (a). K: Quartz with green biotite inclusion. L: Zoned vein quartz. (Sample numbers: A, C-30578; B, C-30579; C, C-29858, 1381 m (4530 ft) depth; D, C-33322; E, C-30563; F, C-30563; G, C-33330; H, C-30499; I, C-33331; J, C-33330; K, C-33344; L, C-33342.)

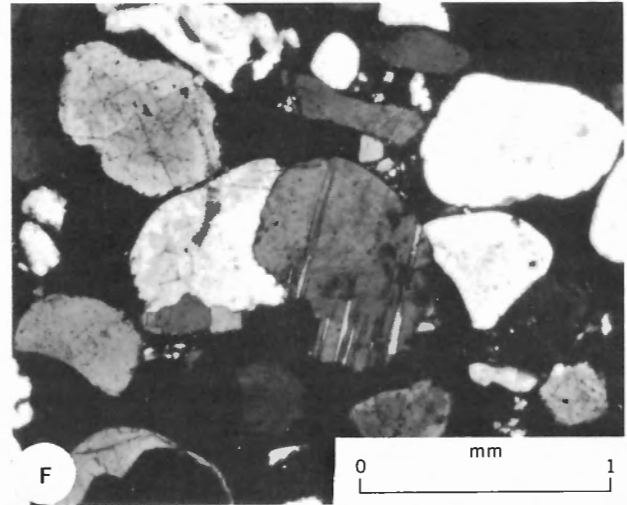
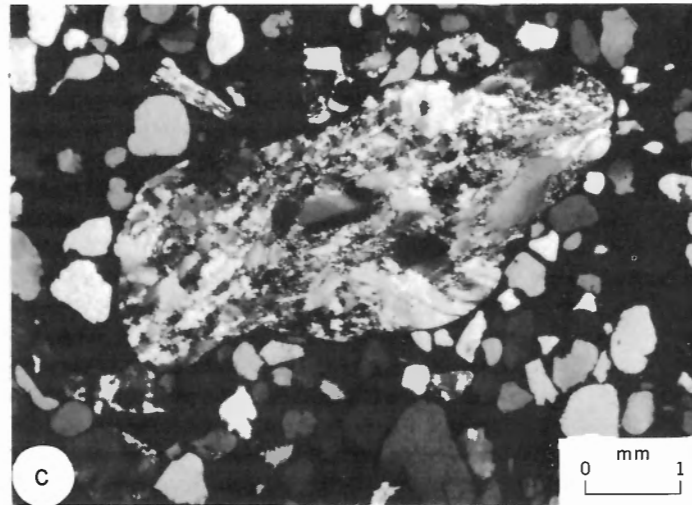
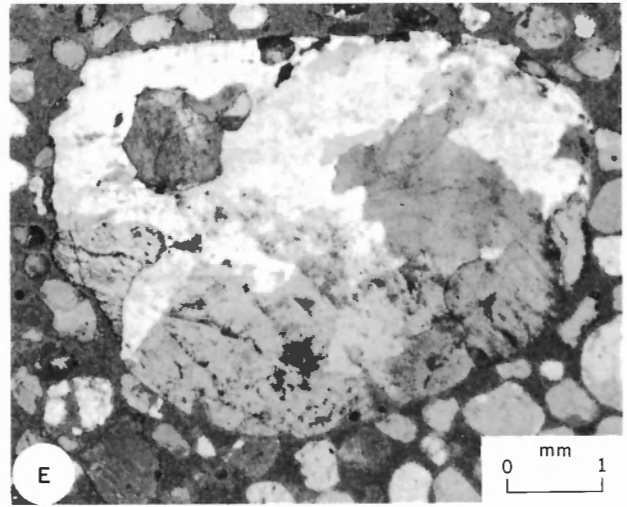
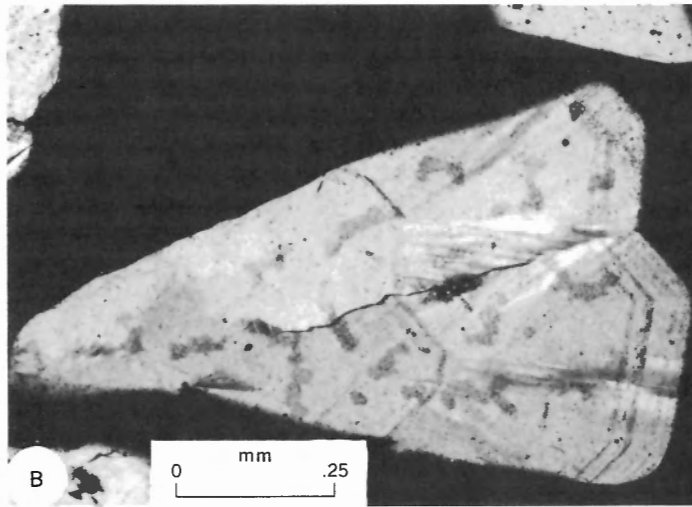
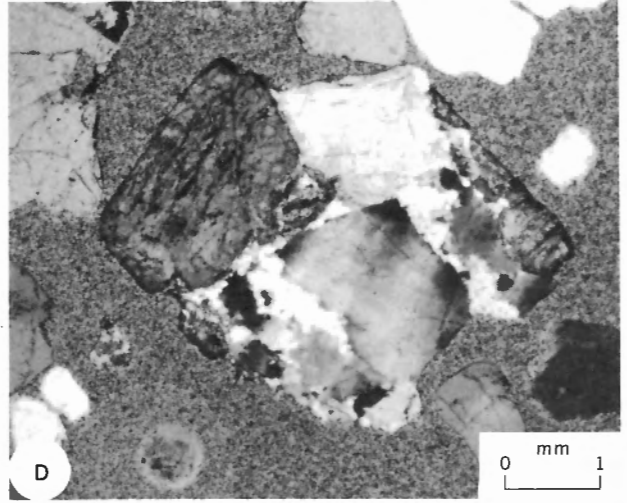
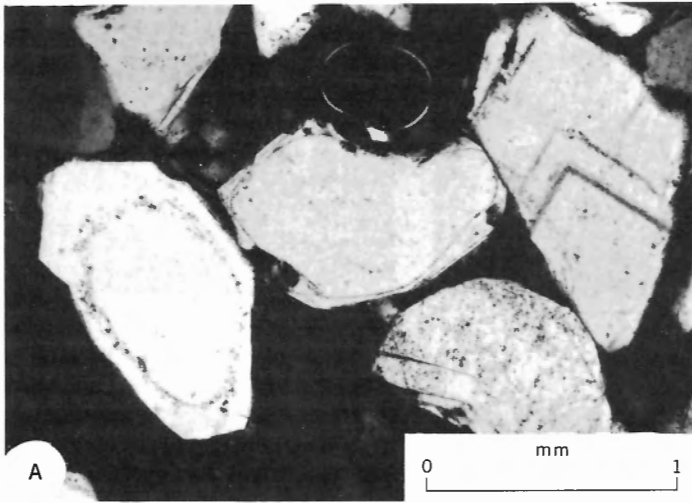


Plate 20. Quartz grains, Isachsen Formation, all under crossed polarizers. A: Zoned quartz and grains with inherited authigenic overgrowths. B: Zoned vein quartz. C: Polycrystalline metamorphic quartz. D–F: Quartz-potassium feldspar intergrowths; feldspar is stained yellow and appears as darker, higher relief areas; note polycrystalline (plutonic) nature of the quartz. (Sample numbers: A, C-30564; B, C-30576; C, C-30578; D, C-33333; E, C-33333; F, C-30579.)

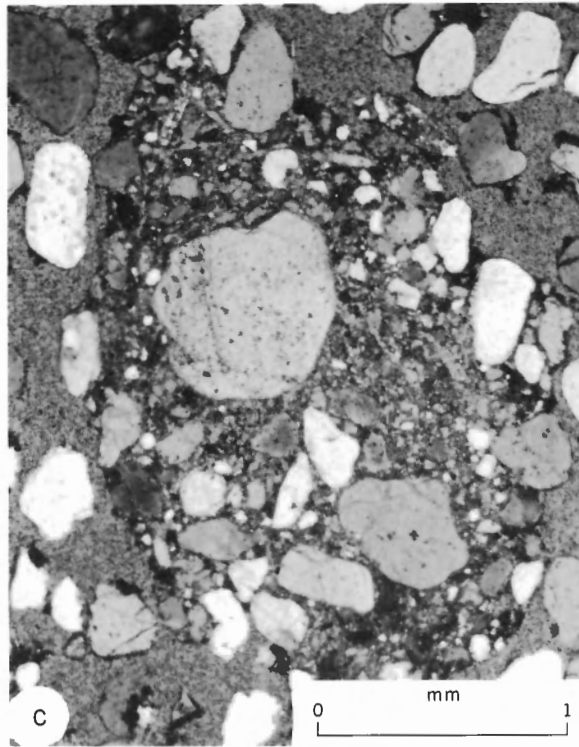
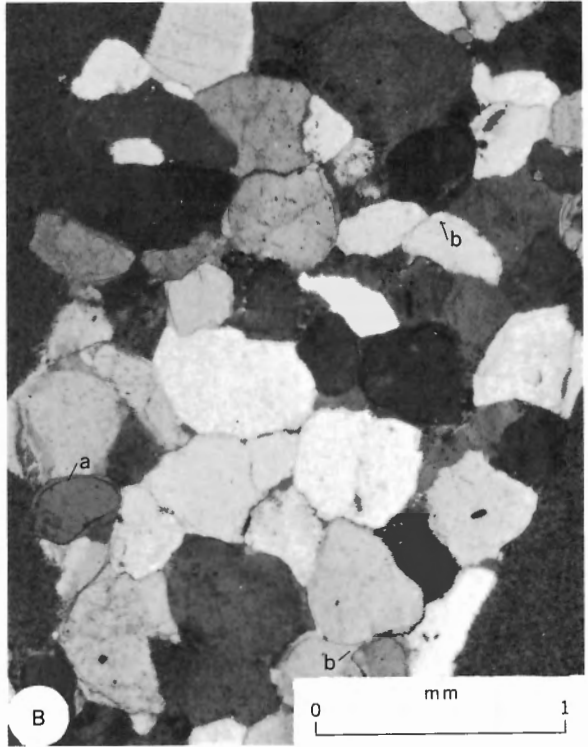
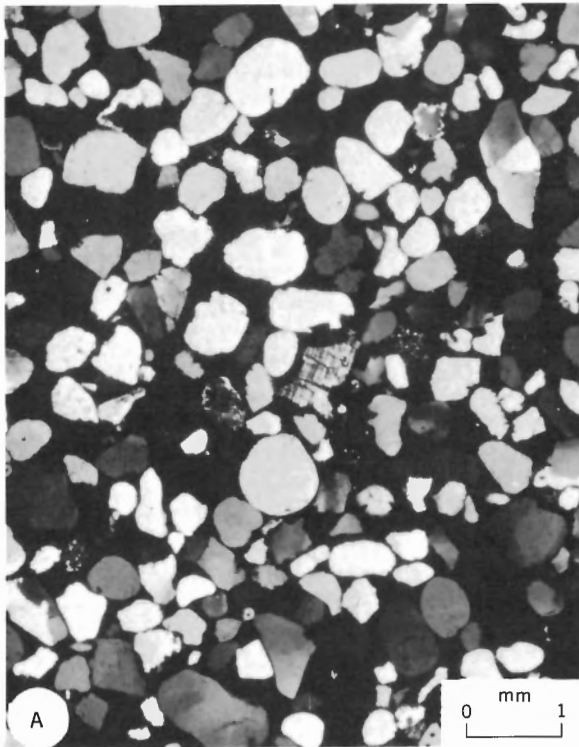


Plate 21. Isachsen Formation, all views under crossed polarizers. A: Typical unconsolidated quartz sand; note grain of microcline at centre. B: Lithified sandstone from lower part of Christopher Formation immediately overlying the Isachsen; inherited (*a*) and in situ (*b*) quartz overgrowths are present. C: Large sandstone fragment; note similarity of large quartz grains to those in enclosing matrix. D: Sandstone (*above*) and chert (*below*) fragments. (Sample numbers: A, C-30578; B, C-29858, 1295 m (4250 ft) depth; C, C-30499; D, C-29858, 1381 m (4530 ft) depth.)

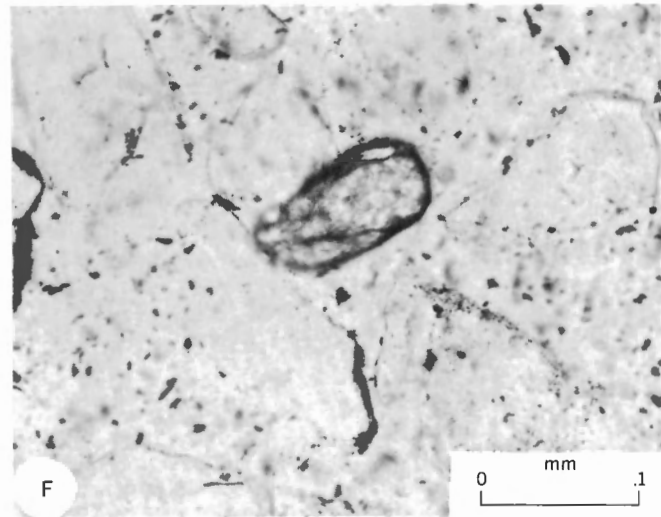
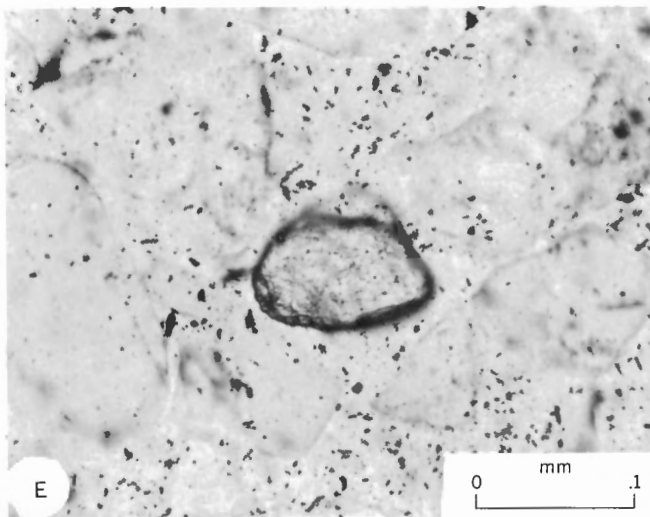
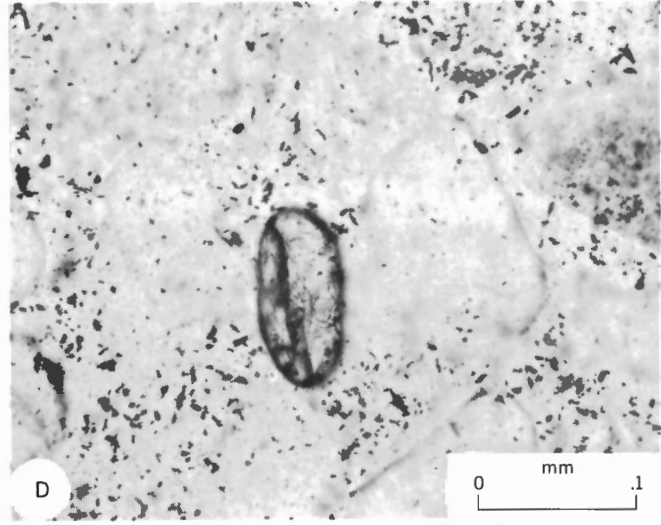
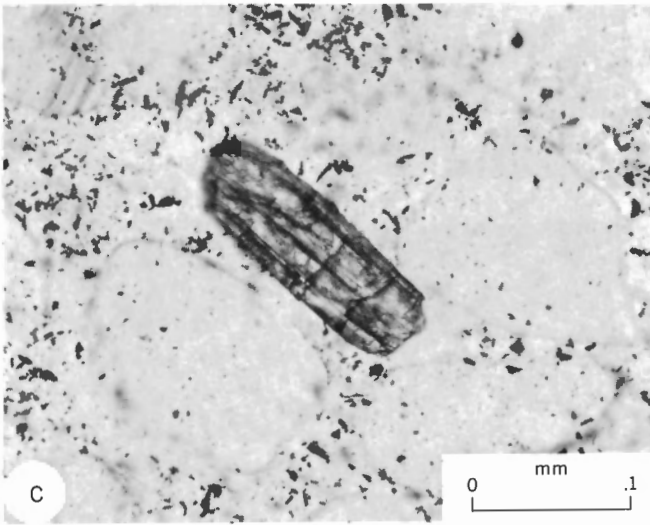
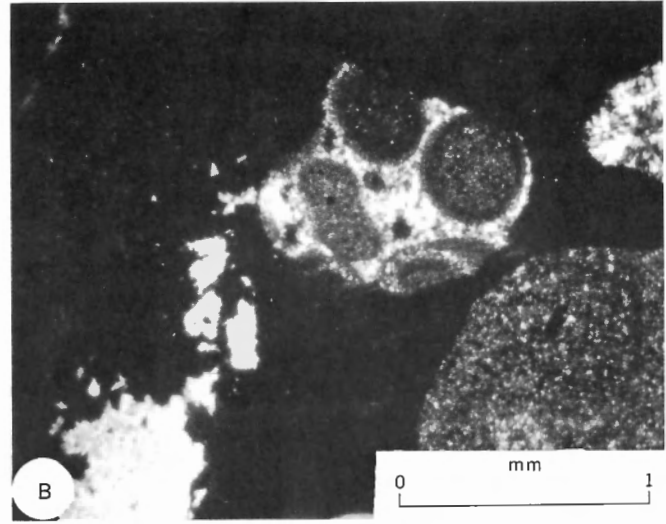
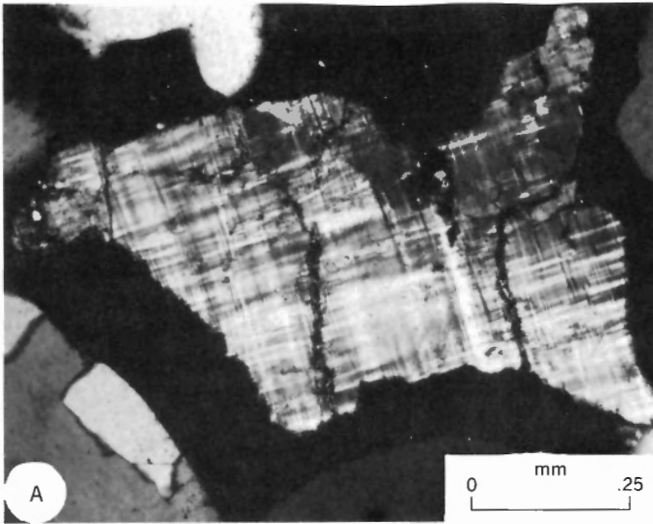


Plate 22. Isachsen Formation, A–B under crossed polarizers, C–F plane polarized light. A: Microcline grain. B: Chert showing radiolarian(?) structures. C–F: Well-rounded zircon grains. (Sample numbers: A, C-30578; B, C-29858, 1381 m (4530 ft) depth; C–F, C-33328.)

intergrown with potassium feldspar crystals are illustrated in Plate 20D–F. Rare quartz grains containing small subhedral crystals of zircon, tourmaline and biotite also have been observed (Pl. 19K). Large polycrystalline quartz grains have been recorded at a few localities (Pl. 20C).

Chert grains (Pl. 21D) vary from pale grey to dark grey and grey-brown, and also show variations in grain size; but preliminary studies showed that gradations between the types would prevent any recognition of distinctive chert types. One grain was observed that shows small spherical structures with faint concentric rings (Pl. 22B). It may be of oolitic or radiolarian origin.

Sandstone grains are seen in a few thin sections (Pl. 21C, D). Various grains show similarities to either the Glenelg sandstones or those of the Melville Island Group. Some of the coarser sandstones contain quartz grains similar in size and roundness to those comprising the bulk of the Isachsen Formation, which is a useful clue to the origin of this material.

Feldspars of several varieties are present. Studies of refractive index and extinction angles of albite twins in plagioclase, as described by Kerr (1959, p. 258), indicate that they are albite or oligoclase in composition. Potassium feldspars include microcline (Pl. 22A) and orthoclase (Pl. 20D–F), some of which shows simple (Carlsbad?) twinning. No sanidine was identified.

Detrital iron oxide grains are seen in many thin sections. Most consist of amorphous limonite or hematite, although some magnetite or ilmenite grains also are present. These grains may represent decomposed mafic minerals such as amphiboles and pyroxenes, which are virtually absent in the Isachsen Formation.

Glauconite has been identified tentatively in three samples, two of them from the Sandhill River section, which has yielded marine foraminifera. This mineral normally is an indicator of marine sedimentation and is not known to be common as detrital (i.e., derived) grains (Pettijohn *et al.*, 1972, p. 228–230).

In one sample detrital limestone grains are abundant. Other rare mineral species are listed in Table 6.

Heavy minerals. Statistical studies of the light minerals described in the previous paragraph have provided an adequate basis for a discussion of sediment sources (*see below*). Because this is the main object of carrying out petrographic analyses, little would be gained by detailed studies of heavy minerals. The following notes are based on qualitative examinations of a limited number of samples.

Minerals common in virtually all samples studied are magnetite, rutile and zircon. Magnetite grains are cubic or triangular and typically exhibit little evidence of rounding. They probably are first-cycle grains from the Proterozoic intrusive rocks. Rutile grains generally are smoky brown, euhedral prisms with 101 terminations. A few samples also contain angular red-brown grains. This mineral also may represent first-cycle derivation from the Proterozoic dykes and sills; most grains appear to be relatively unworn. Zircon grains (Pl. 22C–F) mostly are well rounded and probably are polycyclic in origin. They indicate an acid igneous source but have undoubtedly passed through at least one Proterozoic sedimentary cycle.

Species identified in only a few samples include tourmaline, garnet, kyanite, epidote and sphene. Tourmaline grains were observed only in two heavy mineral samples from southern Banks Island (GSC locs. C-30501, C-30718) but are more common as inclusions in quartz grains in samples from northern Banks Island (Fig. 42), as determined by thin section analysis. Black, relatively unworn, prismatic crystals are typical and probably are recycled from a granitic or pegmatitic source. A distinctive transparent, salmon-pink garnet (spessartite?) occurs in four samples from northern Banks Island (GSC locs. C-33321, C-33337, C-33342, C-33360) and suggests a medium-grade metamorphic or pegmatitic source. Kyanite occurs as colourless or pale blue, bladed, subhedral grains. It has been observed in three samples (GSC locs. C-30501, C-33360, C-30718) and indicates a high-grade metamorphic source. Epidote is fairly common in two samples from southern Banks Island (GSC locs. C-30501, C-30718). The grains exhibit a distinctive yellow or greenish-yellow colour and an angular, fractured outline. Rare prismatic cleavage fragments are present. Epidote is common in low-grade metamorphic rocks. Sphene was identified in one sample (GSC loc. C-30499) from Alexander Milne Point. This is a relatively uncommon mineral, although it has also been observed in the Glenelg sandstones at Nelson Head (Miall, 1976*a*). It suggests a granitic source.

Matrix and cement

Most of the samples examined in thin section lack all but traces of matrix and cement. Fifty-four samples were unconsolidated and were lithified artificially by resin impregnation to enable thin sections to be made. Measurable quantities of detrital clay matrix are present in only one sample.

Many quartz grains are coated with a thin layer of limonite but only two samples contain limonite in sufficient quantities to act as an effective cement. Calcite and siderite are each important as cementing agents in two samples.

Texture

A sample from GSC loc. C-30564 (Station 73-MLA-30) was collected from the lowermost of the planar crossbedded units illustrated in Plate 1. Since it is very loosely cemented with limonite it was possible to make a thin section of a lithified rock rather than loose sand grains. The texture of this sample probably resembles that of much of the sand in the coarse sand facies. The sand is loosely packed, with little or no grain-to-grain suturing or interpenetration. The well rounded grains rarely show subangular authigenic overgrowths. Where present, the overgrowths form the grain-to-grain contacts, demonstrating that the overgrowths were derived with detrital core from a previous sedimentary cycle. Much of the limonite cement is primary, for grain coatings frequently are present at grain contacts. Porosity in this sample was measured by point counter as 24 per cent.

The other consolidated sandstone samples are typical only of the outcrop from which they were collected, and demonstrate a locally different diagenetic history. A sample from GSC loc. C-30478 was collected from the basal conglomeratic sandstone unit at Station 74-MLA-6 in Nelson Head Graben. Quartz grains are angular to subrounded; they contain embayments and commonly are penetrated by rhombs

of carbonate cement. Embayments rarely are filled with clay. Quartz grain contacts show little or no suturing. Cement is rare at the contacts. Authigenic overgrowths are rare and some show evidence of in-place growth. The siderite cement commonly is altered to opaque iron oxides (limonite?). Traces of a clear, colourless, late-stage calcite cement are present.

GSC loc. C-30585 (Station 74-MLA-87; Mercy River) yielded a very fine grained, finely laminated sandstone from the upper part of the formation. Lamination results from the distribution of detrital iron oxide grains. The sample contains 19 per cent rhombic siderite cement.

Quantitative analysis

Analyses are reported in Table 6 to the nearest percentage point.

Sand classification. Figure 37 shows ternary plots of the sand samples; the three poles used are quartz, rock fragments and feldspar (data from Table 6). Rock fragments include chert, sandstone, shale, mica, detrital limestone, detrital iron oxide and heavy minerals. The samples have been divided into two sets according to geographical distribution. Superimposed on the plots is one of the two classification triangles proposed by Okada (1971, Fig. 5A). The arenite triangle is for samples containing less than 15 per cent detrital matrix; the wacke triangle (not shown) uses the same terminology, substituting the word wacke for arenite, and is intended for sandstones containing in excess of 15 per cent detrital matrix. Only one sample (GSC loc. C-30708) falls within the wacke category. One sample (GSC loc. C-33326) rich in detrital limestone

grains is a lithic arenite; the remaining 57 samples are divided between the quartz arenites and quartzose arenite categories.

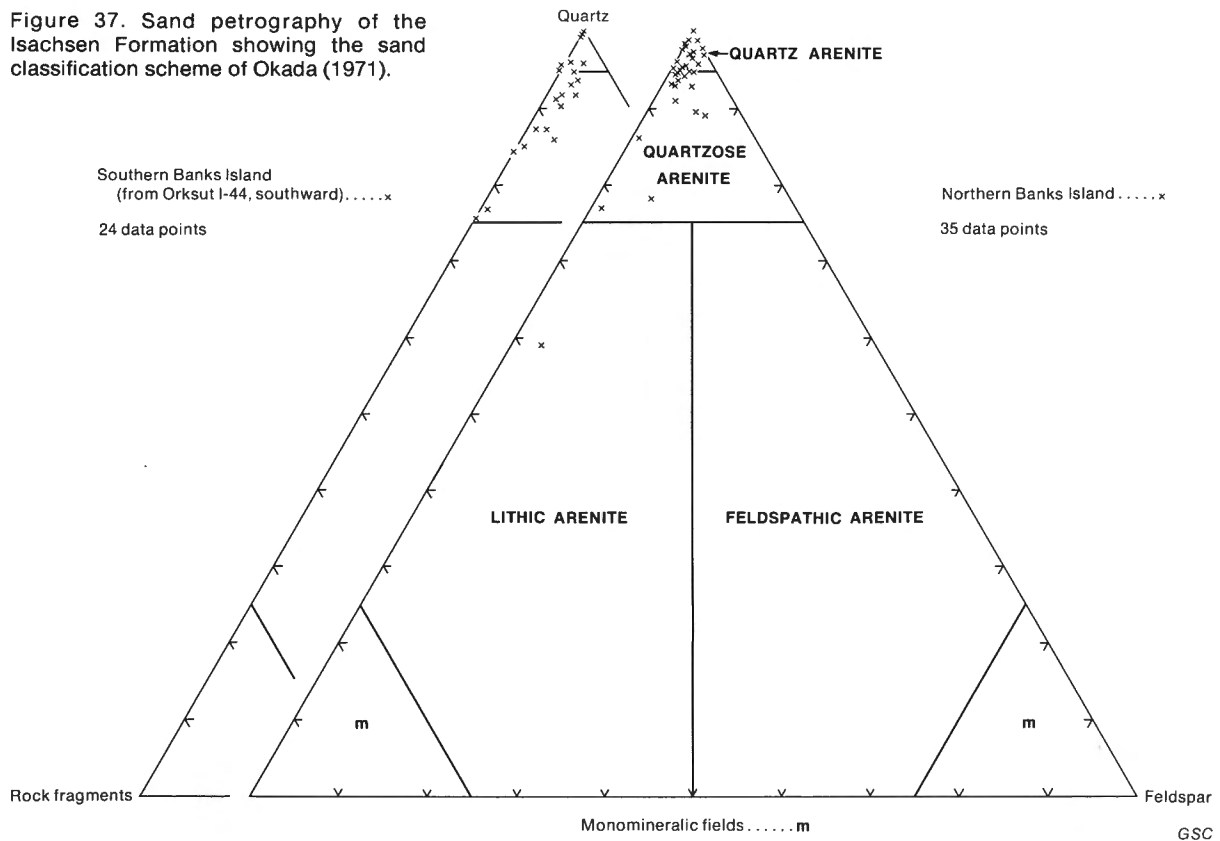
Many alternative classifications have been published; most have been reviewed by Okada (1971). Pettijohn *et al.* (1972, Fig. 5-3) used a slightly different scheme, according to which most of the quartzose arenites shown in Figure 37, would be termed sublitharenites. Two of the quartzose arenites from northern Banks Island, which contain slightly more feldspar than rock fragments, would be classified as subarkoses.

Areal variation in major components. A preliminary test for regional variation in sand content is shown in Figure 37, where the 59 sand samples are plotted on two different ternary diagrams depending on whether they came from northern or southern Banks Island. The diagrams demonstrate that there are no gross differences in composition across the project-area. An analysis for more subtle variations forms the remainder of this section.

Two-dimensional data arrays such as those shown in Table 6 may be analyzed by several different statistical techniques. Factor analysis probably is the most complex but provides the most complete description of the sources of variability in the data. In the present study the related but simpler technique of cluster analysis (Parks, 1966) has been used. This approach, coupled with an analysis, partly qualitative, of the minor constituents in the Isachsen sands, has provided a sufficient basis for a discussion of probable sediment sources.

A Q-mode cluster analysis was performed on the data to

Figure 37. Sand petrography of the Isachsen Formation showing the sand classification scheme of Okada (1971).



test for significant mineral groupings. Rare components (shown by the letter *R* in Table 6) were arbitrarily assigned a percentage of 0.5, and trace components (*T*) a value of 0.1. The results are given in Figure 38. Cluster groupings are gradational and the high degree of correlation in the upper part of the diagram shows that distinctive and mutually exclusive mineral assemblages cannot be recognized. The dendrogram has been divided into five major clusters, as seen on the left-hand side of Figure 38. The composition (major components) of the five clusters is shown in a ternary plot (Fig. 39; note that only the upper half of the diagram is shown, the remainder being empty) and Figure 40 gives their geographic distribution. In Figure 40, where several samples from the same locality fall in the same cluster group, they are shown by one number. The clusters overlap slightly in terms of their major components (Fig. 39), and most of the clusters show wide geographic distribution (Fig. 40). This confirms in more detail the general compositional homogeneity suggested by Figure 37.

Geographically distinct distribution is shown only by cluster 4, which is relatively high in rock fragments and low in feldspar. The cluster is represented by nine samples which, with one exception, are located in southern Banks Island. Six of the fourteen samples forming cluster 1 also are from southern Banks Island. This cluster is characterized by low feldspar content. Table 6 indicates that feldspar is absent, or present only in trace quantities in the six samples.

In summary, Q-mode cluster analysis demonstrates that the sands of the Isachsen Formation are relatively homogeneous in composition. A weak tendency for feldspar content to be more rare in southern Banks Island has been shown. This result is confirmed and amplified by an analysis of minor components in the sand samples.

Areal variation in minor components. Four of the sand components that are frequently found, but in only minor quantities, have been plotted on a ternary diagram as seen in Figure 41. The three end members are chert, sandstone plus shale, and feldspar. The four components were recalculated to 100 per cent for the purpose of this plot and it should be borne in mind that a range of error is associated with each point because of point-count measurement variance. This is particularly important for minor components, for which a few points difference in the count can cause major changes in position within the ternary diagram. Nevertheless, a regional differentiation emerges clearly from this plot: samples from northern Banks Island contain the most chert, and those from southern Banks Island contain the most sedimentary rock fragments.

Lastly, Figure 42 gives the distribution of some rare components. Most of the clast types on this map are present only in trace quantities in the thin section; one or two grains per section is typical. The distribution map shows that most of these clast types are present only along the east side of Northern Banks Basin.

Vertical variation. At Stations 73-MLA-26 and 30 paleocurrent and grain size data demonstrate that the measured sections may each be divided into two segments. The same differentiation cannot be demonstrated on the basis of sand composition, as shown in Figures 43 and 44. Four samples from each

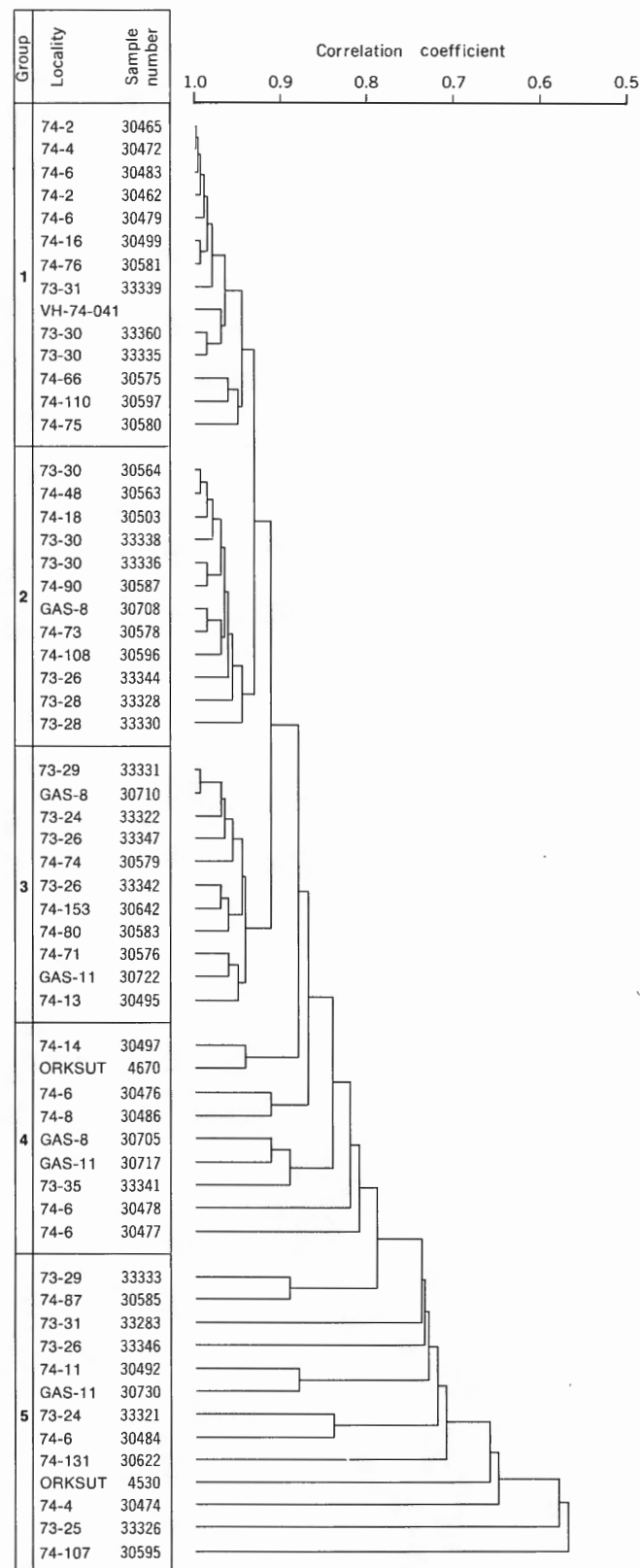


Figure 38. Q-mode cluster analysis of 59 petrographic samples from the Isachsen Formation. Data from Table 6.

GSC

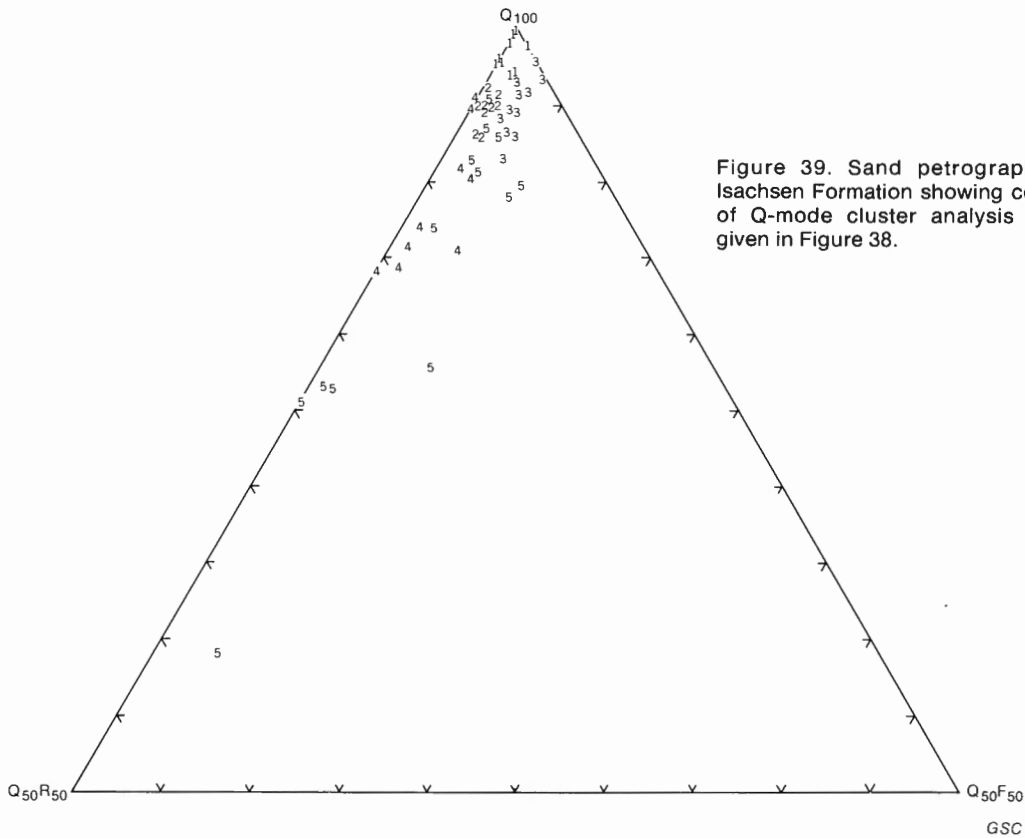


Figure 39. Sand petrography of the Isachsen Formation showing composition of Q-mode cluster analysis groupings given in Figure 38.

of the two sections have been analyzed (grain size, which can influence petrographic composition, is similar in all samples). The upward stratigraphic trend is indicated by the arrows; the position of the samples within the section is shown by the data point symbol, circles for sand derived from the southwest, crosses for sand derived from the southeast. If the circles and the crosses were in recognizable, separate groups it would indicate that the source areas had different surface geology, but such is not the case. If the arrows were straight it would show that the source area geology was changing significantly with time but, again, this is not the case.

Sediment sources

Paleocurrent evidence has shown that most of the Isachsen sands that outcrop within Banks Island were derived from the south or the east, from Coppermine Arch or the craton. Storkerson Uplift, Cape Crozier Anticline, and areas to the west also may have contributed some sediment but, as the discussion which follows attempts to demonstrate, most of the known features of the Isachsen petrography can be explained with reference to source rocks within the craton.

It is assumed at the outset that the geology of the craton has not changed significantly since the Cretaceous. Elsewhere (Miall, 1976a) the writer has suggested that a late Paleozoic or early Mesozoic clastic wedge may have covered part or all of Banks Island and adjacent areas, but there is no direct evidence for such a deposit. In fact, its presence is not required by any features of the Isachsen petrography; the suggestion was made originally to explain the high degree of

thermal alteration in the Devonian rocks. However, a steep geothermal gradient will produce much the same effects as deeper burial.

Figures 3 and 45 show the geology of the potential source area of the Isachsen sediments south and east of Banks Island. A brief description of the clastic grains which would be produced by erosion of these rocks is given below, accompanied by comments on their relative durability based on studies of erosion and transportation in modern environments. A humid environment probably prevailed during Isachsen time; evidence for this is summarized in a later section.

Archean. Rocks of this age make up most of the Shield extending southward from the mainland coast opposite Victoria Island. A small area of Archean rocks also crops out at the east end of Minto Uplift. These rocks form part of the Slave Province of the Canadian Shield. A detailed petrological description of a small area near Great Slave Lake was provided by Heywood and Davidson (1969). Rocks include tonalite, granite, granodiorite, heterogeneous schist and gneiss, various sediments and metasediments, and volcanic rocks. Banks Island is 500 km (300 mi) from the closest present-day outcrops of Slave Province. If any material was derived by rivers flowing directly from these outcrops, it is necessary to consider which of the rocks listed above would survive transportation. Mann and Cavaroc (1973) studied the composition of sands derived from a humid, temperate source area in North Carolina underlain by igneous, metamorphic and sedimentary rocks, and reached the following conclusions (*ibid.*, p. 879):

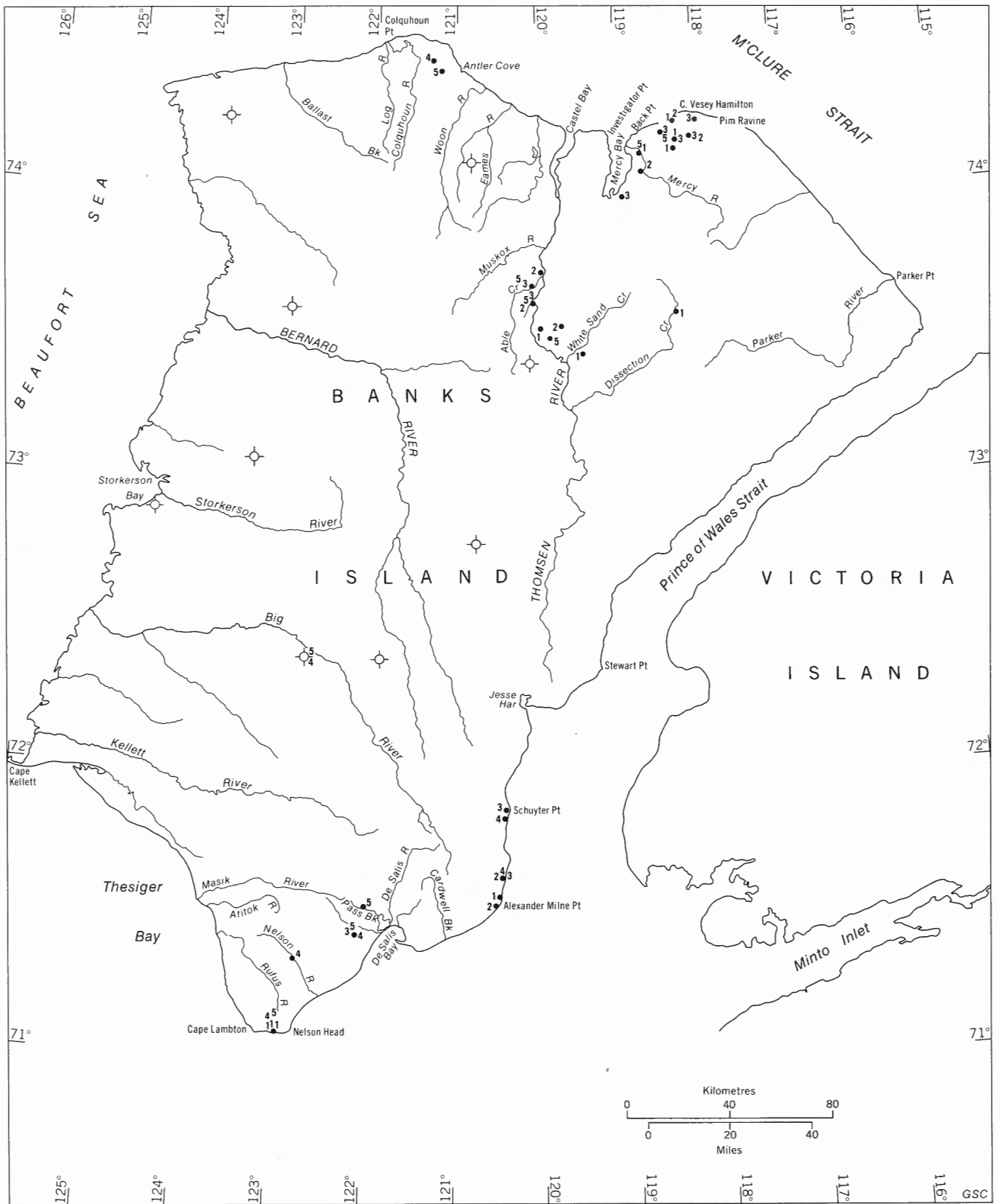


Figure 40. Sand petrography of the Isachsen Formation showing the areal distribution of Q-mode cluster analysis groupings (59 samples, 17 variables, 5 groups) given in Figure 38. Overlapping data points omitted.

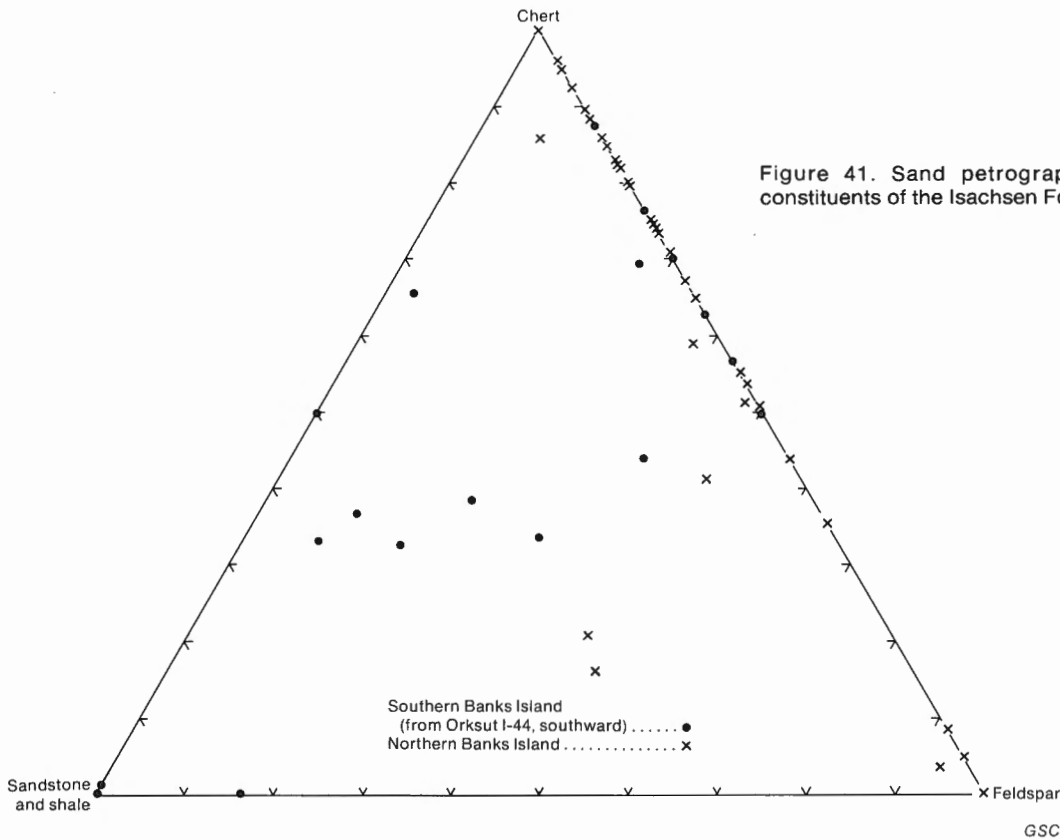


Figure 41. Sand petrography: minor constituents of the Isachsen Formation.

1. From a primary granitic or micaceous-feldspathic metamorphic source, ferromagnesian silicate minerals (and ferromagnesian rock fragments) and plagioclases are almost completely destroyed before leaving the source area.

2. Detrital mica and micaceous rock fragments are reduced to less than 10 per cent of the total sand sample, even from schistose source rocks, within the source area.

3. The proportion of sand-sized quartz released from metamorphic sources is detectably greater than from granitic sources; the converse is true for orthoclase.

Mann and Cavaroc (1973) concluded that sediments reaching the main drainage area are dominated by the more durable quartz varieties, orthoclase and granite/gneissic rock fragments and do not reflect relative mineral proportions in the parent source rocks. A precise comparison with the Isachsen is not intended by this discussion because of probable differences in climate, relief, etc., but the main trends deduced by Mann and Cavaroc probably are of general applicability.

Polycrystalline quartz grains, of both plutonic and metamorphic origin, are rapidly reduced in proportion relative to monocrystalline grains, probably as a result of fracture along crystal boundaries (Blatt, 1967, p. 422). Pittman (1969) confirms the rapid destruction of plagioclase twins during stream transport as a result of breakage along composition and twin planes.

First-cycle sediments derived from an Archean source such as Slave Province and under humid conditions should contain abundant plutonic quartz (predominantly monomineralic) and potassium feldspars, in approximate proportion to

their relative abundance in the source rocks. Minor constituents may include polycrystalline granite gneiss fragments, vein quartz, minor plagioclase and rare accessory minerals such as zircon, tourmaline, epidote, kyanite, garnet and mica. This assemblage is close to that found in the Isachsen Formation. Actual descriptions of the potential Archean sources confirm the correlation.

Heywood and Davidson (1969, p. 16–18) described the abundant granitic rocks of their report-area near Great Slave Lake. Features relevant to the present study include large phenocrysts of microcline, smaller crystals of albite, zoned oligoclase and rare greenish black biotite. Intergrowths of quartz and feldspar are common in some varieties. Accessories include apatite, magnetite, sphene, allanite, tourmaline, beryl and garnet.

Thorsteinsson and Tozer (1962, p. 25) briefly described the granodiorite which outcrops over an area of approximately 6 km² (2.5 sq mi) on the west side of Hadley Bay in northern Victoria Island. The rock is fine to coarse grained and is "composed essentially of varying amounts of plagioclase, microcline, quartz, biotite, muscovite". Quartz veinlets are common.

Although the composition of the grains in the Isachsen Formation is (with the exception of additions such as chert, to be discussed later) such as would be expected from erosion of the Archean rocks of the Slave Province, the abundant evidence of a multicycle origin for the quartz grains indicates that none of the detritus may, in fact, have been derived directly from the Archean, but that it has been cycled through several episodes of erosion and sedimentation. The Proterozoic sedimentary rocks of Minto Uplift are geographically

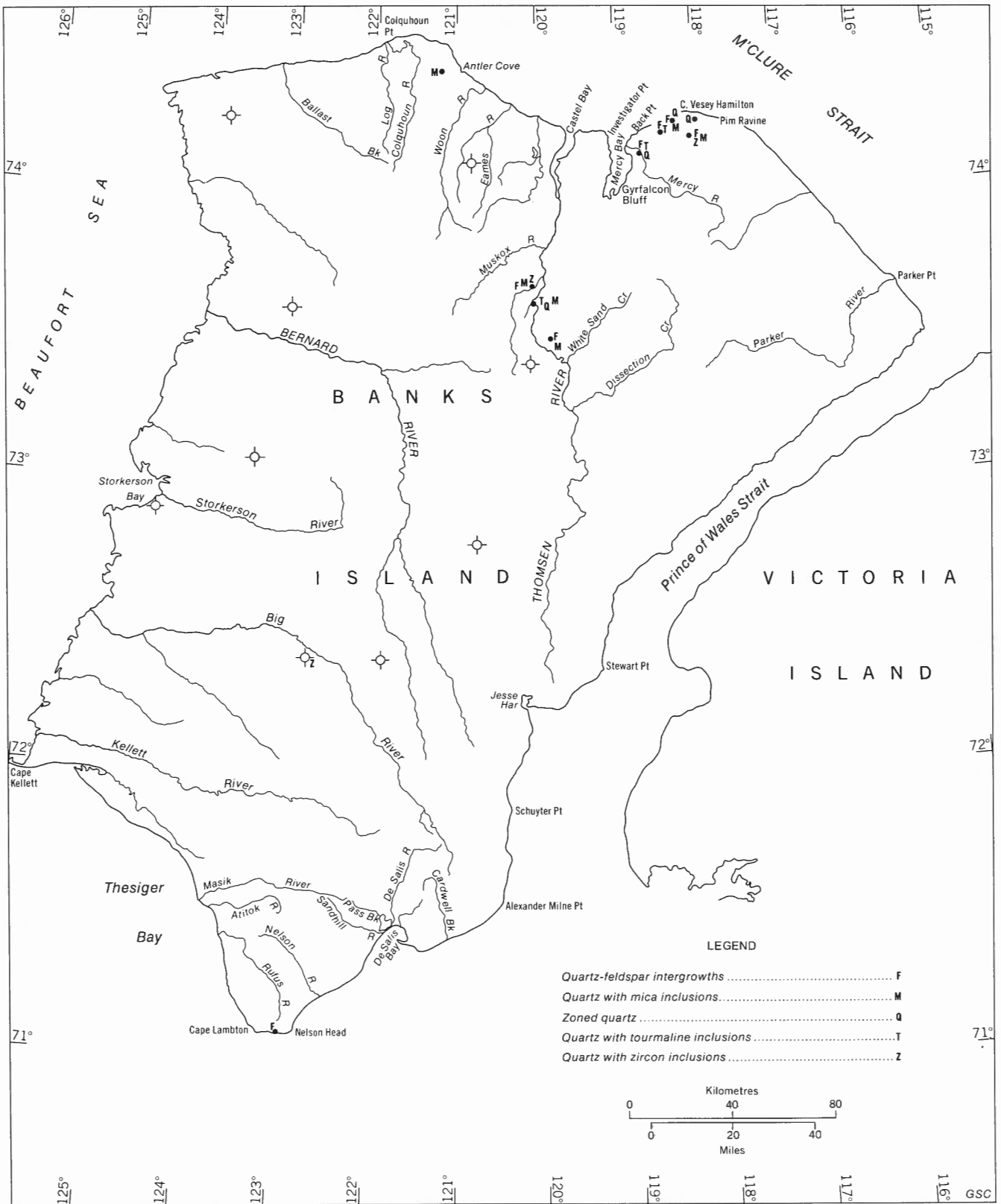


Figure 42. Distribution of some rare components in the Isachsen Formation.

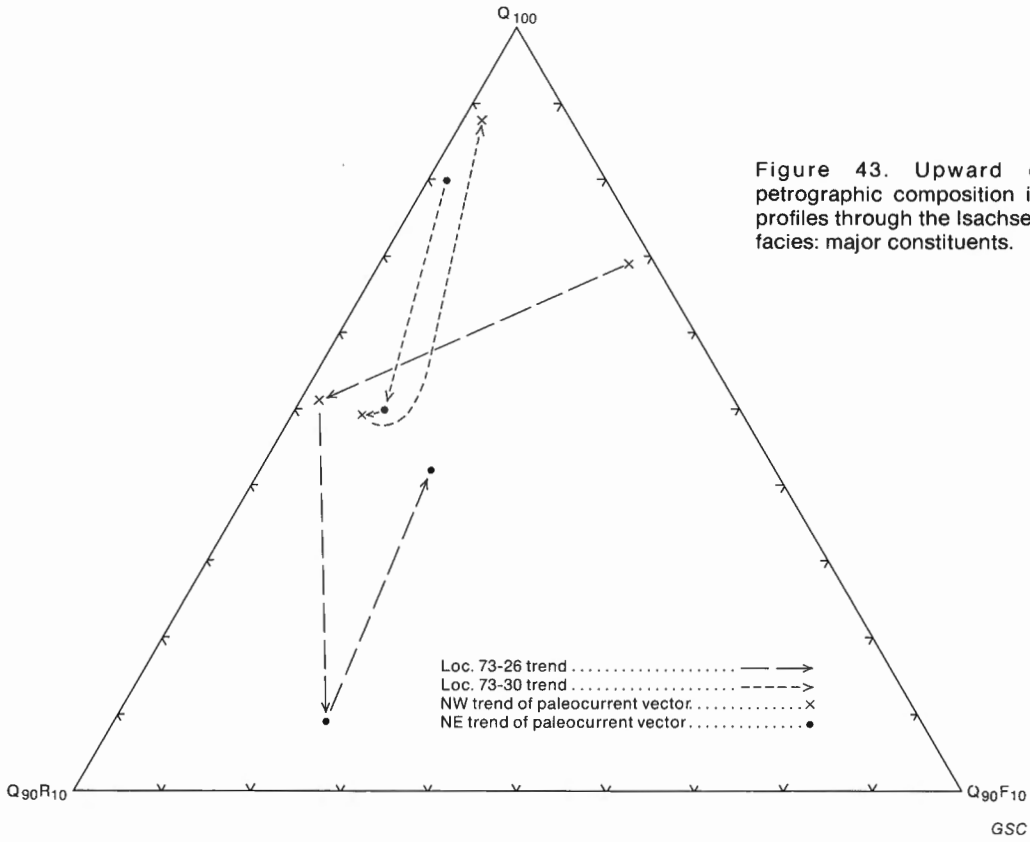


Figure 43. Upward changes in petrographic composition in two vertical profiles through the Isachsen coarse sand facies: major constituents.

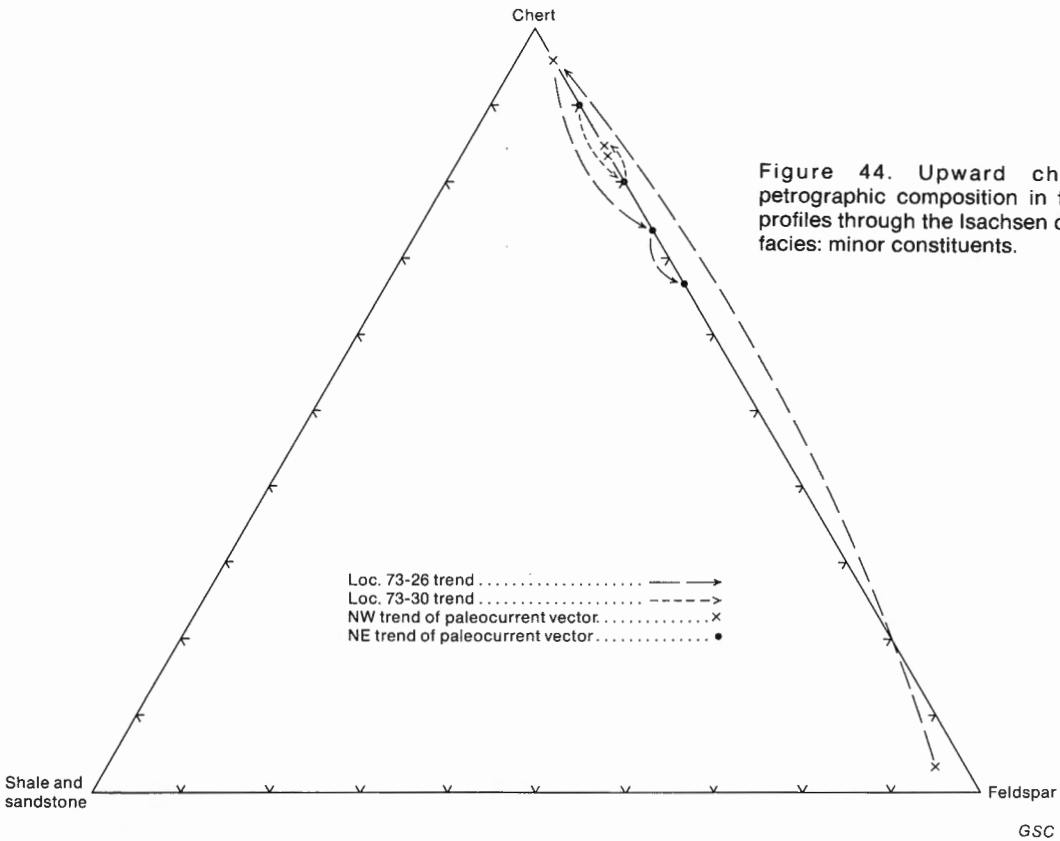


Figure 44. Upward changes in petrographic composition in two vertical profiles through the Isachsen coarse sand facies: minor constituents.

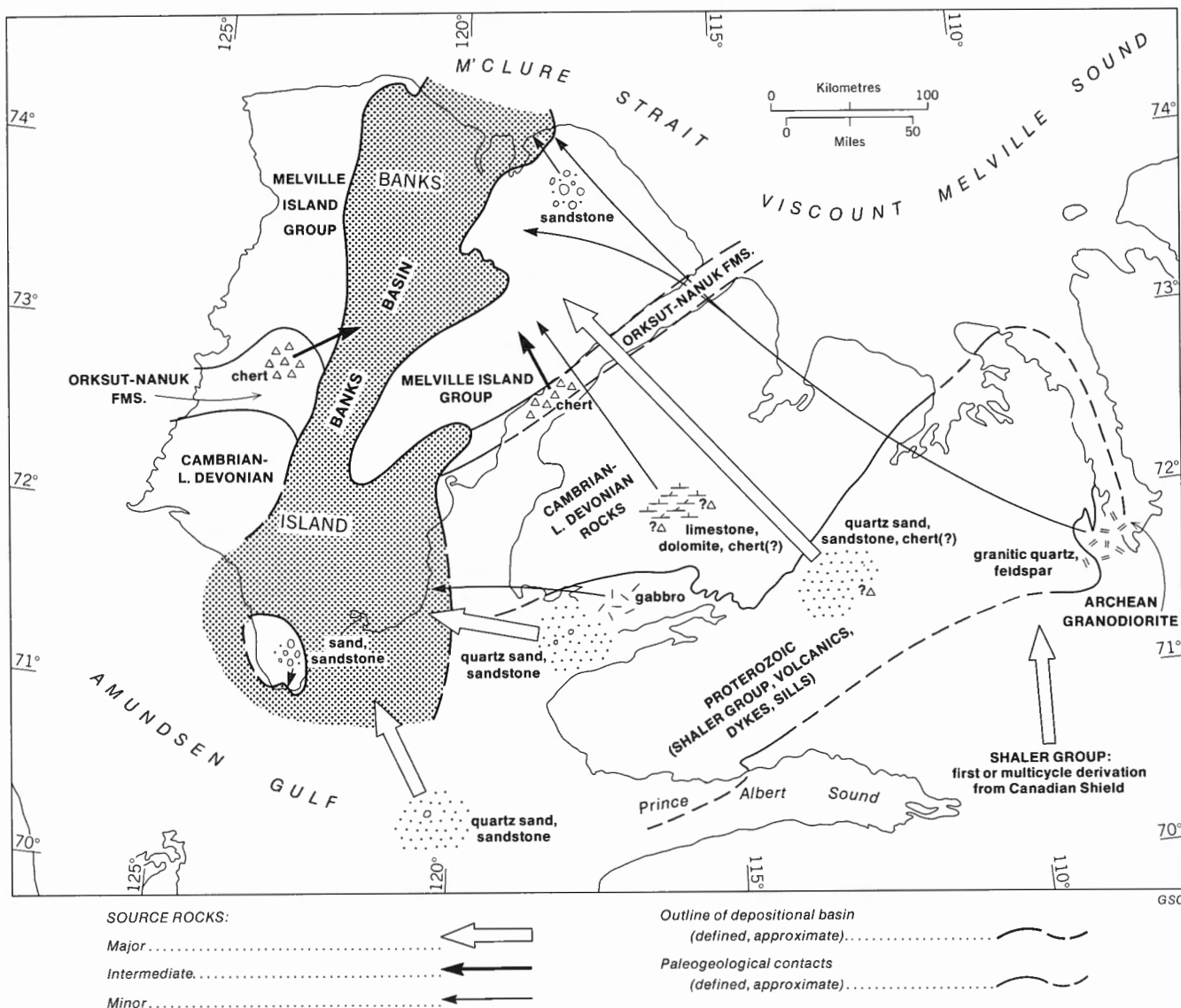


Figure 45. Source rocks of the Isachsen Formation; paleogeography of Banks and western Victoria islands and the Isachsen depositional basin (stipple).

much closer to Banks Island than the Shield and are obvious possibilities as intermediate source rocks between the Isachsen and its ultimate origin. (The possibility of Proterozoic sedimentary sources within the Shield cannot, however, be excluded.)

Proterozoic. Thorsteinsson and Tozer (1962) recognized seven Proterozoic map-units in the Minto Uplift area. Five of these are sedimentary formations comprising the Shaler Group. They consist of a variegated succession of carbonate, clastic and evaporitic rocks. Overlying the Shaler Group is the Natkusiak Formation, consisting of basalt flows and minor amounts of agglomerate; all these rocks are intruded by numerous gabbro dykes and sills.

Many of these sedimentary and intrusive rocks are unlikely sources of detritus for the Isachsen Formation, particularly the carbonates and evaporites which are subject to

rapid dissolution on exposure to the atmosphere or during transportation. The volcanic rocks and the dykes and sills also are of low potential as source rocks for, as discussed above, most of the principal components, including plagioclase feldspars and all the mafic minerals, are subject to rapid first-cycle chemical breakdown. Detrital iron oxides in the Isachsen may represent degraded ferromagnesian minerals and other than these the only contribution of the igneous rocks appears to be a few gabbro pebbles identified at Station 74-MLA-16 (Alexander Milne Point) and, possibly, stable heavy minerals such as magnetite and rutile.

There remain the terrigenous clastic rocks, particularly in the two oldest units of the Shaler Group, the Glenelg and Reynolds Point formations. Few detailed petrographic descriptions of these rocks have been published, but the data available indicate that the grain size and mineralogy of the sandstones are similar to those of the Isachsen Formation.

These two formations are considered to have provided the bulk of the Isachsen detritus. Data provided by G.M. Young (1974) and the author (Miall, 1976a) suggest that they were derived, in turn, from the igneous and metamorphic rocks of the Shield although, as in the Isachsen Formation itself, there is evidence of a polycyclic origin for some of the clasts (G.M. Young, 1974, p. 18). The intermediate steps between the Shield and the Shaler Group are not known and are beyond the scope of this report.

The most direct evidence of derivation from the Shaler Group is provided by the cobbles and boulders of Glenelg sandstone in the basal Isachsen conglomerate at Nelson Head (Station 74-MLA-6; Pl. 5). In spite of the importance of chemical weathering in destroying ferromagnesian minerals, it is surprising that the conglomerates at Nelson Head are completely lacking in gabbro clasts. Presumably this reflects an accident of exposure during the Cretaceous, for the underlying Glenelg Formation is intruded by several thick sills.

At Nelson Head (Miall, 1976a), the Glenelg sandstones are medium to very fine grained. They consist of from 73 to 100 per cent quartz, 4 to 18 per cent orthoclase, traces of chert, plagioclase, microcline and muscovite. Detrital limonite and heavy mineral concentrations locally reach 8 or 9 per cent. Quartz grains are subangular to well rounded. Some samples show sutured grains as a result of pressure solution. Evidence of authigenic growth on detrital cores is sparse.

The Glenelg Formation of Victoria Island (Thorsteinsson and Tozer, 1962; G.M. Young, 1974) includes many units of fine- to medium-grained 'orthoquartzite' and beds of pebble-conglomerate. White vein quartz is the predominant pebble type throughout Victoria Island but subordinate amounts of red and grey quartzite, schist, and red jasper also are present. Paleocurrent evidence in Victoria Island (G.M. Young, 1974) and at Nelson Head (Young and Jefferson, 1975; Miall, 1976a) indicates derivation from the Shield, to the southeast.

The Isachsen Formation includes a significant proportion of coarse-grained to very coarse grained sand, some of which may have been derived by abrasion and breakage of the quartz-pebble conglomerates of the Glenelg. The remainder of the quartz sand in the Isachsen probably was derived, with very little change in roundness or grain size, directly by disaggregation of the Glenelg sandstone strata.

As mentioned previously, clasts of silicified carbonate sediments also may have been derived from the Shaler Group, but the data available are inconclusive.

In the section on quantitative analysis, it was demonstrated that there are several subtle differences between the clast composition of the Isachsen in northern and southern Banks Island. Some of these probably are related to variations in composition of the Shaler Group clastic rocks along the length of the Minto Uplift, or to the proximity of the Isachsen depositional basin to the source area. These differences, and their interpretation, are listed below.

1. Feldspar grains and quartz-feldspar intergrowths are slightly more common in northern Banks Island. It may be that the small Archean granodiorite body at Hadley Bay was a significant first-cycle sediment source for the Shaler Group

rocks in that area and that this local distinctiveness has been carried over to the Isachsen sands.

2. Quartz grains with inclusions of biotite, tourmaline and zircon are indicative of an acid igneous source. They are virtually confined to northern Banks Island, and the same reasoning as in point 1, above, may apply. Vein quartz, also, is found only in this part of the island and quartz veinlets are abundant in the granodiorite (Thorsteinsson and Tozer, 1962, p. 25).

3. Clastic sedimentary rock fragments (sandstone and shale) are more abundant in southern Banks Island (not just in Nelson Head Graben where they form boulder conglomerates). If these clasts are derived from the Minto Uplift, it is not surprising that they are more abundant in areas where the Isachsen rests directly on the Proterozoic rocks.

Cambrian to lower Lower Devonian. Cambrian rocks consist of sandstone, shale, siltstone and dolomite. Most of the detrital material may be derived from the Proterozoic and some may have been re-eroded and included in the Isachsen, but the Cambrian beds are less than 120 m (400 ft) thick, and probably did not provide a major sediment source.

Ordovician to lower Lower Devonian rocks consist predominantly of limestone and dolomite, with minor amounts of chert. Carbonate rocks are not common as clasts in any but the most immature terrigenous rocks and the Isachsen is no exception. Limestone detritus is important only at Station 73-MLA-25 (Able Creek). Chert is more abundant as a clast type and may have been derived very largely from the lower Paleozoic sediments. Quantitative analysis shows that it is more abundant in northern Banks Island, where the Isachsen rests directly on the Devonian.

Upper Lower to Upper Devonian. Chert is abundant in the Nanuk Formation (Miall, 1976a), the outcrop area of which (during the Cretaceous) is shown in Figure 45. Much of the chert in the Isachsen, including some possibly derived from Storkerson Uplift, may have been derived from this unit. Unfortunately, it was not possible to distinguish different chert types in the thin sections and therefore it is impossible to be certain which of the potential chert sources was the most important.

The evidence suggests that, except locally, the Upper Devonian clastic rocks of the Melville Island Group contributed very little detrital material to the Isachsen. Clasts of sandstone and shale up to boulder size are common locally in northern Banks Island (Table 7) but quantitatively this material is insignificant. The writer (Miall, 1976a) and Klovan and Embry (1971) showed that most of the Melville Island sandstone is fine to very fine grained. Medium- to coarse-grained sand is present in the upper part of the succession and may have provided some detritus, but most of the quartz grains are angular (Klovan and Embry, 1971, Pl. 3) and have a somewhat different appearance from the grains of the Isachsen. Authigenic quartz overgrowths do not appear to be common in the Devonian sandstone units, in contrast with the abundant polycyclic overgrowths of the Isachsen quartz grains. One Isachsen sample alone (GSC loc. C-30595; Station 74-MLA-107, White Sand Creek) resembles a Devonian

sandstone. It was collected from close to the Isachsen–Melville Island unconformity.

Summary

A summary of the preceding discussion is provided in diagram form in Figure 45, in which the relative importance of the different source rocks is indicated.

Paleoclimate analysis

Techniques for a formal paleoclimate analysis are available for certain fossil groups but uniquely sedimentological techniques have yet to be developed. However, there is a range of climatic indicators within the Isachsen Formation that can be employed to develop some useful generalizations.

One approach is palynological analysis. Hopkins (1971) carried out a detailed study of the Isachsen Formation on northwestern Melville Island and concluded that the climate was warm-temperate or subtropical. Hopkins (1971, p. 111) visualized from palynological evidence, "a coastal plain dotted with lakes, swamps and meandering rivers. The lowland was clothed in a luxuriant cover of gymnosperms . . . The source of the Isachsen sediments was the higher areas bordering the basin, and these were undoubtedly covered by conifers."

Plant remains in the form of lignite coal chips or seams are common in the Isachsen Formation of Banks Island and there is no reason to suppose that the climate was not warm-temperate and humid as on Melville Island.

This conclusion is confirmed by the nature of the sedimentary structure assemblage. Streams in arid areas, in addition to a lack of marginal vegetation, show evidence in their deposits of strongly fluctuating discharge. Andersen and Picard (1974, p. 176) and Picard and High (1973) listed some distinctive features of waning floods in ephemeral streams. They include abundant small-scale ripple marks, dendritic surge marks (High and Picard, 1968), fluted steps and abundant evidence of desiccation. Fine-grained deposits are formed in abandoned channels during low-water stage. Collinson (1970) described the development of reactivation surfaces in crossbedded strata. They are internal erosion surfaces, which form during periods of waning flow and, as such, provide good evidence of fluctuating discharge. All these features are scarce or absent in the braided stream deposits of the Isachsen Formation, demonstrating that discharge was relatively constant, probably with mild seasonal fluctuations.

In perennial streams floods occur at only very rare intervals. Evidence for these in the Isachsen is provided by the rare pebble beds and scattered boulders (Figs. 27–29).

The existence in the Isachsen sands of numerous quartz grains with solution embayments (Pl. 19A–D) is another useful climatic indicator. Crook (1968) and Cleary and Conolly (1971) have shown that such features typically develop when a sand deposit is saturated with fluids rich in organic compounds, as in soil with a thick vegetation cover. The embayments are, in other words, an indicator of chemical weathering processes occurring in a humid environment. The embayments could represent solution before or during transportation reflecting, therefore, the climate of the source area rather than the depositional basin, but this is regarded as improbable because grains with deep embayments would be structurally

weakened and probably would not survive for long in a high-energy fluvial environment.

Paleohydrological analysis

The purpose of this section is to derive estimates of river sinuosity, slope discharge and drainage area, a knowledge of which can add a new dimension to paleogeographic reconstructions. The methods used are based mainly on comparisons with modern rivers but because of the large number of unknowns involved, they lack precision and the results should be regarded as little more than order-of-magnitude estimates.

Schumm (1963, 1968a, b, 1969, 1972) has developed a series of empirical relationships among water depth, channel width, discharge and sediment load, following his extensive investigations of rivers in the United States and Australia. Other important works are those by Leopold *et al.* (1964), Brice (1964), Allen (1968) and Malde (1968). Very few applications of these data and ideas to ancient rocks have been attempted. Schumm (1968a) investigated the paleohydrology of some Quaternary fluvial deposits in Australia; Friend and Moody-Stuart (1972) studied a Devonian fluvial formation in Spitsbergen. Cotter (1971) investigated a Cretaceous sandstone in Utah and Leeder (1973) studied some Devonian rocks of Scotland.

Part of the discussion that follows has been presented in a slightly different form by the author (Miall, 1976b).

Discharge as a function of climate

Climatic variables, particularly temperature and rainfall, are pre-eminent in determining river discharge rates. Under arid or arctic conditions discharge will be extremely variable, reaching a peak following spring melt or a flash flood, and possibly dropping to zero at other times. Similar variability will persist in a warm-arid or tropical-arid climate but under warm or tropical humid conditions discharge will be far less variable because of the effect of vegetation in trapping and delaying water runoff.

This variability also is reflected in rates of erosion and sediment transportation. Langbein and Schumm (1958) showed that the highest sediment yields, up to 1500 tons per square mile of drainage area (6×10^5 kg/km²) per year, occur in semiarid to semihumid areas in which there is little vegetation cover. With increasingly humid climate, the rate of erosion decreases and, in areas of 45 inches (114 cm) of rainfall per year and greater, the sediment yield appears to be constant at approximately 450 tons per square mile (1.8×10^5 kg/km²) per year.

Evidence for the type of climate prevailing during Barremian and Aptian time was summarized in the preceding section. It was concluded that temperate to subtropical, humid conditions prevailed. Most of the Isachsen rivers, therefore, are thought to have been perennial rather than ephemeral and flash flood conditions would have been rare.

Paleohydrology of the meandering streams

Several workers have shown that an analysis of fining-upward cycles can yield information regarding channel dimensions and meander wavelength (Cotter, 1971; Friend and Moody-Stuart, 1972; Leeder, 1973). These parameters then enable

estimates to be made regarding discharge and drainage area. Such cycles have been identified tentatively in the Orksut I-44 well (Fig. 19) and are the subject of the analysis that follows (the cycles in the Castel Bay C-68 well have not been studied at the time of writing this report).

Estimation of channel parameters. Fining-upward cycles develop as a result of a lateral accretion on a point bar surface. As shown in Figure 46 (redrawn from Leeder, 1973, Figs. 1, 4), the coarse sand member in each cycle represents simultaneous deposition over the entire accretion surface and over virtually the entire depth range of the channel. The thickness of the sand member is therefore equal to the bankfull depth of the channel, allowing for postdepositional thickness changes such as compaction. In the Orksut I-44 well three cycles have been identified and each have sand members approximately 10 m (33 ft) thick. This value is used as the starting point in the analysis.

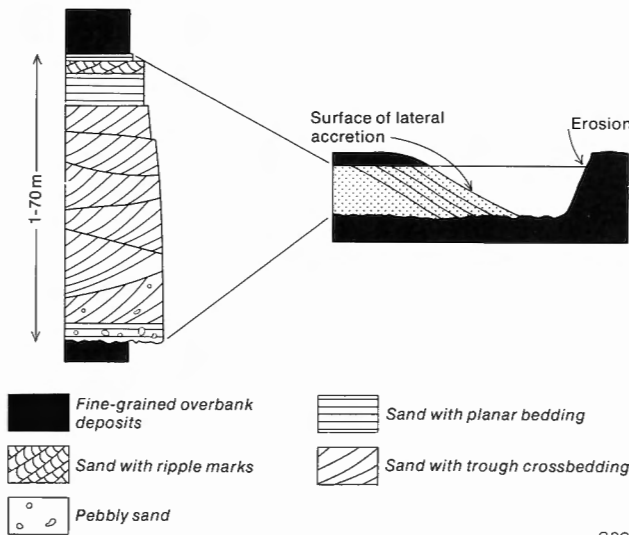


Figure 46. Development of a fining-upward sequence by lateral accretion (after Leeder, 1973).

Cotter (1971, p. 133) summarized various estimates that have been made regarding the relationship between width and depth in meandering channels. Leeder (1973) investigated this relationship on a more rigorous basis using published data from modern rivers, and arrived at the following equation for sinuous rivers:

$$\log w = 1.54 \log h + 0.83 \quad (1)$$

where w = bankfull width, in metres, h = bankfull depth, in metres. This relationship has a 95 per cent confidence limit of $\pm 0.7 \log$ units. Therefore the channels at Orksut I-44 have channel widths in the order of 230 m (750 ft) with 95 per cent confidence limits of 50 and 1200 m (160 and 3900 ft). Width:depth ratios F show a possible range of 5 to 120. Schumm (1963) stated that for sinuous rivers F is typically less than 10.

Schumm (1972) gave these equations for the relationship between slope s , sinuosity (P ; the ratio of channel length to

valley length) and the channel dimensions w and F (all in imperial units):

$$s = 30(F^{0.95}/w^{0.98}) \quad (2)$$

$$P = 3.5 F^{-0.27} \quad (3)$$

From the estimated values of w and F in Table 8, a range of values for P and s has been calculated (converted to metric units in Table 8).

Values for slope are somewhat high. Data summarized by Eicher (1969, p. 1085) and Friend and Moody-Stuart (1972, Table 1) indicate a range of 20 to 330 cm/km for sandy, braided rivers. Sinuous, suspension load streams would be expected to show gentler slopes. The sinuosity value of 2.3 calculated from the minimum channel dimensions is comparable with the data summarized by Schumm (1963), which showed that sinuosities greater than 2 were typical for suspension load streams. The lower values of 1.5 and 1 are regarded as improbable and virtually impossible, respectively.

Sinuosity also can be calculated from paleocurrent information. At Pass Brook (Station 74-MLA-11) and Sandhill River (Station 74-MLA-12), current directions are strongly bimodal (Figs. 21, 22). The two modes in each case may represent different channel reaches in a highly sinuous river. Differences in mean azimuth between the modes are 210° and 149° , respectively (Table 3). Langbein and Leopold (1966, p. H5) provided an equation relating angular change to sinuosity. Rewriting the equation using degrees instead of radians, the relationship is as follows:

$$P = 1/1 - (\theta/252)^2 \quad (4)$$

where θ is the maximum angular range in channel orientation. This gives sinuosity estimates of 3.2 (Pass Brook) and 1.5 (Sandhill River). There is no evidence that the modal directions at these localities represent the maximum divergence from the river valley orientation and the two values should be regarded as local minima only.

Leopold *et al.* (1964, Fig. 7-41) showed that there is a linear, logarithmic relationship between channel width and meander wavelength and they provided the following relationship:

$$Lm = 10.9 w^{1.01} \quad (5)$$

where Lm = meander wavelength, in feet, and w = channel width, in feet. Meander wavelength, therefore, can be calculated using the values for channel width derived above; the results are given in Table 8 in metric units.

Estimation of discharge and drainage area. A relationship between meander wavelength and mean annual discharge Qm has been provided by Carlston (1965); it is given in imperial units as:

$$Lm = 106 Qm^{0.46} \quad (6)$$

Values for discharge derived using this equation are shown in Table 8.

There are two methods by which drainage area (A) may be derived from these results. Dury (quoted in Leopold *et al.*, 1964, p. 312) showed that a linear, logarithmic relationship exists between drainage area and meander wavelength. Comparisons with their data suggest a range of values for the total drainage area for the trunk stream flowing past the Orksut location (Table 8).

Table 8. Paleohydrology of the meandering river at Orksut I-44

PARAMETER	SYMBOL	LOW	MEDIAN	HIGH	UNIT	EQUATION	AUTHOR OF EQUATION
Channel width	w	50	230	1200	m	1	Leeder (1973, p. 268)
Width : depth ratio	F	5	23	120	—	—	
Channel slope	s	85	365	1750	cm/km	2	Schumm (1972, p. 101)
Sinuosity	P	2.3	1.5	1	—	3	Schumm (1972, p. 104)
Meander wavelength	Lm	560	2700	14 000	m	5	Leopold <i>et al.</i> (1964, p. 297)
Mean annual discharge	Qm	14	410	15 500	m ³ /sec	6	Carlston (1965)
Drainage area	A ₁	780	23 300	52 000	km ²	—	Leopold <i>et al.</i> (1964, p. 312)
Drainage area	A ₂	1300	37 900	1 400 000	km ²	—	Leopold <i>et al.</i> (1964, p. 320)

GSC

Table 9. Paleohydrology of the braided streams, Isachsen Formation

PARAMETER	SYMBOL	LOW	MEDIAN	HIGH	UNIT	EQUATION	AUTHOR OF EQUATION
Mean depth	d _s	2.5	3.6	4.1	m	7	Allen (1968)
Bankfull depth	d _b	4.7	5.7	5.9	m	8	Schumm (1972)
Sinuosity	P	1.03	1.08	1.13	—	4	Langbein and Leopold (1966)
Width/depth ratio	F	93	78	66	—	3	Schumm (1972)
Mean annual discharge	Qm	350	600	670	m ³ /sec	—	—
Mean annual flood	Qma	1600	2500	2710	m ³ /sec	9	Schumm (1972)
Maximum flood	Qmax	7000	10 000	9000	m ³ /sec	—	—
Drainage area	A ₁	10 000	20 000	60 000	km ²	—	Leopold <i>et al.</i> (1964)
Drainage area	A ₂	32 000	55 000	61 000	km ²	—	Leopold <i>et al.</i> (1964)

GSC

Table 10. Hydrology of some modern braided rivers

RIVER	d _b	w	Qm	Qma	Qmax	v	AUTHOR
Brahmaputra	15	13	19 000	40 000	71 000	2.4	Coleman, 1969
Ganga	<10	—	—	43 300	—	3.4	Singh and Kumar, 1974
Donjek	3	.4-2.2	—	1400	—	3.6	Rust, 1972
Durance	6.6	.7	188	—	5200	6	Doeglas, 1962
L. Platte	—	.4-6	109	—	3200	—	Smith, 1971a
Slims	5	.3-1.8	—	570	—	>2	Fahnestock, 1969
Amite	6.7	.07	—	1400	—	—	McGowen and Garner, 1970
Tana	15	.6-2	150	1800	3500	—	Collinson, 1970
Bijou Creek	2.4-3.6	.2-.7	—	—	13 000	6	McKee <i>et al.</i> , 1967

Bankfull depth (in metres)d_b Mean annual flood (m³/sec)Qma
 Channel width (in kilometres)w Maximum flood (m³/sec)Qmax
 Mean annual discharge (m³/sec)Qm Flood velocity (m/sec)v

GSC

A second method derives from the general relationship

$$Q \propto aA^b$$

presented by Leopold *et al.* (1964). The values for a and b vary according to climatic factors and the magnitude of the river system (Gregory and Walling, 1973, p. 267). Leopold *et al.* (1964, p. 251) suggested a value of 1 for exponent b in humid regions, when using Q as a measure of mean annual flood (bankfull discharge). Hack (1957, p. 54) determined that for the Potomac River mean annual discharge in ft³/sec was equal to the drainage area in square miles. An examination of data provided by Leopold *et al.* (1964, Table 7-13) indicates that such a relationship is in fact common. A second estimate of the drainage area upstream from Orksut I-44 is therefore possible, as shown in Table 8. This approximation has been used by several authors (Eicher, 1969, p. 1082; Cotter, 1971, p. 136) in similar exercises of paleohydrological reconstruction.

A comparison of the two sets of results shows that the mean and minimum values are of a similar order of magnitude but that the maximum values are completely different. The larger figure is regarded as completely unrealistic.

It must be emphasized that all the equations and data sets used in these calculations involve a considerable margin for error and that, in using one estimate as a basis for a successive estimate, errors may become additive. For this reason the results in Table 8 should be regarded as providing no more than order-of-magnitude approximations. A useful check on the validity of the estimates can be carried out by relating the different values for drainage area to known details of local paleogeography. Second, paleohydrological reconstructions from the proximal, braided stream facies upstream should be consistent with those given in Table 8, in that differences between them should be explainable in terms of their derivation from different parts of the same catchment area. A discussion along these lines is presented at the end of the section on paleohydrological analysis.

Paleohydrology of the braided streams

The five vertical profiles discussed earlier in this chapter provide the necessary data for estimating the various hydrological parameters. The similarity between all five profiles justifies grouping of certain data items for the purpose of generalized calculations.

Estimation of channel parameters. In the absence of fining-upward cycles a different approach must be used to estimate channel depth and width. Allen (1968, Fig. 6.4) has shown that the mean height of large-scale ripple marks (which includes trough and planar cross-stratification in his terminology) is proportional to mean water depth. The relationship is expressed as follows:

$$H = 0.086d_s^{1.19} \quad (7)$$

where H = mean ripple height, in metres, and d_s = mean water depth over the sedimentary structure, in metres. Allen's data indicate a ± 50 per cent variation in water depth for a given ripple height; nevertheless the equation provides a method of obtaining estimates of mean water depth in the Isachsen streams using H = mean crossbed set thickness at each locality (Table 4). There is some doubt that planar crossbeds formed from advancing bars (rather than migrating

dunes) can be used in such calculations, but trough crossbeds also are present and these probably represent the type of dune structure studied by Allen. They have a similar H distribution to the planar crossbeds; the mean value for all trough crossbeds from all five profiles is 40 cm (16 in.). Estimated values for d_s are shown in Table 9.

Sinuosity can be estimated from paleocurrent data in the five profiles. As discussed in the section on paleocurrent analysis, the moving average azimuth is interpreted as a measure of the orientation of the braided channel system. It is, in other words, the mean orientation of all the minor channels within the system at a given time. The vertical change in mean azimuth is interpreted as a result of slow downstream meander migration. Therefore the range in values of the mean azimuth is a measure of θ , the maximum angular range in channel orientation, and Langbein and Leopold's (1966) equation for determining sinuosity may be used (equation 4, above). Values for θ for each vertical profile were discussed earlier in this report. The estimates of sinuosity derived from them are given in Table 9. Schumm (1963) reported that bedload streams typically have sinuosities less than 1.3. The Isachsen examples thus are well within the defined range.

Width:depth ratios may be derived by substituting values of sinuosity into equation 3. For values of P ranging from 1.03 to 1.13, F is calculated at between 93 and 66. Schumm (1963) stated that low sinuosity, bedload streams have width:depth ratios of over 40. Smith (1971a, p. 3409) reported values of F ranging from 36 to 341 for the braided lower Platte River.

From estimates of depth and width an approximation of channel cross-section area can be obtained.

Estimation of flow velocity and discharge. Leopold *et al.* (1964, p. 243) stated that water flow is less than or equal to the mean annual discharge 75 per cent of the time. Such discharge typically fills a channel to approximately one third of its maximum (bankfull) depth (*ibid.*, p. 243). As stated previously, 63 per cent of the total thickness of the five profiles comprises planar crossbedded sand. The remaining 37 per cent of the sands represent departures from these flow conditions and may represent either higher or lower energy conditions. If the percentage of crossbedding in a section is accepted as an estimate of the proportion of the total depositional time under which conditions were suitable for crossbed formation, then it follows that such conditions must have been close to those defined by the term mean annual discharge.

Assuming that material of all sizes is available for transportation, the grain size of a deposit formed by bedload transportation will be directly related to flow velocity. The mean grain size of the sands in the planar crossbedded units ranges from approximately 0.2 to 0.5 mm (medium to coarse grained). Sundborg (1967, Fig. 1) showed that material of this size will commence movement at velocities of approximately 40 cm/sec. Friend and Moody-Stuart (1972, Fig. 27), using the data of Guy *et al.* (1966), showed that medium to coarse sand deposits, characterized by large-scale bedforms such as dunes, will form at mean flow velocities of 50 to 100 cm/sec.

Pebble beds and scattered boulders are interpreted as indicating greater flow velocities. Several empirical equations are available for calculating threshold movement velocities from clast diameter, as summarized by Malde (1968, p. 46)

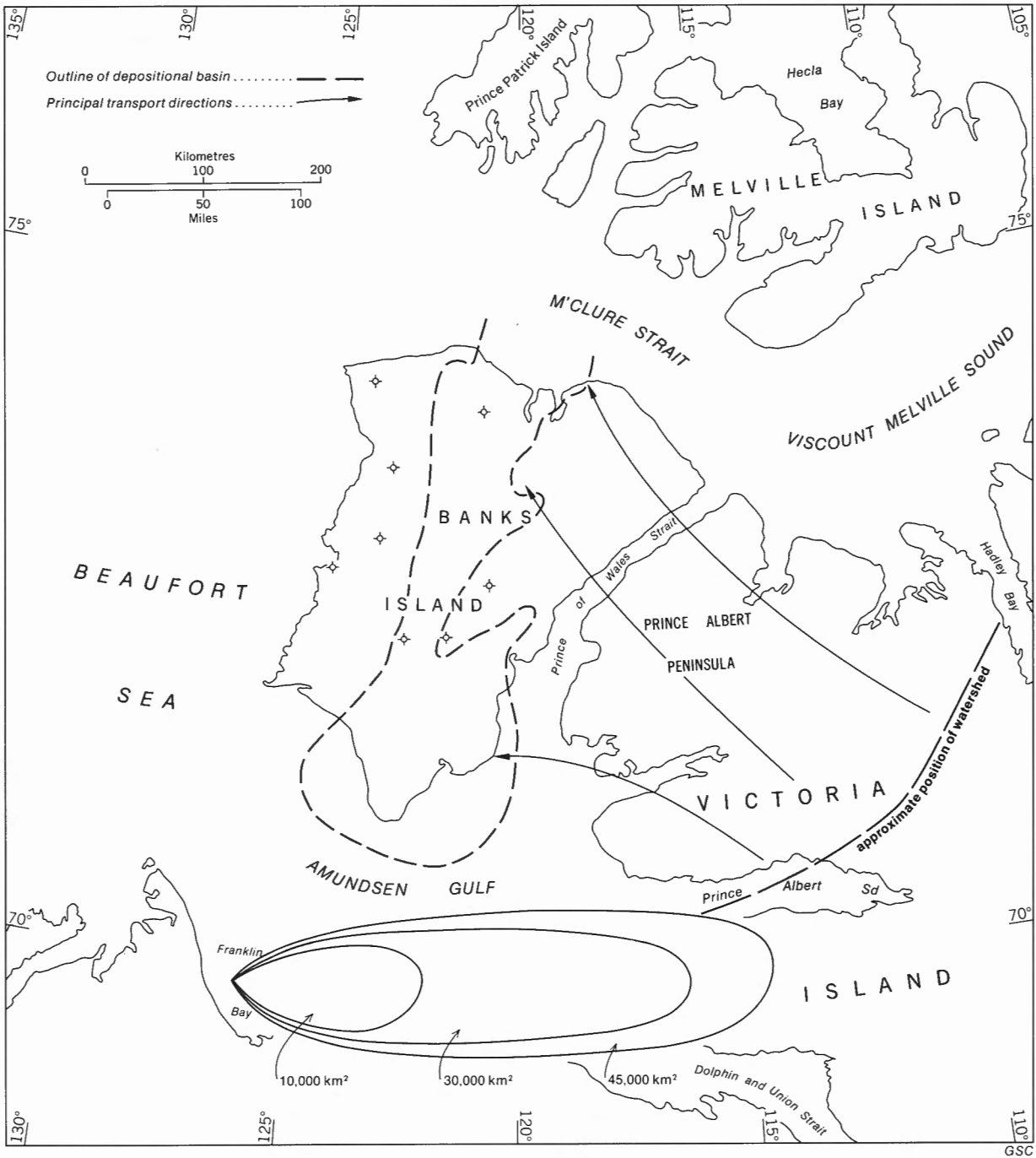


Figure 47. The main drainage pattern on the east side of Banks Basin. At bottom is shown a range of areas at the same scale as the map to illustrate the range of drainage basin areas given in Table 9.

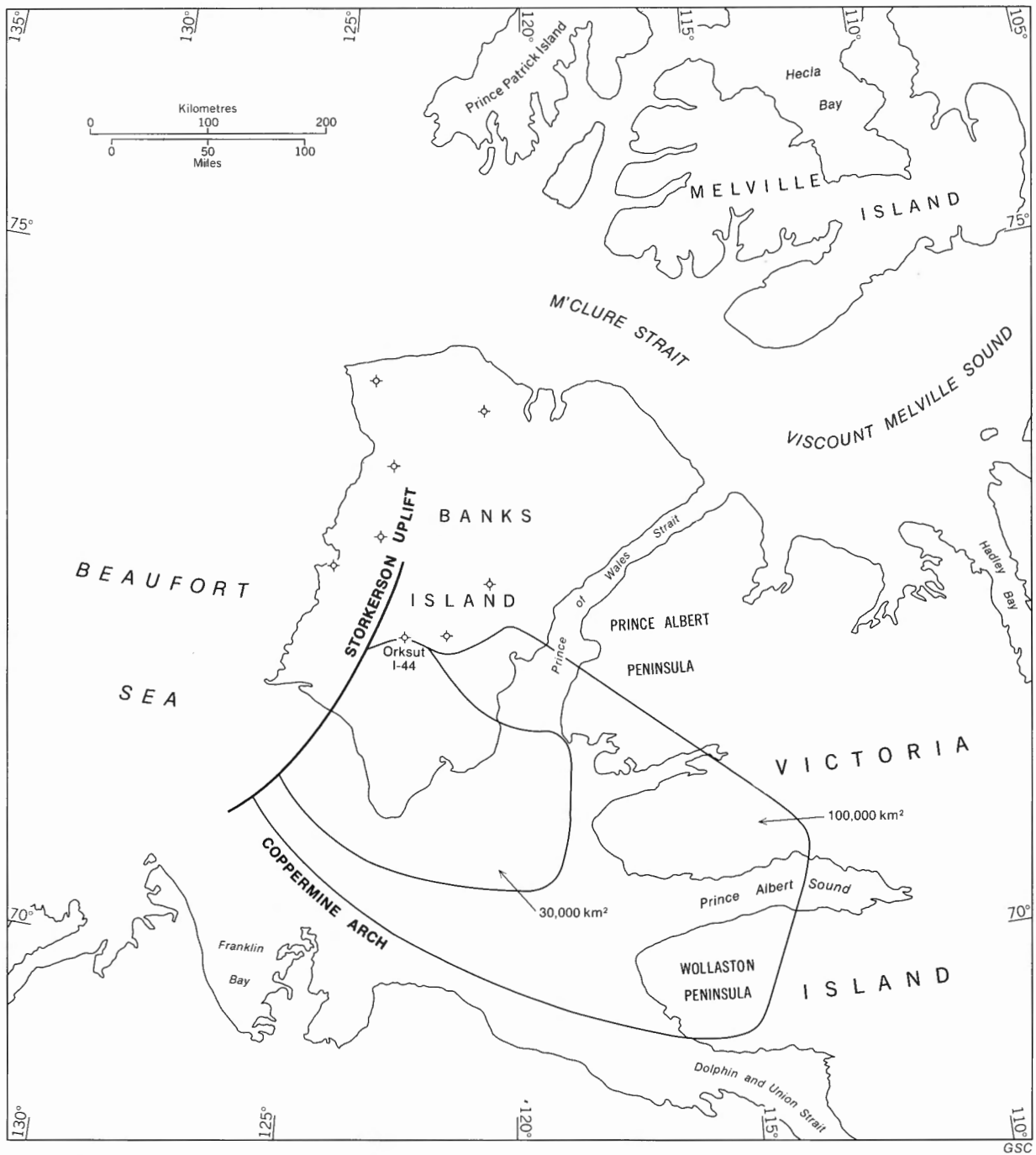


Figure 48. Estimated drainage area, meandering stream at Orksut I-44. The configuration of the drainage area is hypothetical, but is drawn to comply with paleogeographic constraints such as the probable existence of Coppermine Arch and Storkerson Uplift as watershed areas.

and Dott (1974, p. 245). The largest boulder found in the Isachsen Formation has a diameter of 75 cm. Assuming no debris flood transportation (for which there is no evidence), the calculated flow velocity required to move this boulder is 4 m/sec. There is a small probability that larger material may be present, indicating even faster flow rates.

By using estimates of cross-section area and mean and maximum flow velocity, it is possible to calculate discharge both for average flow conditions and for flood conditions. Mean annual discharge is the product of mean annual cross-section area and mean annual flow velocity. An estimate of maximum flood discharge also can be arrived at in the same manner, using bankfull depth and the same width:depth ratio. Empirical work by Schumm (1969, p. 256) has resulted in the following equations:

$$d_b = 0.6M^{0.34}Qm^{0.29} \quad (8)$$

$$d_b = 0.09M^{0.35}Qma^{0.42} \quad (9)$$

where d_b is bankfull depth of river tract, in feet, M is the percentage of silt plus clay in the stream channel perimeter, Qm is the mean annual discharge, in cubic feet per second, and Qma is mean annual flood, in cubic feet per second. For bedload streams, M is typically 5 per cent or less (Schumm, 1968a, b). By using $M = 5$ per cent and values in Table 9 for Qm , bankfull depth can be estimated. Then, using estimated bankfull depth, mean annual flood values can be derived from equation 9.

Values for $Qmax$ are considerably greater than those calculated for mean annual flood, indicating that boulders were moved only by the rare catastrophic floods which occurred at intervals of several years or tens of years.

Data from some modern braided rivers are given in Table 10 for purposes of comparison. Some of the figures are provided by the quoted authors; others, particularly depth and width values, are interpolated from the authors' illustrations. Data from many other rivers are available (e.g., in Schumm, 1968a, and Leopold *et al.*, 1964), but the rivers used in Table 10 are the only ones which are known to contain sediments and sedimentary structures similar to those of the Isachsen Formation.

A comparison of the values in Table 9 with those in Table 10 shows that the estimated paleohydrological parameters of the streams that deposited the Isachsen Formation are of the same order of magnitude as those of many of the smaller modern braided rivers, rather than such major rivers as the Brahmaputra.

Estimation of drainage area. Two estimates of drainage area can be made using the relationship between drainage area and discharge discussed earlier in this section. The first estimate A_1 is derived from an examination of Leopold *et al.*'s (1964, Table 7-13) data on bankfull discharge (mean annual flood) and area. The second estimate A_2 is obtained by using the approximation quoted by Eicher (1969, p. 1082) to the effect that mean annual discharge in ft^3/sec is equal to drainage area in square miles.

Paleogeographic implications

Estimates of drainage area and discharge have been obtained independently for two different parts of the Isachsen river system. The estimates should be compatible with one another,

in that the proximal, braided streams should have smaller discharges and drainage areas than the river at Orksut I-44. Moreover, the river at the Orksut locality may represent the combined discharges of more than one tributary braided stream. A third constraint is that the drainage areas of the tributary streams cannot overlap, and a fourth constraint is that a close relationship exists between drainage area and length (Leopold *et al.*, 1964, Fig. 5-6).

Proximal, braided stream deposits are known in three areas on Banks Island: Cape Vesey Hamilton, Baker Creek and Alexander Milne Point. A minimum of three rivers therefore are required to produce these accumulations. A single river meandering laterally over an alluvial plain in the area of Alexander Milne Point could have produced at different times all the known deposits between De Salis Bay and Schuyter Point. Lateral migration across its own deposits is a common feature of braided streams (Gole and Chitale, 1966; Miall, 1976b). Similarly, a river flowing northwest through the White Sand Creek area and debouching into Banks Basin in the area of Baker Creek could explain all the deposits that outcrop along Thomsen River. The area between Thomsen River and Mercy Bay probably was a watershed in Isachsen time, for the Christopher Formation rests directly on the Devonian basement. On the north side of the watershed, a third stream may have been responsible for all the Isachsen coarse sand facies found between Mercy Bay and Cape Vesey Hamilton. The major shift in paleocurrent patterns at Station 73-MLA-30 has been interpreted as the result of tectonic readjustment of a river pattern. Possibly it represents a river capture event within the same drainage area, as a result of differential uplift.

Nothing is known regarding the area between Schuyter Point and Dissection Creek. Braided stream deposits, in fact, may be absent within much or all of this area. Figure 47 shows the distribution of possible source areas for the three known braided streams.

The drainage basin represented by the Isachsen deposits at Orksut I-44 must have been large enough to embrace that of the upstream, braided river portion headward from Alexander Milne Point, assuming the paleocurrent analysis is correct. Some estimates of the total drainage area are shown in Figure 48, in which the shape has been drawn to fit certain constraints of local paleogeography. Coppermine Arch (Lerand, 1973) is assumed to have been a watershed at the time. Contemporaneous rocks to the southwest are in part marine (Young *et al.*, 1976) and therefore rivers cannot have originated anywhere to the southwest of the present-day Amundsen Gulf. The importance of Storkerson Uplift as a water and sediment source is unknown. It is presumed to be small for the sake of this analysis. The largest of the areas shown, at 100 000 km^2 (39 000 sq mi), is approximately the right area to allow the inclusion of major streams entering the basin from the east, on the scale suggested in Figure 47.

Christopher Formation

Lithofacies and sedimentary structures

As shown in Chapter 2, most of the Christopher Formation consists of shale and clay, much of it silty. Silt, siltstone, sand

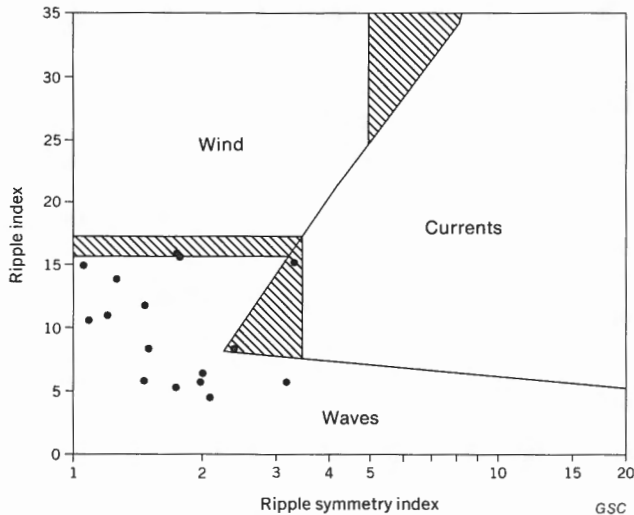


Figure 49. Plot of ripple index and ripple symmetry index for 16 ripple marks at Stations 74-GAS-4 (Rufus River) and 74-GAS-13 (Atitok River). Environment fields are from Tanner (1967).

and sandstone are prominent locally, as at Atitok River (Station 74-GAS-13; Pl. 8). Most of these coarser grained rocks occur in beds less than 4 m (13 ft) thick, although a few thicker units have been recorded. The lowermost unit exposed at Atitok River is a sandstone bed 8 m (26 ft) thick.

Sedimentary structures are rare in the Christopher Formation. None are observable in the shale apart from local bioturbation. Most of the coarser grained units exhibit planar bedding, lamination or flaser bedding. Rare, low-angle planar crossbeds are present in a few places. More common are small-scale, slightly asymmetrical ripple marks, and these are particularly well displayed in some of the siderite-cemented sandstone units. The top surface of such units, as at Rufus River (Station 74-GAS-4) and Atitok River (Station 74-GAS-13) may be covered with a train of ripple marks. They show slightly wavy crests and rare bifurcation. Small vertical burrows 1 cm deep are abundant locally in the ripple surface. A plot of ripple index and ripple symmetry index of these ripples (Fig. 49) suggests that all may have been wave formed, by comparison with the data of Tanner (1967, Fig. 1) and Reineck and Singh (1973, Figs. 27, 28). Ripple orientation is relatively consistent, with a vector magnitude per cent of 92.4. The steep side of the ripples is oriented in a weighted mean direction of 197°.

Depositional environment

As recorded in Chapter 2, there is abundant evidence throughout the Christopher Formation of a marine origin for the formation in the form of the invertebrate fauna. This includes ammonites, pelecypods, crustaceans, dinoflagellates and abundant foraminifera. Interpretations by J.H. Wall (*pers. com.*, 1974) based on the foraminiferal assemblages, suggest an inner to outer shelf environment for the fine-grained (shale and clay) units.

A shallower water, nearshore, possibly shallow subtidal or intertidal origin is indicated for some of the coarser grained units. The laterally persistent pelecypod-bearing sandstone

exposed at Atitok River (Pl. 8A) is interpreted as a nearshore sand bar containing local shell concentrations. Vertical burrows are, according to Heckel (1972, Fig. 7), most typical of a littoral environment, within a tidal flat zone or in the subtidal environment above wave base. Ripple symmetry suggests a wave-formed origin. The interpretation is confirmed by the nature of the pelecypod assemblages, according to J.A. Jletzky (*pers. com.*, 1976). There is an overall similarity with some of the tidal flat deposits described by Klein (1971).

The sandstone at Rufus River is near the base of the formation, at a point where the Christopher shows a rapid southward thinning. It probably represents a shoreline deposit in an onlapping sea that was slowly inundating the Cape Lambton Uplift. Other sandstone units represent local shoals within the Christopher sea.

The Hassel Formation (next section) probably is a facies variant of the Christopher, representing a major regression at the end of Albian time.

Grain size analysis of sand units

Grain size distribution curves and values for phi mean (*M*) and standard deviation (σ) for three sand samples are shown in Figure 50. Each sample is dominated by a well sorted fraction of very fine sand grade, and has a less well sorted coarser fraction. The fine fraction (<4.25 ϕ) constitutes between 2 and 24 per cent of the samples; it was not analyzed and therefore values for mean grain size are slightly too coarse.

Curve shapes shown in Figure 50 are unlike any published by Glaister and Nelson (1974). They do, however, show similarities to the shoreline sand curves of Visser (1969, Fig. 6). Four separate fractions may be recognized. The suspension

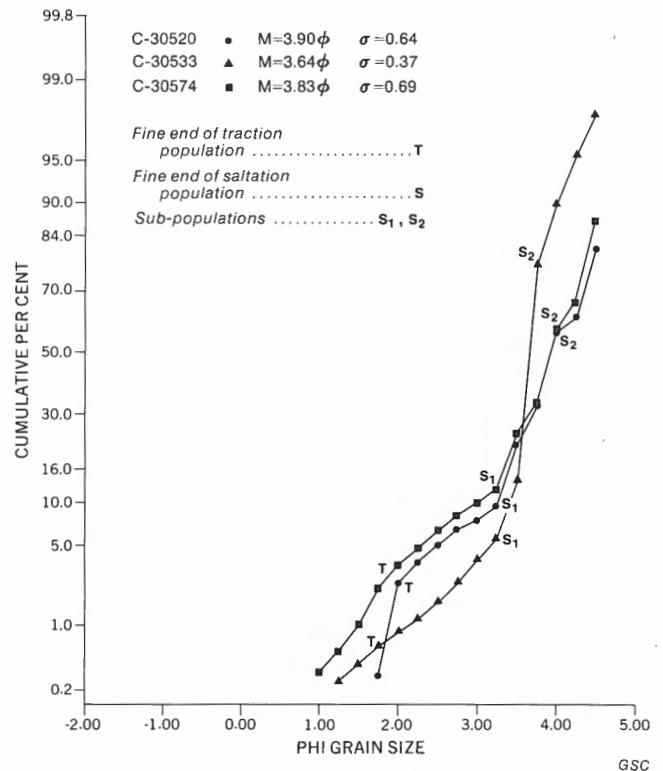


Figure 50. Grain size distribution curves, sand from the Christopher Formation.

population constitutes between 21 and 33 per cent of the distributions. It is shown in Figure 50 by the upper end of the curves and is finer than 3.75 phi. The bulk of the sand comprises a saltation load which, according to Visher's (1969) analysis, may be divided into two subpopulations. Visher (1969, p. 1080) stated that wave swash and backwash constitute two different transport conditions and that they produce two separate saltation populations in opposite flow directions. The two subpopulations are identified on the curves as segments TS_1 and S_1S_2 ; the letters *T* and *S* beside the curves mark the fine limit of the traction and saltation subpopulations, respectively. Traction load ranges from 0.2 per cent to possibly as much as 4 per cent of the sand, although the traction-suspension separating is not sharp, owing to population mixing. In many of Visher's (1969) samples a distinct coarse fraction is composed predominantly of shell fragments, but this is not the case in the Christopher Formation.

Although the curve shapes are similar to those of Visher (1969, Fig. 6), the limits of the various subpopulations in the Christopher samples are all finer. There are several possible reasons for this. As Visher (1969, p. 1083) noted to explain differences within his own samples, different sand provenances and different particle shapes will influence the final grain size distributions. In addition energy level will be of major importance, for the sorting and transporting power of waves will vary with wave magnitude. The constant factor in shoreline sands, according to Visher (*ibid.*), is the presence of the concave-upward break in slope in the saltation population. It is of interest to note that such a break in slope was, in fact, not noted in any of Glaister and Nelson's (1974) samples from this environment. The latter authors attribute this to limited sampling but it may relate perhaps more to fundamental problems with the analytical technique. Curve-shape analysis starts from the assumption that grain size distributions are controlled predominantly by transportation modes, but most sand units are derived largely from a pre-existing sand body and the effects of varying provenance, coupled with variations in grain shape and energy level, cannot but influence the final curve shape.

Petrographic analysis

Sand, sandstone

Point count analyses were performed on eight thin sections of arenaceous rocks. The results are shown in Table 11.

In most details these rocks are very similar to the sands and sandstones of the Isachsen Formation, and so detailed petrographic descriptions are not necessary in this section. The reader is referred to Plates 19 to 22 for illustrations of typical mineral species, in particular to Plate 21B, which is a view of a well cemented quartz arenite from the base of the Christopher Formation in the Orksut I-44 well.

Principal differences between the Isachsen and Christopher sands are as follows:

1. Embayed and polycrystalline quartz grains are rare or absent in the Christopher Formation.
2. Many quartz grains are angular, in contrast to the good rounding exhibited by the coarser grained Isachsen sands.
3. Glauconite is present in many of the Christopher sands.
4. The cementing medium in the lithified sandstone units commonly contains a high percentage of siderite. Quartz grains commonly exhibit corroded margins in such sandstones, indicating that some diagenetic dissolution has taken place (*see* next section for a discussion of the origin of the siderite).

The Christopher sands probably were derived from the same source areas as were the Isachsen sands. Some probably represent Isachsen sands that were reworked as the Christopher sea transgressed over the Isachsen fluvial basin. Embayments in quartz grains would not develop in a marine environment and those inherited from the Isachsen Formation may have been fragmented by wave action. The angularity of the majority of the quartz grains suggests that such fragmentation may have been important, for the Isachsen sands typically are relatively well rounded. The presence of glauconite in the sands is not unexpected, as glauconite is characteristic of the marine environment.

Table 11. Petrographic analyses of sand and sandstone from the Christopher Formation

STATION OR WELL	C NO. OR DEPTH (Ft)	PER CENT CLASTIC GRAINS									PER CENT ALL POINTS				PER CENT			ROCK TYPE (follows classification of Okada, 1971)
		QUARTZ	CHERT	K-FELDSPAR	PLAGIOCLASE	MUSCOVITE	BIOTITE	GLAUCONITE	SHALE, CLAY	DETRITAL FEOX	POROSITY	QUARTZ CEMENT	CARB. CEMENT	CLAY MATRIX	FEOX MATRIX	QUARTZ	ROCK FRAGMENTS	
74-25	30520	74	2	6	R	T	T	R	16	1					74.6	19.5	5.9	LTHC AREN
74-35	30533	74	2	13	1	R	R	R	6	3					74.3	11.6	14.1	FSPC AREN
74-65	30574	77	1	4	T	1	T	-	T	17					76.9	18.7	4.4	QTZS AREN
GAS-6	30832	100	-	-	-	-	-	-	T	T	-	-	41	-	99.8	.2	.0	QTZ AREN
GAS-17	30768	56	3	21	T	-	-	T	-	19	-	-	77	-	56.4	22.2	21.4	LTHC AREN
GAS-25	30786	91	T	8	T	T	-	-	R	R					91.2	.8	8.0	QTZS AREN
STKSON	(5120)	95	-	5	-	T	-	-	-	-	-	-	89	-	94.6	.1	5.3	QTZS WACK
ORKSUT	(4250)	97	3	T	-	-	-	-	-	-	-	22	5	-	97.4	2.6	.1	QTZ AREN

GSC

Less than 1%R Trace quantitiesT Quartz QTZ Quartzose QTZS
Lithic LTHC Arenite AREN Wacke WACK Feldspathic FSPC

Shale, silty shale

Seven samples were analyzed semiquantitatively, by X-ray diffraction, to determine mineral content. The results are given in Table 12.

Clay mineral content ranges from 9 to 42 per cent. The origin and diagenetic history of clay minerals is an exceedingly complex subject, and it is not possible to arrive at final conclusions regarding the clay mineralogy of the Christopher Formation on the basis of the limited amount of data available. Some general remarks follow.

Kaolinite is typically produced by weathering of aluminum silicate rocks, particularly those rich in K⁺ and Na⁺. It is thus a common weathering product of granites, for the feldspars that are common in granites (albite, orthoclase, microcline) are of the appropriate composition (Keller, 1970, p. 798). As shown in Table 12, feldspar is found in all the samples studied. Petrographic analysis of Isachsen and Christopher sand samples shows that sodic and potassic feldspars are important constituents and that much of the detritus was derived ultimately from an acid igneous source.

Chlorite may form diagenetically, particularly in a marine environment, but it appears to be a stable species and many occurrences of the mineral in sediments may simply reflect derivation from a chlorite-bearing source rock (Keller, 1970, p. 808). The limited quantities of chlorite observed in the Christopher Formation may reflect derivation of minor quantities of sediment from a low-grade metamorphic source, presumably within the Shield. Polycyclic derivation through Proterozoic sediments is a possibility.

Illite may be a detrital mineral or a product of diagenesis, particularly of mica, kaolinite and montmorillonite (Keller, 1970, Table 8). Kaolinite is prone to destructive dissolution in seawater but the evidence suggests that it does not convert to illite until the containing sediments have been subjected to deep burial (Keller, 1970, p. 804).

Quartz and feldspar are present as detrital grains, probably as silt-grade material. Gypsum probably represents an oxidation product of pyrite, possibly produced during recent weathering.

Siderite typically is produced under acidic reducing conditions such as are caused by decaying organic matter (Pettijohn *et al.*, 1972, p. 48). There is no independent evidence of such conditions persisting during the Albian but it

is noteworthy that most of the large sideritic concretions (Cape Crozier) and siderite-cemented sandstones (Rufus River, Colquhoun Point) are located on, or close to, structural highs. One of the themes of this report is that most of the large-scale structural elements (Fig. 4) were in existence throughout the Cretaceous and Paleogene. They controlled sedimentation trends during this time period and also may have influenced diagenesis. The Christopher Formation was subjected to erosion prior to the Kanguk transgression in Turonian time; it is known to be thin over Cape Lambton Uplift (Fig. 11) and probably also was reduced in thickness over Cape Crozier Anticline. Possibly a hydrodynamic regime was established during or following the period of erosion which favoured downward percolation of formation waters from structurally high areas. The basal Kanguk contains ample evidence of a reducing, possibly acidic, environment and may have been the source of the ferrous iron.

Hassel Formation

Lithofacies and sedimentary structures

Three typical surface sections through the Hassel Formation are shown in Figure 51. Four major facies are recognizable on the basis of lithology and sedimentary structures. These are described below, and the environment of deposition interpreted for each facies is discussed in the subsequent section. The Hassel section at Castel Bay C-68 is different in that it contains a significant proportion of shale. In the absence of continuous core, a detailed description and facies analysis cannot be attempted.

Facies types

Facies A. This facies, invariably present at the base of the Hassel Formation, represents a gradational contact between the Hassel and the underlying Christopher. It consists of interbedded very fine sand or silt and silty shale. Lenticular bedding, as defined by Reineck and Wunderlich (1968), is common. Ironstone nodules containing ammonites and pelecypods may be present and bioturbation is important locally. Sand lenticles diminish in number and thickness downward and the facies passes imperceptibly into the shale of the Christopher Formation.

Facies B. This facies has been recorded in several localities (Stations 74-MLA-44, 119) but is present in only one of the three sections shown in Figure 51. It consists of very fine sand or sandy silt, structureless or showing fine lamination. Nodules containing pelecypods are rare.

Facies C. The coarsest deposits in the Hassel Formation constitute facies C. Sand is typically fine grained, but lenticles of coarse sand and scattered pebbles may be present. Several different assemblages of sedimentary structures are present. The most common assemblage is defined as facies C₁ and is typified by low-angle planar cross-stratification similar to xi-crossbedding, as defined by Allen (1963, p. 108). This consists of sets of low-angle planar crossbeds underlain by erosional or nonerosional surfaces. The cross-strata are discordant to the lower bounding surface. The most distinctive features of this structure are the low angle of foreset dip

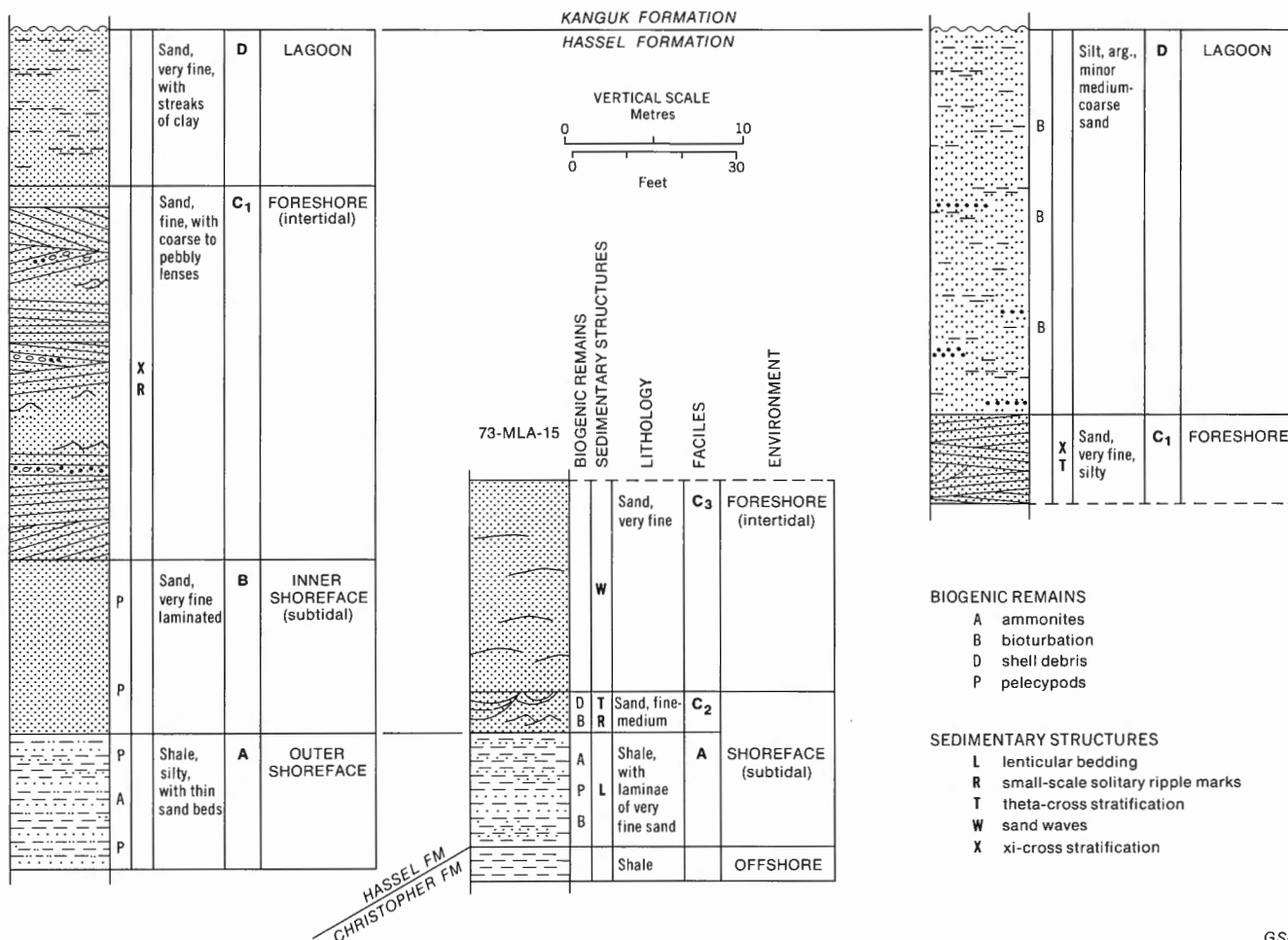
Table 12. Semiquantitative X-ray diffraction analyses of fine-grained rocks from the Christopher Formation

STATION NO. OR WELL NAME	SAMPLE GSC LOC. NO. OR WELL DEPTH (Ft)	Undifferentiated clay minerals		Kaolinite	Kaolinite + chlorite	Mixed layers	Quartz	Feldspar	Calcite	Siderite	Gypsum	Pyrite
		Illite										
73-MLA-27	C-26406	-	10	-	13	2	68	5	-	1	1	-
74-MLA-4	C-30473	-	7	19	-	5	64	2	-	-	3	-
74-GAS-7	C-30687	-	3	-	3	3	46	11	34	-	-	-
74-GAS-7	C-30693	-	19	-	20	3	45	7	-	-	6	-
74-GAS-7	C-30695	-	9	-	9	6	59	11	-	-	6	-
74-GAS-25	C-30785	-	8	21	-	5	47	13	-	1	5	-
NANUK D-76	(3720)	10	-	-	-	-	87	tr	-	-	-	3

GSC

74-MLA-44

74-MLA-104



GSC

Figure 51. Typical sections through the Hassel Formation.

(generally less than 10°) and the apparently random orientation of the indicated current directions. An outcrop containing xi-cross-stratification is illustrated in Plate 9A. Owing to the low angle of foreset dip it is often difficult to determine whether a particular sand unit is a crossbed or a planar-bedded deposit and this renders paleocurrent analysis virtually impossible. Rare trough crossbeds and solitary, small-scale ripple marks may be present in this subfacies. Biogenic remains include lenses of pelecypod shells (Pl. 9B) and rare vertical burrows.

Facies C₂ consists of similar lithologies and contains the same type of biogenic remains but is characterized by different sedimentary structures. Small-scale ripple marks of various types are abundant. Oscillation ripples, in which the internal structure mirrors the external morphology, are common locally (Pl. 23A). Most ripples, however, show foresets internally and these are truncated by the stoss (up-current) side of the ripple (Pl. 23A). Interfering and crosscutting ripples, similar to small-scale pi-cross-stratification (Allen, 1963, p. 110) have been observed at one locality. Where the sediment supply was slightly greater, ripple trains developed into the climbing type (Pl. 23B), typically kappa-cross-stratification, which is characterized by wavy ripple

crests (Allen, 1963, p. 106). Facies C₂ may also contain trough crossbeds.

Facies C₃ consists of fine to very fine sand showing lamination, undulatory bedding or low-amplitude sand waves. The latter have wavelengths of about 1.5 m (4.9 ft) and amplitudes of less than 10 cm (4 in.). No biogenic remains have been recorded.

Facies D. The predominant lithology is mottled silt or silty, very fine sand. Argillaceous content is high and seams of clay may be common. Bioturbation is abundant; bedding is faint or absent.

Depositional environment

The facies sequence A-B-C-D is similar to the regressive-marine sequences of Bernard *et al.* (1963), Visher (1965), Davies *et al.* (1971), Dickinson *et al.* (1972), Spearing (1974) and Harms *et al.* (1975, Chap. 5). There are some similarities to the regressive cycle described by Howard (1972), although his sequence is characterized by more abundant trace fossils and generally coarser grain size. A significant part of many of the sequences described in the literature consists of eolian

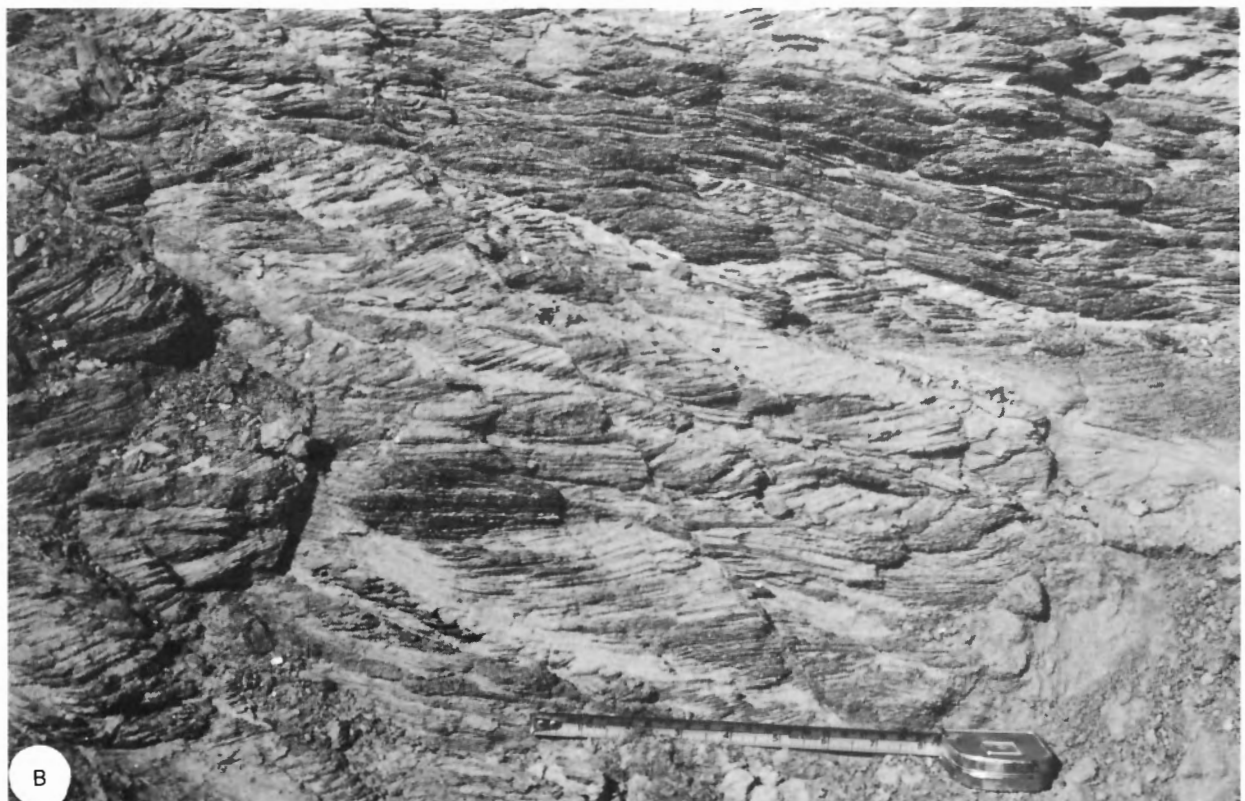


Plate 23. Small-scale ripple marks, Hassel Formation. A: Current ripples (*centre*) and oscillation ripples (*near top*), near Thomsen River (Station 73-MLA-17). GSC 199166. B: Superimposed sets of climbing ripple marks, near Colquhoun River (Station 74-MLA-145). GSC 199183.

deposits; they apparently are absent in the Hassel Formation. A distinction between the shoreline environment and the barrier island environment often is made in the literature (e.g., Spearing, 1974) and yet, unless the geometry of the sand body and the nature of the surrounding facies are known, it may be impossible to distinguish between the two in a succession of ancient rocks. In the present case the probable elongate nature of the Hassel sand bodies and the existence of a lagoonal facies in at least two localities (Fig. 51) favours an interpretation of the Hassel as a barrier island sand body. The position of the shoreline probably corresponds closely to the present-day erosional limits of the formation (Fig. 12). The shale-bearing Hassel Formation at Castel Bay C-68 probably represents a deeper water, offshore marine environment. Refinements on this model are possible on the basis of paleocurrent analysis (next section). A discussion of the environments of deposition of the various subfacies in the Hassel Formation is given below.

Facies A. The fine-grained nature of this facies and the lenticular bedding would suggest a close similarity between these rocks and tidal deposits, as described by Reineck and Wunderlich (1968) and Klein (1971). "Tidal bedding", as named by Wunderlich (1970, p. 106) and Klein (1971, Table 1), refers to an alternation of silt or sand transported as bedload during flood tide, and clay deposited from suspension during periods of slack water. There is no doubting the distinctiveness of this bedding type or the fact that it indicates marked fluctuations in depositional energy level, but it has been shown that it is not confined to the tidal environment. McCave (1970, p. 4157) and Oertel (1973, p. 36) suggested that alternation of fine and coarse sediments and the presence of ripple marks and flasers can be accounted for by long-term fluctuations in energy level in the subtidal environment. Clay will be the deposit formed most of the time but, during strong spring tides or a storm, bed-load transportation of sand will occur. Oertel (1973, Fig. 2) illustrated 'typical' flaser, wavy and lenticular bedding in a core taken 5.5 m (18 ft) below mean low tide level in a tidal inlet in Georgia.

In the present case, facies A is interpreted as originating in a subtidal environment near wave base, i.e., on a shoreface. This interpretation fits the interpretations made of the other facies better than does the alternative of an intertidal environment.

Facies B. This facies is of uncertain origin. Visher's (1965, Fig. 2) model includes a 'wave zone' unit above the shoreface zone, characterized by very fine sand or silt and by parallel bedding or ripple marks. There is a correspondence between this unit and facies B, but Clifton *et al.* (1971) have shown from work on modern high-energy beaches in Oregon that the transition from shoreface to beach is marked by a complex and varied assemblage of sedimentary structures which are absent from facies B. Planar bedding can be caused by wave surge in the wave breaker zone (the "outer planar facies" of Clifton *et al.*, 1971), but small-scale asymmetrical ripples and megaripples typically occur seaward of this zone and would be expected to be present in or below facies B. Possibly sedimentary structures have been destroyed by extensive bioturbation. The section at Station 74-MLA-44 (Fig. 51) may not be typical of the Hassel as a whole.

Facies C. The varied assemblages of sedimentary structures comprising facies C are entirely typical of a high-energy shoreline, as shown by Clifton *et al.* (1971). Waves undergo transformation from a broad swell offshore to a steeper, taller crest nearshore; they break and create swash up the beach. Each of these zones is characterized by a different type and energy of water motion and hence by a different type of sedimentary structure. As wave and tide conditions change, these zones migrate seaward or landward so that the internal structures sampled at any one place are likely to reflect deposition in several different wave zones (*ibid.*, p. 665). Facies C₁ is characterized by low-angle planar and trough cross-stratification with randomly oriented foresets. In detail, this structure type probably represents three separate wave zones: the zone immediately seaward of the breaker zone, characterized by megaripples and landward-dipping foresets; the wave surge zone, in which bedding is planar; and the surf zone, where seaward-dipping troughs and large-scale ripples typically develop. The "upper shoreface" facies of Howard (1972, p. 223) and Davies *et al.* (1971) shows similar characteristics.

In facies C₂, trough crossbeds and small-scale ripple marks are dominant. Troughs may occur at the surf-swash transition zone (Clifton *et al.*, 1971, p. 656) or in the wave plunge zone (Howard, 1972, p. 223). A third and more likely possibility is that the facies represents a shallow subtidal, upper shoreface environment. Harms *et al.* (1975, p. 87) have shown that trough crossbeds in this particular setting within the shoreline sequence may represent dunes formed by long-shore currents. Paleocurrent analysis (next section) provides supporting evidence for this interpretation.

Facies C₃ probably represents a single wave zone, the "outer planar facies" of Clifton *et al.* (1971, p. 657), which develops in the surf zone. Planar bedding and broad, gentle undulations a few centimetres high and about 2 m (6.6 ft) in wavelength characterize this part of the foreshore.

Facies D. The fine grain size, poorly developed bedding, the mottling and bioturbation are typical of a lagoonal environment, as described by Visher (1965, p. 45) and Dickinson *et al.* (1972, p. 202-205). Rare medium- to coarse-grained sand lenses probably represent small washover fans, formed during high spring tides or storms when waves may break over the top of the beach (Dickinson *et al.*, 1972, p. 199).

Paleocurrent analysis

The Hassel Formation has a limited distribution (Fig. 12) and limited exposure, so that the number of sedimentary structures available for study is relatively small. In addition, accurate paleocurrent determinations in the low-angle planar crossbeds were impossible because of uncertainty as to which units represented horizontal bedding planes. Also, with low foreset dip it is difficult to measure dip orientation accurately, especially if the rocks are gently tilted.

Forty-one readings were obtained at three different field stations. These were mainly small-scale ripple marks but also included some trough crossbeds. A table of orientation parameters (mean, standard deviation, etc.) is not given; it would be of little value, for the distributions are polymodal. A plot of

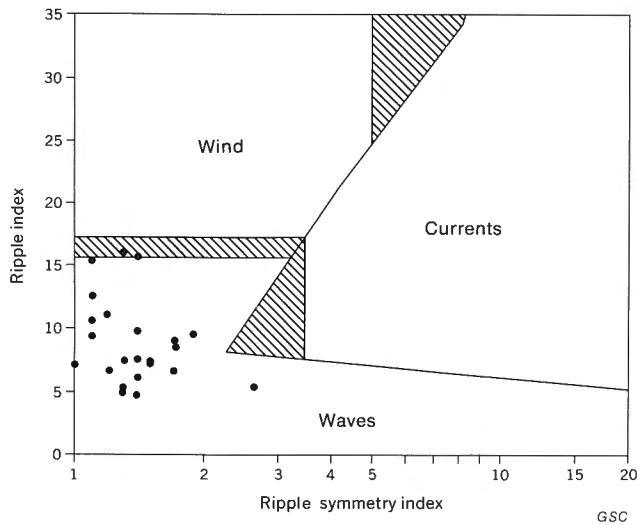


Figure 52. Plot of ripple index and ripple symmetry index for 23 ripple marks at Stations 73-MLA-15, 17 (lower Thomsen River), showing the environment field limits of Tanner (1967).

Table 13. Derivation of wave parameters from field observations on ripple marks, Hassel Formation

Ripple wavelength (cm)	Mean grain size (mm)	Wave height (cm)	Water depth (cm)	Fetch (km)
7.2	0.115	18	93	195
12.4	0.115	28	260	380
19.0	0.115	41	930	530

GSC

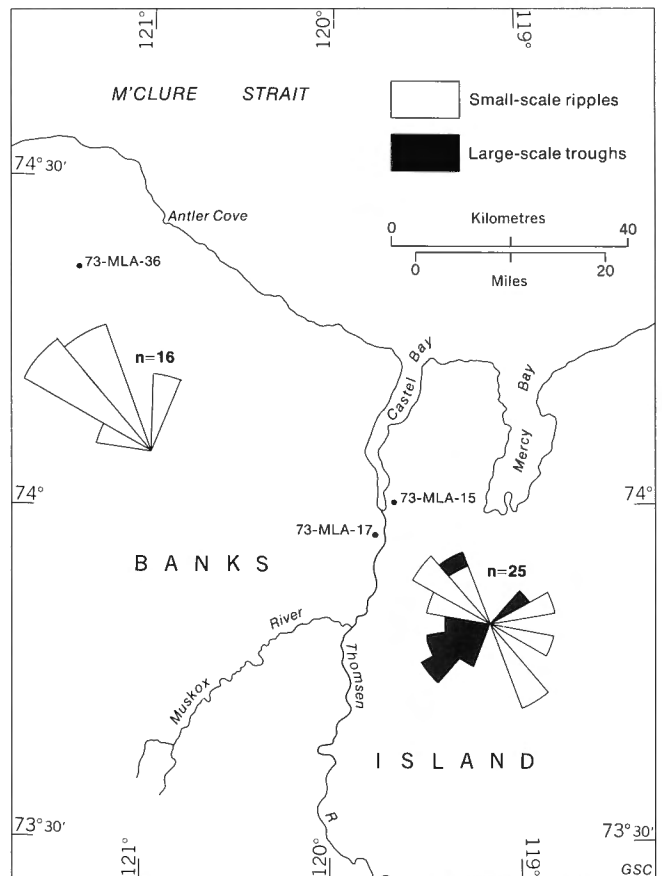


Figure 53. Paleocurrent rose diagrams, Hassel Formation.

ripple index and ripple symmetry index is given in Figure 52 and current rose diagrams are shown in Figure 53.

Analysis of ripple-mark morphology

Most of the small-scale ripple marks plot within the limits of wave-formed structures that were defined empirically by Tanner (1967), as shown in Figure 52. Two ripples are long-wavelength forms that fall within the area of overlap between wave- and wind-formed structures. The internal structure of many of the ripples suggests a current origin because it commonly consists of prograding, truncated foresets with a locally consistent orientation. However, the external morphology, which is what is measured by the ripple indices, indicates a reshaping by water oscillation in a wave environment so that the asymmetry was virtually removed. The external morphology is assumed to have reached equilibrium conditions under wave influence.

Observations and experiments carried out by Tanner (1971) showed that relationships exist between ripple spacing, grain size, water depth, wave size and fetch. Tanner's (1971) data were derived from extensive studies of ripple marks on modern coastlines and lake shores. Regression analyses were performed on various combinations of data items and a series of equations were derived that can be used to obtain useful paleogeographic parameters from field observations on ancient ripple marks. Input (Table 13) consists of ripple spacing (wavelength) and mean grain size (set at an average of 0.115 mm in these calculations; see section on grain size analysis).

Output, derived using the procedure given by Tanner (1971, p. 83), includes wave height, water depth and wave fetch. Three ripple spacings were used in these calculations, a minimum, a mean and a maximum value, to arrive at a range of output values. Even the shortest computed wave fetch is more than double the width of Northern Banks Basin (the distance from Mercy Bay to Cape Crozier is approximately 80 km, 50 mi), so that the waves which formed these ripples may have travelled along the length of the basin from some distant point and arrived at the shoreline by refraction in the shallow offshore region. In any case, the results confirm what is obvious from the faunal content of the Hassel Formation, that Northern Banks Basin was open to a broad marine area during Late Albian time.

Modal analysis

Three modal directions perpendicular to one another are shown by the paleocurrent data (Fig. 53). A northwest-directed mode is shown by ripple marks at Stations 73-MLA-15 and 36. Easterly to southeasterly directed ripples are present at Stations 73-MLA-15 and 17 and a southwest-directed mode is formed through crossbeds at Station 73-MLA-15. Paleocurrent trends have long been known to be polymodal in the marginal marine environment. Clifton *et al.* (1971) and Klein (1970) provided detailed interpretations of the modality based on work in modern intertidal regions. Local topographic irregularities can cause divergence or convergence of tidal currents, thus strengthening or weakening their sediment-moving abili-

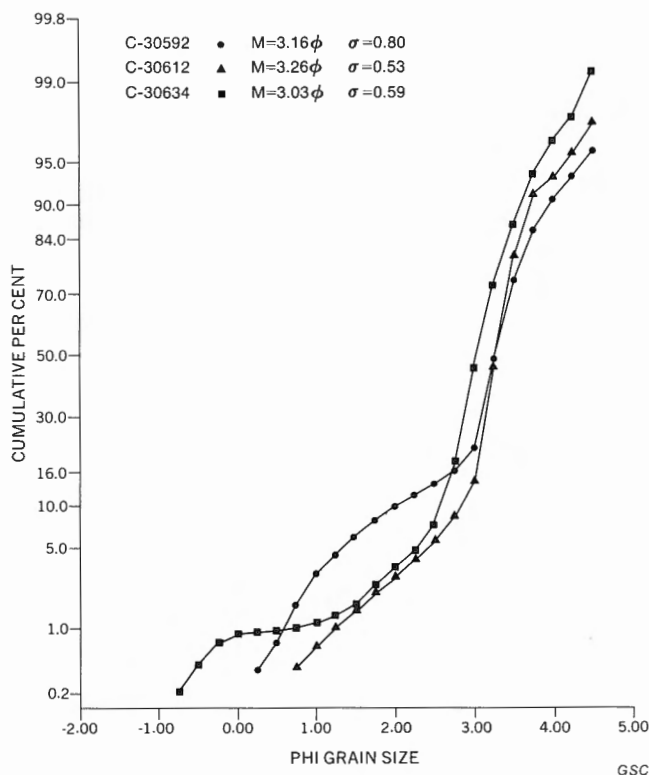


Figure 54. Grain size distribution curves, sand from the Hassel Formation.

ty. Such effects will be different under flood and ebb conditions, so that local areas become flood or ebb dominated and paleocurrent trends may include modes at 180 degrees to each other (Klein, 1970). Diametrically opposed modes also result from ripple development in different parts of the wave environment (Clifton *et al.*, 1971).

It is significant that modal current directions are oriented parallel and perpendicular to the axis of Northern Banks Basin. Klein (1970) has shown that current modes commonly are parallel and perpendicular to the direction of tidal currents and that intertidal sand bars tend to be elongated in the same direction. If tidal currents are parallel to the axis of Banks Basin, it would suggest that, as during Isachsen time, the shape of the basin influenced sedimentary trends. The basin during the Late Albian probably was a broad marine channel along which tidal currents were funnelled. The southwesterly directed mode formed by trough crossbeds probably reflects the direction of tide-influenced longshore drift. The English Channel may be a good modern analogue.

Grain size analysis

Cumulative distribution curves for three sand samples from the Hassel Formation are shown in Figure 54. The sands are very fine grained and sorting is moderately good to moderate. GSC loc. C-30592 is from the upper part of the formation (facies C₃?) at Station 74-MLA-94 on Mercy Bay. GSC loc. C-30612 is from facies B at Station 74-MLA-119 near Muskox River; and GSC loc. C-30634 is from Station 74-MLA-145 at Cape M'Clure, facies unknown.

Curve shapes are similar to those derived from the

Christopher Formation (Fig. 50) and show four relatively distinct segments representing four subpopulations:

1. Relatively well sorted, quantitatively minor, traction load
2. Poorly sorted, coarser grained saltation subpopulation
3. Very well sorted, finer grained saltation subpopulation
4. Less well sorted, quantitatively minor, suspension load

As shown by Visser (1969), these curve shapes are typical of beds deposited in a beach and shoreface environment. The reader is referred to the section on grain size analysis of sand from the Christopher Formation for a further discussion of this type of curve.

Petrographic analysis

Fourteen thin sections from the Hassel Formation were analyzed by point counter. One from Station 73-MLA-12 is a section through a siderite-cemented sand concretion; the remainder are sections through unconsolidated sands. Results are shown in Table 14.

Description of clast types

As noted elsewhere, most of the Hassel sands are fine and very fine grained. Coarser material is present at a few localities and pebbles were observed at only two outcrops. At Station 74-MLA-44 (Antler Cove) clasts of quartz, chert and quartzose sandstone up to 1 cm in diameter occur in facies C₁ in the middle of the formation. At Station 73-MLA-17 (Thomsen River) rare, small pebbles of dolomite are present.

Quartz sand grains typically are monocrystalline, angular and rarely show authigenic overgrowths. However, at GSC loc. C-33314, quartz grains are well rounded, some with overgrowths and rounded detrital cores, others with incipient embayments. These grains are similar to those from the Isachsen Formation illustrated in Plate 19. Chert and feldspar grains also are angular. Potassium feldspars are of all varieties, including simple twinned and untwinned orthoclase, and microcline. Plagioclase feldspars are mainly oligoclase and andesine. At GSC locs. C-30612 and C-30634, many of the feldspar grains are partly altered to sericite.

All the samples examined contained glauconite as fine- to very fine grained sand-size pellets, irregular in shape and green or, less commonly, brown.

Iron oxides typically are dark brown, virtually opaque, and of no definite shape. They probably represent decomposed ferromagnesian minerals. A sample from GSC loc. C-33362 contains opaque magnetite grains, a few of which show subhedral, square or octagonal outlines.

Rare grains showing quartz-feldspar intergrowths similar to those in the Isachsen Formation (Pl. 20D-F) are present in samples from GSC locs. C-30592, C-30634 and C-33311.

A wide variety of heavy minerals is present in the Hassel sands. Magnetite or ilmenite is the most common. An orange-red garnet (almandite?) is abundant in GSC loc. C-33314 and a transparent, delicate pink garnet (spessartite?) is found in samples from GSC locs. C-33308 and C-33310. Less common species include tourmaline (smoky grey to black varieties), rutile, zircon, kyanite (colourless, bladed and prismatic grains), apatite (rounded prisms) and epidote.

Table 14. Petrographic analyses of sand and sandstone from the Hassel Formation

STATION OR WELL	C NO.	PER CENT CLASTIC GRAINS										PER CENT ALL POINTS				PER CENT			ROCK TYPE (follows classification of Okada, 1971)	
		QUARTZ	CHERT	K-FELDSPAR	PLAGIOCLASE	MUSCOVITE	BIOTITE	GLAUCONITE	DETRITAL LS/DOL	SHALE, CLAY	DETRITAL FE OX	POROSITY	QUARTZ CEMENT	CARB. CEMENT	CLAY MATRIX	FE OX MATRIX	QUARTZ	ROCK FRAGMENTS		
73-12	33362	68	2	8	1	-	-	9	-	T	12	-	-	60	-	74.9	14.8	10.3	LTHC	AREN
73-14	33309	79	4	13	1	-	-	2	-	1	1	-	-	-	80.5	6.1	13.4	QTZS	AREN	
73-15	33310	72	5	12	R	T	R	1	-	3	5	-	-	-	73.4	13.8	12.9	LTHC	AREN	
73-15	33311	73	9	10	1	T	T	4	-	1	1	-	-	-	76.0	12.1	11.9	QTZS	AREN	
73-17	33314	76	8	2	R	T	-	R	4	5	4	-	-	-	76.4	21.6	2.0	QTZS	AREN	
74-44	30555	68	8	18	T	-	R	2	-	-	4	-	-	-	69.3	12.4	18.3	FSPC	AREN	
74-44	30556	96	4	T	-	-	-	T	-	T	-	-	-	-	96.3	3.6	.1	QTZ	AREN	
74-94	30592	70	4	3	T	-	-	1	-	15	7	-	-	-	70.5	26.3	3.2	LTHC	AREN	
74-119	30612	60	3	15	2	-	R	2	-	17	1	-	-	-	61.5	21.8	16.7	LTHC	AREN	
74-130	30621	73	5	18	1	-	-	1	-	-	2	-	-	-	74.0	7.3	18.7	FSPC	AREN	
74-145	30634	79	3	9	R	-	-	3	-	4	1	-	-	-	81.4	8.8	9.8	QTZS	AREN	
GAS-23	30778	83	10	5	T	-	-	2	-	-	1	-	-	-	84.1	10.5	5.4	QTZS	AREN	
GAS-36	30803	71	5	17	1	T	R	1	-	3	1	-	-	-	72.1	9.2	18.7	FSPC	AREN	
GAS-42	30813	60	11	14	1	R	-	10	-	2	2	-	-	-	66.9	16.6	16.6	LTHC	AREN	

Less than 1%R
LithicLTHC
Trace quantitiesT
AreniteAREN
QuartzQTZ
WackeWACK
QuartzoseQTZS
GSC

Matrix and cement

Most of the Hassel sands are 'clean' in the sense that they contain very little matrix. Flakes and aggregates of clay minerals are scattered through most samples but normally constitute less than 1 per cent of the rock. Clay-mineral and calcite cementation locally has lithified the Hassel so that it forms friable sandstone, as for example in the pelecypod-bearing lenses at Station 74-MLA-119, near Muskox River (Pl. 9B). Concretions formed by siderite cementation are present in many outcrops. Commonly they contain ammonite or pelecypod remains. At Antler Cove (Station 74-MLA-44) the concretions reach 1.2 m (3.9 ft) in diameter.

Texture

A typical Hassel sand is illustrated in Plate 27A. Porosity estimates are not possible in any of the samples collected because the samples could not be retained in their original loosely bound condition (the sample shown in Pl. 27A has been impregnated with resin).

Quantitative analysis

Sand classification. All the Hassel samples analyzed in this study are arenites, in the classification of Okada (1971), because all contain only trace or rare amounts of detrital matrix. The distribution of detrital grains, in terms of the three main end-members quartz, rock fragments and feldspar, is shown in Figure 55. The composition ranges from lithic arenite (5 samples) to feldspathic arenite (3) to quartzose arenite (5). One sample is a quartz arenite (Table 14).

Areal variation. A Q-mode cluster analysis of the petrographic data given in Table 14 has been performed, as shown in Figure 56. The dendrogram has been divided into two clusters, the distribution of which in terms of major constituents is shown in Figure 55, and the areal distribution in Figure 57.

Cluster 1 is relatively more quartz-rich. It occurs in the

Cape Crozier and Mercy Bay area. Cluster 2 contains more rock fragments and feldspar. With the exception of one sample from Antler Cove, the members of this cluster are located along lower Thomsen River and Muskox River.

Sediment sources

The sand mineralogy of the Hassel Formation superficially resembles that of the Isachsen Formation, except that some of the sand samples in the Hassel contain a larger proportion of feldspar grains. One sample (GSC loc. C-33314) contains quartz grains very similar to those in the Isachsen Formation; they are well rounded and contain authigenic overgrowths from an earlier sedimentary cycle, and some show embayments. This sample may have been derived, in whole or in part, from the Isachsen Formation. It is unlikely to have been derived directly from the same source as the Isachsen (the Proterozoic rocks of Minto Uplift) for paleocurrent evidence indicates that longshore drift probably took place from north to south.

The fine to very fine grain size, poor roundness and general mineralogy of the Hassel sands are consistent with their having been derived from Devonian rocks, principally the Melville Island Group. Most of the Melville Island Group sands consist of angular grains, as illustrated by Miall (1976a, Pl. 10A) and Klován and Embry (1971, Pl. 3), and most are fine to very fine grained. Detrital chert is not common in the Melville Island Group (Miall, 1976a, Table 4) and that present in the Hassel may have been derived from other chert-bearing Devonian rocks such as the Nanuk Formation. Both the Nanuk Formation and the Melville Island Group probably cropped out in cliff exposures along the Hassel shoreline near Cape Vesey Hamilton and Cape Crozier. Presumably the heavy minerals in the Hassel were derived from the same source.

Scanty evidence from trough crossbedding orientation (Fig. 53) indicates possible longshore drift from the north.

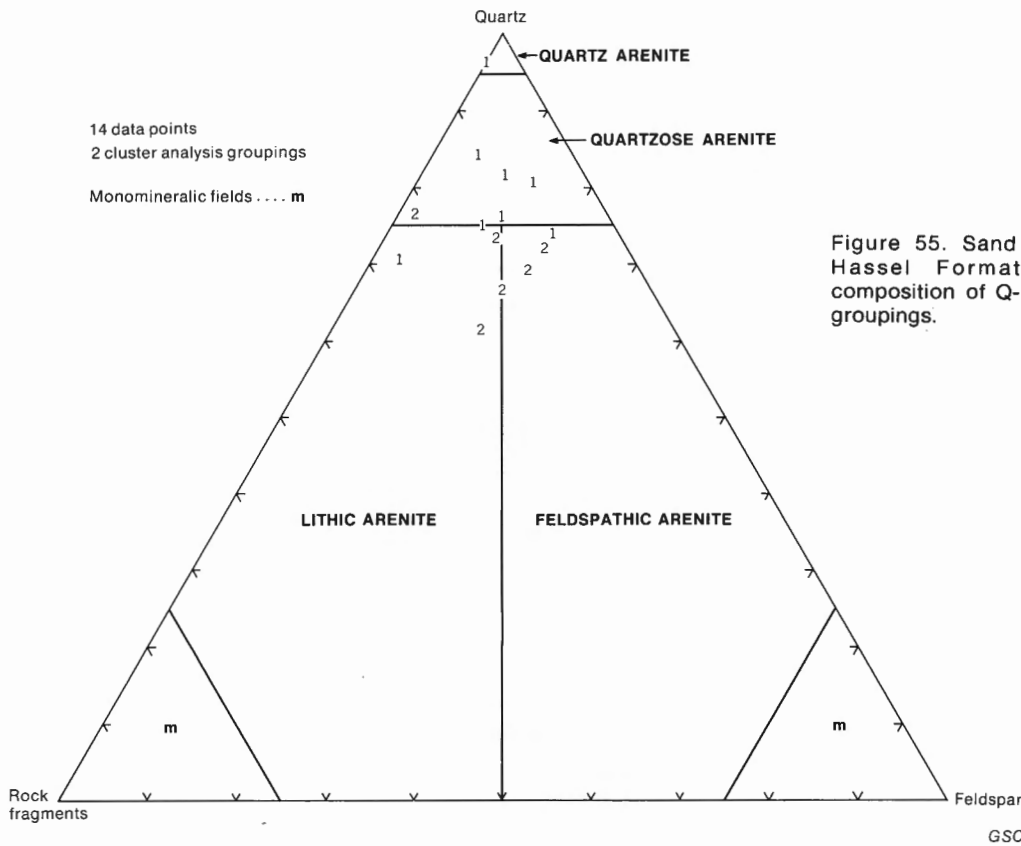


Figure 55. Sand petrography of the Hassel Formation showing the composition of Q-mode cluster analysis groupings.

Calculations from ripple marks (Table 13) indicate that waves reaching the Hassel shoreline may have had a fetch of up to 500 km (310 mi). This distance, in a northerly direction, suggests a wave origin from as far away as Mackenzie King Island, which is well into Sverdrup Basin. It is possible that longshore drift carried detritus along the coast from sources within the Sverdrup Basin, such as Devonian or upper Paleozoic rocks. One exposure of the upper sand member of the Kanguk Formation, which is similar in origin to the Hassel Formation, contains fragments of Early Permian corals that may have been derived from the Belcher Channel Forma-

tion of Sverdrup Basin (E. W. Bamber, *pers. com.*, 1973, as reported in Miall, 1976a), presumably by longshore drift.

Two lines of evidence suggest that most of the Hassel Formation may have been of very local origin. The formation thins and disappears to the north, on the west side of Mercy Bay, indicating that the barrier islands from which it was formed were not laterally extensive. This militates against extensive longshore drift. Secondly, the textural immaturity of the Hassel sands suggests that they have not had extensive exposure to the abrasive effects of the wave environment and probably are derived locally.

This also may explain the lateral variations in mineralogy that were demonstrated by cluster analysis. If the Hassel sands were derived by long-distance longshore drift, it would be unlikely that the mineralogy of the sands would vary markedly between Mercy Bay and Muskox River. All the detritus would have been thoroughly homogenized during transportation. Local derivation from Upper Devonian sands, which themselves showed lateral differences in mineralogy, would be a more likely explanation of the differences in the Hassel Formation. Not enough is known yet about the mineralogy of the Melville Island Group in the Banks Island area to assess this hypothesis. However, it is known that in the eastern Arctic the lower part of the Melville Island Group contains a larger percentage of feldspar and generally is more mineralogically immature than the upper part (H. P. Trettin, *pers. com.*, 1975). The more feldspar-rich part of the Hassel (cluster 2) lies close to the exposures of the pre-Mercy Bay-Melville Island Group, whereas the more quartz-rich part (cluster 1) overlies the upper part of this unit. The correlation is suggestive.

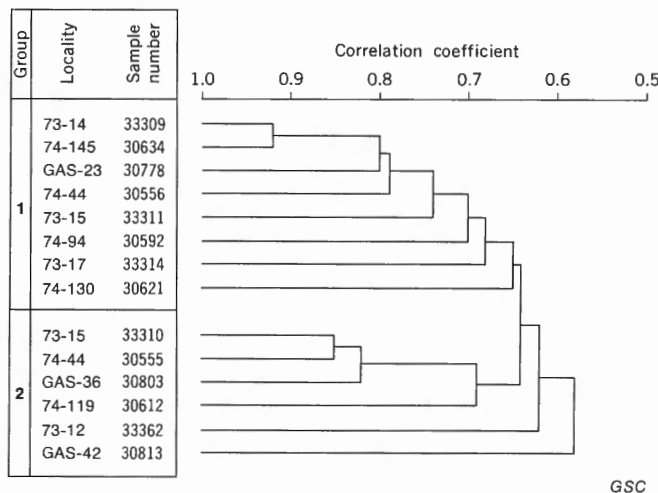


Figure 56. Q-mode cluster analysis of 14 samples from the Hassel Formation. Data from Table 14.

Kanguk Formation

Lithofacies and sedimentary structures were described fully in the chapter on stratigraphy. More detailed descriptions of the sedimentary structure types are necessary only for the sand members. These are given later in the section.

Bituminous shale member

Several unusual lithologies are present in this member, including tuff, bentonite beds and manganese spherulites. None of these lithologies is confined exclusively to the basal Kanguk; manganese spherulites are found in the upper part of the silty shale member in the subsurface of east-central Banks Island, and tuff fragments are present in several sand beds in the sand members and in the Eureka Sound Formation. The most typical occurrences are, however, in the bituminous shale member. Petrographic analyses and discussions of their origin are provided below.

Petrographic analysis

Tuff beds

Tuff beds have been identified at two localities: Station 74-MLA-28, near Masik River (GSC locs. C-30526, C-30527), where locally they reach 21 cm (8 in.) in thickness (Pl. 10B), and Station 74-VH-024 at Worth Point (GSC loc. C-37216). Angular glass shards with a modal size range of 5 to 6 ϕ (coarse silt grade) comprise, in each case, almost the entire sample (Pl. 24A), although trace or rare amounts of unabraded quartz, plagioclase, biotite and iron oxide also are present. Soft shale layers interbedded with the tuff commonly contain scattered glass fragments and abundant radiolarians (Pl. 24B). Locally the tuff is cemented with calcite and the cement has partly replaced the glass fragments and the radiolarian tests.

Wet-chemical analyses have been performed on two tuff samples, the results of which are shown in Table 15. These analyses correspond to an andesite-dacite composition, by comparison with data given by Turner and Verhoogen (1960).

Bentonite beds

Throughout most of Banks Island the basal 2 m (6.6 ft) of the Kanguk contain at least two layers, typically 5 to 15 cm (2–6 in.) thick, of grey or yellow clay. Four samples of this material were analyzed by X-ray diffraction, the results of which are given in Table 16.

Montmorillonite commonly originates by marine hydrolysis of volcanic ash (Keller, 1970, p. 801). Mixed layer clays typically are montmorillonite-mica mixtures (A.E. Foscolos, *pers. com.*, 1975). Clinoptilolite is a zeolite mineral, and zeolites are a common alteration product of volcanic glass (Pettijohn *et al.*, 1972, p. 267).

Jarosite may have been derived by decomposition of orthoclase (Parker, 1972).

Manganese spherulites

The writer (Miall, 1974d) provided descriptions and analyses of two subsurface samples from the basal Kanguk that contain abundant manganese spherulites. Subsequently, similar spherulites were recorded in the basal Kanguk in the Orksut I-44 well and at the surface near Mercy Bay (Station 74-GAS-23). (Similar spherulites also are present in the upper part of the

Table 15. Chemical analyses of tuff samples, basal Kanguk Formation

Constituent	C-30526	C-37216
SiO ₂	68.0%	65.6%
Al ₂ O ₃	12.1	12.1
TiO ₂	.2	.2
Fe ₂ O ₃	1.5	1.6
Na ₂ O	2.8	2.6
K ₂ O	4.3	3.7
MnO	.05	.06
MgO	.17	.23
Loss on ignition	9.05	11.22
Total	98.17	97.31

Note: CaO analysis not performed; CaO content plus total cannot exceed 100%, therefore CaO less than 3% in each case.

GSC

Table 16. Semiquantitative X-ray diffraction analyses of bentonitic beds, basal Kanguk Formation

SAMPLE	Montmorillonite	Mixed layers	Quartz	Feldspars	Calcite	Gypsum	Jarosite	Clinoptilolite
C-33296	—	74	6	—	—	20	—	—
C-30518	72	—	11	3	—	11	—	3
C-30792	92	—	2	2	1	2	1	—
C-30814	—	—	—	—	—	—	—	100

GSC

Table 17. Spherulitic carbonate, basal Kanguk Formation: partial chemical analyses in weight per cent (acid extractable fraction and organic compounds only)

Constituents	Uminmak H-07 Sample	Nanuk D-76 Sample
CaO	6.37	8.95
MgO	1.20	0.70
MnO	31.6	37.4
FeO	3.8	3.3
BaO	0.45	0.45
SrO	0.01	0.01
H ₂ O	0.7	0.0
CO ₂	28.4	32.8
Organics	0.9	0.0
Total	73.43	81.61

GSC

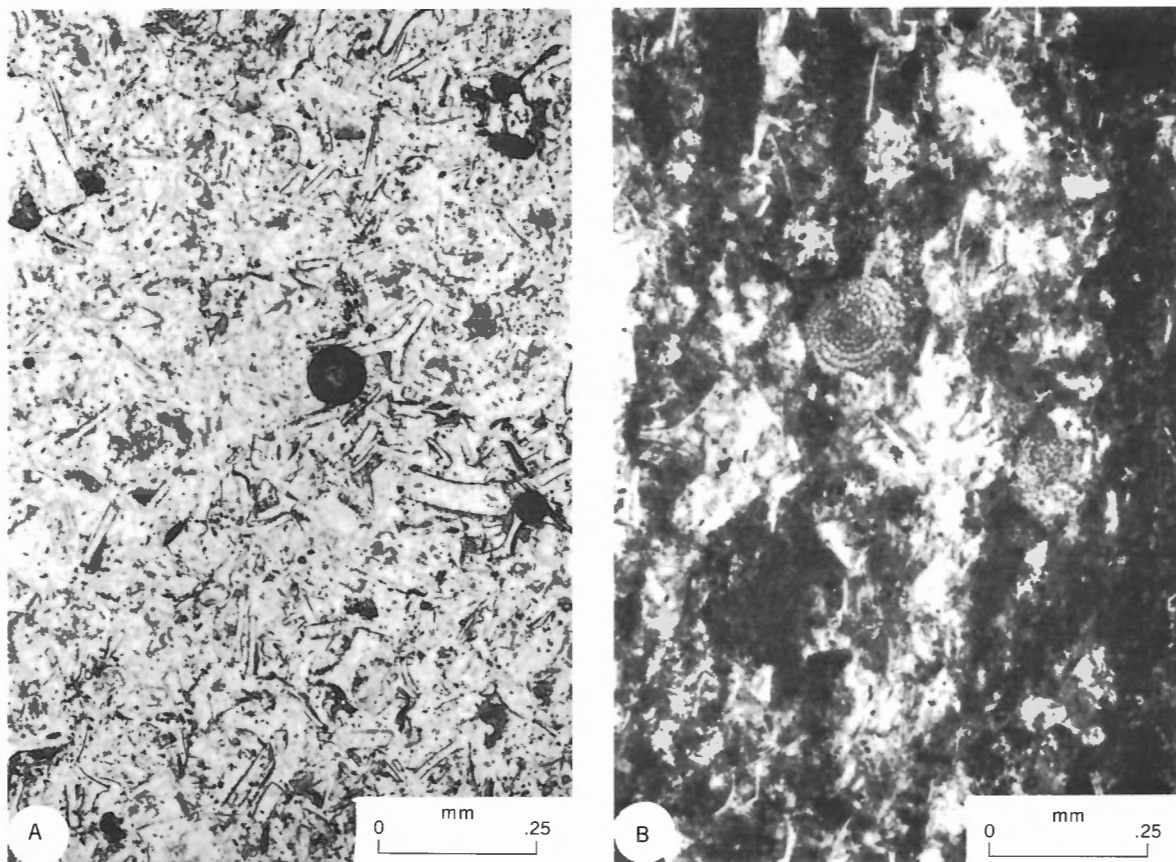


Plate 24. Tuffaceous rocks from the basal Kanguk Formation. A: Vitric tuff, upper Sachs River (Station 74-MLA-28). B: Calcareous, tuffaceous shale with radiolarians, same locality as A. Both views under plane polarized light. (Sample numbers: A, C-30526; B, C-30527.)

silty shale member at the Ikkariktok M-64 and Tiritchik M-48 wells.) Illustrations of the spherulites are given in Plate 25 and a brief description and analysis are provided below.

The spherulites in the Nanuk and Uminmak wells consist of rhodochrosite (MnCO_3) and range in diameter from 10 to 700μ . They show radial-fibrous texture with little or no evidence of a detrital nucleus. One or two brown concentric laminae may be present near the outer edge of each spherulite. The spherulites are set in a matrix of clay minerals and late-stage sparry dolomite. Silt-size detrital quartz particles are found in the matrix and also within some of the spherulites, indicating that the present outline of the spherulites is diagenetic in origin. Partial chemical analyses of the rocks containing the spherulites are provided in Table 17. These samples also contain amorphous iron and manganese oxides, as determined by X-ray fluorescence.

The structures at Station 74-GAS-23 appear somewhat different (Pl. 25B) and may not be of identical origin. Some show radial-fibrous texture but most show concentric, oolitic texture in which outer layers may truncate inner laminae. Many of these structures are similar to the coated caliche grains described by various workers (e.g., James, 1972) from the vadose zone in modern carbonate environments. The ooids consist predominantly of calcite and are rimmed with fine dolomite crystals. The matrix primarily consists of structureless or pelletoid, fine-grained dolomite with traces of ferroan

dolomite. Scattered detrital quartz, chert, plagioclase and microcline grains also are found in the matrix. X-ray fluorescence indicates that manganese is a major component of this rock but its distribution and chemical compounds are not known.

Depositional environment

The bituminous shale member was deposited in a marine environment, as indicated by the rare presence of fish fragments (plates and vertebrae), radiolarians and *Inoceramus* sp. However, the large bituminous content and the tuff and bentonite beds and manganese spherulites indicate that the environment was unusual. Conant and Swanson (1961) discuss the black, bituminous Chattanooga Shale of Tennessee and conclude that the deposit was formed in shallow water in which currents and wave action were not strong enough to prevent stagnant conditions from developing. Similar rocks were forming up until approximately 2000 years B.P. in the central Black Sea. Ross and Degens (1974, p. 196) suggested that an H_2S -rich zone became so well established in the deep basin that incoming, oxygenated waters were unable to break up the stagnant water mass. Such conditions inhibit the decomposition of contained organic matter. However, explanation of the widespread paleogeographic distribution of the bituminous shales in the Kanguk remains a problem.

Volcanic activity is known to have been widespread

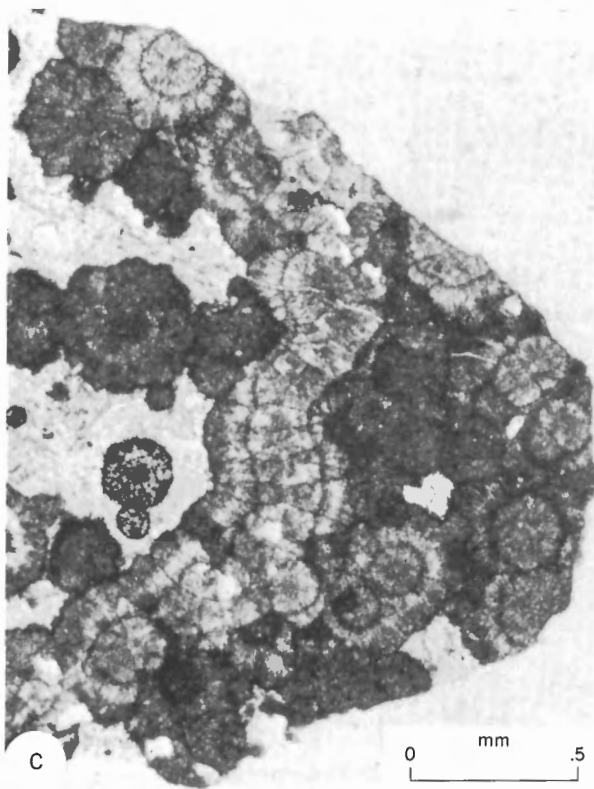
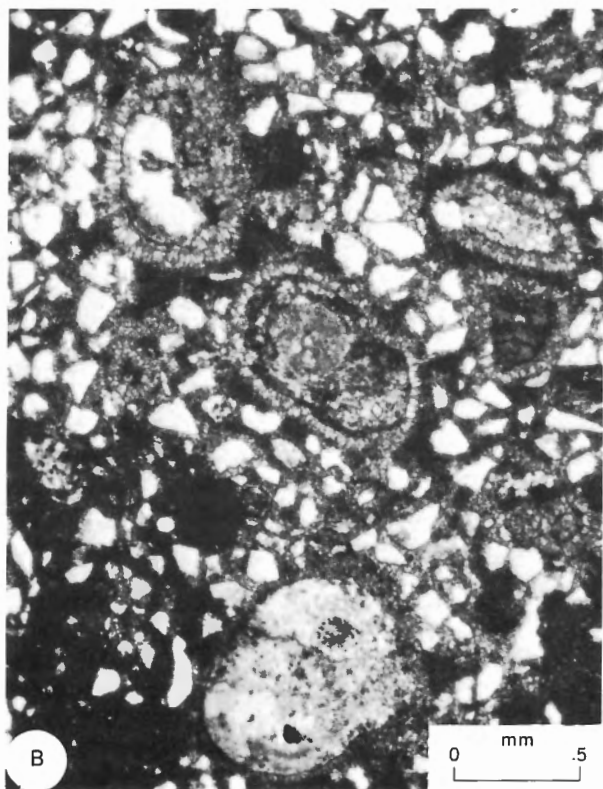
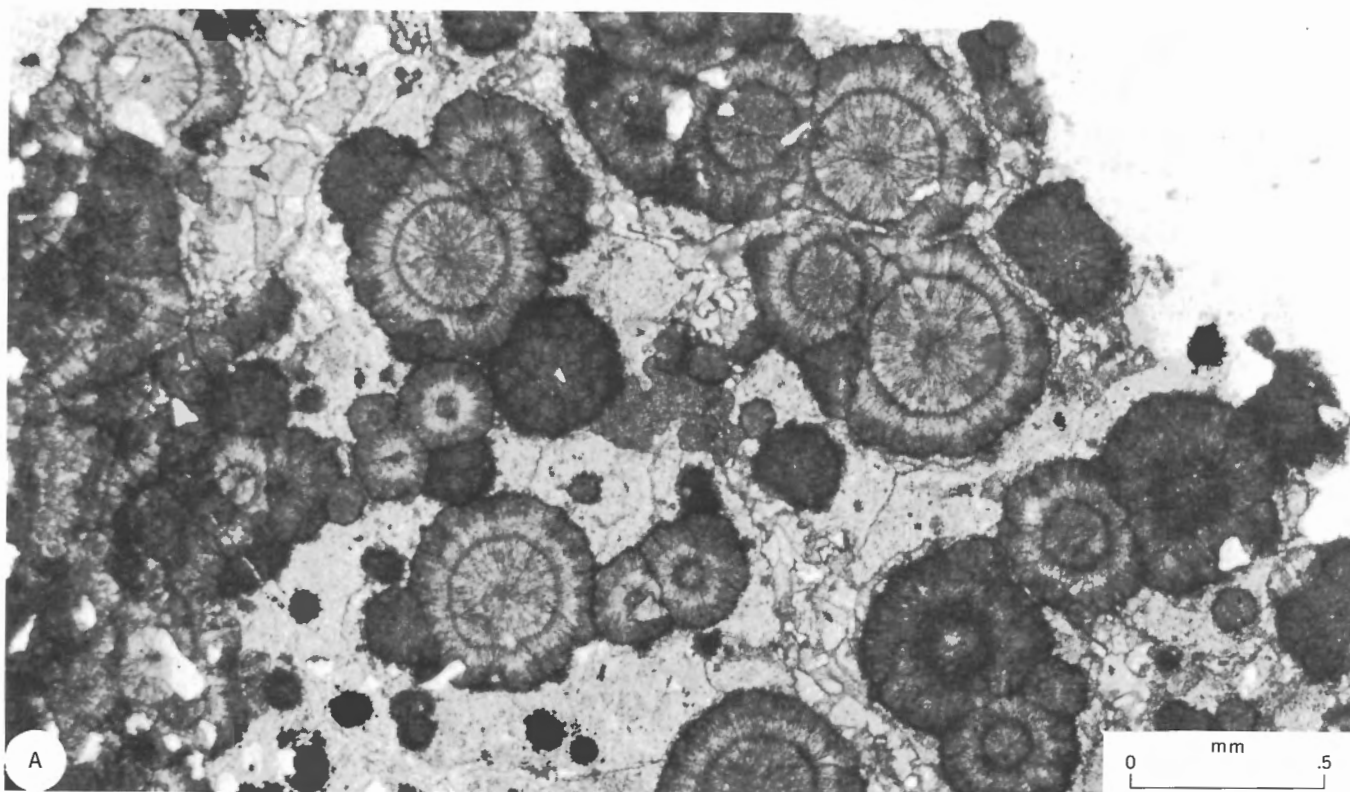


Plate 25. Manganese spherulites from the basal Kanguk Formation. A: Uminak H-07 well; note clay minerals and sparry dolomite in matrix, and detrital quartz grains. B: Caliche(?) ooids, Mercy Bay (Station 74-GAS-23). C: Coagulated spherulites. All views under plane polarized light. (Sample numbers: A, C-39381, 712-718 m (2337-2356 ft) depth; B, C-30780; C, same as A.)

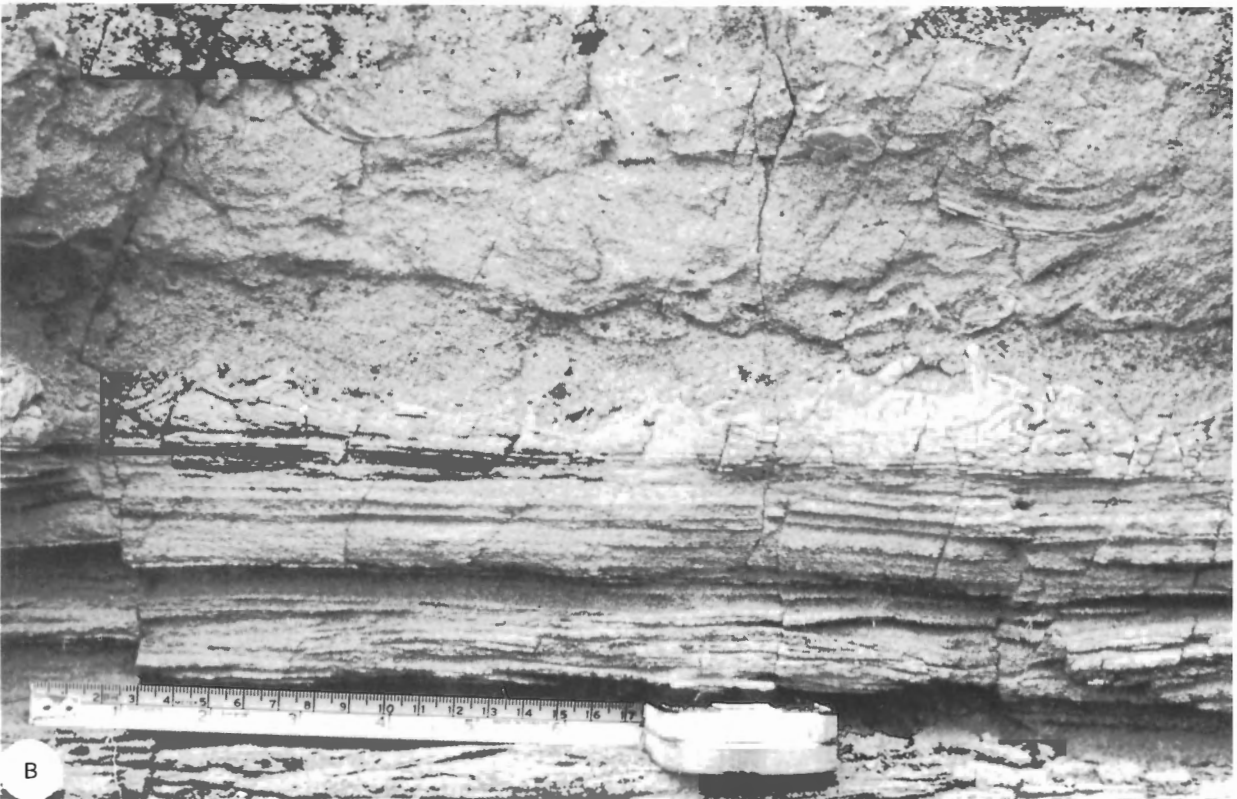


Plate 26. Sedimentary structures in the upper sand member of the Kanguk Formation. A: Superimposed sets of planar crossbedding near Antler Cove (Station 73-MLA-9). GSC 199163. B: Deformed small-scale ripple marks and water-escape structures near Antler Cove (Station 73-MLA-11). GSC 199165.

during the Late Cretaceous. The volcanic Strand Fiord Formation of Axel Heiberg Island (Souther, 1963, p. 441, 442) consists of 85 to 180 m (280–600 ft) of superimposed basalt flows and minor pyroclastic deposits, and is Cenomanian or Turonian in age (H.R. Balkwill, *pers. com.*, 1974). Myhr (1975) reported that much of the Upper Cretaceous succession of Anderson Plains and Tuktoyaktuk Peninsula also shows evidence of extensive volcanic activity in the form of tuffaceous and bentonitic beds. The tuffs of southern Banks Island are andesite-dacite in composition, which indicates a different origin to the Strand Fiord volcanics. The location of the volcanic source is unknown and possibly lay offshore west of Banks Island, or in the northern Cordillera. Scheidegger and Potter (1968) showed that tuff grains of coarse silt grade can be transported by wind for 500 to 1000 km (300–600 mi). Wind rather than water transportation seems more probable for the tuff and bentonite beds, in spite of their being interbedded with shales bearing marine fossils, for their great lateral, blanketlike extent points to an origin in single eruptions and virtually contemporaneous deposition over areas of many thousands of square kilometres.

According to Dickinson (1974), andesite-dacite tuffs often form in volcanic arcs above continental or semicontinental crust. It is of interest to speculate whether there is any possible connection between the occurrence of the volcanic rocks and a sea-floor spreading event in the Arctic Ocean. This will be discussed in a later chapter.

In the Kanguk Formation radiolaria typically are found only in tuffaceous horizons. J.H. Wall (*pers. com.*, 1975) commented that radiolaria are preserved only where geochemical conditions inhibit silica dissolution. Excess silica in the formation waters as a result of volcanic activity would provide such conditions.

A genetic association between volcanic activity and the presence of manganese spherulites was suggested tentatively by the author (Miall, 1974*d*) because, at that time, evidence of both had been found only in the same basal few metres of the Kanguk Formation. Tuffaceous and manganese-bearing rocks are now known from higher in the Kanguk but this does not negate the hypothesis. The arguments presented (Miall, 1974*d*, p. 1712–1714) to explain the origin of the spherulites may be summarized as follows. Decomposition of volcanic glass could have provided a source of manganese and also certain catalytic compounds controlling sedimentary manganese accretion (Morganstein and Felsher, 1971). Enrichment and concentration then may have taken place by ionic or molecular diffusion in pore solutions. Lynn and Bonatti (1965) suggested that manganese dissolves upon burial in a reducing environment, and then slowly migrates and accumulates in the more oxidized upper strata. The presence of organic matter is believed to be of primary importance in the creation of reducing conditions in the newly buried sediments. Hodgson (1966) has shown by a study of carbon and oxygen isotope ratios that the carbonate carbon of spherulitic and concretionary rocks is derived from carbon dioxide liberated during the early stages of decomposition of organic matter. Liberation of ammonia during decomposition would cause a rise in pH and consequent localized increase in carbonate solubility (Hodgson, 1968, p. 1262). Excess carbon would be trapped in the sediments and would be precipitated whenever the pH of the

waters dropped to that of normal sea water at the completion of organic decomposition. Areas of high organic content, where reducing conditions prevailed, gave rise to bituminous shale without manganese spherulites (siderite concretions are present locally and commonly contain vertebrate or invertebrate remains).

The present form of the spherulites resulted from diagenesis. Miall (1974*d*, p. 1714) listed some occurrences of similar radial-fibrous diagenetic textures developed in other minerals. Strong evidence for such an origin lies in the distribution of the detrital quartz grains, which are scattered through the spherulitic rock both in the matrix and within the spherulites themselves. They clearly were enclosed passively by the spherulites during growth. As noted earlier, the ooid structures at Station 74-GAS-23 may be partly of oolitic and/or caliche origin.

Spherulites and amorphous manganese oxide concentrations are found at other levels within the Kanguk Formation but bituminous shale is characteristic only of the basal Kanguk Formation. Myhr (1975) reported several bituminous horizons in the Upper Cretaceous rocks of the Tuktoyaktuk Peninsula, indicating that in Beaufort-Mackenzie Basin the unusual geochemical conditions discussed above were established at several different times.

Silty shale member

Petrographic analysis

Several sand samples from this member were studied in thin section. For convenience, they are described together with those from the sand members.

Shale, silty shale

Semiquantitative X-ray diffraction analyses have been performed on eight samples of shale and silty shale from the silty shale member. Five samples are from a measured section on lower Thomsen River and are numbered in order of decreasing age. Results are given in Table 18 in terms of weight per cent.

The clay mineralogy of a given sample may have had a complex origin, as discussed in the section on fine-grained rocks of the Christopher Formation, and a complete depositional and diagenetic history cannot be developed on the basis of the few samples available. The presence of montmorillonite in one sample and clinoptilolite (a zeolite mineral) in another suggests continued volcanic activity, for both minerals may be produced by degradation of volcanic ash, as discussed earlier in this chapter. Many of the well chip samples from the Kanguk Formation of western Banks Island are considered to be bentonitic because they are swollen from water absorption in the drilling mud stream (Fig. 8). Rhodochrosite has been identified by X-ray diffraction in one sample, 245 m (805 ft) above the base of the formation in the Nanuk D-76 well. This occurrence is related, possibly, to the manganese spherulites high in the Kanguk in the Ikkariktok and Tiritchik wells, in that all the occurrences may represent a single manganese-rich horizon originating during a single volcanic episode.

Concretions

Cone-in-cone limestone and concretions of various types locally are common in the silty shale member. Analyses have

Table 18. Semiquantitative X-ray diffraction analyses of fine-grained rocks from the silty shale member, Kanguk Formation

STATION NO. OR WELL NAME	GSC LOC. OR DEPTH (Ft)	Montmorillonite		Kaolinite + chlorite	Mixed layers	Quartz	Feldspars	Calcite	Dolomite	Siderite	Gypsum	Rhodochrosite	Clinoptilolite
		Illite											
Nanuk D-76	(2370)	—	—	5	—	72	3	16	2	—	—	2	—
74-MLA-114	C-30602	25	22	—	—	50	—	—	—	—	3	—	—
74-GAS-21	C-30770	—	3	—	—	52	6	—	4	2	20	—	13
74-GAS-21	C-30772	—	10	6	17	52	5	—	—	—	10	—	—
74-GAS-21	C-30773	—	13	9	16	48	8	—	—	—	6	—	—
74-GAS-21	C-30774	—	10	5	7	72	4	—	—	—	2	—	—
74-GAS-21	C-30775	—	8	6	4	63	15	—	—	—	4	—	—
74-GAS-48	C-30826	—	12	8	5	67	4	—	—	—	4	—	—

GSC

been performed on four of these by semiquantitative X-ray diffraction, as shown in Table 19.

X-ray fluorescence showed that all these samples contain abundant amorphous iron and that GSC loc. C-33294 also contains abundant amorphous manganese, both elements probably in the form of oxides. Most of the samples examined show concentric lamination, and several periods of growth are suggested by truncations of inner by outer laminae. A few layers also contain smaller scale laminated concretions less than 1 mm in diameter within them.

Table 19. Semiquantitative X-ray diffraction analyses of concretions from the silty shale member, Kanguk Formation

STATION NO.	GSC LOC. NO.	Illite	Quartz	Feldspar	8.85Å	Dolomite	Siderite	Gypsum	Pyrite
73-MLA-8	C-33294	—	—	7	—	86	—	7	—
73-MLA-14	C-33297	1	28	1	—	—	70	—	—
73-MLA-42	C-33299	—	25	11	—	23	9	25	7
73-MLA-42	C-33300	—	19	—	23	43	5	10	—

GSC

Depositional environment

The faunal content of the silty shale, including reptiles, fish, marine pelecypods, sponges, dinoflagellates, foraminifera and radiolarians, provides abundant evidence of a marine environment for the silty shale member. The presence of montmorillonite, clinoptilolite and rhodochrosite in minor quantities in several of the samples taken from this member indicates a continuation of the volcanic influence on sedimentation on a very minor scale.

Lower and upper sand members

Lithofacies and sedimentary structures

The lower sand member consists of a coarsening-upward succession, grading from interbedded sandstone and shale at the base to coarse, pebbly sand at the top (see Chap. 2). Core is available for only the upper part of the lower sand member in the Orksut I-44 well and shows that flaser bedding and bioturbation are common.

The lithological succession of the upper sand member is

similar to that of the lower sand member. There is also a strong similarity with the Hassel Formation. Trough and planar crossbedding (Pls. 12A, 26A) and low-angle planar crossbedding are abundant. Small-scale ripple marks also are seen, many of them deformed by penecontemporaneous soft-sediment fluidization and slumping (Pl. 26B).

The main difference between the upper sand member and the Hassel Formation appears to be an absence of any beds equivalent to Hassel facies D, the lagoonal facies.

Depositional environment

The Hassel Formation was considered to comprise shoreface, foreshore and lagoonal facies. The sand members of the Kanguk likely were deposited under similar conditions, except for the absence of a lagoonal facies. The sand bodies probably represent shallow subtidal to intertidal sand bars localized over shoals in the Kanguk sea. Planar crossbed sets may represent point bar deposits in tidal channels. The occurrences at Uminmak H-07 and Orksut I-44 wells probably indicate shallow water over a mildly positive Storkerson Uplift, the Antler Cove exposures represent deposition near the Cape Crozier Anticline, and the presence of the upper sand member in the Tiritchik M-48 and Ikkariktok M-64 wells indicates shallow water at the shelf edge. The sand members were not formed in deeper water conditions, as in Big River Basin (Storkerson Bay A-15 and Nanuk D-76 wells).

The reader is referred to the discussion of the sedimentology of the Hassel Formation for further details on facies interpretations.

Paleocurrent analysis

Orientation measurements were carried out on 36 current structures in the upper sand member, including small-scale ripple marks and large-scale trough and planar crossbeds. Results are shown in Figure 58. The results are similar to those obtained from the Hassel Formation and, as with the latter, are interpreted as the product of wave activity and tidal currents. The principal modal directions in the data from Stations 73-MLA-4, 5, 6, 7 and 9 are oriented parallel to the axis of Banks Basin.

Grain size analysis

Grain size curves of three sand samples from the upper sand member near Antler Cove are shown in Figure 59. The sands

are medium to fine grained and sorting is good to moderately good.

The sample from GSC loc. C-33293 was collected from a planar crossbedded unit at Station 73-MLA-6. A sample from GSC loc. C-33295 was taken from an indistinctly bedded sand bed at Station 73-MLA-9, and the sample from GSC loc. C-33302 represents a planar crossbedded unit at the same station.

Although the depositional environment of the upper sand member may have been similar to that of the Hassel Formation, grain size curve shapes of the two sand units are different. The two saltation subpopulations are perhaps recognizable in the curve representing the sample from GSC loc. C-33295 but not in the other two samples. The latter are similar to the "mature beach deposits" of Glaister and Nelson (1974, Figs. 7, 12). The bulk of the distribution comprises a relatively well sorted saltation population in each case, although finer and coarser grained populations also are present. Both these samples (GSC locs. C-33293, C-33302) are from planar crossbedded units.

Petrographic analysis

For convenience, all the sand samples collected from the silty shale member and the sand members are described in this section. The petrographic characters are similar, except that many of the samples from the silty shale member contain in excess of 15 per cent matrix and are sandy or silty shales (wackes) rather than arenites.

Table 20 gives point count analyses of 26 samples.

Description of clast types

Scattered, well rounded pebbles of chert up to 2 cm (0.8 in.) or, rarely, 4 cm (1.6 in.) in diameter, are common in the sand members. They also occur in rare, thin, sand beds in the silty shale member, as at Station 73-MLA-42 (near Muskox River). At Station 73-MLA-6 a lens of conglomerate 50 cm (1.6 ft) thick contains pebbles up to 6 cm (2.4 in.) in diameter. Clast types include the following (count of 100 pebbles): dark grey to black chert, 53 per cent; light grey chert, 31 per cent; quartz, 16 per cent; plus rare green and red chert, quartzose sandstone and silicified coral and other fossil fragments. The corals have been identified by E.W. Bamber (*pers. com.*, 1973), who provided the following faunal list (GSC loc. C-26204):

- bryozoans indet.
- horn corals indet.
- lophophyllid coral
- ?*Bothrophyllum* sp.
- Protowentzelella* sp.

Bamber states that the assemblage is Early Permian, probably Artinskian, in age. *Protowentzelella* is common in the Belcher Channel Formation and its equivalents but has not been reported from northern Yukon or Alaska.

Quartz sand grains are variable in the Kanguk Formation. Many of the finer grained sands (e.g., GSC loc. C-30627) consist very largely of angular quartz (Pl. 27B) whereas coarser sand units (e.g., GSC locs. C-30589 and C-30788) consist of well rounded grains, with or without detrital cores and authigenic overgrowths (Pl. 27C, D). Very rare multiple

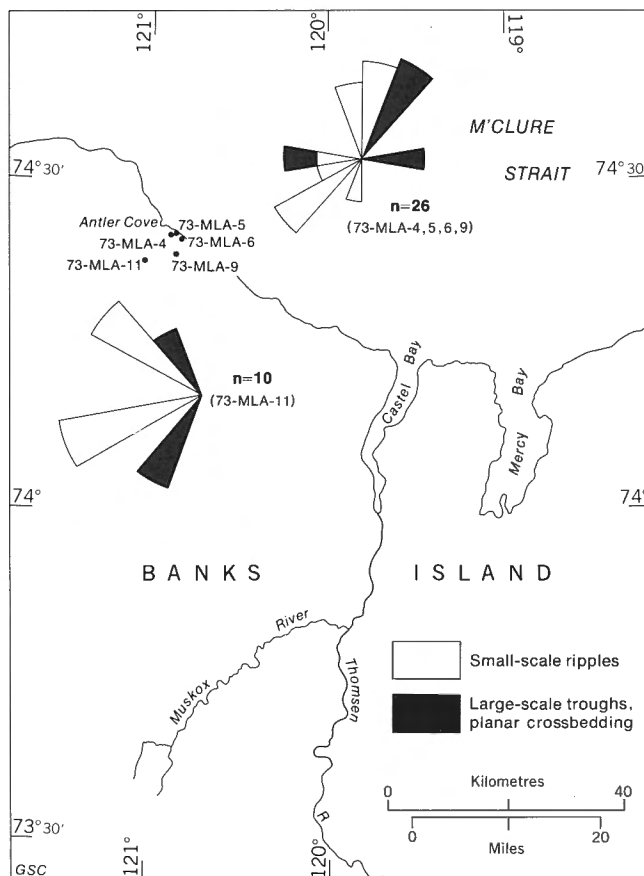


Figure 58. Paleocurrent rose diagrams, upper sand member of the Kanguk Formation.

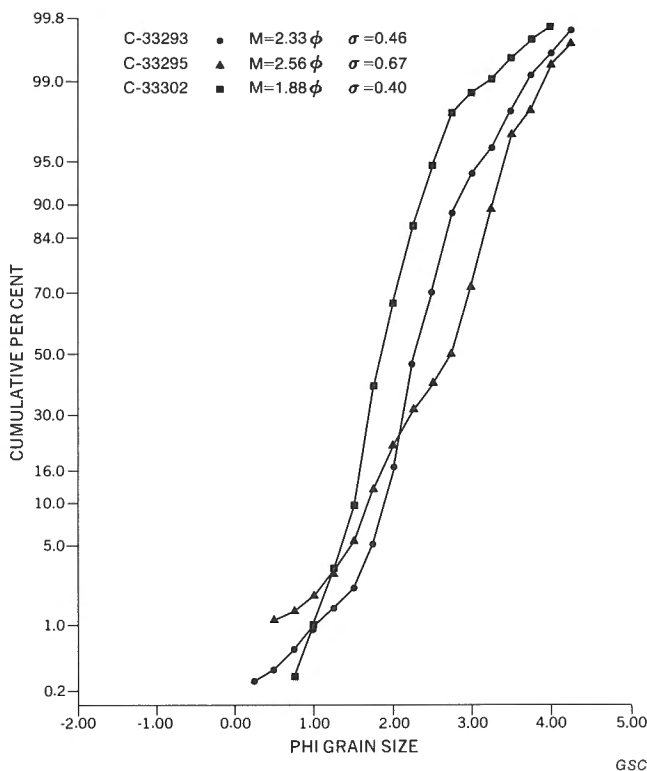


Figure 59. Grain size distribution curves, sand from the upper sand member, Kanguk Formation.

Table 20. Petrographic analyses of sand and sandstone from the Kanguk Formation

STATION OR WELL	C. NO. OR DEPTH (FT.)	FORMATION	PER CENT CLASTIC GRAINS											PER CENT ALL POINTS			PER CENT			ROCK TYPE <i>(follows classification of Okada, 1971)</i>					
			QUARTZ	CHERT	SANDSTONE	K-FELDSPAR	PLAGIOCLASE	MUSCOVITE	BIOTITE	GLAUCONITE	PLANT DEBRIS	DETRITAL LS/DOL	SHALE. CLAY	DETRITAL FE OX	TUFF. PUMICE	MICROFOSSILS	POROSITY	CARB. CEMENT	CLAY MATRIX			QUARTZ	ROCK FRAGMENTS	FELDSPAR	
73-1	33290	KKS	89	5	-	6	T	-	-	R	-	-	T	-	-	-	-	-	89.2	4.7	6.1	QTZS	AREN		
73-4	33291	KKS	51	20	4	3	1	-	T	-	T	18	2	18	2	T	-	-	51.3	45.2	3.5	LTHC	AREN		
73-5	33357	KKS	74	1	-	2	2	T	-	T	18	-	3	-	-	-	-	-	89.6	5.0	5.4	QTZS	AREN		
73-6	33293	KKS	92	5	-	4	-	-	-	T	-	-	-	T	-	-	-	-	91.6	4.6	3.8	QTZS	AREN		
73-9	33295	KKS	95	3	-	2	R	-	-	-	-	-	-	T	-	-	-	-	95.1	2.7	2.2	QTZ	AREN		
73-9	33303	KKS	93	3	-	2	-	-	-	T	-	-	-	R	1	-	-	-	93.2	4.7	2.1	QTZS	AREN		
73-11	33306	KKS	38	25	6	4	R	R	T	-	2	1	22	3	-	-	-	-	37.5	57.8	4.7	LTHC	AREN		
73-22	33319	KKS	78	4	-	5	-	-	-	8	-	-	-	4	-	1	-	-	85.7	9.0	5.3	QTZS	AREN		
73-41	33353	KKS	76	4	-	10	R	1	1	7	-	-	-	R	-	-	-	-	81.9	6.5	11.6	QTZS	AREN		
73-42	33279	KK	73	1	-	3	2	-	-	12	-	-	2	-	-	7	-	-	37	90.8	3.2	6.0	QTZS	WACK	
73-42	33278	KK	88	1	-	3	T	1	T	5	-	-	-	3	-	-	-	-	40	92.0	5.3	2.7	QTZS	WACK	
74-56	30568	KKS	48	7	-	2	T	-	-	T	-	37	4	R	-	-	-	-	-	48.4	49.3	2.3	LTHC	AREN	
74-54	30565	KK	67	5	-	3	2	-	-	T	-	4	14	4	-	-	-	-	-	66.9	28.0	5.1	LTHC	AREN	
74-93	30589	KK	96	1	-	R	-	-	-	-	-	2	-	-	-	-	-	-	3	38	96.2	3.4	.4	QTZ	WACK
74-114	30602	KK	24	-	-	-	T	-	-	67	-	-	-	4	-	5	-	-	47	85.2	14.4	.4	QTZS	WACK	
74-114	30830	KK	45	T	-	T	1	-	-	35	-	-	-	7	-	12	-	-	69	85.1	12.6	2.3	QTZS	WACK	
74-114	30603	KK	97	T	-	R	T	T	T	T	-	-	1	R	-	-	-	-	34	97.4	2.1	.5	QTZ	WACK	
74-124	30615	KK	94	3	-	T	1	-	-	1	-	-	-	1	-	-	-	-	25	9	94.7	4.7	.6	QTZS	AREN
74-125	30616	KK	75	1	-	5	T	2	-	9	-	-	-	7	T	2	-	-	66	83.7	11.2	5.1	QTZS	WACK	
74-129	30620	KKS	85	1	T	2	T	-	-	-	-	-	-	12	-	-	-	-	29	-	84.6	13.4	2.0	QTZS	AREN
74-136	30627	KK	84	4	-	2	1	1	-	3	-	-	-	6	-	-	-	-	46	86.5	10.3	3.2	QTZS	WACK	
GAS-26	30788	KK	98	1	-	1	-	-	-	-	-	-	-	R	-	-	-	-	15	15	97.6	1.2	1.2	QTZ	WACK
UMINMAK (2195)	KKS	96	3	-	T	T	-	-	T	-	-	-	-	-	-	-	-	-	7	29	96.4	3.4	.2	QTZ	AREN
ORKSUT (3050)	KKS	33	2	-	1	-	2	T	2	21	1	5	1	28	2	-	-	-	61	44.5	54.0	1.5	LTHC	WACK	
ORKSUT (3917)	KKS	90	2	-	4	T	1	-	1	-	-	-	-	2	-	-	-	-	41	91.0	5.3	3.7	QTZS	WACK	
TRTCHK (2480)	KK	65	6	-	12	T	2	-	T	-	2	-	13	-	-	-	-	-	63	-	65.4	22.7	11.9	LTHC	AREN

Less than 1%R AreniteAREN QuartzoseQTZS
 LithicLTHC QuartzQTZ Kanguk Formation; silty shale memberKK
 Trace quantitiesT WackeWACK Kanguk Formation; sand membersKKS

GSC

overgrowths were noted in one sample (GSC loc. C-30603). Some of the larger quartz grains show pitting and embayments similar to those illustrated in Plate 19 (e.g., GSC loc. C-30603). Quartz with inclusions of zircon (GSC loc. C-30603) or tourmaline (GSC locs. C-33293, C-33295) are rare.

Most other detrital grains are similar to those observed in the Hassel or Isachsen formations and will not be described in detail. Glauconite is very abundant locally (Pl. 28A), and radiolarians and siliceous sponge spicules also are common at some horizons (Pl. 28A). Glassy tuff fragments are abundant in one sample (Orksut I-44, 3050 ft, 930 m) and are found in trace amounts in two others. Detrital carbonate fragments are abundant in one sample (GSC loc. C-30568).

Matrix and cement

Most of the samples from the silty shale member contain abundant clay matrix, the mineralogy of which was described in the section on that member. Three samples contain carbonate cement. A sample from GSC loc. C-33357 (Station 73-MLA-5) is a very fine, silty sand with a matrix of finely comminuted carbonaceous debris and a cement of ferroan dolomite. Similar cements are in two subsurface samples, as shown in Table 20.

The remaining samples are unconsolidated sands containing little or no matrix and no cement.

Texture

Most of the sands and sandstones are loosely packed, with little or no evidence of grain interpenetration or suturing. Where detrital matrix and secondary cement are absent, porosity is high, reaching 29 per cent at GSC loc. C-30620. In these cases, cementation depends on the presence of thin, clay mineral or iron oxide films on the detrital grains. Sandstones cemented by carbonate, such as at GSC loc. C-33357, show no grain framework, which suggests that the cement has replaced an earlier detrital matrix. Many of the grains also show evidence of replacement by the carbonate cement.

Sand classification

A ternary QRF diagram of the 26 samples from the Kanguk Formation is given in Figure 60. Most of the samples are quartzose or lithic arenites and wackes (Okada, 1971). Those richest in rock fragments contain unusually high concentrations of grain types that normally are rare or absent, such as sedimentary rock fragments (shale, sandstone, limestone), or tuff.

Sediment sources

The bulk of the sand grains in the Kanguk Formation are fine to very fine grained and angular. Like the Hassel sands, they have been derived mainly from the Devonian Melville Island

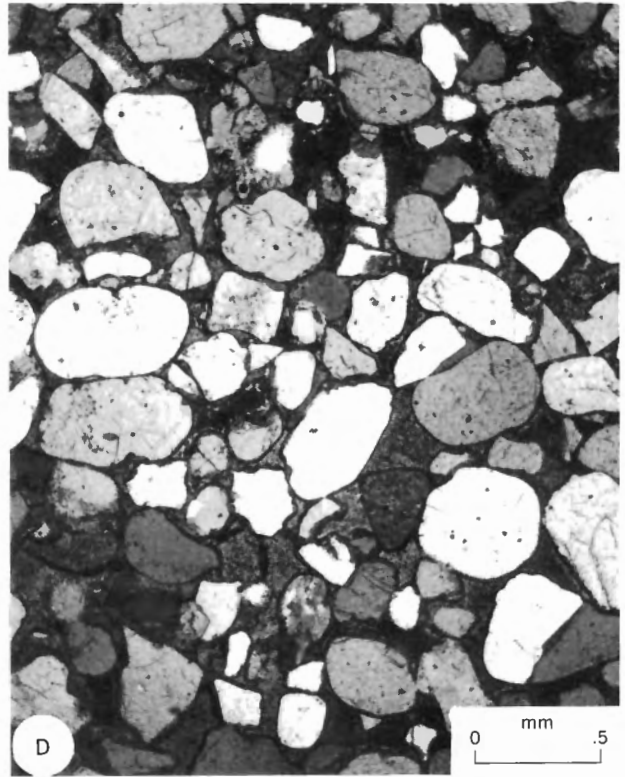
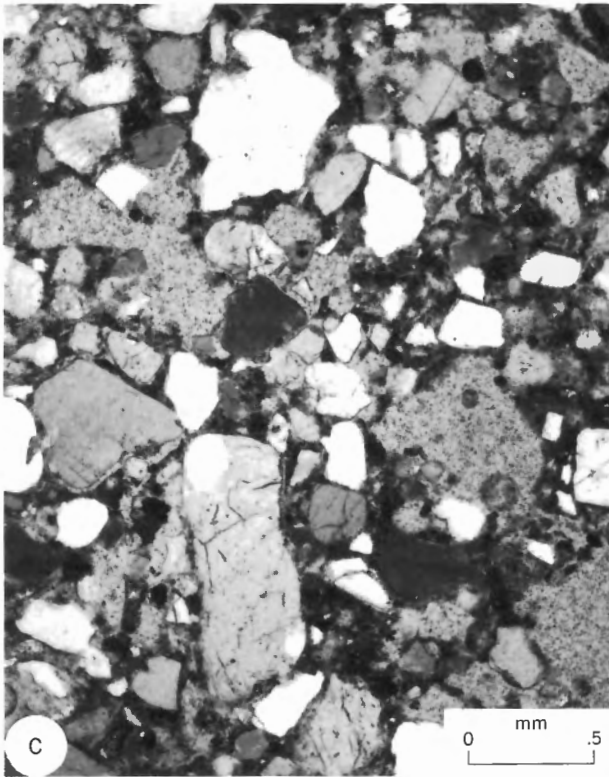
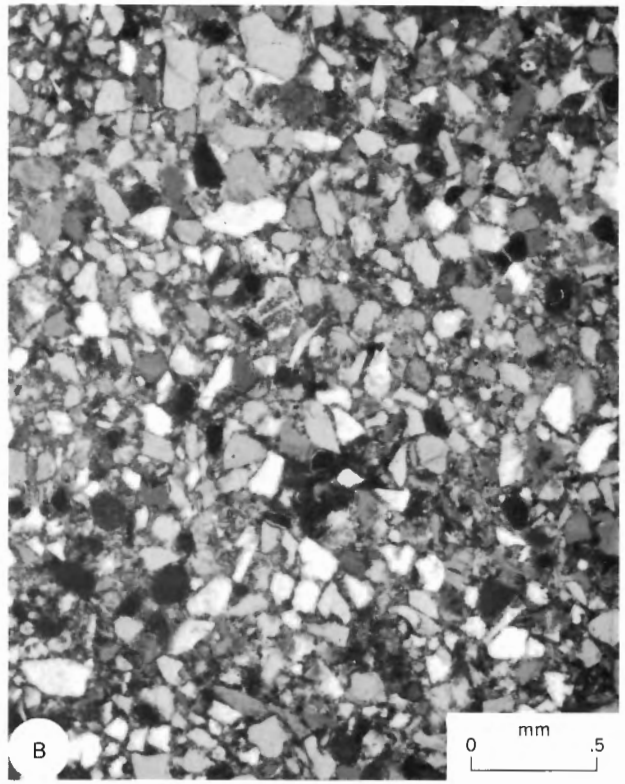
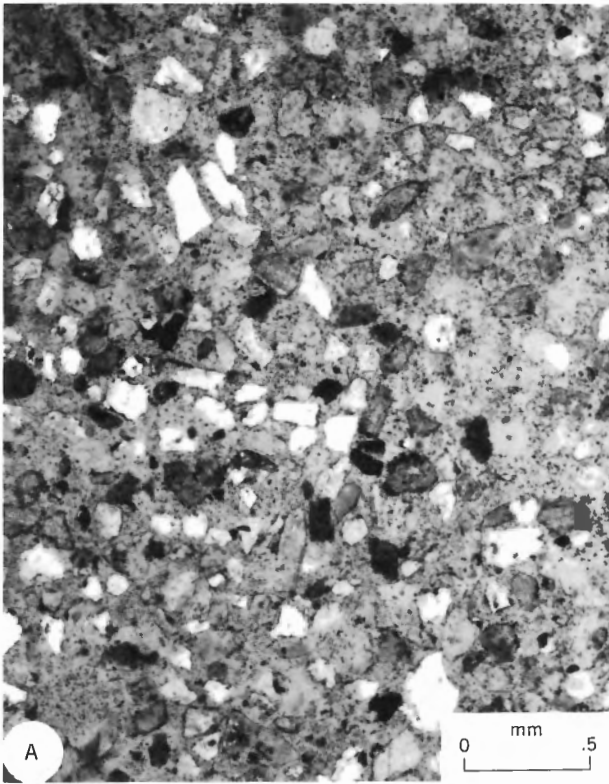


Plate 27. Photomicrographs of sand from the Hassel and Kanguk formations, all under partially crossed polarizers. A: Typical fine-grained sand of Hassel Formation, resin impregnated. B: Typical fine-grained sand from a sand unit within the silty shale member of the Kanguk, resin impregnated. C,D: Medium-grained sandstones from near the top of the silty shale member. (Sample numbers: A, C-30634; B, C-30627; C, C-30589; D, C-30788.)

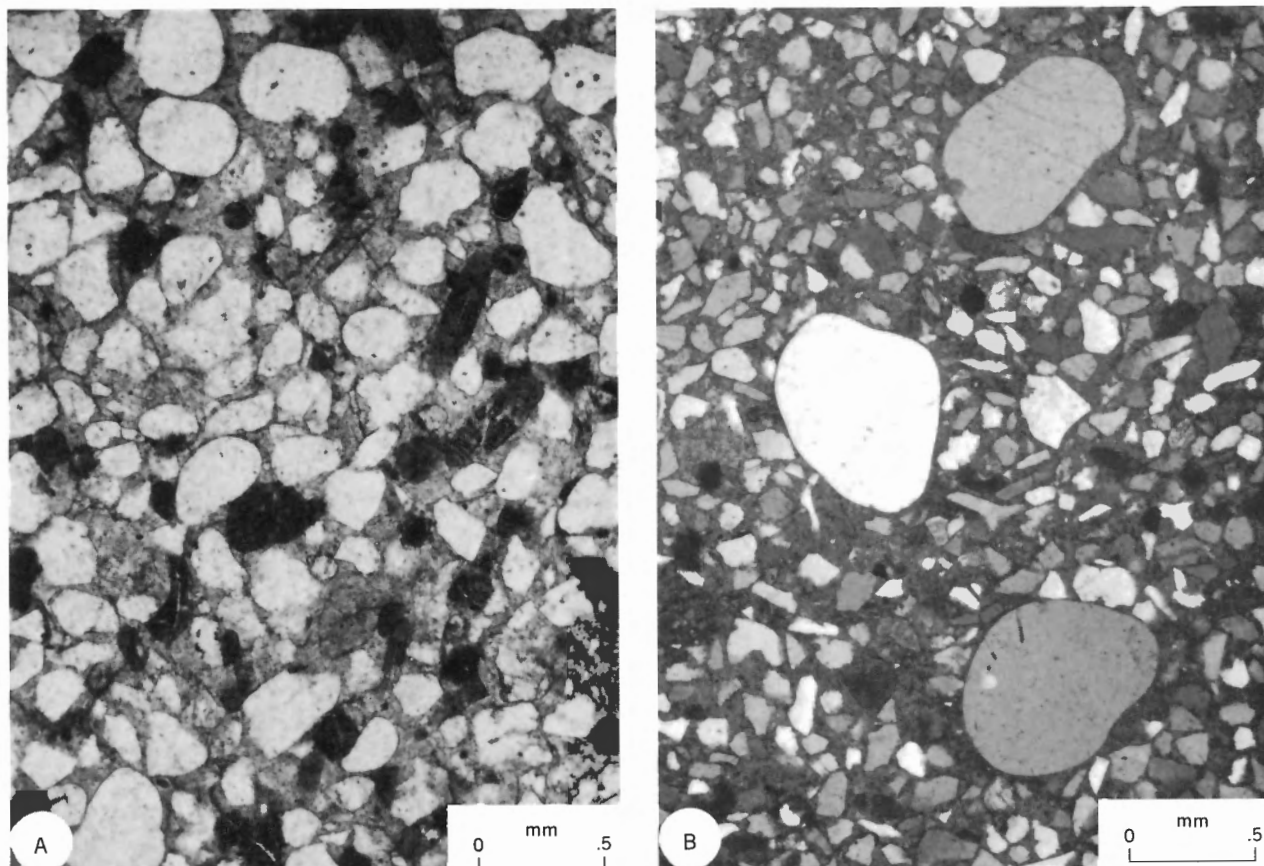


Plate 28. Photomicrographs of sandstone from the Kanguk Formation. A: Sandstone containing glauconite (*dark, amorphous grains*) and sponge spicules (*rod-shaped grains*), silty shale member, plane polarized light. B: Sandstone showing bimodal grain size distribution, silty shale member, partially crossed polarizers. (Sample numbers: A, C-33279; B, C-30603.)

Group which probably cropped out in cliff exposures on the margins of Banks Basin. There are, however, minor but significant admixtures of other grains with a distinctly different origin.

In some samples (Pl. 27C, D), there are numerous quartz grains identical in character to those comprising the Isachsen Formation. They are medium to coarse grained, well rounded, and show detrital cores with overgrowths or embayments. Others contain small crystals of zircon or tourmaline. Generally such grains form a distinct population within the sand, distinguishable mainly because they are larger and rounder (Pl. 28B). Probably this material was derived from exposures of the Isachsen along the margins of Banks Basin. The Lower Cretaceous rocks were uplifted and partially eroded in the mid-Cretaceous (Table 1; Chap. 2) and exposures of the Isachsen Formation probably appeared at that time.

Many of the chert clasts, particularly the pebbles, probably were derived from the Nanuk Formation exposed on Storkerson Uplift or in the present Prince of Wales Strait area. Rare green and red types may have been derived from Proterozoic rocks; the presence of such lithotypes as clasts in the Glenelg Formation is recorded by G.M. Young (1974, p. 18).

Permian coral fragments probably indicate long-range

transportation from the Sverdrup Basin, for there is no evidence of a Permian source within the report-area. Long-shore drift was presumably the mechanism by which these unusual clasts reached their present outcrop area near Antler Cove. Such a distance of transport is by no means improbable. Allen (1972) postulated distances of up to at least 800 km (500 mi) for transportation of sandy and pebbly material in the deltaic Lower Cretaceous rocks of southern Europe.

Eureka Sound Formation

The lithologies in the Shale Member are very similar to those of the silty shale member of the Kanguk Formation and their sedimentology will not be considered in detail. One thin section from a sand unit in the Shale Member at Station 73-MLA-7 (Antler Cove) is described with the samples from the Cyclic Member.

Lithofacies and sedimentary structures

—1. General description.

For the other units described in this chapter, a description of the lithofacies and sedimentary structures leads directly to deductions regarding depositional environment. For the Cyclic Member of the Eureka Sound Formation, the nature of

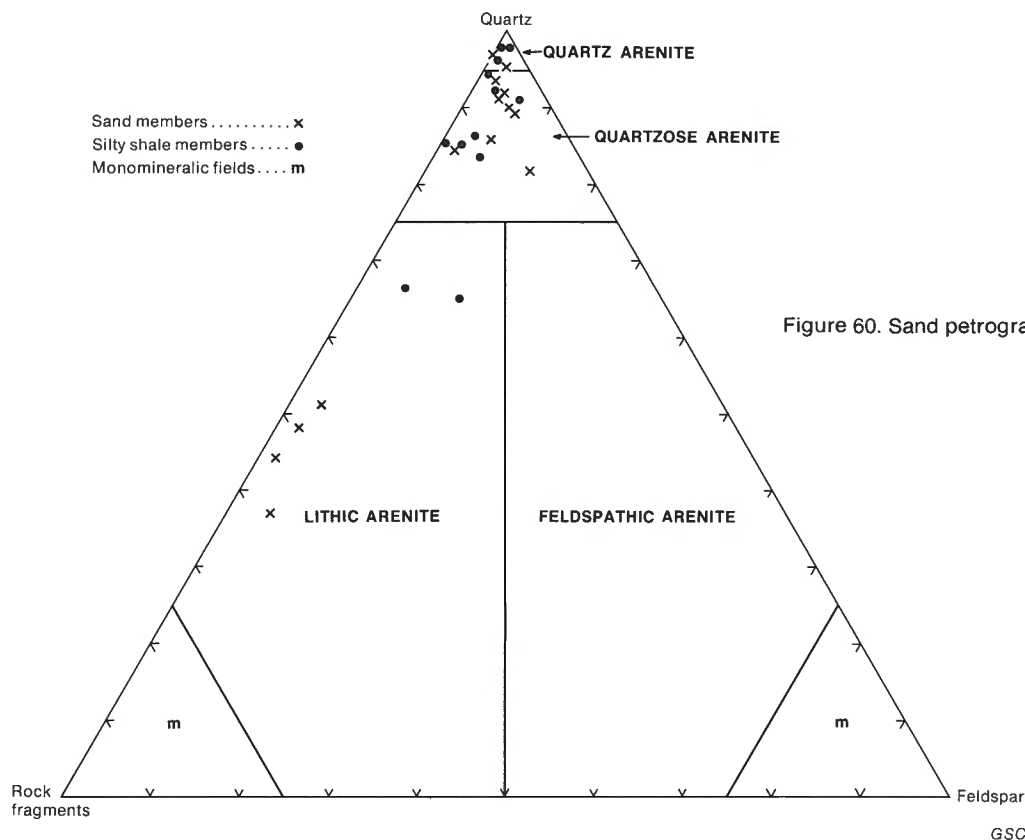


Figure 60. Sand petrography of the Kanguk Formation.

the vertical lithological sequence must be considered first. The depositional environment of the member is discussed in a later section.

The Cyclic Member consists of five lithofacies, as described in the section on the lithology of the Eureka Sound Formation (Chap. 2). These are assigned code letters for the purpose of statistical analysis.

Facies A: shale, dark brown-grey or mottled, micaceous, abundant plant remains, friable

Facies B: interbedded shale and silt or very fine sand, laminated to medium bedded

Facies C: sand, fine to very fine grained, with abundant large- and small-scale sedimentary structures, mottled 'salt and pepper' coloration, plant rootlets, unconsolidated

Facies D: soil, sandy, commonly sideritic, abundant plant rootlets

Facies E: lignite, with or without thin laminae of dark grey shale

The fine-grained rocks (facies A, B) contain few sedimentary structures. Interbedded sand or silt and shale horizons rarely show small-scale contorted bedding as a result of diagenetic density flowage. Elsewhere flaser and lenticular bedding (Reineck and Wunderlich, 1968) have been observed.

A wide variety of sedimentary structures is present in the sand beds (facies C). Planar crossbeds of alpha type (Allen, 1963, p. 101) locally are common. They occur as solitary sets,

large in scale and typically bound by nonerosional upper and lower surfaces (Pl. 29B). They are similar in most respects to the planar crossbeds of the coarse sand facies in the Isachsen Formation, except that rarely are they superimposed as seen in Plate 1. Set thickness ranges from 5 to 150 cm (2–59 in.). Larger crossbed sets, in which the foresets are of varying lithology and may themselves contain small-scale sedimentary structures are rare. These are epsilon crossbeds of Allen (1963, p. 102). Plate 29A shows an example from near Castel Bay.

Trough crossbeds are very abundant in facies C of the Cyclic Member but also occur in facies B. They normally are solitary and are underlain by erosional surfaces. Set thickness ranges from 1.5 to 100 cm (0.6–39 in.). The smaller examples are similar to nu cross-stratification (*ibid.*, p. 107) but most are classified as theta cross-stratification (*ibid.*, p. 105). Large-scale, grouped and overlapping trough crossbeds (pi cross-stratification of Allen, 1963, p. 110) were observed at one locality. Examples of theta cross-stratification are shown in Plate 30. Low-angle "hummocky cross-stratification" (Harms *et al.*, 1975, p. 88) is present at one locality (Pl. 13B).

Small-scale ripple marks also are abundant in facies C. Climbing ripple lamination in which the ripples have slightly wavy crests (kappa cross-stratification of Allen, 1963, p. 106) is the most common type but irregular, superimposed and crosscutting ripple marks also are abundant locally (Pl. 31A).

Ball and pillow structures were observed at a few localities (Pl. 32). They consist of masses of contorted strata in which laminae have been deformed but remain largely unfractured. The structures are enclosed between planar-bedded

layers indicating a very early origin, before later beds were deposited on top of them. They indicate fluidization and flow on a gentle depositional slope, as the result of earthquake-induced or other types of shock. Similar deformation structures in some Pennsylvanian rocks are illustrated by Rascoe (1975), who showed that they are confined to areas of active, contemporaneous uplift.

Sand volcanoes were observed at one locality (Pl. 31B); they resulted from local dewatering processes (perhaps also shock-induced, as shown by Rascoe, 1975).

Analysis of cyclic sedimentation

Markov chain analysis of surface sections

Field observations indicate a coarsening-upward clastic cycle, commonly capped by soil and lignite beds, in many of the surface sections throughout the Cyclic Member. To evaluate statistically the importance of this cyclicity and to test for its regional variability, the stratigraphic sections were analyzed by single dependency Markov chain analysis.

A Markov process is one "in which the probability of the process being in a given state at a particular time may be deduced from knowledge of the immediately preceding state" (Harbaugh and Bonham-Carter, 1970, p. 98). A simple statistical routine is available to calculate these probabilities from coded stratigraphic data, as described by the author (Miall, 1973) and Davis (1973) among others.

The starting point in the analysis is the transition count matrix. This is a two-dimensional array which tabulates the number of times that all possible vertical lithological transitions occur in a given stratigraphic succession. The lower bed of each transition couplet is given by the row number of the matrix, and the upper bed by the column number, each lithofacies being assigned a code number for the purpose of the computer routines. In the present case, numbers 1 to 5 are applied to facies A to E of the Cyclic Member. The transitions in this study have been derived by the "embedded chain" method (Krumbein and Dacey, 1969), in which all lithological transitions are recorded, regardless of bed thickness. Transitions between discrete beds composed of the same lithofacies are not recorded so that the principal diagonal in the transition count matrix is composed of zeros.

Two data sets have been used in the analysis, one comprising grouped data from all sections of Paleocene age and one consisting of Eocene sections. Results from the two data sets are compared later in this section to test for changes in cyclicity with time.

Transition count matrices for the two data sets are given in Tables 21 and 22 and difference probability matrices in Tables 23 and 24. Positive values in the difference matrix indicate which transitions have occurred with greater than random frequency. From these matrices, transition path diagrams have been constructed as shown in Figure 61. Significance tests (Table 25) show that the Markov property (memory) is at a confidence level of at least 99.9 per cent.

In Figure 61, all the lithological transitions that occur with a greater than random frequency are shown by arrows. Where a lithofacies has a greater than random probability of passing up into two different facies, the least probable of the two transitions is indicated by an arrow with a dashed tail.

Table 21. Transition count matrix, grouped Paleocene data from the Cyclic Member, Eureka Sound Formation

Lithofacies and code	A	B	C	D	E	Row sums
Shale (A)	0	39	8	3	7	57
Shale and sand (B)	17	0	36	4	1	58
Sand (C)	26	10	0	8	5	49
Soil (D)	5	2	4	0	5	16
Lignite (E)	10	5	3	1	0	19
Total						199

GSC

Table 22. Transition count matrix, grouped Eocene data from the Cyclic Member, Eureka Sound Formation

Lithofacies and code	A	B	C	D	E	Row sums
Shale (A)	0	34	38	0	5	77
Shale and sand (B)	15	0	26	2	3	46
Sand (C)	41	11	0	12	11	75
Soil (D)	4	1	2	0	7	14
Lignite (E)	19	3	3	0	0	25
Total						237

GSC

Table 23. Difference probability matrix, grouped Paleocene data from the Cyclic Member, Eureka Sound Formation

Lithofacies and code	A	B	C	D	E
Shale (A)	.00	.28	-.20	-.06	-.01
Shale and sand (B)	-.11	.00	.27	-.04	-.12
Sand (C)	.15	-.18	.00	.06	-.02
Soil (D)	.00	-.19	-.02	.00	.21
Lignite (E)	.21	-.06	-.11	-.04	.00

GSC

Table 24. Difference probability matrix, grouped Eocene data from the Cyclic Member, Eureka Sound Formation

Lithofacies and code	A	B	C	D	E
Shale (A)	.00	.15	.02	-.09	-.09
Shale and sand (B)	-.08	.00	.17	-.03	-.07
Sand (C)	.07	-.14	.00	.07	-.01
Soil (D)	-.06	-.13	-.19	.00	.39
Lignite (E)	.40	-.10	-.23	-.07	.00

GSC

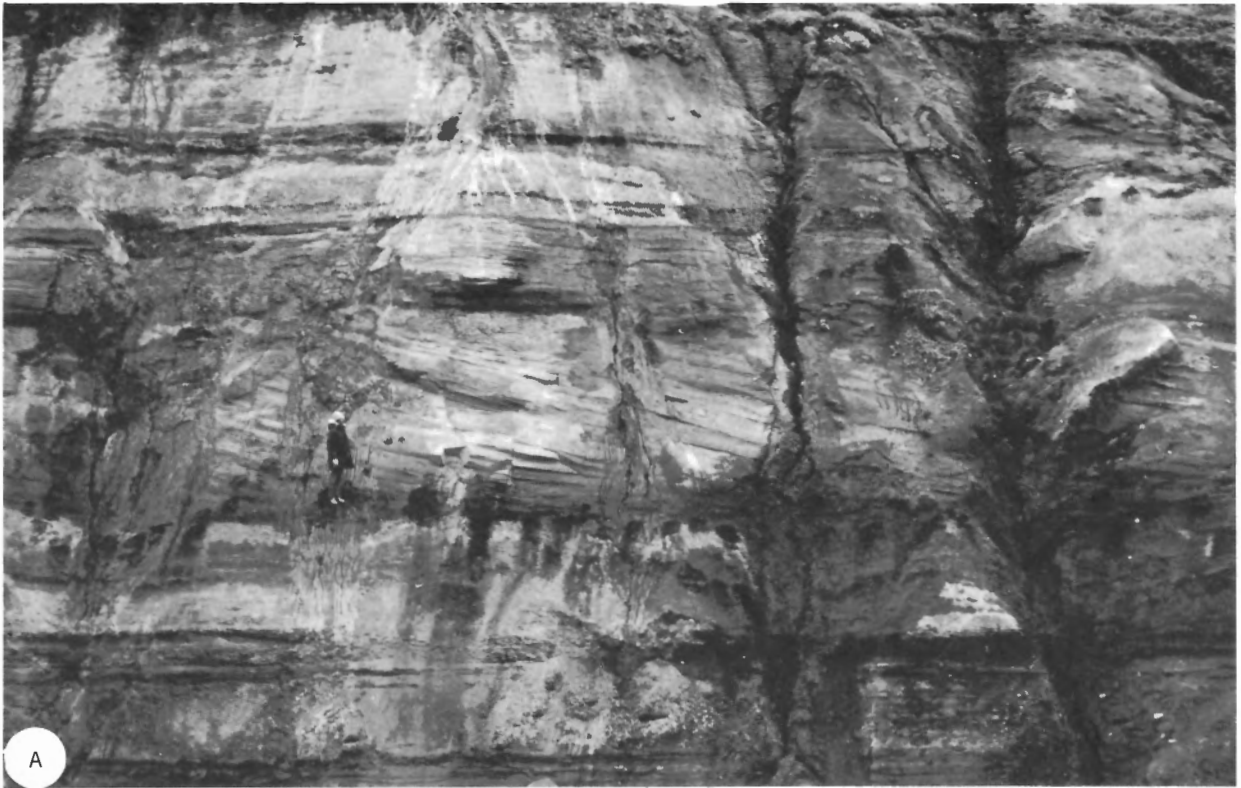


Plate 29. Planar crossbedding, Cyclic Member, Eureka Sound Formation. A: Large-scale (epsilon) crossbed unit, near Castel Bay (Station 74-MLA-156). GSC 199210. B: Large-scale (alpha) crossbed unit (A), overlain by sand with ripple marks (F) and trough crossbeds (T), Nangmagvik Lake (Station 73-MLA-20). Outcrop is 17 m (56 ft) high. GSC 199169.



Plate 30. Trough crossbedding, Cyclic Member, Eureka Sound Formation. A: At Nangmagvik Lake (Station 73-MLA-21). Trough unit is 20 cm (8 in.) thick. GSC 199170. B: At Castel Bay (Station 74-MLA-156). Shovel handle is 50 cm long. GSC 199212.



Plate 31. Small-scale sedimentary structures, Cyclic Member, Eureka Sound Formation. A: Superimposed and crosscutting current ripples near Eames River (Station 74-MLA-118). GSC 199206. B: Sand volcano, showing cones of several generations, Nangmagvik Lake (Station 73-MLA-20). GSC 199168.



Plate 32. Ball and pillow structures, Cyclic Member, Eureka Sound Formation. A: Near lower Thomsen River (Station 74-MLA-126). GSC 199205. B: At Eames River (Station 73-MLA-44). GSC 199161.

Other transitions are present, as can be seen from an examination of Tables 21 and 22, but they can be explained on the basis of random changes in depositional environment. The coarsening-upward clastic cycle (facies succession A-B-C) is shown to be the most important transition sequence and this commonly is followed by a soil-lignite couplet (D-E).

The two diagrams in Figure 61 show slight differences, the significance of which has been tested using the stationarity test provided by Harbaugh and Bonham-Carter (1970, p. 124) and the writer (Miall, 1973, p. 352). The test yields a χ^2 value of 31.48 with 20 degrees of freedom, which is just barely significant at the 95 per cent confidence level (limiting value at 20 degrees of freedom is 31.41). The differences consist mainly of a slightly greater tendency in the younger rocks for the clastic cycle to be capped by soil and by lignite. The A-C transition shown in Figure 61B may or may not be geologically significant; it means that the shale-sand transition tended to be more abrupt in Eocene than in Paleocene time.

Examination of the data shows 91 cycles of the A-C or A-B-C type in the total 1336.5 m (4385.1 ft) of measured sections. They have a mean thickness of 7.36 m (24.15 ft) and comprise 50.1 per cent of the total measured thickness.

Sedimentological interpretations of these results are given in a later section.

Fourier analysis of subsurface sections

The clastic cycles in the surface sections consist of beds which show an upward increase in grain size. Silt- and clay-size material diminishes in importance considerably between facies A and C. X-ray diffraction analyses of typical shale samples show that they consist of at least 25 per cent clay minerals, whereas grain size analyses of sand samples show that the silt plus clay fraction may drop as low as 1 per cent by weight. These variations are recorded accurately in the subsurface by the gamma ray log. This log measures the natural radioactivity in the rocks and, because in sedimentary rocks radioactive elements tend to concentrate in clays and shales, it is a useful

Table 25. Tests of significance, Markov chain analysis of stratigraphic successions from the Cyclic Member, Eureka Sound Formation

Data set	Test equation*	χ^2	Degrees of freedom	Probability of randomness
PALEOCENE	1	62.08	15	< 99.9%
PALEOCENE	2	175.28	11	< 99.9%
EOCENE	1	73.21	15	< 99.9%
EOCENE	2	217.81	11	< 99.9%

*Equation 1 from Billingsley (1961, p. 17)

*Equation 2 from Harbaugh and Bonham-Carter (1970, p. 121)

GSC

indicator of clay content in a sedimentary succession. If clastic cycles are present in the subsurface, it would be expected that the gamma ray log would reveal them by a series of funnel-shaped deflections, the gamma count decreasing upward. Such is, in fact, the case. Figure 8 shows that all the gamma ray logs through the Cyclic Member indicate coarsening-upward cycles (some fining-upward cycles also are indicated). Cycles considerably thicker and thinner than the average surface cycle are present in these logs, although the range of thicknesses in the surface and subsurface is similar. A portion of a gamma ray log is shown in Figure 62 to illustrate the comparison. Sand units of the same range of thickness suggested by the gamma ray logs have been observed at the surface, although very thick units are rare. Six sand beds 14 m (46 ft) or more in thickness have been recorded. The thickest is 33.1 m (108.6 ft) at Station 74-MLA-46 (Log River).

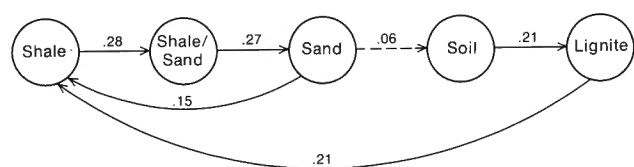
The existence of megacycles in the subsurface logs is shown by a tendency for the cycles to become thicker upward, or to contain a more prominent coarse member. This tendency is particularly evident in the Storkerson Bay A-15 well (Fig. 8) in which three megacycles can be recognized:

- megacycle 3, 2255–1791 ft (687–546 m) interval
- megacycle 2, 2622–2255 ft (799–687 m) interval
- megacycle 1, 3102–2622 ft (945–799 m) interval

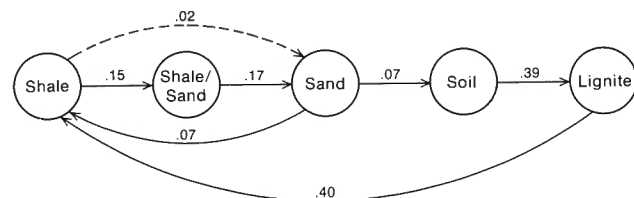
Megacycles also are present in the Nanuk D-76 well (Fig. 8).

Statistical analysis of the subsurface sections cannot be based on a visual subdivision of the log into cyclic units, because it is impossible to achieve a rigorous operational definition of what constitutes a cycle. In many cases a given vertical interval could be subdivided into cycles in several different ways. An alternative approach using Fourier analysis has been employed. In this technique the digitized log is analyzed as if it were a wave form and the relative amplitudes of all possible harmonics are quantified. The basic statistics are described by Preston and Henderson (1964).

Four subsurface logs have been analyzed with this technique using the lower 512 feet (156 m) of each section through the Cyclic Member (upper 512 ft in the Orksut well). The amplitude spectra are shown in Figure 63. It can be seen that the spectra are different for each well, with the exception of one peak corresponding to a harmonic wavelength of about 6 m (20 ft), which appears to be capable of correlation, with slight wavelength variations, among all four wells. The variations in wavelength are shown in Figure 63; they range from



A. Paleocene data



B. Eocene data

GSC

Figure 61. Transition path diagrams, Cyclic Member of the Eureka Sound Formation. Probability values from the difference matrices (Tables 23, 24) are shown.

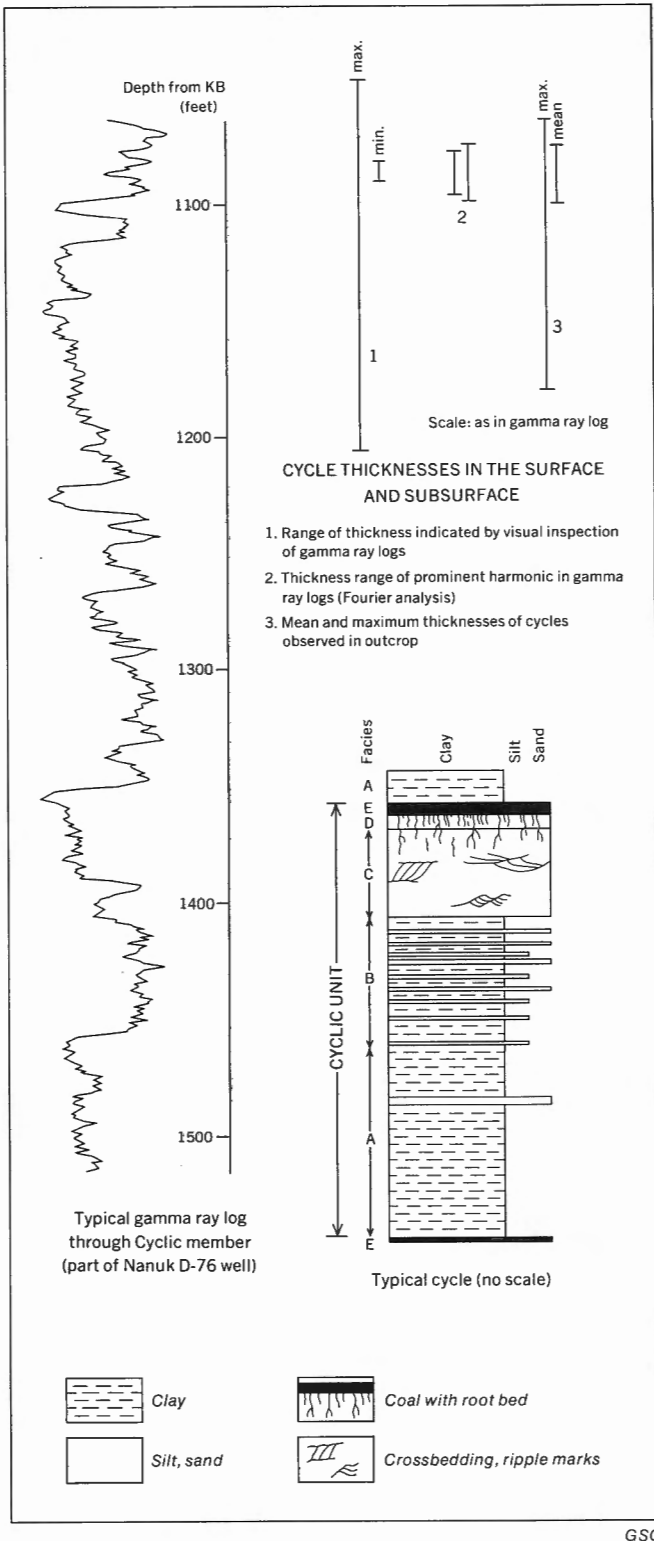


Figure 62. Comparison of cycles in the surface and subsurface.

5.8 to 6.8 m (19–22.3 ft). This persistent type of subsurface cycle is about as thick as the surface cycles; the mean thickness suggests that the subsurface cycles comprise the same type of depositional unit as those studied in the surface outcrops. The slight differences in thickness may be significant, however, and will be discussed in a later section.

Lithofacies and sedimentary structures
–2. Regional variation

Vertical variation

Complete sections through the Cyclic Member are not available but upper and lower parts of the member can be compared by grouping the data into Paleocene and Eocene categories and calculating various parameters for each data set. This has been done already for the cycles within the succession, by using Markov chain analysis. Other variables are considered below. It is important to bear in mind that a component of lateral variability cannot be eliminated from these data because outcrops of Paleocene age are confined to the eastern flank of Northern Banks Basin, whereas the Eocene parts of the succession are exposed in the central and western parts of the basin. Some of the differences discussed below appear more significant when shown in map form (see next section).

Differences between the Paleocene and Eocene for six important parameters are listed in Table 26. The variance for each parameter has been calculated (not shown) and a difference-of-means test carried out, using the *t*-statistic. The probabilities of the differences being statistically significant are shown in the right-hand column.

Mapping suggested that the sand/shale ratio increases in younger beds, and the data very nearly support this conclusion at a 95 per cent confidence level. Lateral variability probably is masking a vertical change in this parameter. Lignite distribution undergoes no change between the lower and upper parts of the Cyclic Member (even the variances of the distribution are not significantly different). This is regarded as fairly conclusive proof that the subdivision of the sand-bearing part of the Eureka Sound into two members by Jutard and Plauchut (1973, p. 213) is not of regional significance. These authors established a subdivision on the basis of an apparent upward decrease in lignite content but their conclusions can have validity only for the few sections that they measured.

Table 26. Vertical variations in stratigraphic parameters, Cyclic Member of the Eureka Sound Formation

PARAMETER	PALEOCENE	EOCENE	t	p
Sand/shale ratio	1.0	1.8	-1.59*	.92
Per cent lignite	2.3	2.3	0.0*	.0
Mean sand bed thickness (m)	2.9	4.3	-0.23*	.55
Mean cycle thickness (m)	6.8	7.7	-0.73*	.75
Per cent section which is cyclic	40.8	56.4	-1.91	.97
Sand/shale ratio within cycles	3.2	2.6	0.42*	.65

Level of probability reached p
 2-tailed difference-of-means *t* test t
 Not significantly different at 95% confidence level 0.33*

GSC

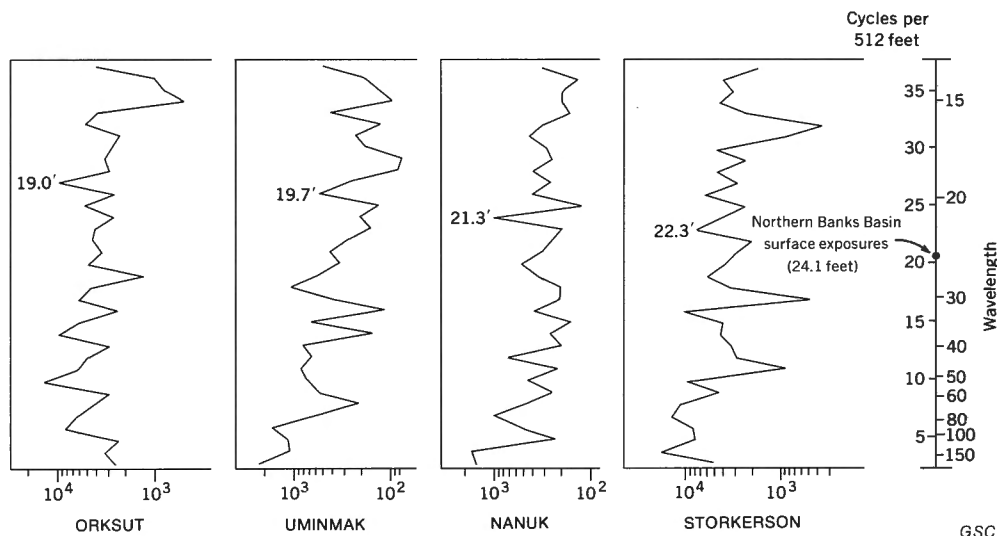


Figure 63. Amplitude spectra for parts of four gamma ray logs which were analyzed to test for cyclicity in the Cyclic Member of the Eureka Sound Formation. Corresponding mean thickness of cycles in the surface outcrops also is shown.

If the sand/shale ratio increases with decreasing age, it is of interest to determine whether this is due to an increase in the number of sand beds in the section or to an increase in sand bed thickness. No significant differences in bed thickness are present, as shown in Table 26, and therefore the change in sand/shale ratio is assumed to be the result of a greater number of sand beds in the succession.

The remaining three parameters shown in Table 26 relate to the clastic cycles which were discussed in an earlier section. The younger parts of the Cyclic Member contain a significantly greater percentage of the section that is composed of cycles. However, cycle thickness and sand/shale ratio within the cycles both show no appreciable change.

Lateral variation

Table 27 provides values for a series of parameters calculated for each of the twenty-three sections measured through the Eureka Sound Formation in Banks Basin. For many of these sections, the thickness exposed probably is inadequate to provide a completely reliable estimate of such values as cycle thickness or sand/shale ratio within cycles. However, when the data are plotted in map form, many of the variables show regional trends, suggesting that the magnitudes of such trends are larger than the measurement error (some of the trends are weak, and the interpretations suggested below may be subject to modification if more data become available). Location numbers and age of the sections are shown in Figure 64.

Table 27. Summary of stratigraphic data, Cyclic Member of the Eureka Sound Formation

Location (All MLA)	73-19	73-20	73-21	73-37	73-38	73-39	73-40	73-43	73-44	74-43	74-45	74-46	74-113	74-115	74-116	74-118	74-126	74-150	74-154	74-155	74-157	74-158	74-159
Age (PALEOCENE , EOCENE)	P	P	P	E?	E	E	E?	E?	E?	P	E	E	P	P	P	E	P?	E	E?	E	E?	E	P?
Section thickness (metres)	54.2	60.5	78.0	53.0	20.0	71.0	78.0	44.0	53.0	64.4	79.5	81.8	41.0	71.0	63.0	52.0	36.6	40.0	49.7	113.5	37.6	29.2	65.5
Number of measured units	28	10	28	22	7	20	27	11	16	18	20	22	28	31	31	17	19	19	19	43	15	13	20
Per cent shale	29.5	38.8	31.2	24.2	21.5	46.5	49.0	12.5	27.3	15.2	35.7	20.8	45.9	29.7	32.9	20.4	30.6	41.8	58.6	53.3	27.7	48.6	53.9
Per cent shale/sand	49.6	38.0	46.4	30.2	0.0	7.0	22.4	28.4	3.3	17.4	19.6	0.6	37.0	26.2	41.6	28.5	45.1	8.5	12.7	16.6	8.8	21.2	15.1
Per cent sand	16.4	23.1	19.0	43.6	76.5	45.1	27.6	47.7	66.8	64.4	40.0	72.6	12.4	41.3	25.1	50.8	11.2	46.5	27.2	27.8	63.3	29.1	30.8
Per cent soil	0.7	0.0	3.1	1.9	1.0	1.4	0.0	2.3	1.1	0.5	0.0	1.7	0.5	0.4	0.5	0.4	0.0	1.0	0.6	0.3	0.0	0.3	0.0
Per cent lignite	3.7	0.0	0.4	0.2	1.0	0.0	1.0	9.1	1.5	2.5	4.7	4.3	4.1	2.4	0.0	0.0	13.1	2.3	1.0	2.1	0.3	1.0	0.2
Sand/shale ratio	0.56	0.60	0.61	1.8	3.6	0.97	0.56	3.8	2.4	4.2	1.1	3.5	0.27	1.4	0.76	2.5	0.37	0.90	0.46	0.52	2.3	0.59	0.57
Mean sand bed thickness (metres)	1.3	14.0	3.0	2.6	5.1	4.0	3.1	7.5	7.1	5.2	6.4	8.5	1.3	3.3	1.6	4.4	1.4	3.3	2.3	2.3	4.8	2.8	2.9
Sedimentary structure assemblage no. *	2	1	2	3	2	3	3	1	2	2	1	2	4	4	4	3	3	3	2	3	2	3	3
Number of cycles	4	1	2	5	1	6	6	0	4	1	4	5	4	6	7	2	1	4	5	11	4	2	6
Mean cycle thickness (metres)	5.3	15.0	8.6	5.7	4.8	7.7	7.8	-	9.0	10.5	8.2	12.0	4.1	7.3	6.4	5.8	4.6	7.7	8.3	7.3	4.1	8.5	7.4
Per cent section which is cyclic	39.1	24.8	22.7	53.6	24.0	64.8	60.1	0.0	67.8	16.3	41.3	73.3	40.0	61.7	71.1	22.3	12.6	76.7	83.1	70.7	43.6	58.2	67.4
Sand/shale ratio within cycles	1.2	14.0	0.43	8.6	2.7	0.70	1.6	-	2.1	0.27	8.0	3.8	1.1	1.1	1.3	2.1	1.1	0.88	0.87	1.1	2.4	0.9	10.1

* Numbers are explained in text

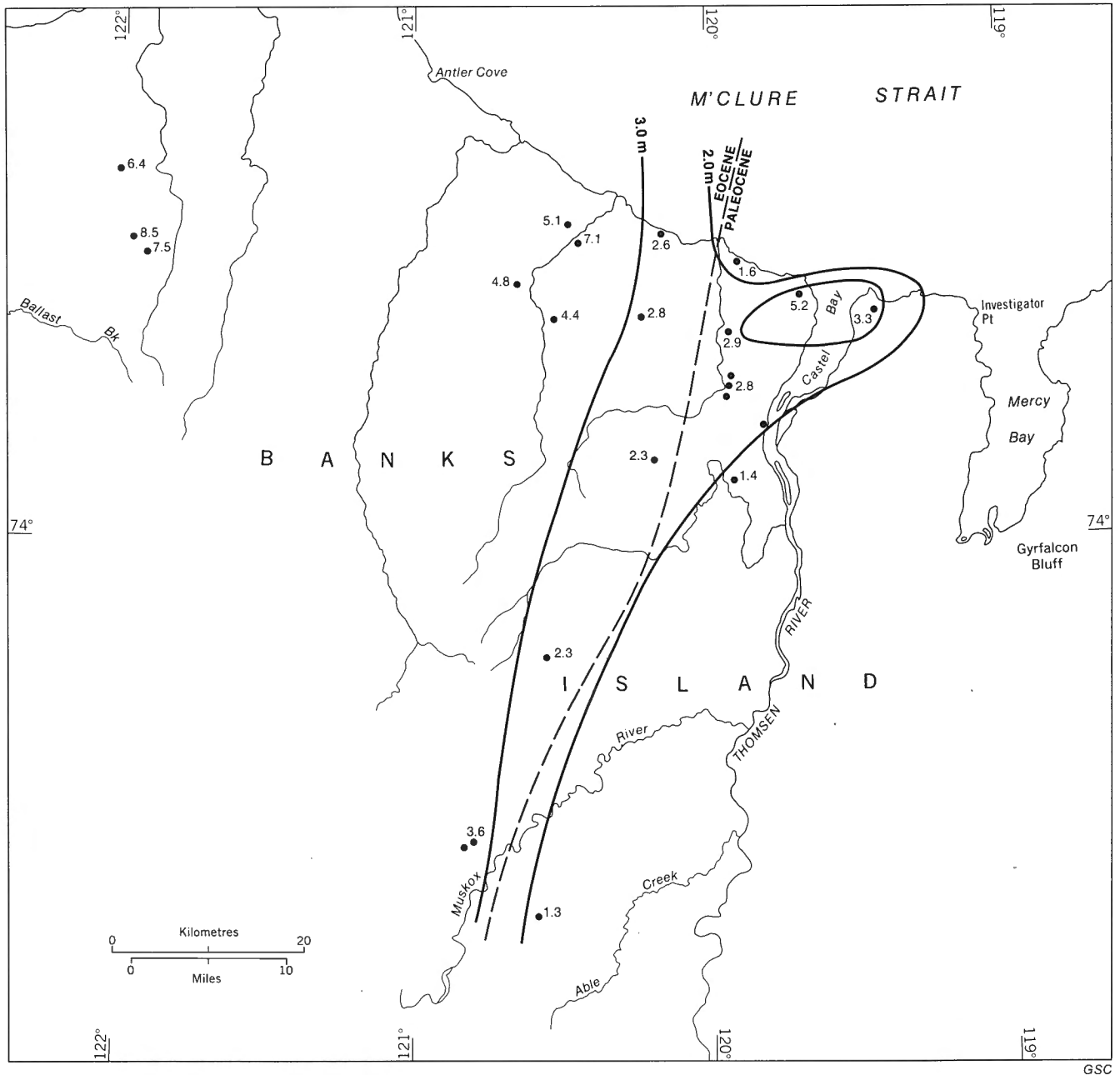


Figure 66. Mean sand bed thickness, Cyclic Member of the Eureka Sound Formation.

Sound Formation of Banks Island was deposited under marine conditions. This is discussed in later sections.

Cyclic models

Coarsening-upward clastic cycles typically occur in marginal marine environments. The regressive-marine, shoreline or barrier island cycle has been discussed earlier in this chapter in connection with the Hassel Formation. The other main type of cycle is the coarsening-upward deltaic sequence. It was first recognized by Scruton (1960), based on detailed work in the Mississippi delta, and represents the progradation of silts and sands from a distributary mouth. Subsequently very similar

cycles have been recognized in many modern deltas, including the Niger (Allen, 1970a) and the Rhône (Oomkens, 1970), and in many ancient rock sequences (Duff and Walton, 1962; Read and Dean, 1967; Fisher *et al.*, 1969; Curtis, 1970; and many others).

It is important to distinguish among wave-, tide- and river-dominated deltas, because the vertical sequence is superficially similar. In the wave- and tide-dominated deltas such as the Niger, tidal channel and beach deposits comprise the upper, coarse members of the deltaic sequence (Allen, 1970a; Oomkens, 1974). In river-dominated deltas these deposits will be of less importance and distributary mouth bars, bar-finger

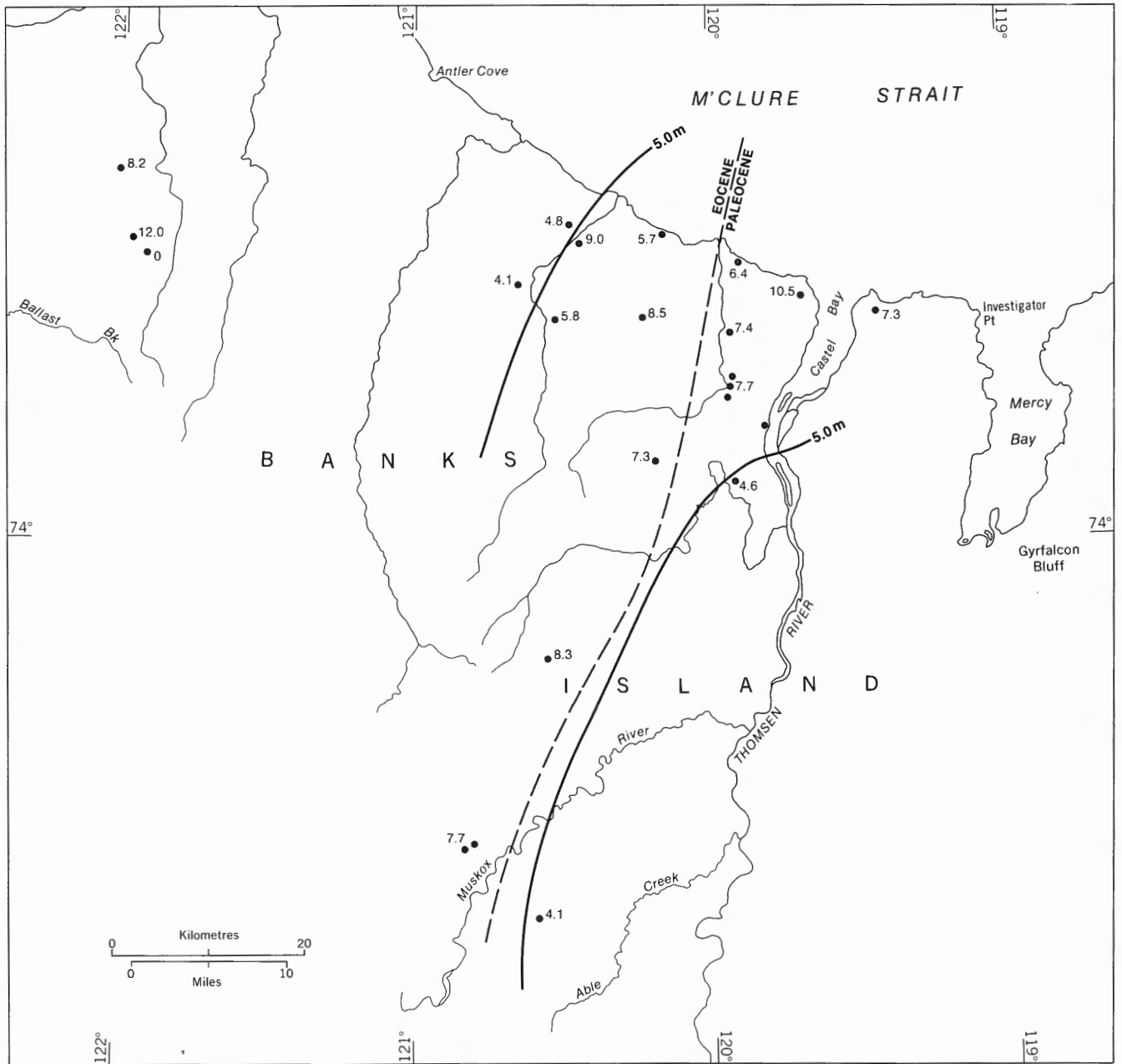


Figure 67. Mean cycle thickness, Cyclic Member of the Eureka Sound Formation.

sands and fining-upward, fluvial point-bar sequences will predominate, as in the Mississippi (Fisk, 1955, 1961; Coleman and Gagliano, 1964; Gould, 1970) and the Colorado (Kanes, 1970).

Another important consideration is that of scale. For major deltas the vertical, coarsening-upward sequence may range from 50 to 150 m (160–490 ft) or more in thickness (Klein, 1974). But coarsening-upward sequences also occur on a much smaller scale within deltas. Coleman and Gagliano (1964) and Elliott (1974) described crevasse splay and minor mouth bar sequences ranging from 2 to 14 m (6.6–46 ft) thick. A complete deltaic wedge may consist of many such small

cycles superimposed one upon the other. Both large- and small-scale cycles are present in the Cyclic Member, as has been demonstrated in a previous section. A detailed interpretation of the cycles follows.

Small-scale cycles

The scarcity of invertebrate remains, the abundance of high-angle cross-stratification, the unimodal nature of the paleocurrents (next section) and the abundance of coal in the cycles of Northern Banks Basin indicate that they were formed by river-dominated deltas. A direct analogy is proposed herein between these cycles and the small-scale cycles described by

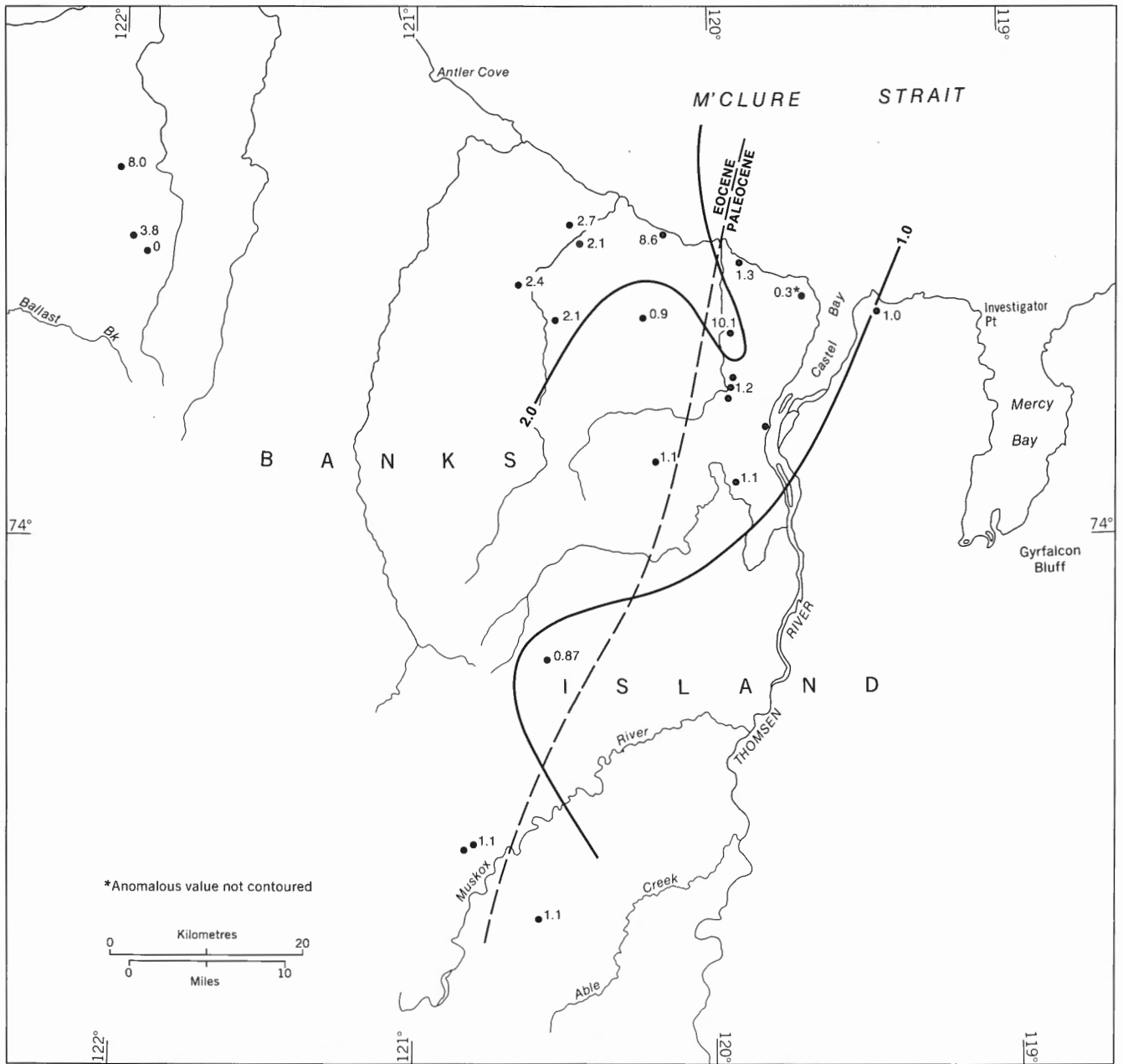


Figure 68. Sand/shale ratio within the clastic cycles, Cyclic Member of the Eureka Sound Formation.

GSC

Elliott (1974). As will be shown, the deltas probably were lobate or birdsfoot-shaped. Elliott's deltaic cycles range from 2 to 14 m (6.6–46 ft) thick, the thickest of which he interpreted as minor mouth bar sequences. In the Mississippi delta, which he discusses, such cycles certainly are minor in scale but, in smaller scale deltas, such as those which probably gave rise to the Cyclic Member, they probably represent the progradation of principal distributary channels.

The shale units (facies A) represent quiet-water, probably marine or brackish sedimentation in prodelta areas or in interdistributary bays. In rare instances, shale units contain one or more laterally discontinuous sand lenses up to 1 m (3.3

ft) thick, commonly in the form of shallow troughs infilled with trough cross-laminated sand (Pl. 33A). Some of these lenses may represent frontal splays from advancing distributary mouth bars. Others are interpreted as the product of overbank floods and thus represent small-scale crevasse-splay deposits (Elliott, 1974, Fig. 1A, B). The development of new distributary channels in a delta depends on the occurrence of such crevasing. The channels are widened gradually and a new prograding sequence is begun.

Shale units commonly pass upward into interbedded shale and silt or shale and very fine sand (facies B). This facies represents the further development and influence of a cre-

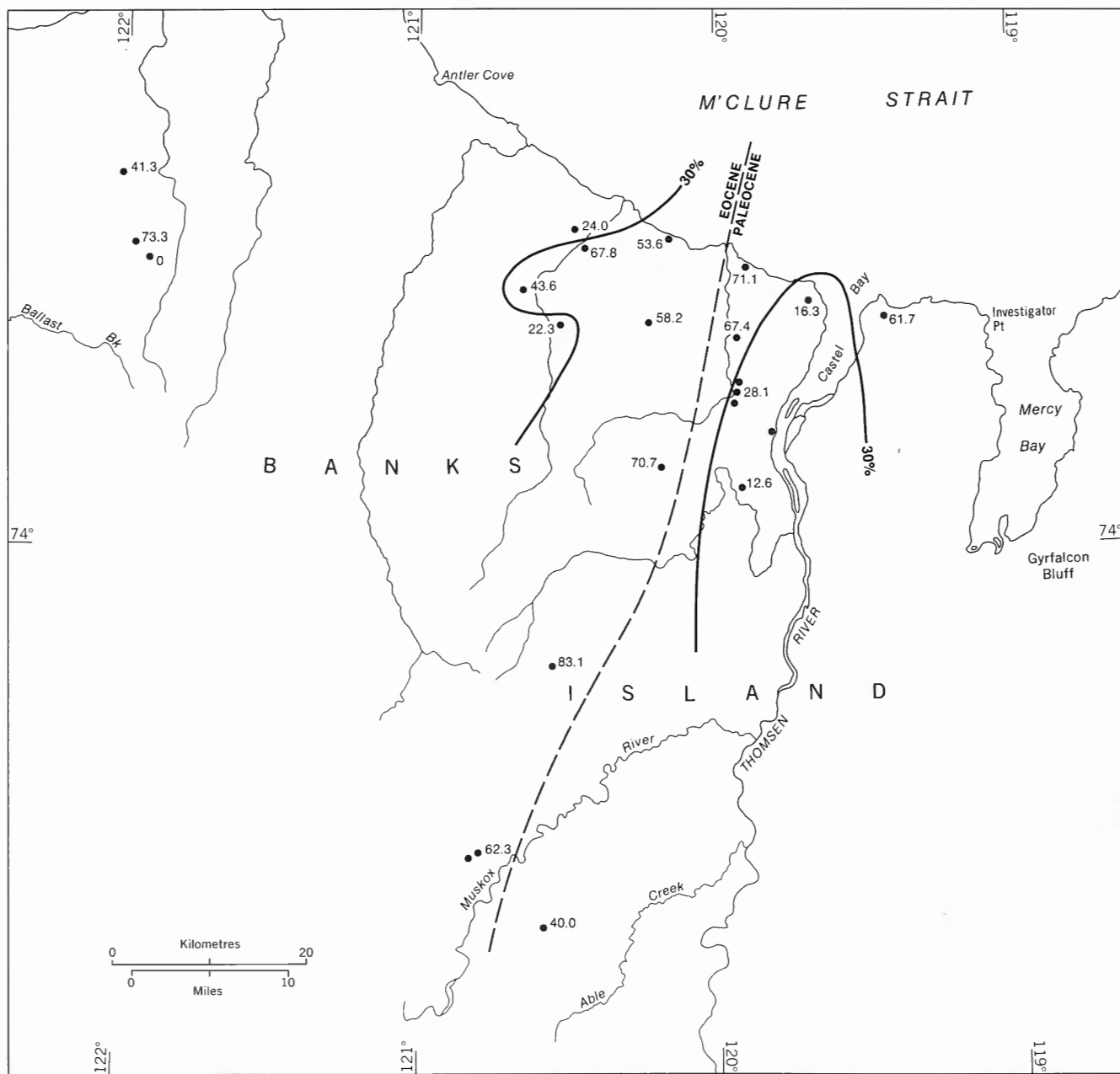


Figure 69. Percentage of section that is cyclic, Cyclic Member of the Eureka Sound Formation.

vasse, or the first appearance of prograding clastic sheets from a distant distributary mouth. The sedimentary succession would be virtually identical in each case.

Facies C represents the result of continued progradation. A distributary deposits most of its bedload when it debouches into the delta-front area or into an interdistributary bay, and the result is a mouth bar deposit which consists of a laterally extensive lens of sand (Elliott, 1974, Fig. 2). Depending on the relative strengths of river or tidal currents, the geometry, internal stratification and biogenic remains within the bar deposits may show considerable variation from delta to delta. Most of the sand beds in the Cyclic Member contain trough

crossbeds (of dune origin) and small-scale ripple marks (Pls. 30, 31A), indicating a fluctuation in discharge rates. However, with some exceptions (discussed below), current directions are unimodal and thus fluvial currents must have predominated. Many of the sand units were colonized by plants (Pl. 34A), suggesting that the bar became emergent and that the distributary channel was abandoned slowly as a result of crevassing upstream.

In one instance, near Eames River, a sand unit contains abundant remains of the trace fossil *Ophiomorpha* (Pl. 13B). As Howard (1972) and DeWindt (1974) have shown, this characteristic fossil type represents the burrows of a callianassid

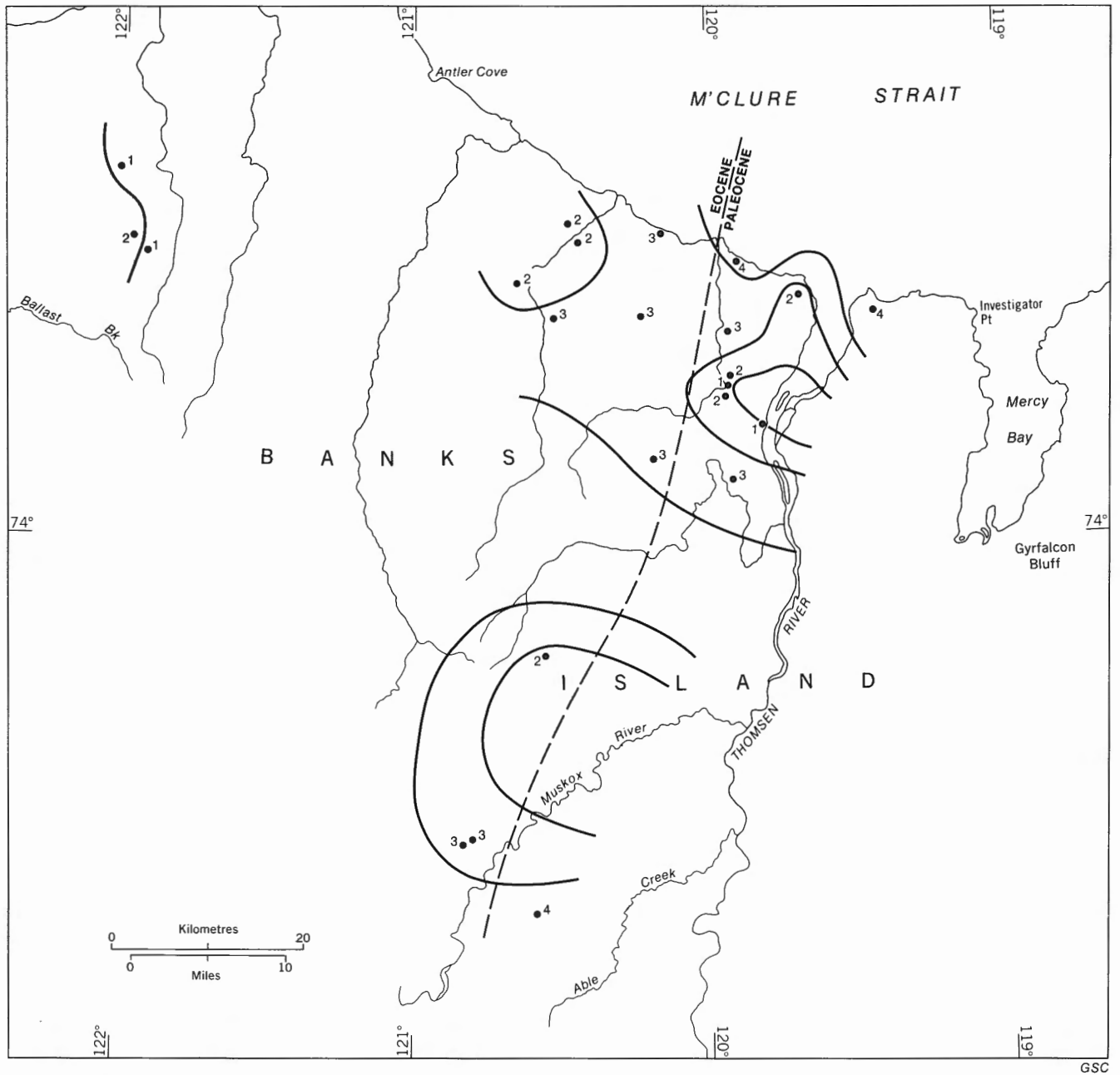
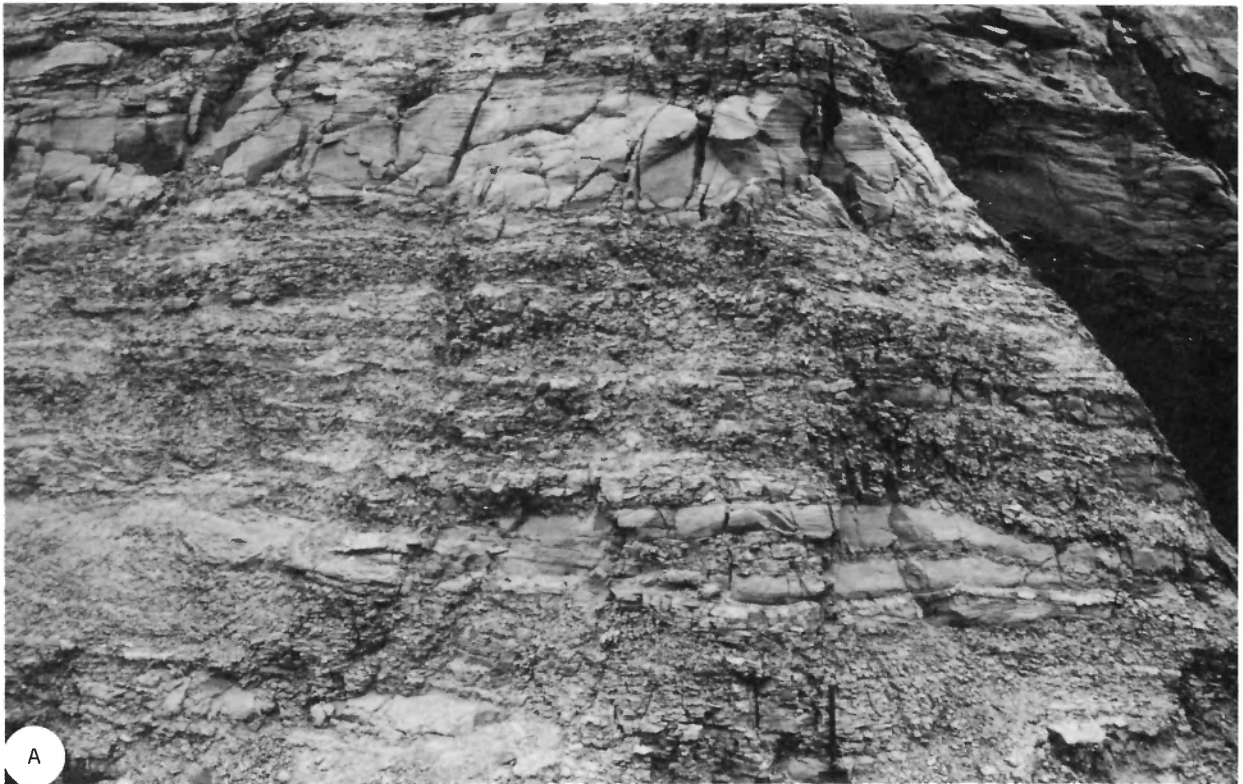


Figure 70. Distribution of sedimentary structure assemblages, Cyclic Member of the Eureka Sound Formation.

shrimp, and it is an excellent indication of the very shallow marine or intertidal environment. The burrows occur in low-angle 'hummocky' cross-stratified sand, a structure which Harms *et al.* (1975, p. 88) interpret to be of storm-wave origin. The sand unit near Eames River probably represents an abandoned mouth bar that was reworked by wave and tide activity, but this type of event must have been rare for only one such occurrence has been noted. In bars that were in the process of formation, the rate of sedimentation probably was too rapid to allow the colonization by marine organisms. It probably is significant that the *Ophiomorpha* locality is near the centre of the basin in a relatively distal delta front

position. Current directions locally are bimodal in this area (*see later section*) which also suggests a marine (wave, tide) influence.

The clastic cycles may or may not be followed by a soil-lignite couplet; the statistically high probability of such a transition has been demonstrated by Markov chain analysis. Where present, as illustrated in Plate 14A, the lignite indicates that the distributary had prograded farther into the prodelta region and the bar became part of the delta-plain marsh. Thick vegetation must have developed in these regions to have given rise to the extensive lignite beds and, in some instances,



A



B

Plate 33. Features of deltaic sedimentation, Cyclic Member, Eureka Sound Formation. A: Shale with thin sand lenticles. The latter are interpreted as crevasse-splay deposits; Castel Bay (Station 74-MLA-156). GSC 199211. B: Crosscutting of deltaic lobes, Log River (Station 74-MLA-45). Approximately 40 m (130 ft) of section are visible. GSC 199196.

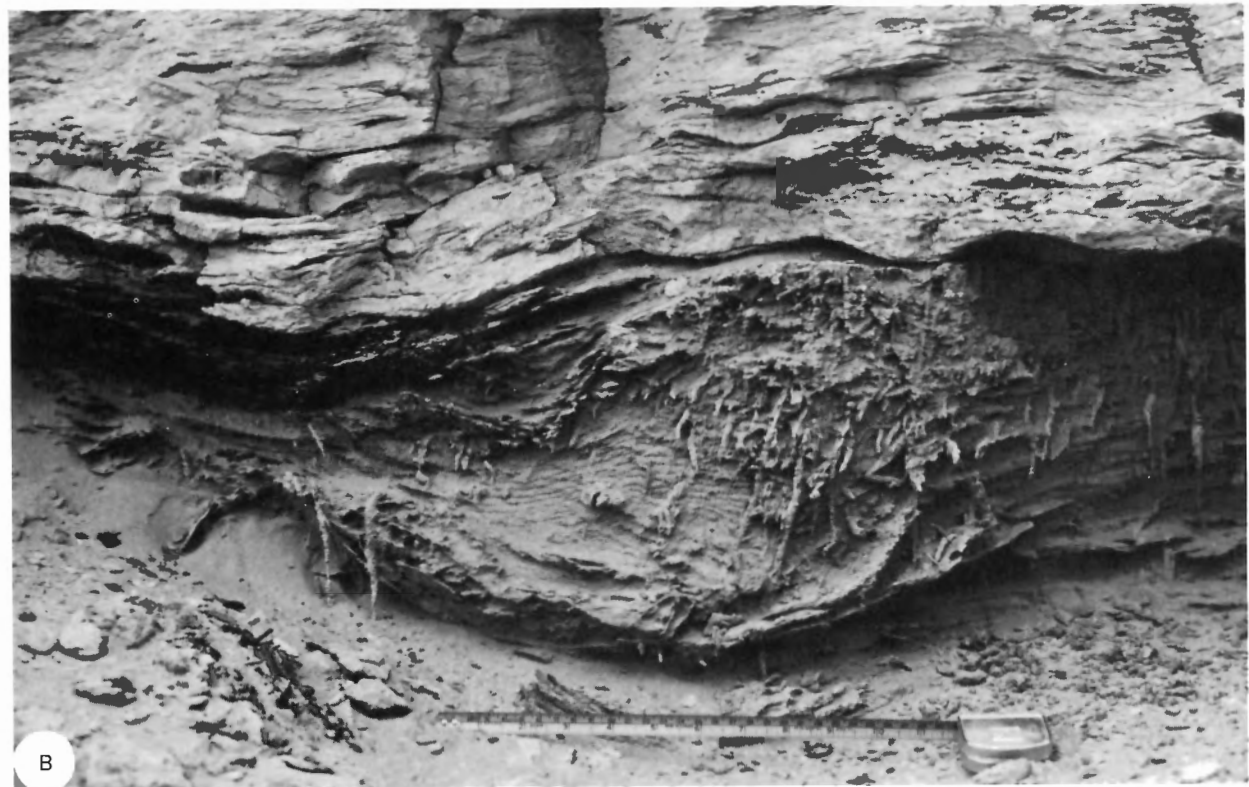


Plate 34. Plant and lignite remains, Cyclic Member, Eureka Sound Formation. A: Sand with roots, followed directly by shale, Eames River (Station 73-MLA-37). GSC 199182. B: Sand with roots and an erosional remnant of a lignite bed (*left*) overlain by shale, Eames River (Station 73-MLA-38). GSC 199179.

large trees became established as is indicated by the presence of petrified trunks and stumps (Pl. 14B).

In some instances, the sand of facies C is followed abruptly by shale (facies A) and a new scale cycle is started. Erosional remnants of a lignite seam may (Pl. 34B) or may not (Pl. 34A) be present at the contact. In any event, the base of each cycle normally is abrupt and indicates a period of erosion. The interpretation of this feature is that sooner or later each distributary was abandoned and, at this point, subsidence due to compaction or to tectonic basin sinking began to exceed the rate of sediment buildup. For a time marsh development and plant colonization may have occurred but sooner or later the sediment-water interface dropped to a point where wave erosion would have commenced and an erosion surface then developed. A new cycle would then begin, and eventually the new area of low topography would be ripe for the reception of sediment from a new crevasse or prograding distributary.

In a few places delta top-set deposits are preserved in the form of distributary channel sediments. These are characterized by medium- or large-scale planar crossbeds of structure assemblage 1 (Fig. 70, Pl. 29). They represent point bars or linguoid bars within distributary channels, and may have developed in part by lateral accretion. A further examination of these structures is presented in the discussion on paleocurrent analysis.

Examination of logs in the wells of western Banks Island indicates that much of the upper part of the Cyclic Member may consist of coarse (proximal) delta top-set deposits.

Noncyclic units

Between 17 and 100 per cent of the section at each surface exposure consists of units that cannot be fitted conveniently into a coarsening-upward cycle sequence. This by no means damages the validity of the deltaic model. Many of the beds probably comprise coarsening-upward cycles smaller in scale than the level of field observation. Others comprise parts of cycles that were not completed because of a random event such as a flood or channel avulsion, causing major changes in the distributary pattern (Elliott, 1974, p. 620).

Regional variability in small-scale cycles

As shown in Figure 63, cycle thickness varies from one region to another in the subsurface. In the exposures in Northern Banks Basin there is a weak and statistically nonsignificant tendency for cycles to be thicker in the Eocene (Table 26) but no trends are detectable when the data are shown in map form (Fig. 67).

All these results, shown together in Figure 71, demonstrate that on a broader, regional scale the small-scale cycles do show noticeable lateral thickness variations. Figure 71 also shows the zero Bouguer gravity contour and the map is patterned to emphasize gravity highs and lows. Thickness contours can be drawn parallel to the gravity lines, suggesting that cycle thickness varies with position within the depositional basins (thicker cycles occurring nearer the centre of the basins). It should be emphasized that, because of the paucity of data points, the map could be contoured in other ways, and so the interpretation shown should be regarded as suggestive only.

Read and Dean (1975) have shown that in seven differ-

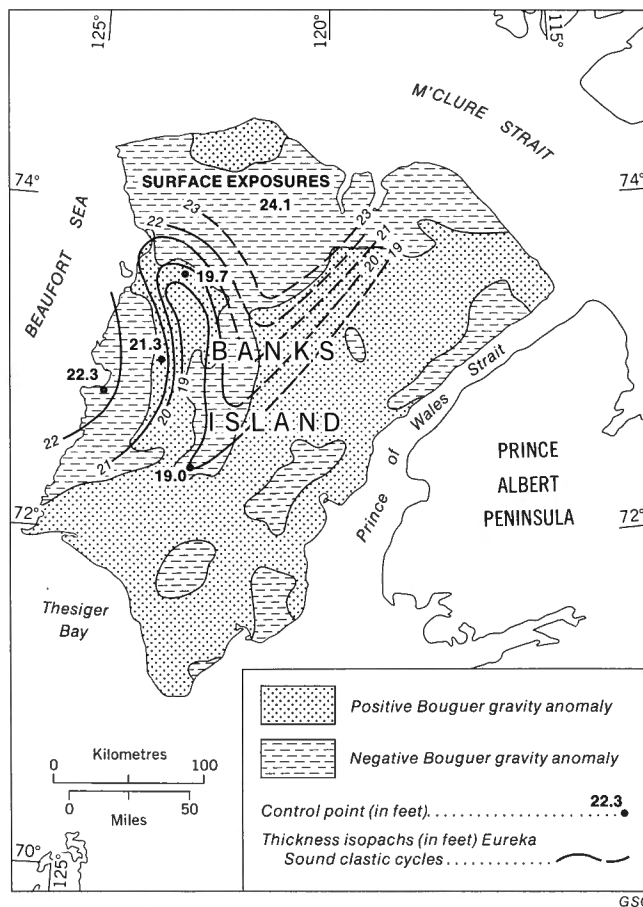


Figure 71. Regional variations in clastic cycle thickness in the Cyclic Member of the Eureka Sound Formation. Data points derived from amplitude spectra, as shown in Figure 63.

ent Carboniferous coal-bearing successions in the United Kingdom a close linear relationship exists between number of cycles and total thickness of strata in a given stratigraphic interval. Thus the number of cycles is proportional to the net subsidence of the basin. The relationship is given by

$$c = a + bt$$

where c = number of cycles, t = total thickness of strata (in metres) and a , b are coefficients. It is also the case that

$$c = t/T$$

where T = mean cycle thickness (in metres). Therefore, if a is zero, b should be equal to the reciprocal of the mean cycle thickness. This is not the case. In five of Read and Dean's examples, b is less than $1/T$ and a is greater than zero. For example, Read and Dean's data set D gives the following relationship:

$$c = 0.11t + 4.9$$

If $t = 300$, $c = 37.9$ and $T = 7.9$. If $t = 60$, $c = 11.5$ and $T = 5.2$. In other words, the mean cycle thickness increases as the thickness of the stratigraphic interval increases. This is similar to the result suggested by Fourier analysis of the Cyclic Member. Read and Dean (1967, Fig. 2B) showed the same result for some Namurian cycles in Scotland.

The delta model

The small-scale cycles discussed above represent the progradation of individual distributary mouths. At the Storkerson Bay A-15 and Nanuk D-76 wells these cycles are superimposed on megacycles of much greater thickness (Fig. 8). At Storkerson Bay the cycles are 146, 112 and 141 m (480, 367 and 464 ft) thick (in stratigraphic order). At Nanuk D-76 three similar megacycles are present, with thicknesses of 89, 77 and 60 m (293, 252, 196 ft). These megacycles are considered to represent the progradation of delta lobes into Big River Basin. As with the small-scale cycles, vertical and lateral accretion gradually overtook subsidence and each lobe was eventually abandoned as the river distributaries switched into topographically lower areas. This event was followed by a period of predominantly fine-clastic sedimentation and a new megacycle commenced. Progradation may have begun earlier at Storkerson Bay than elsewhere within Big River Basin, as shown by the greater abundance of sand in the Shale Member here than in the other wells (Fig. 8).

The same process may be seen in a general way in the surface outcrops of the Cyclic Member. The westward progradation across Northern Banks Basin is shown by the fact that, at Castel Bay (east side of Northern Banks Basin) the base of the Cyclic Member is Paleocene in age, whereas at Cape Crozier the member is entirely Eocene (Table 1).

Further evidence of westward progradation is provided by the increase toward the west and up the succession of the sand/shale ratio (Fig. 65), sand bed thickness (Fig. 66), sand/shale ratio within the cycles (Fig. 68), and per cent of section that is cyclic (Fig. 69, Table 26). The position and shape of the deltaic lobes within this progradation is suggested by the distribution of sedimentary structure assemblages, as shown in Figure 70. (An important check on the validity of this pattern is provided by paleocurrent analysis, as discussed in the next section.) That such a pattern was obtained by sampling sections not closely age-equivalent suggests that the delta lobes must have retained the same overall position for a considerable time, indicating that rates of sedimentation and subsidence were in approximate balance (Curtis, 1970, p. 293-295). However, different parts of each lobe probably were active at different times, in much the same way that an alluvial fan is built up by as few as one distributary that slowly migrates over the entire fan surface. Plate 33B shows a rare example of an exposure where the intersection of two deltaic lobes is visible. The accretion surfaces are at different angles and their intersection has the appearance of an angular unconformity.

Paleocurrent analysis

A total of 254 sedimentary structures in the Eureka Sound Formation were measured to determine paleocurrent direction. They comprise 156 large-scale structures, mainly planar and trough crossbedding, and 98 small-scale structures, mainly ripple marks of various types. The data were collected at fourteen field stations, all but one located in Northern Banks Basin. Statistical data for the readings are given in Table 28 and current rose diagrams are shown in Figure 72. All the data have been weighted according to the method of the author (Miall, 1974e). In two cases data from more than one

station have been grouped because of geographic proximity. The Nangmagvik Lake data (Stations 73-MLA-19, 20, 21) are shown in greater detail by the author (Miall, 1974e, Table 3).

Interpretation

Most of the paleocurrent distributions at individual field stations are unimodal; vector strength L is high, and the probability of randomness p is low. However, the indicated mean transport directions appear to show no consistent orientation (Table 28, Fig. 72). Field stations between Castel Bay and Eames River have yielded readings that fall within one or other of two main trends, northwest or southeast. This is perpendicular to the axis of Northern Banks Basin; it suggests that the basin was actively subsiding during the Paleogene and that sediment was transported into the basin from both sides.

A much more meaningful pattern emerges when the paleocurrent trends are considered in conjunction with the distribution of sedimentary structure assemblages, as shown in Figure 73. The apparently high paleocurrent variability is then seen to be the result of sedimentation within individual deltas that were formed by distributaries fanning out from the main trunk streams. This is clear particularly near Castel Bay, where the data suggest a lobate or birdsfoot outline for the delta. A north-trending distributary (or distributary system) built a lobe of the delta north along the west side of Castel Bay, as shown by the paleocurrent data at Station 74-43. At Nangmagvik Lake (Stations 73-19, 20, 21) the distributary system was oriented northwest and at Station 74-156, near the mouth of Thomsen River, a third lobe is suggested by paleocurrents oriented south-southeast.

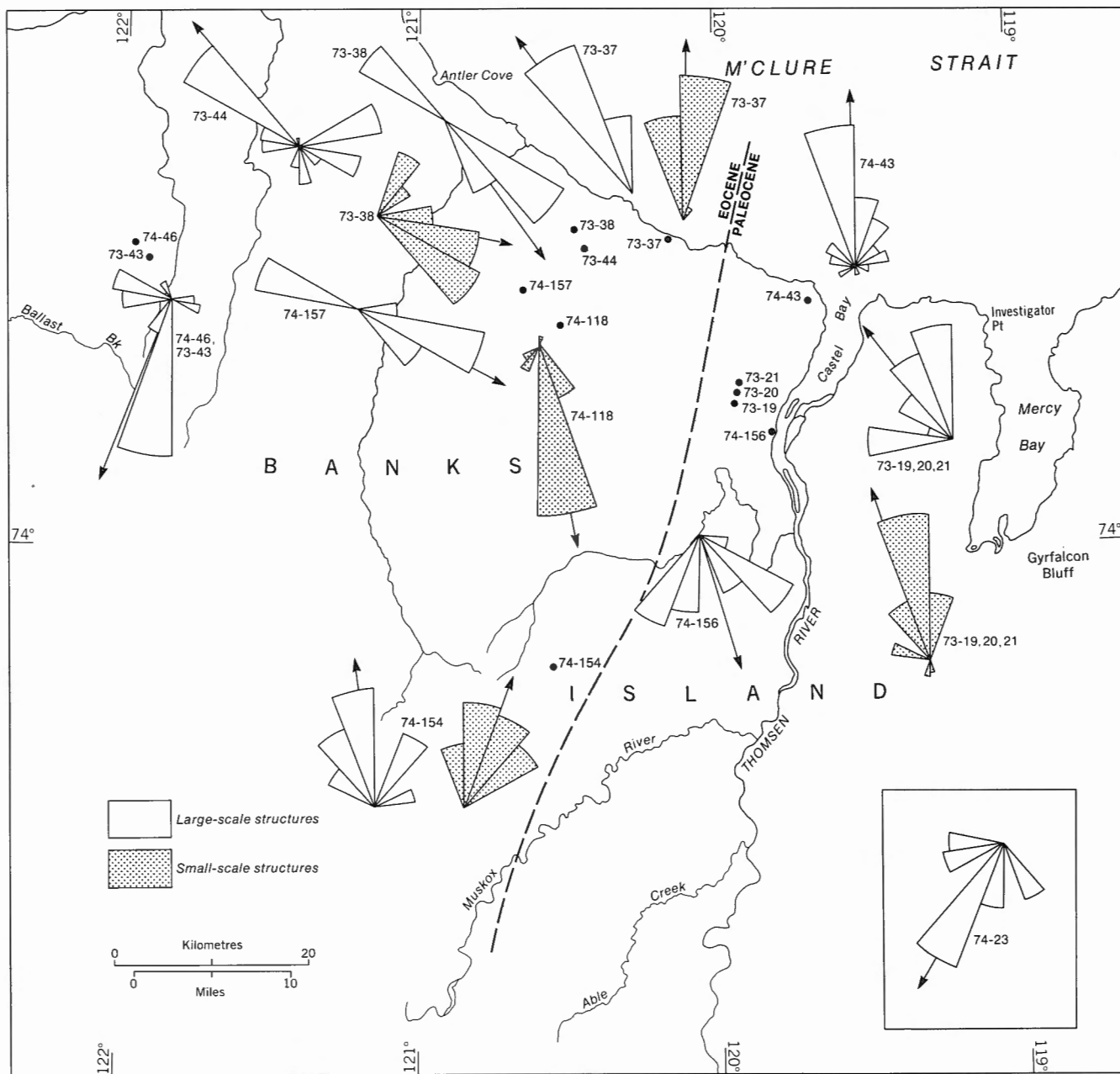
The Thomsen River and Nangmagvik Lake field locations are situated within a zone characterized by high-energy structures (assemblage 1). These are interpreted as the product

Table 28. Paleocurrent data, Eureka Sound Formation

STATION NUMBER (MLA)	STATION NAME	STRUCTURE TYPE	n	$\bar{\theta}$	L	p
73-19, 20, 21	Nangmagvik Lake	$\alpha \epsilon \theta \pi$	36	323	86	$<10^{-11}$
73-19, 20, 21	Nangmagvik Lake	κ	24	342	94	$<10^{-9}$
73-37	Eames River	θ	3	325	99	0.053*
73-37	Eames River	κ	10	002	99	$<10^{-4}$
73-38	Eames River	α	5	145	42	0.409*
73-38	Eames River	κ	22	103	84	$<10^{-6}$
73-43, 74-46	Log River	$\alpha \theta$	21	202	78	$<10^{-5}$
73-44	Eames River	$\alpha \theta$	27	320	34	0.043
74-23	Masik River	α	8	210	87	0.003
74-43	Castel Bay	$\alpha \theta$	26	359	92	$<10^{-9}$
74-118	Eames River	κ	15	169	98	$<10^{-6}$
74-154	Muskox River	$\alpha \theta$	10	353	89	$<10^{-3}$
74-154	Muskox River	κ	27	020	94	$<10^{-10}$
74-156	Thomsen River	$\alpha \theta$	14	164	85	$<10^{-4}$
74-157	Eames River	α	6	117	37	0.439*

GSC

Number of observations n
 Weighted mean azimuth (Miall, 1974e) $\bar{\theta}$
 Vector magnitude (per cent) L
 Probability of directional randomness (Rayleigh test) p
 Mean azimuth not significant at 95% confidence level *
 Greek-letter structure names assigned by Allen, 1963 $\alpha, \epsilon, \theta, \kappa, \pi$



GSC

Figure 72. Paleocurrent rose diagrams, Eureka Sound Formation. Station 74-23 is located in southern Banks Island (see Fig. 2).

of distributary channel and crevasse splay deposition in the delta plain environment. A high sinuosity (meandering) channel at Station 74-156 is suggested by an unusually large scale planar crossbed set (Pl. 29A), which is interpreted to be epsilon crossbedding, in the terminology of Allen (1963). The set is 4 m (13 ft) thick, has a foreset dip of 15 degrees and a foreset orientation of 270 degrees (due west). The westerly foreset orientation is perpendicular to the mean paleocurrent trend. This structure is considered to be a point bar deposit built by lateral accretion on the inside of a channel meander. The term epsilon crossbedding is confined now to very large scale crossbeds which show foreset orientation at steep angles

to the mean transport direction, and which are stated to be formed only in point bar deposits (Allen, 1970b; Miall, 1974e). But such structures are, in fact, rare in ancient rocks (Allen, 1970b; Leeder, 1973).

Three other deltas are indicated by the distribution of sedimentary structure assemblages (Fig. 70). A westerly-prograding system is present near Muskox River. The outline of the delta probably is more complex than that shown but field stations are insufficient for a more precise definition. A northward-oriented lobe is indicated by paleocurrent data at Station 74-154. The source stream presumably originated in the craton.

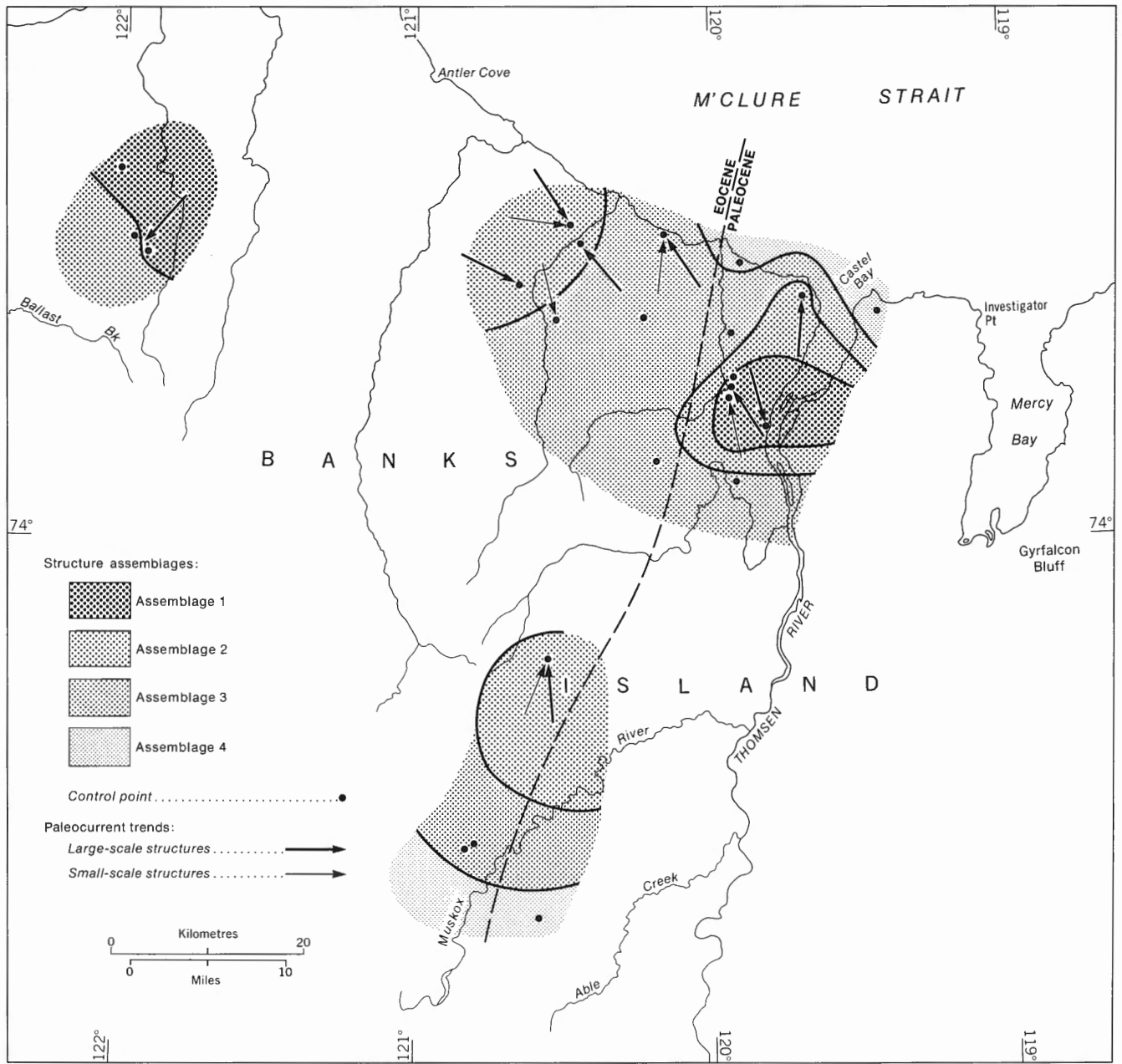


Figure 73. Sedimentary structure assemblages and paleocurrent trends, Eureka Sound Formation.

At Eames River a southeasterly-directed delta is suggested both by structure assemblages (Fig. 70) and paleocurrent trends (Figs. 72, 73). The rocks in this area are Eocene in age and, therefore, the delta may postdate entirely the deltas on the east side of the basin.

The bimodal paleocurrent patterns at Stations 73-38, 73-44 and 74-157 may reflect the influence of marine (wave, tide) currents in reworking the sediment. It is noteworthy that the one occurrence of the marine trace fossil *Ophiomorpha* is located in the same area (Station 73-37). The westward-directed modes at Stations 73-38 and 74-157 are represented by only one reading each. Probably contemporaneous with the

Eames River delta is a fourth example at Log River, which built out in a southward direction. Both reflect uplift along Cape Crozier Anticline.

Not shown in the illustrations are the data from near Masik River in southern Banks Island (Station 74-23). The mean current direction is south-southwest, but the field station may be situated on the south side of a delta showing a general westward progradation.

In summary, paleocurrent trends provide evidence of delta progradation westward from the craton commencing during the Paleocene, and south and east from Cape Crozier Anticline (Prince Patrick Uplift) in the Eocene.

Grain size analysis

Fourteen samples from the Cyclic Member were analyzed by sonic sifter (Table 29). Some of these samples contain a significant percentage of silt and clay grade material (up to 34% in the sample from GSC loc. C-30600) but this has not been analyzed beyond the limits of the sifter, which is 4.5 ϕ (coarse silt). The higher moment measures, in particular skewness and kurtosis, are strongly affected by the tails of the distribution. Therefore, although they are given in Table 29, they are not discussed in this section.

All the samples from the northern Banks Island are very fine grained sand. Those from the southern part of the island range up to medium grained.

Table 29. Grain size data, Cyclic Member, Eureka Sound Formation

MLA STATION NO.	GSC LOC. NO.	PHI MEAN	MEAN (mm)	PHI VAR.	PHI STD. DEV.	PHI SKEW.	PHI KURT.
74-20	C-30504	2.0513	.2413	.3881	.6230	0.6063	3.6984
74-21	C-30508	3.6840	.0778	.3384	.5817	-1.1863	10.3351
74-22	C-30511	1.9412	.2604	.8187	.9048	0.2355	1.1204
74-23	C-30514	2.9451	.1299	.3293	.5739	0.2069	1.4565
74-39	C-30543	3.7644	.0736	.1593	.3991	-0.2359	4.0849
74-45	C-30560	3.1259	.1146	.1950	.4416	0.1877	2.7212
74-46	C-30561	3.5727	.0840	.3200	.5657	-0.2843	3.4046
74-113	C-30600	3.8812	.0679	.3643	.6036	-1.0884	7.6126
74-115	C-30605	3.7649	.0736	.3281	.5728	-1.0743	9.6287
74-116	C-30607	3.2976	.1017	.4547	.6743	0.0180	1.1877
74-118	C-30609	3.4363	.0924	.2459	.4959	-0.5886	7.8338
74-148	C-30636	2.2607	.2087	.2381	.4879	0.7558	5.5040
74-150	C-30639	3.1869	.1098	.2340	.4837	0.2003	2.7890
74-154	C-30644	3.7648	.0736	.5682	.7538	-0.9785	5.4739

GSC

Interpretation

Three typical grain size curves are shown in Figure 74. Many of the other samples show curves similar to the sample from GSC loc. C-30560. The distributions are similar to those of the Isachsen Formation, particularly those at Station 73-MLA-26 (Figs. 31, 32), although the Eureka Sound curves are shifted to the right, reflecting the finer grain size of the younger unit. It should be pointed out also that the Eureka Sound curves are similar to those of the Hassel Formation (Fig. 54), in terms of both curve shape and size distribution. The similarities are the result of similar depositional environments or similar sediment sources.

The Eureka Sound sands are mainly distributary mouth bars or crevasse splay deposits and the curve shapes compare with the distributary channel and mouth bar samples analyzed by Visser (1969, Fig. 11) and Glaister and Nelson (1974, Fig. 8). The main difference is a higher degree of sorting exhibited by the central portions of the Eureka Sound curves than in the curves shown by the authors quoted. The higher degree of sorting may be a reflection of the grain size distribution of the sand from which the Eureka Sound was derived. As discussed in the next section, most of the Eureka Sound sand probably represents reworked Middle and Upper Devonian sediments. The same is true of the Hassel Formation and, therefore, both sand units tend to show similar grain size distributions although deposited under very different environmental conditions.

Because insufficient samples were collected a complete

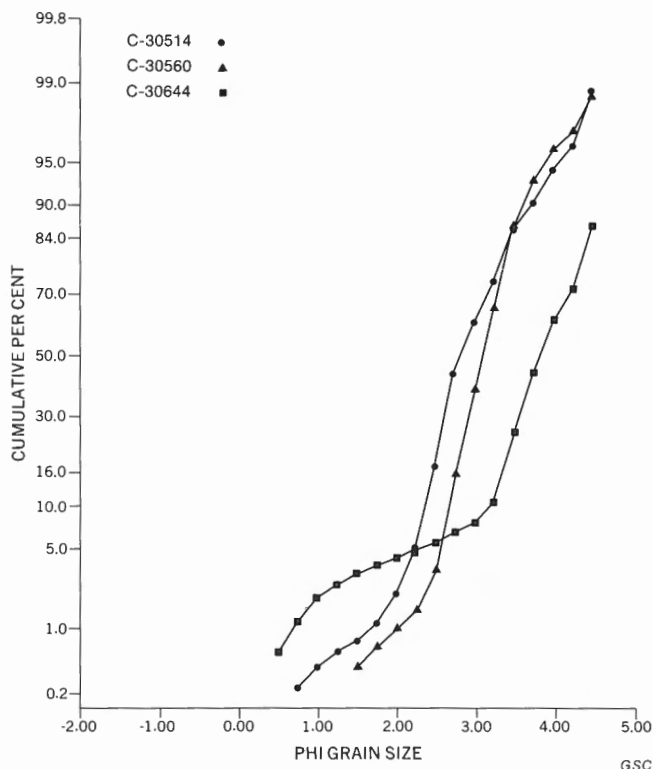


Figure 74. Grain size distribution curves, sand from the Eureka Sound Formation.

study of regional grain size variations could not be carried out. Since local depositional environments and energy level varied greatly during Eureka Sound sedimentation, a large sampling would be necessary for such a study. The coarser grained sands, for example from GSC loc. C-30514, tend to occur, as would be expected, in beds characterized by large-scale sedimentary structures, particularly planar crossbedding (structure assemblage 1). The sections with few structures (structure assemblage 4) contain sand beds that are very fine grained and silty. Coarse, pebbly beds are present only in southern Banks Island and in the subsurface of the western part of the island.

Petrographic analysis

Point count analyses were performed on 42 thin sections of arenaceous rocks from the Eureka Sound Formation. Results are given in Table 30. In addition, Table 31 gives clast counts of five pebble beds.

Description of clast types

Pebbles and cobbles. Clasts coarser than sand grade are found only in the Nelson Head area and in the three wells near Storkerson Uplift. At Nelson Head, locally, they reach 12 cm (4.7 in.) in diameter. Quartz sandstone and quartzite in the pebble beds in this area probably were derived from the Glenelg Formation (Proterozoic), which crops out immediately to the south of the Eureka Sound exposures (Miall, 1976a). Silicified carbonate sediments similar to those occurring in the Isachsen Formation are common as clasts in the Nelson Head area, as are medium grey to black varieties of chert. Both the

Table 30. Petrographic analyses of sand and sandstone from the Eureka Sound Formation

STATION OR WELL	C. NO. OR DEPTH (FT)	PER CENT CLASTIC GRAINS												PER CENT ALL POINTS					PER CENT			ROCK TYPE (follows classification of Okada, 1971)			
		QUARTZ	CHERT	SANDSTONE	K-FELDSPAR	PLAGIOCLASE	MUSCOVITE	BIOTITE	GLAUCONITE	PLANT DEBRIS	DETRITAL LS/DOL	SHALE, CLAY	DETRITAL FE OX	TUFF, PUMICE	MICROFOSSILS	POROSITY	QUARTZ CEMENT	CARB. CEMENT	CLAY MATRIX	FE OX MATRIX	QUARTZ			ROCK FRAGMENTS	FELDSPAR
73-7	33358	66	20	-	6	2	1	T	T	4	T	2	-	-	-	-	-	69	-	-	67.9	23.9	8.2	LTHC	AREN
73-19	33315	42	16	1	3	R	1	1	-	1	-	15	5	14	T	-	-	-	-	41.8	55.4	2.8	LTHC	AREN	
73-19	33316	61	13	-	3	1	2	T	-	-	-	15	5	-	-	-	-	-	-	61.2	34.7	4.1	LTHC	AREN	
73-20	33317	34	49	-	5	R	1	T	-	-	-	7	5	-	-	-	-	-	-	33.7	61.2	5.1	LTHC	AREN	
73-37	33349	69	17	-	4	T	T	-	-	-	-	7	2	-	-	-	-	-	-	69.3	26.8	3.9	LTHC	AREN	
73-38	33350	64	18	-	3	R	T	-	-	-	-	11	3	-	-	-	-	-	-	64.2	32.0	3.8	LTHC	AREN	
73-39	33351	41	46	-	9	T	R	-	-	-	-	4	R	-	-	-	-	-	-	41.2	49.7	9.1	LTHC	AREN	
73-40	33352	63	24	-	4	-	-	-	-	-	-	6	2	-	-	-	-	-	-	63.4	32.5	4.1	LTHC	AREN	
73-43	33354	51	31	2	4	R	R	-	1	-	-	8	3	T	-	-	-	-	-	51.2	44.9	3.9	LTHC	AREN	
73-43	33354	46	33	2	3	1	-	T	1	-	-	11	4	T	-	-	-	-	-	45.9	50.1	4.0	LTHC	AREN	
73-44	33355	43	32	1	8	2	R	-	T	-	-	8	6	-	-	-	-	-	-	43.0	47.2	9.7	LTHC	AREN	
74-20	30504	60	11	3	2	T	-	-	-	R	6	17	2	-	-	-	-	-	-	60.1	38.2	1.7	LTHC	AREN	
74-21	30508	58	10	-	8	1	-	-	-	-	-	24	T	-	-	-	-	-	-	57.4	33.3	9.3	LTHC	AREN	
74-22	30511	66	18	-	1	T	-	-	-	-	3	9	3	-	-	-	-	-	-	65.7	33.2	1.1	LTHC	AREN	
74-23	30514	43	5	-	1	R	-	-	-	-	44	5	1	-	-	-	-	-	-	42.9	55.4	1.7	LTHC	AREN	
74-39	30543	83	1	-	10	1	T	T	-	-	-	4	2	-	-	-	-	-	-	82.6	6.9	10.5	QTZS	AREN	
74-43	30550	40	31	2	6	T	R	T	-	-	-	15	5	-	-	-	-	-	-	40.3	53.2	6.5	LTHC	AREN	
74-45	30560	47	12	2	3	1	-	-	-	-	-	30	5	T	-	-	-	-	-	47.3	49.0	3.7	LTHC	AREN	
74-46	30561	63	4	-	2	T	T	T	-	1	-	23	2	5	T	-	-	-	-	62.7	34.9	2.4	LTHC	AREN	
74-46	30561	43	18	-	4	T	T	-	-	3	-	18	1	12	T	-	-	-	-	42.8	53.1	4.1	LTHC	AREN	
74-113	30600	67	5	-	1	T	T	-	T	-	-	25	2	T	-	-	-	-	-	67.1	31.5	1.4	LTHC	AREN	
74-115	30605	58	5	-	3	2	T	-	T	-	1	30	2	T	-	-	-	-	-	58.2	37.6	4.2	LTHC	AREN	
74-115	30606	60	18	-	1	1	R	-	-	-	-	5	16	-	-	-	-	-	13	59.6	38.4	2.0	LTHC	AREN	
74-116	30607	52	12	-	7	T	-	R	-	-	-	28	1	-	-	-	-	-	-	51.6	41.7	6.7	LTHC	AREN	
74-118	30609	63	8	-	3	R	R	R	-	-	-	22	2	-	-	-	-	-	-	62.8	34.3	2.9	LTHC	AREN	
74-127	30617	43	25	1	2	1	-	T	-	-	-	20	8	-	-	-	-	-	21	42.7	54.4	2.9	LTHC	WACK	
74-148	30636	52	27	-	3	-	-	-	-	-	-	10	8	-	-	-	-	-	-	51.7	45.7	2.6	LTHC	AREN	
74-149	30638	56	34	1	3	T	-	-	-	-	-	1	4	-	-	-	-	-	-	56.4	40.6	3.0	LTHC	AREN	
74-150	30639	86	12	-	1	-	-	-	-	-	-	R	R	-	-	-	-	-	-	86.2	13.0	.8	QTZS	AREN	
74-154	30644	66	16	-	2	-	R	T	-	-	-	12	3	-	-	-	-	-	-	66.0	31.6	2.4	LTHC	AREN	
GAS-43	30816	73	17	-	2	R	T	1	T	-	-	6	1	-	-	-	-	-	-	72.6	25.1	2.3	LTHC	AREN	
GAS-43	30819	32	54	3	2	-	R	-	-	-	-	3	6	-	-	-	-	-	-	32.0	66.1	1.9	LTHC	AREN	
STKSON	(1130)	41	52	2	4	-	-	-	-	1	-	-	R	-	-	-	-	-	-	40.6	55.8	3.6	LTHC	AREN	
STKSON	(1350)	56	41	-	1	-	-	-	-	T	-	R	2	-	-	-	-	-	-	55.5	43.7	.8	LTHC	AREN	
STKSON	(1630)	46	53	-	R	-	-	-	-	T	-	R	-	-	-	-	-	-	-	46.0	53.6	.4	LTHC	AREN	
STKSON	(1770)	41	56	-	1	-	-	-	-	-	-	-	2	-	-	-	-	-	-	40.9	58.3	.8	LTHC	AREN	
NANUK	(845)	36	58	T	1	T	-	-	-	T	-	-	4	-	-	-	-	-	-	36.4	62.7	.9	LTHC	AREN	
NANUK	(955)	46	49	R	1	-	-	-	-	T	-	-	3	-	-	-	-	-	-	46.2	52.4	1.4	LTHC	AREN	
NANUK	(1025)	37	59	-	1	-	-	-	-	-	-	1	2	-	-	-	-	-	-	37.2	61.7	1.1	LTHC	AREN	
UMINMAK	(830)	60	27	-	3	-	-	-	T	-	-	9	1	-	-	-	-	-	-	60.3	36.9	2.8	LTHC	AREN	
ORKSUT	(1880)	20	2	-	T	T	-	-	-	39	-	10	4	23	2	-	-	-	-	34.5	65.1	.3	LTHC	WACK	
TRTCHK	(1280)	93	4	-	3	T	T	-	-	-	-	-	T	-	-	-	-	-	-	92.5	4.2	3.3	QTZS	AREN	

Less than 1%.....R Trace quantities.....T Quartz.....QTZ Quartzose.....QTZS GSC
Lithic.....LTHC Arenite.....AREN Wacke.....WACK

silicified carbonates and the chert could have been derived from the Proterozoic rocks of Minto Uplift or the Paleozoic rocks of Prince Albert Homocline. Insufficient information is available concerning the sedimentology of either of these groups of rocks to allow more precise source determinations. Shale clasts and quartz (probably of vein origin) are abundant locally. Igneous rocks, including gabbro and pink granite, are rare and were identified only in the outcrops near Nelson Head. Gabbro clasts were presumably derived from the sills and dykes which intrude the Shaler Group. Granite clasts are unusual, none having been identified in any other sedimentary unit in the report-area. Possibly they were derived from a conglomerate in the Proterozoic rocks, although no such clast types are recorded from these rocks in Victoria Island (Thorsteinsson and Tozer, 1962; G.M. Young, 1974).

Sand. Quartz constitutes between 20 and 93 per cent of the Eureka Sound sand units. Most grains are fine or very fine grained, monocrystalline, angular to subrounded (Pl. 35A). Authigenic overgrowths are rare but have been observed in a few samples (e.g., GSC locs. C-30606, C-30609). Both strained and unstrained varieties are present, but no attempt has been made to quantify the distribution. Many samples contain polycrystalline grains in trace amounts; in some (e.g., GSC locs. C-30504, C-30511) a foliated variety indicates a metamorphic origin. Several samples from southern Banks Island (GSC locs. C-30504, C-30511) consist predominantly of fine to coarse sand reminiscent of the Isachsen Formation (Pl. 35B). Quartz grains commonly are well rounded and many show authigenic overgrowths. Pits and embayments are rare, however, in contrast to the Isachsen sands (Pl. 19A-D).

Table 31. Conglomerate clast types, Eureka Sound Formation

STATION OR WELL NAME	SECTION HEIGHT OR WELL DEPTH (in metres)							Maximum clast size (cm)	
		Granite	Gabbro	Silicified Limestone	Quartzite	Shale	Chert		Quartz
74-MLA-20	—	—	—	C	C	—	C	—	6
74-MLA-22	—	R	—	C	C	—	C	C	10
74-MLA-23	3	—	R	C	A	—	C	—	12
Storkerson	655	—	—	—	C	C	A	C	?
Uminmak	185	—	—	—	C	C	A	A	?

GSC

Abundant A Common C Rare R

Grains of this type are present in trace amounts in several samples of fine-grained sand (e.g., GSC loc. C-30600), giving rise to a strongly bimodal size distribution. A similar texture observed in some of the sand samples from the Kanguk Formation is illustrated in Plate 28B.

Rare quartz types include zoned quartz (Storkerson Bay A-15, 1350 ft), quartz with inclusions of zircon (Storkerson Bay A-15, 1130 ft) and intergrowths of quartz with feldspar or mica (GSC locs. C-30560, C-33349, Storkerson Bay A-15, 1130 and 1350 ft).

Chert grains are similar to those in the other Cretaceous and Tertiary units. They vary from pale to dark grey to grey-brown (Pl. 35C). Chert grains with small spherical structures, of oolitic or radiolarian origin, are present in trace amounts, particularly in Big River Basin (Nanuk D-76, 845, 955 and 1025 ft; Storkerson Bay A-15, 1130 and 1770 ft, GSC loc. C-30550). A similar example from the Isachsen Formation is illustrated in Plate 22B. Many grains are penetrated by veinlets of quartz.

Feldspars are of various types, including orthoclase, microcline and plagioclase. Measurements on extinction angles of albite twins (Kerr, 1959, p. 258) show that most plagioclase grains probably are andesine or oligoclase.

Sedimentary rock fragments abound in the Eureka Sound Formation. Almost every sample contains shale or claystone clasts, except some from Big River Basin. They vary from structureless to bedded or foliated. One sample (GSC loc. C-33354) has a fragment of folded shale. Sandstone clasts are in several samples, always as a minor constituent. Detrital carbonate grains are present mainly in samples from southern Banks Island.

Volcanic rock fragments are abundant locally. Most are angular glass shards with the shape of fractured lava bubbles (Pl. 35D). A few larger fragments (pumice) are present, notably in samples from GSC loc. C-30561 and Orksut I-44 (1880 ft). Commonly associated with volcanic fragments are sponge spicules. These are similar to those in the Kanguk Formation (Pl. 28A). They are cylindrical, siliceous fragments with a central canal. In rare cases, triaxial junctions are preserved.

Six samples contain trace amounts of glauconite (Table 30), probably detrital in origin. In two other samples, both from GSC loc. C-33354, glauconite constitutes approximately 1 per cent of the sample. It may or may not be authigenic.

Iron oxides are similar to those in the other units described in this report. Many are dark brown, semiopaque and amorphous. They probably represent degraded ferromagnesian minerals. One grain in a sample from GSC loc. C-30617 is veined and is reminiscent of serpentinized olivine. Other grains are black and opaque and include magnetite and/or ilmenite.

Other detrital species are listed in Table 30.

Heavy minerals. The most widely distributed minerals are magnetite, epidote and rutile. All are fractured or subhedral grains showing little evidence of water wear. Cleavage faces are present on some magnetite grains but most are irregular in outline. Epidote grains are bottle-green or yellowish green and mostly irregular in shape. A few prismatic grains with ragged terminations have been observed. Rutile grains usually occur as fragments of euhedral prisms. One example (broken) of a geniculate twin also was observed.

Less common species are zircon, tourmaline, apatite, spessartite(?), kyanite, andalusite and sphene. The last two were observed only in one sample from Station 74-MLA-23 near Masik River (GSC loc. C-30514). Andalusite occurs as clear, transparent, colourless or slightly pinkish grains with irregular subrounded outlines. Sphene grains are dark brown and mostly irregular in shape but one example of the characteristic lozenge-shaped crystal form also is found in the sample. Zircon grains are yellowish and well rounded; tourmaline is a black variety; apatite and kyanite both occur as colourless prisms, the former often subrounded.

Metamorphic and basic igneous sources appear to have predominated in creating these assemblages. Kyanite, andalusite, spessartite and epidote indicate a metamorphic source and kyanite indicates high-rank metamorphism; rutile and magnetite are abundant in a wide variety of rock types. They may have been derived from the sills and dykes of Minto Uplift. Zircon, tourmaline, sphene and apatite generally are derived from acidic igneous sources, although the rareness of these species and the roundness of many of the grains indicate that they may all be second cycle or multicycle in origin.

Matrix and cement

Most of the Eureka Sound sands lack cement and all but traces of matrix, and are unconsolidated. One sample from the Shale Member (GSC loc. C-33358) contains 69 per cent cement, primarily ferroan dolomite. At each of two localities near the base of the Cyclic Member (Station 74-MLA-115, Castel Bay; Station 74-MLA-127, Woon River), a resistant sandstone unit 3 m and 6 m (10, 20 ft) thick, respectively, is exposed. The sandstone is cemented by up to 17 per cent clay minerals but retains a porosity as high as 21 per cent. Some of the subsurface samples also contain clay matrix or carbonate cement and are consolidated.

Texture

The unconsolidated sands are extremely porous and are assumed to be loosely packed. The two sandstone units referred to above both show these characteristics, although they contain more clay matrix than is typical in the Eureka Sound sand.

In the sandstone cemented by carbonate minerals, a detrital grain framework commonly is lacking. Some detrital

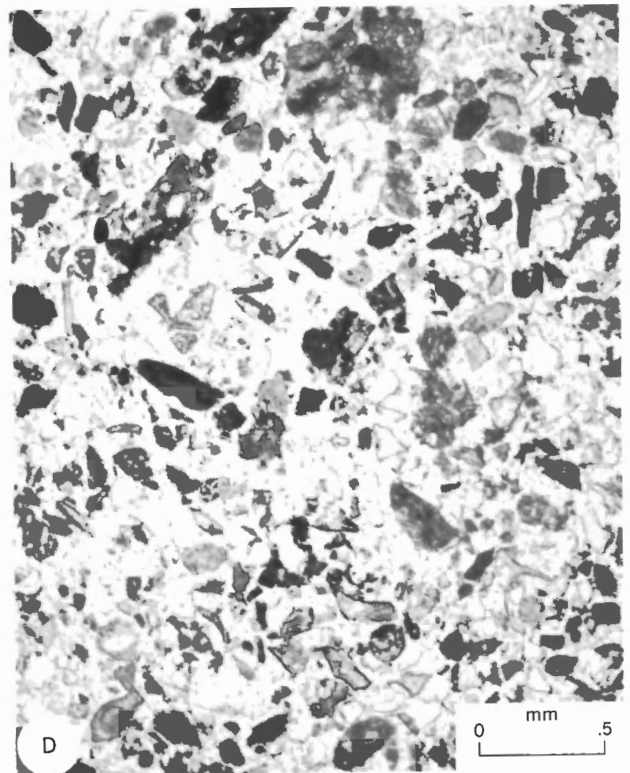
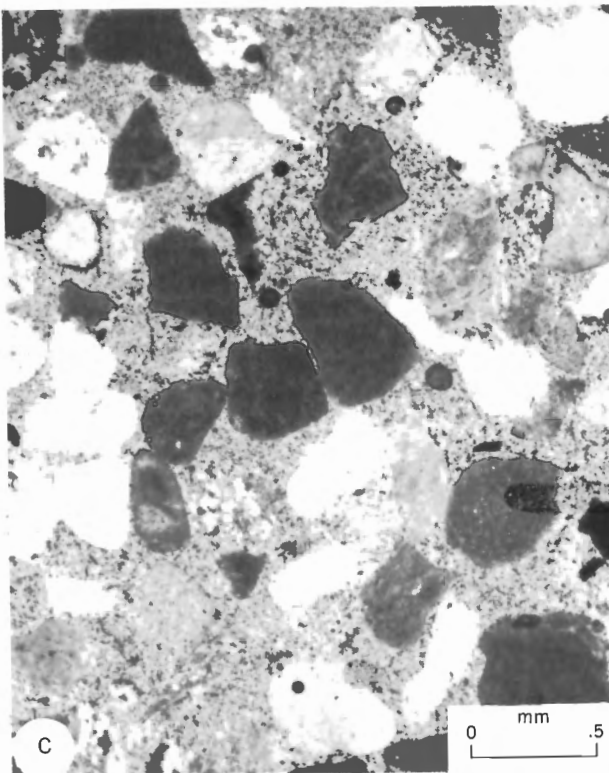
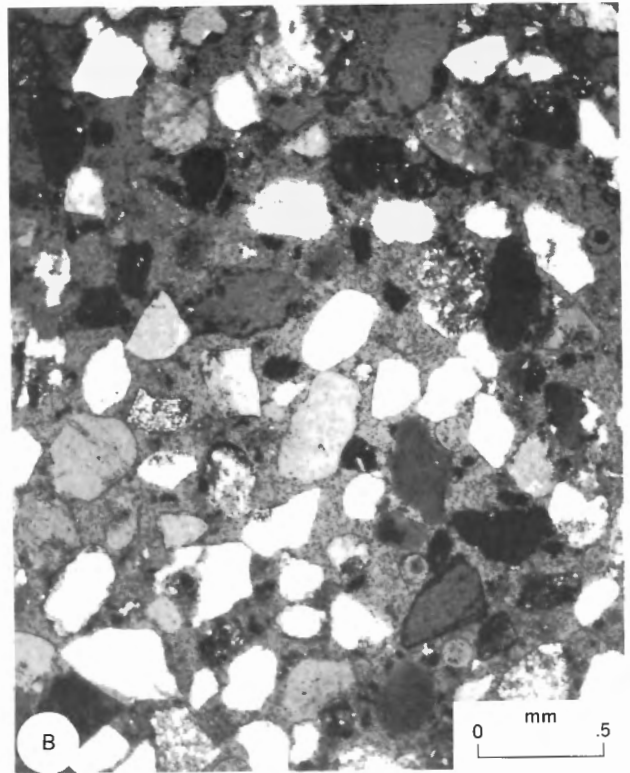
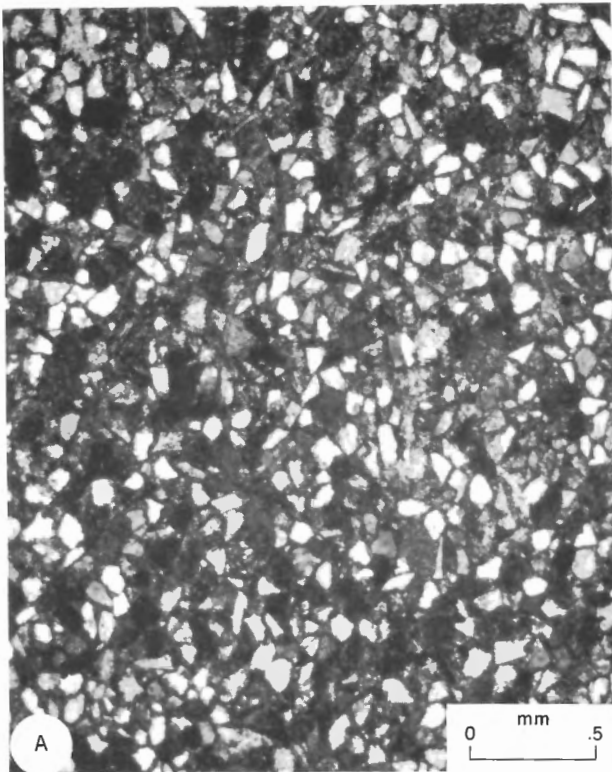


Plate 35. Photomicrographs of sand from the Eureka Sound Formation. A: Typical very fine grained sand, partially crossed polarizers. B: Medium-grained sand, with many quartz grains similar to those in the Isachsen Formation, partially crossed polarizers. C: Chert-rich sand, partially crossed polarizers. D: Fine-grained sand with abundant volcanic glass fragments, plane polarized light. (Sample glass numbers: A, C-30606; B, C-24069, 291 m (955 ft) depth; C, C-30504; D, C-33315.)

grains may have been replaced by the cement and others are partly replaced, as shown by ragged grain-cement contacts.

Quantitative analysis

Sand classification. The composition of the Eureka Sound Formation sand samples in terms of the three principal rock-forming components is shown in a ternary QRF plot, Figure 75. The arenite classification of Okada (1971) is superimposed on the plot. Two samples that contain more than 15 per cent detrital matrix, and are therefore wackes, are shown on the same plot for convenience. Three samples are quartzose arenites, 37 are lithic arenites.

In terms of the sand classification of Pettijohn *et al.* (1972, Fig. 5-3), the single sample with 92.5 per cent quartz (Tiritchik M-48, 1280 ft) is a quartz arenite, and the other two quartzose arenites of Figure 75 become a subarkose and sublitharenite. The lithic arenites all retain the same name in the Pettijohn *et al.* scheme.

Areal composition variations. The data points in Figure 75 are differentiated according to sample origin. Three geographically distinct regions have been defined: Northern Banks Basin; Big River Basin–Storkerson Uplift; and central and southern Banks Island, from Orksut I-44 southward. It can be seen that gross composition does not vary significantly from region to region, although a wide range of compositions exists in each region.

A Q-mode cluster analysis has been performed on the data given in Table 30. The analytical procedure followed is the same as that used for the Isachsen Formation, and the

reader is referred to the section on the sedimentology of that unit for the details. The cluster dendrogram is given in Figure 76, the composition of the clusters in Figure 77, and their areal distribution in Figure 78. The dendrogram has been divided into six clusters and these form the basis of the ensuing discussion.

Cluster 1 contains a relatively large percentage of rock fragments and a small percentage of quartz and feldspar. Examination of the data shows that the chert component is significantly large in these samples, and that most are from the vicinity of Storkerson Uplift.

Clusters 2, 3 and 4 are widely distributed throughout Banks Island. Cluster 2 is characterized by a large quartz content, cluster 3 by intermediate compositions in which sedimentary rock fragments (sandstone) are significant, and cluster 4 includes the samples with the largest feldspar content.

Clusters 5 and 6 are groups of dissimilar samples. They are confined to the northern and southern parts of the island, respectively, but the meaning of this trend is hard to interpret.

Associations of detrital components have been investigated using R-mode cluster analysis, the results of which are shown in Figure 79. The seventeen components can be grouped into seven assemblages. The first is an assemblage of dissimilarity because few samples contain the four components, commonly in trace amounts. The association between tuff and microfossils has been referred to earlier; the fossils are siliceous sponge spicules. Glauconite is a rare component and forms a cluster on its own. Cluster 4 represents an assemblage of mafic minerals comprising iron oxide, including

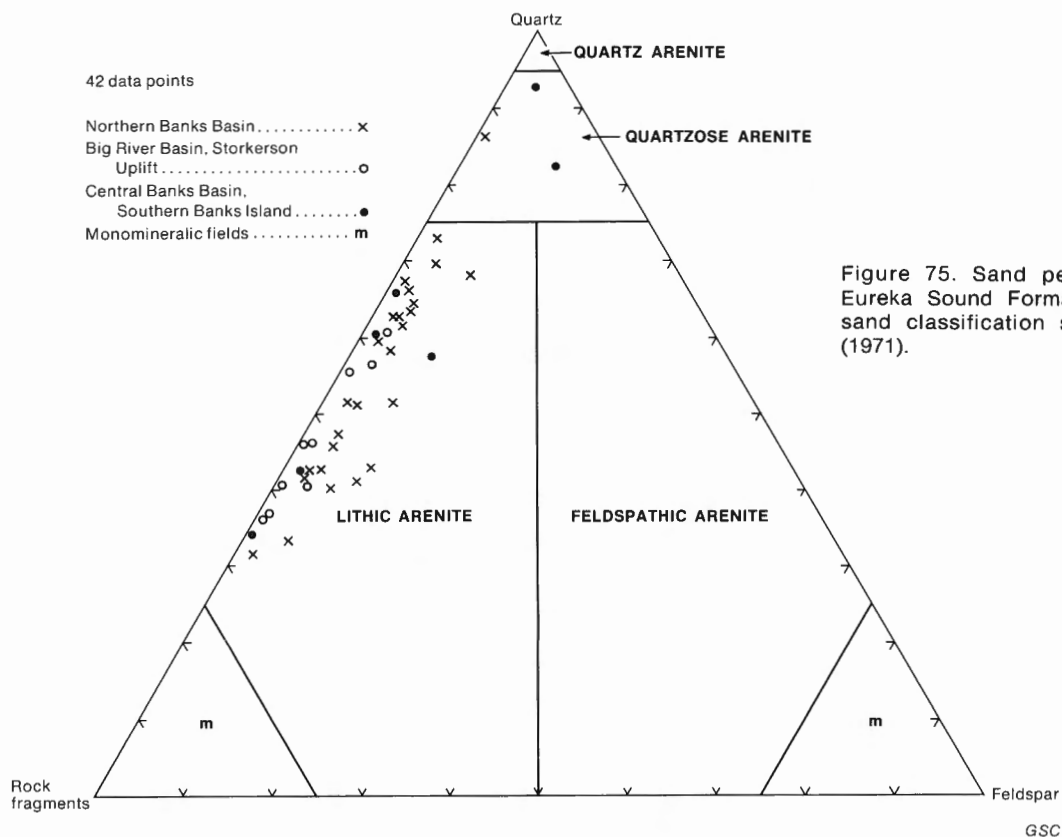


Figure 75. Sand petrography of the Eureka Sound Formation showing the sand classification scheme of Okada (1971).

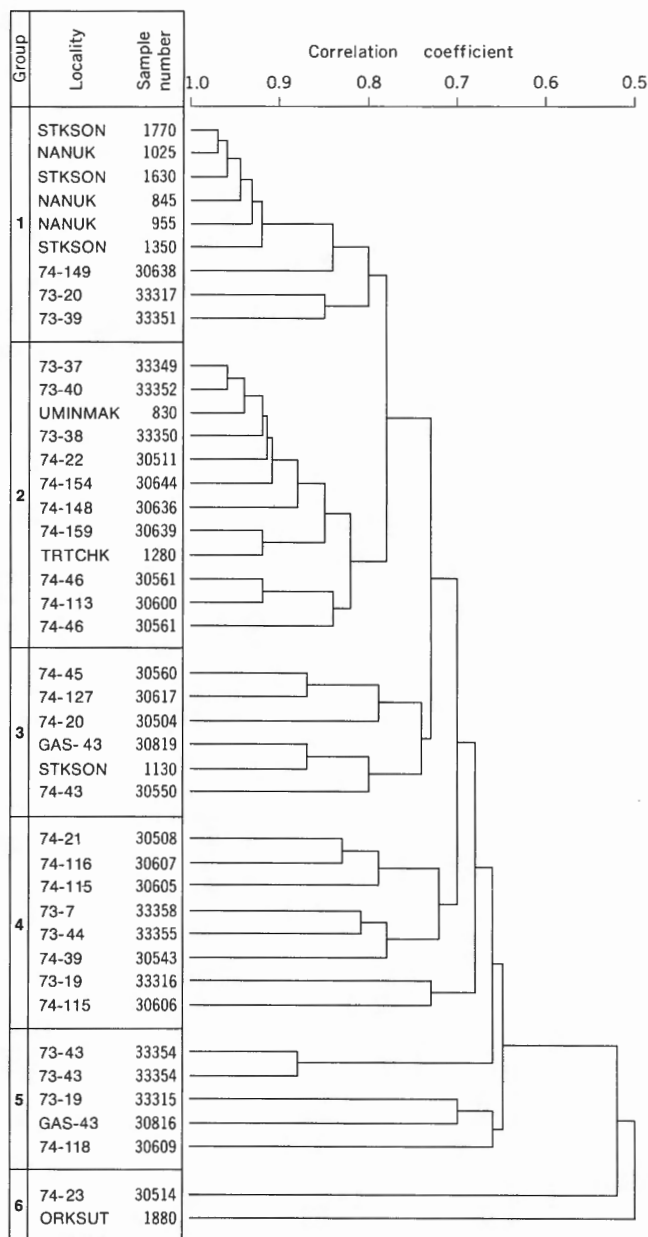


Figure 76. Q-mode cluster analysis of 42 samples from the Eureka Sound Formation. Data from Table 30.

magnetite/ilmenite and degraded ferromagnesian grains. Cluster 6 includes granitic rock fragments (quartz, feldspar), many of which probably are multicyclic in origin. Sandstone and chert are each seen to show distinctive distributions.

The distinctiveness of the chert distribution is emphasized by a ternary plot of three rock-forming components in which percentage compositions have been recalculated to total 100 per cent (Fig. 80). The largest chert content is shown by samples from Big River Basin and Storkerson Uplift. The remaining samples show a wide range of compositions and no other geographic trends are discernible.

Vertical composition variations. No composition changes can be demonstrated between older and younger parts of the Cyclic Member, in either the surface or the subsurface.

Sediment sources

Paleocurrent evidence shows that, along the eastern side of the Banks Basin, detritus in the Paleocene part of the Cyclic Member was derived from the craton to the east. The Eocene rocks of north-central Banks Island were derived at least in part from the north, from Prince Patrick Uplift. Petrographic evidence is consistent with these conclusions and it can be shown also that the Eureka Sound of the Big River Basin area was derived at least in part from the Storkerson Uplift.

The principal source rocks undoubtedly were Devonian sediments, in contrast with the Isachsen Formation, in which detritus from Devonian rocks is of minor importance. The very fine grain size and angularity of the quartz grains is consistent with derivation from the Melville Island Group, which itself consists predominantly of fine-grained to very fine grained quartzose sand (Miall, 1976a; Klován and Embry, 1971). The Melville Island crops out throughout northeastern Banks Island and at Cape M'Clure and Cape Crozier at the southern end of Prince Patrick Uplift. The outcrop area probably was larger during the Tertiary.

Chert probably was derived mainly from the Middle Devonian Nanuk Formation (Miall, 1976a). During Tertiary time it cropped out along Prince of Wales Strait (within the craton) and probably also over an extensive area on Storkerson Uplift. (In the Nanuk D-76 well, the Nanuk Formation occurs immediately below the Devonian-Cretaceous contact.) Chert content is highest in samples from Big River Basin. Chert with oolitic or radiolarian structures and spicular remains is found most abundantly in the same samples. Similar rocks are known from the Nanuk Formation. Storkerson Uplift, therefore, appears to have been an important source area for the Eureka Sound of the Big River Basin.

Rocks of Cambrian to Early Devonian age provided minor but locally significant quantities of detritus. Some chert may have been derived from the Ordovician-Silurian succession of Prince Albert Peninsula (map-unit 10b of Thorsteinson and Tozer, 1962). Detrital carbonate grains are abundant in three samples from southern Banks Island near the area where the Cretaceous-Tertiary succession probably rests directly on the lower Paleozoic rocks.

A few samples contain abundant fine to coarse quartz grains similar to those that form the bulk of the Isachsen Formation. They may possibly have been derived directly from the Isachsen, for that formation must have been exposed along the edge of the depositional basin. However, the samples in which this material is most abundant (GSC locs. C-30504, C-30511) are located in southern Banks Island where the Cretaceous-Tertiary succession rests directly on Proterozoic sedimentary rocks such as the Glenelg Formation and therefore these coarser Eureka Sound sands are assumed to have derived from the same Precambrian source. Rare gabbro pebbles at Station 74-MLA-23 and silicified carbonate rocks probably are derived from the Proterozoic rocks of Minto Uplift.

Nine samples from widely scattered parts of Banks Island contain tuff fragments—glass shards and pumice. It is important to note also that they are not necessarily present in all the samples from a given locality. This suggests that they were not derived by fluvial erosion of a volcanic source but reflect single volcanic episodes. However, there must have been more

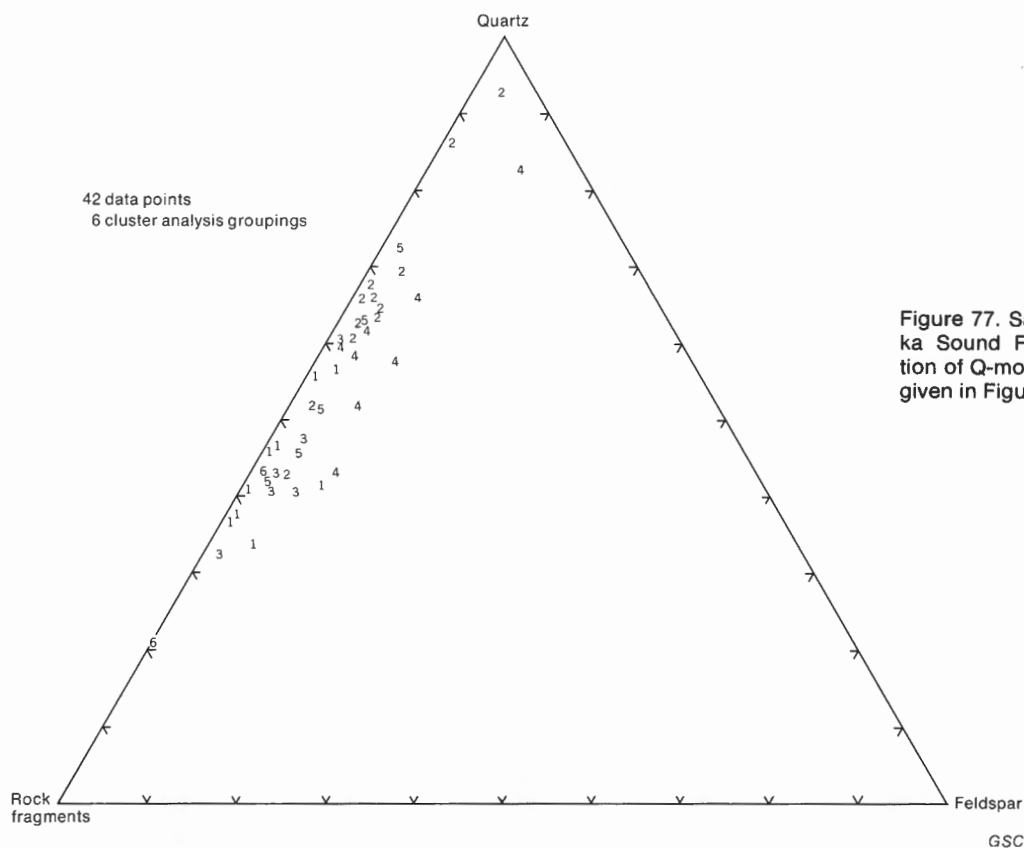


Figure 77. Sand petrography of the Eureka Sound Formation showing composition of Q-mode cluster analysis groupings given in Figure 76.

than one such episode and more than one resultant ash fall, since tuffaceous sands are present both in Paleocene and Eocene parts of the Cyclic Member. The origin of the material is uncertain. The only evidence of volcanism of approximately this age in the Arctic Islands is a single andesite flow in southeastern Bathurst Island (Kerr, 1974, p. 64). In Beaufort-Mackenzie Basin and northern Yukon, bentonitic and tuffaceous rocks are abundant in Tertiary sediments (F.G. Young and D.W. Myhr, *pers. com.*, 1974). The location of the volcanic source or sources is unknown. Fine-grained material can be transported by wind for many hundreds of kilometres but Scheidegger and Potter (1968) showed that material of medium sand grade is unlikely to be carried for more than 200 km (120 mi). Possibly a volcanic source lay offshore west of Banks Island. Tuff or ash beds have not been observed in the Eureka Sound Formation but as discrete beds their preservation potential in a fluvial and deltaic setting would be small.

Heavy minerals in the Cyclic Member probably were derived from several sources. Rutile and magnetite may be first-cycle derivatives of the sills and dykes of Minto Uplift. The origin of the extensive metamorphic suite consisting of kyanite, andalusite, spessartite and epidote is problematic. First-cycle derivation from the Canadian Shield is unlikely, as is second-cycle origin from the Shaler Group, because the evidence of the light minerals shows that quantitatively such sources are of minor importance. Possibly this suite originated in the Devonian clastic rocks. No information is available to

the writer regarding heavy minerals in the Melville Island Group but the sediments are known to have been derived from Pearya Geanticline and, also, probably from the Greenland Caledonides and the Greenland Shield, all of which contain metamorphic rock assemblages (Trettin *et al.*, 1972; Haller, 1971).

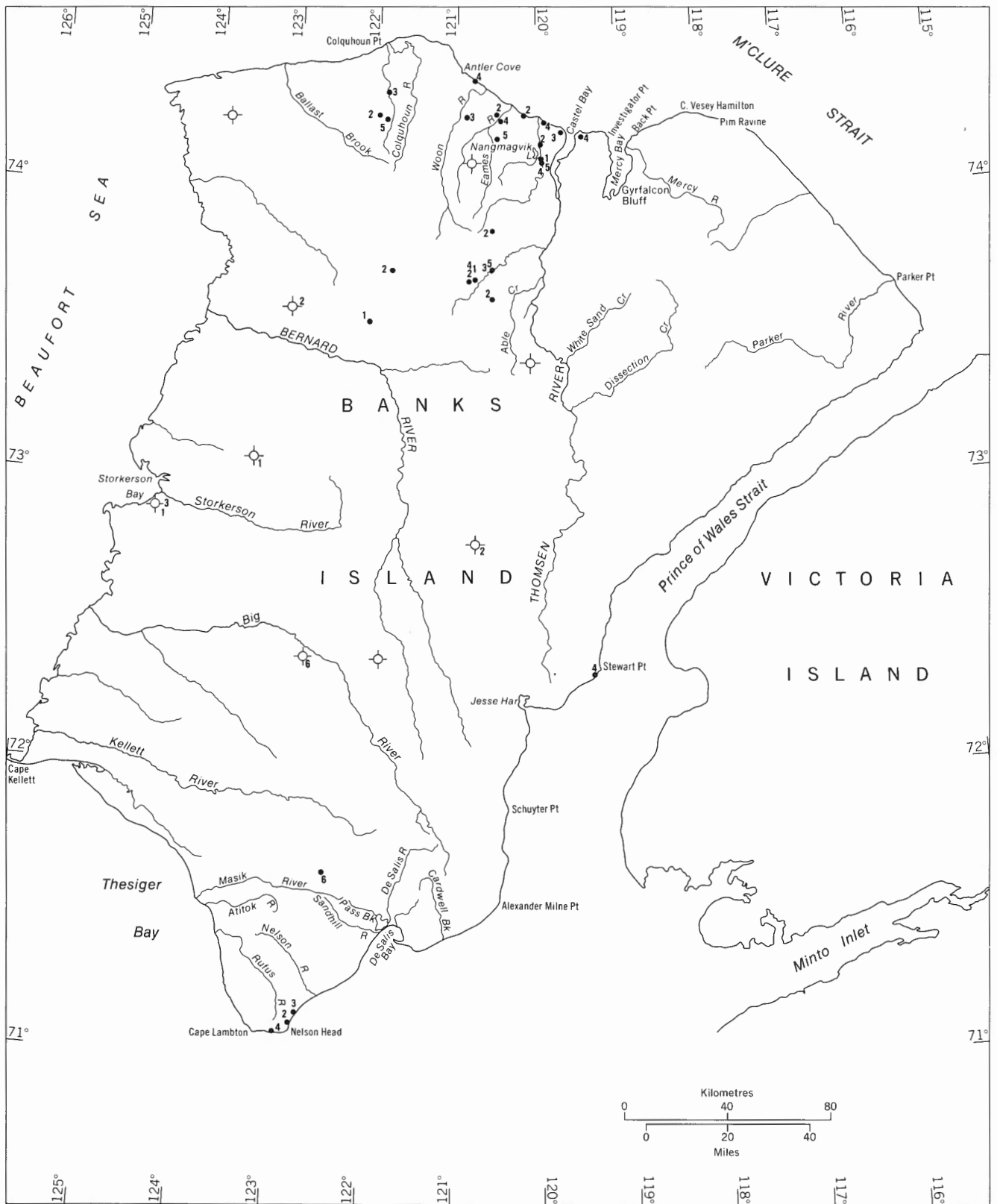
A summary of the conclusions reached in the preceding paragraphs is shown in Figure 81.

Paleohydrological analysis

Sufficient information is available to permit an analysis to be performed on the channel dimensions and the water discharge of some of the streams that deposited the Cyclic Member. Each of the calculations that follows relates to delta distributaries, several of which are presumed to fan out from the main trunk stream at the head of each delta. The data regarding sedimentary structures are taken from the delta lobe that has been mapped between Nangmagvik Lake and Castel Bay (Fig. 73). A humid climate is assumed on the basis of the abundant vegetative remains.

An analysis based on epsilon crossbedding

Epsilon crossbeds are typical of point bar deposits, which form on the inside of bends in sinuous river channels (Allen, 1963; Leeder, 1973). They accumulate by lateral accretion and their thickness is thought to correspond to the bankfull depth



GSC

Figure 78. Sand petrography of the Eureka Sound Formation showing the areal distribution of Q-mode cluster analysis groupings (42 samples, 14 variables, 6 groups) given in Figure 76.

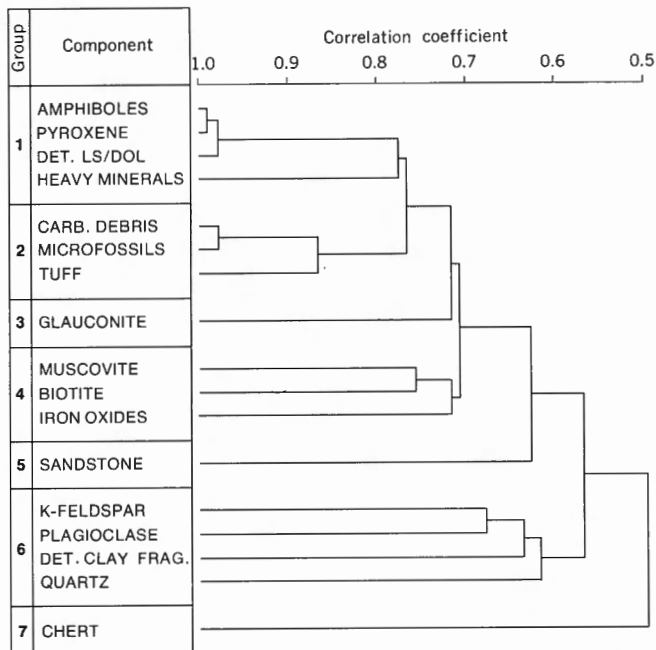


Figure 79. R-mode cluster analysis of sand samples from the Eureka Sound Formation. Data from Table 30.

of the river channel. As Leeder (1973) has shown, identification of this structure can provide an extremely valuable guide to the magnitude of the channel and from this data water discharge rates can then be calculated.

A single example of epsilon crossbedding has been identified in the Cyclic Member at Station 74-MLA-156 (Pl. 29A). The structure is 4 m (13 ft) thick and has a foreset dip of 15 degrees. Data collected by Leeder (1973) on the relationship between channel width and depth show that for high sinuosity streams (such as this channel was shown to be in the section on paleocurrent analysis) the following equation applies widely (equation 1 of this report):

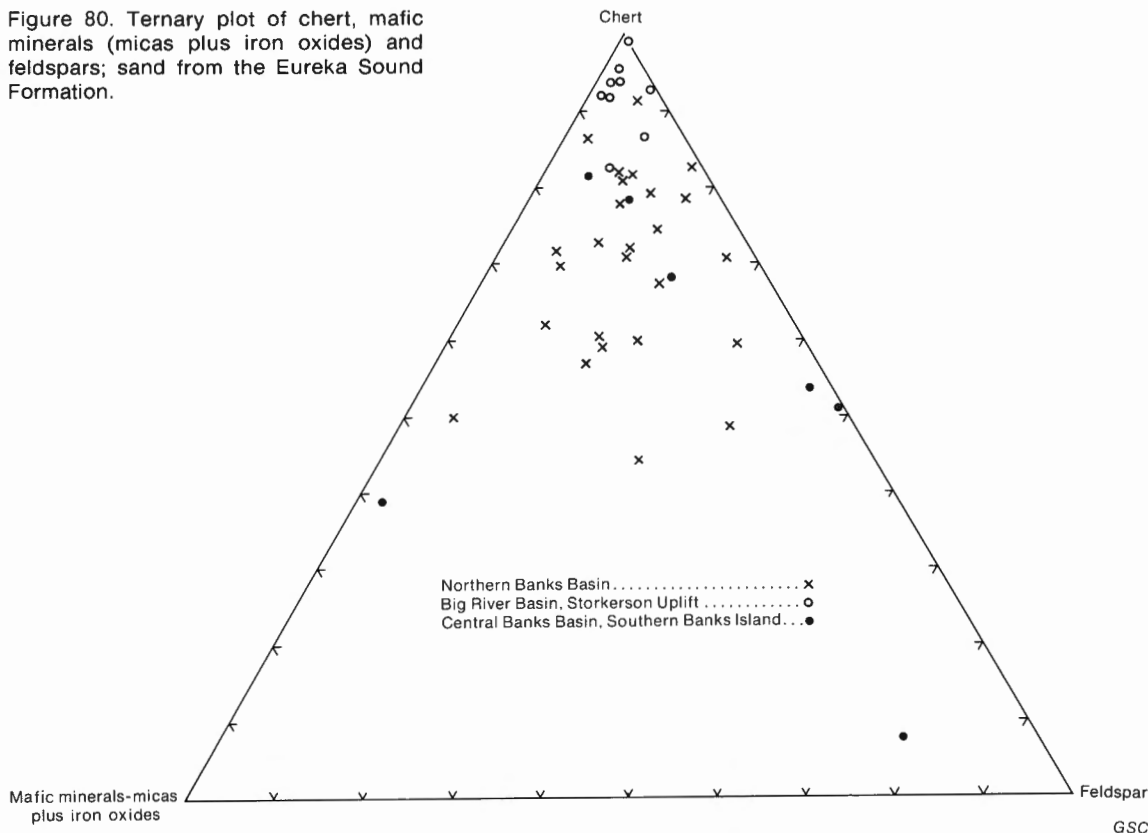
$$w = 6.8 h^{1.54}$$

where w = channel width and h = bankfull depth, in metres. By using the confidence limits provided by Leeder (1973, p. 268), a range of possible values for channel width can be calculated, as shown in Table 32. An alternative method of calculating channel width is based on the relationship (Leeder, 1973, p. 269)

$$\tan \beta = h/0.67 w \tag{10}$$

where β is the angle of foreset dip of the epsilon crossbed. This gives a value of 22 m for w , which is well within the range of values listed in Table 32. Width/depth ratio for the channel thus lies between 3 and 72, with a median value of 14. This suggests a comparison with the 'mixed load' stream type of Schumm (1972), a comparison that is reasonably well borne out by grain size and sinuosity data. According to Schumm (1972, Table 1) delta distributaries are commonly of this type.

Figure 80. Ternary plot of chert, mafic minerals (micas plus iron oxides) and feldspars; sand from the Eureka Sound Formation.



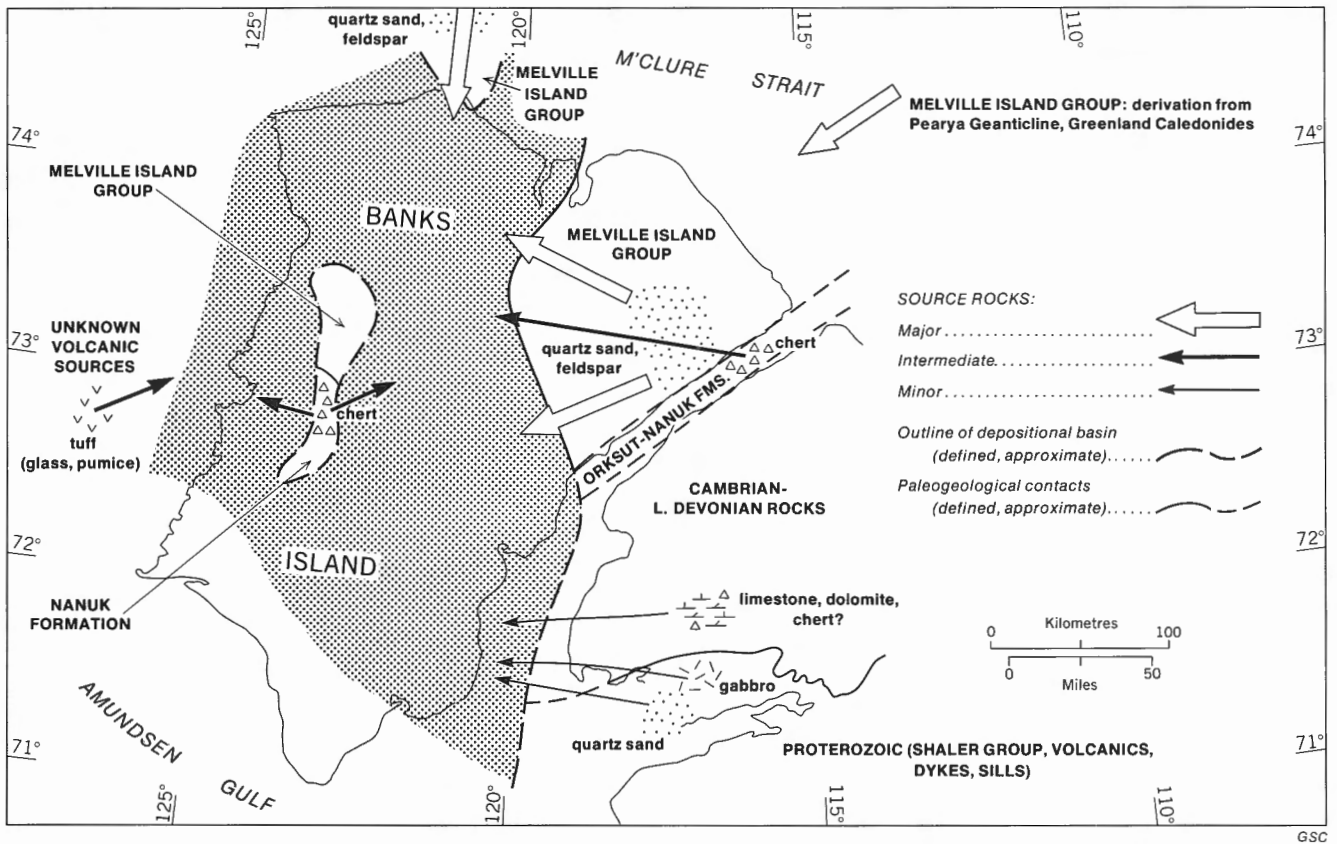


Figure 81. Source rocks of the Eureka Sound Formation, showing paleogeography of the report-area and the Eureka Sound depositional basin (stipple).

Three methods are available to calculate discharge from channel dimensions. Leopold *et al.* (1964) have demonstrated a relationship between channel width and meander wavelength L_m (equation 5 of this report) and Carlston (1965) related the latter to mean annual discharge Q_m (equation 6 of this report). By using these equations a range of values for L_m and Q_m can be calculated, as shown in Table 32 (the two equations are based on imperial units but the results have been converted to their metric equivalents).

A second method of calculating discharge relies on the family of equations developed by Schumm (1972). By substituting in his equations, Leeder (1973, p. 272) was able to show that bankfull discharge was directly related to channel depth and width, as follows (in imperial units):

$$Q_m a = w^{2.43} / 18 (w^{1.13} / h) \quad (11)$$

The second set of discharge values for $Q_m a$ in Table 32 were derived using this equation. The low and median values are similar but the high values are somewhat different. Normally, bankfull discharge would be expected to be greater than mean annual discharge.

The third method of estimating discharge is based on assessing the probable mean water velocity and multiplying this by the channel cross-section area. The water velocity can be estimated fairly reliably using the mean grain size of the sediments. In the Cyclic Member most of the sands are very fine grained. Sundborg (1967) and Friend and Moody-Stuart

(1972, Fig. 27) showed that sediment of this size is eroded and transported at a minimum velocity of approximately 30 cm/sec. The bankfull cross-section area of the channel is assumed to be approximately one half the product of width and depth, in the region opposite a point bar (Fig. 46). Results of this discharge estimation are shown in Table 32 and, again, the figures are of a similar order of magnitude to those derived earlier.

An analysis based on trough crossbedding

An alternative approach to paleohydrological analysis, based on the relationship between ripple height and water depth (Allen, 1968; equation 7 of this report), was utilized in the hydrological analysis of the Isachsen braided streams. As was suggested in that section, trough crossbeds probably represent dunes that migrated along the channel bottom and, as such, they conform to the definition of ripples followed by Allen (1968). In the present case, adequate data from Stations 73-MLA-19, 20, 21 (Nangmagvik Lake) are available to provide a reliable estimate of ripple height in that area; the mean is 41.2 cm (16.2 in.). Assuming a possible 50 per cent range of error in the estimation of water depth from ripple height, a range of depth values can be calculated, as shown in Table 33. Note that the median value is close to that indicated by the height of the epsilon crossbedding.

Channel width can be calculated from depth, assuming a range of possible width/depth ratios similar to that arrived at

in the previous section. From these estimates discharge can then be derived using any of the three methods described above. Values are given in Table 33. The range of values calculated for Q_m in the two distributaries are fairly similar but Q_{ma} is an order of magnitude greater in the Nangmagvik Lake distributary.

Estimation of river discharge and drainage area

It can be assumed that within a delta more than one distributary will be operating at any given time. The delta near Castel Bay contains evidence of three different distributaries flowing south, northwest and north, respectively (Fig. 73). However, there is no evidence that all three were active at the same time. As an approximation, it would seem reasonable to assume that the discharge of the trunk river feeding the delta would be between two and four times that of any of the typical distributaries. Mean annual river discharge at Castel Bay, therefore, can be estimated at the following low, median and high values: 5, 95 and 5000 m³/sec (using averages of the low, median and high mean annual distributary discharges and multiplying factors of 2, 3 and 4, respectively).

As discussed in the paleohydrological analysis of the Isachsen Formation, an estimate of drainage area may be obtained from the approximate equality known to exist between mean annual discharge (in cfs) and drainage area (in sq mi) (Hack, 1957; Eicher, 1969; Cotter, 1971). Low, median and high estimates are thus 13, 250 and 13 000 km² (5, 96 and 5000 sq mi).

Dury (quoted in Leopold *et al.*, 1964, p. 312) showed that a linear, logarithmic relationship exists between drainage area

and meander wavelength. Comparisons with their data suggest the following low, median and high values for drainage area: 1300, 2600, 52 000 km² (500, 1000 and 20 000 sq mi). These are considerably higher than the estimates derived by the first method, even though the meander wavelengths used in the estimation relate to single distributaries rather than to the entire river. The reasons for the discrepancy are not clear. However, the estimates provide some limits on the possible size of the Eureka Sound drainage system, which are of considerable paleogeographic utility.

Paleogeographic implications

The drainage area estimates for the delta at Castel Bay are, for the most part, much smaller than those obtained for the Isachsen braided streams. This is consistent with petrographic data, which show that the Eureka Sound sediment could have been derived from areas immediately adjacent to the depositional basin (Fig. 81), in contrast to that of the Isachsen Formation, most of which probably was derived from Minto Uplift (Fig. 45). The drainage area estimates derived in the preceding section, plus data from paleocurrent determinations and facies distributions, have been used to construct a tentative paleodrainage map for the Paleogene (Fig. 82). The principal deltaic systems are known to have been derived from the north and from the east. Lesser quantities of detritus were derived from Storkerson Uplift and must have formed deltas prograding into Big River Basin. The uplift became reduced in relief by erosion and covered by deltaic systems prograding from the east at some time during the Paleogene.

Table 32. Paleohydrology of the distributary channel at Station 74—MLA—156 (Castel Bay)

PARAMETER	SYMBOL	LOW	MEDIAN	HIGH	UNIT	EQUATION	AUTHOR OF EQUATION
Channel width	w	11	57	290	m	1	Leeder (1973)
Meander wavelength	L _m	123	654	3380	m	5	Leopold <i>et al.</i> (1964)
Mean annual discharge	Q _{m1}	0.5	20	700	m ³ /sec	6	Carlston (1965)
Mean annual discharge	Q _{m2}	7	34	170	m ³ /sec	—	This report
Bankfull discharge	Q _{ma}	2	18	152	m ³ /sec	11	Leeder (1973)

GSC

Table 33. Paleohydrology of an average distributary channel at Stations 73—MLA—19, 20, 21 (Nangmagvik Lake)

PARAMETER	SYMBOL	LOW	MEDIAN	HIGH	UNIT	EQUATION	AUTHOR OF EQUATION
Water depth	h	1.9	3.7	5.6	m	7	Allen (1968)
Width/depth ratio	—	3	14	72	—	—	Leeder (1973)
Channel width	w	5.7	52	400	m	1	Leeder (1973)
Meander wavelength	L _m	63	590	4660	m	5	Leopold <i>et al.</i> (1964)
Mean annual discharge	Q _{m1}	0.3	41	3740	m ³ /sec	6	Carlston (1965)
Mean annual discharge	Q _{m2}	1.6	30	340	m ³ /sec	—	This report
Bankfull discharge	Q _{ma}	0.4	152	3304	m ³ /sec	11	Leeder (1973)

GSC

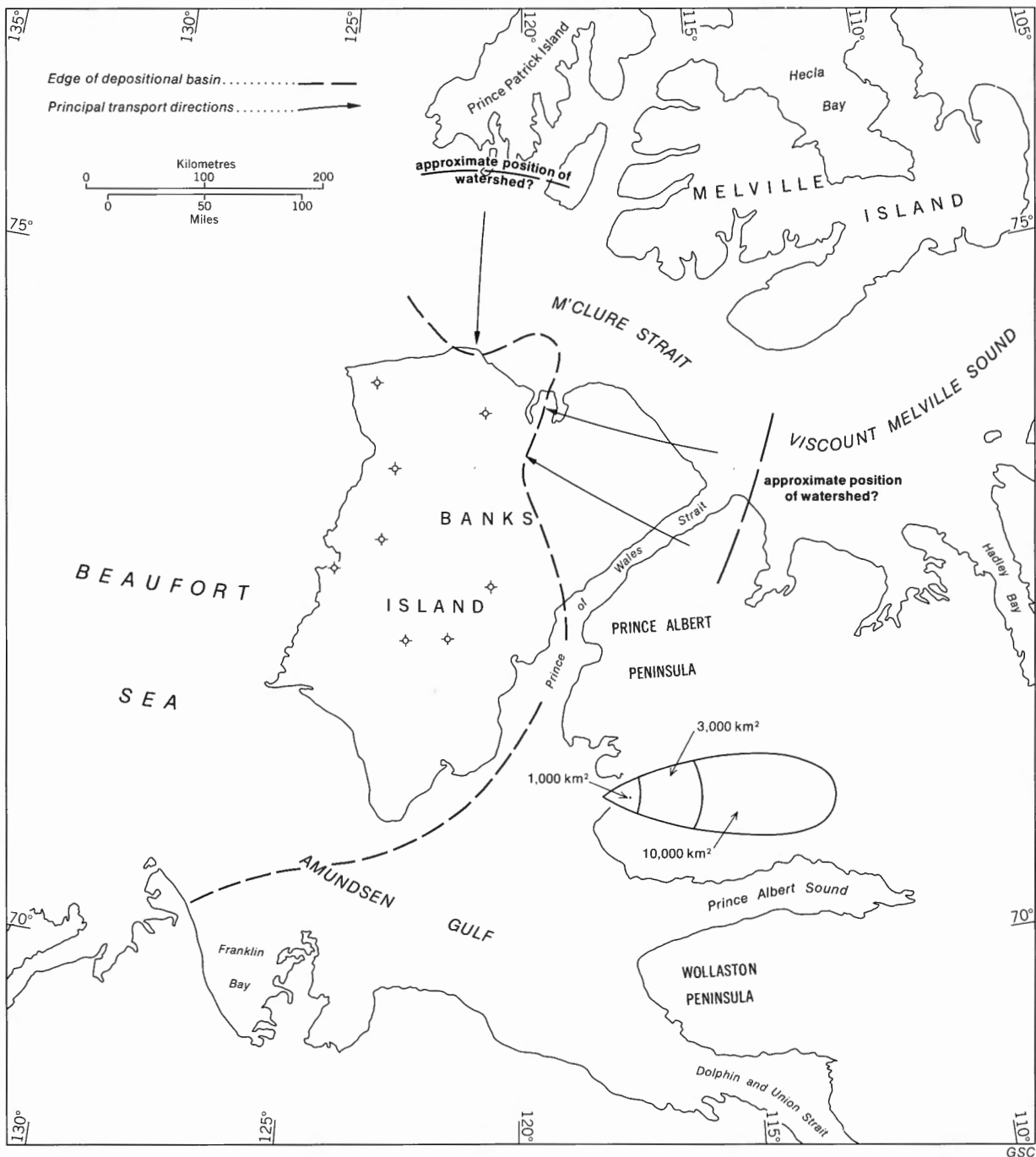


Figure 82. The main drainage pattern for rivers entering Northern Banks Basin. A range of possible areas for individual drainage basins is shown in the lower right, at the same scale as the map.

Beaufort Formation

Detailed sedimentological studies have not been carried out on the Beaufort Formation by the writer. The following brief notes are derived from the work of Hills (1969) and Hills and Fyles (1973).

On northwestern Banks Island the Beaufort comprises a lower unit of cross-stratified, medium-grained sand, and an upper unit of interbedded clay and ripple-laminated, fine- to medium-grained sand. Each unit is truncated to the east and along the lower reaches of Ballast Brook a channel eliminates

all but the lowest beds. Reworked palynomorphs and sandstone composition indicate that the lower unit had a predominantly Mesozoic provenance, whereas the upper part of the Beaufort contains evidence of the increasing importance of Paleozoic source rocks. Paleocurrent data indicate westerly flow directions. The formation is presumably fluvial in origin.

Plant spores, pollen and megafossils indicate that the temperature during the early phases of deposition of the Beaufort was similar to that of the Great Lakes region today. A cooling trend is suggested by a change in floral assemblage in the upper part of the formation.

4. Structural Geology

Introduction

The structural geology of Banks Island is dominated by a series of small pericratonic basins and highs, as shown in Figure 4. These features were described in Chapter 1 under "Regional geological setting" and a discussion of their influence on sedimentation throughout Cretaceous and Paleogene time has been one of the main themes of this report.

Two generalized structural contour maps of the report-area, based on gravity data and subsurface well information, are given in Figures 83 and 84. A structural cross-section is provided with the geological maps (*in pocket*). Figure 83 shows approximate structure contours for the base of the Mesozoic. Figure 84 provides contours on the base of the Beaufort, which marks a major unconformity. The contours show how the Arctic Coastal Plain dips steeply toward the Beaufort Sea near the west coast of Banks Island.

The remainder of this chapter deals with the smaller scale structures in the Mesozoic and Tertiary rocks that have been defined by detailed field mapping (the structural geology of the older rocks was described by Miall, 1976a).

The dominant structure in Banks Island consists of flat-lying beds or broad, gentle folds with very low flanking dips, cut by numerous normal faults. Most faults are oriented between north and northeast; all but a few show small displacement.

Folds

The majority of outcrops of the Mesozoic and Tertiary rocks (Pls. 8A, 10A, 15A) exhibit horizontal strata but locally dips of up to 20 degrees have been recorded, especially in the Eureka Sound Formation (Pl. 13A). Such dips are of little structural importance for they are not persistent over wide areas. Few folds of more than a few kilometres in lateral extent have been mapped. The most important is the syncline corresponding to the axis of Northern Banks Basin. The fold trends north-northeast (azimuth approximately 020°) and the axial trace is located approximately 10 km (6 mi) east of Eames River. The fold can be traced by surface mapping for approximately 30 km (19 mi) south from M'Clure Strait. It is 80 km (50 mi) wide between Devonian outcrops at Cape Crozier and Cape Vesey Hamilton, and involves all the Mesozoic and lower Tertiary units between. The amplitude of the fold is about 2100 m (7000 ft), this being the combined thickness of the Mesozoic-Tertiary section. Regional dip, therefore, is approximately 3 degrees on each flank of the fold but locally dips are up to 15 degrees (Investigator Point). Subsidiary folds are present on the flanks of the main syncline: a minor faulted anticline east of Antler Cove; a

minor anticline and syncline near Woon River; a minor anticline and syncline near Castel Bay, shown only by dip symbols on the geological map because of uncertainty as to the position of the axial traces.

The other major fold in the report-area has been named Cape Crozier Anticline by Thorsteinsson and Tozer (1960, 1962). At the core of the anticline are the faulted inliers of Devonian Melville Island Group at Cape Crozier, Cape M'Clure and Cape Wrottesley. Rocks of the Mesozoic-Tertiary succession are exposed on the flanks of the structure, which plunges to the south along an axial trace that is followed by the upper part of Colquhoun River.

Other broad fold structures probably are present, corresponding in position to the depositional basins and highs described earlier in this report, but because of insufficient exposure they cannot be defined on a geological map. For example, the outcrops of Proterozoic rocks at De Salis Bay probably are part of the core of an anticline corresponding to De Salis Uplift (Fig. 4), a feature defined on the basis of gravity data. The Beaufort Formation also appears to be very gently folded (Fig. 84), indicating gentle post-Miocene movement.

Faults

The most prominent fault in the report-area is a north-south trending structure at Nelson Head, which juxtaposes Eureka Sound Formation against Proterozoic rocks. The fault is indicated by a prominent fault-line scarp, 300 m (1000 ft) high, near the coast (Pl. 36B), but the relief becomes more subdued inland to the north. Maximum throw on the fault is about 900 m (3000 ft), diminishing to the north, where the fault splays out into several subsidiary structures.

Nelson Head Graben is between Nelson Head and Cape Lambton. The graben has a maximum width of 3 km (1.9 mi), which diminishes to the north, and a downthrow of approximately 300 m (1000 ft). The Isachsen Formation is 200 m (660 ft) thick within the graben but probably is absent on either side, indicating that the fault was active in Early Cretaceous time. The easterly bounding fault of the graben extends northward into the headwaters of Rufus River, where it splays into several minor structures involving the Christopher and lowermost Kanguk formations, with displacements of a few tens of metres.

Another small graben is tentatively mapped south of Alexander Milne Point. The Christopher Formation is present in the downdropped fault block and the Isachsen Formation on the flanks.

In northern Banks Island the core of Cape Crozier



Plate 36. Faults. A: Devonian rocks at Cape M'Clure (*distance*) and at Cape Crozier (*foreground*) with a small graben in between, in which the Christopher Formation is present. GSC 199122. B: Proterozoic rocks, capped by thin Cretaceous shale (*left*) upfaulted against Eureka Sound Formation (Te^2). A faulted inlier of Christopher Formation (Kc) is present in the small bay at lower left; Nelson Head. (P = Glenelg Formation.) GSC 199123.

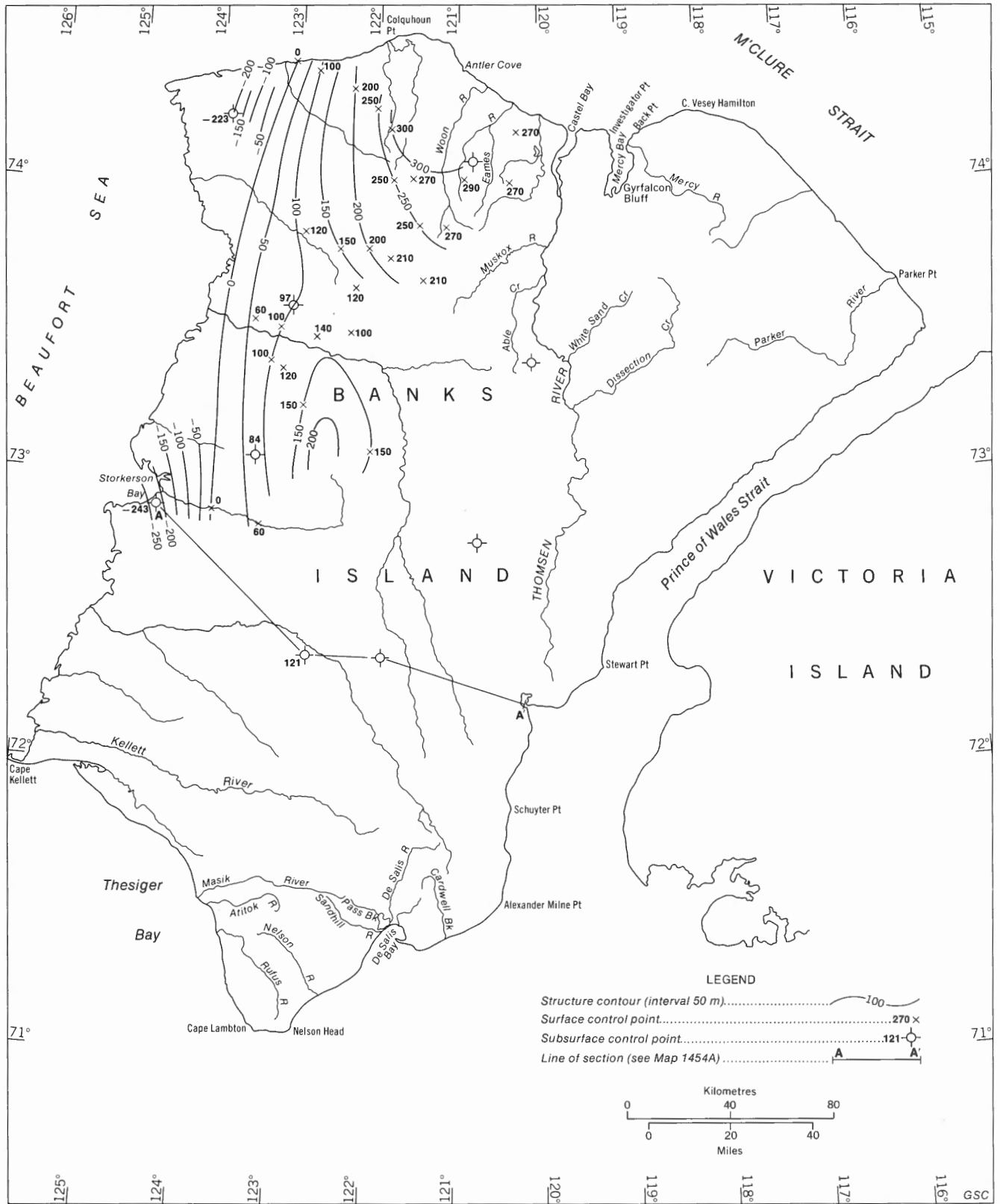
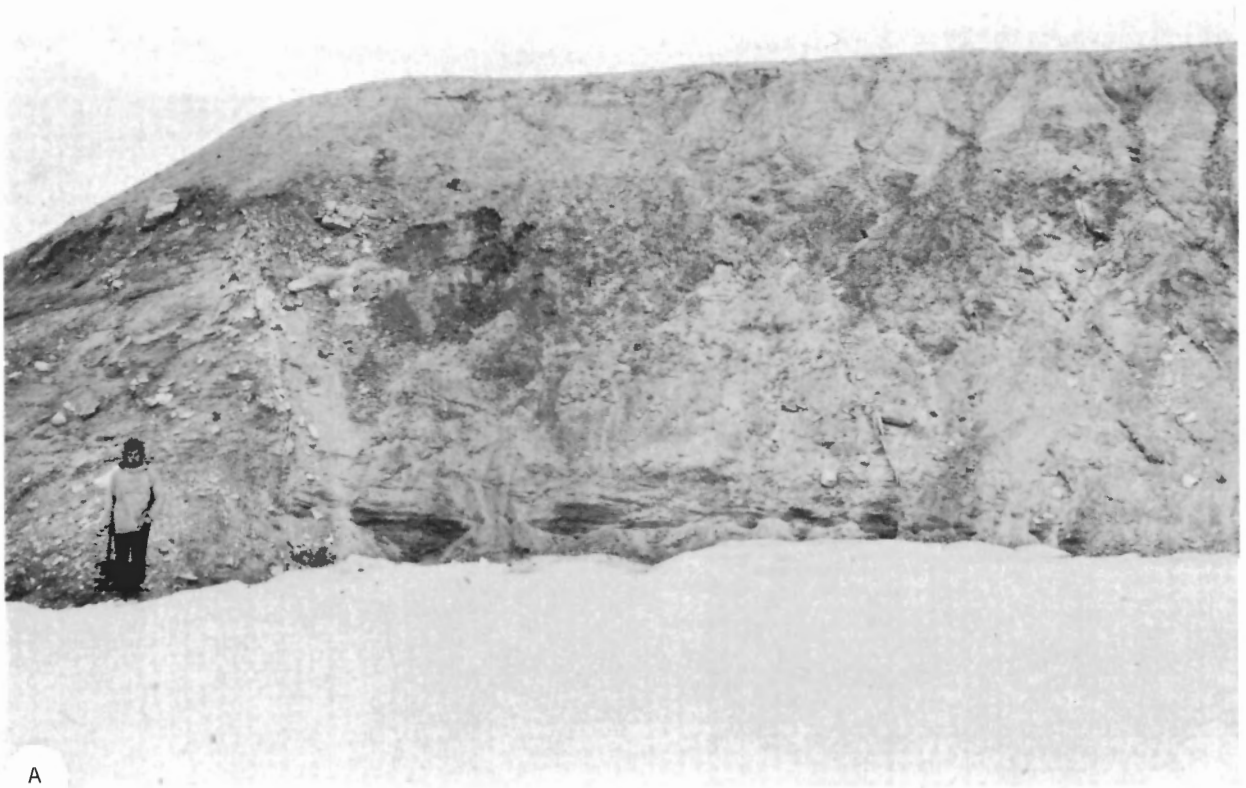


Figure 84. Structural contours on the base of the Beaufort Formation. Contours are not drawn south of Storkerson River because the position of the Beaufort–Eureka Sound contact is uncertain.



Plate 37. Superficial structures in the Eureka Sound Formation. A: Large slumped mass of Eureka Sound Formation, which has rotated into the form of a small syncline, north of Muskox River (near Station 74-MLA-154). GSC 199207. B: Normal faults in the Cyclic Member, related to superficial slumping, Eames River (Station 73-MLA-44). GSC 199160.



A



B

Plate 38. Small-scale structures. A: Minor faults and joints filled with crushed breccia, Cape Vesey Hamilton (Station 74-MLA-76). GSC 199199. B: Folding and faulting in the basal Kanguk Formation, Able Creek (Station 74-GAS-30). GSC 199214.

Anticline is an area of complex normal faulting. The most prominent fault forms the southeastern boundary of the Devonian inlier, where the Melville Island Group and the Kanguk Formation are juxtaposed by a downthrow (to the east) of approximately 300 m (1000 ft). In the northern part of the inlier several faults divide the strata into a series of blocks, of which Cape M'Clure is one. To the east of the Cape a graben structure 1 km (0.6 mi) wide is occupied by the Christopher Formation, which rests here directly on the Devonian (Pl. 36A).

The lower part of Thomsen River follows a normal fault which has a maximum downthrow to the west of approximately 300 m (1000 ft). The fault is oriented approximately north-south and cuts obliquely across the strike of the beds, so that progressively younger beds (up to and including the Eureka Sound Formation) are involved toward the north. The fault may extend northward beneath Castel Bay.

East of Mercy Bay the Isachsen-Melville Island contact is partly fault controlled. Downthrow may reach locally as much as 180 m (600 ft), based on the disposition of the Isachsen Formation on either side of the fault at Cape Vesey Hamilton. Part of the fault movement probably took place in Early Cretaceous time, for the Isachsen here contains boulders up to 75 cm (30 in.) in diameter, indicating local strong relief. In addition, there is evidence from the study of sedimentary structures that stream direction and competency changed suddenly during Isachsen sedimentation, possibly as a result of contemporaneous fault movement. Direct evidence of post-Isachsen movement is provided by an exposure of Isachsen Formation 3.2 km (2 mi) east of Station 73-MLA-29 where, adjacent to a major fault, the sand is cut by a series of fracture planes filled with a cemented crush-breccia (Pl. 38A). These are interpreted as minor faults subsidiary to, and parallel to, the main fault plane.

Possible evidence of relatively recent movement is visible on aerial photographs of the region near the mouth of Bernard River. A lineament is present which extends parallel to the coast, and airphoto interpretation suggests that it may be a fault between the Beaufort Formation and the Eureka Sound Formation. Other lineaments are present within the Beaufort Plateau between Ballast Brook and Log River but airphoto

interpretation indicates that vertical movement on them is negligible.

Many additional faults are shown on the accompanying geological maps and many others probably have not been detected for lack of good exposure. The sedimentological evidence of faulting during Isachsen time at Cape Vesey Hamilton and Nelson Head Graben probably is of regional significance, and it is considered likely that many or all of the areas where the Devonian rocks are overlain by the Christopher Formation without any intervening Isachsen were fault-bounded structural highs during Isachsen sedimentation. This would apply to Storkerson Uplift, Cape Crozier Anticline and the craton-edge region penetrated by the Tiritchik M-48 and Ikkariktok M-64 wells. The fact that few faults have been mapped in the Beaufort Formation, yet many displace the Eureka Sound Formation, indicates that the second main period of fault movement was during the mid-Tertiary.

Superficial structures

Superficial structures are common in the Mesozoic and Tertiary rocks. They are interpreted as landslip features which develop as a result of stream undercutting or saturation of potential glide planes such as clay beds. Large masses of Eureka Sound Formation commonly are involved in rotational slumps and develop small-scale anticlines and synclines as a result (Pl. 37A). The glide planes may be steeper locally, in which case the slump has the same appearance in outcrop as a major fault but is, in fact, of limited lateral extent (Pl. 37B). Small folds, probably of surficial origin, have also been observed in the Kanguk Formation (Pl. 38B).

Such structures render measurement of sections and bed-to-bed correlation difficult or impossible. Jutard and Plauchut (1973) provided a composite section through the Eureka Sound Formation based on a compilation of many short sections measured on the east flank of Northern Banks Basin. However, the present writer feels that this type of exercise does not have a very high potential for accuracy.

Similar superficial slumps have been recorded in the Devonian rocks of northeastern Banks Island by Klován and Embry (1971, Pl. 4).

5. Economic Geology

Oil and gas

Nine exploratory wells have been drilled in Banks Island up to the time of writing (February 1976) and at least seven of them had Mesozoic clastic units as primary objectives. No shows have been reported from any of these wells, and no seepages are known to be present at the surface. Drillstem test results are summarized in Table 34. Geological and geochemical data relating to the Mesozoic and Tertiary clastic rocks are not encouraging, as summarized in the ensuing paragraphs.

The oldest potential reservoir unit in the succession is the basal Jurassic sandstone encountered in the Orksut I-44 well at a depth of 1813 m (5948 ft). The sandstone is 16 m (52 ft) thick at this locality; its lateral extent is unknown. A single thin section of this unit has been studied and reveals that the rock contains an abundance of clay matrix. The operator reports that a core through the sandstone shows porosities averaging 28.9 per cent and permeabilities averaging 768 millidarcies.

The Isachsen Formation is the best potential reservoir unit in the Mesozoic and Tertiary succession. Data available to date indicate that the formation reaches a maximum thickness of 200 m (660 ft) and contains several units of

medium- to coarse-grained sand with porosities up to 24 per cent. The Isachsen consists almost exclusively of sand at the margins of the depositional basins but passes into interbedded sandstone and shale at the centre, as a result of a facies change from a braided to a meandering stream environment. The distribution of the Isachsen Formation is shown in Figure 9. The formation is present throughout Banks Basin but is absent over Storkerson Uplift and in Big River Basin.

In outcrop sections the Hassel Formation is predominantly sand and locally is as much as 50 m (160 ft) thick. However, as Figure 12 shows, the formation becomes more argillaceous toward the centre of Northern Banks Basin and therefore is of very little interest as a potential reservoir.

Various sand units are found in the Kanguk Formation. The lower sand member was penetrated by the Uminmak H-07 well at a depth of 640 m (2100 ft) and by the Orksut I-44 well at 1186 m (3890 ft). The unit is 36 m (117 ft) and 29 m (96 ft) thick, respectively, in these wells. The sandstone is fine to medium grained, quartzose, and has a porosity of up to 29 per cent. The lower sand member is interpreted as a shallow subtidal to intertidal, offshore sand bar and probably has a limited lateral extent, possibly occurring only as pod-shaped

Table 34. Drillstem test results in the Mesozoic rocks of Banks Island

WELL	DEPTH		FORMATION	RECOVERIES
	Metres	Feet		
Storkerson Bay A-15	No tests			
Nanuk D-76	No tests			
Uminmak H-07	620-659	2035-2163	KANGUK (lower sand member)	400 ft gas cut mud, 850 ft gassy salt water
Orksut I-44	1189-1198	3902-3932	KANGUK (lower sand member)	Misrun
	1372-1384	4500-4540	ISACHSEN	Weak initial puff increasing to good air blow, decreasing toward end of test. 3100 ft water, 300 ft quartz sand
	1810-1835	5940-6020	basal Mesozoic sand	Good initial puff, strong air flow, decreasing to nil in 25 minutes 3950 ft sandy water
Ikkariktok M-64	No tests			
Tiritchik M-48	No tests			

GSC

units near Storkerson Uplift. The upper sand member is more widely distributed but generally is thinner, finer grained and more silty and probably of less value as a reservoir unit.

The Eureka Sound Formation contains numerous sand bodies ranging up to 33.1 m (108.6 ft) in thickness. The sand is composed predominantly of quartz and rock fragments (mainly chert), is typically fine to very fine grained, and shows excellent porosity. Pebbly beds are present in the formation in Big River Basin. The lateral extent of most of the sand units probably is about 0.5 to 5 km (0.3–3.1 mi). Most are considered to be channel sands or distributary mouth bar sands deposited in a deltaic environment. They grade laterally into silts and soft shales.

Both structural and stratigraphic traps are possibilities in the Mesozoic-Tertiary rocks. Lateral porosity pinchouts are to be anticipated in many of the sand units, particularly in the Eureka Sound Formation and in the lower sand member of the Kanguk Formation. Structural traps are likely to be controlled mainly by faulting. However, sedimentological evidence suggests that many of the faults were active during Isachsen sedimentation. This formation is absent on at least some of the known structural highs, as at the Ikkariktok M-64 and Tiritchik M-48 locations, suggesting that the highs were in existence during the Early Cretaceous and may have acted as local sediment sources. If this interpretation is correct, it reduces considerably the potential for structural traps in the Isachsen Formation unless areas can be located where the formation is truncated by a fault in an updip situation.

Geochemical evidence indicates that probably the entire Mesozoic-Tertiary succession is immature, and this is regarded as the most critical factor in reducing the hydrocarbon potential of the report-area. Snowdon and Roy (1975) showed that in the Sverdrup Basin mature levels are not reached until a depth of approximately 2000 m (6500 ft) below the base of the Tertiary and, because of this, Triassic rocks are regarded as showing much higher potential than are Jurassic and Cretaceous strata. The same is undoubtedly the case in Banks Island. Data available to date indicate that nowhere is the base of the Mesozoic as deep as 2000 m (6500 ft) and, subtracting the known thickness of Tertiary sediments from the total, the maximum depth of pre-Tertiary burial may be as little as half the required minimum. Only in parts of Northern Banks Basin and in the offshore part of Big River is it considered possible that the Mesozoic section has been buried to sufficient depths for mature geochemical levels to have been reached.

These conclusions are confirmed by palynological work (W.S. Hopkins, Jr., *pers. com.*, 1974) which has shown that all the palynomorphs are characterized by low carbonization levels. In addition, unpublished geochemical analyses carried out by L.R. Snowdon (*pers. com.*, 1974) show that in the first four wells drilled in the report-area (Storkerson Bay A-15,

Nanuk D-76, Uminmak H-07, Orksut I-44) the entire Mesozoic section yields only minor quantities of biogenic wet gas, mainly methane. According to Evans and Staplin (1970) and Snowdon and Roy (1975), this is characteristic of the immature zone.

An additional negative factor is that formation waters at depth in the Mesozoic succession are of relatively low salinity. The operator reports the following analytical results from the Orksut I-44 well: 1372 to 1384 m (4500–4540 ft), Isachsen Formation, 5935 mg/L; 1810 to 1835 m (5940–6020 ft), basal Mesozoic sand, 7988 mg/L. The freshness of the waters suggests that a strong hydrodynamic system may be in effect, flushing the porous units with water from the surface. Such a system would have detrimental effects on any hydrocarbon pools in the subsurface.

In conclusion, although trap and reservoir possibilities are regarded as fair to good, geochemical data indicate that the section is too immature to have yielded more than small quantities of biogenic wet gas. Probably the best prospects are located offshore to the west of Banks Island, where the Mesozoic section is buried beneath a thick wedge (probably up to at least 3000 m, 9800 ft) of upper Tertiary to recent sediments (Lerand, 1973; Miall, 1975*b*, Fig. 15).

Coal

The Eureka Sound Formation contains numerous seams of lignitic coal. Traces also are present in the Isachsen Formation. Jutard and Plauchut (1973) subdivided the beds referred to here as the Cyclic Member of the Eureka Sound into two units, largely on the basis of a supposed upward decrease in coal content. Detailed work by the writer has shown that this is not of regional validity and can be true only of the specific sections measured by the earlier workers.

Lignite comprises between 0 and 13.1 per cent of the sections measured in the Eureka Sound. The highest percentages are found at Station 74-MLA-126 near the mouth of Thomsen River, and in the general area of Log River. Individual seams range up to 3 m (10 ft) but the thicker seams normally contain laminae or thin beds of carbonaceous shale or siltstone.

The coal in the Eureka Sound Formation is all of low rank. It is friable, and commonly contains identifiable wood and other cellular material, indicating very little alteration. No analyses have been performed on the material and it is regarded as being of little economic value. Thorsteinsson and Tozer (1962, p. 62) reported that at one time the Innuits of Holman Island used coal from the area around Alexander Milne Point, probably from the Isachsen Formation. The present writer is unable to state whether this source is still in use.

6. Synthesis and Conclusions

Regional paleogeographic evolution

Sedimentological and stratigraphic data are summarized in this section and an attempt is made to present a unified geological history for the Jurassic to Neogene time interval. The relationship between Banks Island and adjacent regions to the north (Eglinton Graben, Sverdrup Basin) and the south (Anderson Basin, Beaufort-Mackenzie Basin) is discussed.

Jurassic and early Neocomian

The sedimentary history of Sverdrup Basin commenced in the Mississippian Period, that of Mackenzie Delta region in the Jurassic Period. In this respect, the geology of the report-area is analogous to that of the Delta region because the oldest post-Devonian sediments recorded are the Toarcian to Oxfordian clastics defined by Tozer (1956, p. 18) as the Wilkie Point Formation. On southern Prince Patrick Island the formation comprises up to 180 m (600 ft) of sand and sandstone, which is in part glauconitic, ferruginous and phosphatic. According to Tozer and Thorsteinsson (1964, p. 124), the lower part of the formation is marine and the upper part nonmarine. At the Orksut I-44 well location in southern Banks Island the formation is 185 m (608 ft) thick and consists of silty shale with minor amounts of siltstone. It is marine throughout. The Prince Patrick outcrops probably represent a prograding delta marginal to Sverdrup Basin and derived from the southeast (Meneley *et al.*, 1975), whereas the Orksut I-44 location lies within what was probably a linear, intracratonic trough extending through Eglinton Graben and Northern Banks Basin (Fig. 17). Whether or not this trough was open directly to the Mackenzie Delta region, either by a southward extension from Orksut (as shown in Fig. 17) or along a seaway west of Banks Island, cannot be determined at this time.

A disconformity separates Wilkie Point strata from succeeding Mould Bay Formation in the surface outcrops on Prince Patrick Island but there is as yet no evidence for a disconformity in the subsurface. South of Mould Bay weather station the disconformity becomes an unconformity and to the west of this locality the Mould Bay oversteps the Wilkie Point and rests directly on Devonian rocks. In southwestern Prince Patrick Island and on Eglinton Island the formation is predominantly sandstone but increasing amounts of shale appear to the northeast, into Sverdrup Basin. At Orksut I-44 the Mould Bay Formation virtually is indistinguishable from the Wilkie Point; it consists of silty shale and lesser siltstone. The formation is more sandy at Castel Bay C-68. Thicknesses range from between 60 and 120 m (200–400 ft) on southwestern Prince Patrick Island to 200 m (657 ft) at Orksut I-44.

A generalized paleogeography for the Jurassic Period is shown in Figure 17. A seaway connection to the south is shown on this map but there is considerable uncertainty as to its exact position. It is not known whether Banks Basin and Eglinton Graben existed in their present form. The eastern coastline of the basin can be located because Jurassic strata are everywhere, except on northern Eglinton Island, overstepped by Cretaceous strata and not present at the surface. On Banks Island, Storkerson Uplift may have formed a western margin to the seaway. However, the lack of a sandy, marginal facies in the Jurassic rocks at Orksut I-44 is surprising and it suggests that Storkerson Uplift could not have been a major source-area at that time.

Barremian and Aptian

The Mould Bay Formation ranges up to Valanginian in age at Prince Patrick Island (Tozer and Thorsteinsson, 1964, p. 137) and early Neocomian at Orksut I-44. The Isachsen of northern Banks Island is Barremian to earliest Albian in age. A disconformity exists, therefore, between the two formations within at least part of the project-area, whereas the contact may be conformable within much of Sverdrup Basin (Table 1).

The Isachsen represents a period of great expansion of sedimentation beyond the confines of Sverdrup Basin. To call this event a transgression would be misleading, for the sediments which resulted are almost entirely nonmarine. At least within the present project-area and probably over much of the remaining Arctic Islands the cause for this increased sedimentation is thought to have been a period of epeirogenic disturbance in the craton. The pattern of tectonic activity and sedimentation that resulted is very characteristic of the Unstable Craton Margin province. Uplifts and downwarps were accentuated, probably through block faulting, and the resulting rejuvenation of drainage networks caused large volumes of clastic detritus to be eroded and transported toward the major depocentres. Nonmarine sediments thus were accumulated in pericratonic troughs such as Anderson Basin, Banks Basin and Eglinton Graben, and on cratonic areas which displayed positive tendencies throughout most of post-Paleozoic time, such as the Pim Ravine area of northeastern Banks Island. The maximum thickness is present in Sverdrup Basin, where the Isachsen Formation is about 1200 m (3900 ft). A regional paleogeographic synthesis is shown in Fig. 85.

The Isachsen Formation of the report-area was deposited by both braided and meandering streams. The braided stream facies consists predominantly of medium to coarse, locally pebbly sand (coarse sand lithofacies) and appears to have

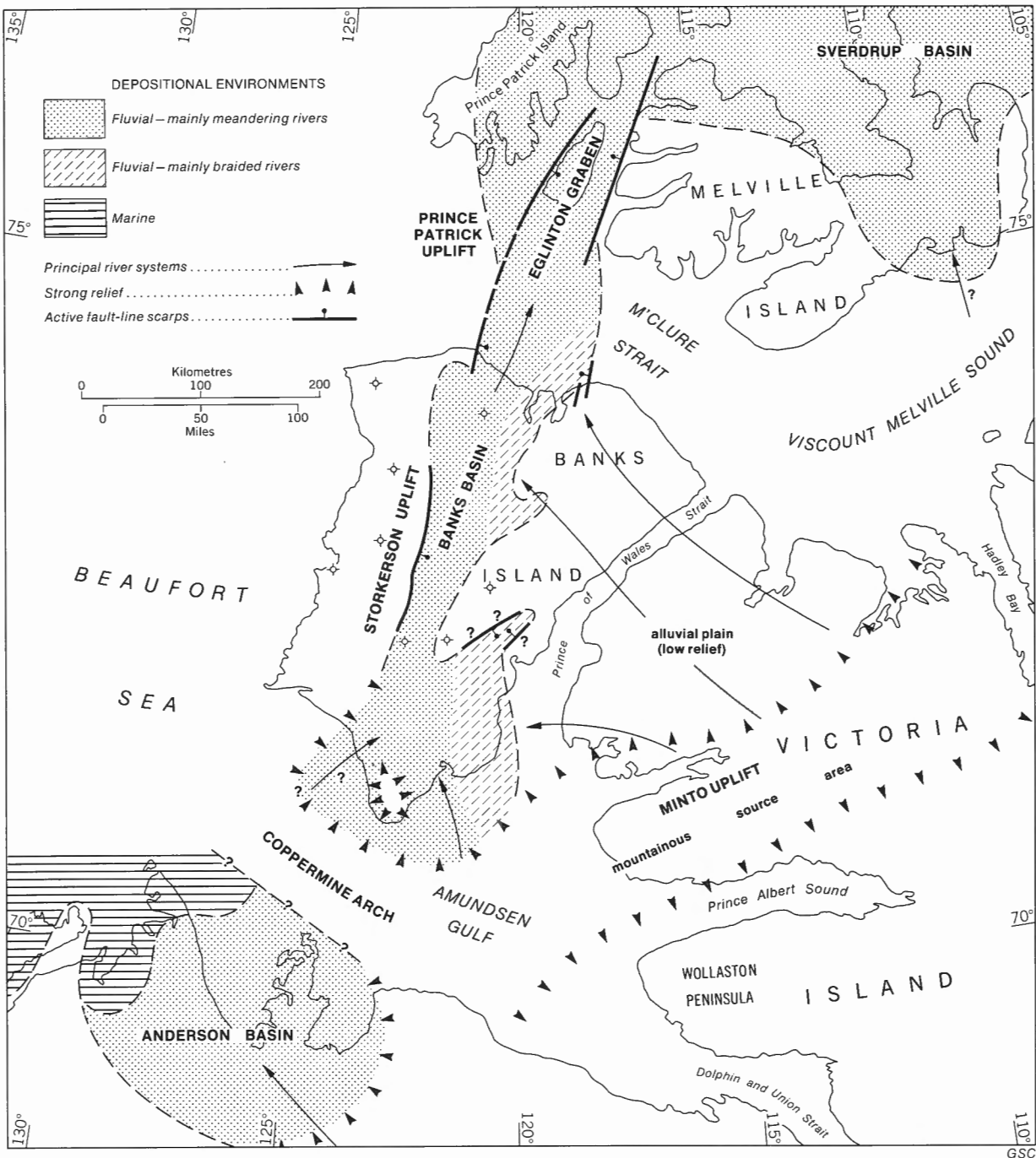


Figure 85. Paleogeographic synthesis for Barremian and Aptian time. Data from areas north and south of Banks Island from Tozer and Thorsteinsson (1964), Yorath *et al.* (1969) and Young *et al.* (1976).

been confined to the margins of the present-day basins, as at Alexander Milne Point in Cardwell Basin and White Sand Creek, Baker Creek and Cape Vesey Hamilton in Northern Banks Basin (Fig. 22). Deposits of meandering streams may (Orksut I-44, Castel Bay C-68) or may not (Sandhill River) contain recognizable fining-upward cycles. They include a higher proportion of shale and silt and are located near present basin centres, such as Orksut I-44 in Central Banks Basin, Castel Bay C-68 in Northern Banks Basin, and Sandhill River, which may represent an extension of Cardwell Basin.

These distributions suggest that the basins of the present day (Fig. 4) were depositional basins during Isachsen sedimentation, because braided stream sediments typically are the more proximal of the two main fluvial facies and thus would be expected to occur at a basin edge, nearer the source-area.

This interpretation is confirmed by paleocurrent data (Figs. 21, 22) which show that rivers entered the sides of the basins and then turned to flow parallel to their axes. Mean current directions are subparallel and subperpendicular to the trends of the present-day basins.

There is abundant evidence of local relief in the Barremian-Aptian period. At Nelson Head the thickest Isachsen section in the report-area (200 m, 660 ft) accumulated in a small graben structure. The graben must have existed at that time since the formation is completely absent on either side, indicating local uplift (Fig. 22). The amount of relief is suggested by the fact that the basal Isachsen is a boulder conglomerate of alluvial fan origin, containing clasts up to 50 cm (20 in.) in diameter. Central and northern Banks Island display similar evidence of local relief. The Isachsen is found in the Orksut I-44 and Castel Bay C-68 wells but is absent in the Bar Harbour E-76, Storkerson Bay A-15, Nanuk D-76, Uminmak H-07, Ikkariktok M-64 and Tiritchik M-48 wells, and at Cape Crozier. The formation probably never was present there, for the Isachsen is followed conformably by the Christopher in most areas and there would not have been time for uplift and erosion. The areas penetrated by these wells, Storkerson Uplift–Big River Basin and Cape Crozier Anticline and the shelf-edge east of Central Banks Basin probably were land areas at the time, possibly fault-bounded, and they may have been minor sources of sediment.

At Cape Vesey Hamilton in northern Banks Island, the Isachsen-Devonian contact is fault-bounded, and the faults there probably also were active during sedimentation. The presence of pebble beds and boulders up to 75 cm (30 in.) in diameter points to the existence of strong local relief. In addition, detailed paleocurrent studies (*see* discussion of Fig. 29) provide evidence that the streams locally changed direction and increased in competency, probably as a result of contemporaneous uplift localized along the bounding faults. Exhumed Cretaceous river valleys have been mapped on the Devonian plateau south and east of Cape Vesey Hamilton (Fig. 24).

Petrographic studies of the Isachsen sand show that the bulk of the detritus must have been derived from the Proterozoic rocks of Minto Uplift, although the Paleozoic rocks of Prince Albert Homocline and Storkerson Uplift were the provenance for small additional amounts of material. Minor amounts of lateral variation within the Proterozoic source rocks are recorded by the distribution of certain rare detrital species, of granitic origin, within the Isachsen. This may have been the time when Minto Uplift first appeared as a recognizable structural feature. There must have been considerable uplift and erosion during Isachsen sedimentation to have provided the requisite quantity of detritus, whereas there is no evidence of any similar clastic wedges having been derived from the uplift at any time prior to the Early Cretaceous.

The detrital material was transported westward and northwestward across Prince Albert Homocline by a system of perennial, low-sinuosity braided, bedload rivers. Physiographically, the setting must have been a smaller scale analogue of the present-day Rocky Mountains and western Interior Plains, a mountainous source area to the south and east, and an alluvial plain of low relief over which braided streams flowed, deriving only small quantities of clastic material from the Paleozoic rocks forming the local bedrock. The braided rivers were similar morphologically to those existing now, such as the Donjek (Yukon) and the Platte (Nebraska), but paleohydrological reconstructions of the Isachsen streams indicate that they had somewhat higher discharge rates, which suggests

larger drainage areas (Tables 9, 10).

At the edges of the depositional basins the streams split into several distributaries and probably fanned out into an 'inland delta', distributing their sediment load laterally over a wide area, as does the modern Kosi River in India (Gole and Chitale, 1966). The facies change into meandering stream deposits in the centre of Banks and Cardwell basins probably reflects a decrease in slope.

As shown in Figure 85, the streams probably flowed northward along Banks Basin. They probably continued through Eglinton Graben and entered the west end of Sverdrup Basin, where their sediment load ultimately was deposited. Contrary to the interpretation of Cassan and Evers (1973), the present writer considers this depositional system to be entirely separate from that forming contemporaneous marine and nonmarine strata in Anderson and Beaufort-Mackenzie basins. Petrographic, paleocurrent and hydrological data can be explained entirely on the basis of the interpretation shown in Figure 85. Coppermine Arch probably was a watershed of low relief and the sediments of Anderson Basin were derived from the craton to the southeast (Yorath *et al.*, 1969, p. 15) and not from the south or southwest. There does not appear to have been any through-going fluvial system, as proposed by Cassan and Evers (1973).

Albian

The Early Albian was marked by a widespread marine transgression throughout western and Arctic Canada (Jelletzky, 1971, p. 42) and there is ample evidence for such a transgression in the report-area. The Christopher Formation overlaps the Isachsen to rest directly on Proterozoic or Paleozoic basement at Rufus River and Nelson Head (Cape Lambton Uplift), Dissection Creek, Storkerson Bay (Big River Basin), the Nanuk D-76 and Uminmak H-07 wells (Storkerson Uplift), and at Cape Crozier. Fluvial and deltaic sedimentation probably persisted for part of Albian time in the Cape Lambton Uplift area, as suggested by the marine Albian foraminifera in the upper part of the Isachsen Formation at Sandhill River (Table 1, Fig. 86). Elsewhere a passive marine inundation took place and the nonmarine Isachsen Formation passes upward abruptly but conformably into the marine shale of the Christopher Formation. Similar contemporaneous rocks in Anderson Basin comprise the Horton River Formation (Table 1).

Sedimentary structures and foraminiferal assemblages indicate an intertidal to outer shelf environment for the report-area during Albian time. Shale, which comprises the bulk of the Christopher Formation, represents offshore sedimentation, probably below wave base. Wave or tide influence is indicated by minor sandy units, which record the development of local shoals or other areas of high energy (such as an area swept by tidal currents). Nearshore sand and shell banks are present locally, as at Atitok River (Pl. 8). The clastic detritus within them is similar to that comprising the bulk of the Isachsen Formation, which suggests that the material was derived from the same Proterozoic source.

The Hassel Formation records a discrete regressive phase at the end of Albian time. This unit is present immediately below a regional mid-Cretaceous disconformity that represents emergence and uplift at the end of the Albian. The

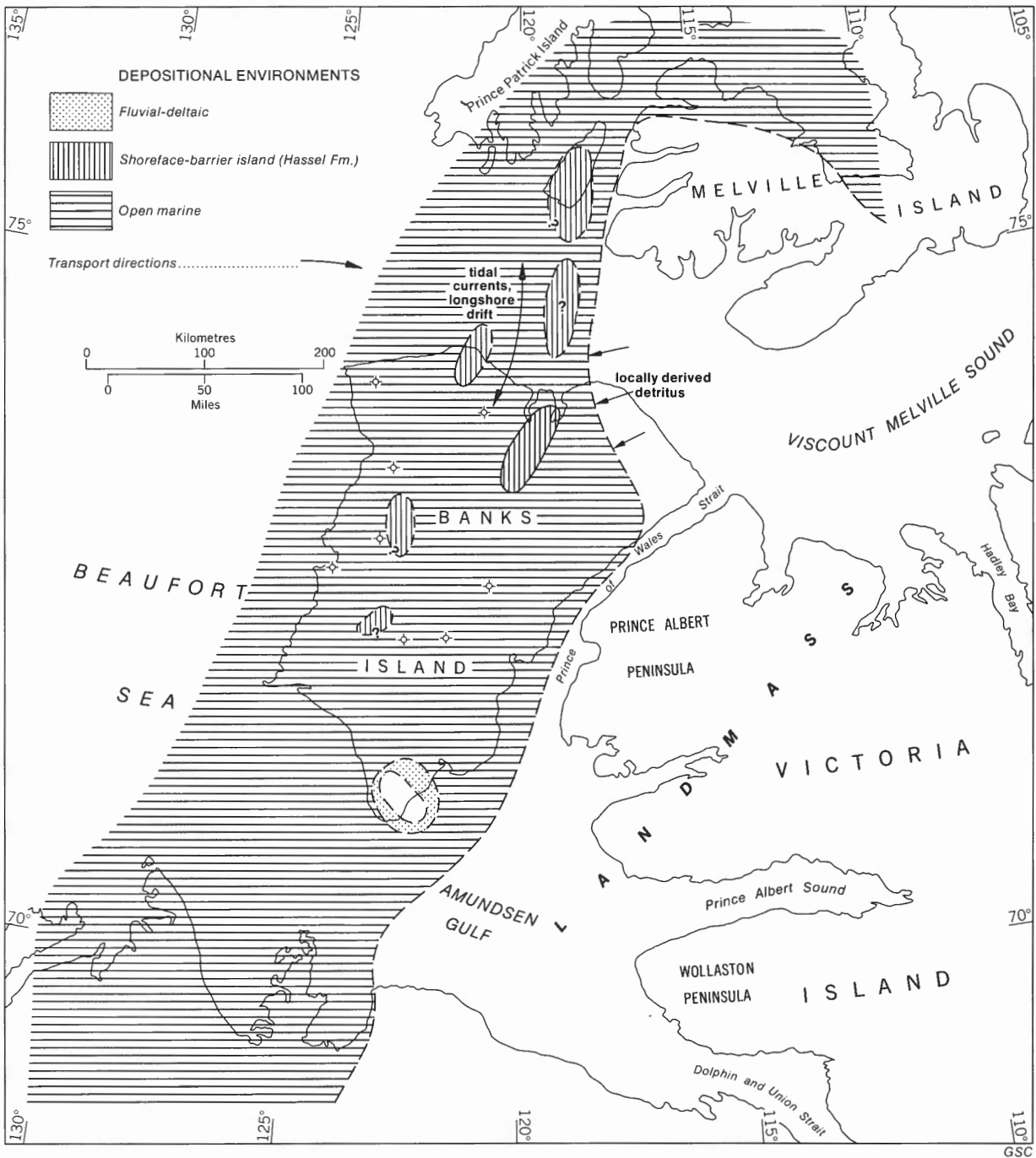


Figure 86. Paleogeographic synthesis for Albian time.

typical Hassel is known only on the margins of Northern Banks Basin, at Cape Crozier Anticline and between Investigator Point and Muskox River (Fig. 12). The Castel Bay C-68 well contains a shaly facies. The formation may have been deposited elsewhere, for example on Storkerson Uplift (as suggested in Fig. 86) and other positive areas, and subsequently removed during mid-Cretaceous erosion. No beds equivalent to the Hassel are present in Anderson Basin, to the south, whereas in Sverdrup Basin the formation is considerably thicker than in the report-area and includes

several different facies.

The Hassel, exposed at the surface in Banks Island, consists of fine-grained sand and sandy silt containing a marine microfauna. The vertical succession, including the basal beds transitional with the Christopher Formation, forms a typical regressive marine sequence up to 50 m (164 ft) thick. Sedimentary structures in the lower and middle parts of the unit are considered to indicate subtidal environments. They include flaser and lenticular bedding in the lowermost beds, probably formed under an alternation of quiet water and

storm or spring-tide conditions, below normal wave base. Above these beds is a facies characterized by a variety of small-scale ripple marks and high- and low-angle planar and trough crossbedding (Fig. 51), probably indicating deposition in various parts of the active wave breaker and surge zone. The sequence commonly is capped by a bioturbated, silty facies thought to be lagoonal in origin. In summary, the Hassel Formation as it outcrops at the surface is interpreted as having been formed in a barrier island environment during a period of marine regression. The shaly Hassel facies in the Castel Bay C-68 well probably represents an offshore, open-marine environment. Paleocurrent measurements (Fig. 53) have a polymodal distribution. As Klein (1970) has shown, this is characteristic of deposits formed under the influence of waves and tides, in which current directions undergo irregular fluctuations and daily reversals. The modes are, however, subparallel or subperpendicular to the axis of Northern Banks Basin, and this indicates that the latter probably controlled the shape and orientation of the sand bars that would presumably parallel the coastline.

Emergence of the surrounding land areas is indicated by the petrography of the Hassel sand. The mineral assemblage is quite different from that of the Isachsen and Christopher sands; it shows a greater degree of mineralogical immaturity, including a significantly higher proportion of feldspar fragments. These characteristics, and the finer grain size of the Hassel, indicate a different provenance, which probably was the Devonian rocks outcropping in northern and northeastern Banks Island—principally the Upper Devonian Melville Island Group. Cliffs in the Devonian sediments probably were present along the Albian shoreline and provided the bulk of the Hassel sand. Short-distance transportation is indicated, rather than extensive longshore drift, and this seems to be confirmed by the fact that the mineralogy of the Hassel varies according to which part of the Melville Island Group the formation overlies.

Cenomanian to Santonian

The Cenomanian and Turonian were times of maximum uplift within the report-area. The sea may have retreated altogether during the Cenomanian but it returned to Big River Basin probably during the Turonian, this being the age of the oldest post-Christopher strata at the Storkerson Bay A-15 well (the basal Kanguk Formation), as based on tentative foraminifera identifications. A regression also took place in Eglinton and Prince Patrick islands and on the Arctic mainland (Anderson Basin) at the end of the Early Cretaceous and, as far as is known from the sedimentary record, the sea has not returned to Prince Patrick Island since that time. A similar break in sedimentation occurred in the Beaufort-Mackenzie Basin and in the Yukon Coastal Plain (Chamney, 1973; Young, 1975) and also in Anderson Basin (Yorath *et al.*, 1975), whereas in parts of Sverdrup Basin sedimentation was continuous from Early to Late Cretaceous time (Stott, 1969).

The return of marine conditions reached Anderson Basin and the flanks of Storkerson Uplift (Nanuk D-76 and Uminmak H-07 locations) in the Santonian but may not have extended over Banks Basin and Eglinton Graben until the Campanian. According to Jeletzky (1971, p. 56), the Conia-

cian to mid-Santonian was the time of maximum extent of Cretaceous seas in the Canadian western interior and the Arctic.

A paleogeographic reconstruction of the report-area is given in Figure 87. Sediments of Turonian to Santonian age in Banks and Eglinton islands form the lower part of the Kanguk Formation. This is discussed in the next section.

Campanian and Maastrichtian

Several distinctive lithologies are present at the base of the Kanguk Formation. The most prominent of these, forming a useful marker bed for mapping purposes, is a unit of black, bituminous shale ranging from 2 to 15.2 m (6.6–49.9 ft) in thickness. Thin bentonite beds typically about 5 cm (2 in.) thick are common and several localities in southern Banks Island have beds of vitric tuff up to 21 cm (8 in.) thick. Spherulites of rhodochrosite (MnCO_3) are present in the basal Kanguk in Central Banks Basin and Big River Basin and, possibly, Northern Banks Basin. The manganese spherulites probably formed as a result of the volcanism, for volcanic rocks are capable of providing a suitable source of manganese, and the geochemical degradation processes which are assumed to have taken place have been observed in modern oceanic volcanic settings (as summarized by Miall, 1974d).

The source of the volcanism is still unknown. Bentonitic and tuffaceous beds of the same age are abundant in the Beaufort-Mackenzie Basin and in the northern Cordillera (D.W. Myhr, C.J. Yorath, *pers. com.*, 1974) and the Banks Island occurrences probably are related to the same source. A volcanic centre may have been located in the offshore to the west of Banks Island, or in the Cordilleran Geosyncline (fine-grained ash can travel for hundreds of kilometres if injected into high atmospheric jet streams). Analyses of tuff from southern Banks Island indicate an andesite-dacite source, a type of volcanism that is characteristic of continental edge (subduction zone?) rather than oceanic (spreading centre?) settings (Dickinson, 1974).

The bituminous shale is a widespread lithofacies, having been recorded in many parts of the Arctic Islands, the Arctic mainland (the Smoking Hills Formation of Yorath *et al.*, 1975), northern Yukon (Boundary Creek Formation of Young, 1975), and northern Alaska (upper member of the Ignek Formation of Keller *et al.*, 1961, p. 206). It records the existence of a euxinic environment of very wide aerial extent. Fish and marine pelecypod remains have been found in the shale, indicating that the sea was not inimical to all forms of life. The cause of the restriction of normal circulation is not clear. Possibly the arch that extends along the edge of the Arctic beneath the Arctic Coastal Plain formed a shallow bar or sill. Elements of this arch include Storkerson Uplift and Cape Crozier Anticline within the report-area, Aklavik Arch on the mainland (Lerand, 1973; Yorath and Norris, 1975) and the Sverdrup Basin rim (Meneley *et al.*, 1975).

The remainder of the Kanguk Formation records a paleogeographic setting very similar to that described for the Albian, as shown in Figure 88. An open-marine environment extended over much of the report-area, with the accumulation of a thick succession of silty shale derived from adjacent, low-lying land areas. Subtidal to intertidal, offshore sand bars formed over shoals such as Storkerson Uplift and Cape

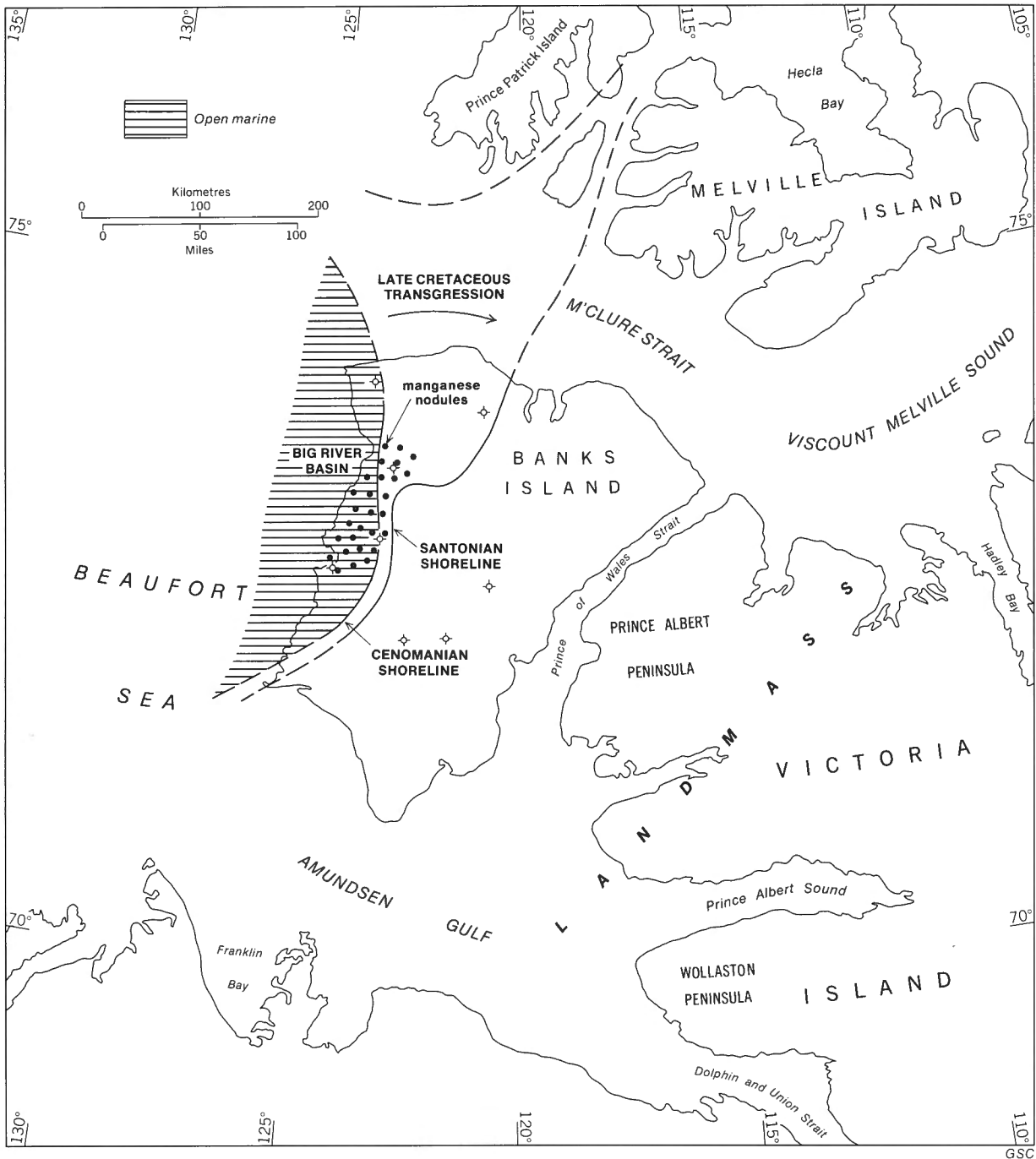


Figure 87. Paleogeographic synthesis for Cenomanian to Santonian time. Facies ornamentation as in Figure 86.

Crozier Anticline and these now comprise the lower and upper sand members of the Kanguk. Some long-range sediment transportation from Sverdrup Basin is indicated by the occurrence of Permian coral fragments in the upper sand member at Antler Cove. Sediments of similar age and lithology accumulated in Eglinton Graben and also in Anderson Basin, where they comprise the Mason River Formation of Yorath *et al.* (1975). The original extent of the Kanguk Formation may have been much greater than the present outcrop distribution would suggest. Dixon *et al.* (1973) recorded the occurrence of

typical Kanguk Formation in a faulted outlier in Somerset Island, 450 km (280 mi) south of the edge of Sverdrup Basin. Similarly, much of eastern Banks Island and Victoria Island may have been covered by the sea during the latest Cretaceous.

Paleocene and Eocene

The Paleogene is represented in Banks Island by the Eureka Sound Formation, a regressive, mainly nonmarine deposit formed in various deltaic environments. Coarse clastic

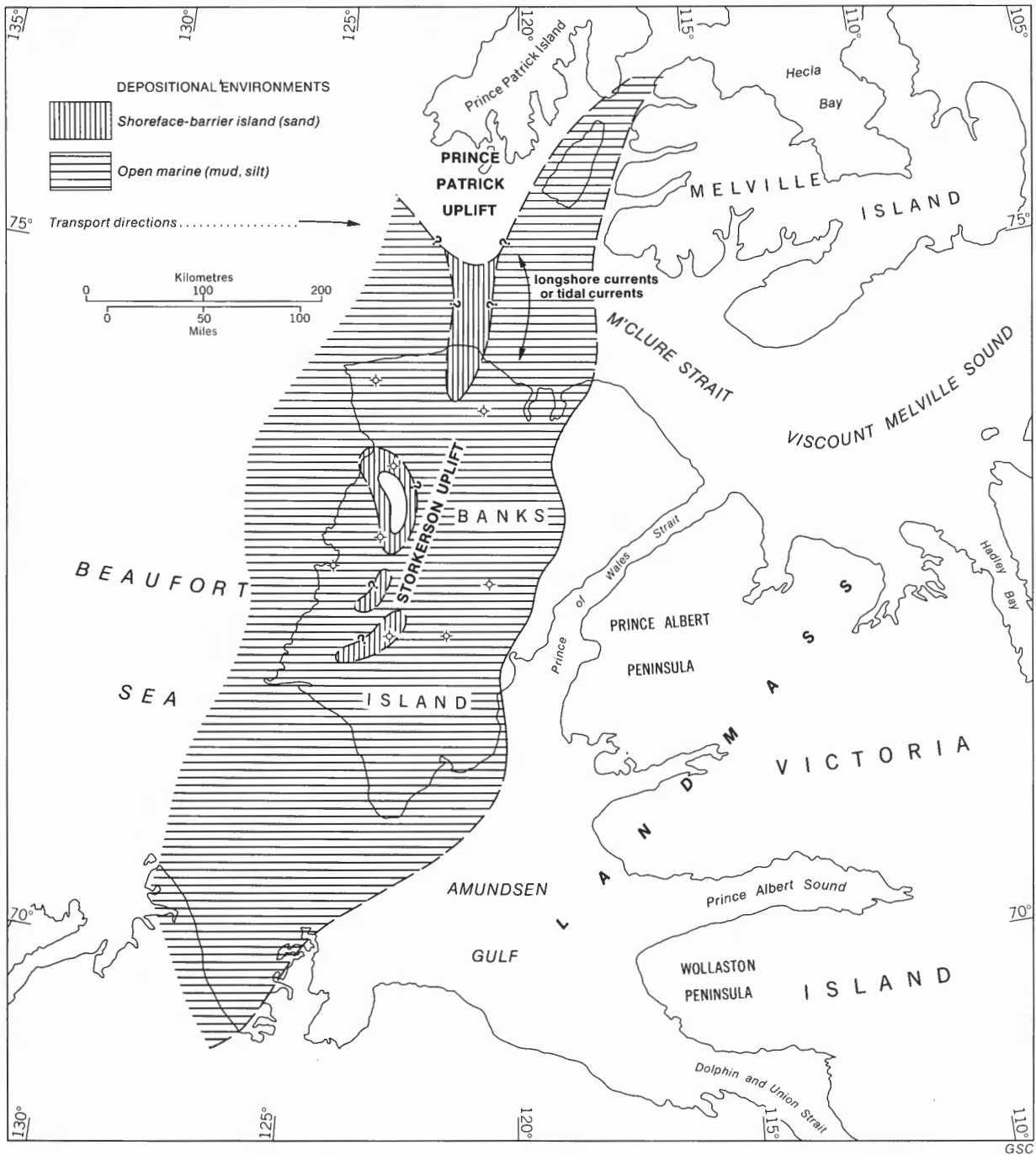


Figure 88. Paleogeographic synthesis for Campanian and Maastrichtian time. The sand members of the Kanguk Formation are not differentiated in this diagram. Facies ornamentation as in Figure 86.

sedimentation commenced at different times in different parts of the report-area, as shown in the two generalized paleogeographic maps (Figs. 89, 90). In Big River Basin the base of the formation, a coal-bearing, probably nonmarine shale, is of late Maastrichtian age, whereas elsewhere it is Paleocene. Coarser clastics of the proximal delta facies (the Cyclic Member) appeared in the Paleocene in Central Banks Basin and the eastern side of Northern Banks Basin, but not until the Eocene in the area of Cape Crozier Uplift and Big River Basin (Table 1). Throughout Eureka Sound sedimentation, marine

incursions are attested to by rare foraminifera, radiolarians, marine microplankton, and the trace fossil *Ophiomorpha*. The marine influence is particularly apparent in the centre of Northern Banks Basin, where locally bimodal current directions suggest wave or tide influence on sedimentation.

The Cyclic Member was formed by the lateral and vertical accretion of delta lobes, building out into the basinal areas by the progradation of distributaries from a few major trunk streams. At least four such lobes can be mapped on the basis of varying energy levels, as revealed by sedimentary

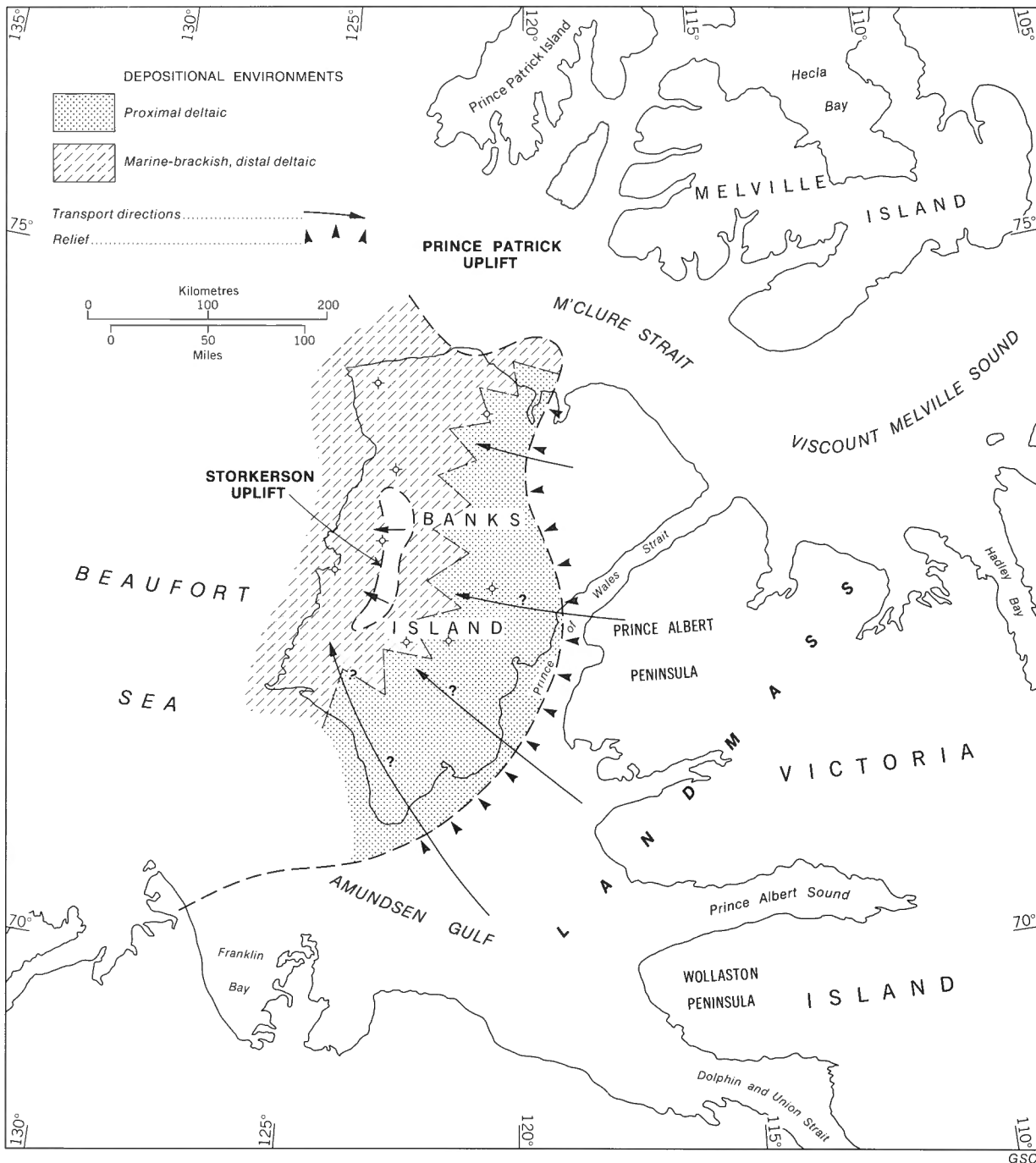


Figure 89. Paleogeographic synthesis for Paleocene time.

structure assemblages (Fig. 73); two lobes of Paleocene age enter the east side of Northern Banks Basin and two of Eocene age prograde out from Cape Crozier Uplift. Others undoubtedly exist in the subsurface. The deltas were about 20 km (13 mi) in radius and appear in plan view to have been of semicircular or birdsfoot shape. They are composed of a series of coarsening-upward cycles grading from shale to sand and commonly capped by soil and lignite coal. The cycles average 7.4 m (24.2 ft) in thickness. They are interpreted as the product of prograding distributaries; the shale represents a

delta front deposit, the sand a mouth bar or channel deposit and the soil-coal couplet a product of the delta-top marsh environment. Vertical repetition of such sequences was achieved by lateral channel migration or avulsion, subsidence, compaction and the commencement of a new cycle of progradation. These minor cycles built thicknesses of up to 140 m (470 ft), forming coarsening-upward megacycles, as seen in subsurface logs (Fig. 8). The thickness of the minor cycles varies according to position within the present-day basins, thicker cycles occurring nearer the basin centres (Fig. 71). This

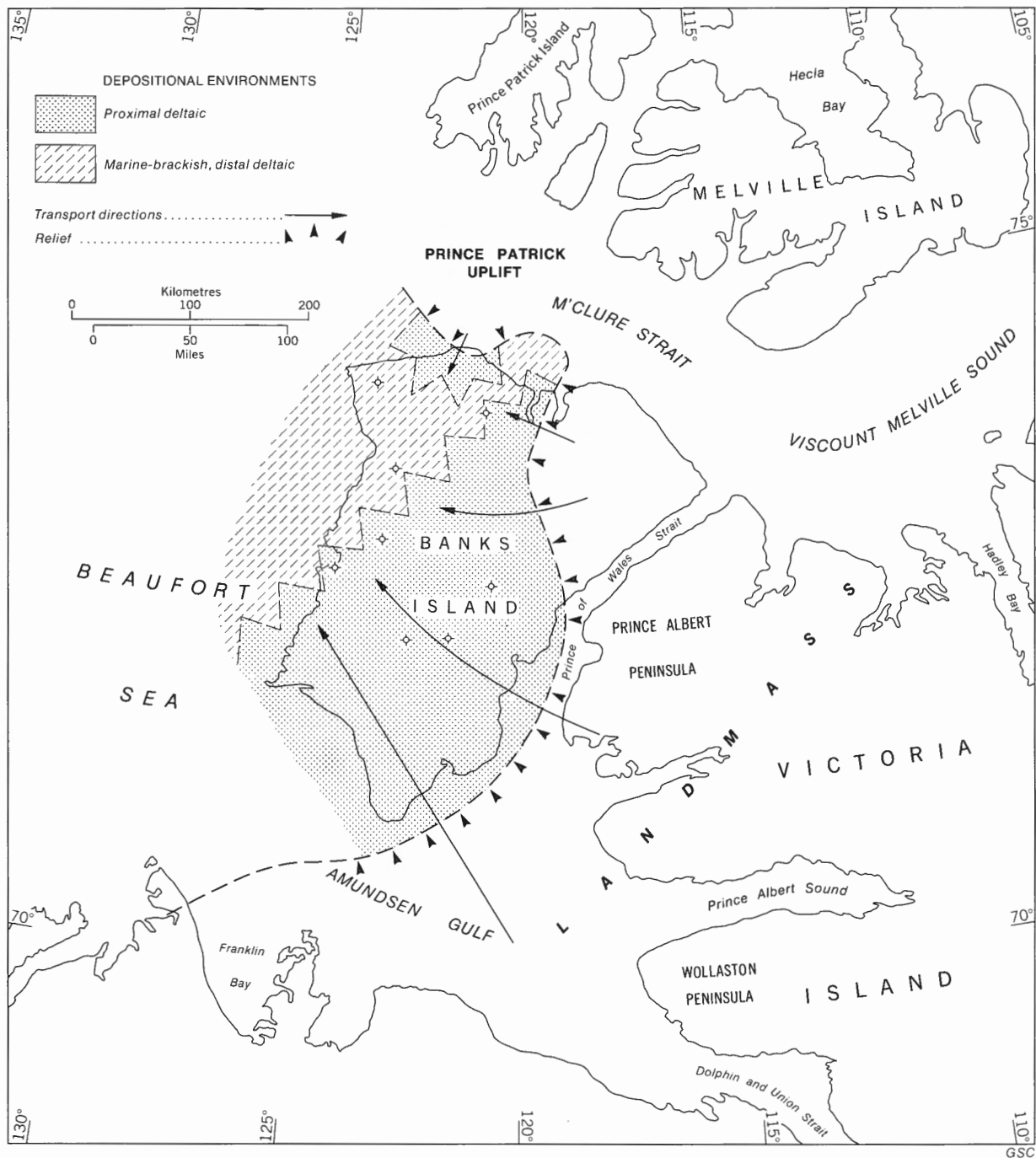


Figure 90. Paleogeographic synthesis for Eocene time.

indicates that the current structurally negative elements were depositional basins during the Paleogene, as they were during much of the Cretaceous.

Studies of paleocurrent patterns confirm the above interpretations. Flow directions fan out within each delta lobe (Figs. 72, 73), but the mean directions are parallel to the present-day structural dip of Banks Basin, as revealed by gravity data (Fig. 4).

Petrographic data indicate that the Eureka Sound Formation was derived mainly from the Upper Devonian Melville

Island Group, although significant quantities of chert must represent erosion of the lower Paleozoic or Proterozoic succession as well. The Nanuk Formation of Middle Devonian age (Miall, 1976a) probably provided a major source of chert, particularly for the Cyclic Member in Big River Basin, which was probably derived in part from Storkerson Uplift. Proterozoic clastic rocks provided an important local source for the Eureka Sound in southern Banks Island. Contemporaneous volcanic activity somewhere outside the report-area is indicated by glass shards and pumice.

Paleohydrological reconstructions (Tables 32, 33) indicate that the rivers flowing into Banks and Big River basins were smaller, in terms of discharge and drainage area, than those which deposited the Isachsen Formation, although the difference is not reflected in the volume of sediment that accumulated because of the different lengths of time represented by the two formations. The Isachsen (Barremian-Aptian) was deposited over a period of no longer than 12 million years, whereas the Eureka Sound (Paleocene-Eocene) represents 20 to 30 million years of sedimentation. The relative relief between basin and source area presumably was maintained or even slightly increased through Paleogene time, because Eocene sections near the centre of Northern Banks Basin contain more sand and a greater number of cycles than do Paleocene sections along the eastern margins of the basin. Storkerson Uplift could never have been a major sediment source because of its small size, and it became submerged beneath a flood of detritus from the craton to the east or possibly from the south, at some time during deposition of the Cyclic Member.

Oligocene and Miocene

Eureka Sound sedimentation terminated at some time during the Eocene, and Beaufort sedimentation commenced in the middle Miocene. During the interval between, uplift and tectonic deformation took place and the structural geology of the report-area assumed approximately its present form. Major fault movements occurred: for example, part or all of the 900 m (3000 ft) throw on the Nelson Head fault and the 300 m (1000 ft) throw on the fault forming the east side of Cape Crozier Anticline. Other faults, such as Nelson Head Graben, were in existence already but show evidence of minor additional movement in the post-Late Cretaceous, probably during the Neogene. The Cape Kellett Fault Zone (Lerand, 1973) off the southwest tip of Banks Island may have been initiated at this time.

Erosion followed uplift, and the next sedimentary unit, the Beaufort Formation, unconformably overlies several different Mesozoic and Tertiary units as a result. Detritus that formed during the Oligocene and Miocene presumably was carried beyond the present report-area, probably into what are now offshore areas to the west, where a prograding wedge of sediment several thousands of metres thick accumulated (stratigraphic relationships shown for the Cape Kellett area by Lerand, 1973, Figs. 15-17, are assumed to be similar to those prevailing throughout the offshore regions west of Banks Island). In middle Miocene time, peneplanation had proceeded far enough for these sediments to 'backfill' on to the present areas of western Banks and Prince Patrick islands, to form the middle to upper Miocene Beaufort Formation. A fluvial mode of origin is assumed for this unit, which consists of sand, gravel, clay and peat. Paleocurrent data indicate that the streams were generally westerly flowing within the report-area (Hills and Fyles, 1973).

Post-Miocene

Very gentle folding and minor fault movement have taken place since the deposition of the Beaufort. As shown in Figure 84, two broad, dome-shaped structures have developed in the

basal Beaufort unconformity surface, which probably have little or no relationship to the shape of the Beaufort depositional surface. Each dome is offset to the east from an older uplift (Cape Crozier Anticline and Storkerson Uplift) for reasons that are not yet clear. Minor post-Beaufort faulting has taken place in Prince Patrick Island (Tozer and Thorsteinsson, 1964, p. 192) and western Banks Island.

Subsequently, downcutting has caused the dissection of

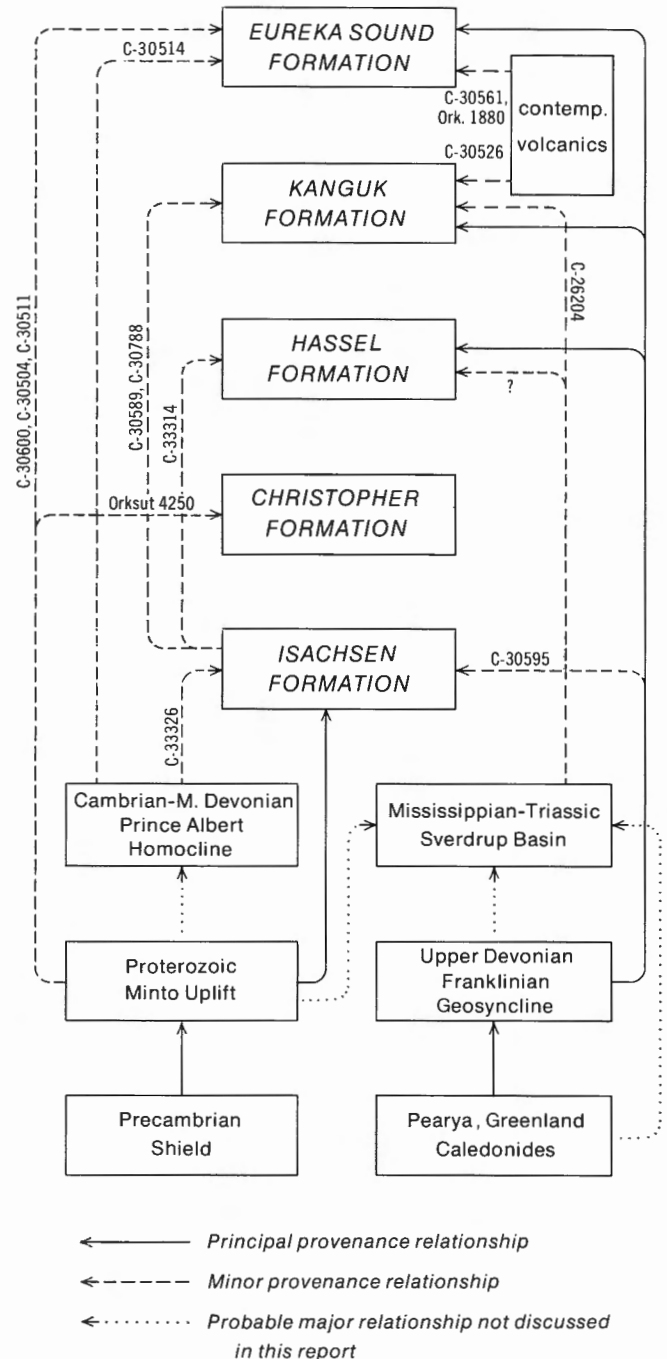


Figure 91. Detrital flow chart showing interpreted relationships among the Mesozoic-Tertiary units of Banks Island and their principal source rocks. The minor relationships are deduced from a very few samples, for which sample numbers are given.

the Beaufort and underlying deposits. The drainage system which evolved at this time probably was modified by rift-faulting in some of the interisland areas such as M'Clure Strait. Trettin *et al.* (1972, Fig. 20) showed the river pattern which has been deduced for the latest Tertiary.

The final major event that affected the report-area was the Quaternary glaciation, which will not be discussed in this report. Sedimentation in the offshore areas probably continued to the present, adding to the upper Tertiary-Quaternary offshore equivalents and successors of the Beaufort Formation.

Detrital flow chart

The various arguments presented in Chapter 3 regarding clastic sources have been summarized in a single diagram, Figure 91. The purpose of the diagram is to demonstrate the varying importance through time of the major and minor source rocks and to summarize the conclusions regarding the ultimate (first-cycle) origin of the detritus.

Regional tectonic considerations

The report-area comprises a series of pericratonic basins and uplifts, many of which are fault controlled. It is situated at the junction of several contrasting structural provinces (Sverdrup Basin, Arctic Platform, Beaufort-Mackenzie Basin) and partly overlaps a series of earlier, Paleozoic cratonic arches and troughs, including Minto Uplift, Coppermine Arch and Hazen Trough (Miall, 1976a). There were major changes in tectonic trends between the mid-Paleozoic (Devonian) and the Mesozoic. Coppermine Arch persisted as a mildly positive axis but Hazen Trough contracted and became divided into two parts by the appearance of Storkerson Uplift and Cape Crozier Anticline. The Ikkariktok M-64 and Tiritchik M-48 well locations were at the edge of the trough during the Devonian but from Jurassic to Paleogene time they formed part of the shelf edge.

Although Mesozoic-Tertiary sedimentation commenced in the Jurassic within the report-area, there is no evidence for the existence of the new tectonic elements until mid-Early Cretaceous time, when the existence of Banks Basin is clearly demonstrated by the distribution and sedimentary history of the Isachsen Formation. Storkerson Uplift and Cape Crozier Anticline probably were land areas at this time. They form part of a tectonic trend that, at least in part, had a much earlier origin. Cape Crozier Anticline is part of Prince Patrick Uplift, as defined by Thorsteinsson and Tozer (1960), and the latter constitutes the southern end of the Sverdrup Basin rim, which Meneley *et al.* (1975) showed to have been active since the Carboniferous. Whether this trend was active in the report-area at the time is not known but the lack of any evidence, such as a clastic wedge in the Jurassic rocks, would suggest that, if present, the uplift could have displayed very little relief.

The differential uplift and clastic sedimentation that ensued in Barremian-Aptian time are a local reflection of what appears to have been a widespread series of tectonic events in the North American Arctic. Minto Uplift and, probably, Storkerson Uplift-Cape Crozier Anticline underwent strong positive movements, while Banks Basin and Cardwell Basin

subsided. This differential movement within what are relatively small tectonic elements is one of the main reasons for classifying Banks Island as part of the Unstable Craton Margin. In the Sverdrup Basin area, cratonic uplift to the south resulted in a flood of detritus entering the basin between Valanginian and Aptian time (Stott, 1969; Roy, 1973, 1974). To the south, clastic sediments of the Langton Bay Formation (Valanginian-Albian) were derived from uplift of the Brock River area of Coppermine Arch (Yorath *et al.*, 1969, 1975). Faulting and syntectonic clastic sedimentation characterized the Beaufort-Mackenzie Basin during the Lower Cretaceous (Hawkings and Hatlelid, 1975, p. 639; Young *et al.*, 1976). Movement was localized along the north side of Aklavik Arch. In northern Yukon, uplift and erosion took place in the late Aptian and a flyschoid succession developed in the Aptian-Albian within a fault-bounded trough (Jeletzky, 1961; Young, 1973, 1974).

Yorath and Norris (1975) suggested that this tectonic activity may be related to sea-floor spreading in the Arctic Ocean and they proposed that the spreading centre was located in the approximate position of the continental slope west of the Canadian Arctic Islands, where a line of prominent, positive, free-air gravity anomalies is situated. Their interpretation of these anomalies is that they represent the uplifted edge of the crustal continental margin over a fossil oceanic ridge. Sobczak (1975a, b) disagreed with this interpretation and related the gravity anomalies to isostatically uncompensated recent sediments underlying the continental slope. Yorath and Norris (1975) suggested that asymmetric spreading on this axis took place in conjunction with transcurrent movement on the Kaltag Fault-Rapid Fault array. The ridge remained coupled to the Arctic Islands continental crust and, following (temporary?) cessation of movement, thermal contraction may have caused the development of tensional features such as grabens, of which Banks Basin-Eglinton Graben may be an example.

This reconstruction is speculative and its application to other parts of the Arctic is beyond the scope of the present report. No plate tectonic reconstructions that have yet appeared have explained satisfactorily all the known features of circum-Arctic geology, although the reader is referred to a synthesis by Hughes (1975, *see especially discussion of Fig. 4*) which appears to answer many of the problems raised by earlier workers.

Volcanism in the Late Cretaceous and Paleogene may have no relationship to an Arctic Ocean spreading centre. The tuffs in southern Banks Island are andesite-dacite in composition, which indicates that they are unlikely to have been derived from any oceanic volcanic activity. Cordilleran volcanism, possibly related to subduction, is a more likely origin for the material.

Maastrichtian to Eocene tectonic movements, which caused elevation of Storkerson Uplift and the shelf and initiated Eureka Sound sedimentation, were part of the Eureka Orogeny. The orogeny is related to a newer pattern of plate movements that has continued to the present day, including the opening of the Atlantic and the westward drift of North America. In the Unstable Craton Margin, including Banks Island, differential movements were relatively gentle, in contrast to the eastern Sverdrup Basin where major thrust

movements and the development of thick clastic wedges occurred. According to Harland (1975, p. 242), Greenland separated from Labrador during the Paleogene and probably was displaced slightly from the Arctic Islands by sinistral movement along Nares Strait. The Canadian Arctic Islands were compressed with an anticlockwise rotation movement. Sinistral displacement along M'Clure Strait–Viscount Melville Sound possibly took place at the same time, accounting for the apparent offset between Banks Basin and Eglinton Graben.

Assessment of sedimentological methods

The bulk of this report has been concerned with the use of various sedimentological techniques in an analysis of depositional environments and paleogeographic evolution. It is worthwhile, finally, to evaluate which techniques have been the most successful or the most efficient in contributing to the final synthesis.

The study of lithofacies variations and sedimentary structure assemblages has permitted direct comparisons with a variety of modern sedimentary environments and has enabled detailed analyses to be carried out of the depositional settings of the various units. Careful observation and classification of sedimentary structures in the field are fundamental to this type of work.

Next in usefulness in this study are petrographic and paleocurrent analyses. Paleocurrent measurements normally are made to investigate the orientation of regional paleoslope. A study of the number of orientation modes can, as in the present case, provide additional information regarding depositional environment. The orientation of these modes relative to tectonic elements has provided important information on the development of basins and highs during the Cretaceous and Tertiary. Detailed local analyses of paleocurrent information have improved the level of interpretation of the fluvial and deltaic rocks in the succession by providing information

regarding channel sinuosity and relative stream competency.

Petrographic analyses of detrital components have been of importance in determining the nature of the source rocks. These have been identified as rocks outcropping mainly to the south and east of Banks Island, as suggested by paleocurrent analysis. The sequence of source rocks that appears in successively younger formations has provided useful information regarding the unroofing history of structurally elevated areas such as Minto Uplift. Most of these conclusions are based on a study of light density minerals in thin section, which generally are easier to study than heavy minerals. Little is known regarding heavy mineral suites in the source rocks, which also makes interpretation of derived assemblages difficult.

Paleohydrological analysis of fluvial and deltaic systems has been attempted but the techniques still are primitive and the results subject to a wide range of possible error. The main contributions of the work have been to allow comparisons with modern rivers and to determine the probable size of the drainage area during the two principal periods of subaerial erosion (mid–Early Cretaceous, Paleogene). The results are not accurate enough to stand on their own but it is significant that they are consistent with conclusions derived from the petrographic work. This would suggest that the techniques can be useful and that they are worth further study and refinement.

Grain size analyses have contributed little to this study. They provide important basic descriptive data but interpretation of the size distributions was beset with difficulties. Many factors influence the latter, including the size distribution of the source sediments, abrasion during transport and the nature of the depositional environment. A considerable number of samples would be necessary to separate out the various effects, whereas much of the information that supposedly can be obtained from grain size studies is more easily derived by other means. Difficulties with the sonic sifter as a result of static electricity have been noted in the section on 'methods'.

References

- Agterberg, F.P., Hills, L.V. and Trettin, H.P.
1967: Paleocurrent trend analysis of a delta in the Bjorne Formation (Lower Triassic) of northwestern Melville Island, Arctic Archipelago; *J. Sediment. Petrol.*, v. 37, p. 852-862.
- Allen, J.R.L.
1963: The classification of cross-stratified units with notes on their origin; *Sedimentology*, v. 2, p. 93-114.
1964: Studies in fluvial sedimentation: six cyclothems from the Lower Old Red Sandstone, Anglo-Welsh Basin; *Sedimentology*, v. 3, p. 163-198.
1965: Fining-upward cycles in alluvial successions; *Geol. J.*, v. 4, p. 229-246.
1966: On bed forms and paleocurrents; *Sedimentology*, v. 6, p. 153-190.
1968: Current ripples, their relation to patterns of water and sediment motion; North Holland Pub. Co., Amsterdam.
1970a: Sediments of the modern Niger delta: a summary and review; in *Deltaic sedimentation: modern and ancient*, J.P. Morgan, ed.; Soc. Econ. Paleontol. Mineral., Spec. Publ. 15, p. 138-151.
1970b: Studies in fluvial sedimentation; a comparison of fining-upward cyclothems, with special reference to coarse-member composition and interpretation; *J. Sediment. Petrol.*, v. 40, p. 298-323.
- Allen, J.R.L. and Banks, N.L.
1972: An interpretation and analysis of recumbent-folded deformed crossbedding; *Sedimentology*, v. 19, p. 257-284.
- Allen, P.
1972: Wealden detrital tourmaline: implications for northwestern Europe; *J. Geol. Soc. London*, v. 128, p. 273-294.
- Allman, M. and Lawrence, D.F.
1972: Geological laboratory techniques; Blandford Press, London.
- Andersen, D.W. and Picard, M.D.
1974: Evolution of synorogenic clastic deposits in the Intermontane Uinta Basin of Utah; in *Tectonics and sedimentation*, W.R. Dickinson, ed.; Soc. Econ. Paleontol. Mineral., Spec. Publ. 22, p. 167-189.
- Balkwill, H.R.
1973: Structure and tectonics of Cornwall Arch, Amund Ringnes and Cornwall Islands, Arctic Archipelago; in *Proc. Symp. Geology of the Canadian Arctic*, Saskatoon, Sask., May 1973, J.D. Aitken and D.J. Glass, eds.; Geol. Assoc. Can. and Can. Soc. Pet. Geol., p. 39-62.
- Balkwill, H.R. and Bustin, R.M.
1975: Stratigraphic and structural studies, central Ellesmere Island and eastern Axel Heiberg Island, District of Franklin; *Geol. Surv. Can.*, Paper 75-1A, p. 513-517.
- Banks, N.L. and Collinson, J.D.
1974: Discussion of "some sedimentological aspects of planar cross-stratification in a sandy braided river"; *J. Sediment. Petrol.*, v. 44, p. 265-267.
- Barnes, C.R., Brideaux, W.W., Chamney, T.P., Clowser, D.R., Dunay, R.E., Fisher, M.J., Fritz, W.H., Hopkins, W.S., Jr., Jeletzky, J.A., McGregor, D.C., Norford, B.S., Norris, A.W., Pedder, A.E.H., Rauwerda, P.J., Sherrington, P.F., Sliter, W.V., Tozer, E.T., Uyeno, T.T. and Waterhouse, J.B.
1974: Biostratigraphic determinations of fossils from the subsurface of the Northwest and Yukon territories; *Geol. Surv. Can.*, Paper 74-11.
- Bennett, C.A. and Franklin, N.L.
1954: Statistical analysis in chemistry and the chemical industry; Wiley, New York.
- Bernard, H.A., Leblanc, R.J. and Major, C.F.
1963: Recent and Pleistocene geology of southeast Texas; in *Geology of the Gulf Coast and central Texas, and guidebook excursions*, E.H. Rainwater and R.P. Zingula, eds.; Houston Geol. Soc., Houston, Texas, p. 175-224.
- Billingsley, P.
1961: Statistical methods in Markov Chains; *Ann. Math. Statist.*, v. 32, p. 12-40.
- Blatt, H.
1967: Original characteristics of clastic quartz grains; *J. Sediment. Petrol.*, v. 37, p. 401-424.
- Blatt, H. and Christie, J.M.
1963: Undulatory extinction in quartz of igneous and metamorphic rocks and its significance in provenance studies of sedimentary rocks; *J. Sediment. Petrol.*, v. 33, p. 559-579.
- Bourne, S.A. and Pallister, A.E.
1973: Offshore areas of Canadian Arctic Islands - geology based on geophysical data; in *Arctic Geology*, M.G. Pitcher, ed.; Am. Assoc. Pet. Geol., Mem. 19, p. 48-56.
- Brice, J.C.
1964: Channel patterns and terraces of the Loup Rivers in Nebraska; U.S. Geol. Surv., Prof. Paper 422-D.
- Brideaux, W.W., Chamney, T.P., Dunay, R.E., Fritz, W.H., Hopkins, W.S., Jr., Jeletzky, J.A., McGregor, D.C., Norford, B.S., Norris, A.W., Pedder, A.E.H., Sherrington, P.F., Sliter, W.V., Sweet, A.R., Uyeno, T.T. and Waterhouse, J.B.
1975: Biostratigraphic determinations of fossils from the subsurface of the Districts of Franklin and Mackenzie; *Geol. Surv. Can.*, Paper 74-39.
- Brideaux, W.W., Clowser, D.R., Copeland, M.J., Jeletzky, J.A., Norford, B.S., Norris, A.W., Pedder, A.E.H., Sweet, A.R., Thorsteinsson, R., Uyeno, T.T. and Wall, J.H.
1976: Biostratigraphic determinations from the subsurface of the Districts of Franklin and Mackenzie and the Yukon Territory; *Geol. Surv. Can.*, Paper 75-10.
- Bull, W.B.
1972: Recognition of alluvial fan deposits in the stratigraphic record; in *Recognition of ancient sedimentary environments*, J.K. Rigby and W.K. Hamblin, eds.; Soc. Econ. Paleontol. Mineral., Spec. Publ. 16, p. 63-83.
- Cant, D.J. and Walker, R.G.
1976: Development of a braided-fluvial facies model for the Devonian Battery Point sandstone, Quebec; *Can. J. Earth Sci.*, v. 13, p. 102-119.
- Carlston, C.W.
1965: The relation of free meander geometry to stream discharge and its geomorphic implications; *Am. J. Sci.*, v. 263, p. 864-885.
- Cassan, J.P. and Evers, J.H.
1973: The Cretaceous Isachsen, Christopher and Hassel Formations on Banks Island, N.W.T. - a sedimentological interpretation (abst.); in *Program and abstracts, Symp. Geology of the Canadian Arctic*, Saskatoon, Sask., May 1973; Can. Soc. Pet. Geol. and Geol. Assoc. Can.
- Chamney, T.P.
1971: Tertiary and Cretaceous biostratigraphic divisions in the Reindeer D-27 borehole, Mackenzie River delta; *Geol. Surv. Can.*, Paper 70-30.
1973: Tuktoyaktuk Peninsula Tertiary and Mesozoic biostratigraphy correlations; *Geol. Surv. Can.*, Paper 73-1B, p. 171-178.

- Christie, R.L.
1972: Central Stable Region; *in* The Canadian Arctic Islands and the Mackenzie Region; XXIV Int. Geol. Congr., Excursion A66, p. 40-87.
- Cleary, W.J. and Conolly, J.R.
1971: Distribution and genesis of quartz in a piedmont-coastal plain environment; *Bull. Geol. Soc. Am.*, v. 82, p. 2755-2766.
- Clifton, H.E., Hunter, R.E. and Phillips, R.L.
1971: Depositional structures and processes in the non-barred high energy nearshore; *J. Sediment. Petrol.*, v. 41, p. 651-670.
- Coleman, J.M.
1969: Brahmaputra River: channel processes and sedimentation; *Sediment. Geol.*, v. 3, p. 129-239.
- Coleman, J.M. and Gagliano, S.M.
1964: Cyclic sedimentation in the Mississippi River deltaic plain; *Gulf Coast Assoc. Geol. Soc., Trans.*, v. 14, p. 67-80.
- Collinson, J.D.
1970: Bedforms of the Tana River, Norway; *Geogr. Ann.*, v. 52A, p. 31-56.
- Conant, L.C. and Swanson, V.E.
1961: Chattanooga Shale and related rocks of central Tennessee and nearby areas; *U.S. Geol. Surv., Prof. Paper* 357.
- Costello, W.R. and Walker, R.G.
1972: Pleistocene sedimentology, Credit River, southern Ontario: a new component of the braided river model; *J. Sediment. Petrol.*, v. 42, p. 389-400.
- Cotter, E.
1971: Sedimentary structures and the interpretation of paleoflow characteristics of the Ferron Sandstone (Upper Cretaceous), Utah; *J. Sediment. Petrol.*, v. 41, p. 129-138.
- Crook, K.A.W.
1968: Weathering and roundness of quartz sand grains; *Sedimentology*, v. 11, p. 171-182.
- Curray, J.R.
1956: The analysis of two dimensional orientation data; *J. Geol.*, v. 64, p. 117-131.
- Curtis, D.M.
1970: Miocene deltaic sedimentation, Louisiana Gulf Coast; *in* Deltaic sedimentation: modern and ancient, J.P. Morgan, ed.; *Soc. Econ. Paleontol. Mineral., Spec. Publ.* 15, p. 293-308.
- Davies, D.K., Ethridge, F.G. and Berg, R.R.
1971: Recognition of barrier environments; *Bull. Am. Assoc. Pet. Geol.*, v. 55, p. 550-565.
- Davis, J.H.
1973: *Statistics and data analysis in geology*; Wiley, New York.
- Detterman, R.L., Reiser, H.N., Brosgé, W.P. and Dutro, J.T., Jr.
1975: Post-Carboniferous stratigraphy, northeastern Alaska; *U.S. Geol. Surv., Prof. Paper* 886.
- DeWindt, J.T.
1974: Callianassid burrows as indicators of subsurface beach trend, Mississippi River Delta Plain; *J. Sediment. Petrol.*, v. 44, p. 1136-1139.
- Dickinson, K.A., Berryhill, H.L., Jr., and Holmes, C.W.
1972: Criteria for recognizing ancient barrier coastlines; *in* Recognition of ancient sedimentary environments, J.K. Rigby and W.K. Hamblin, eds.; *Soc. Econ. Paleontol. Mineral., Spec. Publ.* 16, p. 192-214.
- Dickinson, W.R.
1974: Sedimentation within and beside ancient and modern magmatic arcs; *in* Modern and ancient geosynclinal sedimentation, R.H. Dott, Jr. and R.H. Shaver, eds.; *Soc. Econ. Paleontol. Mineral., Spec. Publ.* 19, p. 230-239.
- Dixon, J., Hopkins, W.S., Jr., and Dixon, O.A.
1973: Upper Cretaceous marine strata on Somerset Island; *Can. J. Earth Sci.*, v. 10, p. 1337-1339.
- Doeglas, D.J.
1962: Structure of sedimentary deposits of braided rivers; *Sedimentology*, v. 1, p. 167-190.
- Dott, R.H., Jr.
1974: Cambrian tropical storm waves in Wisconsin; *Geology*, v. 2, p. 243-246.
- Duff, P. McL. D and Walton, E.K.
1962: Statistical basis for cyclothems: a quantitative study of the sedimentary succession in the East Pennine Coalfield; *Sedimentology*, v. 1, p. 235-256.
- Eicher, D.L.
1969: Paleobathymetry of Cretaceous Greenhorn Sea in eastern Colorado; *Bull. Am. Assoc. Pet. Geol.*, v. 53, p. 1075-1090.
- Elliott, T.
1974: Interdistributary bay sequences and their genesis; *Sedimentology*, v. 21, p. 611-622.
- Evans, C.R. and Staplin, F.L.
1970: Regional facies of organic metamorphism, geochemical prospecting for petroleum and natural gas; *Can. Inst. Min. Met., Spec. Vol.* 11, *Geochemical Explor.*, p. 517-520.
- Fahnestock, R.K.
1969: Morphology of the Slims River; *Icefield Ranges Res. Proj., Sci. Results*, v. 1, p. 161-172.
- Fisher, W.L., Brown, L.F., Scott, A.J. and McGowen, J.H.
1969: Delta systems in the exploration for oil and gas; *Bur. Econ. Geol., Univ. Texas at Austin*.
- Fisk, H.N.
1955: Sand facies of recent Mississippi delta deposits; *Proc. 4th World Pet. Congr., Rome, Sect. 1/C, Paper* 3, p. 377-398.
1961: Bar finger sands of Mississippi delta; *in* Geometry of sandstone bodies; *Am. Assoc. Pet. Geol.* p. 29-52.
- Friend, P.F. and Moody-Stuart, M.
1972: Sedimentation of the Wood Bay Formation (Devonian) of Spitsbergen; *Regional analysis of a late orogenic basin*; *Nor. Polarinst., Skr. Nr.* 157.
- Given, M.M. and Wall, J.H.
1971: Microfauna from the Upper Cretaceous Bearpaw Formation of south-central Alberta; *Bull. Can. Soc. Pet. Geol.*, v. 19, p. 502-544.
- Glaister, R.P. and Nelson, H.W.
1974: Grain-size distributions, an aid in facies identification; *Bull. Can. Pet. Geol.*, v. 22, p. 203-240.
- Gole, C.V. and Chitale, S.V.
1966: Inland delta building activity of Kosi River; *J. Hydraul. Div., Am. Soc. Civ. Eng.*, v. 92, HY2, p. 111-126.
- Gould, H.R.
1970: The Mississippi delta complex; *in* Deltaic sedimentation: modern and ancient, J.P. Morgan, ed.; *Soc. Econ. Paleontol. Mineral., Spec. Publ.* 15, p. 3-30.

- Gregory, K.J. and Walling, D.E.
1973: Drainage basin form and process; Edward Arnold, London.
- Greiner, H.R.
1963: Graham Island; *in* Geology of the north-central part of the Arctic Archipelago, Northwest Territories (Operation Franklin); Geol. Surv. Can., Mem. 320, p. 407-412.
- Griffiths, J.C.
1967: Scientific method in analysis of sediments; McGraw Hill, New York.
- Guy, H.P., Simons, D.B. and Richardson, E.V.
1966: Summary of alluvial channel data from flume experiments, 1956-61; U.S. Geol. Surv., Prof. Paper 462-I.
- Hack, J.T.
1957: Studies of longitudinal stream profiles in Virginia and Maryland; U.S. Geol. Surv., Prof. Paper 294-B, p. 45-97.
- Haller, J.
1971: Geology of the East Greenland Caledonides; Interscience, New York.
- Harbaugh, J.W. and Bonham-Carter, G.
1970: Computer simulation in geology; Wiley Interscience, New York.
- Harland, W.B.
1975: Phanerozoic relative motions of North Atlantic Arctic lands; *in* Canada's continental margins and offshore petroleum exploration, C.J. Yorath, E.R. Parker and D.J. Glass, eds.; Can. Soc. Pet. Geol., Mem. 4, p. 235-256.
- Harms, J.C., Southard, J.B., Spearing, D.R. and Walker, R.G.
1975: Depositional environments as interpreted from primary sedimentary structures and stratification sequences; Soc. Econ. Paleontol. Mineral., Short Course No. 2.
- Hawkings, T.J. and Hatlelid, W.G.
1975: The regional setting of the Taglu Field; *in* Canada's continental margins and offshore petroleum exploration, C.J. Yorath, E.R. Parker and D.J. Glass, eds.; Can. Soc. Pet. Geol., Mem. 4, p. 633-647.
- Heckel, P.H.
1972: Recognition of ancient shallow marine environments; *in* Recognition of ancient sedimentary environments, J.K. Rigby and W.K. Hamblin, eds.; Soc. Econ. Paleontol. Mineral., Spec. Publ. 16, p. 226-286.
- Heywood, W.W.
1955: Arctic piercement domes; Trans. Can. Inst. Min. Met., v. 58, p. 27-32.
1957: Isachsen area, Ellef Ringnes Island, District of Franklin, Northwest Territories; Geol. Surv. Can., Paper 56-8.
- Heywood, W.W. and Davidson, A.
1969: Geology of Benjamin Lake map-area; Geol. Surv. Can., Mem. 361.
- High, L.R., Jr., and Picard, M.D.
1968: Dendritic surge marks ("Dendrophycus") along modern stream banks; Wyoming Univ. Contr. Geol., v. 7, p. 1-6.
1974: Reliability of cross-stratification types as paleocurrent indicators in fluvial rocks; J. Sediment. Petrol., v. 44, p. 158-168.
- Hills, L.V.
1969: Beaufort Formation, northwestern Banks Island, District of Franklin; Geol. Surv. Can., Paper 69-1A, p. 204-207.
- Hills, L.V. and Fyles, J.G.
1973: The Beaufort Formation, Canadian Arctic Islands (abst.); *in* Program and abstracts, Symp. Geology of the Canadian Arctic, Saskatoon, Sask., May 1973; Can. Soc. Pet. Geol. and Geol. Assoc. Can.
- Hills, L.V. and Ogilvie, R.T.
1970: *Picea banksii* n. sp., Beaufort Formation (Tertiary), northwestern Banks Island, Arctic Canada; Can. J. Botany, v. 48, p. 457-464.
- Hodgson, W.A.
1966: Carbon and oxygen isotope ratios in diagenetic carbonates from marine sediments; Geochim. Cosmochim. Acta, v. 30, p. 1223-1233.
1968: The diagenesis of spherulitic carbonate concretions and other rocks from Mangakahia Group sediments, Kaipara Harbour, New Zealand; J. Sediment. Petrol., v. 38, p. 1254-1263.
- Hopkins, W.S., Jr.
1971: Palynology of the Lower Cretaceous Isachsen Formation on Melville Island, District of Franklin; Geol. Surv. Can., Bull. 197, p. 109-133.
- Hopkins, W.S., Jr., and Balkwill, H.R.
1973: Description, palynology and paleoecology of the Hassel Formation (Cretaceous) on eastern Ellef Ringnes Island, District of Franklin; Geol. Surv. Can., Paper 72-37.
- Howard, J.D.
1972: Trace fossils as criteria for recognizing shorelines in the stratigraphic record; *in* Recognition of ancient sedimentary environments, J.K. Rigby and W.K. Hamblin, eds.; Soc. Econ. Paleontol. Mineral., Spec. Publ. 16, p. 215-225.
- Hughes, T.
1975: The case for creation of the North Pacific Ocean during the Mesozoic Era; Palaeogeogr., Palaeoclimatol., Palaeoecol., v. 18, p. 1-43.
- James, N.P.
1972: Holocene and Pleistocene calcareous crust (caliche) profiles: criteria for subaerial exposure; J. Sediment. Petrol., v. 42, p. 817-836.
- Jeletzky, J.A.
1961: Eastern slope, Richardson Mountains: Cretaceous and Tertiary structural history and regional significance; *in* Geology of the Arctic, G.O. Raasch, ed.; Proc. 1st. Int. Symp. Arctic Geol., v. 1, p. 532-583.
1968: Macrofossil zones of the marine Cretaceous of the western interior of Canada and their correlation with the zones and stages of Europe and the western interior of the United States; Geol. Surv. Can., Paper 67-72.
1971: Marine Cretaceous biotic provinces and paleogeography of Western and Arctic Canada: illustrated by a detailed study of ammonites; Geol. Surv. Can., Paper 70-22.
- Jutard, G. and Plauchut, B.P.
1973: Cretaceous and Tertiary stratigraphy northern Banks Island; *in* Proc. Symp. Geology of the Canadian Arctic, Saskatoon, Sask., May 1973, J.D. Aitken and D.J. Glass, eds.; Geol. Assoc. Can. and Can. Soc. Pet. Geol., p. 203-219.
- Kanes, W.H.
1970: Facies and development of the Colorado River delta in Texas; *in* Deltaic sedimentation: modern and ancient, J.P. Morgan, ed.; Soc. Econ. Paleontol. Mineral., Spec. Publ. 15, p. 78-106.

- Keller, A.S., Morris, R.H. and Detterman, R.L.
1961: Geology of the Shaviovik and Sagavanirktok Rivers region, Alaska; U.S. Geol. Surv., Prof. Paper 303-D.
- Keller, W.D.
1970: Environmental aspects of clay minerals; *J. Sediment. Petrol.*, v. 40, p. 788–813.
- Kerr, J.Wm.
1974: Geology of Bathurst Island Group and Byam Martin Island, Arctic Canada (Operation Bathurst Island); *Geol. Surv. Can., Mem.* 378.
- Kerr, P.F.
1959: Optical mineralogy; McGraw Hill, New York.
- Klein, G. de V.
1970: Depositional and dispersal dynamics of intertidal sand bars; *J. Sediment. Petrol.*, v. 40, p. 1095–1127.
1971: A sedimentary model for determining paleotidal range; *Bull. Geol. Soc. Am.*, v. 82, p. 2585–2592.
1974: Estimating water depths from analysis of barrier island and deltaic sedimentary sequences; *Geology*, v. 2, p. 409–412.
- Klovan, J.E. and Embry, A.F. III
1971: Upper Devonian stratigraphy, northeastern Banks Island, N.W.T.; *Bull. Can. Pet. Geol.*, v. 19, p. 705–729.
- Krumbein, W.C.
1941: Measurement and geologic significance of shape and roundness of sedimentary particles; *J. Sediment. Petrol.*, v. 11, p. 64–72.
- Krumbein, W.C. and Dacey, M.F.
1969: Markov chains and embedded Markov chains in geology; *J. Int. Assoc. Math. Geol.*, v. 1, p. 79–96.
- Kumar, S. and Bhandari, L.L.
1973: Paleocurrent analysis of the Athgarh Sandstone (Upper Gondwana), Cuttack District, Orissa (India); *Sediment. Geol.*, v. 10, p. 61–75.
- Langbein, W.B. and Leopold, L.B.
1966: River meanders – theory of minimum variance; U.S. Geol. Surv., Prof. Paper 422-H.
- Langbein, W.B. and Schumm, S.A.
1958: Yield of sediment in relation to mean annual precipitation; *Am. Geophys. Union, Trans.*, v. 39, p. 1076–1084.
- Leeder, M.R.
1973: Fluvial fining-upward cycles and the magnitude of paleochannels; *Geol. Mag.*, v. 110, p. 265–276.
- Leopold, L.B., Wolman, M.G. and Miller, J.P.
1964: Fluvial processes in geomorphology; W.H. Freeman, San Francisco.
- Lerand, M.
1973: Beaufort Sea; *in* The future petroleum provinces of Canada, their geology and potential, R.G. McCrossan, ed.; *Can. Soc. Pet. Geol., Mem.* 1, p. 315–386.
- Lynn, D.C. and Bonatti, E.
1965: Mobility of manganese in diagenesis of deep-sea sediments; *Mar. Geol.*, v. 3, p. 457–474.
- Malde, H.E.
1968: The catastrophic Late Pleistocene Bonneville Flood in the Snake River Plain, Idaho; U.S. Geol. Surv., Prof. Paper 596.
- Mann, W.R. and Cavaroc, V.V.
1973: Composition of sand released from three source areas under humid, low relief weathering in the North Carolina Piedmont; *J. Sediment. Petrol.*, v. 43, p. 870–881.
- McCave, I.N.
1970: Deposition of fine-grained suspended sediment from tidal currents; *J. Geophys. Res.*, v. 75, p. 4151–4159.
- McGowen, J.H. and Garner, L.E.
1970: Physiographic features and stratification types of coarse-grained point bars; modern and ancient examples; *Sedimentology*, v. 14, p. 77–112.
- McKee, E.D., Crosby, E.J. and Berryhill, H.L., Jr.
1967: Flood deposits, Bijou Creek, Colorado; *J. Sediment. Petrol.*, v. 37, p. 829–851.
- Meneley, R.A., Henao, D. and Merritt, R.K.
1975: The northwest margin of the Sverdrup Basin; *in* Canada's continental margins and offshore petroleum exploration, C.J. Yorath, E.R. Parker and D.J. Glass, eds.; *Can. Soc. Pet. Geol., Mem.* 4, p. 531–544.
- Miall, A.D.
1973: Markov chain analysis applied to an ancient alluvial plain succession; *Sedimentology*, v. 20, p. 347–364.
1974a: Stratigraphy of the Elf *et al.* Storkerson Bay A-15 well; *Geol. Surv. Can., Paper* 74-1A, p. 335, 336.
1974b: Bedrock geology of Banks Island; *Geol. Surv. Can., Paper* 74-1A, p. 336–342.
1974c: Subsurface geology of western Banks Island; *Geol. Surv. Can., Paper* 74-1B, p. 278–281.
1974d: Manganese spherulites at an intra-Cretaceous unconformity, Banks Island, Northwest Territories; *Can. J. Earth Sci.*, v. 11, p. 1704–1716.
1974e: Paleocurrent analysis in alluvial sediments: a discussion of directional variance and vector magnitude; *J. Sediment. Petrol.*, v. 44, p. 1174–1185.
1975a: Geology of Banks Island, District of Franklin; *Geol. Surv. Can., Paper* 75-1A, p. 559–564.
1975b: Post-Paleozoic geology of Banks, Prince Patrick and Eglinton Islands, Arctic Canada; *in* Canada's continental margins and offshore petroleum exploration, C.J. Yorath, E.R. Parker and D.J. Glass, eds.; *Can. Soc. Pet. Geol., Mem.* 4, p. 557–588.
1975c: Stratigraphy of the Deminex CGDC FOC Amoco Orkut I-44 well; *Geol. Surv. Can., Paper* 75-1B, p. 257–259.
1976a: Proterozoic and Paleozoic geology of Banks Island, Arctic Canada; *Geol. Surv. Can., Bull.* 258.
1976b: Paleocurrent and paleohydrologic analysis of some vertical profiles through a Cretaceous braided stream deposit, Banks Island, Arctic Canada; *Sedimentology*, v. 23, p. 459–484.
1976c: Sedimentary structures and paleocurrents in a Tertiary deltaic succession, Northern Banks Basin, Arctic Canada; *Can. J. Earth Sci.*, v. 13, p. 1422–1432.
1977: A review of the braided river depositional environment; *Earth-Sci. Rev.*, v. 13, p. 1–62.
- Momin Ul Hoque
1968: Sedimentologic and paleocurrent study of the Mauch Chunk Sandstone (Mississippian) south-central and western Pennsylvania; *Bull. Am. Assoc. Pet. Geol.*, v. 52, p. 246–263.
- Morganstein, M. and Felsher, M.
1971: The origin of manganese nodules; a combined theory with special reference to palagonitization; *Pac. Sci.*, v. 25, p. 301–307.
- Mountjoy, E.W.
1967: Upper Cretaceous and Tertiary stratigraphy, northern Yukon Territory and northwestern District of Mackenzie; *Geol. Surv. Can., Paper* 66-16.

- Myhr, D.W.
1975: Markers within Cretaceous rocks as indicated by mechanical logs from boreholes in the Mackenzie Delta area, Northwest Territories; *Geol. Surv. Can., Paper 75-1B*, p. 267-275.
- Norris, D.K.
1974: Structural geometry and geological history of the Canadian Cordillera; *in Proc. 1973 Nat. Conv., A.E. Wren and R.B. Cruz, eds.; Can. Soc. Expl. Geophys.*, p. 18-45.
- Oertel, G.F.
1973: Examination of textures and structures of mud in layered sediments at the entrance of a Georgia tidal inlet; *J. Sediment. Petrol.*, v. 43, p. 33-41.
- Okada, H.
1971: Classification of sandstone: analysis and proposal; *J. Geol.*, v. 79, p. 509-525.
- Olson, J.S. and Potter, P.E.
1954: Variance components of cross-bedding direction in some basal Pennsylvanian sandstones of the eastern Interior Basin: statistical methods; *J. Geol.*, v. 62, p. 26-49.
- Oomkens, E.
1970: Depositional sequences and sand distribution in the postglacial Rhône delta complex; *in Deltaic sedimentation, modern and ancient, J.P. Morgan, ed.; Soc. Econ. Paleontol. Mineral., Spec. Publ. 15*, p. 198-212.
1974: Lithofacies relations in the Late Quaternary Niger delta complex; *Sedimentology*, v. 21, p. 195-222.
- Parker, A.
1972: Jarosite in Wealden oil-sand from Lulworth Cove; *J. Geol. Soc. London*, v. 128, p. 289, 290.
- Parks, J.M.
1966: Cluster analysis applied to multivariate geologic problems; *J. Geol.*, v. 74, p. 703-715.
- Pettijohn, F.J.
1962: Paleocurrents and paleogeography; *Am. Assoc. Pet. Geol.*, v. 46, p. 1468-1493.
- Pettijohn, F.J., Potter, P.E. and Siever, R.S.
1972: Sand and sandstone; Springer-Verlag, New York.
- Picard, M.D. and High, L.R., Jr.
1973: Sedimentary structures of ephemeral streams; *Dev. Sedimentol.*, No. 17, Elsevier, Amsterdam.
- Pittman, E.D.
1969: Destruction of plagioclase twins by stream transport; *J. Sediment. Petrol.*, v. 39, p. 1432-1437.
- Plass, L. van der and Tobi, A.C.
1965: A chart for judging the reliability of point counting results; *Am. J. Sci.*, v. 263, p. 87-90.
- Plauchut, B.P.
1971: Geology of the Sverdrup Basin; *Bull. Can. Soc. Pet. Geol.*, v. 19, p. 659-679.
- Preston, F.W. and Henderson, J.H.
1964: Fourier series characterization of cyclic sediments for stratigraphic correlation; *Kans. Geol. Surv., Bull. 169*, p. 415-425.
- Rascoe, B., Jr.
1975: Tectonic origin of preconsolidation deformation in Upper Pennsylvanian rocks near Bartlesville, Oklahoma; *Bull. Am. Assoc. Pet. Geol.*, v. 59, p. 1626-1638.
- Read, W.A. and Dean, J.M.
1967: A quantitative study of a sequence of coal-bearing cycles in the Namurian of central Scotland, 1; *Sedimentology*, v. 9, p. 137-156.
1975: A statistical relationship between net subsidence and number of cycles in Upper Carboniferous paralic facies successions in Great Britain; *Septième Congr. Int. de Stratigraphie et de Géologie Carbonifère, Compte Rendu, Band IV*, p. 153-159.
- Reineck, H.E. and Singh, I.B.
1973: *Depositional sedimentary environments*; Springer-Verlag, New York.
- Reineck, H.E. and Wunderlich, F.
1968: Classification and origin of flaser and lenticular bedding; *Sedimentology*, v. 11, p. 99-104.
- Ross, D.A. and Degens, E.T.
1974: Recent sediments of Black Sea; *in The Black Sea - geology, chemistry and biology, E.T. Degens and D.A. Ross, eds.; Am. Assoc. Pet. Geol., Mem. 20*, p. 183-199.
- Roy, K.J.
1973: Isachsen Formation, Amund Ringnes Island, District of Franklin; *Geol. Surv. Can., Paper 73-1A*, p. 269-273.
1974: Transport directions in the Isachsen Formation (Lower Cretaceous), Sverdrup Islands, District of Franklin; *Geol. Surv. Can., Paper 74-1A*, p. 351-353.
- Rust, B.R.
1972: Structure and process in a braided river; *Sedimentology*, v. 18, p. 221-245.
- Scheidegger, A.E. and Potter, P.E.
1968: Textural studies of grading: volcanic ash falls; *Sedimentology*, v. 11, p. 162-170.
- Schumm, S.A.
1963: A tentative classification of alluvial river channels; *U.S. Geol. Surv., Circ. 477*.
1968a: River adjustment to altered hydrologic regimen - Murrumbidgee River and paleochannels, Australia; *U.S. Geol. Surv., Prof. Paper 598*.
1968b: Speculations concerning paleohydrologic controls of terrestrial sedimentation; *Bull. Geol. Soc. Am.*, v. 79, p. 1573-1588.
1969: River metamorphosis; *Am. Soc. Civ. Eng., Proc., J. Hydraul. Div.*, v. 95, p. 255-273.
1972: Fluvial paleochannels; *in Recognition of ancient sedimentary environments, J.K. Rigby and W.K. Hamblin, eds.; Soc. Econ. Paleontol. Mineral., Spec. Publ. 16*, p. 98-107.
- Schwarzacher, W.
1953: Crossbedding and grain size in Lower Cretaceous sands of East Anglia; *Geol. Mag.*, v. 90, p. 322-330.
- Scruton, P.C.
1960: Delta building and the deltaic sequence; *in Recent sediments, northwest Gulf of Mexico, F.P. Shepard, F.B. Phleger, and T.H. van Andel, eds.; Am. Assoc. Pet. Geol.*, p. 82-102.
- Selley, R.C.
1968: A classification of paleocurrent models; *J. Geol.*, v. 76, p. 99-110.
- Simons, D.B., Richardson, E.V. and Nordin, C.F., Jr.
1965: Sedimentary structures generated by flow in alluvial channels; *in Primary sedimentary structures and their hydrodynamic interpretation, G.V. Middleton, ed.; Soc. Econ. Paleontol. Mineral., Spec. Publ. 12*, p. 34-52.
- Singh, I.B. and Kumar, S.
1974: Mega- and giant ripples in the Ganga, Yamuna and Son Rivers, Uttar Pradesh, India; *Sediment. Geol.*, v. 12, p. 53-66.

- Smith, N.D.
 1971a: Transverse bars and braiding in the lower Platte River, Nebraska; *Bull. Geol. Soc. Am.*, v. 82, p. 3407-3420.
 1971b: Pseudo-planar stratification produced by very low-amplitude sand waves; *J. Sediment. Petrol.*, v. 41, p. 69-73.
 1972: Some sedimentological aspects of planar cross-stratification in a sandy braided river; *J. Sediment. Petrol.*, v. 42, p. 624-634.
 1974a: Sedimentology and bar formation in the upper Kicking Horse River, a braided outwash stream; *J. Geol.*, v. 82, p. 205-224.
 1974b: Some sedimentological aspects of planar cross-stratification in a sandy braided river: a reply to N.L. Banks and J.D. Collinson; *J. Sediment. Petrol.*, v. 44, p. 267-269.
- Snowdon, L.R. and Roy, K.J.
 1975: Regional organic metamorphism in the Mesozoic strata of the Sverdrup Basin; *Bull. Can. Pet. Geol.*, v. 23, p. 131-148.
- Sobczak, L.W.
 1975a: Gravity anomalies and passive continental margins, Canada and Norway; *in* Canada's continental margins and offshore petroleum exploration, C.J. Yorath, E.R. Parker and D.J. Glass, eds.; *Can. Soc. Pet. Geol., Mem. 4*, p. 743-762.
 1975b: Gravity and deep structure of the continental margins of Banks Island and Mackenzie Delta; *Can. J. Earth Sci.*, v. 12, p. 378-394.
- Souther, J.G.
 1963: Geological traverse across Axel Heiberg Island from Buchanan Lake to Strand Fiord; *in* Geology of the north-central part of the Arctic Archipelago, Northwest Territories (Operation Franklin); *Geol. Surv. Can., Mem. 320*, p. 426-448.
- Spearing, D.R.
 1974: Summary sheets of sedimentary deposits; *Geol. Soc. Am.*
- Stephens, L.E., Sobczak, L.W. and Wainwright, E.S.
 1972: Gravity measurements on Banks Island, N.W.T. with map no. 150 - Banks Island; *Can. Dep. Energy, Mines, Resour., Gravity Map Ser., Earth Phys. Br.*
- Stott, D.F.
 1969: Ellef Ringnes Island, Canadian Arctic Archipelago; *Geol. Surv. Can., Paper 68-16*.
- Sundborg, A.
 1967: Some aspects on fluvial sediments and fluvial morphology, I: General views and graphic methods; *Geogr. Ann.*, v. 49A, p. 333-343.
- Tanner, W.F.
 1967: Ripple mark indices and their uses; *Sedimentology*, v. 9, p. 89-104.
 1971: Numerical estimate of ancient waves, water depth and fetch; *Sedimentology*, v. 16, p. 71-88.
- Thorsteinsson, R.
 1961: History and geology of Meighen Island; *Geol. Surv. Can., Bull. 75*.
- Thorsteinsson, R. and Tozer, E.T.
 1957: Geological investigations in Ellesmere and Axel Heiberg Islands, 1956; *Arctic*, v. 10, p. 2-31.
 1960: Summary account of structural history of the Canadian Arctic Archipelago since Precambrian time; *Geol. Surv. Can., Paper 60-7*.
- 1962: Banks, Victoria and Stefansson Islands, Arctic Archipelago; *Geol. Surv. Can., Mem. 330*.
- Tozer, E.T.
 1956: Geological reconnaissance, Prince Patrick, Eglinton and western Melville Islands, Arctic Archipelago, Northwest Territories; *Geol. Surv. Can., Paper 55-5*.
 1960: Summary account of Mesozoic and Tertiary stratigraphy, Canadian Arctic Archipelago; *Geol. Surv. Can., Paper 60-5*.
 1963a: Mesozoic and Tertiary stratigraphy; *in* Geology of the north-central part of the Arctic Archipelago, Northwest Territories (Operation Franklin); *Geol. Surv. Can., Mem. 320*, p. 74-95.
 1963b: South side of Strand Fiord; *in* Geology of the north-central part of the Arctic Archipelago, Northwest Territories (Operation Franklin); *Geol. Surv. Can., Mem. 320*, p. 448-456.
- Tozer, E.T. and Thorsteinsson, R.
 1964: Western Queen Elizabeth Islands, Arctic Archipelago; *Geol. Surv. Can., Mem. 332*.
- Trettin, H.P.
 1969: Pre-Mississippian geology of northern Axel Heiberg and northwestern Ellesmere Islands, Arctic Archipelago; *Geol. Surv. Can., Bull. 171*.
- Trettin, H.P., Frisch, T.O., Sobczak, L.W., Weber, J.R., Niblett, E.R., Law, L.K., Delaurier, J.M. and Witham, K.
 1972: The Innuitian Province; *in* Variations in tectonic styles in Canada, R.A. Price and R.J.W. Douglas, eds.; *Geol. Assoc. Can., Spec. Paper 11*, p. 83-179.
- Troelsen, J.C.
 1950: Contributions to the geology of northwest Greenland, Ellesmere and Axel Heiberg Islands; *Medd. om Grønland*, v. 149, no. 7.
- Turner, F.J. and Verhoogen, J.
 1960: *Igneous and metamorphic petrology*; McGraw Hill, New York.
- Visher, G.S.
 1965: Use of vertical profile in environmental reconstruction; *Bull. Am. Assoc. Pet. Geol.*, v. 49, p. 41-61.
 1969: Grain size distributions and depositional processes; *J. Sediment. Petrol.*, v. 39, p. 1074-1106.
 1972: Physical characteristics of fluvial deposits; *in* Recognition of ancient sedimentary environments, J.K. Rigby and W.K. Hamblin, eds.; *Soc. Econ. Paleontol. Mineral., Spec. Publ. 16*, p. 84-97.
- West, R.M., Dawson, M.R., Hutchison, J.H. and Ramaekers, P.
 1975: Paleontologic evidence of marine sediments in the Eureka Sound Formation of Ellesmere Island, Arctic Archipelago, N.W.T., Canada; *Can. J. Earth Sci.*, v. 12, p. 574-579.
- Williams, G.E.
 1968: Formation of large-scale trough cross-stratification in a fluvial environment; *J. Sediment. Petrol.*, v. 38, p. 136-140.
 1971: Flood deposits of the sand-bed ephemeral streams of central Australia; *Sedimentology*, v. 17, p. 1-40.
- Williams, P.F. and Rust, B.R.
 1969: The sedimentology of a braided river; *J. Sediment. Petrol.*, v. 39, p. 649-679.
- Wolfe, J.A., Hopkins, D.M. and Leopold, E.B.
 1966: Tertiary stratigraphy and paleobotany of the Cook Inlet region, Alaska; *U.S. Geol. Surv., Prof. Paper 398-A*.

- Wunderlich, F.
 1970 Genesis and environment of the "Nellenkopfschichten" (Lower Emsian, Rheinian Devonian) at locus typicus in comparison with modern coastal environments of the German Bay; *J. Sediment. Petrol.*, v. 40, p. 102-130.
- Yorath, C.J., Balkwill, H.R. and Klassen, R.W.
 1969: Geology of the eastern part of the northern interior and Arctic coastal plains, Northwest Territories; *Geol. Surv. Can.*, Paper 68-27.
 1975: Franklin Bay and Malloch Hill map-areas, District of Mackenzie; *Geol. Surv. Can.*, Paper 74-36.
- Yorath, C.J. and Norris, D.K.
 1975: The tectonic development of the southern Beaufort Sea and its relationship to the origin of the Arctic Ocean; *in* Canada's continental margins and offshore petroleum exploration, C.J. Yorath, E.R. Parker and D.J. Glass, eds.; *Can. Soc. Pet. Geol.*, Mem. 4, p. 589-612.
- Young, F.G.
 1973: Mesozoic epicontinental, flyschoid and molassoid depositional phases of Yukon's north slope; *in* Proc. Symp. Geology of the Canadian Arctic, Saskatoon, May 1973, J.D. Aitken and D.J. Glass, eds.; *Can. Soc. Pet. Geol. and Geol. Assoc. Can.*, p. 181-202.
- 1974: Cretaceous stratigraphic displacements across Blow Fault Zone, northern Yukon Territory; *Geol. Surv. Can.*, Paper 74-1B, p. 291-296.
- 1975: Upper Cretaceous stratigraphy, Yukon Coastal Plain and northwestern Mackenzie Delta; *Geol. Surv. Can.*, Bull. 249.
- Young, F.G., Myhr, D.W. and Yorath, C.J.
 1976: Geology of the Beaufort-Mackenzie Basin; *Geol. Surv. Can.*, Paper 76-11.
- Young, G.M.
 1974: Stratigraphy, paleocurrents and stromatolites of Hadrynian (Upper Precambrian) rocks of Victoria Island, Arctic Archipelago, Canada; *Precamb. Res.*, v. 1, p. 13-41.
- Young, G.M. and Jefferson, C.W.
 1975: Late Precambrian shallow water deposits, Banks and Victoria Islands, Arctic Archipelago; *Can. J. Earth Sci.*, v. 12, p. 1734-1748.

Summary of subsurface Mesozoic and Tertiary stratigraphy

	Storkerson Bay A-15	Nanuk D-76	Uminmak H-07	Orksut I-44	Ikkariktok M-64	Tiritichik M-48	Castel Bay C-68	Bar Harbour E-76
	feet (metres)							
<i>Log depths</i>								
Surficial deposits	?	?	?	?	0 (0)	0 (0)	?	?
Beaufort Fm.	0 (0)	0 (0)	0 (0)	0 (0)	abs.	abs.	abs.	0 (0)
Eureka Sound Fm.	860 (262)	50 (15)	50 (15)	50 (15)	50 (15)	30 (9)	0 (0)	905 (276)
Cyclic Mbr.	860 (262)	50 (15)	50 (15)	50 (15)	50 (15)	30 (9)	0 (0)	905 (276)
Shale Mbr.	3102 (945)	1643 (501)	1135 (346)	2410 (735)	1315 (401)	475 (145)	?	2510 (765)
Kanguk Fm.	3610 (1100)	1940 (591)	1476 (450)	3010 (917)	1870 (570)	1265 (386)	3080 (939)	2795 (852)
U. sand mbr.	abs.	abs.	abs.	3010 (917)	1870 (570)	1265 (386)	?	2795 (852)
Shale mbr. (upper pt)	3610 (1100)	1940 (591)	1476 (450)	3055 (931)	1940 (591)	1300 (396)	?	2867 (874)
L. sand mbr.	abs.	abs.	2100 (640)	3890 (1186)	2342 (714)	abs.	?	?
Shale mbr. (lower pt)	(undivided)	(undivided)	2217 (676)	3986 (1215)	2442 (744)	(undivided)	?	?
Bituminous shale mbr.	4470 (1362)	?	?	?	?	?	?	?
Hassel Fm.	abs.	abs.	abs.	abs.	abs.	?	4600 (1402)	3630 (1106)
Christopher Fm.	4495 (1370)	3175 (968)	2356 (718)	4230 (1289)	abs.	abs.	4625 (1410)	abs.
Isachsen Fm.	abs.	abs.	abs.	4370 (1332)	abs.	abs.	4768 (1453)	3650 (1112)
Mould Bay Fm.	abs.	abs.	abs.	4683 (1427)	abs.	abs.	5536 (1687)	abs.
Wilkie Point Fm.	abs.	abs.	abs.	5340 (1628)	abs.	abs.	6152 (1875)	abs.
Paleozoic	5136 (1565)	3695 (1126)	2858 (871)	6000 (1829)	2784 (849)	2510 (765)	6487 (1979)	3910 (1192)
<i>Subsea elevations</i>								
Surficial deposits	?	?	?	?	419 (128)	358 (109)	?	?
Beaufort Fm.	64 (20)	327 (100)	368 (112)	448 (136)	abs.	abs.	abs.	173 (53)
Eureka Sound Fm.	-796 (-243)	277 (84)	318 (97)	398 (121)	369 (112)	328 (100)	509 (155)	-732 (-223)
Cyclic Mbr.	-796 (-243)	277 (84)	318 (97)	398 (121)	369 (112)	328 (100)	509 (155)	-732 (-223)
Shale Mbr.	-3038 (-926)	-1316 (-401)	-767 (-234)	-1962 (-598)	-896 (-273)	-117 (-36)	?	-2337 (-712)
Kanguk Fm.	-3546 (-1081)	-1613 (-492)	-1108 (-338)	-2562 (-781)	-1451 (-442)	-907 (-276)	-2571 (-784)	-2622 (-799)
U. sand mbr.	abs.	abs.	abs.	-2562 (-781)	-1451 (-442)	-907 (-276)	?	-2622 (-799)
Shale mbr. (upper pt)	-3546 (-1081)	-1613 (-492)	-1108 (-338)	-2607 (-795)	-1521 (-464)	-942 (-287)	?	-2694 (-821)
L. sand mbr.	abs.	abs.	-1732 (-528)	-3442 (-1049)	-1923 (-586)	abs.	?	?
Shale mbr. (lower pt)	(undivided)	(undivided)	-1849 (-564)	-3538 (-1078)	-2023 (-617)	(undivided)	?	?
Bituminous shale mbr.	-4406 (-1343)	?	?	?	?	?	?	?
Hassel Fm.	abs.	abs.	abs.	abs.	abs.	?	-4091 (-1247)	-3457 (-1054)
Christopher Fm.	-4431 (-1351)	-2848 (-868)	-1988 (-606)	-3782 (-1153)	abs.	abs.	-4116 (-1254)	abs.
Isachsen Fm.	abs.	abs.	abs.	-3922 (-1195)	abs.	abs.	-4259 (-1298)	-3477 (-1060)
Mould Bay Fm.	abs.	abs.	abs.	-4235 (-1291)	abs.	abs.	-5027 (-1532)	abs.
Wilkie Point Fm.	abs.	abs.	abs.	-4892 (-1491)	abs.	abs.	-5643 (-1720)	abs.
Paleozoic	-5072 (-1546)	-3368 (-1027)	-2490 (-759)	-5552 (-1693)	-2365 (-721)	-2152 (-656)	-5977 (-1822)	-3737 (-1139)

Appendix 2

Subsurface logs

The logs which follow are, in part, uncorrected sample logs. Depths and thicknesses may, therefore, be inaccurate because of sample log, etc. Corrected stratigraphic tops are given in Appendix 1 and Figure 8

Depth	Elevation	Thickness	Description
feet (metres)			
Elf et al Storkerson Bay A-15			
Location: lat. 72°54'00"N; long. 124°33'29"W			
Elevation: 64 ft K.B.			
Total depth: 6719 ft			
Completed: December 10, 1971			
Status: dry and abandoned			
Log by A. D. Miall from samples and cores stored at Geological Survey of Canada, Calgary, Alberta, January 22, 1973–May 30, 1973.			
Beaufort Formation			
0	64	40	Surficial sediments, probably Beaufort Formation, no samples available
0	(20)	(12)	
40	24	40	Samples probably cavings. Operator reports ice wedge in 25–80 ft interval
(12)	(7)	(12)	
80	-16	90	Pebbly gravel, abundant pebbles of orange, yellow, brown and black chert, fairly common pebbles of white quartzose sandstone, rare pebbles of green micaceous shale, gabbro; maximum clast size 1 cm, original pebble size probably considerably greater. Abundant sand grains composed of all the above lithologies plus clear quartz, the latter generally rounded to well rounded, commonly highly polished or with pitted surfaces. Rare, slightly carbonized wood fragments
(24)	(-5)	(27)	
170	-106	20	Sand, unconsolidated, medium to coarse grained, pebbly, consisting predominantly of grains of quartz and chert
(52)	(-32)	(6)	
190	-126	130	Pebbly gravel, similar to 80–170 ft interval, partly carbonized wood fragments fairly common, abundant sandy matrix. Matrix clast count: chert 50%, quartz 43%, plant fragments 3%, others 4%
(58)	(-38)	(40)	
320	-256	70	Pebbly sand, predominantly dark grey chert and colourless quartz grains, fairly common buff and orange chert, white quartzose sandstone, black volcanic fragments (basalt?), altered wood
(98)	(-78)	(21)	
390	-326	260	Pebbly gravel, mineralogy similar to 320–390 ft interval, abundant sandy matrix, fairly common fragments of peat. Much of this material may be cavings
(119)	(-99)	(79)	
650	-586	170	Pebbly sand, coarse grained, carbonized wood and brown peat fragments common, mineralogy of sand as in 320–650 ft interval. Coarsest pebble grain size approximately 5 mm
(198)	(-179)	(52)	
820	-756	40	Peat, dark brown, plus partly carbonized wood fragments
(250)	(-230)	(12)	
Eureka Sound Formation			
<i>Cyclic Member</i>			
860	-796	450	Samples described as follows:
(262)	(-243)	(137)	
			Sand, coarse grained, subrounded to subangular grains of white and colourless quartz and dark grey chert, carbonized wood fragments common but are probably cavings (decrease in frequency downward), occasional small pebbles (cavings?), rare fragments of medium brown soft siltstone. Abundant dark red-brown wood fragments at the 1160, 1190, 1220, 1250, 1290 and 1340 ft levels. This interval is interpreted from samples and gamma ray log to consist of alternating coarse-grained sand and soft shale or silty shale, with shale having been absorbed in the mud stream and not appearing in the sample record. Wood material may be present as scattered logs, discrete seams or both
1310	-1246	481	Samples described as follows:
(399)	(-380)	(147)	
			Sand, medium grained, grains mainly colourless quartz and light to dark grey chert, quartz grains subangular to subrounded, chert grains subangular; occasional carbonized wood fragments. Wood and fragments of soft brown silty shale

Depth	Elevation	Thickness	Description
	feet (metres)		
			common in samples from the 1420, 1510–1530, 1560–1580, 1640, 1780–1820 ft intervals. Clast count at 1600 feet: quartz 50%, chert 41%, wood 9%. This interval is interpreted from samples and gamma ray log to consist predominantly of medium-grained quartz- and chert-rich sandstone with interbeds of silty shale, the latter containing lignite seams or wood fragments. This interval is similar lithologically to the 813–1025 ft interval in the Nanuk well
1791 (546)	-1727 (-526)	719 (219)	Samples described as follows: Conglomerate, probably mainly unconsolidated, consisting of pebbles up to at least 6 mm in diameter (larger pebbles probably present but broken by drill bit); very little sand or finer fraction present in samples; pebbles comprise light to dark grey and, less commonly, mottled chert, 44%; white quartzose sandstone, 23%; dark grey to black, well-indurated shale, commonly siliceous and in places containing thin quartz veins, 18%; white and colourless quartz, 12%; other lithologies, 3% (percentages measured in samples from 1820 ft level). Rare fragments show interbedding of quartzose sandstone and dark grey chert. Wood fragments are fairly common in 1950–2020 ft and 2050–2080 ft intervals and abundant at 2010, 2240 and 2310 ft levels. Unbroken pebbles are rounded to well rounded
2510 (765)	-2446 (-746)	30 (9)	Samples described as follows: Pebbly sand. Bimodal grain size distribution; coarser material (very coarse sand to small pebble grade) may be cavings, composed predominantly of chert, siliceous shale, quartzite and some quartz. Finer grained material is of medium sand grade and consists of quartz, 54%; dark grey chert and siliceous shale (difficult to distinguish in small, partly polished grains), 46%; plus rare grains of white quartzite; quartz grains subrounded to well rounded, chert grains subrounded
2540 (774)	-2476 (-755)	650 (198)	Samples described as follows: Conglomerate, very similar to 1791–2510 ft interval, with sand matrix similar to 2510–2540 ft interval. Carbonized wood and lignite fragments fairly common to abundant. Abundant wood ash at 3120 ft level. Conglomerate may be mainly cavings. Core # 1, 2919.8–2920 ft, siderite, medium grey, extremely dense, hard, very fine grained. Remainder of core, 2901–2919.8 and 2920–2927 ft intervals, not recovered <i>Note:</i> 1791–3102 ft interval interpreted as a series of interbedded conglomerate, sandstone and shale or siltstone, the silt and shale material having been absorbed in the mud stream and not present in the samples. Base of Cyclic Member drawn at 3102 ft <i>Shale Member</i>
3190 (972)	-3126 (-953)	10 (3)	Samples consist of conglomerate as in 1791–2510 ft interval (cavings?), plus much casing cement. A few fragments of soft brown shale
3200 (975)	-3136 (-956)	10 (3)	Sample composed mainly of lignite and wood ash
3210 (978)	-3146 (-959)	80 (24)	Samples as follows: Pebbly sand, quartz and chert grains, very coarse sand grade, plus abundant lignite fragments and ash and fairly abundant fragments of soft, friable, light grey shale containing plant remains
3290 (1003)	-3226 (-983)	60 (18)	Samples as follows: Lignite, black, friable, plus some sand as in 3210–3290 ft interval. Rare fragments of medium grey, slightly micaceous, soft shale containing plant fragments appear below 3320 ft level; small fragments of white, quartzose, very fine sandstone at 3340 ft level. Rare fragments of siderite identical to that in core # 1
3350 (1021)	-3286 (-1002)	40 (12)	Samples composed of approximately equal proportions of lignite, soft, friable, black, and shale, silty, medium to light grey, slightly calcareous. Quartz sand grains abundant but may be cavings
3390 (1033)	-3326 (-1014)	70 (21)	Samples are of lignite as in 3350–3390 ft interval, with minor amounts of shale, as in 3350–3390 ft interval, plus some rounded quartz grains (cavings?), fragments of quartzose siltstone and rare fragments of siderite as in core # 1. Shale commonly contains comminuted plant debris. Some fragments of harder, more compact subbituminous coal
3460 (1055)	-3396 (-1035)	60 (18)	Lignite-shale samples, as in 3350–3390 ft interval, plus quartzose siltstone and very fine sandstone

Depth	Elevation	Thickness	Description
	feet (metres)		
3520 (1073)	-3456 (-1053)	110 (34)	Shale, grey and reddish brown, in places silty, minor lignite, minor soft grey ash, minor white, quartzose, very fine sandstone; 3600–3610 ft interval samples almost entirely of coarse-grained quartz and chert sand, probably cavings <i>Note:</i> 3102–3610 ft interval is interpreted as a shale and coal sequence, with a few silty and sandy interbeds. Coal intervals are inserted on the graphic log on the basis of high resistivity, low gamma ray reading and high apparent porosity on sonic log. This interval compares closely with the 1643–1940 ft interval of the Elf Nanuk well. Base of Eureka Sound drawn at 3610 ft
Kanguk Formation			
<i>Silty shale member</i>			
3630 (1106)	-3566 (-1087)	330 (101)	Siltstone, brown and reddish brown, variably argillaceous, and interbedded with minor amounts of grey, slightly bentonitic shale, occasional thin streaks of very fine sandstone, occasional foraminifera, small pelecypod at 3780 ft
3960 (1207)	-3896 (-1187)	10 (3)	Shale, dark grey, carbonaceous, abundant plant remains, foraminifera common. Corrected depth interval 3910–3945 ft (?)
3970 (1210)	-3906 (-1190)	90 (27)	Argillaceous siltstone as in 3630–3970 ft interval, with occasional very fine sandy streaks, and carbonaceous shale containing plant remains, a few subbituminous coal streaks. Samples contain up to 80% chert and quartz sand grains – probably cavings, foraminifera locally abundant
4060 (1237)	-3996 (-1218)	4 (1)	Cone-in-cone calcite
4064 (1239)	-4000 (-1219)	106 (32)	Shale, medium grey, silty, carbonaceous, rare coal streaks, foraminifera fairly common; thin cone-in-cone calcite streak at 4147 ft
4170 (1271)	-4106 (-1251)	40 (12)	Siltstone, argillaceous, brown and reddish brown, foraminifera fairly common; thin cone-in-cone calcite at 4184 and 4202 ft
4210 (1283)	-4146 (-1264)	32 (10)	Shale, pale grey, fissile, compare 'Pale Shale' of northern mainland, rare carbonaceous streaks
4242 (1293)	-4178 (-1273)	4 (1)	Cone-in-cone calcite
4246 (1294)	-4182 (-1275)	144 (44)	Silty shale, light to medium grey, noncalcareous, foraminifera generally rare. Coal fragments (?cavings), rare brown silty shale, rare pyrite, pelecypod fragments.
4390 (1338)	-4326 (-1319)	80 (24)	Silty shale, as above, but slightly bentonitic
<i>Bituminous shale member</i>			
4470 (1362)	-4406 (-1343)	1 (0.3)	Shale, dark brown, containing spherulitic structures, compare 3138–3175 ft interval of Elf Nanuk D-76. Samples very poor
Christopher Formation			
4471 (1363)	-4407 (-1343)	259 (79)	Silty shale, light to medium grey, noncalcareous, arenaceous foraminifera rare in samples, except abundant at 4570–4590 ft. Gamma ray log indicates high radioactivity in upper 24 ft of interval
4730 (1442)	-4666 (-1422)	126 (38)	Argillaceous siltstone, medium grey, some reddish brown siltstone near base, noncalcareous, slightly micaceous, rare pyrite, rare very fine sandy streaks, faint laminations, arenaceous foraminifera fairly common in samples
4856 (1480)	-4792 (-1461)	30 (9)	Samples as in 4730–4856 ft. Mechanical logs indicate otherwise: S.P. and caliper deflections suggest porous zone; high resistivity and high (sonic) density also indicated. Gamma ray deflection is nearly constant through this unit. Interval interpreted tentatively as a porous siltstone or very fine sandstone
4886 (1489)	-4822 (-1470)	169 (52)	Argillaceous siltstone plus, in places, very fine porous sandstone as in 4730–4856 ft interval. Arenaceous foraminifera rare in samples
5055 (1541)	-4991 (-1521)	15 (5)	Samples as in 4730–4856 ft. Mechanical log deflections and presence of dolomite fragments in samples labelled 5100–5120 ft interval together suggest thin dolomite bed in this interval. Strata are fine grained, brown, contain fine sand grains
5070 (1545)	-5006 (-1526)	66 (20)	Argillaceous siltstone with some very fine grained sandy streaks. Foraminifera fairly common
5136 (1565)			Weatherall Formation

Depth	Elevation	Thickness	Description
	feet (metres)		
Elf Nanuk D-76			
Location: lat. 73°05'13"N; long. 123°23'45"W			
Elevation: 327 ft K.B.			
Total depth: 4518 ft			
Completed: March 4, 1972			
Status: dry and abandoned			
Log by A.D. Miall from samples and cores stored at Geological Survey of Canada, Calgary, Alberta, November 20, 1972 – January 12, 1973.			
Beaufort Formation			
0 (0)	327 (100)	160 (49)	Pebble conglomerate, maximum grain size much greater than 1 cm (larger fragments broken by drill bit), abundant clasts of orange, brown and grey chert imparting dark orange-brown hue to sample; clasts of quartz, feldspar, schist, granite gneiss, sedimentary rocks (Proterozoic?) including shale, fine-grained brown sandstone, white quartzose sandstone, brown dolomite, all fairly common. Rare clasts of diabase, pyrite, silicified oolite; fragments of partly carbonized wood up to 1 cm in length in places. A few well rounded quartz grains, commonly with highly polished surfaces; size range 0.5 to 2 mm, probably polycyclic. Roundness (Krumbein, 1941, scale) of 0.5 to 0 ϕ size range, 0.533, for 0–40 ft sample interval
Eureka Sound Formation			
<i>Cyclic Member</i>			
160 (49)	167 (51)	280 (85)	Pebble conglomerate as 0–160 ft interval, quartz grains increased in abundance to $\pm 1\%$. Unit becomes silty and muddy between 380 and 440 ft. Quartz grain roundness at 230–240 ft, 0.5–0 ϕ size range, sample 1, 0.547; sample 2, 0.537
440 (134)	-113 (-34)	69 (21)	Pebble conglomerate, maximum grain size at least 1.3 cm. Orange and brown chert virtually absent. Abundant fragments of medium to dark grey chert, white and grey quartzite, rare grey shale clasts, abundant carbonized wood fragments. Abundant grains of clear and milky quartz, well rounded, highly polished, 0.3 to 2 mm size range, polycyclic? Roundness at 470–480 ft, 0.5 to 0 ϕ size range, 0.517
509 (155)	-182 (-55)	37 (11)	Siltstone, sandy, pebbly, buff to light grey; angular to well rounded clasts of grey chert, quartzite, quartz, fairly abundant polycyclic quartz grains
546 (166)	-219 (-67)	84 (26)	Pebble conglomerate, modal grain size approximately 8 mm, maximum grain size 14 mm, clasts mainly light to dark grey chert, white quartzite, a few clasts of orange chert, polycyclic quartz grains, rare schist, rounded wood pebbles. Wood fragments abundant in 540–550 ft interval, uncommon 550–590 ft, common 590–600 ft, up to 50% 600–630 ft interval
630 (192)	-303 (-92)	55 (17)	Granule conglomerate, modal grain size 2–3 mm, maximum 9 mm, wood fragments $\pm 30\%$, clast lithologies as in 546–630 ft interval. Quartz grain roundness at 640–650 ft interval, 0.5–0 ϕ size range, 0.540
685 (209)	-358 (-109)	25 (8)	?Pebbly sand. Samples are of granule conglomerate, probably cavings
710 (216)	-383 (-117)	40 (12)	Pebbly sand, pebbles mainly grey chert, some quartzite and quartz, sand grains similar mineralogically, wood rare. Roundness of quartz grains at 710–720 ft interval, 0.5–0 ϕ size range, 0.540; chert grains (same interval and size range), 0.405. At 720–730 ft interval, roundness of 0.5–0 ϕ size range: quartz 0.545, chert 0.403. Gradational contact with underlying unit
750 (229)	-423 (-129)	63 (19)	Granule conglomerate, modal grain size 4 mm, fine fraction (sand, silt, mud) virtually absent—possibly washed out in drilling mud, clast lithologies as in 546–630 ft interval. Wood rare in 750–780 ft interval, $\pm 30\%$ in 780–810 ft interval, $\pm 10\%$ in 810–813 ft interval
813 (248)	-486 (-148)	27 (8)	Sand. Samples are of granule conglomerate, probably cavings
840 (256)	-513 (-156)	126 (38)	Sand, coarse grained, modal grain size 0.6 mm, occasional granule-size clasts present (may be cavings); clast count at 840–850 ft interval: dark grey chert 45%, quartz 53%, wood 2%; pyrite, trace. Roundness 0.5–0 ϕ size range: quartz 0.525, chert 0.310. At 950–960 ft interval: chert 57%, quartz 42%, wood 1%. Roundness of quartz 0.523, chert 0.385

Depth	Elevation	Thickness	Description
	feet (metres)		
			Gamma ray log suggests porosity of sands increases downward (possibly due to increased grain size). Sands may be interbedded with thin shale or siltstone beds (shale fragments present in samples from next lower unit)
966 (294)	-639 (-195)	59 (18)	Sand, coarse to very coarse grained. Mineralogy as for 840-966 ft interval. Clast count at 1020-1025 ft interval: quartz 39%, chert 57%, wood 4%. Roundness 0.5-0 ϕ size range: quartz 0.535, chert 0.375
1025 (312)	-698 (-213)	578 (176)	Samples are as described but probably include a considerable proportion of cavings from Beaufort Formation
			Pebble conglomerate, modal grain size 5-6 mm, clasts of dark grey chert, dark grey shale, white quartzite, milky quartz, sparse rounded wood fragments. Sand and finer grades virtually absent from sample. Clasts rounded to well rounded. Modal grain size increases slightly downward, to 10 mm at 1070 ft, then decreases to 5-6 mm at 1280 ft, increases to 10 mm below 1290 ft. Roundness of quartz grains 1310-1400 ft interval, 0.5-0 ϕ size range, 0.480
			This interval interpreted from gamma ray log and regional considerations to consist of coarsening-upward sedimentary cycles, typically (in order of deposition) shale, silt, sandstone and/or conglomerate, and possibly coal or lignite
1603 (489)	-1276 (-389)	40 (12)	Sandstone, very fine grained, silty, quartzose, buff, grains rounded, abundant carbonized plant fragments, rare chert grains, rare pyrite grains, well cemented, very low porosity. Grain size decreasing downward. Gradational contact with unit below
			<i>Shale Member</i>
1643 (501)	-1316 (-401)	17 (5)	?Shale, soft, dark grey, samples very poor
1660 (506)	-1333 (-406)	20 (6)	Shale, soft, dark grey, lignite streaks and sandy interbeds in places
1680 (512)	-1353 (-412)	6 (2)	Coal, soft, friable
1686 (514)	-1359 (-414)	90 (27)	Shale, as in 1660-1680 ft interval
1776 (541)	-1449 (-442)	19 (6)	?Coal, soft, friable, with shale interbeds, presence of coal interpreted from sample log and from low gamma ray response
1795 (547)	-1468 (-447)	43 (13)	?Shale, as in 1660-1680 ft interval
1838 (558)	-1511 (-460)	12 (4)	?Coal, samples mainly cavings of chert and quartzite pebbles
1850 (560)	-1523 (-464)	90 (27)	?Shale, as in 1660-1680 ft interval. Sparse interbeds of light grey, fine-grained siltstone, abundant coal fragments. Very poor samples
			Kanguk Formation
			<i>Shale Member</i>
1940 (591)	-1613 (-492)	122 (37)	Shale, dark grey, soft, occasionally silty. (Much cement in samples at 1960-1970, 1990-2040 ft, also drilling mud, mica and cellophane flakes [lost-circulation inhibitors]. Casing set at 1980 ft.) Samples fair 1940-1990 ft, good 1970-1990 ft, very poor 1990-2062 ft
2062 (628)	-1735 (-529)	28 (9)	Siltstone, light grey, quartzose with calcareous matrix, some minute plant fragments, well cemented, some calcite veins, tight, very poor samples
2090 (637)	-1763 (-537)	91 (28)	Argillaceous siltstone, slightly bentonitic
2181 (665)	-1854 (-565)	15 (5)	Siltstone, as at 2062-2090 ft, fair samples
2196 (669)	-1869 (-570)	20 (6)	Argillaceous siltstone, slightly bentonitic
2216 (675)	-1889 (-576)	7 (2)	Cone-in-cone structure: pure calcite with fibrous crystalline texture
2223 (678)	-1896 (-578)	225 (69)	Siltstone, medium to coarse grained, calcareous, slightly to very argillaceous, comminuted plant debris common, arenaceous foraminifera common in samples
2448 (746)	-2121 (-646)	8 (2)	Cone-in-cone calcite
2456 (749)	-2129 (-649)	52 (16)	Silty shale, finely laminated, rare fine sandy streaks, scattered limonitic ironstone concretions, comminuted plant debris, arenaceous foraminifera common in samples

Depth	Elevation	Thickness	Description
	feet (metres)		
2508 (764)	-2181 (-665)	242 (74)	Siltstone, coarse to medium grained, calcareous quartzose, in places argillaceous, and containing shaly streaks, pink, bentonitic, light. Streaks of cone-in-cone calcite at 2610, 2624, 2710 and 2728 ft levels. Arenaceous foraminifera common in samples
2750 (838)	-2423 (-738)	138 (42)	Argillaceous siltstone, medium to fine grained, light grey, tight, slightly bentonitic, pyrite blebs, arenaceous foraminifera
2888 (880)	-2561 (-781)	17 (5)	Shale, dark grey, micaceous, slightly silty
2905 (885)	-2578 (-786)	211 (64)	Argillaceous siltstone, medium to fine grained, light grey, tight, sparse limonite, pyrite, <i>Inoceramus</i> fragments, in places streaks of well laminated slightly bentonitic shale, reddish brown
3116 (950)	-2789 (-850)	22 (7)	Shale, grey, grey-green and reddish brown, in places silty. Minor minute flecks of ?glauconite. Minor brown limonitic ironstone. This unit corresponds to the 'Bituminous Zone' of the mainland
3138 (956)	-2811 (-857)	37 (11)	Spherulitic concretions. Spherulites average 0.4 mm in diameter, commonly welded together, otherwise poorly consolidated, matrix dolomite? Serrated sonic and resistivity logs suggest interbedding with argillaceous streaks. Dipmeter indicates consistent northeasterly dip at 4-12°, decreasing upward. Spherulites probably of diagenetic origin
Christopher Formation			
3175 (968)	-2848 (-868)	135 (41)	Shale, pale buff to pale grey, scattered buff, quartzose silty streaks
3310 (1009)	-2983 (-909)	385 (117)	Shale, medium grey, poor fissility, slightly micaceous, a few pyrite nodules. Light grey, quartzose, slightly calcareous, coarse siltstone streaks between 3330 and 3400, at 3610 and between 3675 and 3695 ft. ?Belemnite fragment at 3450 ft. Foraminifera rare. Rare <i>Ammodiscus</i> sp.
3695 (1126)			Nanuk Formation

Elf Uminmak H-07

Location: lat. 73°36'29"N; long. 123°00'30"W

Elevation: 368 ft K.B.

Total depth: 5573 ft

Completed: May 7, 1972

Status: dry and abandoned

Log by A. D. Miall from samples and cores stored at Geological Survey of Canada, Calgary, Alberta, February 19, 1973-July 26, 1973.

Beaufort Formation

0 (0)	368 (112)	390 (119)	Pebble conglomerate, unconsolidated, fragments up to 1.5 cm (larger fragments may have been present but broken by drill bit). Predominant lithologies in conglomerate clasts: chert, reddish brown, orange, dark brown and grey, some faintly mottled or laminated; clear quartz; milky quartz; quartzose sandstone, white and reddish brown, fine to medium grained, well cemented; dark grey siliceous shale; matrix of coarse quartz sand; pebbles and sand grains well rounded, rare rounded fragments petrified wood, carbonized wood. Clast count (at 50 ft): orange, brown, buff chert 45%, grey chert 17%, quartz 24%, quartzite 6%, siliceous shale 6%, others 2%. Orange chert virtually absent below 190 ft level. Wood fragments fairly common from 230-290, abundant 290-320, common 320-390 ft
----------	--------------	--------------	--

Eureka Sound Formation*Cyclic Member*

390 (119)	-22 (-7)	120 (37)	Pebble conglomerate, similar to above but with different proportion of clast types. Clast count at 390 ft: grey chert 51%, siliceous shale 18%, quartz 17%, quartzose sandstone 9%, wood 4%, orange, brown chert 1%, rare fragments of mainly unaltered wood
--------------	-------------	-------------	--

Depth	Elevation	Thickness	Description
	feet (metres)		
510 (155)	-142 (-43)	30 (9)	Pebbly sand, very coarse grade, grains mainly of quartz and grey chert, abundant wood and wood ash, a few fragments soft, medium grey shale. Pebbles of chert, siliceous shale and quartzose sandstone
540 (165)	-172 (-52)	140 (43)	Pebble conglomerate, as in 390–510 ft interval, rare fragments of soft, medium grey shale suggest several shale interbeds. Wood fragments present. Clast count at 670 ft level: grey chert 49%, quartz 29%, quartzose sandstone 11%, siliceous shale 7%, wood 4%
680 (207)	-312 (-95)	75 (23)	Samples mainly pebble conglomerate, as above, but containing several fragments of greyish brown, sandy and silty mudstone. Interval probably mudstone with sandy and silty streaks. Rare wood fragments
755 (230)	-387 (-118)	380 (116)	Samples consist mainly of pebble conglomerate, plus carbonized wood fragments, as in 540–680 ft interval. Fragment of silicified oolite noted at 890 ft level. Scattered fragments of friable, fine to very fine grained silty sandstone, consisting of quartz, chert and siliceous shale grains, commonly angular to subrounded, set in a calcareous matrix. Fragments of buff or greyish silty mudstone and reddish brown siltstone also present. Pebble conglomerate may be entirely cavings. Gamma ray log suggests alternation of argillaceous and nonargillaceous lithologies. Interval interpreted as interbedded ?conglomerate, sandstone, siltstone and shale. Some suggestion of serrated funnel-shaped log, indicating possible upward-coarsening sedimentary cycles Abundant wood fragments at 900 ft (cavings?), abundant lignite at 920–940 ft (probably not cavings), lignite and wood ash at 970–1000 ft, lignite at 1050–1060 ft
			<i>Shale Member</i>
1135 (346)	-767 (-234)	13 (4)	Lignite, very dark brown to black, soft, friable, preserving wood texture
1148 (350)	-780 (-238)	26 (8)	Shale and silty shale, pale buff to pale grey, containing abundant lignitic plant fragments. Numerous cavings of quartzose, pebbly sand in sample
1174 (358)	-806 (-246)	10 (3)	Lignite, as in 1135–1148 ft interval
1184 (361)	-816 (-249)	26 (8)	Shale and silty shale with plant fragments, as in 1148–1174 ft interval
1210 (369)	-842 (-257)	61 (19)	Lignite with argillaceous streaks and thin seams of medium to dark grey carbonaceous shale. Samples contain much ash as well as abundant cavings of pebbly, quartz sand
1271 (387)	-903 (-275)	205 (62)	Shale and silty shale with plant fragments as in 1148–1174 ft interval. Probably thin lignite beds at 1327, 1351, 1401 and 1462 ft levels
			<i>Kanguk Formation</i>
			<i>Shale member (upper part)</i>
1476 (450)	-1108 (-338)	74 (23)	Samples predominantly lignite and pebbly quartz sand as in 1271–1476 ft intervals. At 1500 ft level, a few fragments of pale olive-grey silty mudstone are present. This lithology is identical to that comprising the bulk of the samples in the 1550–1640 ft interval. Interval interpreted as comprising silty mudstone. Top of Kanguk Formation placed provisionally at 1476 ft level on the basis of mechanical log interpretation
1550 (472)	-1182 (-360)	70 (21)	Silty mudstone, pale olive-grey, non-bentonitic, slightly micaceous, slightly calcareous (much casing cement in samples from top of interval). In places thin streaks of very fine sand, predominantly quartzose. Minute streaks of carbonaceous material also common. No fossils noted
1620 (494)	-1252 (-382)	60 (18)	Argillaceous siltstone, pale brownish buff, and silty mudstone, similar to 1550–1620 ft interval but reddish brown, slight calcareous content, rare small, highly carbonized (coalified), plant fragments. Several streaks of bright red, very iron-rich (?limonitic) mudstone, rare pyrite concretions. No foraminifera noted
1680 (512)	-1312 (-400)	18 (5)	Sandstone, very fine grained, silty, buff
1698 (518)	-1330 (-405)	212 (65)	Siltstone, slightly argillaceous, slightly micaceous, pale buff to red-brown, slightly calcareous; scattered, highly carbonized and comminuted plant fragments; rare faint lamination; rare thin streaks of very fine grained, quartzose sandstone; scattered, angular, medium sand grade chert grains. No foraminifera noted

Depth	Elevation	Thickness	Description
	feet (metres)		
1910 (582)	-1542 (-470)	102 (31)	Siltstone, slightly argillaceous, slightly micaceous, very slightly calcareous, medium grey or buff-grey; scattered, comminuted plant debris; a few very fine sandy streaks; rare pyrite nodules; foraminifera rare
2012 (613)	-1644 (-501)	88 (27)	Shale, with silty streaks, medium grey or brownish grey, slightly micaceous, calcareous, slightly bentonitic in places. No foraminifera noted
			<i>Lower sand member</i>
2100 (640)	-1732 (-528)	30 (9)	Sand, very coarse grained, well sorted, quartzose, grains well rounded. (Samples contain much shale and siltstone but these are probably cavings.) Strong deflection of gamma ray and spontaneous potential logs suggest very clean, highly porous sand. This is supported by very little evidence of matrix—a few fragments of medium-grained quartzose sandstone. Mineralogy: quartz, clear, milky, or occasionally pinkish, 96%; chert, dark grey or greenish grey, 4%. (Grains classified as chert may include some siliceous shale.) A few chert pebbles up to 1.2 cm
2130 (649)	-1762 (-537)	30 (9)	Sand, as above, but samples contain frequent fragments of medium- to coarse-grained sandstone with silica and (minor) calcite cement, suggesting partial lithification of the unit. Matrix yellowish, contains rare glauconite grains
2160 (658)	-1792 (-546)	57 (17)	Sand, medium to very coarse grained, in places fine to very fine grained as in 2100–2130 ft interval. Mechanical log interpretation suggests interbedding with thin shales or siltstones. Rare coarse sand- to granule-grade clasts. One of silicified oolite noted at 2200 ft; glauconite grains fairly common; rare small limonitic iron concretions; sand contains much limonite cement in places
			<i>Shale member (lower part)</i>
2217 (676)	-1849 (-564)	120 (37)	Shale, slightly silty, medium, slightly brownish grey, fine disseminated mica, minor calcareous content, rare trace of bentonite; rare limonite concretions; rare foraminifera (may be caved)
2337 (712)	-1969 (-600)	19 (6)	Shale, partly chertified and weathered; spherulitic texture common. Compare 3138–3175 ft interval in Elf Nanuk D-76. Southwesterly dip of 5–9° indicated on dipmeter
			Christopher Formation
2356 (718)	-1988 (-606)	344 (105)	Shale, medium, slightly greenish grey, slightly silty, slightly calcareous. Shale in places bright green (ferrous iron compounds present?), foraminifera fairly common, a few pelecypod fragments. One pebble of chert containing silicified foraminifera noted at 2420 ft (?caved). Pyrite concretions fairly common, rare limonite concretions
2700 (823)	-2332 (-711)	112 (34)	Shale, as in 2356–2700 ft interval, plus intercalated layers of siltstone, grey-brown, quartzose, slightly calcareous, shows poor intergranular and vuggy porosity
2812 (857)	-2444 (-745)	13 (4)	Sandstone, brown, very fine grained, silty, slightly glauconitic, low intergranular porosity
2825 (861)	-2457 (-749)	33 (10)	Silty shale as in 2356–2812 ft interval
2858 (871)			Melville Island Group

Deminex CGDC FOC Amoco Orksut I-44

Location: lat. 72°23'44.66"N; long. 122°42'08.81"W

Elevation: 447.7 ft K.B.

Total depth: 10 040 ft

Completed (rig release): March 28, 1973

Status: dry and abandoned

Log by A. D. Miall from samples and cores stored at Geological Survey of Canada, Calgary, Alberta, November 9, 1973–March 15, 1974.

Beaufort Formation

0 (0)	448 (136)	60 (18)	Gravel, samples consist predominantly of coarse sand and pebble-grade material. Pebbles include fragments of quartz sandstone, chert, some metamorphic rock fragments, dolomite. Unbroken pebbles are rounded. Sand grains predominantly quartz, rounded to well rounded. Rare clasts of silicified oolite
----------	--------------	------------	--

Depth	Elevation	Thickness	Description
	feet (metres)		
Eureka Sound Formation			
<i>Cyclic Member</i>			
60 (18)	388 (118)	55 (17)	Mudstone, soft, medium grey, slightly micaceous, silty, a few wood fragments
115 (35)	333 (101)	45 (14)	Gravel, samples consist predominantly of pebble-grade and coarse sand grade material. Pebbles include quartz sandstone and grey chert and are subangular to subrounded. Sand-grade material is similar in composition to pebbles, plus less than 5% quartz grains. Partly lignitized wood fragments are abundant. Some are well rounded, indicating transportation prior to inclusion in the sediment. Grades into unit below
160 (49)	288 (88)	90 (27)	Pebbly sand, pebbles as in 115–160 ft interval, sand-grade material consists of approximately equal proportions of well rounded quartz grains and angular to subangular, medium grey chert grains. Wood fragments, sparse, becoming fairly common below 200 ft level
250 (76)	198 (60)	170 (52)	Gravel, pebble and sand material similar in composition and rounding characteristics to 160–250 ft interval. Wood fragments rare, becoming common below 320 ft level. Sand-grade material present only in minor quantities. Pebble-grade material includes many broken fragments suggesting maximum clast size over 1 cm, but larger clasts broken by drill bit
420 (128)	28 (9)	30 (9)	Mudstone, soft, dark brownish grey, slightly silty and micaceous, contains numerous wood impressions and partly lignitized wood fragments
450 (137)	–2 (–1)	40 (12)	Pebbly sand, similar to 160–250 ft interval. Abundant wood fragments
490 (149)	–42 (–13)	10 (3)	Mudstone, medium brownish grey (sample very poor)
500 (152)	–52 (–16)	53 (16)	Gravel, as in 250–420 ft interval. Samples from 530–560 ft interval contain much casing cement
553 (169)	–105 (–32)	417 (127)	Samples consist predominantly of mudstone, dark grey to black, commonly carbonaceous and containing abundant lignitic coal fragments. Some reddish brown, iron-stained fragments, a few silty fragments, a few very fine to medium sand grade quartz grains This interval is interpreted from mechanical logs and from samples to consist of interbedded mudstone and argillaceous siltstone beds, with sandy streaks in places. Upward-coarsening cycles appear to be indicated on the mechanical log
970 (296)	–522 (–159)	93 (28)	Samples similar to 553–970 ft interval but containing slightly more fine to medium sand grade quartz grains, plus rare coarse to very coarse sand grains Interval interpreted as medium-grained or, in places, coarse-grained silty sand with siltstone and mudstone interbeds
1063 (324)	–615 (–188)	107 (33)	Samples similar to 970–1063 ft interval but log characteristics suggest that the sand material is caved from this interval and that the lithologies are similar to those in the 553–970 ft interval
1170 (357)	–722 (–220)	290 (88)	Samples consist predominantly of dark grey, carbonaceous shale, partly micaceous, commonly containing plant impressions, and siltstone, pale grey, quartzose, noncalcareous, rarely containing very fine sand grade quartz grains and comminuted carbonaceous debris. Abundant lignite debris Interval is interpreted as interbedded shale and siltstone with a few lignitic coal seams
1460 (445)	–1012 (–308)	220 (67)	Siltstone, pale grey, quartzose, noncalcareous, in places containing very fine sand grade quartz grains and comminuted carbonaceous debris. Rare carbonaceous shale fragments also present. Samples to 1710 ft level have this characteristic but log characteristics suggest that the lithologic change takes place at approximately 1680 ft level Interval interpreted as siltstone with minor amounts of shale and fine to very fine sand
1680 (512)	–1232 (–376)	193 (59)	Samples similar to 1460–1680 ft interval but containing approximately 5% rounded quartz grains and subangular to subrounded grey chert grains, all typically coarse sand grade Interval interpreted as interbedded fine to coarse sandstone, siltstone and carbonaceous shale

Depth	Elevation	Thickness	Description
	feet (metres)		
1873 (571)	-1425 (-434)	284 (87)	Samples similar to 1460–1680 ft interval Interval interpreted from log characteristics to be predominantly siltstone with minor amounts of shale, section becoming gradually more shaly and argillaceous downward. Sharp change in log characteristics at 2157 ft level
2157 (657)	-1709 (-521)	113 (34)	Siltstone, pale grey, quartzose, argillaceous, with several fine sandy streaks and a few shale interbeds
2270 (692)	-1822 (-555)	80 (24)	Siltstone, argillaceous, pale grey, slightly bentonitic, a few fine sandy streaks
2350 (716)	-1902 (-580)	60 (18)	Siltstone, argillaceous, pale grey to reddish brown, several fine sandy streaks, a few silty shale interbeds
<i>Shale Member</i>			
2410 (735)	-1962 (-598)	170 (52)	Silty shale, medium grey to pale brown and reddish brown, micaceous. A few strongly red-stained (limonitic) fragments, a few grey or pinkish siltstone interbeds
2580 (786)	-2132 (-650)	60 (18)	Silty shale, pale to medium grey, micaceous, several grey siltstone interbeds. Much dispersed comminuted carbonaceous debris, very slightly calcareous
2640 (805)	-2192 (-668)	140 (43)	As in 2410–2580 ft interval
2780 (847)	-2332 (-711)	230 (70)	As in 2580–2640 ft interval. Silt minor in quantity. Pale colours predominate
Kanguk Formation			
<i>Upper sandstone member</i>			
3010 (917)	-2562 (-781)	45 (14)	Argillaceous siltstone, pale grey, slightly micaceous, several very fine sandy interbeds. Noncalcareous, a few plant impressions, much comminuted carbonaceous debris
<i>Shale member (upper part)</i>			
3055 (931)	-2607 (-795)	145 (44)	Silty shale, pale grey, micaceous, noncalcareous, rare small pyrite nodules
3200 (975)	-2752 (-839)	410 (125)	Shale, slightly silty, pale grey, micaceous, noncalcareous, fragments of siderite nodules, becoming rare below 3300 ft. Much casing cement in samples from 3200–3230 ft interval. Trace of dark brown, finely crystalline dolomite below 3290 ft, rare pyrite nodules, rare bituminous streaks. ?Fish fragments at 3470 ft, rare arenaceous foraminifera observed in samples below 3500 ft
3610 (1100)	-3160 (-964)	120 (37)	Shale, silty, micaceous, very slightly calcareous, pale to medium grey, rare scattered sand grains up to 0.6 mm (coarse sand grade), rare pyrite, a few streaks of fine- to very fine grained quartzose sand containing fine sand and silt-size glauconite grains
3730 (1137)	-3282 (-1000)	10 (3)	Pebbly sand with silty and argillaceous matrix, pebbles of quartz and chert up to at least 6 mm in diameter
3740 (1140)	-3292 (1003)	150 (46)	Silty shale with glauconitic sandy streaks, as in 3610–3730 ft interval. Rare sand grains identifiable as fragments of silicified oolite, shale is micaceous and contains scattered pyrite
<i>Lower sand member</i>			
3890 (1186)	-3442 (-1049)	12 (4)	Sandstone as in 3902–3910 ft interval
3902 (1189)	-3454 (-1053)	9 (3)	Core #1, elevations and thicknesses are approximate owing to partial core loss. Sandstone and shale; sandstone is pale grey, very fine grained, quartzose, with scattered, well rounded quartz grains up to very coarse sand grade. Approximately 5% dark grey, subangular chert grains, 1% glauconite grains and rare pink ?feldspar grains. Shale is dark grey, micaceous. Sandstone-shale interbedding is on the millimetre scale
3911 (1192)	-3463 (-1056)	1 (0.3)	Siltstone, pale grey, very fine grained, quartzose, indurated
3912 (1192)	-3464 (-1056)	20 (6)	Sandstone, as in 3902–3911 ft interval, with scattered muscovite flakes. Abundant small flasers of carbonaceous shale, containing comminuted organic debris, abundant bioturbation. End of core #1
3932 (1198)	-3484 (-1062)	54 (16)	Sandstone and siltstone interbedded. Sandstone is as in core #1, siltstone is quartzose, pale grey

Depth	Elevation	Thickness	Description
	feet (metres)		
			<i>Shale member (lower part)</i>
3986 (1215)	-3538 (-1078)	144 (44)	Interbedded siltstone and shale. Siltstone is argillaceous, micaceous, glauconitic, medium grey, slightly calcareous; shale is pale greenish grey, slightly micaceous, slightly calcareous, rare arenaceous foraminifera observed in samples
4130 (1259)	-3683 (-1122)	100 (30)	Similar to 3986-4130 ft interval, but shale paler and slightly bentonitic in places, siltstone commonly contains glauconitic grains. Traces of spherulitic carbonate at base
			<i>Christopher Formation</i>
4230 (1289)	-3782 (-1153)	24 (7)	Shale, grey
4254 (1297)	-3806 (-1160)	13 (4)	Sandstone, white, quartzose, supermature, medium grained with scattered grains up to 3 mm in diameter, well sorted, variable porosity owing to patchy silica cementation, rare secondary pyrite, rare limonitic grain coatings, trace of calcareous cement. No glauconite noted
4267 (1301)	-3819 (-1164)	2 (0.6)	Silty shale
4269 (1301)	-3821 (-1165)	5 (1.5)	Core #2, no recovery
4274 (1303)	-3826 (-1166)	30 (9)	Core #3. Shale, dark grey, silty, micaceous, with several interbeds of pale greenish grey, bioturbated mudstone and quartzose, argillaceous siltstone. Detrital pods of greenish ?chloritic clay- and silt-size glauconite grains scattered throughout the silty horizons. Flaser and very small scale ripple bedding common
4304 (1312)	-3856 (-1175)	3 (1)	No recovery. End of core #3
4307 (1313)	-3859 (-1176)	63 (19)	Shale, silty, micaceous, medium grey to pale greenish grey, trace of pyrite, trace of microcrystalline brown dolomite, from concretions
			<i>Isachsen Formation</i>
4370 (1332)	-3922 (-1195)	42 (13)	Interbedded sandstone, siltstone and shale. Sandstone is white, quartzose, fine to medium grained, with some grains up to coarse sand grade, rare iron cement, siltstone and shale are medium grey and pale greenish grey, micaceous. Streaks of coal common, pyrite nodules common, no glauconite
4412 (1345)	-3964 (-1208)	18 (5)	Interbedded siltstone and shale similar to 4370-4412 ft interval. Red-brown ironstone and pyrite common, no sandstone and coal, no glauconite
4430 (1350)	-3982 (-1214)	100 (30)	Siltstone and shale, siltstone is medium brown, quartzose, well indurated, shale is silty, micaceous, medium grey to pale greenish grey. Abundant quartz sand grains in samples, may be cavings, trace of coal
4530 (1381)	-4082 (-1244)	30 (9)	Sandstone, white, quartzose, mature, a few pale grey chert fragments, coarse to very coarse grained, grains subangular to subrounded, coal streaks common
4560 (1390)	-4112 (-1253)	34 (10)	Sandstone, siltstone and silty shale, sandstone is similar to 4530-4560 ft interval but coarse grained, siltstone is quartzose, shale is silty and micaceous, coal streaks and pyrite common
4594 (1400)	-4146 (-1264)	89 (27)	As in 4560-4594 ft interval but sandstone is very coarse grained; sandstone contains grass-green clay clasts in places, trace of limonitic cement, occasional pebbles of quartz, chert, up to 7 mm
			<i>Mould Bay Formation</i>
4683 (1427)	-4235 (-1291)	107 (33)	Mudstone, dark brownish grey, soft, plastic when wet, abundant arenaceous foraminifera in samples, abundant pelecypod shell fragments
4790 (1460)	-4342 (-1323)	360 (110)	Shale, silty, medium grey and grey-green, slightly micaceous, noncalcareous, abundant arenaceous foraminifera, pelecypod shell fragments, several streaks of siltstone and sandstone, especially in 4900-4910 ft interval, pyrite common
5150 (1570)	-4702 (-1433)	100 (30)	As in 4790-5150 ft interval, but pelecypod fragments and foraminifera slightly less abundant
5250 (1600)	-4802 (-1464)	120 (37)	As in 4790-5150 ft interval

Depth	Elevation	Thickness	Description
	feet (metres)		
Wilkie Point Formation			
5370 (1637)	-4922 (-1500)	500 (152)	Shale, silty, dark grey, slightly calcareous, and minor amounts of siltstone, argillaceous, dark grey, trace of glauconite, abundant pelecypod fragments and fairly abundant arenaceous foraminifera. Top of formation drawn at 5340 ft on basis of mechanical log interpretation
5870 (1789)	-5422 (-1653)	78 (24)	Shale, slightly silty, very dark grey to black, carbonaceous, slightly calcareous, rare foraminifera
Basal sand member			
5948 (1813)	-5500 (-1676)	12 (4)	Samples composed of shale. Log characteristics indicate lithology similar to that in 5960-5974.5 ft interval of core #4
5960 (1817)	-5512 (-1680)	14.5 (4.4)	Core #4. Sandstone, medium brownish grey, fine grained, well sorted, supermature, less than 1% accessory minerals, predominantly chert, grains well rounded, loosely cemented, high porosity and permeability, massive bedding. A 1-inch lens of silty shale with wood fragments at 5973 ft
5974.5 (1820.9)	-5526.5 (-1684.4)	22.0 (6.7)	Sandstone, pale brownish grey, very fine grained, well sorted, supermature, grains round to subangular, trace of glauconite, chert, high intergranular porosity and permeability, streaks of carbonaceous debris every few centimetres. Faint crossbedding visible, rare burrow structures
5996.5 (1827.6)	-5548.5 (-1691.2)	1 (0.3)	Sandstone, very fine grained, as in 5974.5-5996.5 ft interval, interbedded with carbonaceous, silty shale, containing traces of disseminated pyrite. Interbedding on a millimetre scale
5997.5 (1827.9)	-5549.5 (-1691.5)	2.5 (0.8)	Shale, dark grey, silty, carbonaceous
6000 (1829)			Orksut Formation

Columbia et al Ikkariktok M-64

Location: lat. 72°23'45.8"N; long. 121°50'48.8"W

Elevation: 419 ft K.B.

Total depth: 4226 ft

Completed: April 16, 1974

Status: dry and abandoned

Log by A. D. Miall from samples stored at Geological Survey of Canada, Calgary, Alberta, November 13, 1975 - November 21, 1975.

Note: Samples not available for 0-860 ft interval. The descriptions for this interval are based on operator's descriptions and log interpretation**Surficial deposits**

0 (0)	419 (128)	50 (15)	Sand, coarse to medium grained, consisting of quartz, dolomite, igneous and metamorphic grains, chert, trace of carbonaceous shale and coal
----------	--------------	------------	---

Eureka Sound Formation*Cyclic Member*

50 (15)	369 (112)	200 (61)	Sand and gravel, clasts of quartz, chert, dolomite, igneous and metamorphic fragments, traces of carbonaceous shale and coal
250 (76)	169 (52)	610 (186)	Samples consist of up to 80% pebbles, remainder is soft, grey-brown clay and shale, quartz- and chert-bearing sand and silt, traces of carbonaceous shale, plant fragments, coal. Pebbles may all be cavings; lignite becomes more abundant in samples downward
860 (262)	-441 (-134)	210 (64)	Shale, medium brownish grey, in part silty, slightly micaceous, soft; approximately 20% fine- to coarse-grained sand, composed predominantly of quartz and chert; minor lignite and laminated, carbonaceous shale, a little fine-grained quartz sandstone. Below 900 ft colour varies from light grey-brown to dark grey
1070 (326)	-651 (-198)	40 (12)	Shale and sand, as in 860-1070 ft interval, plus up to 30% pale grey to cream quartzose siltstone
1110 (338)	-691 (-211)	60 (18)	Shale and sand, as in 860-1070 ft interval; carbonaceous shale and coal up to 10%

Depth	Elevation	Thickness	Description
	feet (metres)		
1170 (357)	-751 (-229)	10 (3)	Shale, medium grey; very fine sandstone to siltstone, pale grey, argillaceous, quartzose; shale, dark grey to black, carbonaceous; coal; traces of coarse-grained quartzose sand
1180 (360)	-761 (-232)	20 (6)	As in 1070-1110 ft interval
1200 (366)	-781 (-238)	115 (35)	As in 1170-1180 ft interval, very little sandstone in samples
			<i>Shale Member</i>
1315 (401)	-896 (-273)	95 (29)	Mudstone, pale to medium grey, silty, traces of comminuted plant debris, cavings of gravel, carbonaceous shale and lignite in some samples; traces of bentonitic shale below 1370 ft
1410 (430)	-991 (-302)	300 (91)	Mudstone, silty, pale to medium grey, plus hematite-stained mudstone and minor siltstone. Traces of pyrite in the siltstone; rare traces of fine-grained sandstone, traces of coal, becoming abundant in 1710-1720 ft interval
1710 (521)	-1291 (-393)	160 (49)	Mudstone, variably silty, reddish buff. Traces of dark red hematite-stained mudstone, traces of coal, traces of quartzose siltstone to very fine sandstone
			Kanguk Formation
			<i>Upper sand member</i>
1870 (570)	-1451 (-442)	70 (21)	Siltstone, quartzose, buff-grey, grading into very fine grained sandstone. Log interpretation indicates a downward increase in argillaceous content
			<i>Silty shale member (upper part)</i>
1940 (591)	-1521 (-464)	260 (79)	Shale, medium grey, rare foraminifera, trace of pyrite, spherulitic concretions (manganese?) fairly common in 1940-2100 ft interval, abundant at 2010 ft depth
2200 (671)	-1781 (-543)	68 (21)	Interbedded siltstone, minor amounts of very fine grained sandstone and shale, siltstone and sandstone are pale grey, quartzose
2268 (691)	-1849 (-564)	74 (23)	Shale, medium to dark grey, fissile, slightly micaceous, trace of pyrite, trace of coal (cavings?), trace of spherulitic concretions, rare foraminifera
			<i>Lower sand member</i>
2342 (714)	-1923 (-586)	100 (30)	Sandstone, pale grey, very fine grained to silty, quartzose, fair porosity, trace of glauconite, calcareous matrix, rare foraminifera, trace of pyrite. Shale interbeds in lower part of unit
			<i>Silty shale member (lower part)</i>
2442 (744)	-2023 (-617)	173 (53)	Shale, silty, medium grey, slightly micaceous, trace of pyrite, trace of glauconite, virtually noncalcareous
2615 (797)	-2196 (-669)	145 (44)	Interbedded siltstone and very fine grained sandstone, pale grey, quartzose, glauconitic, fair porosity, trace of pyrite, rare pyritized burrows, calcareous matrix
2760 (841)	-2341 (-714)	24 (7)	Siltstone, pale brown, quartzose, noncalcareous, a few shale interbeds
2784 (849)			Nanuk Formation

Elfex Texaco Tiritichik M-48

Location: lat. 72°47'51"N; long. 120°44'48"W

Elevation: 358 ft K.B.

Total depth: 7268 ft

Completed: April 6, 1974

Status: dry and abandoned

Log by A. D. Miall from samples and cores stored at Geological Survey of Canada, Calgary, Alberta, February 3, 1975 - February 28, 1975.

Surficial deposits

0	358	30	No samples
(0)	(109)	(9)	

Depth	Elevation	Thickness	Description
	feet (metres)		
<i>Eureka Sound Formation</i>			
<i>Cyclic Member</i>			
30 (9)	328 (100)	60 (18)	Sand and gravel, samples composed of coarse to very coarse, well rounded quartz grains; dark grey, subangular chert grains and granules; coarse sand grade to small pebble-size fragments of quartz sandstone; rare diabase; rare bluish opaline chert; occasional fragments of lignite and soft, medium grey, silty mudstone
90 (27)	268 (82)	20 (6)	As in 30–90 ft interval, plus abundant fragments of dark grey, carbonaceous shale
110 (34)	248 (76)	20 (6)	As in 30–90 ft interval, sandstone fragments probably partly derived from Eureka Sound Formation, partly derived from Devonian rocks. Diabase probably derived from Proterozoic diabase sills, well rounded quartz grains probably derived from Isachsen Formation
130 (40)	228 (69)	130 (40)	No samples, lithology probably as in 30–90 ft interval
260 (79)	98 (30)	10 (3)	Samples consist of, in order of decreasing abundance, soft, dark grey, carbonaceous shale; medium to pale grey, fine-grained quartzose sandstone; subangular, pebble-size fragments of pale to medium grey and brownish-grey chert; subrounded, coarse sand grade, milky quartz grains; well rounded, coarse sand grade quartz grains; lignite
270 (82)	88 (27)	100 (30)	No samples
370 (113)	-12 (-4)	105 (32)	Shale, soft, pale to dark grey, noncalcareous, with abundant comminuted plant debris, and siltstone, pale to medium grey. Large pebbles of quartzose sandstone, chert, igneous rock fragments, probably all caved. Log interpretation suggests top of shale at 350 ft depth
<i>Shale Member</i>			
475 (145)	-117 (-36)	25 (8)	Shale, medium grey, trace of very comminuted carbonaceous debris, noncalcareous, trace of gypsum, more compact than shale at shallower depths. Pebbles and sand grains abundant, as in 370–475 ft interval, probably cavings
500 (152)	-142 (-43)	20 (6)	Samples consist mainly of casing cement
520 (158)	-162 (-49)	50 (15)	Samples as in 370–475 ft interval, lithology probably siltstone and shale, the remainder of the sample comprising cavings
570 (174)	-212 (-65)	120 (37)	Shale, medium grey, slightly micaceous, slightly calcareous, commonly silty, traces of comminuted plant debris, traces of red-brown mudstone
690 (210)	-332 (-101)	10 (3)	As in 570–690 ft interval, plus abundant red-brown silty shale
700 (213)	-342 (-104)	250 (76)	Mudstone, medium grey, soft, slightly micaceous, slightly calcareous, rarely silty, becomes softer downward. Trace of pyrite at 860 ft
950 (290)	-592 (-180)	290 (88)	Samples predominantly red-brown shale; chert and quartz sand grains; pyrite; minor, very fine grained sandstone. Geophysical log interpretation suggests lithology probably as in 700–950 ft interval, most of the mudstone having been lost in the mud stream
1240 (378)	-882 (-269)	25 (8)	Samples similar to 950–1250 ft interval, plus abundant lignite and carbonaceous shale fragments. Abundant coarse-grained quartz sand near base of interval. Geophysical log interpretation suggests lignite and carbonaceous shale may be important in this interval
<i>Kanguk Formation</i>			
<i>Upper sand member</i>			
1265 (386)	-907 (-276)	35 (11)	Sandstone, very fine grained, quartzose, abundant iron oxide in matrix, grains angular to subrounded
<i>Shale member</i>			
1300 (396)	-942 (-287)	62 (19)	Shale, pale grey, slightly silty, slightly carbonaceous, probably with interbeds of siltstone and sandstone as in 1265–1300 ft interval. Samples include abundant coarse to very coarse quartz sand grains (cavings?)
1362 (415)	-1004 (-306)	88 (27)	Samples mainly coarse to pebbly quartz sand, minor amounts of ferruginous siltstone and minor chert, interpreted as cavings. Geophysical log interpretation suggests lithology predominantly shale, as in 1300–1362 ft interval. Lignite abundant below 1380 ft depth

Depth	Elevation	Thickness	Description
	feet (metres)		
1450 (442)	-1092 (-333)	30 (9)	Samples consist predominantly of siltstone, pale grey to grey-brown, calcareous, containing scattered fine to coarse sand grains. Minor amounts of pale grey shale below 1470 ft. Geophysical log interpretation suggests lithology is mainly shale; siltstone probably caved from 1300–1362 ft interval
1480 (451)	-1122 (-342)	100 (30)	Shale, pale to medium grey, slightly silty, slightly carbonaceous, scattered pyrite, abundant arenaceous foraminifera including <i>Ammodiscus</i> sp. and <i>Cyclamina</i> sp. Minor reddish nodular carbonate in 1480–1530 ft interval, minor pyrite
1580 (482)	-1222 (-372)	150 (46)	Shale, as in 1480–1580 ft interval, but slightly paler, rare arenaceous foraminifera, rare minute crystals of white and colourless gypsum, in single-bladed crystals or small radiating clusters, becoming common in 1660–1720 ft interval, trace of glauconite, trace of mica, trace of pyrite
1730 (528)	-1372 (-418)	150 (46)	Shale, medium grey, slightly silty, slightly micaceous, slightly calcareous, traces of white gypsum crystals
1880 (573)	-1522 (-464)	20 (6)	Shale, pale grey, soft, virtually noncalcareous
1900 (579)	-1542 (-470)	10 (3)	Sandstone, pale grey, very fine grained, quartzose with ferruginous cement
1910 (582)	-1552 (-473)	70 (21)	Shale, medium grey, as in 1730–1880 ft interval, trace of pyrite, occasional streaks of fine to coarse sand in quartzose siltstone matrix, traces of gypsum
1980 (603)	-1622 (-495)	10 (3)	Sandstone, as in 1900–1910 ft interval
1990 (606)	-1632 (-498)	40 (12)	Shale, medium to dark grey, slightly micaceous, slightly calcareous, arenaceous foraminifera. Samples from 2010–2060 ft interval contain much casing cement
2030 (619)	-1672 (-510)	40 (12)	Siltstone, quartzose, soft, very calcareous, pale grey, with pale grey silty shale interbeds
2070 (631)	-1712 (-522)	70 (21)	Shale, pale to medium, slightly brownish grey, slightly micaceous, slightly silty, calcareous, with interbeds of calcareous siltstone as in 2030–2070 ft interval, a few white gypsum crystals
2140 (652)	-1782 (-543)	110 (34)	Shale, medium to dark grey, slightly micaceous, slightly calcareous, with minor silty interbeds
2250 (686)	-1892 (-577)	100 (30)	Siltstone, pale grey, quartzose, calcareous matrix, cleanest and coarsest grained in uppermost 40 ft of interval, becoming argillaceous below
2350 (716)	-1992 (-607)	115 (35)	Mudstone, medium grey, silty with interbeds of pale grey shale and argillaceous siltstone
2465 (751)	-2107 (-642)	45 (14)	Siltstone, as in 2250–2350 ft interval, glauconitic
2510 (765)			<i>Weatherall Formation</i>

Appendix 3

Stratigraphic sections

Index of field stations

Station	Location	Latitude	Longitude	Formations
		° ' "	° ' "	
73-MLA-7	Antler Cove	74 24	120 47	Eureka Sound
73-MLA-19	Nangmagvik Lake	74 08	119 56	Eureka Sound
73-MLA-20	Nangmagvik Lake	74 08	119 56	Eureka Sound
73-MLA-21	Nangmagvik Lake	74 09	119 55	Eureka Sound
73-MLA-26	Baker Creek	73 37	120 06	Isachsen, Christopher
73-MLA-29	Cape Vesey Hamilton	74 13	118 21	Isachsen
73-MLA-30	Cape Vesey Hamilton	74 15	118 19	Isachsen
73-MLA-31	Mercy River	74 08	118 40	Isachsen
73-MLA-37	Eames River	74 17	120 09	Eureka Sound
73-MLA-38	Eames River	74 17	120 31	Eureka Sound
73-MLA-39	Muskox River	73 42	120 50	Eureka Sound
73-MLA-40	Muskox River	73 42	120 50	Eureka Sound
73-MLA-42	Muskox River	73 46	120 17	Kanguk
73-MLA-43	Log River	74 16	121 56	Eureka Sound
73-MLA-44	Eames River	74 17	120 28	Eureka Sound
74-MLA-2	Nelson Head	71 06	122 57	Isachsen
74-MLA-4	Nelson Head	71 06	122 56	Isachsen
74-MLA-6	Nelson Head	71 06	122 58	Isachsen
74-MLA-17	Alexander Milne Point	71 33	120 30	Isachsen
74-MLA-18	Alexander Milne Point	71 32	120 33	Isachsen
74-MLA-43	Castel Bay	74 13	119 42	Eureka Sound
74-MLA-44	Antler Cove	74 28	121 03	Christopher, Hassel, Kanguk
74-MLA-45	Log River	74 20	122 00	Eureka Sound
74-MLA-46	Log River	74 17	121 57	Eureka Sound
74-MLA-93	Mercy Bay	74 02	119 28	Kanguk
74-MLA-104	Muskox River	73 44	120 24	Hassel, Kanguk
74-MLA-113	Muskox River	73 38	120 35	Eureka Sound
74-MLA-114	Muskox River	73 46	120 24	Kanguk
74-MLA-115	Mahogany Point	74 13	119 27	Eureka Sound
74-MLA-116	Desert Creek	74 15	119 55	Eureka Sound
74-MLA-118	Eames River	74 12	120 34	Eureka Sound
74-MLA-126	Thomsen River	74 03	119 56	Eureka Sound
74-MLA-150	Bernard River	73 29	122 13	Eureka Sound
74-MLA-154	Muskox River	73 53	120 34	Eureka Sound
74-MLA-155	Desert Creek	74 04	120 12	Eureka Sound
74-MLA-157	Eames River	74 14	120 40	Eureka Sound
74-MLA-158	Desert Creek	74 12	120 15	Eureka Sound
74-MLA-159	Desert Creek	74 15	119 55	Eureka Sound
74-GAS-4	Rufus River	71 25	123 28	Christopher
74-GAS-7	Nelson River	71 22	122 45	Christopher
74-GAS-8	Alexander Milne Point	71 37	120 25	Isachsen
74-GAS-11	Sandhill River	71 27	122 09	Isachsen, Christopher
74-GAS-12	Masik River	71 37	123 27	Christopher
74-GAS-13	Atitok River	71 31	123 23	Christopher
74-GAS-21	Thomsen River	73 57	119 50	Kanguk, Hassel
74-GAS-25	Back Point	74 15	118 30	Christopher
74-GAS-46	Cape M'Clure	74 31	121 10	Christopher

Legend. 73, 74: year of measurement; MLA: measured and described by A.D. Miall; GAS: measured and described by A.S. Greene.

Appendix 3 (cont.)

Unit	Lithology	Thickness		Height above base	
		m	(ft)	m	(ft)
Station 73-MLA-7					
<i>Eureka Sound Formation</i>					
<i>Shale Member (part of)</i>					
12	Sandstone, very fine grained, calcareous, silty, medium grey, weathering to orange-brown, with abundant wood impressions and comminuted plant debris	0.5	(1.6)	87.5	(287.1)
11	Shale, poorly exposed	12.0	(39.4)	87.0	(285.5)
10	As in unit 12, persistent lens	1.5	(4.9)	75.0	(246.1)
9	Shale, dark grey, soft, rarely iron-stained to red-brown	5.0	(16.4)	73.5	(241.2)
8	As in unit 12, impersistent lens	1.0	(3.3)	68.5	(224.8)
7	As in unit 9	2.5	(8.2)	67.5	(221.5)
6	As in unit 12. This unit is a prominent ridge-former, traceable laterally for at least 2 km (1.2 mi)	1.5	(4.9)	65.0	(213.3)
5	Sand, fine grained, light grey, calcareous, mainly unconsolidated except at top of unit where it grades into unit 6. Solitary trough crossbeds	0.5	(1.6)	63.5	(208.3)
4	Shale, as in unit 9, with thin, discontinuous sandstone lenticles containing bioturbation structures, very small scale festoon trough crossbedding	20.5	(67.3)	63.0	(206.7)
3	Sandstone, light grey, fine grained, well sorted, no bedding visible, noncalcareous, lithified, slabby weathering	0.2	(0.7)	42.5	(139.4)
2	Shale, as in unit 9, plus rare sideritic ironstone lenses, rare fragments of wood, cone-in-cone limestone	27.3	(89.6)	42.3	(138.8)
1	Covered interval, probably shale, estimated thickness above upper sand member of the Kanguk Formation	15.0	(49.2)	15.0	(49.2)
Station 73-MLA-19					
<i>Eureka Sound Formation</i>					
<i>Cyclic Member (part of)</i>					
31	Shale, dark grey-brown, with rare streaks of very fine sand. Lens of ironstone at top of unit	2.5	(8.2)	54.0	(177.2)
30	Sand, very fine grained, with abundant streaks and thin beds of shale	0.5	(1.6)	51.5	(169.0)
29	Sand, very fine grained, medium grey, slightly argillaceous, solitary trough crossbeds and small-scale festoon crossbedding	0.5	(1.6)	51.0	(167.3)
28	As in unit 31	1.8	(5.9)	50.5	(165.7)
27	Sand, very fine grained	0.1	(0.3)	48.7	(159.8)
26	Shale, dark grey-brown, weathering to pale grey, rests on unit 25 with sharp, flat contact	0.1	(0.3)	48.6	(159.5)
25	As in unit 29. Trough crossbeds up to 3 m (10 ft) wide	2.0	(6.6)	48.5	(159.1)
24	As in unit 30	0.5	(1.6)	46.5	(152.6)
23	Shale, as in unit 22, but weathering pale grey, nonmicaceous	4.0	(13.1)	46.0	(150.9)
22	Shale, dark grey, weathering brown, slightly micaceous. Rests on ripple-marked surface of unit 21 with sharp contact, grades up into unit 23	1.5	(4.9)	42.0	(137.8)
21	As in unit 29	1.5	(4.9)	40.5	(132.9)
20	As in unit 30	1.4	(4.6)	39.0	(128.0)
19	Shale, dark grey, slightly micaceous	0.1	(0.3)	37.6	(123.4)
18	As in unit 29	0.3	(1.0)	37.5	(123.0)

Unit	Lithology	Thickness		Height above base	
		m	(ft)	m	(ft)
17	Shale, black, carbonaceous, with abundant lignite fragments, rests on unit 16 with sharp contact, grades laterally into lignite in places	0.2	(0.7)	37.2	(122.1)
16	As in unit 29	2.0	(6.6)	37.0	(121.4)
15	As in unit 30	3.0	(9.8)	35.0	(114.9)
14	As in unit 19	4.0	(13.1)	32.0	(105.0)
13	As in unit 30, with layer of clay-ironstone nodules	0.5	(1.6)	28.0	(91.9)
12	As in unit 19	0.5	(1.6)	27.5	(90.2)
11	Sand, very fine grained, with argillaceous streaks, laminated, no crossbedding observed, abundant ironstone nodules	9.5	(31.2)	27.0	(88.6)
10	As in unit 30	2.5	(8.2)	17.5	(57.4)
9	Shale, silty, medium to dark grey, slightly micaceous, with very fine grained sand laminae, grades up into unit 10	2.5	(8.2)	15.0	(49.2)
8	Shale, black, laminated, abundant carbonaceous debris	0.3	(1.0)	12.5	(41.0)
7	Shale, pale grey, slightly micaceous, abundant plant debris, laminated, patches of brown iron staining	0.7	(2.3)	12.2	(40.0)
6	As in unit 9	4.5	(14.8)	11.5	(37.7)
5	As in unit 29	1.0	(3.3)	7.0	(23.0)
4	As in unit 19	0.5	(1.6)	6.0	(19.7)
3	Lignite, abundant partly altered plant roots and stems, abundant thin streaks of soft, medium grey, micaceous shale with abundant comminuted carbonaceous debris	2.0	(6.6)	5.5	(18.0)
2	Sand, very fine grained, micaceous with abundant carbonaceous streaks, finely laminated, abundant climbing-ripple lamination	2.5	(8.2)	3.5	(11.5)
1	As in unit 30	1.0	(3.3)	1.0	(3.3)

Station 73-MLA-20***Eureka Sound Formation******Cyclic Member (part of)***

16	Siltstone, pale grey	3.5	(11.5)	60.5	(198.5)
15	Shale, dark grey-brown, slightly micaceous, weathering pale grey	2.0	(6.6)	57.0	(187.0)
14	Sand, very fine grained, with thin interbeds of soft shale, climbing-ripple cross-lamination	8.0	(26.2)	55.0	(180.5)
13	As in unit 15	7.0	(23.0)	47.0	(154.2)
12	As in unit 14	12.5	(41.0)	40.0	(131.2)
11	As in unit 15	5.5	(18.0)	27.5	(90.2)
10	Shale, silty, grey-brown, slightly micaceous, rare climbing-ripple lamination	1.5	(4.9)	22.0	(72.2)
9	Sand, very fine grained, with argillaceous streaks	1.0	(3.3)	20.5	(67.3)
8	As in unit 15	3.0	(9.8)	19.5	(64.0)
7	Sand, fine grained, solitary sets of medium-scale planar crossbedding, climbing-ripple lamination, mineralized tree trunks up to 2 m long, ironstone lenticles up to 30 cm (1 ft) thick, containing wood impressions	6.0	(19.7)	16.5	(54.1)
6	Sand, medium grained, with large-scale superimposed trough crossbeds	3.5	(11.5)	10.5	(34.5)
5	Sand, fine grained, climbing-ripple lamination; wedge-shaped unit draped over underlying bed	1.0	(3.3)	7.0	(23.0)
4	Sand, fine to medium grained with large-scale trough crossbeds infilled with sand showing climbing-ripple lamination, passing laterally into large-scale planar crossbed set, foresets containing wood fragments	2.5	(8.2)	6.0	(19.7)

Unit	Lithology	Thickness		Height above base	
		m	(ft)	m	(ft)
3	Sand, fine grained, argillaceous, finely laminated with climbing-ripple lamination, small-scale solitary trough crossbeds up to 50 cm wide, containing wood fragments	1.0	(3.3)	3.5	(11.5)
2	Shale, dark brown, silty, slightly micaceous	1.0	(3.3)	2.5	(8.2)
1	Sand, medium grey, fine grained, argillaceous with rare shale streaks	1.5	(4.9)	1.5	(4.9)

Station 73-MLA-21***Eureka Sound Formation****Cyclic Member (part of)*

29	Sand, very fine grained, medium grey, laminated with abundant climbing-ripple lamination	4.5	(14.8)	78.0	(255.9)
28	Interbedded shale and very fine grained silty sand, laminated	4.0	(13.1)	73.5	(241.1)
27	Shale, dark grey, weathering to pale grey, lenticles of lignite, carbonized logs up to 1 m (3.3 ft) in length	0.9	(2.9)	69.5	(228.0)
26	Lignite, lenticular, discontinuous	0.1	(0.3)	68.6	(225.1)
25	Interbedded sand and shale, sand is laminated, with abundant climbing-ripple lamination	4.5	(14.8)	68.5	(224.7)
24	Shale, dark grey, with minor sandy streaks, grades up into unit 25	2.0	(6.6)	64.0	(210.0)
23	Sand, very fine grained, with rare argillaceous streaks, large-scale solitary trough crossbeds, large-scale symmetrical ripple marks, climbing-ripple lamination	3.3	(10.8)	62.0	(203.4)
22	Ironstone, lenticular, plant impressions	0.2	(0.7)	58.7	(192.6)
21	Shale, dark grey to dark grey-brown, slightly micaceous, with minor fine sandy and silty streaks	7.3	(24.0)	58.5	(191.9)
20	Ironstone, as in unit 22	0.2	(0.7)	51.2	(168.0)
19	As in unit 28	1.5	(4.9)	51.0	(167.3)
18	Sand, fine grained, medium grey, slightly argillaceous, slightly micaceous, solitary trough crossbeds and, at top of unit, climbing-ripple lamination	2.5	(8.2)	49.5	(162.4)
17	As in unit 28, wavy and flaser bedding	1.5	(4.9)	47.0	(154.2)
16	Shale, dark grey, weathering to pale grey, slightly micaceous, relatively more resistant than the unconsolidated sand units	4.3	(14.1)	45.5	(149.3)
15	As in unit 22	0.2	(0.7)	41.2	(135.2)
14	Shale, medium grey, platy weathering, very slightly micaceous	0.5	(1.6)	41.0	(134.5)
13	Sand, very fine grained, rare wavy-bedded argillaceous streaks, climbing-ripple lamination	2.5	(8.2)	40.5	(132.9)
12	Sand, minor shale beds, shale increasing upward, laminated, climbing-ripple lamination, at top of unit narrow, steep-sided scours	1.8	(5.9)	38.0	(124.7)
11	Lignite, with log fragments and lenses of pale grey shale	0.2	(0.7)	36.2	(118.8)
10	Shale, black, carbonaceous, at base, becoming pale grey at top, with plant fragments	1.0	(3.3)	36.0	(118.1)
9	Sand, as in unit 18	2.0	(6.6)	35.0	(114.8)
8	Interbedded sand and shale, shale is soft, dark grey, slightly micaceous, sand is very fine grained, slightly argillaceous, medium grey, laminated	1.9	(6.2)	33.0	(108.3)
7	As in unit 22	0.1	(0.3)	31.1	(102.0)
6	As in unit 8	2.0	(6.6)	31.0	(101.7)
5	Shale, dark grey, slightly micaceous, soft, friable	5.3	(17.4)	29.0	(95.1)
4	Ironstone, red-brown, platy-weathering	0.2	(0.7)	23.7	(77.8)

Unit	Lithology	Thickness		Height above base	
		m	(ft)	m	(ft)
3	Sand, fine grained, medium grey, quartzose, slightly micaceous, laminated, rare streaks of shale	16.0	(52.5)	23.5	(77.1)
2	Shale, black, slightly micaceous, silty	4.5	(14.8)	7.5	(24.6)
1	Shale, dark grey, laminated, slightly micaceous, thin streaks and lenses of sand showing contortion and rip-up clasts	3.0	(9.8)	3.0	(9.8)

Station 73-MLA-26***Christopher Formation (part of)***

13	Interbedded sand and shale, sand is very fine grained, shale is medium grey, bioturbated, contains clay-ironstone concretions	16.0	(52.5)	37.5	(123.0)
----	---	------	--------	------	---------

Isachsen Formation (part of)

12	Sand, very fine grained, quartzose, with thin laminae of shale and lignite showing flaser bedding, small-scale trough crossbeds; thin cyclic units of sand, root bed, shale, in upward order, cycles commonly 10 cm thick, rarely 15 cm. Abrupt contact with overlying unit	7.5	(24.6)	21.5	(70.6)
11	Sand, medium grained, large-scale planar crossbeds, abundant lignite fragments in toe of foresets	0.5	(1.6)	14.0	(45.9)
10	Sand, medium grained, planar laminated, lignite fragments sparse to abundant, climbing-ripple cross-lamination	0.9	(2.9)	13.5	(44.3)
9	Sand, as in units 10 and 11, in alternating sequence	2.6	(8.5)	12.6	(41.3)
8	Sand, medium to coarse grained, laminated, lignite lenticles, pebbles, small-scale planar and trough crossbedding and climbing-ripple lamination	2.0	(6.6)	10.0	(32.8)
7	Sand, as in unit 9	1.0	(3.3)	8.0	(26.2)
6	Sand, as in unit 8	0.3	(1.0)	7.0	(23.0)
5	Sand, as in unit 9	4.4	(14.4)	6.7	(22.0)
4	Pebble conglomerate, very angular pebbles of silicified carbonate sediments, quartz and chert	0.1	(0.3)	2.3	(7.5)
3	Sand, as in unit 9	1.6	(5.2)	2.2	(7.2)
2	Sand, medium grained, laminated, abundant fragments of lignite, abundant pebbles up to 3.5 cm diameter of quartz, chert, silicified carbonate sediments, quartzose sandstone	0.4	(1.3)	0.6	(2.0)
1	Sand, as in unit 11	0.2	(0.7)	0.2	(0.7)

Station 73-MLA-29***Isachsen Formation (part of)***

7	Sand, coarse grained, argillaceous, laminated	0.3	(1.0)	28.1	(92.2)
6	Sand, medium to coarse grained, with pebbles and cobbles in lower part of unit, abundant large-scale planar crossbedding	6.7	(22.0)	27.8	(91.2)
5	Boulder conglomerate, clasts up to 73 cm (38.7 in.) in long diameter, consisting of quartzose sandstone and silicified carbonate sediments, including flat-pebble conglomerate, stromatolites, clasts angular to subangular, imbricated	0.6	(1.9)	21.1	(69.2)
4	Pebbly sand, small-scale planar crossbeds, wood fragments, clay clasts up to 14 cm (5.5 in.) in diameter	1.0	(3.3)	20.5	(67.3)
3	Sand, medium to coarse grained, with rare argillaceous streaks, angular clasts of quartzose sandstone up to 8 cm (3.1 in.) in diameter, rare planar laminated intervals with small-scale ripple marks, abundant large-scale planar and trough crossbedding	6.3	(20.7)	19.5	(64.0)

Unit	Lithology	Thickness		Height above base	
		m	(ft)	m	(ft)
2	Sand, medium grained, with argillaceous lenticles, angular pebbles up to 3.5 cm (1.4 in.) in diameter at top of unit, abundant planar crossbedding	3.7	(12.1)	13.2	(43.3)
1	Shale, soft, laminated, dark grey, with silty streaks, interbedded with fine- to medium-grained sand containing argillaceous lenticles, planar laminated	9.5	(31.2)	9.5	(31.2)
Station 73-MLA-30					
<i>Isachsen Formation</i>					
35	Sand, very fine grained, silty, with argillaceous streaks, weathering with castellated appearance	2.0	(6.6)	95.5	(313.3)
34	Sand, quartzose, white, medium to coarse grained with abundant large-scale superimposed planar crossbeds	2.0	(6.6)	93.5	(306.8)
33	Sand, fine to medium grained, planar laminated with small, superimposed, low-angle planar crossbeds	1.0	(3.3)	91.5	(300.2)
32	As in unit 34	0.3	(1.0)	90.5	(296.9)
31	As in unit 33	0.3	(1.0)	90.2	(295.9)
30	As in unit 34	2.0	(6.6)	89.9	(295.0)
29	Sand, quartzose, white, fine to medium grained, planar-bedded, rare lignite streaks	2.5	(8.2)	87.9	(288.4)
28	As in unit 34	5.3	(17.4)	85.4	(280.2)
27	Sand, white, quartzose, fine grained, abundant lignite, rare contorted ripple marks	2.2	(7.2)	80.1	(262.8)
26	As in unit 34	0.5	(1.5)	77.9	(255.6)
25	Lignite	0.1	(0.3)	77.4	(253.9)
24	As in unit 34, with large trough crossbed at top of unit	3.4	(11.1)	77.3	(253.6)
23	As in unit 33	0.3	(1.0)	73.9	(242.5)
22	As in unit 34	0.3	(1.0)	73.6	(241.5)
21	As in unit 33	0.4	(1.3)	73.3	(240.5)
20	As in unit 34, with log fragments up to 6 cm (2.4 in.) in diameter	0.6	(2.0)	72.9	(239.2)
19	Cobble- and boulder-conglomerate clast-supported framework, clasts predominantly quartzose sandstone of the Melville Island Group, up to 34 cm (1.1 ft) in diameter, angular to subrounded, coarse sand matrix	0.3	(1.0)	72.3	(237.2)
18	As in unit 34	1.3	(4.3)	72.0	(236.2)
17	Pebble bed, pebbles up to 10 cm (4 in.) in diameter, angular to rounded	0.3	(1.0)	70.7	(232.0)
16	As in unit 34, with minor intervals of planar-laminated, medium-grained sand; large-scale planar crossbeds abundant, smaller scale planar crossbeds and small, superimposed trough crossbeds also present. Lignite streaks common, especially in toe of crossbed foresets	3.3	(10.8)	70.4	(231.0)
15	Sand, medium grained, becoming coarse and pebbly at top. Maximum clast size 15 cm (6 in.), clasts angular, consist predominantly of silicified carbonate debris and quartzose sandstone	0.2	(0.7)	67.1	(220.1)
14	As in unit 34	0.2	(0.7)	66.9	(219.5)
13	As in unit 33, with small-scale climbing-ripple lamination	0.3	(1.0)	66.7	(218.9)
12	Sand, very coarse to gritty, with small pebbles, planar crossbedding	0.1	(0.3)	66.4	(217.9)
11	As in unit 33, with small-scale asymmetric ripple marks	0.1	(0.3)	66.3	(217.5)
10	Pebble conglomerate, modal pebble size 3 cm (1.8 in.), rare clasts up to 14 cm (5.5 in.), angular to rounded, consisting predominantly of quartzose sandstone and silicified carbonate sediments. Matrix of coarse sand with lignite streaks	0.6	(2.0)	66.2	(217.2)

Unit	Lithology	Thickness		Height above base	
		m	(ft)	m	(ft)
9	As in unit 34	1.0	(3.3)	65.6	(215.3)
8	As in unit 33	1.0	(3.3)	64.6	(212.0)
7	As in unit 34	1.5	(4.8)	63.6	(208.7)
6	As in unit 33	0.5	(1.6)	62.1	(203.8)
5	As in unit 34	1.1	(3.4)	61.6	(202.1)
4	As in unit 33, with scattered pebbles up to 2 cm (1 in.) in diameter, fragments of wood up to 50 cm (20 in.) in length, rare large-scale trough crossbeds	0.5	(1.5)	60.5	(198.5)
3	As in unit 34, with scattered pebbles and lignite fragments	1.5	(5.0)	60.0	(196.9)
2	Covered, to base of creek bed	2.0	(6.6)	58.5	(191.9)
1	Mainly covered, along course of creek flowing into the sea with scattered outcrops of sand similar to units 33 and 34	56.5	(185.4)	56.5	(185.4)

Station 73-MLA-31***Christopher Formation (part of)***

10	Shale, dark grey, poorly exposed	2.0	(6.6)	48.5	(159.1)
----	----------------------------------	-----	-------	------	---------

Isachsen Formation (part of)

9	Sand, very fine grained, silty, with argillaceous streaks, weathering with castellated appearance	6.0	(19.7)	46.5	(152.6)
8	Sand, fine grained, planar laminated with rare small-scale ripple marks	2.0	(6.6)	40.5	(132.9)
7	Clay ironstone	0.2	(0.7)	38.5	(126.3)
6	As in unit 9	7.0	(23.0)	38.3	(125.7)
5	Sand, fine grained, interbedded with soft, dark grey shale	13.0	(42.7)	31.3	(102.7)
4	Sand, fine grained, massive, with rare, large-scale, solitary sets of planar and trough crossbedding	3.0	(9.8)	18.3	(60.0)
3	Sand, fine grained, with large-scale trough crossbeds	1.0	(3.3)	15.3	(50.2)
2	Sand, as in unit 4, plus small-scale ripple marks	4.0	(13.1)	14.3	(46.9)
1	Sand, fine to medium grained, with abundant superimposed large-scale planar crossbed sets and less common trough crossbeds, rare small-scale planar crossbeds; thin seams of lignite, lignite fragments abundant, commonly concentrated in toe of foreset beds	10.3	(33.7)	10.3	(33.7)

Station 73-MLA-37***Eureka Sound Formation******Cyclic Member (part of)***

22	Sand, fine grained, medium grey, slightly greenish, argillaceous, laminated, with <i>Ophiomorpha</i> burrows in place	8.1	(26.6)	53.0	(173.9)
21	Shale, dark brown	0.2	(0.7)	44.9	(147.3)
20	Ironstone, nodular, replacing and cementing sand with small-scale ripple marks, roots, plant fragments	0.2	(0.7)	44.7	(146.7)
19	Sand, fine grained, medium grey, slightly greenish, argillaceous, laminated, iron-stained streaks and thin ironstone lenticles	2.0	(6.6)	44.5	(146.0)
18	Interbedded shale, dark brown, and very fine grained, silty sand	1.5	(4.9)	42.5	(139.4)
17	Siltstone, argillaceous, pale grey, laminated, rare argillaceous streaks and lenticles	5.1	(16.7)	41.0	(134.5)

Unit	Lithology	Thickness		Height above base	
		m	(ft)	m	(ft)
16	Lignite	0.1	(0.3)	35.9	(117.8)
15	Siltstone, argillaceous, dark grey, laminated, with rootlets	0.8	(2.6)	35.8	(117.5)
14	As in unit 18, grading up into unit 15	1.0	(3.3)	35.0	(114.8)
13	As in unit 19 plus abundant, symmetrical and asymmetrical ripple marks, abundant rootlets	1.5	(4.9)	34.0	(111.6)
12	Shale, dark grey, weathering dark brown	4.0	(13.1)	32.5	(106.6)
11	As in unit 13	2.0	(6.6)	28.5	(93.5)
10	As in unit 18	2.5	(8.2)	26.5	(86.9)
9	As in unit 19	1.5	(4.9)	24.0	(78.7)
8	As in unit 18	4.5	(14.8)	22.5	(73.8)
7	As in unit 19	0.5	(1.6)	18.0	(59.1)
6	As in unit 18, rare large ironstone concretions	6.5	(21.3)	17.5	(57.4)
5	As in unit 19	1.0	(3.3)	11.0	(36.1)
4	Shale, dark brown	2.0	(6.6)	10.0	(32.8)
3	As in unit 19	1.5	(4.9)	8.0	(26.2)
2	Shale, dark brown	1.5	(4.9)	6.5	(21.3)
1	As in unit 19	5.0	(16.4)	5.0	(16.4)

Station 73-MLA-38***Eureka Sound Formation****Cyclic Member (part of)*

7	Shale, dark grey, weathering brown, abrupt contact with unit 6	3.0	(9.8)	20.0	(65.6)
6	Sand, fine grained, medium grey, argillaceous, with abundant climbing-ripple lamination, abundant roots	3.5	(11.5)	17.0	(55.8)
5	As in unit 7	1.3	(4.3)	13.5	(44.2)
4	As in unit 6	2.5	(8.2)	12.2	(40.0)
3	Lignite	0.2	(0.7)	9.7	(31.8)
2	Soil, dark brown, sandy, with abundant rootlets	0.2	(0.7)	9.5	(31.2)
1	As in unit 6, abundant rootlets in topmost 50 cm below unit 2	9.3	(30.5)	9.3	(30.5)

Station 73-MLA-39***Eureka Sound Formation****Cyclic Member (part of)*

20	Interbedded sand and shale	2.0	(6.6)	71.0	(233.0)
19	Sand, fine grained, medium grey, laminated, trough crossbeds and ripple marks	9.0	(29.5)	69.0	(226.4)
18	Shale, dark brown	7.5	(24.6)	60.0	(196.9)
17	As in unit 19, some carbonaceous streaks, rootlets, grades up into unit 18	1.0	(3.3)	52.5	(172.3)
16	Shale, dark grey, weathering pale brown-grey	2.5	(8.2)	51.5	(169.0)
15	As in unit 19, abundant roots, abrupt contact with unit 16	1.0	(3.3)	49.0	(160.8)
14	Interbedded sand and shale, with rootlets	2.0	(6.6)	48.0	(157.5)
13	As in unit 19	2.0	(6.6)	46.0	(150.9)
12	As in unit 16	10.5	(34.5)	44.0	(144.4)

Unit	Lithology	Thickness		Height above base	
		m	(ft)	m	(ft)
11	As in unit 20	0.5	(1.6)	33.5	(109.9)
10	As in unit 16	3.5	(11.5)	33.0	(108.3)
9	Soil, dark brown, sandy, with root fragments	1.0	(3.3)	29.5	(96.8)
8	Sand, medium grey, small-scale ripple marks, rare roots	1.5	(4.9)	28.5	(93.5)
7	Shale, dark brown	3.0	(9.8)	27.0	(88.6)
6	As in unit 19	2.0	(6.6)	24.0	(78.7)
5	Sand with rare streaks of dark grey, carbonaceous shale	0.5	(1.6)	22.0	(72.2)
4	As in unit 7	1.0	(3.3)	21.5	(70.5)
3	As in unit 19, abrupt contact with unit 4	0.5	(1.6)	20.5	(67.3)
2	Shale, dark grey-brown, rare roots in upper 1 m	5.0	(16.4)	20.0	(65.6)
1	Sand, laminated, fine grained, slightly argillaceous, ironstone lenses, rare streaks of carbonaceous shale, abundant wood fragments	15.0	(49.2)	15.0	(49.2)

Station 73-MLA-40

Eureka Sound Formation

Cyclic Member (part of)

30	Interbedded sand and shale, laminated wavy and flaser bedding, sand becomes dominant near top of unit	3.0	(9.8)	78.0	(255.9)
29	Shale, dark brown, grading up into unit 30	3.0	(9.8)	75.0	(246.1)
28	As in unit 30, rootlets in upper part of unit, followed abruptly by unit 29	5.0	(16.4)	72.0	(236.2)
27	Shale, dark brown, laminated	0.8	(2.6)	67.0	(219.8)
26	Lignite	0.2	(0.7)	66.2	(217.2)
25	Sand, fine grained, medium grey, laminated, a few argillaceous streaks, small-scale ripple marks, abundant rootlets	2.0	(6.6)	66.0	(216.6)
24	As in unit 30	2.0	(6.6)	64.0	(210.0)
23	As in unit 27	4.0	(13.1)	62.0	(203.4)
22	Sand, fine grained, medium grey, some shale streaks	1.0	(3.3)	58.0	(190.3)
21	As in unit 30, grades up into unit 22	2.0	(6.6)	57.0	(187.0)
20	As in unit 27	1.5	(4.9)	55.0	(180.5)
19	Sand, very fine grained, silty, buff	0.5	(1.6)	53.5	(175.5)
18	As in unit 22, ripple marks	2.0	(6.6)	53.0	(173.9)
17	As in unit 19	1.0	(3.3)	51.0	(167.3)
16	As in unit 27	0.5	(1.6)	50.0	(164.1)
15	Lignite, containing log fragments at top, laterally persistent for several hundred metres	0.5	(1.6)	49.5	(162.4)
14	As in unit 25	2.0	(6.6)	49.0	(160.8)
13	As in unit 27, grading up into unit 14	10.9	(35.8)	47.0	(154.2)
12	Lignite, lenticular, with log fragments	0.1	(0.3)	36.1	(118.4)
11	Sand, fine grained, medium grey, laminated, rare argillaceous streaks, ripple marks, ironstone nodules	2.0	(6.6)	36.0	(118.1)
10	Shale, as in unit 27, grading up into unit 11, abrupt contact with unit 9	5.5	(18.0)	34.0	(111.6)
9	Shale with a few streaks of silty sand, rootlets	0.5	(1.6)	28.5	(93.5)
8	Shale, dark brown, scattered ironstone nodules	4.0	(13.1)	28.0	(91.9)
7	As in unit 22	3.0	(9.8)	24.0	(78.7)

Unit	Lithology	Thickness		Height above base	
		m	(ft)	m	(ft)
6	Sand, fine grained, medium grey, laminated, a few argillaceous streaks, small-scale ripple marks	1.5	(4.9)	21.0	(68.9)
5	As in unit 30	1.0	(3.3)	19.5	(64.0)
4	As in unit 27	2.5	(8.2)	18.5	(60.7)
3	As in unit 6	4.0	(13.1)	16.0	(52.5)
2	As in unit 27	5.5	(18.0)	12.0	(39.4)
1	As in unit 6	6.5	(21.3)	6.5	(21.3)

Station 73-MLA-42***Kanguk Formation (part of)***

13	Shale, dark grey, with common sandy streaks	2.0	(6.6)	54.0	(177.2)
12	Shale, dark grey, minor amounts of iron oxide staining, abundant small dolomite-siderite nodules	6.0	(19.7)	52.0	(170.6)
11	Sand, quartzose, coarse grained to gritty	1.0	(3.3)	46.0	(150.9)
10	As in unit 12	1.3	(4.2)	45.0	(147.6)
9	Nodular, sideritic clay ironstone	0.2	(0.7)	43.7	(143.4)
8	As in unit 12	3.4	(11.2)	43.5	(142.7)
7	Sand, very argillaceous, pebbly, pebbles subrounded to well rounded, up to 2 cm in diameter, consist predominantly of dark grey chert	0.1	(0.3)	40.1	(131.5)
6	As in unit 12 with lenses of clay ironstone	1.8	(5.9)	40.0	(131.2)
5	As in unit 7	0.2	(0.7)	38.2	(125.3)
4	As in unit 12	10.0	(32.8)	38.0	(124.7)
3	As in unit 6	2.0	(6.6)	28.0	(91.9)
2	As in unit 12	1.0	(3.3)	26.0	(85.3)
1	Shale, dark grey, sparse iron staining	25.0	(82.0)	25.0	(82.0)

Station 73-MLA-43***Eureka Sound Formation******Cyclic Member (part of)***

11	Interbedded sand and shale; sand is fine grained, medium grey, shale is dark grey, soft, friable	2.0	(6.6)	44.0	(144.4)
10	Shale, dark grey, friable	2.0	(6.6)	42.0	(137.8)
9	Lignite with streaks of pale grey shale	2.0	(6.6)	40.0	(131.2)
8	Shale, as in unit 10	1.0	(3.3)	38.0	(124.7)
7	As in unit 11	0.5	(1.6)	37.0	(121.4)
6	Sand, fine grained, medium grey, with ripple marks, planar crossbedding, log fragments	1.0	(3.3)	36.5	(119.8)
5	As in unit 11	6.0	(19.7)	35.5	(116.5)
4	Lignite interbedded with dark grey, carbonaceous, platy-weathering shale containing abundant wood-impressions	2.0	(6.6)	29.5	(96.8)
3	As in unit 11	4.0	(13.1)	27.5	(90.2)
2	As in unit 10	3.5	(11.5)	23.5	(77.1)
1	Sand, as in unit 6, with abundant shale streaks, large tree roots	20.0	(65.6)	20.0	(65.6)

Unit	Lithology	Thickness		Height above base	
		m	(ft)	m	(ft)
Station 73-MLA-44					
<i>Eureka Sound Formation</i>					
<i>Cyclic Member (part of)</i>					
15	Shale, dark brown, weathering pale grey, laminated	2.0	(6.6)	53.0	(173.9)
14	Lignite	0.5	(1.6)	51.0	(167.3)
13	Sand, fine grained, medium grey, with carbonized logs up to 1 m long	4.1	(13.5)	50.5	(165.7)
12	Shale, as in unit 15	1.2	(3.9)	46.4	(152.2)
11	Lignite	0.3	(1.0)	45.2	(148.3)
10	Sand, fine grained; medium grey, laminated, abundant ripple marks, planar crossbedding	9.4	(30.8)	44.9	(147.3)
9	Sand, as in unit 10, capped by laterally persistent lens of ironstone with plant impressions	0.3	(1.0)	35.5	(116.5)
8	Shale, dark brown, weathered pale grey, laminated	1.0	(3.3)	35.2	(115.5)
7	Sand, very fine grained, silty	0.2	(0.7)	34.2	(112.2)
6	Shale, dark brown, laminated, rare sandy streaks, wood fragments	3.3	(10.8)	34.0	(111.6)
5	Interbedded fine grained, silty sand and shale, laminated	1.7	(5.6)	30.7	(100.7)
4	As in unit 6, gradational contact with unit 5	2.5	(8.2)	29.0	(95.1)
3	Sand, as in unit below, with abundant roots. Abrupt contact with unit 4	0.5	(1.6)	26.5	(87.0)
2	Sand, fine grained, dark grey, laminated with superimposed, interfering ripple marks, climbing-ripple lamination, large solitary trough crossbeds, rare wood fragments	21.5	(70.5)	26.0	(85.3)
1	Shale, dark grey, with lenticles of very fine grained, dark grey sand containing planar and ripple laminations and rare, large-scale trough crossbeds	4.5	(14.8)	4.5	(14.8)
Station 74-MLA-2					
<i>Isachsen Formation (part of)</i>					
22	Sand, medium brown, medium grained, with thin, discontinuous lenticles of coal	5.9	(19.4)	88.0	(288.7)
21	Shale, black, carbonaceous	0.1	(0.3)	82.1	(269.4)
20	Clay, brown, abundant cone-in-cone limestone in lower part of unit	11.0	(36.1)	82.0	(269.1)
19	Sand, fine grained, quartzose, predominantly planar bedded with rare faint symmetrical ripple marks, rare bioturbation, streaks of carbonaceous debris and seams up to 10 cm (4 in.) thick of argillaceous lignite, passing laterally and vertically into carbonaceous shale	3.5	(11.5)	71.0	(233.0)
18	Interbedded clay and sand, clay is yellowish brown, sand is yellowish, quartzose, containing small-scale ripple marks	3.0	(9.8)	67.5	(221.5)
17	Shale, black, carbonaceous, platy-weathering, with abundant pyrite nodules and blocks of sideritic clay-ironstone	0.5	(1.6)	64.5	(211.6)
16	As in unit 18	2.5	(8.2)	64.0	(210.0)
15	As in unit 17	0.5	(1.6)	61.5	(201.8)
14	As in unit 18	3.5	(11.5)	61.0	(200.1)
13	Sand, fine to medium grained, with sparse clay flasers, lenses of sideritic clay ironstone concretions and spherical pyrite concretions	1.5	(4.9)	57.5	(188.7)
12	Clay, brown to black, with lesser amounts of sandy lenticles, thin carbonaceous shale lens at top of unit	4.4	(14.4)	56.0	(183.7)
11	As in unit 18	0.6	(2.0)	51.6	(169.3)

Unit	Lithology	Thickness		Height above base	
		m	(ft)	m	(ft)
10	Lignite grading laterally into carbonaceous shale, friable, conchoidal fracture	0.1	(0.3)	51.0	(167.3)
9	Clay, medium grey, with rare sandy streaks, clay ironstone nodules, spherical pyrite nodules up to 3 cm (1.2 in.) in diameter	6.8	(22.3)	50.9	(167.0)
8	As in unit 18, clay is lenticular to flaser bedded	0.6	(2.0)	44.1	(144.7)
7	Clay, soft, black, with rare ironstone lenses, carbonaceous plant fragments at top of unit	2.3	(7.5)	43.5	(142.7)
6	As in unit 18	0.2	(0.7)	41.2	(135.2)
5	As in unit 7	5.7	(18.7)	41.0	(134.5)
4	As in unit 18	0.3	(1.0)	35.3	(115.8)
3	As in unit 7	5.0	(16.4)	35.0	(114.8)
2	Covered	5.0	(16.4)	30.0	(98.4)
1	Sand, medium to coarse grained, quartzose, pale pink, with rare streaks of green clay	25.0	(82.0)	25.0	(82.0)
	Unit 1 is underlain by pink to medium brown quartzose, pebbly sandstone of the Glenelg Formation (Proterozoic)				

Station 74-MLA-4***Isachsen Formation (part of)***

11	Shale, dark grey, with a few sandy streaks, lenticular to flaser bedded	27.0	(88.6)	78.0	(255.9)
10	Sand, medium grained with minor laminae and thin beds of shale, laminated in part, small-scale ripple marks with random orientations (no paleocurrent measurement possible), lenses of sand with green shale flakes	11.0	(36.1)	51.0	(167.3)
9	Covered	20.3	(66.6)	40.0	(131.2)
8	Shale, dark grey, soft, with a few sandy beds, finely laminated, bulbous pyrite concretions, abundant carbonaceous debris, small-scale ripple marks and trough crossbedding	5.2	(17.1)	19.7	(64.7)
7	Sand, fine to medium grained, pale yellowish cream, minor shale laminae	1.0	(3.3)	14.5	(47.6)
6	Shale, dark grey, soft, with intercalated sandy beds, finely laminated, large clay-ironstone blocks with plant impressions	0.5	(1.6)	13.5	(44.3)
5	Sand, as in unit 7	3.0	(9.8)	13.0	(42.7)
4	Shale, as in unit 11	3.0	(9.8)	10.0	(32.8)
3	Sand, medium grained, white to medium grey	3.0	(9.8)	7.0	(23.0)
2	Clay, dark grey, carbonaceous, with scattered streaks of pale, yellowish-brown, medium-grained sand	3.5	(11.5)	4.0	(13.1)
1	Sand, medium grained, quartzose, pink, with angular blocks of sandstone from underlying unit. Possibly a soil horizon	0.5	(1.6)	0.5	(1.6)
	Unit 1 is underlain by pink quartzose sandstone of the Glenelg Formation				

Station 74-MLA-6***Isachsen Formation (part of)***

6	Sand, medium to rarely coarse grained with abundant argillaceous partings and abundant thin beds of coal up to 2 cm (1 in.) thick. Rare, well consolidated, planar-bedded sandstone units. No crossbedding observed, cone-in-cone limestone	33.0	(108.3)	199.0	(653.0)
5	Coal, lignitic, friable, with sandy and argillaceous interbeds	1.0	(3.3)	166.0	(544.6)
4	As in unit 6, no cone-in-cone limestone observed	77.0	(252.6)	165.0	(541.4)
3	Coal, lignitic, friable, with sandy partings	1.0	(3.3)	88.0	(288.7)

Unit	Lithology	Thickness		Height above base	
		m	(ft)	m	(ft)
2	Sand, white, quartzose, fine grained, with abundant partings of black carbonaceous shale and grey shale; sand is planar bedded, no crossbedding observed	12.0	(39.4)	87.0	(285.4)
1	Sandstone, pink, quartzose, medium to very coarse grained with abundant interbeds of pebble-, cobble- and boulder-conglomerate. Clasts up to 50 cm (20 in.) in diameter, consisting of Precambrian quartzose sandstone and greenish shale. Clasts angular to subrounded, set in sandy or argillaceous matrix. Most conglomerate layers are clast supported. They decrease in thickness southward within a few hundred metres and pass into sandstone. Rare trough and planar crossbeds in sandstone units	75.0	(246.0)	75.0	(246.0)

Unit 1 is underlain by the Glenelg Formation

Station 74-MLA-17***Christopher Formation?***

8	Clay, dark grey, passing up into black, very carbonaceous clay	0.1	(0.3)	52.6	(172.6)
---	--	-----	-------	------	---------

Isachsen Formation

7	Sand, white, quartzose, fine to very fine grained with abundant thin laminae of clay. The sand is laminated and contains abundant rootlets at the top. Gradational contact with unit 8	7.0	(23.0)	52.5	(172.2)
6	Shale, black, highly carbonaceous	0.5	(1.6)	45.5	(149.3)
5	Sand, white, quartzose, fine grained with minor clay laminae, small-scale planar crossbeds	6.0	(19.7)	45.0	(147.7)
4	As in unit 1	5.0	(16.4)	39.0	(128.0)
3	Mudstone, medium grey, silty, slightly micaceous, castellated weathering	4.7	(15.4)	34.0	(111.6)
2	Sand, white, quartzose, fine grained with clay laminae	0.4	(1.3)	29.3	(96.1)
1	Siltstone and shale interbedded. The siltstone is medium grey, slightly micaceous, the shale is dark grey and contains thin beds and laminae of fine-grained sand up to 10 cm (4 in.) thick. Some sideritic ironstone layers	28.9	(94.8)	28.9	(94.8)

Station 74-MLA-18***Isachsen Formation (part of)***

15	Sand, medium to coarse grained, quartzose, pale buff, with abundant large-scale trough and planar crossbeds	2.0	(6.6)	11.9	(39.0)
14	Sand, medium to coarse grained, planar bedded, some small-scale planar crossbedding	0.3	(1.0)	9.9	(32.5)
13	Sand, as in unit 15	0.5	(1.6)	9.6	(31.5)
12	Sand, as in unit 14 with thin beds of carbonaceous shale	0.7	(3.3)	9.1	(29.9)
11	Sand, as in unit 15	1.1	(3.6)	8.4	(27.6)
10	Sand, as in unit 12	1.0	(3.3)	7.3	(24.0)
9	Sand, as in unit 15	0.9	(3.0)	6.3	(20.7)
8	Sand, as in unit 12	0.7	(2.3)	5.4	(17.7)
7	Sand, as in unit 15	1.1	(3.6)	4.7	(15.4)
6	Sand, coarse grained, pebbly	0.2	(0.7)	3.6	(11.8)
5	Sand, as in unit 15	0.8	(2.6)	3.4	(11.2)
4	Sand, as in unit 12	0.9	(3.0)	2.6	(8.5)
3	Sand, medium to coarse grained, in part planar bedded, in part planar crossbedded	1.3	(4.3)	1.7	(5.6)

Unit	Lithology	Thickness		Height above base	
		m	(ft)	m	(ft)
2	Sand, coarse grained, with pebbles of quartz and chert up to 1 cm in diameter	0.2	(0.7)	0.4	(1.3)
1	Sand, as in unit 15	0.2	(0.7)	0.2	(0.7)

Station 74-MLA-43***Eureka Sound Formation****Cyclic Member (part of)*

18	Sand, quartzose, fine grained	2.2	(7.2)	64.4	(211.2)
17	Shale, medium grey, silty, micaceous	8.3	(27.2)	62.2	(204.1)
16	Sand, medium grained, laminated, carbonaceous, abundant plant fragments, abundant trough and planar crossbedding	13.9	(45.6)	53.9	(176.8)
15	Silt, dark grey, argillaceous, slightly micaceous, slightly sandy	5.0	(16.4)	40.0	(131.2)
14	Sand, fine grained with mineralized logs	8.0	(26.2)	35.0	(114.8)
13	Lignitic coal	0.3	(1.0)	27.0	(88.6)
12	Mudstone, light grey, with abundant plant fragments	0.3	(1.0)	26.7	(87.6)
11	Lignite, argillaceous streaks at base	0.9	(3.0)	26.4	(86.6)
10	Shale, silty, micaceous, with abundant plant debris	1.5	(4.9)	25.5	(83.7)
9	Sand, very fine grained, laminated, with common argillaceous streaks, small-scale trough crossbeds and small-scale ripple marks	3.0	(9.8)	24.0	(78.7)
8	Lignite	0.2	(0.7)	21.0	(68.9)
7	Sand, as in unit 9	3.3	(10.8)	20.8	(68.2)
6	Interbedded silt and shale, silt is sandy, both lithologies are soft, poorly consolidated, micaceous, laminated, with carbonaceous streaks	2.9	(9.5)	17.5	(57.4)
5	Silt, sandy, unconsolidated	0.3	(1.0)	14.6	(47.9)
4	Shale, silty, micaceous, a few sandy streaks, laminated	3.3	(10.8)	14.3	(46.9)
3	Sand, fine to very fine grained, micaceous, laminated, with streaks of carbonaceous shale	5.5	(18.0)	11.0	(36.1)
2	Lignite with shale streaks. Sharp lower contact with unit 1, upward gradation into unit 3	0.2	(0.7)	5.5	(18.0)
1	Sand, as in unit 3	5.3	(17.4)	5.3	(17.4)

Station 74-MLA-44***Kanguk Formation (part of)***

7	Shale, soft, medium to pale grey	8.0	(26.2)	58.0	(190.3)
6	Shale, dark grey to black, laminated, with thin beds of bentonitic clay, mudstone concretions containing flattened <i>Inoceramus</i> fragments	2.0	(6.6)	50.0	(164.1)

Hassel Formation

5	Sand, medium grey, fine to very fine grained, argillaceous, with thin streaks of grey clay	9.0	(29.5)	48.0	(157.5)
4	Sand, fine grained, glauconitic, laminated, with low-angle planar crossbedding, small-scale asymmetrical ripple marks; rare layers of coarse to pebbly sand, pebbles up to 1 cm in diameter, consist of quartz, chert, quartzose sandstone; rare ironstone lenses and nodules, containing desiccation cracks	21.2	(69.6)	39.0	(128.0)
3	Shale, dark grey, soft, silty, with ironstone nodules containing pelecypods	9.1	(29.9)	17.8	(58.4)

Unit	Lithology	Thickness		Height above base	
		m	(ft)	m	(ft)
2	Sand, quartzose, very fine grained, laminated	1.0	(3.3)	8.7	(28.5)
1	Shale, dark grey, soft, silty, micaceous, interbedded with thin laminae and thin beds up to 30 cm (1 ft) thick of very fine grained, quartzose sand; ironstone nodules containing pelecypods, ammonites. Sand dies out at base of unit, representing gradation into the Christopher Formation	7.7	(25.2)	7.7	(25.2)

Station 74-MLA-45***Eureka Sound Formation****Cyclic Member (part of)*

20	Shale, black, carbonaceous, locally lignitic	1.4	(4.6)	79.5	(260.8)
19	Shale, medium grey, soft, slightly silty	4.6	(15.1)	78.1	(256.2)
18	Sand, fine grained, unconsolidated, 'salt and pepper' texture	0.5	(1.6)	73.5	(241.1)
17	Interbedded shale and sand, finely laminated, sand is very fine grained, silty	3.0	(9.8)	73.0	(239.5)
16	As in unit 19	1.5	(4.9)	70.0	(229.7)
15	Shale, dark grey, carbonaceous, lignitic, abundant wood fragments	1.8	(5.9)	68.5	(224.7)
14	As in unit 17	1.7	(5.6)	66.7	(218.9)
13	As in unit 19	11.7	(38.4)	65.0	(213.3)
12	As in unit 18 with rare argillaceous streaks	10.8	(35.4)	53.3	(174.9)
11	As in unit 19	0.5	(1.6)	42.5	(139.4)
10	As in unit 18	2.5	(8.2)	42.0	(137.8)
9	Shale, as in unit 19, weathering pale grey	1.0	(3.3)	39.5	(129.6)
8	As in unit 18 with clay-ironstone lenses	11.5	(37.7)	38.5	(126.3)
7	As in unit 19	1.6	(5.2)	27.0	(88.6)
6	As in unit 17	2.4	(7.9)	25.4	(83.3)
5	As in unit 19 with clay-ironstone nodules	2.0	(6.6)	23.0	(75.5)
4	Lignite	0.5	(1.6)	21.0	(68.9)
3	As in unit 19	5.5	(18.0)	20.5	(67.3)
2	As in unit 17 with clay-ironstone lenses	8.5	(27.9)	15.0	(49.2)
1	Sand, medium grained, with lenses of wood fragments	6.5	(21.3)	6.5	(21.3)

Station 74-MLA-46***Beaufort Formation (part of)***

23	Gravel, clasts up to 15 cm in diameter	29.8	(97.7)	111.6	(366.2)
----	--	------	--------	-------	---------

Eureka Sound Formation*Cyclic Member (part of)*

22	Sand, fine to medium grained, abundant argillaceous partings at top of unit, large-scale planar and trough crossbeds	5.0	(16.4)	81.8	(268.4)
21	Siltstone, argillaceous, laminated	1.2	(3.9)	76.8	(252.0)
20	Lignite, comprising mainly flattened log fragments, rests on unit 19 with sharp, flat contact	1.9	(6.2)	75.6	(248.0)

Unit	Lithology	Thickness		Height above base	
		m	(ft)	m	(ft)
19	Sand, very fine grained, soft, laminated, abundant small-scale asymmetric ripple marks, rare roots in top few centimetres	3.2	(10.5)	73.7	(241.8)
18	Shale, medium grey, abundant large flattened logs at base	3.7	(12.1)	70.5	(231.3)
17	Shale, lignitic, abundant wood fragments	0.8	(2.6)	66.8	(219.2)
16	Shale, medium grey	1.3	(4.3)	66.0	(216.6)
15	Lignite, large log fragments	0.1	(0.3)	64.7	(212.3)
14	Shale, medium grey	0.7	(2.3)	64.6	(212.0)
13	Shale, carbonaceous, abundant plant fragments, platy weathering	0.4	(1.3)	63.9	(209.6)
12	Clay, soft, brownish, abundant plant fragments, probably a soil horizon	0.1	(0.3)	63.5	(208.3)
11	Sand, fine to medium grained, silty, with minor argillaceous streaks near the top	1.4	(4.6)	63.4	(208.0)
10	Shale, medium grey	5.9	(19.4)	62.0	(203.4)
9	Sand, fine to medium grained, medium grey, abundant carbonaceous debris	33.1	(108.6)	56.1	(184.1)
8	Shale, soft, dark grey	2.8	(9.2)	23.0	(75.5)
7	Sand, fine grained	1.9	(6.2)	20.2	(66.3)
6	Shale, carbonaceous, abundant wood fragments	0.3	(1.0)	18.3	(60.0)
5	Clay, soft, dark grey, abundant plant debris, possibly fossil soil	1.3	(4.3)	18.0	(59.1)
4	Sand, fine grained, thin root zone in upper few centimetres	2.5	(8.2)	16.7	(54.8)
3	Shale	1.4	(4.6)	14.2	(46.6)
2	Sand, fine grained, intercalated argillaceous streaks, abundant lenticles of clay-ironstone containing plant impressions	12.3	(40.3)	12.8	(42.0)
1	Interbedded silty, fine-grained sand and shale, climbing-ripple lamination	0.5	(1.6)	0.5	(1.6)

Station 74-MLA-93***Kanguk Formation****Silty shale member (part of)*

3	Shale, dark grey	30.0	(98.4)	108.0	(354.3)
2	Sandstone, medium grained, quartzose, argillaceous, resistant, bluff forming; abundant pebbles of grey and black chert, white quartz, and quartzose sandstone up to 3.5 cm in diameter; layer of dark red-brown iron oxide cemented sandstone at top of unit	2.5	(8.2)	78.0	(255.9)
1	Shale, dark grey, soft, rare scattered and disarticulated reptilian bones, rare ironstone concretions, commonly surrounded by sulphurous exhalations	75.5	(247.8)	75.5	(247.8)

Station 74-MLA-104***Kanguk Formation****Silty shale member (part of)*

5	Shale, dark grey, soft, slightly silty	13.8	(45.3)	45.0	(147.6)
<i>Bituminous shale member</i>					
4	Shale, black, bituminous, papery weathering, oxidizing to red at surface, flattened <i>Inoceramus</i> , calcareous mudstone concretions with fish remains, two thin bentonite layers at base, wood fragments	4.2	(13.8)	31.2	(102.4)

Hassel Formation (part of)

3	Silt, dark grey, mottled, argillaceous, bioturbated; becoming less argillaceous at top	3.0	(9.8)	27.0	(88.6)
---	--	-----	-------	------	--------

Unit	Lithology	Thickness		Height above base	
		m	(ft)	m	(ft)
2	As in unit 3, with thin laminae of coarse-grained, quartzose sand	19.0	(62.3)	24.0	(78.7)
1	Sand, very fine grained, silty, quartzose, low-angle trough and planar crossbedding	5.0	(16.4)	5.0	(16.4)

Station 74-MLA-113***Eureka Sound Formation****Cyclic Member (part of)*

28	Sand, very fine grained, laminated	2.7	(8.9)	41.0	(134.6)
27	Interbedded sandy silt and silty shale	3.4	(11.2)	38.3	(125.7)
26	Shale, grey-brown, soft	0.9	(3.0)	34.9	(114.5)
25	As in unit 27, small-scale ripple marks	3.2	(10.5)	34.0	(111.6)
24	As in unit 26	2.2	(7.2)	30.8	(101.1)
23	As in unit 27	1.4	(4.6)	28.6	(93.8)
22	As in unit 26	2.6	(8.5)	27.2	(89.2)
21	As in unit 27	0.6	(2.0)	24.6	(80.7)
20	As in unit 26	2.2	(7.2)	24.0	(78.7)
19	As in unit 27, shale is silty, micaceous; unit is laminated	4.0	(13.1)	21.8	(71.5)
18	Lignitic shale	0.6	(2.0)	17.8	(58.4)
17	As in unit 26	2.2	(7.2)	17.2	(56.4)
16	Sand, very fine grained, quartzose	0.2	(0.7)	15.0	(49.2)
15	As in unit 27	1.1	(3.6)	14.8	(48.6)
14	As in unit 26	1.7	(5.6)	13.7	(44.9)
13	Lignitic shale	0.5	(1.6)	12.0	(39.4)
12	As in unit 26; sharp, flat contact with unit 11	1.7	(5.6)	11.5	(37.8)
11	Sand, very fine grained	0.8	(2.6)	9.8	(32.2)
10	As in unit 27	0.2	(0.7)	9.0	(29.5)
9	As in unit 26	2.1	(6.9)	8.8	(28.9)
8	Shale, carbonaceous, lignitic	0.2	(0.7)	6.7	(22.0)
7	Mudstone, pale grey, abundant plant fragments; soil zone	0.1	(0.3)	6.5	(21.3)
6	Sand, soft, yellowish, quartzose, very fine grained, laminated	1.4	(4.6)	6.4	(21.0)
5	Shale, silty, soft, grey-brown, interbedded with yellowish, sandy silt	1.3	(4.3)	5.0	(16.4)
4	As in unit 26	0.4	(1.3)	3.7	(12.1)
3	Shale, lignitic, carbonaceous, large wood fragments	0.4	(1.3)	3.3	(10.8)
2	Mudstone, pale grey, with abundant rootlets; soil zone	0.1	(0.3)	2.9	(9.5)
1	Shale, dark grey-brown, micaceous	2.8	(9.2)	2.8	(9.2)

Station 74-MLA-114***Kanguk Formation****Silty shale member (part of)*

7	Shale, dark grey, soft	4.7	(15.4)	29.0	(95.1)
6	Sandstone, pale grey, medium grained	0.3	(1.0)	24.3	(79.8)
5	Shale, fairly resistant, with sponge spicules	12.5	(41.0)	24.0	(78.7)

Unit	Lithology	Thickness		Height above base	
		m	(ft)	m	(ft)
4	Siltstone, glauconitic, abundant	0.3	(1.0)	11.5	(37.8)
3	As in unit 7	0.6	(2.0)	11.2	(36.8)
2	Siderite-dolomite nodules	0.1	(0.3)	10.6	(34.8)
1	As in unit 7	10.5	(34.4)	10.5	(34.4)

Station 74-MLA-115***Eureka Sound Formation****Cyclic Member (part of)*

31	Sandstone, fine grained, faintly laminated, medium grey, indurated, bluff forming	3.0	(9.8)	71.0	(233.0)
30	Sand, quartzose, very fine grained	3.6	(11.8)	68.0	(223.1)
29	Interbedded very fine grained silty sand or sandy siltstone and silty shale, laminated	0.2	(0.7)	64.4	(211.3)
28	Lignite	0.3	(1.0)	64.2	(210.6)
27	Silt, dark brown, micaceous, sandy, unconsolidated, probably a soil zone	0.3	(1.0)	63.9	(209.7)
26	Silt, fine grained, sandy	1.7	(5.6)	63.6	(208.7)
25	As in unit 29	0.4	(1.3)	61.9	(203.1)
24	Lignite	0.6	(2.0)	61.5	(201.8)
23	Shale, dark grey	2.0	(6.6)	60.9	(199.8)
22	Sand, very fine grained, silty	0.5	(1.6)	58.9	(193.3)
21	Shale, dark grey-brown	1.4	(4.6)	58.4	(191.6)
20	Lignite, argillaceous	0.8	(2.6)	57.0	(187.0)
19	As in unit 29	1.2	(3.9)	56.2	(184.4)
18	Silt, argillaceous, poorly exposed	1.3	(4.3)	55.0	(180.5)
17	Shale, dark grey	0.2	(0.7)	53.7	(176.2)
16	Sand, very fine grained, silty	0.5	(1.6)	53.5	(175.5)
15	As in unit 29	1.5	(4.9)	53.0	(173.9)
14	Shale, black, carbonaceous, with plant fragments	0.2	(0.7)	51.5	(169.0)
13	Shale, dark grey-brown, black and carbonaceous at base	2.5	(8.2)	51.3	(168.3)
12	As in unit 29	2.5	(8.2)	48.8	(160.1)
11	Shale, dark grey-brown to black, in part carbonaceous	1.4	(4.6)	46.3	(151.9)
10	Sand, very fine grained	1.3	(4.3)	44.9	(147.3)
9	As in unit 29	1.5	(4.9)	43.6	(143.1)
8	Shale, soft, dark grey-brown	1.8	(5.9)	42.1	(138.1)
7	Sand, very fine grained, faintly laminated, with 'salt and pepper' coloration	9.0	(29.5)	40.3	(132.2)
6	As in unit 29	6.7	(22.0)	31.3	(102.7)
5	Shale, dark grey-brown	10.1	(33.1)	24.6	(80.7)
4	As in unit 29	4.5	(14.8)	14.5	(47.6)
3	Sand, very fine grained, silty, laminated, with argillaceous streaks	2.5	(8.2)	10.0	(3.3)
2	Shale, dark grey-brown	1.5	(4.9)	7.5	(24.6)
1	Sand, as in unit 3	6.0	(19.7)	6.0	(19.7)

Unit	Lithology	Thickness		Height above base	
		m	(ft)	m	(ft)
Station 74-MLA-116					
<i>Eureka Sound Formation</i>					
<i>Cyclic Member (part of)</i>					
31	Sand, very fine grained, 'salt and pepper' coloration	2.5	(8.2)	63.0	(206.7)
30	Interbedded quartzose, sandy silt and silty shale	0.2	(0.7)	60.5	(198.5)
29	Shale, dark grey to grey-brown	4.8	(15.8)	60.3	(197.8)
28	As in unit 30	6.3	(20.7)	55.5	(182.1)
27	Clay-ironstone	0.1	(0.3)	49.2	(161.4)
26	Sand, very fine grained, very silty	0.2	(0.7)	49.1	(161.1)
25	As in unit 29	3.9	(12.8)	48.9	(160.4)
24	As in unit 30	3.1	(10.2)	45.0	(147.6)
23	As in unit 31	0.3	(1.0)	41.9	(137.5)
22	As in unit 30	0.2	(0.7)	41.6	(136.5)
21	As in unit 29	0.6	(2.0)	41.4	(135.8)
20	As in unit 31	1.8	(5.9)	40.8	(133.9)
19	As in unit 30, becoming sandier near top of unit	9.5	(31.2)	39.0	(128.0)
18	As in unit 29	2.8	(9.2)	29.5	(96.8)
17	As in unit 31	1.3	(4.3)	26.7	(87.6)
16	Clay-ironstone	0.1	(0.3)	25.4	(83.3)
15	As in unit 31	4.4	(14.4)	25.3	(83.0)
14	As in unit 30	1.2	(3.9)	20.9	(68.6)
13	As in unit 29	0.2	(0.7)	19.7	(64.6)
12	As in unit 31	0.7	(2.3)	19.5	(64.0)
11	As in unit 30, becoming coarser grained (more sandy) near top of unit	1.3	(4.3)	18.8	(61.6)
10	As in unit 29	2.8	(9.2)	17.5	(57.4)
9	As in unit 30	1.8	(5.9)	14.7	(48.2)
8	As in unit 29	1.2	(3.9)	12.9	(42.3)
7	Clay-ironstone with mineralized log fragments	0.1	(0.3)	11.7	(38.4)
6	Sand, fine to medium grained, quartzose	2.2	(7.2)	11.6	(38.1)
5	As in unit 30	0.5	(1.6)	9.4	(30.8)
4	As in unit 31	0.6	(2.0)	8.9	(29.2)
3	As in unit 30	2.1	(6.9)	8.3	(27.2)
2	As in unit 29	4.4	(14.4)	6.2	(20.3)
1	As in unit 31	1.8	(5.9)	1.8	(5.9)

Station 74-MLA-118*Eureka Sound Formation**Cyclic Member (part of)*

17	Sand, very fine grained, with minor brown, silty laminae	6.7	(22.0)	52.0	(170.6)
16	Clay-ironstone, with ripple marks	0.1	(0.3)	45.3	(148.6)
15	As in unit 17	1.0	(3.3)	45.2	(148.3)

Unit	Lithology	Thickness		Height above base	
		m	(ft)	m	(ft)
14	Shale, dark brown	0.3	(1.0)	44.2	(145.0)
13	Interlaminated silt and silty shale	5.1	(16.7)	43.9	(144.0)
12	Shale, dark brown	4.3	(14.1)	38.8	(127.3)
11	As in unit 17, sharp contact with unit 12	1.0	(3.3)	34.5	(113.2)
10	As in unit 13	2.2	(7.2)	33.5	(109.9)
9	Clay-ironstone	0.1	(0.3)	31.3	(102.7)
8	As in unit 17	2.8	(9.2)	31.2	(102.4)
7	Sand with interbedded silty shale and siltstone, becoming siltier at the top	3.9	(12.8)	28.4	(93.2)
6	Shale, grey-brown	3.5	(11.5)	24.5	(80.4)
5	As in unit 13, with abundant ripple marks, including solitary trains and climbing ripples	3.0	(9.8)	21.0	(68.9)
4	Shale, dark grey	2.5	(8.2)	18.0	(59.1)
3	Sand, fine grained, 'salt and pepper' coloration	11.1	(36.4)	15.5	(50.9)
2	Shale, medium grey-brown, interbedded with sand	0.6	(2.0)	4.4	(14.4)
1	As in unit 3	3.8	(12.5)	3.8	(12.5)

Station 74-MLA-126***Eureka Sound Formation****Cyclic Member (part of)*

19	Interlaminated silty shale and silt	9.6	(31.5)	36.6	(120.1)
18	Shale, silty	1.4	(4.6)	27.0	(88.6)
17	Sand, fine grained, massive	1.6	(5.2)	25.6	(84.0)
16	As in unit 19	1.1	(3.6)	24.0	(78.8)
15	Lignite	1.2	(3.9)	22.9	(75.1)
14	Shale, grey, with plant fragments (not rootlets) near top of unit	3.7	(12.1)	21.7	(71.2)
13	Lignite	0.3	(1.0)	18.0	(59.1)
12	Siltstone, dark grey, carbonaceous with plant fragments, white weathering	0.1	(0.3)	17.7	(58.1)
11	Lignite	2.6	(8.5)	17.6	(57.8)
10	As in unit 14	1.7	(5.6)	15.0	(49.2)
9	Lignite	0.3	(1.0)	13.3	(43.6)
8	Shale, medium grey, weathering pale grey, silty, micaceous, top few centimetres contain lignite streaks	3.0	(9.8)	13.0	(42.7)
7	Sandy silts and silty sands, very fine grained, sand beds contain climbing-ripple cross-stratification, unit grades up into unit 8	0.9	(2.9)	10.0	(32.8)
6	Shale, silty, micromicaceous, with small-scale ripple marks, silty beds and large, slumped mass of fine-grained sand	4.2	(13.8)	9.1	(29.9)
5	Sand, planar laminated, fine grained, 'salt and pepper' coloration	1.0	(3.3)	4.9	(16.1)
4	Sand, very fine grained, silty, micaceous, with penecontemporaneous deformation structures; top and bottom of unit are undisturbed and show small-scale ripple marks	0.6	(2.0)	3.9	(12.8)
3	Siltstone, laminated, micaceous, with argillaceous streaks	1.6	(5.2)	3.3	(10.8)
2	Shale, carbonaceous in part, silty, micaceous	1.4	(4.6)	1.7	(5.6)
1	Lignite	0.3	(1.0)	0.3	(1.0)

Unit	Lithology	Thickness		Height above base	
		m	(ft)	m	(ft)
Station 74-MLA-150					
<i>Beaufort Formation</i>					
19	Sand, pebbly, abundant chert clasts, commonly orange	10.0	(32.8)	50.0	(164.0)
<i>Eureka Sound Formation</i>					
<i>Cyclic Member (part of)</i>					
18	Sand, fine to very fine grained	5.0	(16.4)	40.0	(131.2)
17	Lignite with large log fragments	0.5	(1.6)	35.0	(114.8)
16	Shale, dark grey-brown	1.8	(5.9)	34.5	(113.2)
15	Shale, lignitic, black	0.2	(0.7)	32.7	(107.3)
14	Sand, very fine grained, 'salt and pepper' coloration, large log fragments	3.5	(11.5)	32.5	(106.6)
13	As in unit 16	2.4	(7.9)	29.0	(95.1)
12	Shale, lignitic	0.2	(0.7)	26.6	(87.3)
11	Mudstone, silty, pale grey grading into dark brown at top of unit, rootlets and plant fragments	0.4	(1.3)	26.4	(85.6)
10	As in unit 14	1.0	(3.3)	26.0	(85.3)
9	As in unit 16	6.3	(20.7)	25.0	(82.0)
8	Silt, interbedded with minor silty shale	0.6	(2.0)	18.7	(61.4)
7	Shale, as in unit 16	0.6	(2.0)	18.1	(59.4)
6	Sand, very fine grained, silty, quartzose, becoming fine grained with 'salt and pepper' coloration near top of unit. Plant fragments in top few centimetres.	3.7	(12.1)	17.5	(57.4)
5	Interbedded silt and silty shale	2.8	(9.2)	13.8	(45.3)
4	As in unit 16	3.5	(11.5)	11.0	(36.1)
3	Sand, very fine grained, quartzose, pale grey, with rare carbonaceous streaks, small-scale ripple marks, tree roots in place	3.0	(9.8)	7.5	(24.6)
2	Silt, quartzose, pale grey, slightly micaceous, abundant planar crossbedding and climbing-ripple crossbedding	0.5	(1.6)	4.5	(18.8)
1	Shale, soft, grey-brown	4.0	(13.1)	4.0	(13.1)

Station 74-MLA-154*Eureka Sound Formation**Cyclic Member (part of)*

19	Shale, silty, medium grey-brown	6.6	(21.7)	49.7	(163.1)
18	Lignite, lenticular	0.1	(0.3)	43.1	(141.4)
17	Soil, sandy, argillaceous, dark grey, with abundant plant fragments, rare roots in place	0.3	(1.0)	43.0	(141.1)
16	Sand, very fine grained, silty, scattered argillaceous streaks, medium grey, abundant tree stems in place, gradational contact with unit 15	2.2	(7.2)	42.7	(140.1)
15	Interbedded shale and very fine grained, silty sand	2.5	(8.2)	40.5	(132.9)
14	Shale, grey, a few sandy steaks	6.9	(22.6)	38.0	(124.7)
13	Lignite	0.1	(0.3)	31.1	(102.0)
12	Sand, a few argillaceous lenses, rare large roots in place	1.2	(3.9)	31.0	(101.7)
11	Interbedded shale or silty shale, and argillaceous silt	3.8	(12.5)	29.8	(97.8)

Unit	Lithology	Thickness		Height above base	
		m	(ft)	m	(ft)
10	Shale	0.6	(2.0)	26.0	(85.3)
9	Lignite	0.2	(0.7)	25.4	(83.3)
8	Sand, very fine grained, very silty, micaceous, laminated, rootlets at top and large wood fragments throughout	1.0	(3.3)	25.2	(82.7)
7	Lignite	0.1	(0.3)	24.2	(79.4)
6	Sand, as in unit 8	2.6	(8.5)	24.1	(79.1)
5	Shale, resting on unit 4 with sharp contact, grading up into unit 6	1.5	(4.9)	21.5	(70.5)
4	Silt, argillaceous, sandy, massive	0.7	(2.3)	20.0	(65.6)
3	Shale, brownish grey, grading up into unit 4	6.5	(21.3)	19.3	(63.3)
2	Sand, fine grained, medium greenish grey with 'salt and pepper' mottling	5.8	(19.0)	12.8	(42.0)
1	Shale, brownish grey	7.0	(23.0)	7.0	(23.0)

Station 74-MLA-155***Eureka Sound Formation****Cyclic Member (part of)*

43	Sand, very fine grained, with occasional roots	5.0	(16.4)	113.5	(372.4)
42	Interbedded shale and silt with small-scale trough crossbeds and ripple marks	2.0	(6.6)	108.5	(356.0)
41	Shale, brownish grey	0.4	(1.3)	106.5	(349.4)
40	Silt, quartzose, pale grey	0.6	(2.0)	106.1	(348.1)
39	Shale, brownish grey, sparse clay-ironstone	3.8	(12.5)	105.5	(346.1)
38	Silt, quartzose, becoming very fine grained sand at top, intercalated carbonaceous streaks, rare roots	2.1	(6.9)	101.7	(333.7)
37	Shale, brownish grey, sparse clay-ironstone	1.1	(3.6)	99.6	(326.8)
36	Sand, very fine grained	3.9	(12.8)	98.5	(323.2)
35	Shale, brownish grey, sparse clay-ironstone	4.4	(14.4)	94.6	(310.4)
34	Sand, very fine grained, rare roots	3.5	(11.5)	90.2	(295.9)
33	As in unit 35	6.8	(22.3)	86.7	(284.5)
32	Silt, pale grey, quartzose	1.5	(4.9)	79.9	(262.2)
31	Shale, resting on unit 30 with sharp, flat contact	3.0	(9.8)	78.4	(257.2)
30	Sand, very fine grained, silty, rare roots	0.9	(3.0)	75.4	(247.4)
29	Interbedded silt and silty shale	0.7	(2.3)	74.5	(244.4)
28	Shale, resting on unit 27 with sharp, flat contact	0.4	(1.3)	73.8	(242.1)
27	Lignite, lenticular	0.1	(0.3)	73.4	(240.8)
26	Interbedded shale and silty shale, rare small log fragments, abundant roots in place	2.5	(8.2)	73.3	(240.5)
25	Shale, brownish grey	3.8	(12.5)	70.8	(232.3)
24	Interbedded silty shale and argillaceous silt	1.3	(4.3)	67.0	(219.9)
23	Shale, brownish grey, rare logs	4.1	(13.5)	65.7	(215.6)
22	Clay-ironstone	0.3	(1.0)	61.6	(202.1)
21	Silt, quartzose, laminated	1.3	(4.3)	61.3	(201.1)
20	Interbedded silt and shale, grading up into unit 21	2.2	(7.2)	60.0	(196.9)
19	Sand, silty	0.5	(1.6)	57.8	(189.6)

Unit	Lithology	Thickness		Height above base	
		m	(ft)	m	(ft)
18	Interbedded silt and shale	0.4	(1.3)	57.3	(188.0)
17	As in unit 35	3.4	(11.2)	56.9	(186.7)
16	Sand, very fine grained, 'salt and pepper' mottling, wood fragments	4.9	(16.1)	53.5	(175.5)
15	As in unit 35	17.1	(56.1)	48.6	(159.5)
14	Interbedded laminated silt and brown shale, abundant clay-ironstone	6.1	(20.0)	31.5	(103.4)
13	Shale, carbonaceous to lignitic, abundant large logs up to 2 m long	2.1	(6.9)	25.4	(83.3)
12	As in unit 35	2.3	(7.5)	23.3	(76.4)
11	Interbedded silt and silty shale	1.2	(3.9)	21.0	(68.9)
10	As in unit 35	2.1	(6.9)	19.8	(65.0)
9	Sand, very fine grained	0.9	(3.0)	17.7	(58.1)
8	Interbedded sand shale and argillaceous silt	1.1	(3.6)	16.8	(55.1)
7	Lignite	0.2	(0.7)	15.7	(51.5)
6	Sand, very fine grained, climbing-ripple cross-stratification, abundant wood fragments	2.0	(6.6)	15.5	(50.9)
5	Interbedded sand and shale, abundant wood fragments	1.3	(4.3)	13.5	(44.3)
4	As in unit 35	3.3	(10.8)	12.2	(40.0)
3	Sand, very fine grained, silty, laminated, minor clay-ironstone	2.8	(9.2)	8.9	(29.2)
2	Shale, brownish, sparse clay ironstone	4.5	(14.8)	6.1	(20.0)
1	Sand, very fine grained, silty, laminated	1.6	(5.2)	1.6	(5.2)

Station 74-MLA-157

Eureka Sound Formation

Cyclic Member (part of)

15	Shale, grey-brown	1.0	(3.3)	37.6	(123.4)
14	Sand, very fine grained	1.4	(4.6)	36.6	(120.1)
13	Shale, grey-brown	0.3	(1.0)	35.2	(115.5)
12	Sand, very fine grained, followed with sharp, flat contact by unit 13	5.7	(18.7)	34.9	(114.5)
11	Interbedded silty sand and shale	1.6	(5.2)	29.2	(95.8)
10	Shale, brown-grey	0.7	(2.3)	27.6	(90.6)
9	Sand, fine grained	0.2	(0.7)	26.9	(88.3)
8	Shale, brown-grey	1.1	(3.6)	26.7	(87.6)
7	Lignite	0.1	(0.3)	25.6	(84.0)
6	Sand, fine grained	0.5	(1.6)	25.5	(83.7)
5	As in unit 11	1.2	(3.9)	25.0	(82.0)
4	Shale	3.5	(11.5)	23.8	(78.1)
3	Interbedded shale and silt	0.5	(1.6)	20.3	(66.6)
2	Shale, brown-grey	3.8	(12.5)	19.8	(65.0)
1	Sand, fine grained, planar laminated, 'salt and pepper' mottling	16.0	(52.5)	16.0	(52.5)

Unit	Lithology	Thickness		Height above base	
		m	(ft)	m	(ft)
Station 74-MLA-158					
<i>Eureka Sound Formation</i>					
<i>Cyclic Member (part of)</i>					
13	Interbedded shale and silt, laminated	2.2	(7.2)	29.2	(95.8)
12	Shale, dark grey-brown	1.5	(4.9)	27.0	(88.6)
11	Sand, very fine grained	3.5	(11.5)	25.5	(83.7)
10	As in unit 13	0.5	(1.6)	22.0	(72.2)
9	Shale, silty, pale weathering, interbedded with dark brown laminated shale	3.4	(11.2)	21.5	(70.5)
8	As in unit 13	1.1	(3.6)	18.1	(59.4)
7	Shale, brownish, silty	5.1	(16.7)	17.0	(55.8)
6	Sand, laminated, abundant small-scale, superimposed ripple marks, rare roots at top of unit. Abrupt contact with unit 7	3.0	(9.8)	11.9	(39.0)
5	Shale and silt, laminated, grading up into unit 6	2.4	(7.9)	8.9	(29.2)
4	Shale, as in unit 9, grading up into unit 5	4.2	(13.8)	6.5	(21.3)
3	Lignite	0.3	(1.0)	2.3	(7.5)
2	Soil, pale mudstone with rootlets	0.1	(0.3)	2.0	(6.6)
1	Sand, very fine grained, laminated, 'salt and pepper' coloration, vertical roots up to 1 m long	1.9	(6.2)	1.9	(6.2)
Station 74-MLA-159					
<i>Eureka Sound Formation</i>					
<i>Cyclic Member (part of)</i>					
20	Shale, dark grey-brown	17.1	(56.1)	65.5	(214.9)
19	Sand, fine grained, laminated, with climbing-ripple cross-stratification	6.2	(20.3)	48.4	(158.8)
18	Shale, as in unit 20	0.2	(0.7)	42.2	(138.5)
17	Sand, fine grained	5.5	(18.0)	42.0	(137.8)
16	As in unit 20	0.2	(0.7)	36.5	(119.8)
15	Sand, fine grained, 'salt and pepper' coloration, sharp contact with unit 16	1.9	(6.2)	36.3	(119.1)
14	Interbedded shale and silty shale	3.0	(9.8)	34.4	(112.9)
13	As in unit 20	9.0	(29.5)	31.4	(103.0)
12	Sand, fine grained	2.8	(9.2)	22.4	(73.5)
11	Interbedded shale and silty sand	1.3	(4.3)	19.6	(64.3)
10	Sand, very fine grained, minor argillaceous streaks	1.2	(3.9)	18.3	(60.0)
9	As in unit 14, grading up into unit 10	1.6	(5.2)	17.1	(56.1)
8	Shale, dark grey-brown, silty in part	2.0	(6.6)	15.5	(50.9)
7	Silt, sandy, quartzose, laminated	0.5	(1.6)	13.5	(44.3)
6	Interbedded shale and silt, laminated	2.3	(7.5)	13.0	(42.6)
5	As in unit 8	0.8	(2.6)	10.7	(35.1)
4	Lignite, lenticular	0.1	(0.3)	9.9	(32.5)
3	Sand, fine grained	2.1	(6.9)	9.8	(32.2)
2	As in unit 6	1.7	(5.6)	7.7	(25.3)
1	As in unit 8	6.0	(19.7)	6.0	(19.7)

Unit	Lithology	Thickness		Height above base	
		m	(ft)	m	(ft)
Station 74-GAS-4					
<i>Christopher Formation</i>					
<i>Lower member</i>					
16	Clay, pale grey to buff, silty, interbedded with dark grey clay	2.5	(8.2)	80.5	(264.1)
15	Clay, dark brown, or dark grey and carbonaceous, abundant siderite concretions	11.5	(37.7)	78.0	(255.9)
14	Sand, very fine grained, interbedded with laminated, carbonaceous clay and silty clay	2.5	(8.2)	66.5	(218.2)
13	Clay, grey, with interbedded silty beds at base of unit	2.0	(6.6)	64.0	(210.0)
12	Sandstone, siderite-cemented, top surface covered with small-scale asymmetric ripple marks	0.7	(2.3)	62.0	(203.4)
11	Covered	3.8	(12.5)	61.3	(201.1)
10	Siltstone, white, quartzose, or grey, argillaceous; interlaminated with soft grey shale and black, carbonaceous shale	13.5	(44.3)	57.5	(188.7)
9	Shale, grey to black, soft	2.0	(6.6)	44.0	(144.4)
8	Silt to very fine grained sand, pyrite nodules	1.5	(4.9)	42.0	(137.8)
7	As in unit 9	2.5	(8.2)	40.5	(132.9)
6	Shale, grey to black and carbonaceous, interbedded with laminae and thin streaks of very fine sand and silt	11.0	(36.1)	38.0	(124.7)
5	Covered	16.0	(52.5)	27.0	(88.6)
4	Sand, medium to very fine grained, quartzose, buff, with streaks and thin beds of grey clay	5.0	(16.4)	11.0	(36.1)
3	Covered	4.0	(13.1)	6.0	(19.7)
2	Clay, grey	1.0	(3.3)	2.0	(6.6)
1	Sand, medium to coarse grained with red-brown iron oxide (limonite?) staining, laminae of clay	1.0	(3.3)	1.0	(3.3)
Unit 1 is underlain by quartzose sandstone of the Glenelg Formation					

Station 74-GAS-7*Christopher Formation**Upper member*

10	Clay, grey	13.0	(42.7)	275.0	(902.3)
9	Sand, greenish grey, fine grained to silty, interbedded with grey clay, sideritic siltstone lens at centre of unit	4.0	(13.1)	262.0	(859.6)
8	Clay, dark grey, with reddish-brown, sideritic ironstone concretions, hedgehog concretions (radiating calcite crystals), wood fragments, gastropods	138.2	(453.4)	258.0	(846.5)
7	Siltstone, siderite cemented, rusty brown, pelecypods, wood fragments	3.4	(11.2)	119.8	(393.1)
6	Clay, dark grey, in part carbonaceous, with thin laminae of silt and very fine grained sand	33.8	(110.9)	116.4	(381.9)
5	Sand and silt, very fine grained, buff to greenish or yellowish, locally siderite-cemented, interbedded with grey clay in laminae and thin beds. Pelecypods in lithified sandstone bed at base of unit	3.1	(10.2)	82.6	(271.0)
4	Clay, grey to greenish grey, minor interbedded silt laminae and sand beds up to 10 cm (4 in.) thick, shell fragments	5.3	(17.4)	79.5	(260.8)
3	Sand, grey to brown, fine grained, with sideritic, silty sandstone concretions and thin laminae of clay, shell fragments	0.7	(2.3)	74.2	(243.5)

Unit	Lithology	Thickness		Height above base	
		m	(ft)	m	(ft)
2	Shale, soft, grey, carbonaceous in part, with minor amounts of silt laminae	5.5	(18.0)	73.5	(241.1)
1	Covered, above estimated top of Isachsen Formation	68.0	(223.1)	68.0	(223.1)
Station 74-GAS-8					
<i>Isachsen Formation (part of)</i>					
8	Interbedded clay and silt with thin streaks of lignitic coal and scattered plant fragments	8.0	(26.2)	36.0	(118.1)
7	Lignite with intercalated clay beds	1.5	(4.9)	28.0	(91.9)
6	Sand, coarse grained to pebbly, minor lenses of clay, abundant planar crossbeds	5.2	(17.1)	26.5	(86.9)
5	Lignite with minor amounts of carbonaceous shale	0.3	(1.0)	21.3	(69.9)
4	Clay, grey-brown	7.0	(23.0)	21.0	(68.9)
3	Interbedded silt and fine-grained sand, minor silty clay lenticles, concretions up to 14 m (46 ft) in width, consisting of coarse-grained sand in red-brown iron oxide matrix	2.0	(6.6)	14.0	(46.0)
2	Sand, medium grey, slightly micaceous, with some thin, irregular laminae of grey clay, planar bedded	10.5	(34.5)	12.0	(39.4)
1	Covered interval. Section measured from sea level	1.5	(4.9)	1.5	(4.9)
Station 74-GAS-11					
<i>Christopher Formation</i>					
<i>Lower member</i>					
21	Clay, grey to buff, interbedded with white, fine-grained, quartzose sand	4.0	(13.1)	165.0	(541.4)
20	Sand, white, quartzose, fine grained, with minor clay streaks	4.0	(13.1)	161.0	(528.2)
19	Clay, silty, with minor amounts of fine-grained sand interbeds up to 50 cm (1.6 ft) thick	9.3	(30.5)	157.0	(515.1)
18	Coal	0.2	(0.7)	147.7	(484.6)
17	Clay, grey to buff, with thin interbeds of fine-grained sand and silt	4.7	(15.4)	147.5	(483.9)
<i>Isachsen Formation</i>					
16	Coal, lignitic with pyritic nodules	0.8	(2.6)	142.8	(468.5)
15	Sand, fine to medium grained, quartzose, passing laterally into gravel, planar crossbedding	5.5	(18.0)	142.0	(465.9)
14	Clay, grey, with thin beds of fine- to medium-grained sand	1.5	(4.9)	136.5	(447.9)
13	Sand, quartzose, fine grained, low-amplitude ripple marks	3.5	(11.5)	135.0	(443.0)
12	Clay, with thin beds and laminae of silt and fine- to medium-grained sand, pyrite nodules, sideritic concretions, minor coal streaks	8.1	(26.6)	131.5	(431.5)
11	Coal	0.1	(0.3)	123.4	(404.9)
10	Interbedded sand and clay; sand is medium grained, with planar crossbeds, abundant thin beds and laminae of grey clay and black carbonaceous shale, rare thin coal seams, pyrite nodules	11.3	(37.1)	123.3	(404.5)
9	Coal	0.5	(1.6)	112.0	(367.5)
8	Clay, brown, laminated	4.0	(13.1)	111.5	(365.8)
7	Clay, red-brown to grey or black and carbonaceous, with laminae of sand and silt, sand units locally thicken to thin to medium beds; rare trough crossbeds in sand units, sideritic nodules	18.5	(60.7)	107.5	(352.7)

Unit	Lithology	Thickness		Height above base	
		m	(ft)	m	(ft)
6	Sand, medium grained, white, quartzose, planar bedded, pyrite nodules	4.5	(14.8)	89.0	(292.0)
5	Interbedded sand and clay, as in unit 7	18.0	(59.1)	84.5	(277.2)
4	Covered	9.5	(31.2)	66.5	(218.2)
3	Sand, medium to coarse grained, thin laminae of coal, abundant planar crossbeds, climbing ripples, pyrite nodules	7.5	(24.6)	57.0	(187.0)
2	Interbedded sand and clay as in unit 7	19.5	(64.0)	49.5	(162.4)
1	Covered interval above the approximate position of the Precambrian-Isachsen contact, as estimated from photogeological interpretation	30.0	(98.4)	30.0	(98.4)

Station 74-GAS-12

Christopher Formation (part of)

14	Clay, grey-brown	9.2	(30.2)	147.0	(482.3)
13	Siltstone, ferruginous, calcite veins	0.3	(1.0)	137.8	(452.1)
12	Clay, grey, with impersistent lenses or concretions of ferruginous siltstone; clay-ironstone, mineralized wood, ammonite fragments	5.5	(18.0)	137.5	(451.1)
11	Clay, silty, medium grey	26.5	(86.9)	132.0	(433.1)
10	Silt, argillaceous, abundant clay-ironstone concretions, dark grey, some beds of medium grey, silty clay	12.5	(41.0)	105.5	(346.1)
9	Shale, carbonaceous, with several beds of clay and silt, clay-ironstone concretions, ammonite fragments	23.5	(77.1)	93.0	(305.1)
8	Clay, silty, medium grey	2.0	(6.6)	69.5	(228.0)
7	Clay, dark grey, carbonaceous, interbedded grey and brown beds, becoming silty near top of unit, ironstone concretions	6.0	(19.7)	67.5	(221.5)
6	Clay, silty, with thin laminae of pale grey silt	6.0	(19.7)	61.5	(201.8)
5	Silt, overlain by carbonaceous shale	1.5	(4.9)	55.5	(182.1)
4	Clay, medium grey, clay-ironstone concretions up to 1 m in diameter	5.5	(18.0)	54.0	(177.2)
3	Clay, dark grey, carbonaceous	4.0	(13.1)	48.5	(159.1)
2	Clay, with thin beds and laminae of silt and very fine grained sand; silt and sand are red-brown; clay-ironstone concretions	7.5	(24.6)	44.5	(146.0)
1	Clay, dark grey to grey-brown, clay-ironstone concretions	37.0	(121.4)	37.0	(121.4)

Station 74-GAS-13

Christopher Formation (part of)

9	Clay, grey to grey-brown, rarely carbonaceous, rare silt beds, clay-ironstone concretions, 'hedgehog' concretions, mineralized wood, shell fragments	67.0	(219.9)	182.0	(597.1)
8	Siltstone, ferruginous, abundant pelecypods, bluff-forming	1.0	(3.3)	115.0	(377.3)
7	Clay, grey, shell fragments, mineralized wood	12.0	(39.4)	114.0	(374.0)
6	Sand, very fine grained, and silt	1.0	(3.3)	102.0	(334.7)
5	Siltstone-sandstone, calcareous, slightly argillaceous, abundant pelecypods, bluff-forming, laterally persistent	3.5	(11.5)	101.0	(331.4)
4	Clay, silty, medium to dark grey, lenses and pods of calcareous siltstone, pelecypods, rare cone-in-cone limestone	49.5	(162.4)	97.5	(319.9)
3	Clay, grey to black, carbonaceous	16.0	(52.5)	48.0	(157.5)
2	Covered	24.0	(78.7)	32.0	(105.0)
1	Sandstone-siltstone, planar bedded, weathers grey to buff, laminated, climbing ripples and small-scale crossbedding	8.0	(26.2)	8.0	(26.2)

Unit	Lithology	Thickness		Height above base	
		m	(ft)	m	(ft)
Station 74-GAS-21					
<i>Kanguk Formation</i>					
<i>Silty shale member (part of)</i>					
7	Shale, grey, friable, thin bedded	2.5	(8.2)	154.0	(505.3)
6	Clay, grey, interbedded with fine-grained, quartzose sand containing small-scale trough crossbedding	1.5	(4.9)	151.5	(497.1)
5	Clay, grey-brown, uniform, numerous siderite-dolomite concretions	60.0	(196.9)	150.0	(492.1)
4	Shale, dark grey, friable, soft	70.4	(231.0)	90.0	(295.3)
<i>Bituminous shale member</i>					
3	Shale, dark grey, bituminous, very fissile, numerous ellipsoidal concretions flattened along bedding planes and containing pelecypods	10.0	(32.8)	19.6	(64.3)
2	Shale, as in unit 3, interbedded with thin seams of yellowish bentonitic clay	1.6	(5.2)	9.6	(31.5)
<i>Hassel Formation (part of)</i>					
1	Sand, silty, greenish	8.0	(26.2)	8.0	(26.2)
Station 74-GAS-25					
<i>Christopher Formation</i>					
<i>Lower member</i>					
5	Shale, dark grey-brown, uniform, rare carbonaceous shale and thin beds of fine-grained quartzose sand and silt	42.0	(137.8)	72.0	(236.2)
4	Interbedded brown shale and very fine grained quartzose sand; unit becomes predominantly sand near top	8.3	(27.2)	30.0	(98.4)
3	Coarsening upward unit as in unit 4	1.7	(5.6)	21.7	(71.2)
2	As in unit 5	10.0	(32.8)	20.0	(65.6)
1	Covered interval above estimated position of Isachsen-Christopher contact, which is 10 m (33 ft) above sea level	10.0	(32.8)	10.0	(32.8)
Station 74-GAS-46					
<i>Christopher Formation (part of)</i>					
14	Sand, fine grained, with thin beds and laminae of carbonaceous shale, lenses of siltstone up to 2 m thick	6.0	(19.7)	67.0	(219.9)
13	Shale, black, carbonaceous, with interbedded silt and very fine grained sand, hedgehog concretions	11.5	(37.7)	61.0	(200.1)
12	Sandstone, and siltstone, red-brown, thin bedded	2.0	(6.6)	49.5	(162.4)
11	Shale, silty, carbonaceous, with rusty streaks of silt	7.5	(24.6)	47.5	(155.8)
10	Shale, dark grey, carbonaceous, poorly exposed	19.5	(64.0)	40.0	(131.2)
9	Sand, fine grained, quartzose	0.5	(1.6)	20.5	(67.3)
8	Siltstone, massive	1.0	(3.3)	20.0	(65.6)
7	Shale, medium to dark grey and carbonaceous, silty in part, with thin laminae of silt	7.5	(24.6)	19.0	(62.3)
6	Sand, fine grained, red-brown, with thin laminae of carbonaceous clay	1.0	(3.3)	11.5	(37.7)

Unit	Lithology	Thickness		Height above base	
		m	(ft)	m	(ft)
5	Shale, dark grey, carbonaceous, with thin laminae of sand at base of unit, mineralized wood	3.3	(10.9)	10.5	(34.5)
4	Sandstone and siltstone interbedded, red-brown, massive, pelecypod fragments	1.2	(3.9)	7.2	(23.6)
3	Sand interbedded with silt, with thin beds of carbonaceous clay	2.5	(8.2)	6.0	(19.7)
2	Sandstone and siltstone interbedded, thin bedded to laminated, small-scale ripple marks, abundant pelecypod fragments	0.5	(1.6)	3.5	(11.5)
1	Sand and silt interbedded, as in unit 3	3.0	(9.8)	3.0	(9.8)

